



THE ARBOVIRUS PROFILES AND INTERACTIONS WITH HOSTS – PREPARING FOR EMERGING DISEASES

EDITED BY: Shu Shen, Fei Deng, Na Jia, Han Xia and Ali Zohaib
PUBLISHED IN: Frontiers in Microbiology



frontiers

Frontiers eBook Copyright Statement

The copyright in the text of individual articles in this eBook is the property of their respective authors or their respective institutions or funders. The copyright in graphics and images within each article may be subject to copyright of other parties. In both cases this is subject to a license granted to Frontiers.

The compilation of articles constituting this eBook is the property of Frontiers.

Each article within this eBook, and the eBook itself, are published under the most recent version of the Creative Commons CC-BY licence.

The version current at the date of publication of this eBook is CC-BY 4.0. If the CC-BY licence is updated, the licence granted by Frontiers is automatically updated to the new version.

When exercising any right under the CC-BY licence, Frontiers must be attributed as the original publisher of the article or eBook, as applicable.

Authors have the responsibility of ensuring that any graphics or other materials which are the property of others may be included in the CC-BY licence, but this should be checked before relying on the CC-BY licence to reproduce those materials. Any copyright notices relating to those materials must be complied with.

Copyright and source acknowledgement notices may not be removed and must be displayed in any copy, derivative work or partial copy which includes the elements in question.

All copyright, and all rights therein, are protected by national and international copyright laws. The above represents a summary only. For further information please read Frontiers' Conditions for Website Use and Copyright Statement, and the applicable CC-BY licence.

ISSN 1664-8714

ISBN 978-2-83250-354-6

DOI 10.3389/978-2-83250-354-6

About Frontiers

Frontiers is more than just an open-access publisher of scholarly articles: it is a pioneering approach to the world of academia, radically improving the way scholarly research is managed. The grand vision of Frontiers is a world where all people have an equal opportunity to seek, share and generate knowledge. Frontiers provides immediate and permanent online open access to all its publications, but this alone is not enough to realize our grand goals.

Frontiers Journal Series

The Frontiers Journal Series is a multi-tier and interdisciplinary set of open-access, online journals, promising a paradigm shift from the current review, selection and dissemination processes in academic publishing. All Frontiers journals are driven by researchers for researchers; therefore, they constitute a service to the scholarly community. At the same time, the Frontiers Journal Series operates on a revolutionary invention, the tiered publishing system, initially addressing specific communities of scholars, and gradually climbing up to broader public understanding, thus serving the interests of the lay society, too.

Dedication to Quality

Each Frontiers article is a landmark of the highest quality, thanks to genuinely collaborative interactions between authors and review editors, who include some of the world's best academicians. Research must be certified by peers before entering a stream of knowledge that may eventually reach the public - and shape society; therefore, Frontiers only applies the most rigorous and unbiased reviews. Frontiers revolutionizes research publishing by freely delivering the most outstanding research, evaluated with no bias from both the academic and social point of view. By applying the most advanced information technologies, Frontiers is catapulting scholarly publishing into a new generation.

What are Frontiers Research Topics?

Frontiers Research Topics are very popular trademarks of the Frontiers Journals Series: they are collections of at least ten articles, all centered on a particular subject. With their unique mix of varied contributions from Original Research to Review Articles, Frontiers Research Topics unify the most influential researchers, the latest key findings and historical advances in a hot research area! Find out more on how to host your own Frontiers Research Topic or contribute to one as an author by contacting the Frontiers Editorial Office: frontiersin.org/about/contact

THE ARBOVIRUS PROFILES AND INTERACTIONS WITH HOSTS – PREPARING FOR EMERGING DISEASES

Topic Editors:

Shu Shen, Wuhan Institute of Virology, Chinese Academy of Sciences (CAS), China

Fei Deng, Wuhan Institute of Virology, Chinese Academy of Sciences (CAS), China

Na Jia, Beijing Institute of Microbiology and Epidemiology, China

Han Xia, Wuhan Institute of Virology, Chinese Academy of Sciences (CAS), China

Ali Zohaib, Islamia University of Bahawalpur, Pakistan

Citation: Shen, S., Deng, F., Jia, N., Xia, H., Zohaib, A., eds. (2022). The Arbovirus Profiles and Interactions With Hosts – Preparing for Emerging Diseases. Lausanne: Frontiers Media SA. doi: 10.3389/978-2-83250-354-6

Table of Contents

- 05** *microRNAs, the Link Between Dengue Virus and the Host Genome*
Yinghua Su, Ting Lin, Chun Liu, Cui Cheng, Xiao Han and Xiwen Jiang
- 18** *Non-structural Proteins of Severe Fever With Thrombocytopenia Syndrome Virus Suppress RNA Synthesis in a Transcriptionally Active cDNA-Derived Viral RNA Synthesis System*
Fuli Ren, Shu Shen, Yun-Jia Ning, Qiongya Wang, Shiyu Dai, Junming Shi, Min Zhou, Hualin Wang, Chaolin Huang, Ding-Yu Zhang and Fei Deng
- 34** *The Antiviral Effect of Novel Steroidal Derivatives on Flaviviruses*
Luping Zhang, Dengyuan Zhou, Qiuyan Li, Shuo Zhu, Muhammad Imran, Hongyu Duan, Shengbo Cao, Shaoyong Ke and Jing Ye
- 50** *The 5' and 3' Untranslated Regions of the Japanese Encephalitis Virus (JEV): Molecular Genetics and Higher Order Structures*
Hong Liu, Jun Zhang, Yuzhen Niu and Guodong Liang
- 66** *Peptide OPTX-1 From Ornithodoros papillipes Tick Inhibits the pS273R Protease of African Swine Fever Virus*
Jingjing Wang, Mengyao Ji, Bingqian Yuan, Anna Luo, Zhenyuan Jiang, Tengyu Zhu, Yang Liu, Peter Muiruri Kamau, Lin Jin and Ren Lai
- 73** *Recent Advances in Bunyavirus Reverse Genetics Research: Systems Development, Applications, and Future Perspectives*
Fuli Ren, Shu Shen, Qiongya Wang, Gang Wei, Chaolin Huang, Hualin Wang, Yun-Jia Ning, Ding-Yu Zhang and Fei Deng
- 86** *Co-circulation of Orthobunyaviruses and Rift Valley Fever Virus in Mauritania, 2015*
Nicole Cichon, Yahya Barry, Franziska Stoek, Abdellah Diambar, Aliou Ba, Ute Ziegler, Melanie Rissmann, Jana Schulz, Mohamed L. Haki, Dirk Höper, Baba A. Doumbia, Mohamed Y. Bah, Martin H. Groschup and Martin Eiden
- 98** *Virome and Blood Meal-Associated Host Responses in Ixodes persulcatus Naturally Fed on Patients*
Liang-Jing Li, Nian-Zhi Ning, Yuan-Chun Zheng, Yan-Li Chu, Xiao-Ming Cui, Ming-Zhu Zhang, Wen-Bin Guo, Ran Wei, Hong-Bo Liu, Yi Sun, Jin-Ling Ye, Bao-Gui Jiang, Ting-Ting Yuan, Jie Li, Cai Bian, Lesley Bell-Sakyi, Hui Wang, Jia-Fu Jiang, Ju-Liang Song, Wu-Chun Cao, Tommy Tsan-Yuk Lam, Xue-Bing Ni and Na Jia
- 108** *Dissecting the Species-Specific Virome in Culicoides of Thrace*
Konstantinos Konstantinidis, Maria Bampali, Michael de Courcy Williams, Nikolas Dovrolis, Elisavet Gatzidou, Pavlos Papazilakis, Andreas Nearchou, Stavroula Veletza and Ioannis Karakasiliotis
- 124** *SUMOylation Is Essential for Dengue Virus Replication and Transmission in the Mosquito Aedes aegypti*
Shih-Che Weng and Shin-Hong Shiao
- 136** *Discovery of Tick-Borne Karshi Virus Implies Misinterpretation of the Tick-Borne Encephalitis Virus Seroprevalence in Northwest China*
Yuan Bai, Yanfang Zhang, Zhengyuan Su, Shuang Tang, Jun Wang, Qiaoli Wu, Juan Yang, Abulimiti Moming, Yujiang Zhang, Lesley Bell-Sakyi, Surong Sun, Shu Shen and Fei Deng

151 *Potential Mechanisms of Transmission of Tick-Borne Viruses at the Virus-Tick Interface*

Mahvish Maqbool, Muhammad Sohail Sajid, Muhammad Saqib, Faisal Rasheed Anjum, Muhammad Haleem Tayyab, Hafiz Muhammad Rizwan, Muhammad Imran Rashid, Imaad Rashid, Asif Iqbal, Rao Muhammad Siddique, Asim Shamim, Muhammad Adeel Hassan, Farhan Ahmad Atif, Abdul Razzaq, Muhammad Zeeshan, Kashif Hussain, Rana Hamid Ali Nisar, Akasha Tanveer, Sahar Younas, Kashif Kamran and Sajjad ur Rahman

171 *The Potential Vector Competence and Overwintering of West Nile Virus in Vector Aedes Albopictus in China*

Ying-mei Zhang, Xiao-xia Guo, Shu-fang Jiang, Chun-xiao Li, Dan Xing, Heng-duan Zhang, Yan-de Dong and Tong-yan Zhao

178 *Dengue Virus-2 Infection Affects Fecundity and Elicits Specific Transcriptional Changes in the Ovaries of Aedes aegypti Mosquitoes*

Fabiana Feitosa-Suntheimer, Zheng Zhu, Enzo Mameli, Gargi Dayama, Alexander S. Gold, Aditi Broos-Caldwell, Andrea Troupin, Meagan Rippee-Brooks, Ronald B. Corley, Nelson C. Lau, Tonya M. Colpitts and Berlin Londoño-Renteria



microRNAs, the Link Between Dengue Virus and the Host Genome

Yinghua Su^{1†}, Ting Lin^{1†}, Chun Liu^{1†}, Cui Cheng¹, Xiao Han^{1*} and Xiwen Jiang^{2*}

¹College of Biological Science and Engineering, Fuzhou University, Fujian, China, ²DAAN Gene Co., Ltd. of Sun Yat-sen University, Guangdong, China

OPEN ACCESS

Edited by:

Han Xia,

Wuhan Institute of Virology, Chinese Academy of Sciences (CAS), China

Reviewed by:

Yang Qiu,

Wuhan Institute of Virology, Chinese Academy of Sciences (CAS), China

Day-Yu Chao,

National Chung Hsing University, Taiwan

*Correspondence:

Xiao Han

hanxiao@fzu.edu.cn

Xiwen Jiang

yuanyecat@vip.sina.com

[†]These authors have contributed equally to this work

Specialty section:

This article was submitted to Virology, a section of the journal Frontiers in Microbiology

Received: 25 May 2021

Accepted: 16 July 2021

Published: 11 August 2021

Citation:

Su Y, Lin T, Liu C, Cheng C, Han X and Jiang X (2021) microRNAs, the Link Between Dengue Virus and the Host Genome. Front. Microbiol. 12:714409. doi: 10.3389/fmicb.2021.714409

Dengue virus (DENV) is a small envelope virus of Flaviviridae that is mainly transmitted by *Aedes aegypti* and *Aedes albopictus*. It can cause dengue fever with mild clinical symptoms or even life-threatening dengue hemorrhagic fever (DHF) and dengue shock syndrome (DSS). At present, there are no specific drugs or mature vaccine products to treat DENV. microRNAs (miRNAs) are a class of important non-coding small molecular RNAs that regulate gene expression at the post-transcriptional level. It is involved in and regulates a series of important life processes, such as growth and development, cell differentiation, cell apoptosis, anti-virus, and anti-tumor. miRNAs also play important roles in interactions between host and viral genome transcriptomes. Host miRNAs can directly target the genome of the virus or regulate host factors to promote or inhibit virus replication. Understanding the expression and function of miRNAs during infection with DENV and the related signal molecules of the miRNA-mediated regulatory network will provide new insights for the development of miRNA-based therapies.

Keywords: microRNA, dengue virus, host-pathogen interaction, virus replication, signaling/signaling pathways

INTRODUCTION

Dengue virus (DENV) is an important infectious agent of flavivirus, which is mainly transmitted by vector insects such as *Aedes aegypti* and *Aedes albopictus*. It can cause severe diseases in humans, such as dengue fever, dengue hemorrhagic fever (DHF), and dengue shock syndrome (DSS). DENV, an infectious virus prevalent in tropical and subtropical areas (Lambrechts et al., 2010) is widely distributed among humans, has a high incidence, and causes great harm. microRNAs (miRNAs), a small noncoding RNA (18–25 nucleotides) that exists widely in all kinds of plants, animals, and microorganisms, are a key transcription factor that affects gene expression. miRNAs can combine with 3'-untranslated regions (3'-UTRs) of messenger RNA (mRNA) to prevent translation events by degrading mRNA or inhibiting translation (Bartel, 2004), which may play an important role in the direct or indirect regulation of viral and host genome transcriptomes. At present, research on the interaction mechanism of miRNAs between DENV and host genome transcriptomes is lacking. Understanding miRNA expression and related target signaling pathways during DENV infection will provide new ideas for miRNA-based therapies. This paper reviews the regulatory role and mechanism of miRNA in DENV infection.

Introduction to DENV

Dengue virus is a single-stranded positive-strand RNA (+ssRNA) virus that belongs to *Flaviviridae*. DENV can be divided into four serotypes according to its antigenicity: 1, 2, 3, and 4. The DENV genome is about 11 kb in length and 45–55 nm in diameter. The 5' and 3' ends of the virus

RNA have untranslated regions containing several 100 nucleotides. The remaining DENV fragment is a single open reading frame. After infecting host cells, the viral genome is transcribed and translated into a total protein, which is cleaved into three structural proteins (C protein, prM/M protein, and E protein) and seven nonstructural proteins (NS1, NS2A, NS2B, NS3, NS4A, NS4B, and NS5; Perera and Kuhn, 2008) by viral and cellular proteases. Among them, E protein is the largest structural protein and the main envelope protein of DENV particles. Nonstructural proteins have many functions: They provide enzyme activity for biochemical reactions, and they provide suitable internal environments for viral RNA replication, including remodeling of the cell membrane and the inhibition of host antiviral reaction. Nonstructural protein 1 (NS1) has multiple polymer structures. In the early stages of infection, NS1 binds to the endoplasmic reticulum (ER) in the form of a dimer and anchors the viral replication complex (RCS) to the membrane. As the infection subsides, NS1 is secreted out of the cell in the form of a hexamer, which results in the body's immune response to the virus (Muller and Young, 2013). NS2A, NS2B, NS4A, and NS4B are membrane binding proteins and components of the viral genome RCS. Among the four serotypes of DENV, NS5 has more than 70% homology and is the most conservative protein. NS5 has a variety of enzyme functions, including roles in N-terminal methyltransferase activity and C-terminal RNA-dependent RNA polymerase activity (Koonin, 1991; Klema et al., 2016). NS3 protein, a hydrophilic multifunctional protein with protease, RNA helicase, and RNA polymerase activity, plays an important role in processes, such as viral genome replication, packaging, and maturation (Tian et al., 2013).

PATHOGENESIS OF DENV AND HOST IMMUNITY

Invasion and Replication of DENV

Dengue virus infection begins with the bite of *A. aegypti* or *A. albopictus* infected by DENV, which can infect many kinds of cells, such as dendritic cells, macrophages, endothelial cells, and hepatocytes (Fang et al., 2013). The virus enters host cells through receptor-mediated endocytosis, in which the envelope glycoprotein E protein binds to receptors on the surfaces of host cells. Under neutral and slightly alkaline conditions, the E protein on the surface of the mature virus is in the form of a homodimer (Modis et al., 2004). In the acidic environment of the nucleosome, the E protein is restructured from a dimer to a trimer (Modis et al., 2004). This conformational change provides the energy required to bind the viral envelope to the host cell membrane and fuse the viral lipid bilayer and the cell membrane (Modis et al., 2004). E protein interacts with proteins on the surfaces of various mammalian and mosquito host cells during the invasion of the virus, but the real receptor for the virus has not yet been determined (Perera-Lecoin et al., 2013). The main receptors studied to date include heparin sulfate (Chen et al., 1997), dendritic cell-specific intracellular adhesion molecule-3-grabbing non-integrin (DC-SIGN) on dendritic cells (Tassaneetrithep et al., 2003), and mannose

receptor (Miller et al., 2008). The virus enters the cell mainly through clathrin-mediated endocytosis (van der Schaar et al., 2008), which enables the viral genome to enter the cytoplasm. Subsequently, it uses the organelles and nutrients of host cells to synthesize genes and various proteins. The newly synthesized genome combines with capsids to form a nucleoprotein complex that sprouts into the ER cavity to infect the lipid bilayer (Yu et al., 2008). At the same time, the virus E protein and prM protein were produced (Yu et al., 2008). Immature virus particles are transmitted through the secretory pathway. In the Golgi network, prM protein lysis mediated by furin results in the rearrangement of E protein, homodimerization, and the formation of mature virus particles that are then released (Yu et al., 2008).

Immune Regulation of Host Resistance to DENV

Once the virus invades cells and replicates, host cells can quickly recognize pathogen-associated molecular patterns through pattern recognition receptors (PRRs). For example, viral RNA, replication intermediates formed by virus nonstructural protease NS5, double-stranded RNA, and various proteins synthesized by the virus can initiate innate immune responses and guide adaptive immune responses to resist invasion by pathogenic microorganisms. PRRs include toll-like receptors (TLRs; Tsai et al., 2009), retinoic acid inducible gene I protein/melanoma differentiation factor 5 (RIG-I/MDA5; Nasirudeen et al., 2011), and miRNAs (Trobaugh et al., 2014). The ability of these innate components to recognize DENV may have different effects on the life cycle of the virus and the host's response to infection. In fact, the mutual recognition pattern of PAMP-PRR activates interferon regulatory factors, including IRF3, IRF7, and NF- κ B. Interferon type I (IFN), chemokines, and cytokines are expressed to promote the expression of antiviral genes and the inflammatory response. When the virus infects the body, it can proliferates in the capillary endothelial cells and releases into the blood to form viremia, and it then further infects mononuclear macrophages in the blood and tissue to cause dengue fever. The occurrence of severe DHF and DSS may be mainly due to the effects of antibody-dependent enhancement (ADE; Halstead, 1982), cross-reactive T cell response (Mongkolsapaya et al., 2003), and cytokine storm (Clark, 2007).

microRNA

RNA interference (RNAi) is a post-transcriptional gene-silencing mechanism mediated by small RNAs with length of 20–30 nucleotides, including miRNAs, small interfering RNAs (siRNAs), and PIWI-associated RNAs (piRNAs; Malone and Hannon, 2009; Castel and Martienssen, 2013). They can guide sequence-specific gene silencing in complex with an Argonaute protein (AGO protein) and cofactors and then involves the degradation of mRNA molecules, thereby preventing gene expression. It has demonstrated that RNAi phenomenon plays essential roles across eukaryotic organisms in genome defense against viruses and transposons: when the siRNAs are derived from viruses, they function as guides to specifically target the invading viruses

for RNAi and thereby inhibit viral replication and infection (Castel and Martienssen, 2013). However, a role for cellular miRNAs in the defense against viral infection in mammalian organisms has thus far remained elusive (Cullen, 2006). Delightfully, RNA-based therapeutics, such as siRNAs, miRNAs, antisense oligonucleotides (ASOs), aptamers, synthetic mRNAs, and CRISPR-Cas9, have great potential to target a large part of the currently undruggable genes and gene products and to generate entirely new therapeutic paradigms in disease (Dowdy, 2017). A classical case is a liver-specific miRNA- miR-122, which is expressed almost exclusively in liver cells with more than 50,000 copies per cell (Filipowicz and Grosshans, 2011). It has been revealed that miR-122 is an essential host factor for hepatitis C virus (HCV) infection and an antiviral target, and clinical proof-of-concept studies have demonstrated that an miR-122 inhibitors Miravirsin, an LNA-modified anti-miR-122, can efficiently reduce viral load in chronically infected HCV patients without detectable resistance (Janssen et al., 2013; Bandiera et al., 2015).

Biosynthesis of miRNA

In animals, miRNA genes are transcribed into primary transcripts (pri-miRNAs) by RNA polymerase II (RNA Pol II) in the nucleus, with a length of about 300–1,000 bases (Lee et al., 2004). In the nucleus exists a nuclear protein complex called a microprocessor complex that contains ribonuclease III endonuclease Drosha; DiGeorge syndrome chromosomal region 8 (DGCR8); and some minor cofactors, such as DEAD box RNA helicase P68 (DDX5) and p72 (DDX17). This microprocessor complex processes pre-miRNAs into hairpin structures of 70–90 nucleotides (Lee et al., 2003), namely, miRNA precursors. Subsequently, pre-miRNAs are transported from the nucleus to the cytoplasm by exportin5 protein (Bohnsack et al., 2004) and cleaved to form a Mir/Mir* complex of about 22 nt by Dicer1, an RNase III (Knight and Bass, 2001). Finally, one chain of the Mir/Mir* complex combines with ago (ago1 and ago2) protein to form the RNA-induced silencing complex (RISC). The chain that binds to the protein is called miRNA, and the other chain is called miRNA*. Mature miRNA is retained in the RISC, and miR* is released to and degraded in the cytoplasm (Krol et al., 2010). miRNA-bound RISCs mediate posttranscriptional silencing through two different mechanisms depending on their complementarity with target mRNA sequences (Bartel, 2004). Because of the endonuclease activity of ago2, complete complementary matching of miRNA and the target sequence usually leads to the degradation of mRNA, whereas an incomplete complementary combination of miRNA and the target sequence inhibits translation (Bartel, 2004).

Regulation of miRNA

microRNA is an important factor regulating gene expression and is widely involved in physiological and pathological processes, such as early development, cell proliferation, apoptosis, cell death, the metabolism of fat, and so on

(Bushati and Cohen, 2007). Each miRNA can have multiple target genes, and several miRNAs can regulate the same gene. This complex regulatory network can not only regulate the expression of multiple genes through one miRNA but also regulate the expression of a single gene through a combination of several miRNAs (Catalanotto et al., 2016). Mammalian miRNAs may control the activity of about 30% of protein coding genes and participate in the regulation of most cells; they are also closely related to most diseases (Filipowicz et al., 2008). Studies have shown the effects of miRNA deletion (Giraldez et al., 2005) and the role of miRNAs in signal transduction pathways (Boehm and Slack, 2005; Hu et al., 2020), cell proliferation (Brennecke et al., 2003), cell differentiation and apoptosis (Yin et al., 2020), and lipid metabolism (Xu et al., 2003). miRNAs also play an important role in infection with viruses. Viruses can use miRNAs to evade host immune monitoring and regulate host factors to promote their own replication. In contrast, miRNAs in host cells can promote or inhibit viral replication by targeting viral genome RNA and regulating their own host factors. A microarray study that used the blood of patients with acute DENV infection showed that the expression of 348 miRNAs changed after DENV infection; 17 miRNAs were found that may be used to distinguish mild dengue fever from severe DHF with complications (Tambyah et al., 2016). In another study, expression of broad-spectrum miRNAs in serum samples of three patients with DENV type 1 (DENV-1) and three healthy volunteers was analyzed with miRNA PCR array technology. A total of 41 miRNAs were upregulated and 12 miRNAs were downregulated in the serum of DENV-1 patients compared to healthy controls (Ouyang et al., 2016). Analyses of receiver operating characteristic (ROC) curves showed that serum hsa-miR-21-5p and hsa-miR-146a-5p can distinguish patients with dengue fever infection with good sensitivity and specificity. Moreover, functional analyses of these miRNAs show that they are involved in inflammation and cell proliferation. Therefore, these miRNAs are expected to be potential biomarkers for a diagnosis of DENV (Wen et al., 2015; Ouyang et al., 2016). Increasing numbers of studies have shown that miRNA plays an important role in DENV, which is discussed in detail below.

THE ROLE OF miRNA IN REGULATING DENV AND RELATED SIGNALING PATHWAYS

miRNAs Target the DENV Genome Directly to Inhibit or Promote DENV Replication miRNAs That Inhibit DENV Replication by Targeting Viral Genomes

microRNAs usually induce translation inhibition by binding to MRE sites of target mRNAs. To date, many miRNAs have been identified that can affect DENV replication by directly targeting viral genome sequences. For example, miR-548 g-3p can regulate the replication of DENV-1, -2, -3, and -4 by

directly targeting the stem ring structure of the virus 5'-UTR promoter element and can also interfere with the translation of DENV, thus inhibiting expression of the virus protein (Giraldez et al., 2005). Previous studies have found that the 5'-UTR of the DENV genome contains two defined elements essential for viral replication. At the 5' end, a large stem-loop (SLA) structure functions as the promoter for viral polymerase activity. Next to the SLA, there is a short stem-loop that contains a cyclization sequence known as the 5' upstream AUG region (5'UAR). The cis-acting elements in the 5'-UTR may involve in controlling viral protein translation, RNA synthesis, and encapsidation (Lodeiro et al., 2009; Gebhard et al., 2011). At the same time, overexpression of miR-484 and miR-744 can inhibit virus replication by acting on 3'-UTRs of the four serotypes of DENV, which indicates that miR-484 and miR-744 are two possible host factors inhibiting DENV infection (Castrillón-Betancur and Urcuqui-Inchima, 2017). Similarly, the 3'-UTR of the DENV is indispensable for their replication as they can promote the translation of the virus (Gebhard et al., 2011; Manzano et al., 2011). Castillo et al. (2016) found through bioinformatics analysis that host miR-133a can target 3'-UTRs of all four DENV serotypes and 3'-UTR of DENV downregulates endogenous expression of miRNA-133a in Vero cells during the first hours of infection. In addition, miR-133a overexpression inhibited DENV replication and this antiviral effect may be mediated by regulation of the host factor polypyrimidine tract binding (PTB) protein, a target of miR-133a (Castillo et al., 2016).

Yan et al. (2014) showed that miR-252 was highly expressed (more than three times uninfected) in a DENV-2 infection model of the mosquito C6/36 cell line and could downregulate expression of E protein through E protein gene targeting DENV-2, thus inhibiting DENV replication. It is noteworthy that the E protein of DENV plays an essential role in the process of virus attachment, fusion with host cell membrane and virus assembly, and can induce a protective immune response by neutralizing antibodies (Yu et al., 2008; Anasir et al., 2020). Therefore, understanding the impact of miRNA on DENV E protein has led to the exploration of miRNA-based drug discovery of antiviral. Finally, Lee et al. (2017) found that the water extract of *Flos Lonicerae* can upregulate expression of Let-7a in human and mouse blood, and Let-7a in turn can target the NS1 region of DENV-2 (nt 3,313–3,330) to inhibit the replication of DENV-2. Recent studies have

revealed that DENV NS1 directly promotes vascular permeability by inducing a strong proinflammatory vasoactive response by mediating TLR 4 signaling (Stacey et al., 2015) and endothelial glycocalyx disruption (Puerta-Guardo et al., 2016). And it can activate platelets *via* TLR 4, leading to thrombocytopenia and hemorrhage (Chao et al., 2019). Therefore, this study provides a new insight for prevention and treatment of DENV infection through induction of the innate miRNA Let-7a by honeysuckle (Lee et al., 2017).

miRNAs That Promote DENV Replication by Targeting Viral Genomes

However, limited miRNAs can directly target viral genomes to promote viral replication but the specific mechanism remains to be investigated. Researchers screened a miRNA that was significantly differentially expressed after DENV-2 infection in HepG2 cells, namely, miR-21, and found that expression of miR-21 increased significantly and promoted the replication of DENV-2 after viral infection of HepG2 cells. However, prior to DENV infection of HepG2 cells, a significant reduction in DENV-2 production was observed after treatment with the miR-21 antagonist anti-miR-21 (AMO-21); thus, miR-21 is expected to be an intervention target for dengue treatment (Kanokudom et al., 2017). However, the mechanism of the replication of DENV induced by miR-21 is unclear; miR-21 may directly target the NS1 protein sequence of the DENV-2 genome (Miranda et al., 2006). Besides, Zhou et al. (2014) found a midgut-specific miRNA in an *A. albopictus* vector, namely, miR-281, after mosquito C6/36 cells were infected with DENV-2. miR-281 may target the 5'-UTR of DENV-2 genomic RNA and upregulate in response to viral infection, thus promoting DENV replication, whereas antagonism or knockout of miR-281 reduces the viral RNA level in *A. albopictus* (Zhou et al., 2014). These miRNAs, which inhibit or promote viral replication by targeting viral genomes, play a direct role in regulating viral infection and reasonable regulation of miRNAs expression and may avoid the excessive production of cellular inflammatory factors, thus avoiding the risk of DHF. miRNA-based therapeutics, such as miRNA mimics and inhibitors of miRNAs may have great potential to directly regulate virus replication and thus treat DENV-related diseases.

Relevant summaries of miRNA are shown in **Table 1** and in the schematic diagram in **Figure 1**.

TABLE 1 | microRNAs that directly target viral genomes to inhibit or promote viral replication.

miRNA	Experimental model	Target	Effects	References
miR-548 g-3p	U937	DENV 5'-UTR	Inhibit	Wen et al., 2015
miR-484, miR-744	Vero	DENV 3'-UTR	Inhibit	Castrillón-Betancur and Urcuqui-Inchima, 2017
miR-133a	Vero	DENV 3'-UTR	Inhibit	Castillo et al., 2016
miR-252	C6/36	Viral gene E	Inhibit	Yan et al., 2014
Let-7a	Blood of humans and mice	NS1 sequence (nt:3,313–3,330)	Inhibit	Lee et al., 2017
miR-21	HepG2	NS1 sequence	Promote	Miranda et al., 2006; Kanokudom et al., 2017
miR-281	C6/36	DENV 5'-UTR	Promote	Zhou et al., 2014

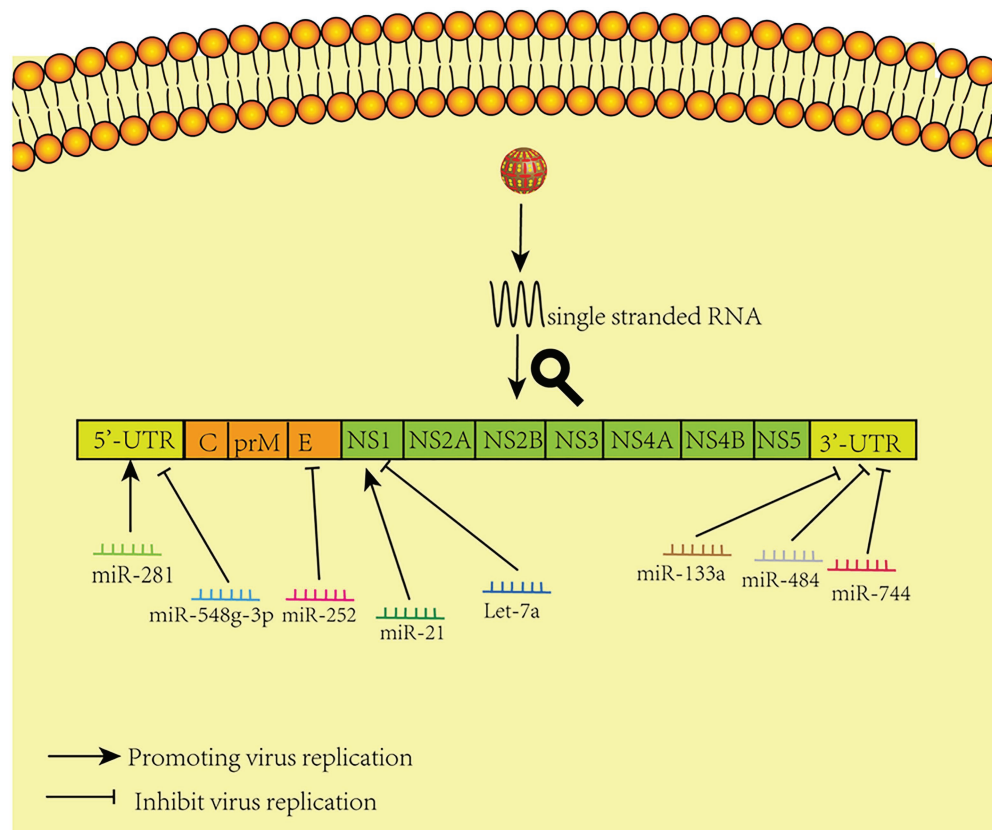


FIGURE 1 | Model of miRNAs that directly target viral genomes. The figure shows that different microRNAs promote and inhibit virus replication by acting directly on corresponding sites in the virus genome.

miRNAs Inhibit or Promote DENV Replication by Regulating Host Factors

Since viruses are parasitic organisms that rely on a range of host cytokines for replication and infection, many miRNAs have been shown to indirectly regulate DENV replication by regulating host factors or immune responses. miRNAs can affect the process of viral translation and replication by acting on related cytokines and regulating related signaling pathways. A large number of studies have clarified how related miRNAs affect related signaling pathways and thus regulate viral replication and disease progression (Barbu et al., 2020). Besides, miRNAs can also enhance or limit cellular responses to infection, such as immune responses or defense mechanisms (Trobaugh et al., 2014).

miRNAs That Inhibit DENV Replication by Regulating Host Factors

miRNAs That Inhibit DENV Replication by Regulating IFN System

After the virus invasion, the body will take the lead in initiating the innate immune response. And the type I interferon system inhibits viral infection by establishing a homeostasis in both infected and uninfected cells. DENV infection triggers the production of type I IFN after viral RNA is detected by TLRs

and RIG-I-like (RLR) receptors, and signaling cascades are initiated *via* connector molecules, such as MyD88, MAVs, or STING (Diamond and Pierson, 2015). Type I IFN binding to cells induces a JAK-STAT-dependent signaling cascade that ultimately leads to the expression of hundreds of IFN-stimulating genes (ISGs), some of which block specific steps in the DENV lifecycle (Schoggins et al., 2012). However, DENV is able to resist the production of type I IFN and signal transduction of key myeloid targets. In addition to regulating DENV replication, the antagonistic type I IFN signaling pathway in antigen-presenting cells attenuated or skewed the adaptive immune response (Diamond and Pierson, 2015).

A previous study has demonstrated that mammals can use cellular miRNAs to fight viral infections through the interferon system (Pedersen et al., 2007), and several studies have confirmed that dysregulated miRNAs can mediate the interferon system to regulate viral replication after DENV infection. For example, expression of Let-7c is upregulated and it has been shown to have a positive effect on protecting cells from oxidative stress and inflammation when DENV infects the human hepatoma cell line Huh-7 and monocyte macrophage line U937-DC-SIGN, and Let-7c directly targets the Basic Leucine Zipper Transcription Factor-1 (BACH1; Escalera-Cueto et al., 2015). However, BACH1 inhibited the expression of heme oxygenase-1 (HO-1) and antioxidant genes involved in oxidative stress response.

Therefore, the upregulation of Let-7c expression indirectly inhibits the replication of DENV-2 and DENV-4 in Huh-7 cells through the modulation of host factors like BACH1 and HO-1. The research of miRNAs that modulate their expression after DENV infection in other cell types may give useful clues about the host molecules that may participate during viral infection (Escalera-Cueto et al., 2015). Another study showed that the antiviral effects of HO-1 are related to the recovery of the antiviral IFN immune response signal pathway and the inhibition of DENV protease activity by biliverdin, a byproduct of heme degradation catalyzed by HO-1 (Tseng et al., 2016). A recent study found that overexpression of miR-155 in Huh-7 cells inhibits virus replication *in vitro* (Su et al., 2020). *In vivo*, overexpression of miR-155 can protect ICR suckling mice from the threat of DENV infection, and miR-155 also induces HO-1-mediated antiviral response by targeting BACH1 (Su et al., 2020). Finally, the HO-1-mediated inhibition of NS2B/NS3 protease activity enhances induction of antiviral interferons and inhibits virus replication (Su et al., 2020). These studies suggest that HO-1 and related miRNAs can be used as potential therapeutic targets to control DENV replication. Related studies have shown that miR-155 regulates immune cells, including dendritic cells, B cells, and T cells, and targets essential molecules involved in regulating the immune system as well as participating in multiple signaling pathways, including MAPK, insulin, Wnt, and MAPK/NF- κ B (Pashangzadeh et al., 2021). In view of this, miR-155 may also play a crucial role in the immune regulation of DENV by targeting a wide range of pathways across different immune responses. Zhu et al. (2014) found that expression of miR-30e* is upregulated in HeLa cells and U937 cells infected by DENV and then activates the NF- κ B pathway by targeting I κ B α , an inhibitor of the innate immune signaling pathway of the virus 3'-UTR. Thus, it promotes expression of IFN- β and its downstream genes, such as oligoadenylate synthase-1 gene (OAS1), myxovirus resistance protein A gene (MxA), and interferon-induced transmembrane protein 1 gene (IFITM1), thus inhibiting virus replication (Zhu et al., 2014). In a previous study on cancer, microRNA-30e* was also reported to promote human glioma cell invasion in an orthotopic xenograft model by directly targeting the I κ B α 3'-UTR and suppresses I κ B α expression and then disrupting the NF- κ B/I κ B α negative feedback loop (Jiang et al., 2012). This miRNA-mediated epigenetic regulation may lead to a more efficient and direct activation of NF- κ B in a cascading manner than the phosphorylation and ubiquitination mediated activation by IKK-induced phosphorylation. Hence, these studies emphasize the direct regulation of miR-30e* on NF- κ B signaling pathway, which is an important intracellular nuclear transcription factor involved in the body's inflammatory response and immune response. Another study found that the miR-34 family (including miR-34a, miR-34c, miR-449a, and miR-449b) has similar natural regulatory effects in response to a variety of flavivirus infections, including DENV (Smith et al., 2017). Upregulation of miR-34 family expression inhibits the Wnt signaling pathway, resulting in the inhibition of phosphorylation of glycogen synthase kinase 3 (GSK3 β). GSK3 β sends positive feedback to the IFN signal pathway by interacting with serine kinase TBK1, which promotes phosphorylation of IRF3 and subsequent transcriptional activation

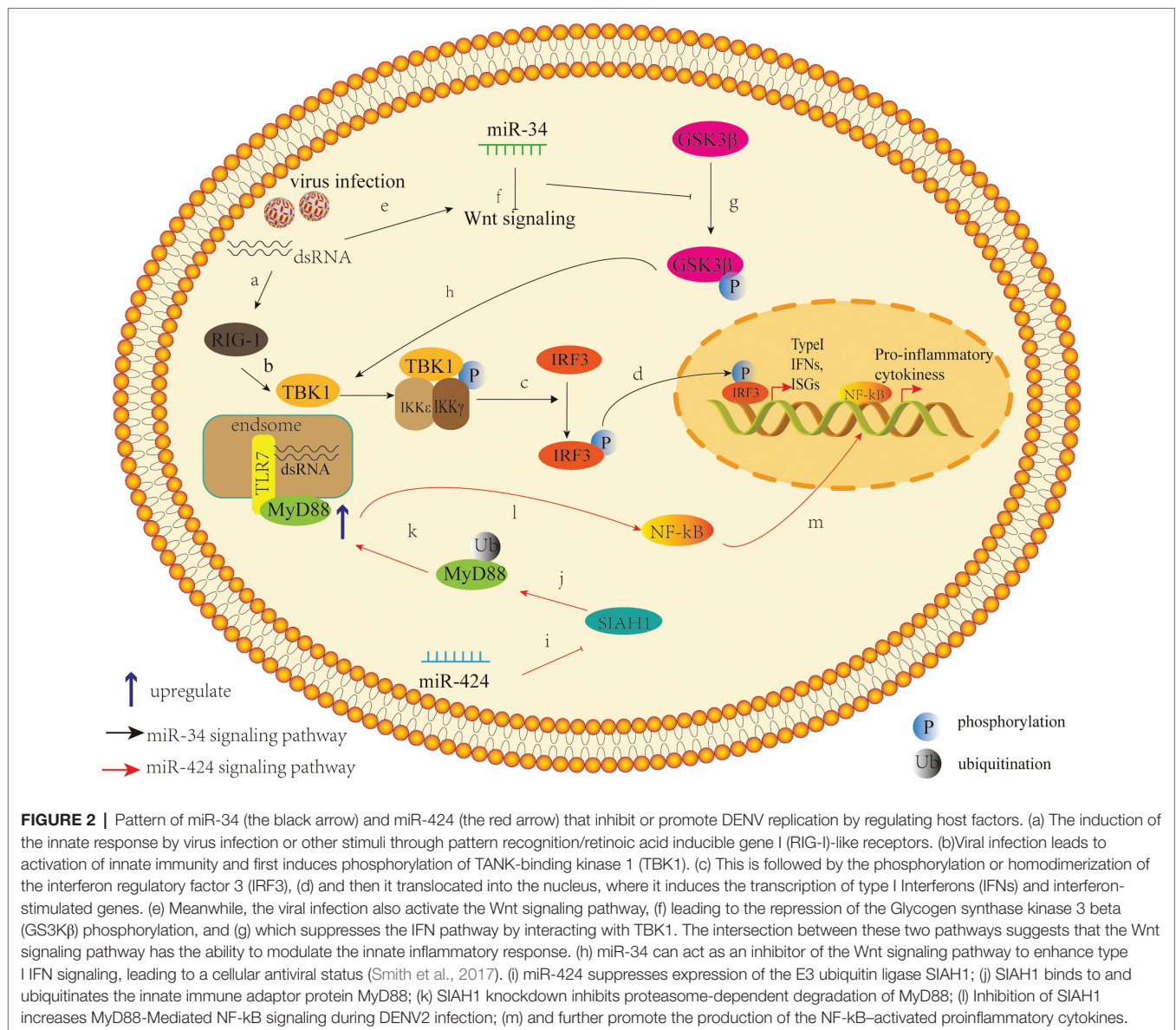
of IFN-I and other ISGS, thus promoting antiviral response (Smith et al., 2017). The miR-34 family increases production of IFN-I and expression of ISGS by inhibiting the Wnt signaling pathway and thus inhibits virus replication (Smith et al., 2017; **Figure 2**). In fact, miR-34a has demonstrated various regulatory effects on cancer cells by targeting multiple genes and signaling pathways, and has shown great promise in animal models of myeloma, hepatocellular carcinoma, lung cancer, and breast cancer (Misso et al., 2014). It is currently being tested in human trials on the efficacy of hepatic and hematologic cancers (Misso et al., 2014). These studies highlight the role of miR-34a in the antiviral response and the possibility that small molecule antagonists in the Wnt signaling pathway that have been suggested as anticancer therapies (Dihlmann and von Knebel, 2005) may be important antiviral targets.

In short, these studies emphasize that miRNA mediates the regulation of interferon system in immune response by related target genes, and then triggers the host's antiviral response.

miRNAs That Inhibit DENV Replication by Regulating Other Host Factors

The intracellular environment is complex and involves numerous signaling pathways, which are also crucial for cellular metabolism. Many miRNAs can also influence viral replication by regulating cytokines other than immune responses. Diosa-Toro and other scholars have found another miRNA with antiviral effects, namely, miR-3614-5p (Diosa-Toro et al., 2017). They found that when human macrophages were not infected with DENV, expression of miR-3614-5p was upregulated, and this overexpression reduced the infectivity of DENV (Diosa-Toro et al., 2017). The researchers predicted that adenosine deaminase acting on RNA1 (ADAR1), a protein that can promote viral replication, is one of the targets of miR-3614-5p and proved that ADAR1 can improve the infectivity of DENV in the early stages of cell infection with the virus (Diosa-Toro et al., 2017). This study extends the knowledge of the contribution of human miRNAs in the construction of networks of interactions between DENV and its human host cells. Wu et al. (2014) showed that miR-223 was significantly decreased after infection with DENV-2 in human endothelial Eahy926 cells and that this overexpression inhibited the replication of DENV-2. This is because miR-223 downregulates the expression of STMN1 through the STMN1 gene, a microtubule instability protein targeting the 3'-UTR of viral RNA, thus inhibiting virus replication (Wu et al., 2014). STMN1 is a microtubule depolymerization protein that is closely related to the formation of spindle bodies in cell mitosis. Therefore, STMN1 can regulate mitosis and may affect the life cycle of DENV. However, the exact mechanism of how STMN1 affects the replication of DENV-2 remains to be elucidated.

Ritu Mishra and other scholars have explored the role of miRNA in mediating the regulation of deubiquitinases in the host proteasome (Mishra et al., 2019). Ubiquitin-specific proteinase 42 (USP42) is a deubiquitination enzyme that is widely expressed in various human tissues (Quesada et al., 2004). USP42 is co-localized with RNA Pol II in the nucleus, binds with histone H2B, and deubiquitinates H2B. The decrease in USP42 expression regulates the ubiquitination of H2B and



inhibits the basic and induced transcription of many promoters (Hock et al., 2014). DENV infection causes a dose-dependent downregulation of host DUB-USP42, and the DENV-NS5 gene alone is enough to cause this downregulation (Mishra et al., 2019). When NS5 is overexpressed, miR-590 is upregulated in a dose-dependent manner. Luciferase assay confirmed the direct regulatory interaction between miR-590 and the 3'-UTR of USP42 (Mishra et al., 2019). This study showed that DENV infection upregulates expression of miR-590 in human microglia, then downregulates expression of host ubiquitinase protein-USP42, thus inhibiting the replication of DENV (Mishra et al., 2019). Besides, the regulation of miR-590 by mimics and antagonists also affects the expression level of TRAF6, a major regulator of host inflammatory response (Mishra et al., 2019). This study provides a new insight for miR-590 to regulate virus replication by mediating host proteasome. Besides, miR-590 also showed dysregulation in the sera of dengue infected patients

(Ouyang et al., 2016). These results hint us that miR-590 plays a crucial role in DENV infection, but its exact regulatory mechanism remains to be elucidated.

Another study found that miR-424 inhibits expression of E3 ubiquitin ligase SIAH1 by activating unfolded protein response (UPR) during the infection of HeLa cells by DENV-2 (Murphy Schafer et al., 2020). The downregulation of SIAH1 can inhibit the replication of DENV, which indicates that this target plays a role in the antiviral activity of miR-424, at least to a certain extent (Murphy Schafer et al., 2020). SIAH1 binds to MyD88, an important transducing protein in the TLR signaling pathway, and ubiquitinates it. Moreover, the antiviral effect of SIAH1 is reduced in cells from which MyD88 has been deleted by CRISPR/Cas9 gene editing (Murphy Schafer et al., 2020). In addition, in cells in which SIAH1 has been downregulated by miR-424 or siRNA knockout by SIAH1, the MyD88-mediated NF-κB signaling pathway is enhanced by

DENV-2 infection or by imiquimod, a TLR7 ligand (Murphy Schafer et al., 2020; **Figure 2**). This study indicates that the target SIAH1 plays an important role in the antiviral activity of miR-424 to some extent and hints us that an additional pathway by which DENV2 harnesses aspects of the UPR to dampen the host innate immune response and promote viral replication.

miRNAs That Promote DENV Replication by Regulating Host Factors

As viruses continue to evolve, they have also gradually evolved a set of new mechanisms to evade host immune monitoring or use host factors to promote their own replication. After viral infection, some dysregulated miRNAs perform a role of promoting viral replication.

As we know, immune-mediated cytokine storms plays a vital role in understanding the pathogenesis of dengue fever (Srikiatkachorn et al., 2017). DENV infection induces massive immune activation and the production of high amounts of proinflammatory cytokines, such as tumor necrosis factor- α (TNF- α) and IFN, which may contribute to the immunopathogenesis of severe DENV infection, such as DHF/DSS (Srikiatkachorn et al., 2017). Wu et al. (2013) found that expression of miR-146a was significantly upregulated after DENV-2 infection of human primary monocytes and human peripheral blood monocytes and that miR-146a inhibits the production of IFN- β by targeting tumor necrosis factor receptor-associated factor 6 (TRAF6). Another study found that Enterovirus 71 upregulates expression of miR-146a through mediating activator protein 1 (Ho et al., 2014). Moreover, miR-146a targets interleukin-1 receptor-associated kinase (IRAK1) and TRAF6 to mediate the TLR signaling pathway and reduce the production of IFN-I, to escape the immune attack of the host (Ho et al., 2014). Knockout or neutralization of virus-induced miR-146a blocks this signaling cascade, restores IRAK1 and TRAF6 expression, increases IFN-I production, and thus inhibits viral replication and improves mouse survival (Ho et al., 2014). This study provides new insight into whether other viruses also evade host immune defense mechanisms through similar mechanisms. Pu et al. (2017) confirmed that miR-146a negatively regulates the autophagy process of A549 cells and THP-1 cells by targeting TRAF6; that is, overexpression of miR-146a significantly blocks DENV-2 induced autophagy, whereas the inhibition of miR-146a expression mediated by locked nuclear acid (LNA) counteracts this effect. Based on this finding, the miR-146a antagonist may play an essential role in restoring the production of host IFN and inhibiting viral replication.

And some cytotoxic molecules, such as perforin and granzymes may involve in cytokine storms (Mongkolsapaya et al., 2006; Mathew and Rothman, 2008). Liu et al. (2016) identified the regulatory role of miR-378 in a serine esterase granzyme B (Grzb), which can induce target cell death through multiple pathways, and the protective effects of Grzb in inhibiting DENV replication *in vivo*. Expression of miR-27a *, miR-30e, and miR-378 was downregulated in patients with DENV infection, and expression of Grzb in natural killer (NK) cells and CD8+

T cells was significantly increased by DENV infection (Liu et al., 2016). Further studies have shown that the main source of Grzb is NK cells. miR-378 rather than miR-27a * or miR-30e inhibits expression of Grzb in NK cells, and overexpression of miR-378 in DENV-infected mice can inhibit expression of Grzb and promote the replication of DENV (Liu et al., 2016). Previous studies have found that I type IFN stimulation enhanced the expression of cytolytic molecules by downregulating miRNA-378 and miR-30e, two kinds of miRNAs with abundant expression, and thus enhanced the cytotoxicity of human NK cells through analysis of miNome in human NK cells (Wang et al., 2012). Therefore, the possibility of miR-378 regulating viral replication by mediating the interferon system cannot be ruled out.

Finally, miR-927 can promote replication of the virus in C6/36 mosquito cells during acute and persistent infection with DENV-2 (Avila-Bonilla et al., 2020). A double luciferase gene reporter experiment confirmed that Filamin (FLN) is a direct target of miR-927 and that FLN is essential in actin rearrangement and related to the regulation of the toll pathway (Avila-Bonilla et al., 2020). Several studies have demonstrated that the Toll pathway plays an essential role as an anti-DENV mechanism in both *A. aegypti* mosquitoes (Xi et al., 2008; Luplertlop et al., 2011) and mosquito cells (Sim and Dimopoulos, 2010). Overexpression or downregulation of miR-927 leads to changes in Cecropin A, G, and Defensin D expression in toll pathway reactions (Avila-Bonilla et al., 2020). In conclusion, this study confirmed that miR-927 is an important factor regulating DENV-2 acute and persistent infection in mosquito cells, and may regulate innate immune response by inhibiting FLN to promote DENV infection, thereby performing a pro-viral activity (Avila-Bonilla et al., 2020). Relevant miRNAs are summarized in **Table 2**.

In conclusion, these findings highlight opportunities to use miRNAs as tools for discovering and describing the unique cytokines involved in promoting or limiting viral replication, which will open up new avenues for antiviral research. The feasibility of miRNA-based treatments for DENV is worthy of further study.

miRNAs Can Be Used as Diagnostic Markers

Nowadays, a series of studies has revealed that miRNAs can be used as biomarkers in the diagnosis of some diseases. For example, miR-486-5p (Tian et al., 2019) and miR-200a-3p (Di et al., 2020) have been identified as potential diagnostic and prognostic markers for lung cancer and colorectal cancer, respectively. In addition, several miRNAs related to cardiac metabolism have been found that can participate in lipid metabolism and can be regarded as potential biomarkers for the early diagnosis or progress of type II diabetes and coronary heart disease (Mens et al., 2020). Dynamic changes in serum miR-122 and its content at weeks 12 and 24 can be used as independent predictors of virologic response in patients with chronic hepatitis B with high viral loads being treated with nucleoside analogues (Wu et al., 2019). Chen et al. (2014) revealed the relationship between miR-150 and suppressors of cytokine signaling (SOCS1) in DENV-2 infection of peripheral

TABLE 2 | microRNAs that inhibit or promote dengue virus (DENV) replication by regulating host factors.

miRNA	Experimental model	Target	Effects	References
Let-7c	Huh-7, U937-DC-SIGN	BACH1	Inhibit	Escalera-Cueto et al., 2015; Tseng et al., 2016
miR-155	Huh-7	BACH1	Inhibit	Su et al., 2020
miR-30e*	HeLa, U937, PBMCs	IκBα	Inhibit	Zhu et al., 2014
miR-34 family	HeLa	Wnt pathway	Inhibit	Smith et al., 2017
miR-3,614-5p	Primary human macrophage	ADAR1 mRNA	Inhibit	Diosa-Toro et al., 2017
miR-223	EAhy926 cells	STMN1 mRNA	Inhibit	Wu et al., 2014
miR-590	Human microglia cells	USP42	Inhibit	Mishra et al., 2019
miR-424	HeLa	SIAH1	Inhibit	Murphy Schafer et al., 2020
miR-146a	Primary human monocytes and THP1 cells	TRAF6	Promote	Wu et al., 2013
miR-378	Human NK cells	Gzmb in NK cells	Promote	Liu et al., 2016
miR-927	C6/36	FLN	Promote	Avila-Bonilla et al., 2020

blood mononuclear cells (PBMCs). In this study, expression of SOCS1 and gamma interferon (IFN- γ), an antiviral, antitumor, and immunoregulatory agent, was significantly reduced in monocytes of DHF patients. Moreover, 24 h after infection of PBMCs with DENV-2, increased SOCS1 expression and decreased miR-150 expression were detected. When miR-150 simulators were transfected into CD14(+) cells infected with DENV-2, it inhibited the induction of SOCS1 expression in a dose-dependent manner (Chen et al., 2014). This study emphasized that the upregulation of miR-150 expression in CD14(+) cells is related to the downregulation of SOCS1 expression, and the pathogenesis of DHF and miR-150 may serve as a potential biomarker (Chen et al., 2014). Another study investigated some dysregulated miRNAs in 20 patients with dengue fever and 20 patients with severe dengue fever. It was found that the expression of miR-150 in peripheral blood cells of patients with severe dengue fever was significantly higher than that of patients with dengue fever, and miR-150 could target zeste homolog 2 enhancer (EZH2; Hapugaswatta et al., 2020), a factor which is involved in the induction of multiple inflammatory, stress, and antipathogen pathways (Arbuckle et al., 2017). Therefore, in the early stage of dengue infection, the differential expression of miR-150 and EZH2 may be serve as reliable biomarkers of disease severity. Furthermore, in a recent study, high-throughput sequencing of RNA from plasma samples of 39 dengue patients revealed that circulating microRNAs could distinguish different stages of dengue disease, so they have the potential to serve as a marker for dengue disease progression (Saini et al., 2020).

Limitations of Research on DENV-Associated miRNAs

Taken together, we summarized the existing relationship between cellular miRNAs and viral infection, miRNAs can not only directly target the viral genome to regulate the life cycle of the virus, but also mediate host innate and adaptive immune processes by regulating various host factors, which may closely be related to the incidence and severity of dengue fever. Although growing evidence has demonstrated the association between cellular miRNAs and viral infection and some miRNAs involved in inflammatory response has been described, these studies

have mainly focused on cell models and little is known about the relationship between miRNAs and the pathogenesis of DHF. A recent study sequenced miRNomes from six deaths and compared them with five controls to characterize microRNAs expression profiles in human liver tissue during DHF (de Oliveira et al., 2021). Eight microRNAs were found to be differentially expressed, including endothelial cell regulatory molecule miR-126-5p, liver specific homeostasis regulator miR-122-5p, and interferon regulator miR-146a-5p. Enrichment analysis with predicted target genes of microRNAs revealed regulatory pathways of apoptosis, involving MAPK, RAS, CDK, and FAS (de Oliveira et al., 2021). Immune response pathways were related to NF- κ B, CC and CX families, IL, and TLR. This is the first description of the human microRNA and isomicroRNA profile in liver tissues from DHF cases and the results demonstrated the association of miR-126-5p, miR-122-5p, and miR-146a-5p with DHF liver pathogenesis, involving endothelial repair and vascular permeability regulation, control of homeostasis, and expression of inflammatory cytokines (de Oliveira et al., 2021). However, in clinical treatment, tissue samples are not readily available, and it is desirable to study the relationship between miRNA and the pathogenesis of DENV infection and DHF in serum or blood samples. Above, we referred to enhanced miR-150 expression is associated with depressed SOCS1 expression involved in DHF (Chen et al., 2014) and we have discussed how differential expression of miRNAs in blood samples in clinical patients can be used to distinguish between the severity of dengue patients (Tambyah et al., 2016), and dysregulated miRNAs in serum samples may mediate inflammatory responses and cell proliferation (Ouyang et al., 2016), which expands our understanding of the pathogenesis of miRNAs and DHF *in vivo* studies.

Existing research has shown that serum miRNAs have many innate advantages: they exist widely in eukaryotes and are highly conserved and it is only expressed in specific tissues and is tissue specific; miRNA has specific expression in different growth and development stages of cells, which has a time sequence. Besides, the expression of miRNA was inhibited at the level of protein translation, so the change of miRNA in disease was earlier than that of protein markers (Brase et al., 2010). The above characteristics make miRNAs have the potential to become a new disease detection marker.

At present, the detection of serum miRNA is still in the early stage of research, and there are several problems as follows: the detection method is complicated, and the price is relatively expensive, which is not conducive to extensive clinical application. In addition, the detection of serum miRNAs needs to be standardized and the reference range of serum miRNA as disease-related markers needs further demonstration. Finally, the sample size of clinical trials is generally small, and there is a lack of long-term follow-up data (Brase et al., 2010). Furthermore, secreted miRNAs, especially those in Extracellular Vesicles (EVs) such as exosomes, may mediate paracrine and endocrine communication between different tissues and thus modulate gene expression and the function of distal cells (Mori et al., 2019).

SUMMARY

Several studies have shown that miRNA plays an important role in DENV infection. However, studies of the targets of miRNAs and the regulatory network associated with the host or viral genome transcriptome of miRNA are still limited, and descriptions of the relevant signaling pathways of miRNA in DENV infection, replication, and host immunity are lacking. At present, some researchers are trying to develop more scientific and accurate methods of predicting miRNA targets (Quillet et al., 2019) and to integrate multiple regulatory networks to predict the function of miRNA (Deng et al., 2019), but these studies are far from sufficient. Moreover, because of the lack of suitable animal models for studying DENV infection, the functions of many host factors still need to be evaluated *in vivo*. One biological characteristic of miRNA is that it can target multiple mRNAs, so the pathophysiological effects observed

by regulating miRNA expression may be related to subtle changes in the mRNA levels of different targets (Nguyen et al., 2018). Meanwhile, each mRNA molecule may contain several or even dozens of potential miRNA targets, so the specificity of miRNA inhibition on target genes requires further study, and accurate means of evaluating the miRNA genome transcriptome should be developed. In addition, because miRNA may be the main factor regulating disease and inflammation, the improper design of miRNA operations may have unexpected side effects, so it is necessary to develop excellent vectors to precisely limit the release of miRNA mimics and inhibitors to infected and inflammatory tissue (Nguyen et al., 2018). Moreover, abnormal expression of miRNA may lead to innate immune and adaptive immune deregulation, resulting in failure to resist invasive pathogens and autoimmune diseases (Lee et al., 2014), which have negative impacts on host health. In conclusion, in-depth understanding of miRNAs and miRNA-mediated signaling pathways in DENV replication and pathology will provide insights for the development of targeted drugs.

AUTHOR CONTRIBUTIONS

YS, TL, and CL: literature search. YS, TL, CL, and CC: figures. XH and XJ: study design. YS: writing. All authors contributed to the article and approved the submitted version.

FUNDING

This work was supported by the Scientific Research Foundation of Fuzhou University (GXRC-19025) and Research Fund of Fujian Provincial Department of Finance (202102).

REFERENCES

- Anasir, M. I., Ramanathan, B., and Poh, C. L. (2020). Structure-based design of antivirals against envelope glycoprotein of dengue virus. *Viruses* 12:367. doi: 10.3390/v12040367
- Arbuckle, J. H., Gardina, P. J., Gordon, D. N., Hickman, H. D., Yewdell, J. W., Pierson, T. C., et al. (2017). Inhibitors of the histone methyltransferases EZH2/1 induce a potent antiviral state and suppress infection by diverse viral pathogens. *MBio* 8, e01141–e01117. doi: 10.1128/mBio.01141-17
- Avila-Bonilla, R. G., Yocupicio-Monroy, M., Marchat, L. A., Pérez-Ishiwara, D. G., Cerecedo-Mercado, D. A., Del Ángel, R. M., et al. (2020). miR-927 has proviral effects during acute and persistent infection with dengue virus type 2 in C6/36 mosquito cells. *J. Gen. Virol.* 101, 825–839. doi: 10.1099/jgv.0.001441
- Bandiera, S., Pfeffer, S., Baumert, T. F., and Zeisel, M. B. (2015). miR-122—a key factor and therapeutic target in liver disease. *J. Hepatol.* 62, 448–457. doi: 10.1016/j.jhep.2014.10.004
- Barbu, M. G., Condrat, C. E., Thompson, D. C., Bugnar, O. L., Cretoiu, D., Toader, O. D., et al. (2020). MicroRNA involvement in signaling pathways during viral infection. *Front. Cell Dev. Biol.* 8:143. doi: 10.3389/fcell.2020.00143
- Bartel, D. P. (2004). microRNAs: genomics, biogenesis, mechanism, and function. *Cell* 116, 281–297. doi: 10.1016/S0092-8674(04)00045-5
- Boehm, M., and Slack, F. (2005). A developmental timing microRNA and its target regulate life span in *C. elegans*. *Science* 310, 1954–1957. doi: 10.1126/science.1115596
- Bohnsack, M. T., Czaplinski, K., and Gorlich, D. (2004). Exportin 5 is a RanGTP-dependent dsRNA-binding protein that mediates nuclear export of pre-miRNAs. *RNA* 10, 185–191. doi: 10.1261/rna.5167604
- Brase, J. C., Wuttig, D., Kuner, R., and Sultmann, H. (2010). Serum microRNAs as non-invasive biomarkers for cancer. *Mol. Cancer* 9:306. doi: 10.1186/1476-4598-9-306
- Brennecke, J., Hipfner, D. R., Stark, A., Russell, R. B., and Cohen, S. M. (2003). Bantam encodes a developmentally regulated microRNA that controls cell proliferation and regulates the proapoptotic gene *hid* in drosophila. *Cell* 113, 25–36. doi: 10.1016/S0092-8674(03)00231-9
- Bushati, N., and Cohen, S. M. (2007). microRNA functions. *Annu. Rev. Cell Dev. Biol.* 23, 175–205. doi: 10.1146/annurev.cellbio.23.090506.123406
- Castel, S. E., and Martienssen, R. A. (2013). RNA interference in the nucleus: roles for small RNAs in transcription, epigenetics and beyond. *Nat. Rev. Genet.* 14, 100–112. doi: 10.1038/nrg3355
- Castillo, J. A., Castrillón, J. C., Dios-Toro, M., Betancur, J. G., St Laurent, G., 3rd, Smit, J. M., et al. (2016). Complex interaction between dengue virus replication and expression of miRNA-133a. *BMC Infect. Dis.* 16:29. doi: 10.1186/s12879-016-1364-y
- Castrillón-Betancur, J. C., and Urcuqui-Inchima, S. (2017). Overexpression of miR-484 and miR-744 in Vero cells alters dengue virus replication. *Mem. Inst. Oswaldo Cruz* 112, 281–291. doi: 10.1590/0074-02760160404
- Catalanotto, C., Cogoni, C., and Zardo, G. (2016). MicroRNA in control of gene expression: an overview of nuclear functions. *Int. J. Mol. Sci.* 17:1712. doi: 10.3390/ijms17101712
- Chao, C. H., Wu, W. C., Lai, Y. C., Tsai, P. J., Perng, G. C., Lin, Y. S., et al. (2019). Dengue virus nonstructural protein 1 activates platelets via toll-like receptor 4, leading to thrombocytopenia and hemorrhage. *PLoS Pathog.* 15:e1007625. doi: 10.1371/journal.ppat.1007625

- Chen, Y., Maguire, T., Hileman, R. E., Fromm, J. R., Esko, J. D., Linhardt, R. J., et al. (1997). Dengue virus infectivity depends on envelope protein binding to target cell heparan sulfate. *Nat. Med.* 3, 866–871. doi: 10.1038/nm0897-866
- Chen, R. F., Yang, K. D., Lee, I. K., Liu, J. W., Huang, C. H., Lin, C. Y., et al. (2014). Augmented miR-150 expression associated with depressed SOCS1 expression involved in dengue haemorrhagic fever. *J. Inf. Secur.* 69, 366–374. doi: 10.1016/j.jinf.2014.05.013
- Clark, I. A. (2007). The advent of the cytokine storm. *Immunol. Cell Biol.* 85, 271–273. doi: 10.1038/sj.icb.7100062
- Cullen, B. R. (2006). Is RNA interference involved in intrinsic antiviral immunity in mammals? *Nat. Immunol.* 7, 563–567. doi: 10.1038/nri1352
- Deng, L., Wang, J., and Zhang, J. (2019). Predicting gene ontology function of human microRNAs by integrating multiple networks. *Front. Genet.* 10:3. doi: 10.3389/fgene.2019.00003
- de Oliveira, L. F., de Andrade, A. A. S., Pagliari, C., de Carvalho, L. V., Silveira, T. S., Cardoso, J. F., et al. (2021). Differential expression analysis and profiling of hepatic miRNA and isomiRNA in dengue hemorrhagic fever. *Sci. Rep.* 11:5554. doi: 10.1038/s41598-020-72892-w
- Di, Z., Di, M., Fu, W., Tang, Q., Liu, Y., Lei, P., et al. (2020). Integrated analysis identifies a nine-microRNA signature biomarker for diagnosis and prognosis in colorectal cancer. *Front. Genet.* 11:192. doi: 10.3389/fgene.2020.00192
- Diamond, M. S., and Pierson, T. C. (2015). Molecular insight into dengue virus pathogenesis and its implications for disease control. *Cell* 162, 488–492. doi: 10.1016/j.cell.2015.07.005
- Dihlmann, S., and von Knebel, D. M. (2005). Wnt/beta-catenin-pathway as a molecular target for future anti-cancer therapeutics. *Int. J. Cancer* 113, 515–524. doi: 10.1002/ijc.20609
- Diosa-Toro, M., Echavarría-Consuegra, L., Flipse, J., Fernández, G. J., Kluiver, J., van den Berg, A., et al. (2017). MicroRNA profiling of human primary macrophages exposed to dengue virus identifies miRNA-3614-5p as antiviral and regulator of ADAR1 expression. *PLoS Negl. Trop. Dis.* 11:e0005981. doi: 10.1371/journal.pntd.0005981
- Dowdy, S. F. (2017). Overcoming cellular barriers for RNA therapeutics. *Nat. Biotechnol.* 35, 222–229. doi: 10.1038/nbt.3802
- Escalera-Cueto, M., Medina-Martínez, I., del Ángel, R. M., Berumen-Campos, J., Gutiérrez-Escolano, A. L., and Yocupicio-Monroy, M. (2015). Let-7c overexpression inhibits dengue virus replication in human hepatoma Huh-7 cells. *Virus Res.* 196, 105–112. doi: 10.1016/j.virusres.2014.11.010
- Fang, S., Wu, Y., Wu, N., Zhang, J., and An, J. (2013). Recent advances in DENV receptors. *TheScientificWorldJOURNAL* 2013:684690. doi: 10.1155/2013/684690
- Filipowicz, W., Bhattacharyya, S. N., and Sonenberg, N. (2008). Mechanisms of post-transcriptional regulation by microRNAs: are the answers in sight? *Nat. Rev. Genet.* 9, 102–114. doi: 10.1038/nrg2290
- Filipowicz, W., and Grosshans, H. (2011). The liver-specific microRNA miR-122: biology and therapeutic potential. *Prog. Drug Res.* 67, 221–238. doi: 10.1007/978-3-7643-8989-5_11
- Gebhard, L. G., Filomatori, C. V., and Gamarnik, A. V. (2011). Functional RNA elements in the dengue virus genome. *Viruses* 3, 1739–1756. doi: 10.3390/v3091739
- Giraldez, A. J., Cinalli, R. M., Glasner, M. E., Enright, A. J., Thomson, J. M., Baskerville, S., et al. (2005). microRNAs regulate brain morphogenesis in zebrafish. *Science* 308, 833–838. doi: 10.1126/science.1109020
- Halstead, S. B. (1982). Immune enhancement of viral infection. *Prog. Allergy* 31, 301–364.
- Hapugaswatta, H., Amarasena, P., Premaratna, R., Seneviratne, K. N., and Jayatilaka, N. (2020). Differential expression of microRNA, miR-150 and enhancer of zeste homolog 2 (EZH2) in peripheral blood cells as early prognostic markers of severe forms of dengue. *J. Biomed. Sci.* 27:25. doi: 10.1186/s12929-020-0620-z
- Ho, B. C., Yu, I. S., Lu, L. F., Rudensky, A., Chen, H. Y., Tsai, C. W., et al. (2014). Inhibition of miR-146a prevents enterovirus-induced death by restoring the production of type I interferon. *Nat. Commun.* 5:3344. doi: 10.1038/ncomms4344
- Hock, A. K., Vigneron, A. M., and Vousden, K. H. (2014). Ubiquitin-specific peptidase 42 (USP42) functions to deubiquitylate histones and regulate transcriptional activity. *J. Biol. Chem.* 289, 34862–34870. doi: 10.1074/jbc.M114.589267
- Hu, H., He, X., Zhang, Y., Wu, R., Chen, J., Lin, Y., et al. (2020). MicroRNA alterations for diagnosis, prognosis, and treatment of osteoporosis: A comprehensive review and computational functional survey. *Front. Genet.* 11:181. doi: 10.3389/fgene.2020.00181
- Janssen, H. L., Reesink, H. W., Lawitz, E. J., Zeuzem, S., Rodriguez-Torres, M., Patel, K., et al. (2013). Treatment of HCV infection by targeting microRNA. *N. Engl. J. Med.* 368, 1685–1694. doi: 10.1056/NEJMoa1209026
- Jiang, L., Lin, C., Song, L., Wu, J., Chen, B., Ying, Z., et al. (2012). MicroRNA-30e* promotes human glioma cell invasiveness in an orthotopic xenotransplantation model by disrupting the NF- κ B/I κ B α negative feedback loop. *J. Clin. Invest.* 122, 33–47. doi: 10.1172/JCI58849
- Kanokudom, S., Vilaivan, T., Wikan, N., Thepparit, C., Smith, D. R., and Assavalapsakul, W. (2017). miR-21 promotes dengue virus serotype 2 replication in HepG2 cells. *Antivir. Res.* 142, 169–177. doi: 10.1016/j.antiviral.2017.03.020
- Klema, V. J., Ye, M., Hindupur, A., Teramoto, T., Gottipati, K., Padmanabhan, R., et al. (2016). Dengue virus nonstructural protein 5 (NS5) assembles into a dimer with a unique Methyltransferase and polymerase Interface. *PLoS Pathog.* 12:e1005451. doi: 10.1371/journal.ppat.1005451
- Knight, S. W., and Bass, B. L. (2001). A role for the RNase III enzyme DCR-1 in RNA interference and germ line development in *Caenorhabditis elegans*. *Science* 293, 2269–2271. doi: 10.1126/science.1062039
- Koonin, E. V. (1991). The phylogeny of RNA-dependent RNA polymerases of positive-strand RNA viruses. *J. Gen. Virol.* 72, 2197–2206. doi: 10.1099/0022-1317-72-9-2197
- Krol, J., Loedige, I., and Filipowicz, W. (2010). The widespread regulation of microRNA biogenesis, function and decay. *Nat. Rev. Genet.* 11, 597–610. doi: 10.1038/nrg2843
- Lambrechts, L., Scott, T. W., and Gubler, D. J. (2010). Consequences of the expanding global distribution of *Aedes albopictus* for dengue virus transmission. *PLoS Negl. Trop. Dis.* 4:e646. doi: 10.1371/journal.pntd.0000646
- Lee, Y., Ahn, C., Han, J., Choi, H., Kim, J., Yim, J., et al. (2003). The nuclear RNase III Drosha initiates microRNA processing. *Nature* 425, 415–419. doi: 10.1038/nature01957
- Lee, Y., Kim, M., Han, J., Yeom, K. H., Lee, S., Baek, S. H., et al. (2004). MicroRNA genes are transcribed by RNA polymerase II. *EMBO J.* 23, 4051–4060. doi: 10.1038/sj.emboj.7600385
- Lee, H. M., Nguyen, D. T., and Lu, L. F. (2014). Progress and challenge of microRNA research in immunity. *Front. Genet.* 5:178. doi: 10.3389/fgene.2014.00178
- Lee, Y. R., Yeh, S. F., Ruan, X. M., Zhang, H., Hsu, S. D., Huang, H. D., et al. (2017). Honeysuckle aqueous extract and induced let-7a suppress dengue virus type 2 replication and pathogenesis. *J. Ethnopharmacol.* 198, 109–121. doi: 10.1016/j.jep.2016.12.049
- Liu, S., Chen, L., Zeng, Y., Si, L., Guo, X., Zhou, J., et al. (2016). Suppressed expression of miR-378 targeting gzmB in NK cells is required to control dengue virus infection. *Cell. Mol. Immunol.* 13, 700–708. doi: 10.1038/cmi.2015.52
- Lodeiro, M. F., Filomatori, C. V., and Gamarnik, A. V. (2009). Structural and functional studies of the promoter element for dengue virus RNA replication. *J. Virol.* 83, 993–1008. doi: 10.1128/JVI.01647-08
- Luplertlop, N., Surasombatpattana, P., Patramool, S., Dumas, E., Wasinpiyamongkol, L., Saune, L., et al. (2011). Induction of a peptide with activity against a broad spectrum of pathogens in the *Aedes aegypti* salivary gland, following infection with dengue virus. *PLoS Pathog.* 7:e1001252. doi: 10.1371/journal.ppat.1001252
- Malone, C. D., and Hannon, G. J. (2009). Small RNAs as guardians of the genome. *Cell* 136, 656–668. doi: 10.1016/j.cell.2009.01.045
- Manzano, M., Reichert, E. D., Polo, S., Falgout, B., Kasprzak, W., Shapiro, B. A., et al. (2011). Identification of cis-acting elements in the 3'-untranslated region of the dengue virus type 2 RNA that modulate translation and replication. *J. Biol. Chem.* 286, 22521–22534. doi: 10.1074/jbc.M111.234302
- Mathew, A., and Rothman, A. L. (2008). Understanding the contribution of cellular immunity to dengue disease pathogenesis. *Immunol. Rev.* 225, 300–313. doi: 10.1111/j.1600-065X.2008.00678.x
- Mens, M. M. J., Maas, S. C. E., Klap, J., Weverling, G. J., Klatser, P., Brakenhoff, J. P. J., et al. (2020). Multi-omics analysis reveals microRNAs associated with cardiometabolic traits. *Front. Genet.* 11:110. doi: 10.3389/fgene.2020.00110
- Miller, J. L., de Wet, B. J., Martinez-Pomares, L., Radcliffe, C. M., Dwek, R. A., Rudd, P. M., et al. (2008). The mannose receptor mediates dengue virus infection of macrophages. *PLoS Pathog.* 4:e17. doi: 10.1371/annotation/98b92fca-fa6e-4bf3-9b39-13b66b640476

- Miranda, K. C., Huynh, T., Tay, Y., Ang, Y. S., Tam, W. L., Thomson, A. M., et al. (2006). A pattern-based method for the identification of MicroRNA binding sites and their corresponding heteroduplexes. *Cell* 126, 1203–1217. doi: 10.1016/j.cell.2006.07.031
- Mishra, R., Sood, V., and Banerjee, A. C. (2019). Dengue NS5 modulates expression of miR-590 to regulate ubiquitin-specific peptidase 42 in human microglia. *FASEB Bioadv.* 1, 265–278. doi: 10.1096/fba.2018-00047
- Misso, G., Di Martino, M. T., De Rosa, G., Farooqi, A. A., Lombardi, A., Campani, V., et al. (2014). Mir-34: a new weapon against cancer? *Mol. Ther. Nucleic Acids* 3:e194. doi: 10.1038/mtna.2014.47
- Modis, Y., Ogata, S., Clements, D., and Harrison, S. C. (2004). Structure of the dengue virus envelope protein after membrane fusion. *Nature* 427, 313–319. doi: 10.1038/nature02165
- Mongkolsapaya, J., Dejnirattisai, W., Xu, X. N., Vasanawathana, S., Tangthawornchaikul, N., Chairunsri, A., et al. (2003). Original antigenic sin and apoptosis in the pathogenesis of dengue hemorrhagic fever. *Nat. Med.* 9, 921–927. doi: 10.1038/nm887
- Mongkolsapaya, J., Duangchinda, T., Dejnirattisai, W., Vasanawathana, S., Avirutnan, P., Jaiungsri, A., et al. (2006). T cell responses in dengue hemorrhagic fever: are cross-reactive T cells suboptimal? *J. Immunol.* 176, 3821–3829. doi: 10.4049/jimmunol.176.6.3821
- Mori, M. A., Ludwig, R. G., Garcia-Martin, R., Brandão, B. B., and Kahn, C. R. (2019). Extracellular miRNAs: From biomarkers to mediators of physiology and disease. *Cell Metab.* 30, 656–673. doi: 10.1016/j.cmet.2019.07.011
- Muller, D. A., and Young, P. R. (2013). The flavivirus NS1 protein: molecular and structural biology, immunology, role in pathogenesis and application as a diagnostic biomarker. *Antivir. Res.* 98, 192–208. doi: 10.1016/j.antiviral.2013.03.008
- Murphy Schafer, A. R., Smith, J. L., Pryke, K. M., DeFilippis, V. R., and Hirsch, A. J. (2020). The E3 ubiquitin ligase SIAH1 targets MyD88 for proteasomal degradation during dengue virus infection. *Front. Microbiol.* 11:24. doi: 10.3389/fmicb.2020.00024
- Nasirudeen, A. M., Wong, H. H., Thien, P., Xu, S., Lam, K. P., and Liu, D. X. (2011). RIG-I, MDA5 and TLR3 synergistically play an important role in restriction of dengue virus infection. *PLoS Negl. Trop. Dis.* 5:e926. doi: 10.1371/journal.pntd.0000926
- Nguyen, T. H., Liu, X., Su, Z. Z., Hsu, A. C., Foster, P. S., and Yang, M. (2018). Potential role of microRNAs in the regulation of antiviral responses to influenza infection. *Front. Immunol.* 9:1541. doi: 10.3389/fimmu.2018.01541
- Ouyang, X., Jiang, X., Gu, D., Zhang, Y., Kong, S. K., Jiang, C., et al. (2016). Dysregulated serum MiRNA profile and promising biomarkers in dengue-infected patients. *Int. J. Med. Sci.* 13, 195–205. doi: 10.7150/ijms.13996
- Pashangzadeh, S., Motallebzadeh, M., Vafashoar, F., Khalvandi, A., and Mojtavani, N. (2021). Implications the role of miR-155 in the pathogenesis of autoimmune diseases. *Front. Immunol.* 12:669382. doi: 10.3389/fimmu.2021.669382
- Pedersen, I. M., Cheng, G., Wieland, S., Volinia, S., Croce, C. M., Chisari, F. V., et al. (2007). Interferon modulation of cellular microRNAs as an antiviral mechanism. *Nature* 449, 919–922. doi: 10.1038/nature06205
- Perera, R., and Kuhn, R. J. (2008). Structural proteomics of dengue virus. *Curr. Opin. Microbiol.* 11, 369–377. doi: 10.1016/j.mib.2008.06.004
- Perera-Lecoin, M., Meertens, L., Carnec, X., and Amara, A. (2013). Flavivirus entry receptors: an update. *Viruses* 6, 69–88. doi: 10.3390/v6010069
- Pu, J., Wu, S., Xie, H., Li, Y., Yang, Z., Wu, X., et al. (2017). miR-146a inhibits dengue-virus-induced autophagy by targeting TRAF6. *Arch. Virol.* 162, 3645–3659. doi: 10.1007/s00705-017-3516-9
- Puerta-Guardo, H., Glasner, D. R., and Harris, E. (2016). Dengue virus NS1 disrupts the endothelial Glycocalyx, leading to hyperpermeability. *PLoS Pathog.* 12:e1005738. doi: 10.1371/journal.ppat.1005738
- Quesada, V., Díaz-Perales, A., Gutiérrez-Fernández, A., Garabaya, C., Cal, S., and López-Otín, C. (2004). Cloning and enzymatic analysis of 22 novel human ubiquitin-specific proteases. *Biochem. Biophys. Res. Commun.* 314, 54–62. doi: 10.1016/j.bbrc.2003.12.050
- Quillet, A., Saad, C., Ferry, G., Anouar, Y., Vergne, N., Lecroq, T., et al. (2019). Improving bioinformatics prediction of microRNA targets by ranks aggregation. *Front. Genet.* 10:1330. doi: 10.3389/fgene.2019.01330
- Saini, J., Bandyopadhyay, B., Pandey, A. D., Ramachandran, V. G., Das, S., Sood, V., et al. (2020). High-throughput RNA sequencing analysis of plasma samples reveals circulating microRNA signatures with biomarker potential in dengue disease progression. *mSystems* 5, e00724–e00720. doi: 10.1128/mSystems.00724-20
- Schoggins, J. W., Dorner, M., Feulner, M., Imanaka, N., Murphy, M. Y., Ploss, A., et al. (2012). Dengue reporter viruses reveal viral dynamics in interferon receptor-deficient mice and sensitivity to interferon effectors in vitro. *Proc. Natl. Acad. Sci. U. S. A.* 109, 14610–14615. doi: 10.1073/pnas.1212379109
- Sim, S., and Dimopoulos, G. (2010). Dengue virus inhibits immune responses in *Aedes aegypti* cells. *PLoS One* 5:e10678. doi: 10.1371/journal.pone.0010678
- Smith, J. L., Jeng, S., McWeeney, S. K., and Hirsch, A. J. (2017). A MicroRNA screen identifies the Wnt Signaling pathway as a regulator of the interferon response during Flavivirus infection. *J. Virol.* 91, e02388–e02316. doi: 10.1128/JVI.02388-16
- Srikiathachorn, A., Mathew, A., and Rothman, A. L. (2017). Immune-mediated cytokine storm and its role in severe dengue. *Semin. Immunopathol.* 39, 563–574. doi: 10.1007/s00281-017-0625-1
- Stacey, K. J., Watterson, D., Modhiran, N., and Young, P. R. (2015). Response to comment on “dengue virus NS1 protein activates cells via toll-like receptor 4 and disrupts endothelial cell monolayer integrity” and “dengue virus NS1 triggers endothelial permeability and vascular leak that is prevented by NS1 vaccination.” *Sci. Transl. Med.* 7:318r314. doi: 10.1126/scitranslmed.aad8657
- Su, Y. C., Huang, Y. F., Wu, Y. W., Chen, H. F., Wu, Y. H., Hsu, C. C., et al. (2020). MicroRNA-155 inhibits dengue virus replication by inducing heme oxygenase-1-mediated antiviral interferon responses. *FASEB J.* 34, 7283–7294. doi: 10.1096/fj.201902878R
- Tambyah, P. A., Ching, C. S., Sepramaniam, S., Ali, J. M., Armugam, A., and Jeyaseelan, K. (2016). microRNA expression in blood of dengue patients. *Ann. Clin. Biochem.* 53, 466–476. doi: 10.1177/0004563215604001
- Tassaneetrithep, B., Burgess, T. H., Granelli-Piperno, A., Trumpfheller, C., Finke, J., Sun, S., McWeeney, S. K., and Hirsch, A. J. (2003). DC-SIGN (CD209) mediates dengue virus infection of human dendritic cells. *J. Exp. Med.* 197, 823–829. doi: 10.1084/jem.20021840
- Tian, Y., Chen, W., Yang, Y., Xu, X., Zhang, J., Wang, J., et al. (2013). Identification of B cell epitopes of dengue virus 2 NS3 protein by monoclonal antibody. *Appl. Microbiol. Biotechnol.* 97, 1553–1560. doi: 10.1007/s00253-012-4419-z
- Tian, F., Wang, J., Ouyang, T., Lu, N., Lu, J., Shen, Y., et al. (2019). MiR-486-5p serves as a good biomarker in nonsmall cell lung cancer and suppresses cell growth With the involvement of a target PIK3R1. *Front. Genet.* 10:688. doi: 10.3389/fgene.2019.00688
- Trobaugh, D. W., Gardner, C. L., Sun, C., Haddow, A. D., Wang, E., Chapnik, E., et al. (2014). RNA viruses can hijack vertebrate microRNAs to suppress innate immunity. *Nature* 506, 245–248. doi: 10.1038/nature12869
- Tsai, Y. T., Chang, S. Y., Lee, C. N., and Kao, C. L. (2009). Human TLR3 recognizes dengue virus and modulates viral replication in vitro. *Cell Microbiol.* 11, 604–615. doi: 10.1111/j.1462-5822.2008.01277.x
- Tseng, C. K., Lin, C. K., Wu, Y. H., Chen, Y. H., Chen, W. C., Young, K. C., et al. (2016). Human heme oxygenase 1 is a potential host cell factor against dengue virus replication. *Sci. Rep.* 6:32176. doi: 10.1038/srep32176
- van der Schaar, H. M., Rust, M. J., Chen, C., van der Ende-Metselaar, H., Wilschut, J., Zhuang, X., et al. (2008). Dissecting the cell entry pathway of dengue virus by single-particle tracking in living cells. *PLoS Pathog.* 4:e1000244. doi: 10.1371/journal.ppat.1000244
- Wang, P., Gu, Y., Zhang, Q., Han, Y., Hou, J., Lin, L., et al. (2012). Identification of resting and type I IFN-activated human NK cell miRNomes reveals microRNA-378 and microRNA-30e as negative regulators of NK cell cytotoxicity. *J. Immunol.* 189, 211–221. doi: 10.4049/jimmunol.1200609
- Wen, W., He, Z., Jing, Q., Hu, Y., Lin, C., Zhou, R., et al. (2015). Cellular microRNA-miR-548g-3p modulates the replication of dengue virus. *J. Inf. Secur.* 70, 631–640. doi: 10.1016/j.jinf.2014.12.001
- Wu, Y., Gao, C., Cai, S., Xia, M., Liao, G., Zhang, X., et al. (2019). Circulating miR-122 is a predictor for virological response in CHB patients with high viral load treated with nucleos(t)ide analogs. *Front. Genet.* 10:243. doi: 10.3389/fgene.2019.00243
- Wu, N., Gao, N., Fan, D., Wei, J., Zhang, J., and An, J. (2014). miR-223 inhibits dengue virus replication by negatively regulating the microtubule-destabilizing protein STMN1 in EAhy926 cells. *Microbes Infect.* 16, 911–922. doi: 10.1016/j.micinf.2014.08.011
- Wu, S., He, L., Li, Y., Wang, T., Feng, L., Jiang, L., et al. (2013). miR-146a facilitates replication of dengue virus by dampening interferon induction by targeting TRAF6. *J. Inf. Secur.* 67, 329–341. doi: 10.1016/j.jinf.2013.05.003

- Xi, Z., Ramirez, J. L., and Dimopoulos, G. (2008). The *Aedes aegypti* toll pathway controls dengue virus infection. *PLoS Pathog.* 4:e1000098. doi: 10.1371/journal.ppat.1000098
- Xu, P., Vernooy, S. Y., Guo, M., and Hay, B. A. (2003). The drosophila microRNA Mir-14 suppresses cell death and is required for normal fat metabolism. *Curr. Biol.* 13, 790–795. doi: 10.1016/S0960-9822(03)00250-1
- Yan, H., Zhou, Y., Liu, Y., Deng, Y., and Chen, X. (2014). miR-252 of the Asian tiger mosquito *Aedes albopictus* regulates dengue virus replication by suppressing the expression of the dengue virus envelope protein. *J. Med. Virol.* 86, 1428–1436. doi: 10.1002/jmv.23815
- Yin, H., He, H., Cao, X., Shen, X., Han, S., Cui, C., et al. (2020). MiR-148a-3p regulates skeletal muscle satellite cell differentiation and apoptosis via the PI3K/AKT Signaling pathway by targeting Meox2. *Front. Genet.* 11:512. doi: 10.3389/fgene.2020.00512
- Yu, I. M., Zhang, W., Holdaway, H. A., Li, L., Kostyuchenko, V. A., Chipman, P. R., et al. (2008). Structure of the immature dengue virus at low pH primes proteolytic maturation. *Science* 319, 1834–1837. doi: 10.1126/science.1153264
- Zhou, Y., Liu, Y., Yan, H., Li, Y., Zhang, H., Xu, J., et al. (2014). miR-281, an abundant midgut-specific miRNA of the vector mosquito *Aedes albopictus* enhances dengue virus replication. *Parasit. Vectors* 7:488. doi: 10.1186/s13071-014-0488-4
- Zhu, X., He, Z., Hu, Y., Wen, W., Lin, C., Yu, J., et al. (2014). MicroRNA-30e* suppresses dengue virus replication by promoting NF- κ B-dependent IFN production. *PLoS Negl. Trop. Dis.* 8:e3088. doi: 10.1371/journal.pntd.0003088
- Conflict of Interest:** XJ is employed by DAAN Gene Co., Ltd. of Sun Yat-sen University.
- The remaining authors declare that the research was conducted in the absence of any commercial or financial relationships that could be construed as a potential conflict of interest.
- Publisher's Note:** All claims expressed in this article are solely those of the authors and do not necessarily represent those of their affiliated organizations, or those of the publisher, the editors and the reviewers. Any product that may be evaluated in this article, or claim that may be made by its manufacturer, is not guaranteed or endorsed by the publisher.

Copyright © 2021 Su, Lin, Liu, Cheng, Han and Jiang. This is an open-access article distributed under the terms of the Creative Commons Attribution License (CC BY). The use, distribution or reproduction in other forums is permitted, provided the original author(s) and the copyright owner(s) are credited and that the original publication in this journal is cited, in accordance with accepted academic practice. No use, distribution or reproduction is permitted which does not comply with these terms.



Non-structural Proteins of Severe Fever With Thrombocytopenia Syndrome Virus Suppress RNA Synthesis in a Transcriptionally Active cDNA-Derived Viral RNA Synthesis System

OPEN ACCESS

Edited by:

Keun Hwa Lee,
Hanyang University, South Korea

Reviewed by:

Ok Sarah Shin,
Korea University, South Korea
Nam-Hyuk Cho,
Seoul National University,
South Korea

*Correspondence:

Ding-Yu Zhang
zhangdy63@hotmail.com
Fei Deng
df@wh.iov.cn

Specialty section:

This article was submitted to
Virology,
a section of the journal
Frontiers in Microbiology

Received: 14 May 2021

Accepted: 23 July 2021

Published: 16 August 2021

Citation:

Ren F, Shen S, Ning Y-J, Wang Q,
Dai S, Shi J, Zhou M, Wang H,
Huang C, Zhang D-Y and Deng F
(2021) Non-structural Proteins
of Severe Fever With
Thrombocytopenia Syndrome Virus
Suppress RNA Synthesis in a
Transcriptionally Active cDNA-Derived
Viral RNA Synthesis System.
Front. Microbiol. 12:709517.
doi: 10.3389/fmicb.2021.709517

Fuli Ren^{1,2,3}, Shu Shen^{2,3}, Yun-Jia Ning^{2,3}, Qiongya Wang¹, Shiyu Dai^{2,3}, Junming Shi^{2,3},
Min Zhou^{2,3}, Hualin Wang^{2,3}, Chaolin Huang^{1,4}, Ding-Yu Zhang^{1*} and Fei Deng^{2,3*}

¹ Research Center for Translational Medicine, Wuhan Jinyintan Hospital, Wuhan, China, ² State Key Laboratory of Virology, Wuhan Institute of Virology, Chinese Academy of Sciences, Wuhan, China, ³ National Virus Resource Center, Wuhan Institute of Virology, Chinese Academy of Sciences, Wuhan, China, ⁴ Department of Infectious Diseases, Wuhan Jinyintan Hospital, Wuhan, China

Severe fever with thrombocytopenia syndrome (SFTS) is an emerging infectious disease caused by the tick-borne SFTS bunyavirus (SFTSV) resulting in a high fatality rate up to 30%. SFTSV is a negative-strand RNA virus containing three single-stranded RNA genome segments designated as L, M, and S, which respectively, encode the RNA-dependent RNA polymerase (RdRp), glycoproteins Gn and Gc, and nucleoprotein (N) and non-structural proteins (NSs). NSs can form inclusion bodies (IBs) in infected and transfected cells. A previous study has provided a clue that SFTSV NSs may be involved in virus-like or viral RNA synthesis; however, the details remain unclear. Our work described here reveals that SFTSV NSs can downregulate virus-like RNA synthesis in a dose-dependent manner within a cDNA-derived viral RNA synthesis system, i.e., minigenome (–) and minigenome (+) systems based on transfection, superinfection, and luciferase reporter activity determination; meanwhile, NSs also show a weak inhibitory effect on virus replication. By using co-immunoprecipitation (Co-IP) and RT-PCR combined with site-directed mutagenesis, we found that NSs suppress virus-like RNA or virus replication through interacting with N but not with RdRp, and the negative regulatory effect correlates closely with the IB structure it formed but is not associated with its role of antagonizing host innate immune responses. When the cytoplasmic structure of IB formed by SFTSV NSs was deprived, the inhibitory effect of NSs on virus-like RNA synthesis would weaken and even disappear. Similarly, we also evaluated other bandavirus NSs that cannot form IB in neither infected nor transfected cells, and the results showed that the NSs of Heartland bandavirus (HRTV) did not

show a significant inhibitory effect on virus-like RNA synthesis within a minigenome system. Our findings provide experimental evidence that SFTSV NSs participate in regulating virus-like or viral RNA synthesis and the negative effect may be due to the NSs–N interaction.

Keywords: bunyavirus, RNA synthesis, HRTV, SFTSV RNA synthesis and regulation, NSs, SFTSV, minigenome

INTRODUCTION

Severe fever with thrombocytopenia syndrome virus (SFTSV) is an emerging tick-borne bunyavirus first isolated and identified in 2009 in the rural areas of Henan Province, China (Yu et al., 2011). SFTSV is now classified into the genus *Bandavirus*, family *Phenuiviridae*, and order *Bunyavirales* by the International Committee on Taxonomy of Viruses (ICTV) (Kuhn et al., 2020). In addition, it is the causative pathogen of severe fever with thrombocytopenia syndrome (SFTS) and is mainly prevalent in East Asian countries, including China, Japan, South Korea, and Vietnam (Takahashi et al., 2014; Kim et al., 2018; Tran et al., 2019). SFTS is mainly characterized by thrombocytopenia syndrome (Yu et al., 2011; Lei et al., 2015), and in some severe patients, it can lead to multiple organ failure or even death (Li et al., 2018; Song et al., 2018), resulting in high fatality rates varying from 12 to 30% in different areas (Park et al., 2019). However, there is no available vaccine or therapeutic drugs for SFTSV. Recently, several tick-borne bunyavirus related to SFTSV, including HRTV and Guertu virus (GTV), have been isolated and identified in United States and China, respectively (McMullan et al., 2012; Shen et al., 2018; Staples et al., 2020). Although the pathogenicity of GTV to human remains unclear, patients with infection of HRTV presented very similar clinical symptoms to SFTS patients. Our previous data showed that SFTSV, HRTV, and even GTV have the potential to undergo genome reassortment (Ren et al., 2020), which may lead to the generation of unknown progeny viruses, thus highlighting growing public health threat posed by bandaviruses.

In segmented negative-strand RNA genome viruses, genomic and antigenomic viral RNA (vRNA and cRNA) but not mRNA are always found assembled with multiple copies of a nucleoprotein (N) into nucleocapsids (Mir and Panganiban, 2006; Reguera et al., 2014; Te Velthuis and Fodor, 2016; Sun et al., 2018). During viral replication, the genomic RNA undergoes encapsidation, and the coated viral genomic RNAs assemble with the viral polymerase (RdRp) to form RNPs (vRNP), which are central to the viral life cycle and can be packaged into progeny virus particles (Hornak et al., 2016; Wichgers Schreur et al., 2018). Then, the viral polymerase RdRp synthesizes full-length antigenomic RNA (cRNA) using vRNA as template in a primer-independent manner, and cRNA subsequently can be used as template for the synthesis of progeny genomic RNA (vRNA) (Reguera et al., 2016). Meanwhile, viral mRNA encoding viral structural and non-structural proteins (NSs) (e.g., RdRp, glycoprotein Gn, Gc, N, and NSs) can be synthesized through the so-called secondary transcription by using newly synthesized vRNA as templates. SFTSV RdRp and N are both implicated in viral RNA synthesis and play indispensable roles

(Kolakofsky and Hacker, 1991; Guu et al., 2012; Amroun et al., 2017; Sun et al., 2018). However, besides these two proteins, other viral proteins may also participate in the viral RNA synthesis, for example, the NSs.

Unlike L and M segments, the S segment of SFTSV adopts ambisense coding strategies to encode N and NSs. It has been demonstrated that N can form oligomers, such as tetramer, pentamer, and hexamer, and is associated with viral RNA encapsidation (Jiao et al., 2013), an important process for viral RNP formation and RNA synthesis (Dong et al., 2013; Li et al., 2013; Reguera et al., 2013; Zheng and Tao, 2013). Although the NSs of bunyaviruses share poor amino acid similarity, the strategies they utilize to hijack host cells are similar (Ly and Ikegami, 2016). SFTSV NSs mainly distribute in the cytoplasm and can form inclusion bodies (IBs) in virus-infected cells and plasmid-transfected cells, and it can suppress the activities of the beta interferon (IFN- β) promoter by interacting with host kinases TBK1/IKK ϵ (Ning et al., 2014, 2015; Wu et al., 2014). In HRTV bandavirus, the NSs disrupt host defenses by blocking the TBK1 kinase–IRF3 transcription factor interaction and signaling required for interferon induction (Ning et al., 2017). In newly isolated Guertu virus (GTV), the NSs can form IBs and extended filamentous structures (FSs) that can diminish the IFN induction through sequestering TBK1 and STAT2 (Min et al., 2020). Interestingly, Wu et al. (2014) and Brennan et al. (2015) have separately provided clues that SFTSV NSs may also play roles in virus-like or viral RNA synthesis and virus replication; Wu also reported that NSs-formed viroplasm-like structures or IBs co-localize with viral S segment. However, the mechanisms of bandavirus including SFTSV and HRTV NSs participating in and regulating viral RNA synthesis were not fully elucidated as yet.

Effect of virus proteins on cDNA-derived virus-like RNA expression has been shown for several important bunyaviruses utilizing minigenome systems, in which the altered levels of virus-like RNA synthesis can be quantified by using the reporter protein as an indicator. For example, Ikegami et al. (2005) have used the reverse genetics system to demonstrate that the NSs of Rift Valley Fever virus (RVFV) promote viral RNA synthesis in an RVFV T7 RNA polymerase-driven minigenome system; a further study revealed that RVFV NSs lead to a specific degradation of PKR that is responsible for translational arrest of cellular and virus mRNAs (Habjan et al., 2009). Meanwhile, RVFV NSs also inhibit cellular transcription by targeting the cellular TFIIH transcription factor (Le May et al., 2004). In the case of Bunyamwera virus (BUNV), it has been reported that the NSs of BUNV inhibit viral RNA synthesis in a minigenome system (Weber et al., 2001) and host cell transcription (Leonard et al., 2006). Previously, we have established the mouse polymerase I (pol I)-driven minigenome (–) system to dissect the genome reassortment potential between

SFTSV and HRTV and to identify the elements located in the UTR affecting viral promoter activity (Ren et al., 2020). Here, we established a minigenome (+) that can generate antigenome cRNA analog; by using the cDNA-derived virus-like RNA synthesis systems including minigenome (−) and minigenome (+) systems, we revealed the involvement of SFTSV NSs in genomic vRNA–minigenome and antigenomic cRNA–minigenome synthesis and evaluated the association between SFTSV NSs and N, RdRp, or viral RNA. Our findings not only provide the details of SFTSV NSs participating in viral RNA transcription and replication by using reverse genetics systems, but also contribute to better understanding of the multiple roles of SFTSV NSs in the virus replication cycle.

MATERIALS AND METHODS

Cells and Virus

BHK-21 (baby hamster kidney) cells (CCL-10, ATCC; United States) were grown in Dulbecco's modified Eagle's medium (DMEM; GIBCO, United States) supplemented with 10% fetal bovine serum (FBS) at 37°C with 5% CO₂. Hela (CCL-2, ATCC; United States) and Vero E6 (African green monkey kidney) cells (CRL-1586, ATCC; United States) were grown in Eagle's Minimal Essential Medium (EMEM; GIBCO, United States) supplemented with 10% fetal bovine serum (FBS) at 37°C with 5% CO₂. SFTSV (WCH97 strain) was grown in Vero E6 cells and handled in a biosafety level 3 laboratory as previously described (Ning et al., 2015, 2019; Feng et al., 2019).

Plasmid Construction

To generate the minigenome transcription plasmids, pRF42 containing the murine pol I promoter and terminator was used as the backbone vector (Flick and Pettersson, 2001). For minigenome reporter plasmids, firefly luc or *EGFP* reporter genes flanked by viral UTR sequences were amplified by PCR and cloned into pRF42 in antisense orientation using the restriction-free clone method with an In-Fusion HD Clone kit (Clontech, Japan). The plasmid pRF42-luc (−)/(+) containing the antisense or sense reporter genes (firefly luc) not flanked by the viral UTR sequence was used as the control.

The helper plasmids of the minigenome reporter system, which encode SFTSV N (pCAG-SV-N), RdRp (pCAG-SV-RdRp), and NSs encoding plasmid pCAG-SV-NSs, were constructed by cloning the corresponding cDNA fragments into the expression vector pCAGGSP7 using double restriction enzyme (*KpnI* and *NotI*) digestion and DNA ligation. Mutant NS plasmid was also constructed by cloning the mutant ORF of NS encoding gene with two proline residues (aa 66 and aa 69) changing to alanine into the expression vector pCAGGSP7 using double restriction enzyme (*KpnI* and *NotI*) digestion and DNA ligation. The GenBank accession numbers of the viral segment reference sequences involved in the cloning of this study are as follows: JQ341188.1 (SFTSV L), JQ341189.1 (SFTSV M), and JQ341190.1 (SFTSV S); NC_024495.1 (HRTV L), NC_024494.1 (HRTV M), and NC_024496.1 (HRTV S). All cloning constructs were confirmed using sequencing.

Antibodies

As previously described (Ning et al., 2015, 2017), rabbit anti-SFTSV NSs, NP, and RdRp or HRTV-NSs antiserum were respectively, raised against the corresponding viral proteins generated by *Escherichia coli*. The antibody anti-β-actin (ABclonal, China) was purchased from the manufacturer. For the secondary antibodies, goat anti-rabbit IgG conjugated with Alexa Fluor 488 (Thermo Fisher Scientific, United States) and goat anti-rabbit IgG conjugated with Alexa Fluor 555 (Thermo Fisher Scientific, United States) used in the IFA assay were purchased from the manufacturer; goat anti-rabbit IgG antibodies conjugated with HRP (Abcam, United States) were used for Western blot and Co-IP analysis.

Minigenome Reporter Assays

BHK-21 cells cultured in 12-well plates were co-transfected with the indicated minigenome transcription plasmid (1.0 μg), RdRp expression plasmid (pCAG-SV-RdRp; 500 ng), N expression plasmid (pCAG-SV-N; 500 ng), and Renilla luciferase control plasmid (pRL-TK; 10 ng) per well using the Lipofectamine 3000 reagent (Invitrogen, United States) following the manufacturer's instructions. In the *EGFP* system, the minigenome-luc reporter plasmid was replaced by the corresponding minigenome-*EGFP* plasmid, with the control plasmid pRL-TK omitted. After transfection for 48 h, cells were delivered to luc activity measurement using a dual-luciferase reporter kit (Promega, United States), and the firefly and Renilla luciferase activities (Luc. Act.) were measured as described previously (Ning et al., 2015, 2017). In the *EGFP* reporter system, *EGFP* expression was visualized under fluorescence microscopy.

Protein–Protein Co-immunoprecipitation Assays

Lysates of the co-transfected or virus-infected cells were incubated with the specific antibodies at room temperature for 30 min and precipitated with protein A/G magnetic beads (MCE, United States). After incubation for 2 h, the beads were firstly washed four times with the binding buffer (PBST: 1 × PBS + 0.5% Triton X-100 at pH 7.4) and eluted with elution buffer (0.15 M glycine, 0.5% Triton X-100, or Tween-20 at pH 2.5–3.1). The immunoprecipitates were subjected to sodium dodecyl sulfate–polyacrylamide gel electrophoresis (SDS-PAGE), transferred onto PVDF membranes (Millipore, United States), and incubated with primary antibodies at a dilution of 1:2,000 at room temperature for 2 h and horseradish peroxidase (HRP)-conjugated secondary antibodies at a dilution of 1:2,000 for 2 h at room temperature. Signals on blots were developed by ECL reagents (Invitrogen, United States).

Immunofluorescence Assay

BHK-21 or Hela cells transfected with plasmids encoding NSs or mutant NSs were washed twice with PBS, fixed with 4% paraformaldehyde for 20 min, permeabilized with 0.1% Triton X-100 for 10 min, and washed thrice with PBS. The cells were blocked with 5% bovine serum albumin in PBS for 1 h at 37°C and incubated with anti-NSs antibodies at 1:2,000 dilution at

37°C for 1 h. After three washes with PBST, the cells were incubated with goat anti-rabbit IgG (H + L) Highly Cross-Adsorbed Secondary Antibody (Alexa Fluor Plus 488, 1:1,000; Invitrogen, United States) at 37°C for 1 h and then washed and stained for 5 min with Hoechst 33342 (Invitrogen, United States). After washing, the cells were visualized under an EVOS FL Auto confocal microscope (Invitrogen, United States).

Immunoblot Analysis

To ensure that NSs, N, and RdRp are expressed within the minigenome reporter systems as indicated on BHK-21 and Hela cells, Western blotting was performed with specific antibodies (anti-NSs, anti-N, or anti-RdRp antibodies) by using β -actin as an internal control. Briefly, equal amounts of SDS-loading buffer treated cell lysates of the transfected cells were subjected to SDS-PAGE, transferred onto PVDF membrane (Millipore, United States), and incubated with primary antibodies, rabbit-derived anti-N/NSs/RdRp, or mouse-derived anti- β -actin antibodies (Thermo Fisher Scientific, United States), at room temperature for 2 h. They were further incubated with HRP-conjugated secondary antibodies for 2 h at room temperature. Signals on blots were developed by ECL reagents (Invitrogen, United States).

Protein–RNA Co-immunoprecipitation Assays

Immunoprecipitation combined with RT-PCR was conducted to detect virus-like RNA in immunoprecipitates. Briefly, cell lysates of the transfected or co-transfected cells were incubated with specific anti-NSs antibodies overnight at 4°C with an RNase inhibitor (Takara, Japan) and precipitated with protein A/G magnetic beads (MCE, United States). After 2-h incubation at 4°C, the beads were washed four times with the binding buffer and eluted with the elution buffer. Viral RNA was isolated from the immunoprecipitates with the TRIzol reagent (Invitrogen, United States) and subjected to RT-PCR. Primers used to amplify L/M/SUTR-Luc are as follows: LUTR-Luc, forward primer 5'-acacaaagaccgcccag-3', reverse primer 5'-cttcacgttctctggcc-3'; MUTR-Luc, forward primer 5'-acacaaagaccggccaaand-3', reverse primer 5'-ggccaacaatgatgaaa-3'; SUTR-Luc: forward primer 5'-acacaaagacccttc-3', reverse primer 5'-aggaagacgcaaagga-3'. Primers used to amplify 2,000 bp of viral L, M, and S are as follows: L, forward primer 5'-ttaaccccacattctg-3', reverse primer 5'-ttgcttcaggtacactg-3'; M, forward primer 5'-ctaagccagcttgctc-3', reverse primer 5'-tcaaagggcattggta-3'; S, forward primer 5'-atgtcgctgagcaaatg-3', reverse primer 5'-atgtcagagtgtccag-3'.

Virus Titration by Immunofluorescence Assay (IFA)

To analyze whether the overexpressed wild-type or mutant NSs could affect virus replication, we performed IFA to determine and compare the titer of virus supernatants collected at various times. Briefly, BHK-21 or Hela cells cultured in 12-well plates were transfected with 0.5, 1.0, and 2.0 μ g of NSs expression plasmid DNA. After 12 h, the cells were infected with SFTSV at a multiplicity of infection (MOI) of 1.0. Supernatants were harvested at 12, 24, 36, 48, 72, 96, and 120 h post infection

(hpi). Vero E6 cells (1×10^5 cells/well) were seeded on 96-well plates and incubated for 24 h at 37°C in 5% CO₂ to produce a confluent monolayer, inoculated with serial 10-fold dilutions of the virus supernatants obtained above, and titrated for infectious virus titration (TCID₅₀) using indirect immunofluorescence as described previously (Ren et al., 2020). Infectious virus titers (TCID₅₀/ml) were calculated based on the Reed and Muench method.

Superinfection Assays

To further reveal the effect of NSs on viral RNA synthesis under infection. We adopted superinfection assays as previously described to compare the levels of viral RNA synthesis through analyzing the luciferase activities of minigenome (–) and minigenome (+) with overexpressed NSs or mutant NSs (Ren et al., 2020). Briefly, BHK-21 cells cultured in 12-well plates were transfected with 2.0 μ g of NSs- or mutant NSs-expression plasmid DNA and 1.0 μ g of L/M/S (–)/(+) minigenome plasmid; at 12 hpi, the cells above were infected with SFTSV at a MOI of 3.0, respectively, and the luciferase activities of minigenome (–) and minigenome (+) were measured at 48 hpi.

Real-Time Quantitative PCR (RT-qPCR)

To measure the RNA levels of the indicated L, M, and S minigenome RNA, the total intracellular RNA content was extracted from cells transfected with minigenome plasmids using TRIzol reagent (Takara, Japan), and the first strand cDNA was synthesized by using the PrimeScriptTM RT reagent kit and quantitated by qPCR using TB Green[®] Premix Ex TaqTM II (Takara, Japan) as previously described (Ning et al., 2015; Mo et al., 2020). The data shown represent the relative abundance of the indicated RNA normalized to that of GAPDH. The primer sequences for GAPDH and SFTSV L, M, and S minigenome RNA were as follows: GAPDH: 5'-ACCACAGTCCATGCCATCAC-3' (forward) and 5'-TCCACCACCCTGTTGCTGTA-3' (reverse); L, M, and S minigenome RNA: 5'-GCCGCAGTTCCAGGAACACTA-3' (forward) and 5'-GCAATGAGTTTCTAGATGTAA-3' (reverse). All RT-qPCR experiments were performed on an ABI 7500 system according to the manufacturer's instructions.

Statistical Analysis

Statistical analyses were accomplished by GraphPad Prism 8, and data were analyzed using one-way analysis of variance (ANOVA). All data are presented as the mean \pm SEM. $p < 0.05$ was considered statistically significant.

RESULTS

The cDNA-Derived Virus-Like RNA Synthesis Systems Consisting of Genomic and Antigenomic Minigenomes of SFTSV Were Constructed

Minigenome (–) of SFTSV driven by murine pol I has been described in our previous study (Ren et al., 2020). The minigenome (+) system constructed in this work consists of

SFTSV RdRp and N expression plasmids and the reporter plasmid that was inserted with the antisense orientation ORF of firefly luciferase (*luc*) or enhanced green fluorescent protein (*EGFP*) cassette flanked by the UTRs of SFTSV L, M, and S segments, respectively, to develop the minigenome (+) system (see section “Materials and Methods”) (Figure 1A).

The minigenome (–)/(+) generated the initial virus-like genome or anti-genome RNA (vRNA or cRNA), respectively, and completely simulated transcription and replication during infection. In the two systems, virus-like RNA synthesis, including replication and transcription, can occur, resulting in the expression of the reporter protein, which can be used as an indicator of the RNA synthesis level (Figure 1B). It is of significance to note that the number of vRNA-minigenome templates available for use in transcription is dependent on virus-like genome replication. An increase in virus-like genome replication leads to an increase in templates available for transcription, and thus, can lead to an increase in both mRNA levels and reporter activity. Therefore, the reporter activity as well as the mRNA amount reflects not only viral transcription but also viral genome replication in the minigenome systems we used.

SFTSV NSs Decreases the Reporter Activity Within Minigenome (–)/(+) Systems

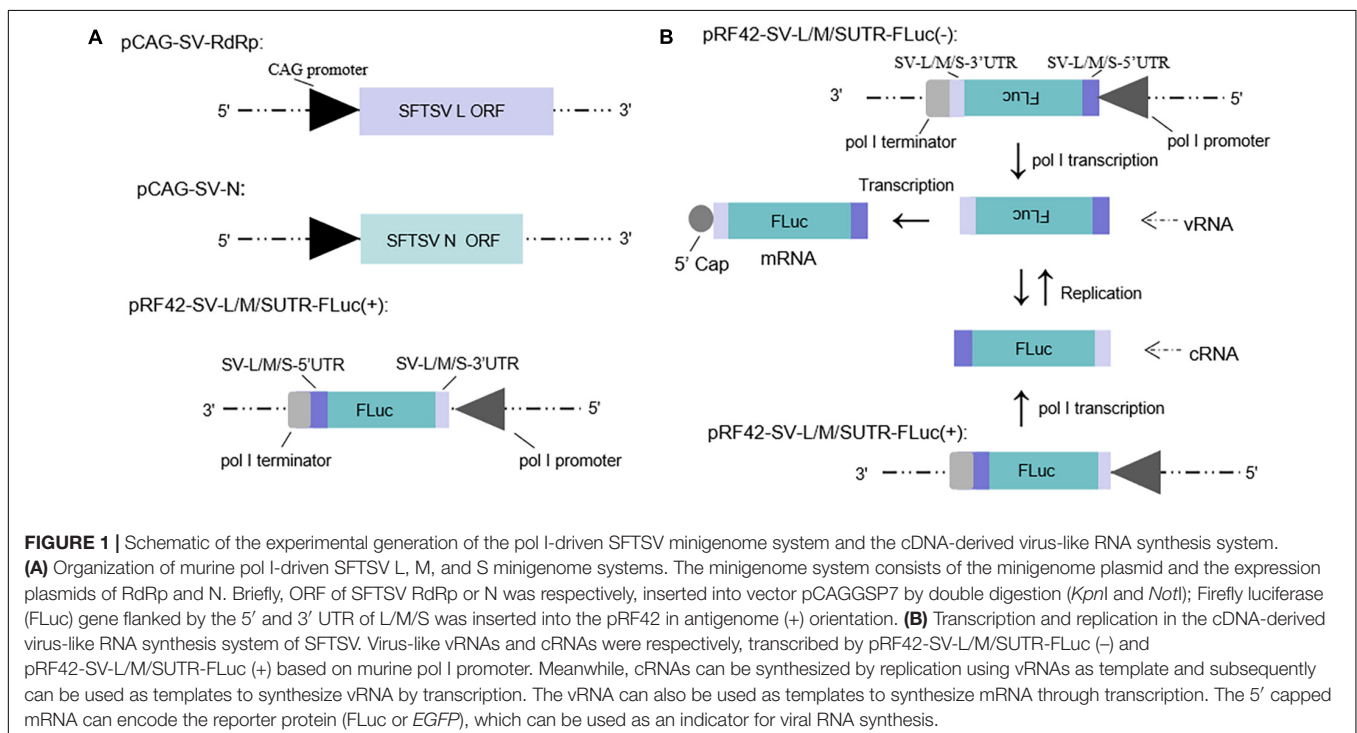
To investigate the role of NSs in virus-like RNA synthesis within the minigenome systems, we exploited multi-plasmid co-transfection combined with firefly luciferase activity determination assays to accurately quantify altered efficiencies in viral RNA synthesis levels.

In the L, M, and S segment-based SFTSV minigenome (–)/(+) systems, functional RNPs efficiently assembled to express reporter protein compared with the groups where RdRp was omitted and negative controls. Luciferase activations (Luc. Act.) for L (–), M (–), S (–), L (+), M (+), and S (+) decreased significantly when NSs encoding plasmids (0.5 μ g for each test) were co-transfected (Figures 2A,B), and they decreased by 32.3, 34.9, 26.2, 26.0, 33.6, and 27.3%, respectively. These results suggest that the NSs downregulated virus-like RNA synthesis in both minigenome (–) and minigenome (+) systems, but not in the manner of significant difference for the two systems.

SFTSV NSs Downregulate Virus-Like RNA Synthesis in a Dose-Dependent Manner

As the initial cDNA-derived product is vRNA for the minigenome (–) system, the genomic minigenome is more suitable than the antigenomic minigenome to mimic authentic viral RNA synthesis in mammalian cells (Kolakofsky and Hacker, 1991; Guu et al., 2012). We next investigated whether SFTSV NSs downregulate the virus-like RNA synthesis in a dose-dependent manner using the minigenome (–) system.

As shown in Figure 3, when the NSs-expression plasmids were added to the mixed plasmids of the minigenome systems, the L (–), M (–), and S (–) minigenomes all showed decreased viral RNA synthesis levels compared with the corresponding minigenome systems without the involvement of NSs. In the L/M/S (–) minigenome, upon the addition of NSs-expression plasmid at 0.5, 1.0, 2.0, and 3.0 μ g (Figures 3A–C, bottom), the levels of viral RNA synthesis decreased significantly as evidenced



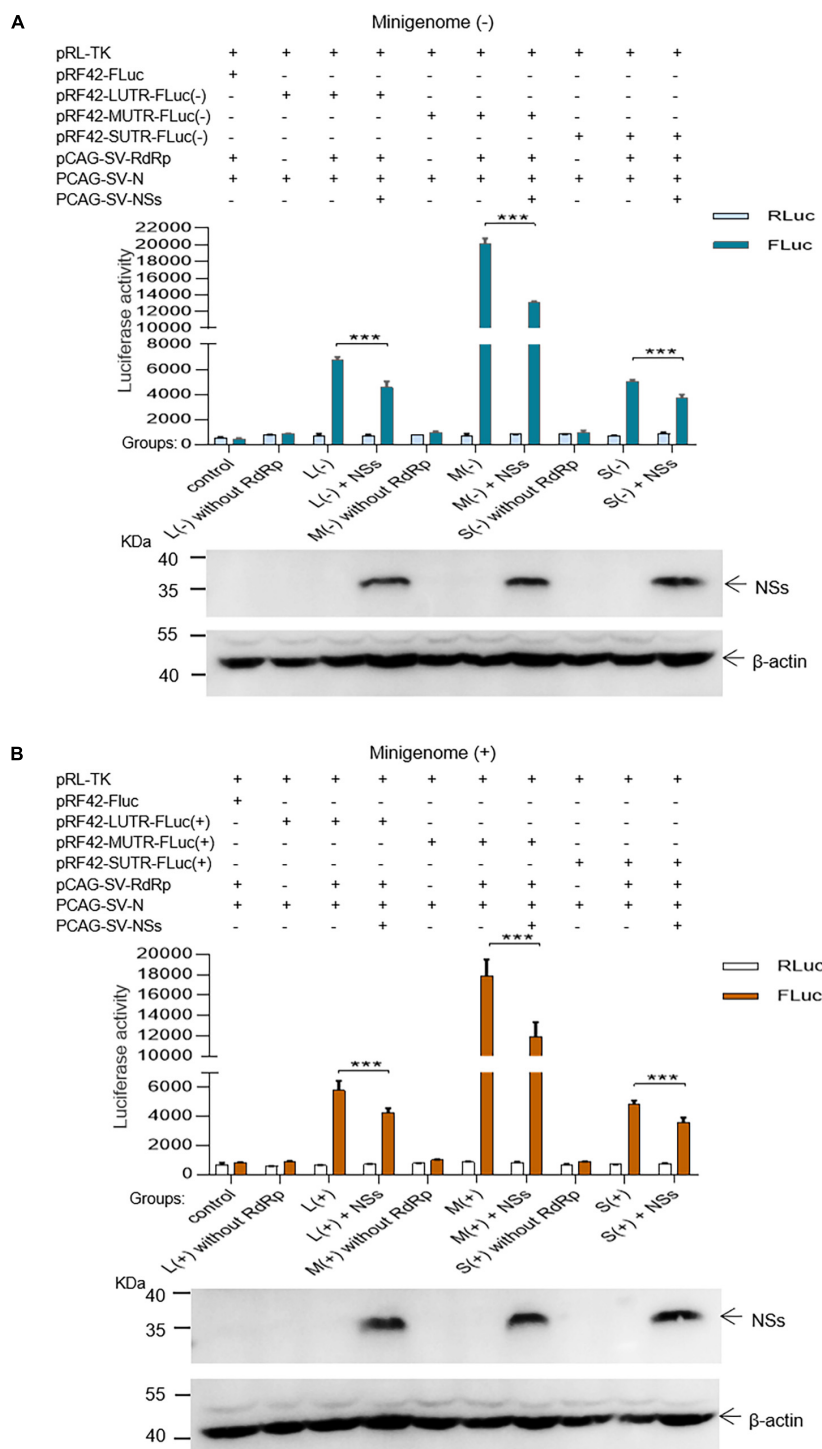
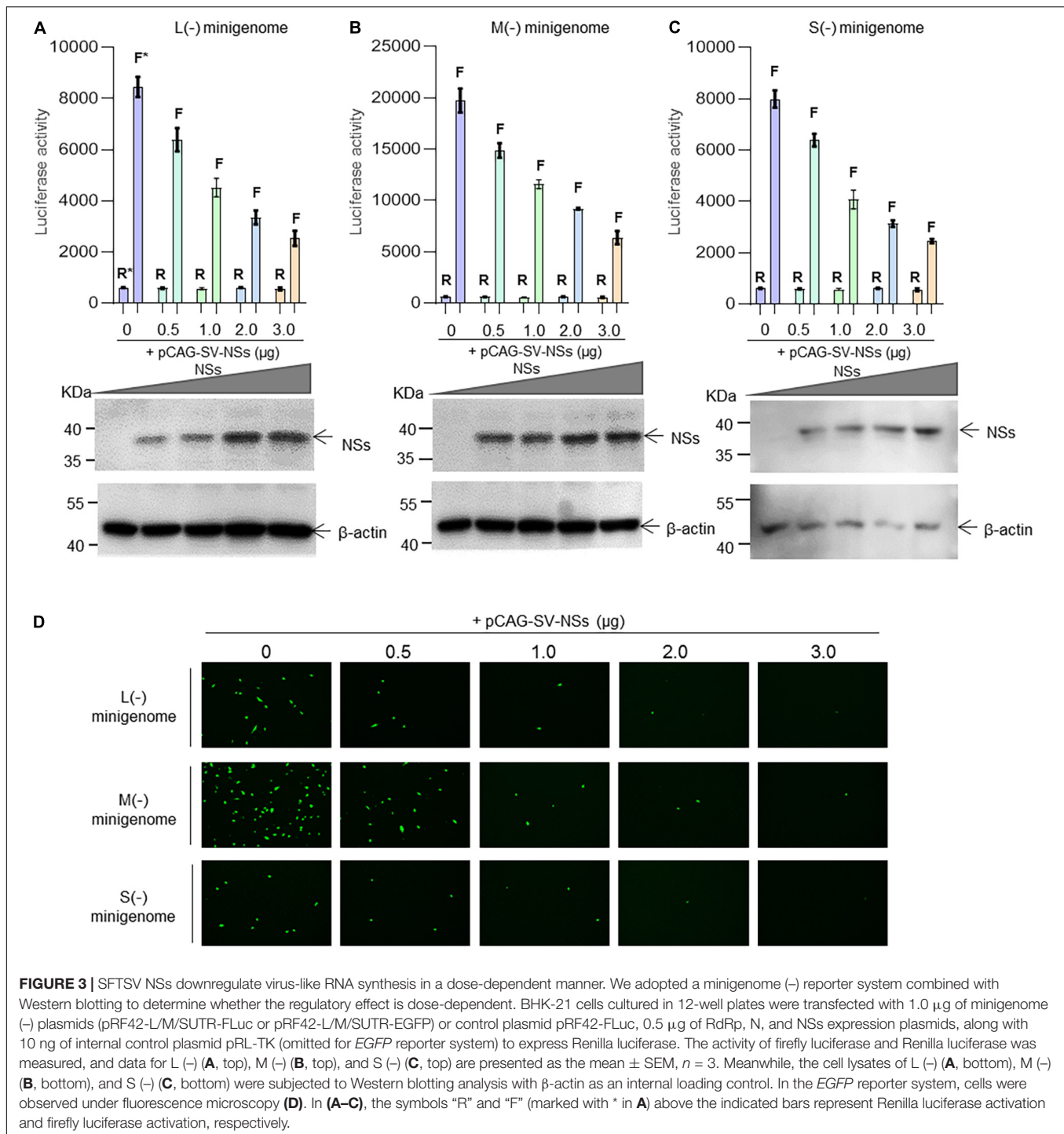


FIGURE 2 | SFTSV NSs decrease the minigenome (-)/(+)-encoded reporter activity. NSs downregulated reporter activity within the minigenome (-) and minigenome (+) systems based on viral L, M, and S denoted as L (-)/(+), M (-)/(+), and S (-)/(+), respectively. Briefly, groups of various plasmid mixes indicated in (A,B) were transfected into BHK-21 cells cultured in 12-well plates with Lipo 3000, respectively. The symbol “+” means the presence of designated plasmid in plasmid mixes and “-” means the absence of designated plasmid in plasmid mixes. Cells were transfected with 1.0 μ g of minigenome (+)/(-) plasmids or control plasmids pRF42-FLuc, 0.5 μ g RdRp, N, and NSs expression plasmids, along with 10 ng of internal control plasmid pRL-TK to express Renilla luciferase. Meanwhile, negative control groups including L (-)/M (-)/S (-) without RdRp and L (+)/M (+)/S (+) without RdRp were independently set up to check that the integrity of the minigenome system is important for virus-like RNA synthesis in both minigenome (-) and minigenome (+) systems. At 48 hpt, firefly luciferase and Renilla luciferase were measured by using Dual-Glo Luciferase Assay System kit as the technical manual and data are presented as the mean \pm standard error of mean (SEM), $n = 3$. *** $p < 0.001$ (A,B). Meanwhile, the NSs expression levels were analyzed by Western blotting by using β -actin as internal control (A,B).



by the decreased luciferase activity, respectively, of 24.5, 46.6, 60.3, and 70.0% for L (–) compared with the control group (Figure 3A) of 24.7, 41.3, 53.5, and 67.8% for the M (–) minigenome (Figure 3B) and of 20.0, 48.9, 60.8, and 69.3% for the S (–) minigenome (Figure 3C). Similar results were observed from the *EGFP*-reporter systems in that the *EGFP* signals reduced upon the increase of co-transfected NS plasmid in the L (–), M (–), and S (–) minigenome systems (Figure 3D).

SFTSV NSs Are Associated With N but Not RdRp Within the Minigenome Reporter Systems and Virus-Infected Cells

Since the NSs downregulate the virus-like RNA synthesis within minigenome reporter systems, it would be urgent to elucidate the possible mechanism of how NS protein regulates

viral RNA synthesis. Here, we utilized protein–protein/RNA co-immunoprecipitation and RT-PCR assays to dissect what components of SFTSV RNP are associated with the NSs within L (–), M (–), and S (–) minigenome systems and virus-infected cells.

The results indicate that when BHK-21 cells were co-transfected with the plasmids of the L/M/S (–) minigenome system comprising pCAG-SV-N, pCAG-SV-RdRp, pRF42-L/M/SUTR-luc (–), and NSs-expression plasmid pCAG-SV-NSs or were infected with SFTSV, viral proteins, including RdRp, N, and NSs, were detected in the cell lysates by Western blotting (Figure 4A, left). To reveal the viral components associated with the NSs, we co-immunoprecipitated the designated cell lysates with anti-NSs antibodies by using Protein A/G Magnetic Beads kits (MCE, United States) and then the immunoprecipitates were subjected to Western blotting analyses. Meanwhile, the viral RNA was extracted from cell lysate and immunoprecipitates with TRIzol reagent and then was subjected to RT-PCR analysis. Our results suggest that NSs are associated with N, not with RdRp (Figure 4A, right). Intriguingly, the amount of N in the immunoprecipitates increased with the amount of NSs (data not shown), further supporting the interaction between NSs and N.

Viral L-, M-, or S-like RNA (denoted as LUTR-luc, MUTR-luc, and SUTR-luc, respectively) was only detected in the cell lysates but not in co-immunoprecipitates (Figure 4B). However, Viral L, M, or S could be obviously detected both in the cell lysates and co-immunoprecipitates but not in the control group (Figure 4B).

The Negative Regulatory Effect of NSs on Virus-Like RNA Synthesis Could Be Outcompeted by Increasing the Expression Levels of N

We next assessed whether the inhibitory effect of NSs on virus-like RNA synthesis could be reversed. We found that when the amount of transfected N-expression plasmid DNA increased, the inhibitory effect of NSs on L, M, and S virus-like RNA synthesis decreased. In the L/M/S (–) minigenome system, the activations of firefly luciferase decreased significantly with the presence of overexpressed NSs. When the amount of additional N-expression plasmid DNA was increased sequentially from 0 to 0.5, 1.0, and 2.0 μ g (Figures 5A–C, right), the activations of firefly luciferase (Luc. Act.) were restored significantly compared with the control groups (Figures 5A–C, left). The Luc. Act. increased by 16.8,

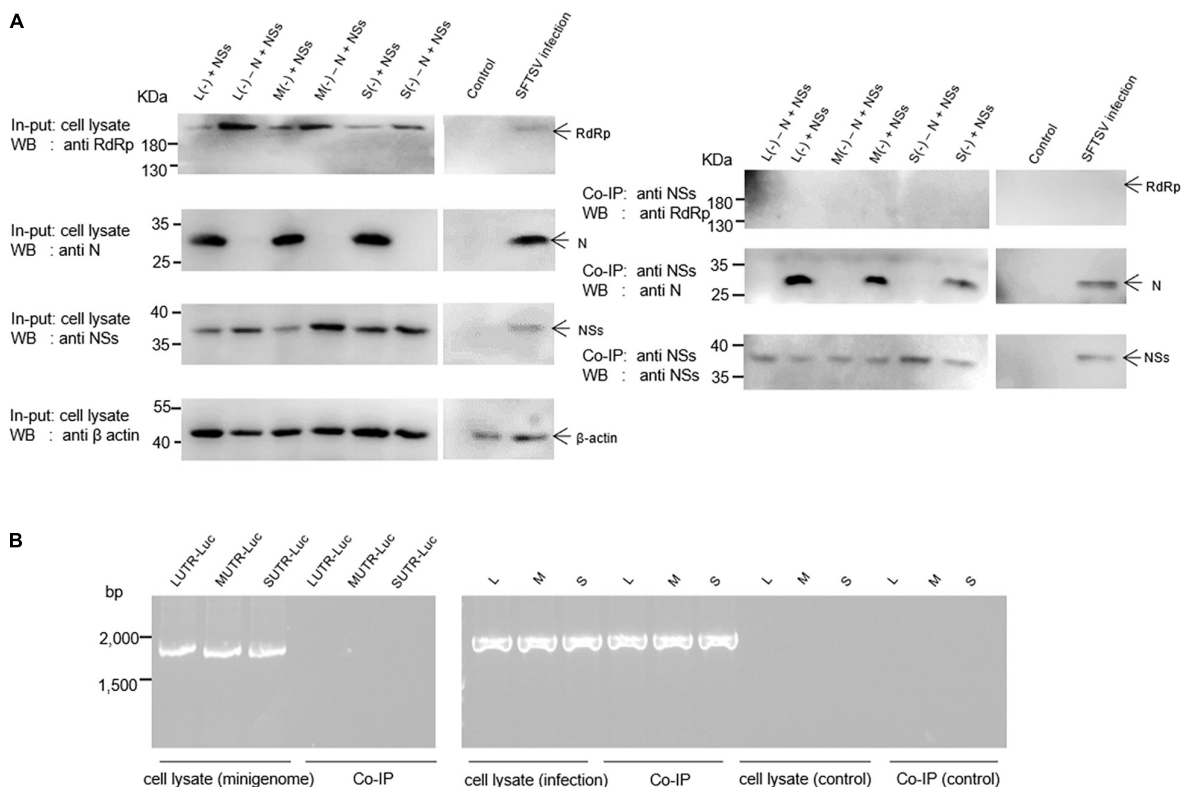


FIGURE 4 | SFTSV NSs are associated with N but not RdRp within the minigenome reporter systems and virus-infected cells. Co-IP assays and RT-PCR were used to identify the viral components interacting with NSs. Minigenome assays were carried out as previously described, and the amounts of expression plasmid and transcription plasmid were 0.5 μ g and 1.0 μ g, respectively. The amount of NSs expression plasmids was 1.0 μ g. Meanwhile, L (–), M (–), and S (–) that do not contain N expression plasmid were set up as negative controls, denoted as L (–)/M (–)/S (–) + NSs, respectively. At 48 hpt, cell lysates of L (–), M (–), and S (–)-transfected and virus-infected cells were subjected to Western blotting analysis (A, left) and Co-IP (A, right), respectively. Meanwhile, cell lysates and co-immunoprecipitates of L (–), M (–), and S (–)-transfected and virus-infected or control cells were all treated with TRIzol reagent to extract virus-like and viral RNA, which were then subjected to RT-PCR analysis (B).

34.9, 56.8, and 65.8%, respectively, for the L (–) minigenome system (**Figure 5A**, left). Similarly, in the M (–) minigenome system, the activations of firefly luciferase increased by 14.1, 30.7, 47.5, and 51.9%, respectively (**Figure 5B**, left), and in the S (–) minigenome system, the activations of firefly luciferase increased by 15.7, 35.1, 53.5, and 57.2%, respectively (**Figure 5C**, left). In contrast, when the amount of RdRp-expression plasmid DNA increased, the inhibitory effect of NSs did not significantly change (see **Supplementary Figure 1**). These results showed that NSs exert negative regulatory effects on virus-like RNA synthesis and that the accumulation of N but not RdRp can reverse the inhibitory effect.

Formation of IBs Induced by NSs Is Associated With Its Inhibitory Effect on Virus-Like RNA Synthesis

To investigate whether the interaction between NSs and N is associated with the IB formed by NSs, we introduced the mutant NSs in which two prolines at positions of 66 and 69 were mutated to alanines (designated as mutant) by site-directed mutagenesis (**Figure 6A**). As shown in **Figure 6B**, when the two prolines at positions 66 and 69 were mutated to alanine, the structure of IB formed by the NSs can hardly be observed compared with the wild-type NSs in both BHK-21 and Hela cells. Meanwhile, HRTV NSs that cannot form IB structure in the cytoplasm was also introduced as a comparison (**Figure 6C**).

When BHK-21 cells were transfected with the same amount (0.5 μ g) of plasmid DNA encoding SFTSV NSs/mutant NSs or HRTV NSs together with mixed plasmids of the minigenome reporter system and internal control plasmid pRL-TK, there was no significant difference in firefly luciferase activation in the L (–), M (–), and S (–) minigenome systems with mutant NSs, whereas with wild-type NSs, the firefly luciferase activations decreased significantly (**Figure 6C**). However, the NSs of HRTV exerted no significant activity-inhibition or -promotion effect on HRTV L, M, and S minigenomes (–) (**Figure 6C**). These results suggest that the suppressive effect of NSs on virus-like RNA synthesis is due to its interaction with N, and the interaction is closely associated with the structure of IB formed by NSs.

NSs Exert a Negative Effect on Viral RNA Synthesis and Virus Replication in Immunodeficient and Non-immunodeficient Cells

To further reveal the role of NSs in authentic virus replication and the potential correlation between NSs regulating viral RNA synthesis and antagonizing the host's antiviral responses, we adopted transfection combined with the superinfection method to compare the efficiencies of virus-like RNA synthesis and virus replication in immunodeficient (BHK-21) and non-immunodeficient (Hela) cells (Andzhaparidze et al., 1981; Matskevich et al., 2009), respectively.

As shown in **Figures 7A,B**, when BHK-21 cells transfected with L/M/S minigenome (–)/(+) and NSs-expression plasmid were infected with SFTSV at a MOI of 3.0, the levels of virus-like RNA synthesis decreased significantly for both minigenome (–)

and minigenome (+) by measuring and comparing the luciferase activities, while similar changes were not observed when the NSs-expression plasmid was replaced with the NSs-mutant-expression plasmid. As shown in **Figures 7C,D**, when immunodeficient BHK-21 cells and non-immunodeficient Hela cells were infected with SFTSV at a MOI of 3.0, there were no obvious differences in the one-step growth curves of the cells when the amount of transfected NSs-expression plasmid DNA was 0.5 and 1.0 μ g, respectively; upon the transfection of 2.0 μ g NSs-expression plasmid DNA, the virus titers were lower than the control groups at various time points. However, when the NSs-expression plasmid was replaced with the plasmid DNA encoding mutant NSs, there were no significant differences in the titers at various time points compared with the control group. Meanwhile, the RT-qPCR results showed that the NSs can directly decrease the synthesis of L-, M-, and S-minigenome RNA significantly compared with the controls (**Figure 7E**). These results indicate that low levels of overexpressed NSs and mutant NSs do not affect SFTSV replication on both BHK-21 and Hela cells and it seems that there are no correlations between regulating viral RNA synthesis and antagonizing antiviral innate immunity by NSs.

DISCUSSION

Reverse genetics systems have been utilized to study the roles of virus components played in the viral RNA replication and transcription. In a typical minigenome system, the minigenome transcripts expressed by either host RNA pol I or T7 RNA polymerase contain an internal ORF of a reporter gene instead of a viral ORF flanked by viral UTRs (Hoenen et al., 2011). The expressed minigenome RNA transcripts undergo RNA replication and transcription in the presence of co-expressed viral proteins including RdRp and N, or co-infected helper virus. The levels of reporter expression indicate the efficiency of the minigenome RNA replication and transcription. The regulatory effect of NSs on viral RNA synthesis has been previously reported in many other bunyaviruses by using minigenome systems. For instance, Weber et al. (2001) have reported that the NSs derived from BUNV, Guaro virus, and Lumbo virus inhibit virus-like RNA synthesis in T7-polymerase-driven minigenome systems by regulating the activity of the viral polymerase in a highly conserved mechanism. Similar to BUNV NSs, Blakqori et al. (2003) have reported that the NSs of La Crosse virus (LACV) can downregulate the activity of the minigenome, thus leading to the downregulation of virus-like RNA synthesis. On the contrary, the NSs of bunyaviruses may also exert a positive regulatory effect on viral RNA synthesis. Rift Valley fever virus (RVFV) NSs locating in both the cytoplasm and nucleus of infected cells can enhance virus-like RNA replication and transcription in a novel RVFV minigenome system (Ikegami et al., 2005). These suggest that the NSs of bunyaviruses adopt various strategies in regulating virus-like or viral RNA synthesis. Our results here showed that SFTSV NSs play a negative regulatory role in virus-like RNA synthesis and that the underlying mechanism of which is not associated with its previously identified role in counteracting antiviral innate immunity.

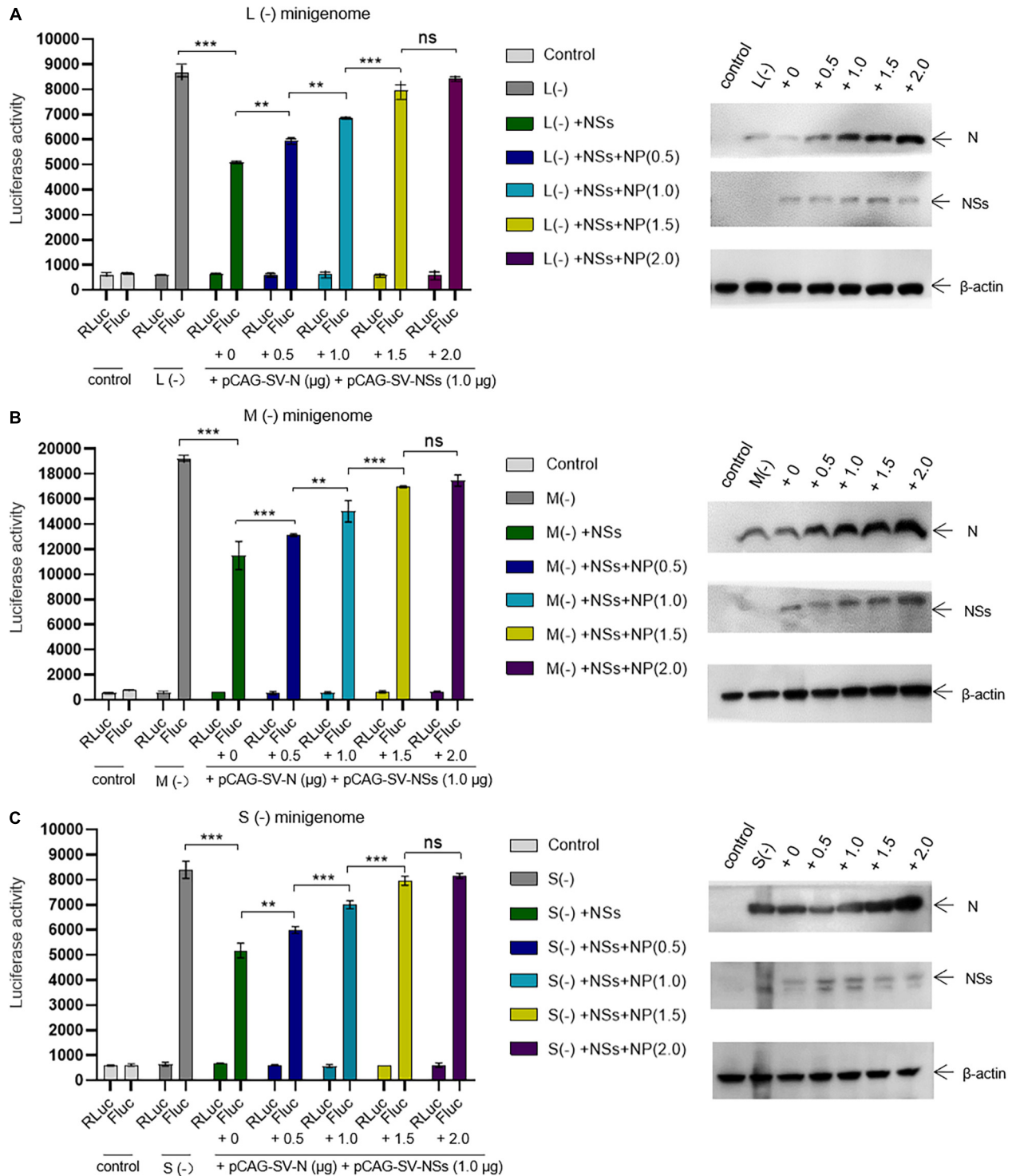


FIGURE 5 | The negative regulatory effect of NSs on virus-like RNA synthesis can be outcompeted by increasing the level of N. Minigenome reporter assays combined with Western blotting analysis was carried out to investigate whether the accumulation of N reverses the negative regulatory effect on virus-like RNA synthesis. Minigenome reporter assays were carried out as described above. Briefly, BHK-21 cells cultured in 12-well plates were transfected with 1.0 μ g of pRF42-L/M/SUTR-FLuc (-), 0.5 μ g of pCAG-SV-RdRp, and 0.5 μ g of pCAG-SV-N together with 10 ng of internal control plasmid (pRL-TK). Meanwhile, control groups with pRF42-L/M/SUTR-FLuc (-) being replaced with pRF42-FLuc were set, respectively. Moreover, cells transfected with plasmid mixes of L (-), M (-), and S (-) with 0.5 μ g of NSs protein expression plasmids pCAG-SV-NSs are also transfected with various amount of additional N expression plasmids pCAG-SV-N (0, 0.5, 1.0, 1.5, and 2.0 μ g, respectively). After 48 h, firefly and Renilla luciferase were measured. Data are presented as the mean \pm SEM ($n = 3$). ** $p < 0.01$; *** $p < 0.001$; ns, non-significant (A–C, left). To confirm the expression of NSs and the accumulation of N, Western blotting was conducted (A–C, right).

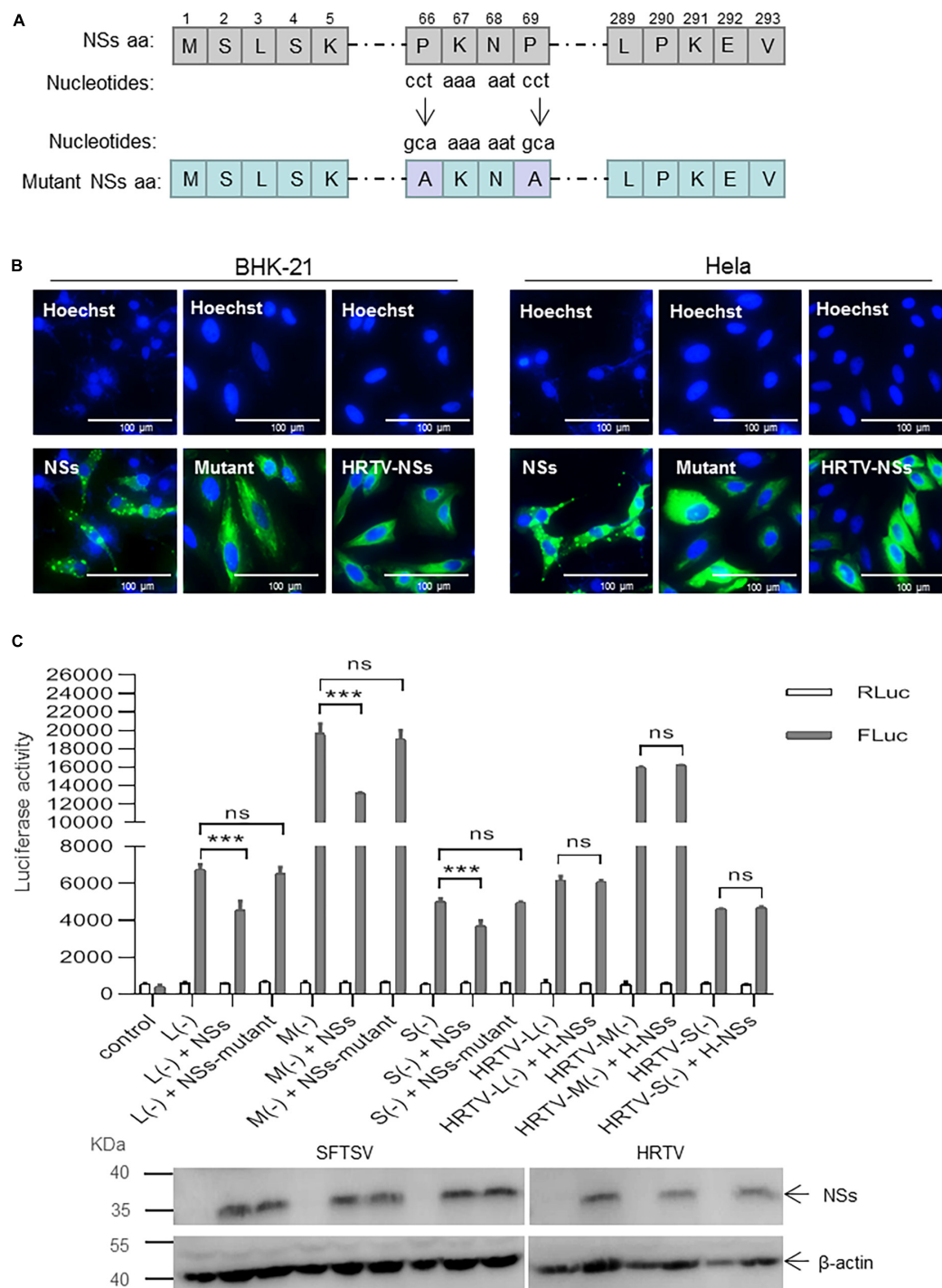


FIGURE 6 | Formation of NSs-induced IB structure is important for the suppression of virus-like RNA synthesis. **(A)** Schematic of mutant NSs clone. The amino acids at positions 66 and 69 were substituted by alanine via the introduction of mutant nucleotides to NSs encoding gene ("cct" were mutated to "gca"). Mutant clone (pCAG-SV-NSs-mutant) was constructed by double restriction enzyme digest (*KpnI* and *NotI*) and In-Fusion technology (Clontech, Japan). **(B)** When BHK-21 and HeLa cells were respectively, transfected with pCAG-SV-NSs, pCAG-SV-NSs-mutant, or pCAG-HRTV-NSs, IFA was performed 48 hpt to observe wild-type, mutated SFTV NSs and HRTV NSs under immunofluorescence microscopy. **(C)** Minigenome reporter assays were performed as previously described. BHK-21 cells in a 12-well plate were transfected with 1.0 μ g of pRF42-SV/HRTV-L/M/SUTR-FLuc (-), 0.5 μ g of pCAG-SV-RdRp, and 0.5 μ g of pCAG-SV-N together with 0.5 μ g of SFTSV NSs/mutant NSs-expression plasmid DNA or HRTV NSs-expression plasmid DNA and 10 ng of internal control plasmid pRL-TK. Meanwhile, a control group with pRF42-FLuc replacing pRF42-SV/HRTV-L/M/SUTR-FLuc was also set up. The activities of firefly and Renilla luciferase were measured at 48 hpt, respectively. Data are presented as the mean \pm SEM ($n = 3$). *** $p < 0.001$; ns, non-significant. The expression levels of SFTSV NSs/mutant NSs and HRTV NSs were analyzed, respectively, by Western blot.

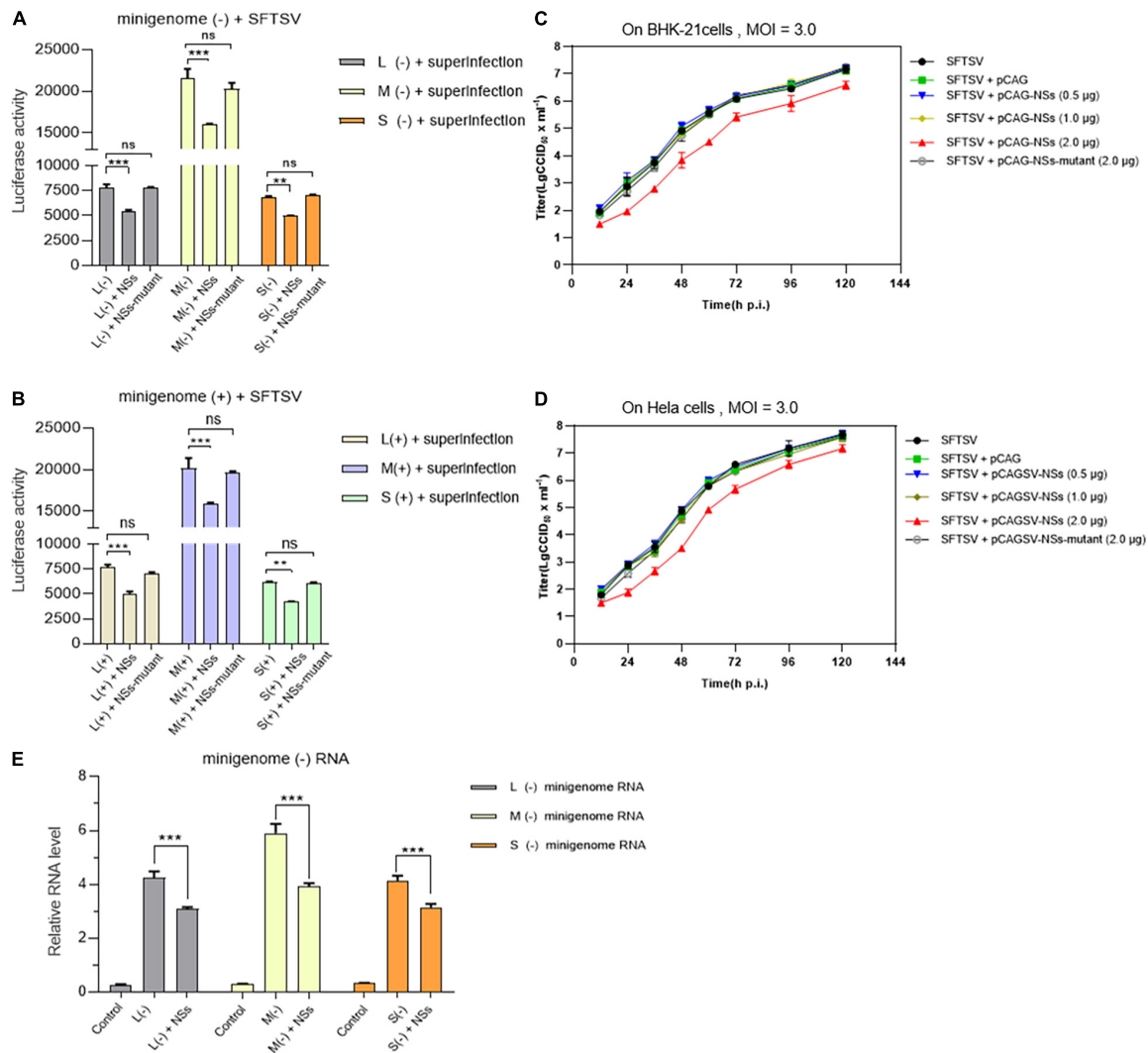


FIGURE 7 | NSs exert a negative regulatory effect on virus-like RNA synthesis and virus replication in both immunodeficient cells and non-immunodeficient cells. To further investigate the role of overexpressed NSs in virus-like RNA synthesis, virus replication, and the correlation between NSs regulating RNA synthesis and antagonizing host antiviral responses, we adopted superinfection and infection methods to analyze virus-like RNA synthesis and virus replication under different conditions. Briefly, when BHK-21 cells transfected with 1.0 µg of L/M/S minigenome (-) or minigenome (+) and 2.0 µg of NSs- or mutant NSs-expression plasmids were infected with SFTSV at a MOI of 3.0, the luciferase activity (Luc. Act.) of the indicated groups were measured at 48 hpi, respectively. Data are presented as the mean ± SEM ($n = 3$) for minigenome (-) (**A**) and minigenome (+) (**B**). $^{**}p < 0.01$; $^{***}p < 0.001$; ns, non-significant. The immunodeficient (BHK-21) or non-immunodeficient cells (HeLa) were transfected with various amounts (0.5, 1.0, and 2.0 µg) of NSs- or mutant NSs-expression plasmids, DNA, respectively. At 12 hpi, the indicated cells above were infected with SFTSV at a MOI of 3.0, respectively, and the supernatants were harvested at 12, 24, 36, 48, 72, 96, and 120 hpi. The supernatants then were titrated for infectious virus titration (TCID₅₀) using indirect immunofluorescence assays. Infectious virus titers (TCID₅₀/ml) were calculated based on the Reed and Muench method. Data are presented as the mean ± SEM ($n = 3$) (**C,D**). The minigenome RNA levels of L (-), M (-), and S (-) were quantified by qRT-PCR using the gene encoding GAPDH as an internal control and the relative RNA levels were presented (**E**). In the qPCR analyses, relative RNA levels over the control groups (wild-type cells or the cells transfected with the control plasmids) were calculated for L (-), M (-), and S (-) minigenome RNA, respectively. Data show mean ± SEM ($n = 3$). $^{***}p < 0.001$.

We have previously employed a cDNA-derived RNA synthesis system, i.e., minigenome (-), that generates RNA replication and transcription products to identify the elements affecting viral promoter activity (Ren et al., 2020). In this study, we utilized pol I-driven minigenome (-)/(+) systems to generate the virus-like RNAs, including vRNA and cRNA, involved in transcription and replication. Using these established systems, we found that SFTSV NSs encoded by the S segment downregulate vRNA-

and cRNA-minigenome synthesis by sequestering N through blocking the interaction between N and naked transcripts of the minigenome (-)/(+) and the RNA derived from the intermediate process (cRNA or vRNA), while SFTSV NSs cannot seem to efficiently block the interaction between viral transcripts and N, which may be due to the sequence differences between virus-like and viral RNA (Figures 4A,B). Wu et al. (2014) have reported that SFTSV NSs are associated with N and viral S segments and

may serve as a virus replication factory in infected cells. Similarly, in the pol I-driven minigenome systems, we found that NSs did interact with N; however, RdRp and virus-like RNA were not detected in the immunoprecipitates by NSs even though viral RNA could be detected (**Figures 4A,B**). Intriguingly, when BHK-21 or Hela cells transfected with low amounts of plasmids DNA (0.5 or 1.0 μ g) expressing NSs were superinfected with SFTSV, NSs did not affect virus replication significantly (**Figures 7C,D**). According to the results of **Figures 5A–C**, we speculate that the accumulation of N due to virus replication reversed the inhibitory effect. However, when the transfected plasmid DNA expressing NSs was increased to 2.0 μ g, the negative effect of NSs on virus replication was obviously observed, whereas the mutant NSs showed no regulatory effect. Meanwhile, we observed no cell apoptosis when the amount of NSs-expression plasmid increased to the maximum extent in this research through morphology analysis, which prove that the cytotoxicity effect of NSs on host cells was negligible. These results altogether indicate that the IB formed by NSs is critical for its regulatory role in virus-like RNA synthesis and virus replication.

Severe fever with thrombocytopenia syndrome virus NSs can form IBs by its own self in both virus-infected cells and NSs-expression plasmid-transfected cells (Wu et al., 2014; Moriyama et al., 2018). Previous studies have speculated on the possible mechanism underlying the viral immune evasion strategy adopted by SFTSV NSs that NSs can sequester critical signaling molecules from the mitochondrial antiviral platform through spatial isolation (Qu et al., 2012; Ning et al., 2014; Santiago et al., 2014). A clue that SFTSV NSs may be involved in virus-like and viral RNA synthesis has been provided by other researchers, though their results suggested that NSs seem to have exerted an opposite regulating effect on virus-like and viral RNA synthesis (Wu et al., 2014; Brennan et al., 2015). However, the details of SFTSV NSs regulating virus-like or viral RNA synthesis are not well elucidated yet. Here, we provide details that SFTSV NSs suppresses virus-like RNA synthesis through blocking the interaction between N and naked virus-like RNA by utilizing pol I-driven minigenome reporter systems and superinfection assays and thereby proposed a possible mechanism. As shown in **Figure 8A**, following the expression of viral RdRp, N, and naked minigenomes within the minigenome system, encapsidation will occur to reconstitute a viable RNP complex that can serve as a template for further transcription and replication. After the encapsidation of virus-like vRNA by N, the coated N can recruit RdRp to form functional vRNP, which can be transcribed into virus-like cRNA and mRNA. The mRNA can then be translated into reporter protein, which can be used to quantify the RNA synthesis level. Additionally, the N-coated virus-like cRNA can recruit RdRp to form functional cRNP, which can be transcribed into progeny virus-like vRNA. However, like the NSs of BUNV and LACV, our results showed that SFTSV NSs can decrease the virus-like RNA synthesis, resulting in decreased minigenome-encoded reporter activity, which can be presumably explained as the encapsidation of vRNA and cRNA were partially blocked *via* the NSs–N interaction (**Figure 8B**). Meanwhile, NSs exert a negative regulatory effect on SFTSV replication

in both immunodeficient cells and non-immunodeficient cells, supporting that its inhibitory effect on virus-like RNA synthesis is not associated with NSs-mediated viral immune evasion. Interestingly, mutant SFTSV NSs cannot form IB, and it does not affect virus-like or viral RNA synthesis, and a similar effect is also detected in HRTV minigenome (–) systems with the involvement of HRTV NSs (**Figures 6A–C**). These results suggest that the inhibitory effect of SFTSV NSs on virus-like RNA synthesis and virus replication is caused by the NSs–N interaction, which may block the encapsidation of naked virus-like RNA.

Viral genomes of segmented negative RNA viruses are always assembled with many copies of a single nucleoprotein (N) to form highly stable nucleocapsids (Ruigrok et al., 2011; Sun et al., 2018), which is critical for transcription and replication. Similarly, in the case of a viral minigenome system based on plasmids or with a helper virus, encapsidation of naked minigenomes is indispensable for virus-like RNA transcription and replication. Although this step is particular to reverse genetics systems and has no strictly equivalent in the virus life cycle, it is of great significance to reveal the factors affecting the interaction between N and virus-like RNAs, especially when minigenome systems are used as tools to investigate viral genome transcription and replication, virus replication and pathogenesis. We here demonstrate the details that SFTSV NSs inhibit virus-like RNA synthesis through NSs–N interaction and in a dose-dependent manner. However, NSs of SFTSV seem to have little effect on virus replication until large amounts of overexpressed NSs were used, which can be presumably explained as the high-level expression of N by virus that can reverse the effect of NSs on virus replication to some extent. To further evaluate the effect of NSs on viral RNA synthesis or virus replication, it is crucial to rescue NSs deletant SFTSV using reverse genetics technology. It has been reported that a NSs deletant SFTSV was successfully rescued and the recombinant virus replicated more efficiently than wild-type virus in cells that had a defective interferon response (A549-NPro) but not in interferon competent cells (A549); meanwhile, their results also suggested that the NSs were not necessary for virus rescue or virus replication, even in cells with a functional IFN response (Brennan et al., 2017). These results consist of what we obtained by using minigenome reporter systems, revealing that the overexpressed NSs show a weak inhibitory effect on virus replication.

In conclusion, we have demonstrated that SFTSV NSs are involved in and inhibit virus-like RNA synthesis by using minigenome systems based on transfection or superinfection *via* a NSs–N interaction. In contrast, for virus replication or viral RNA synthesis, the effect is weak. Based on these results, we hypothesize that the NSs–N interaction partially blocked the encapsidation of naked virus-like RNA or viral RNA, resulting in decreased transcription and replication of minigenomes or the viral genome. The majority of bunyaviruses can encode NSs; although NSs in different bunyaviruses possess different amino acid sequences, the characterization of their common biological functions is important to better understand the life cycle of bunyavirus and to develop effective antiviral drugs and vaccines (Ly and Ikegami, 2016). With this in mind, further studies to

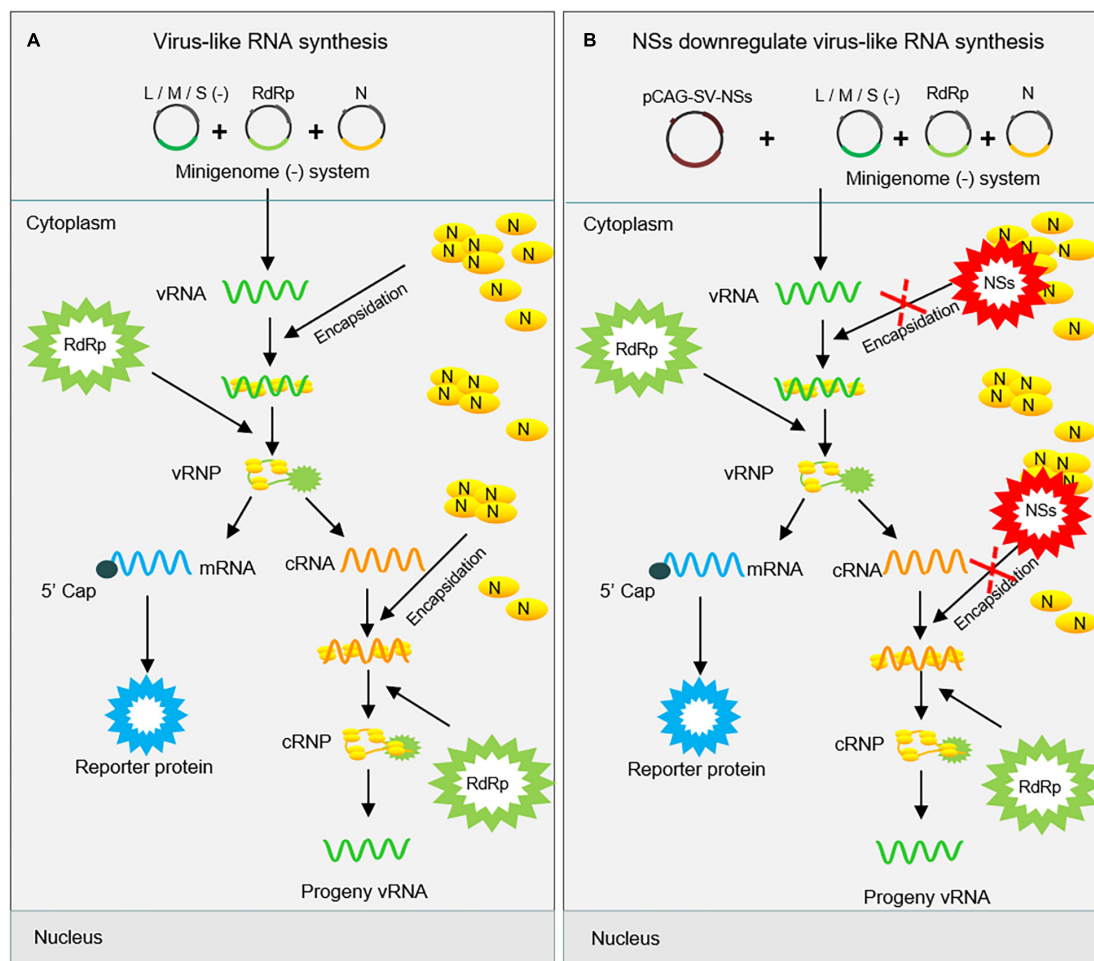


FIGURE 8 | Proposed mechanism for the downregulation of virus-like RNA synthesis by SFTSV NSs within the minigenome reporter system. SFTSV NSs inhibit virus-like RNA synthesis by blocking the N-RNA interaction through sequestering N into inclusion bodies within minigenome reporter systems. As shown in **(A)**, initial genome virus-like RNA (vRNA) is generated by pol I transcription using cDNA as templates. After encapsidation by N, the coated nascent vRNA can assemble with RdRp to form vRNP. Then, mRNA and progeny cRNA and vRNA are generated by transcription and replication, respectively. However, overexpressed NSs block the encapsidation of viral RNAs by competing with nascent RNA to interact with N **(B)**. This, downregulates the synthesis of viral RNA, thus leading to decreased levels of the reporter protein.

reveal novel biological functions of NSs in emerging bunyaviruses are needed. For example, the roles in viral RNA synthesis for the NSs of other pathogenic bunyaviruses (Guertu virus and Bhanja virus, for instance), remain to be studied.

and JS performed the experiments and analyzed the data. HW, Y-JN, and QW helped with experimentation, data processing, and data analysis. FR and SS wrote the original manuscript. All authors contributed to the article and approved the submitted version.

DATA AVAILABILITY STATEMENT

The original contributions presented in the study are included in the article/ **Supplementary Material**, further inquiries can be directed to the corresponding authors.

AUTHOR CONTRIBUTIONS

FD, D-YZ, CH, and FR conceived and designed the study, analyzed the data, and wrote the manuscript. FR, SD, MZ,

FUNDING

This work was funded by the National Major Scientific and Technological Special Project for “Significant New Drugs Development” (Grant Number: 2020ZX09201-001), the National Natural Science Foundation of China (U20A20135), the National Program on Key Research Project of China (2018YFE0200402), and the Innovation Team Project of Hubei Provincial Health Commission (WJ2019C003).

ACKNOWLEDGMENTS

We extend our greatest thanks to Wuhan Institute of Virology and Wuhan Jinyintan Hospital for the Core Facility and technical assistance.

REFERENCES

- Amroun, A., Priet, S., de Lamballerie, X., and Querat, G. (2017). Bunyaviridae RdRps: structure, motifs, and RNA synthesis machinery. *Crit. Rev. Microbiol.* 43, 753–778. doi: 10.1080/1040841X.2017.1307805
- Andzhaparidze, O. G., Bogomolova, N. N., Boriskin, Y. S., Bektemirova, M. S., and Drynov, I. D. (1981). Comparative study of rabies virus persistence in human and hamster cell lines. *J. Virol.* 37, 1–6. doi: 10.1128/JVI.37.1.1-6.1981
- Blakqori, G., Kochs, G., Haller, O., and Weber, F. (2003). Functional L polymerase of la crosse virus allows in vivo reconstitution of recombinant nucleocapsids. *J. Gen. Virol.* 84(Pt 5), 1207–1214. doi: 10.1099/vir.0.18876-0
- Brennan, B., Li, P., Zhang, S., Li, A., Liang, M., Li, D., et al. (2015). Reverse genetics system for severe fever with thrombocytopenia syndrome virus. *J. Virol.* 89, 3026–3037. doi: 10.1128/JVI.03432-14
- Brennan, B., Rezeli, V. V., and Elliott, R. M. (2017). Mapping of transcription termination within the S segment of SFTS phlebovirus facilitated generation of NSs deletant viruses. *J. Virol.* 9:e00743. doi: 10.1128/JVI.00743-17
- Dong, H., Li, P., Elliott, R. M., and Dong, C. (2013). Structure of *Schmallenberg orthobunyavirus* nucleoprotein suggests a novel mechanism of genome encapsidation. *J. Virol.* 87, 5593–5601. doi: 10.1128/JVI.00223-13
- Feng, K., Deng, F., Hu, Z., Wang, H., and Ning, Y. J. (2019). Heartland virus antagonizes type I and III interferon antiviral signaling by inhibiting phosphorylation and nuclear translocation of STAT2 and STAT1. *J. Biol. Chem.* 294, 9503–9517. doi: 10.1074/jbc.RA118.006563
- Flick, R., and Pettersson, R. F. (2001). Reverse genetics system for Uukuniemi virus (Bunyaviridae): RNA polymerase I-catalyzed expression of chimeric viral RNAs. *J. Virol.* 75, 1643–1655. doi: 10.1128/JVI.75.4.1643-1655.2001
- Guu, T. S., Zheng, W., and Tao, Y. J. (2012). Bunyavirus: structure and replication. *Adv. Exp. Med. Biol.* 726, 245–266. doi: 10.1007/978-1-4614-0980-9_11
- Habjan, M., Pichlmair, A., Elliott, R. M., Overby, A. K., Glatzer, T., Gstaiger, M., et al. (2009). NSs protein of rift valley fever virus induces the specific degradation of the double-stranded RNA-dependent protein kinase. *J. Virol.* 83, 4365–4375. doi: 10.1128/JVI.02148-08
- Hoenen, T., Groseth, A., de Kok-Mercado, F., Kuhn, J. H., and Wahl-Jensen, V. (2011). Minigenomes, transcription and replication competent virus-like particles and beyond: reverse genetics systems for filoviruses and other negative stranded hemorrhagic fever viruses. *Antiviral Res.* 91, 195–208. doi: 10.1016/j.antiviral.2011.06.003
- Hornak, K. E., Lanchy, J. M., and Lodmell, J. S. (2016). RNA encapsidation and packaging in the phleboviruses. *Viruses* 8:194. doi: 10.3390/v8070194
- Ikegami, T., Peters, C. J., and Makino, S. (2005). Rift valley fever virus nonstructural protein NSs promotes viral RNA replication and transcription in a minigenome system. *J. Virol.* 79, 5606–5615. doi: 10.1128/JVI.79.9.5606-5615.2005
- Jiao, L., Ouyang, S., Liang, M., Niu, F., Shaw, N., Wu, W., et al. (2013). Structure of severe fever with thrombocytopenia syndrome virus nucleocapsid protein in complex with suramin reveals therapeutic potential. *J. Virol.* 87, 6829–6839. doi: 10.1128/JVI.00672-13
- Kim, Y. R., Yun, Y., Bae, S. G., Park, D., Kim, S., Lee, J. M., et al. (2018). Severe fever with thrombocytopenia syndrome virus infection, South Korea, 2010. *Emerg. Infect. Dis.* 24, 2103–2105. doi: 10.3201/eid2411.170756
- Kolakofsky, D., and Hacker, D. (1991). Bunyavirus RNA synthesis: genome transcription and replication. *Curr. Top. Microbiol. Immunol.* 169, 143–159. doi: 10.1007/978-3-642-76018-1_5
- Kuhn, J. H., Adkins, S., Alioto, D., Alkhovsky, S. V., Amarasinghe, G. K., Anthony, S. J., et al. (2020). 2020 taxonomic update for phylum Negarnaviricota (Riboviria: Orthornavirae), including the large orders *Bunyavirales* and *Mononegavirales*. *Arch. Virol.* 165, 3023–3072. doi: 10.1007/s00705-020-04731-2
- Le May, N., Dubaele, S., Proietti De Santis, L., Billecocq, A., Bouloy, M., and Egly, J. M. (2004). TFIIF transcription factor, a target for the Rift Valley hemorrhagic fever virus. *Cell* 116, 541–550. doi: 10.1016/s0092-8674(04)00132-1
- Lei, X. Y., Liu, M. M., and Yu, X. J. (2015). Severe fever with thrombocytopenia syndrome and its pathogen SFTSV. *Microbes Infect.* 17, 149–154. doi: 10.1016/j.micinf.2014.12.002
- Leonard, V. H., Kohl, A., Hart, T. J., and Elliott, R. M. (2006). Interaction of Bunyamwera Orthobunyavirus NSs protein with mediator protein MED8: a mechanism for inhibiting the interferon response. *J. Virol.* 80, 9667–9675. doi: 10.1128/JVI.00822-06
- Li, B., Wang, Q., Pan, X., Fernandez de Castro, I., Sun, Y., Guo, Y., et al. (2013). Bunyamwera virus possesses a distinct nucleocapsid protein to facilitate genome encapsidation. *Proc. Natl. Acad. Sci. U.S.A.* 110, 9048–9053. doi: 10.1073/pnas.1222552110
- Li, S., Li, Y., Wang, Q., Yu, X., Liu, M., Xie, H., et al. (2018). Multiple organ involvement in severe fever with thrombocytopenia syndrome: an immunohistochemical finding in a fatal case. *Virol. J.* 15:97. doi: 10.1186/s12985-018-1006-7
- Ly, H. J., and Ikegami, T. (2016). Rift Valley fever virus NSs protein functions and the similarity to other bunyavirus NSs proteins. *Virol. J.* 13:118. doi: 10.1186/s12985-016-0573-8
- Matskevich, A. A., Jung, J. S., Schumann, M., Cascallo, M., and Moelling, K. (2009). Vero cells as a model to study the effects of adenoviral gene delivery vectors on the RNAi system in context of viral infection. *J. Innate Immun.* 1, 389–394. doi: 10.1159/000191408
- McMullan, L. K., Folk, S. M., Kelly, A. J., MacNeil, A., Goldsmith, C. S., Metcalfe, M. G., et al. (2012). A new phlebovirus associated with severe febrile illness in Missouri. *N. Engl. J. Med.* 367, 834–841. doi: 10.1056/NEJMoa1203378
- Min, Y. Q., Shi, C., Yao, T., Feng, K., Mo, Q., Deng, F., et al. (2020). The nonstructural protein of guertu virus disrupts host defenses by blocking antiviral interferon induction and action. *ACS Infect. Dis.* 6, 857–870. doi: 10.1021/acsinfecdis.9b00492
- Mir, M. A., and Panganiban, A. T. (2006). The bunyavirus nucleocapsid protein is an RNA chaperone: possible roles in viral RNA panhandle formation and genome replication. *RNA* 12, 272–282. doi: 10.1261/rna.2101906
- Mo, Q., Xu, Z., Deng, F., Wang, H., and Ning, Y. J. (2020). Host restriction of emerging high-pathogenic bunyaviruses via MOV10 by targeting viral nucleoprotein and blocking ribonucleoprotein assembly. *PLoS Pathog.* 16:e1009129. doi: 10.1371/journal.ppat.1009129
- Moriyama, M., Igarashi, M., Koshiba, T., Irie, T., Takada, A., and Ichinohe, T. (2018). Two conserved amino acids within the NSs of severe fever with thrombocytopenia syndrome phlebovirus are essential for anti-interferon activity. *J. Virol.* 92:e00706. doi: 10.1128/JVI.00706-18
- Ning, Y. J., Feng, K., Min, Y. Q., Cao, W. C., Wang, M., Deng, F., et al. (2015). Disruption of type I interferon signaling by the nonstructural protein of severe fever with thrombocytopenia syndrome virus via the hijacking of STAT2 and STAT1 into inclusion bodies. *J. Virol.* 89, 4227–4236. doi: 10.1128/JVI.00154-15
- Ning, Y. J., Feng, K., Min, Y. Q., Deng, F., Hu, Z., and Wang, H. (2017). Heartland virus NSs protein disrupts host defenses by blocking the TBK1 kinase-IRF3 transcription factor interaction and signaling required for interferon induction. *J. Biol. Chem.* 292, 16722–16733. doi: 10.1074/jbc.M117.805127
- Ning, Y. J., Mo, Q., Feng, K., Min, Y. Q., Li, M., Hou, D., et al. (2019). Interferon-gamma-directed inhibition of a novel high-pathogenic phlebovirus and viral antagonism of the antiviral signaling by targeting STAT1. *Front. Immunol.* 10:1182. doi: 10.3389/fimmu.2019.01182
- Ning, Y. J., Wang, M., Deng, M., Shen, S., Liu, W., Cao, W. C., et al. (2014). Viral suppression of innate immunity via spatial isolation of TBK1/IKKε from mitochondrial antiviral platform. *J. Mol. Cell Biol.* 6, 324–337. doi: 10.1093/jmcb/mju015

SUPPLEMENTARY MATERIAL

The Supplementary Material for this article can be found online at: <https://www.frontiersin.org/articles/10.3389/fmicb.2021.709517/full#supplementary-material>

- Park, S. J., Kim, Y. I., Park, A., Kwon, H. I., Kim, E. H., Si, Y. J., et al. (2019). Ferret animal model of severe fever with thrombocytopenia syndrome phlebovirus for human lethal infection and pathogenesis. *Nat. Microbiol.* 4, 438–446. doi: 10.1038/s41564-018-0317-1
- Qu, B., Qi, X., Wu, X., Liang, M., Li, C., Cardona, C. J., et al. (2012). Suppression of the interferon and NF-kappaB responses by severe fever with thrombocytopenia syndrome virus. *J. Virol.* 86, 8388–8401. doi: 10.1128/JVI.00612-12
- Reguera, J., Cusack, S., and Kolakofsky, D. (2014). Segmented negative strand RNA virus nucleoprotein structure. *Curr. Opin. Virol.* 5, 7–15. doi: 10.1016/j.coviro.2014.01.003
- Reguera, J., Gerlach, P., and Cusack, S. (2016). Towards a structural understanding of RNA synthesis by negative strand RNA viral polymerases. *Curr. Opin. Struct. Biol.* 36, 75–84. doi: 10.1016/j.sbi.2016.01.002
- Reguera, J., Malet, H., Weber, F., and Cusack, S. (2013). Structural basis for encapsidation of genomic RNA by La crosse orthobunyavirus nucleoprotein. *Proc. Natl. Acad. Sci. U.S.A.* 110, 7246–7251. doi: 10.1073/pnas.1302298110
- Ren, F., Zhou, M., Deng, F., Wang, H., and Ning, Y. J. (2020). Combinatorial minigenome systems for emerging banyangviruses reveal viral reassortment potential and importance of a protruding nucleotide in genome “panhandle” for promoter activity and reassortment. *Front. Microbiol.* 11:599. doi: 10.3389/fmicb.2020.00599
- Ruigrok, R. W., Crepin, T., and Kolakofsky, D. (2011). Nucleoproteins and nucleocapsids of negative-strand RNA viruses. *Curr. Opin. Microbiol.* 14, 504–510. doi: 10.1016/j.mib.2011.07.011
- Santiago, F. W., Covaleta, L. M., Sanchez-Aparicio, M. T., Silvas, J. A., Diaz-Vizarreta, A. C., Patel, J. R., et al. (2014). Hijacking of RIG-I signaling proteins into virus-induced cytoplasmic structures correlates with the inhibition of type I interferon responses. *J. Virol.* 88, 4572–4585. doi: 10.1128/Jvi.03021-13
- Shen, S., Duan, X., Wang, B., Zhu, L., Zhang, Y., Zhang, J., et al. (2018). A novel tick-borne phlebovirus, closely related to severe fever with thrombocytopenia syndrome virus and Heartland virus, is a potential pathogen. *Emerg. Microbes Infect.* 7:95. doi: 10.1038/s41426-018-0093-2
- Song, P., Zheng, N., Liu, Y., Tian, C., Wu, X., Ma, X., et al. (2018). Deficient humoral responses and disrupted B-cell immunity are associated with fatal SFTSV infection. *Nat. Commun.* 9:3328. doi: 10.1038/s41467-018-05746-9
- Staples, J. E., Pastula, D. M., Panella, A. J., Rabe, I. B., Kosoy, O. L., Walker, W. L., et al. (2020). Investigation of heartland virus disease throughout the United States, 2013–2017. *Open Forum Infect. Dis.* 7:ofaa125. doi: 10.1093/ofid/ofaa125
- Sun, Y., Li, J., Gao, G. F., Tien, P., and Liu, W. (2018). Bunyavirales ribonucleoproteins: the viral replication and transcription machinery. *Crit. Rev. Microbiol.* 44, 522–540. doi: 10.1080/1040841X.2018.1446901
- Takahashi, T., Maeda, K., Suzuki, T., Ishido, A., Shigeoka, T., Tominaga, T., et al. (2014). The first identification and retrospective study of severe fever with thrombocytopenia syndrome in Japan. *J. Infect. Dis.* 209, 816–827. doi: 10.1093/infdis/jit603
- Te Velthuis, A. J. W., and Fodor, E. (2016). Influenza virus RNA polymerase: insights into the mechanisms of viral RNA synthesis. *Nat. Rev. Microbiol.* 14, 479–493. doi: 10.1038/nrmicro.2016.87
- Tran, X. C., Yun, Y., Van An, L., Kim, S. H., Thao, N. T. P., Man, P. K. C., et al. (2019). Endemic severe fever with thrombocytopenia syndrome. *Vietnam. Emerg. Infect. Dis.* 25, 1029–1031. doi: 10.3201/eid2505.181463
- Weber, F., Dunn, E. F., Bridgen, A., and Elliott, R. M. (2001). The *Bunyamwera* virus nonstructural protein NSs inhibits viral RNA synthesis in a minireplicon system. *Virology* 281, 67–74. doi: 10.1006/viro.2000.0774
- Wichgers Schreur, P. J., Kormelink, R., and Kortekaas, J. (2018). Genome packaging of the *Bunyavirales*. *Curr. Opin. Virol.* 33, 151–155. doi: 10.1016/j.coviro.2018.08.011
- Wu, X., Qi, X., Liang, M., Li, C., Cardona, C. J., Li, D., et al. (2014). Roles of viroplasm-like structures formed by nonstructural protein NSs in infection with severe fever with thrombocytopenia syndrome virus. *FASEB J.* 28, 2504–2516. doi: 10.1096/fj.13-243857
- Yu, X. J., Liang, M. F., Zhang, S. Y., Liu, Y., Li, J. D., Sun, Y. L., et al. (2011). Fever with thrombocytopenia associated with a novel bunyavirus in China. *N. Engl. J. Med.* 364, 1523–1532. doi: 10.1056/NEJMoa1010095
- Zheng, W., and Tao, Y. J. (2013). Genome encapsidation by orthobunyavirus nucleoproteins. *Proc. Natl. Acad. Sci. U.S.A.* 110, 8769–8770. doi: 10.1073/pnas.1306838110

Conflict of Interest: The authors declare that the research was conducted in the absence of any commercial or financial relationships that could be construed as a potential conflict of interest.

Publisher's Note: All claims expressed in this article are solely those of the authors and do not necessarily represent those of their affiliated organizations, or those of the publisher, the editors and the reviewers. Any product that may be evaluated in this article, or claim that may be made by its manufacturer, is not guaranteed or endorsed by the publisher.

Copyright © 2021 Ren, Shen, Ning, Wang, Dai, Shi, Zhou, Wang, Huang, Zhang and Deng. This is an open-access article distributed under the terms of the Creative Commons Attribution License (CC BY). The use, distribution or reproduction in other forums is permitted, provided the original author(s) and the copyright owner(s) are credited and that the original publication in this journal is cited, in accordance with accepted academic practice. No use, distribution or reproduction is permitted which does not comply with these terms.



The Antiviral Effect of Novel Steroidal Derivatives on Flaviviruses

Luping Zhang^{1,2,3†}, Dengyuan Zhou^{1,2,3†}, Qiuyan Li^{1,2,3}, Shuo Zhu^{1,2,3},
Muhammad Imran^{1,2,3}, Hongyu Duan^{1,2,3}, Shengbo Cao^{1,2,3}, Shaoyong Ke^{4*} and
Jing Ye^{1,2,3*}

¹ State Key Laboratory of Agricultural Microbiology, Huazhong Agricultural University, Wuhan, China, ² Laboratory of Animal Virology, College of Veterinary Medicine, Huazhong Agricultural University, Wuhan, China, ³ The Cooperative Innovation Center for Sustainable Pig Production, Huazhong Agricultural University, Wuhan, China, ⁴ National Biopesticide Engineering Research Center, Hubei Biopesticide Engineering Research Center, Hubei Academy of Agricultural Sciences, Wuhan, China

OPEN ACCESS

Edited by:

Ali Zohaib,
Islamia University, Pakistan

Reviewed by:

Manjula Kalia,
Regional Centre for Biotechnology
(RCB), India
Bibo Zhu,
Mayo Clinic, United States

*Correspondence:

Shaoyong Ke
shaoyong.ke@nberc.com
Jing Ye
yej@mail.hzau.edu.cn

[†]These authors have contributed
equally to this work

Specialty section:

This article was submitted to
Virology,
a section of the journal
Frontiers in Microbiology

Received: 18 June 2021

Accepted: 09 September 2021

Published: 06 October 2021

Citation:

Zhang L, Zhou D, Li Q, Zhu S,
Imran M, Duan H, Cao S, Ke S and
Ye J (2021) The Antiviral Effect
of Novel Steroidal Derivatives on
Flaviviruses.
Front. Microbiol. 12:727236.
doi: 10.3389/fmicb.2021.727236

Flaviviruses are the major emerging arthropod-borne pathogens globally. However, there is still no practical anti-flavivirus approach. Therefore, existing and emerging flaviviruses desperately need active broad-spectrum drugs. In the present study, the antiviral effect of steroidal dehydroepiandrosterone (DHEA) and 23 synthetic derivatives against flaviviruses such as Japanese encephalitis virus (JEV), Zika virus (ZIKV), and Dengue virus (DENV) were appraised by examining the characteristics of virus infection both *in vitro* and *in vivo*. Our results revealed that AV1003, AV1004 and AV1017 were the most potent inhibitors of flavivirus propagation in cells. They mainly suppress the viral infection in the post-invasion stage in a dose-dependent manner. Furthermore, orally administered compound AV1004 protected mice from lethal JEV infection by increasing the survival rate and reducing the viral load in the brain of infected mice. These results indicate that the compound AV1004 might be a potential therapeutic drug against JEV infection. These DHEA derivatives may provide lead scaffolds for further design and synthesis of potential anti-flavivirus potential drugs.

Keywords: antiviral activity, flavivirus, steroids, DHEA derivatives, therapy

INTRODUCTION

Flaviviruses belonging to the family *Flaviviridae* are a group of more than 70 enveloped RNA viruses. They cause severe diseases in humans and animals. Most of them are arthropod-borne viruses (arboviruses) transmitted to humans or other vertebrate hosts by insect vectors (Gubler, 2007; Fernandez-Garcia et al., 2009). The Flavivirus genus including Japanese encephalitis virus (JEV), Zika virus (ZIKV), Dengue virus (DENV), West Nile virus (WNV), tick-borne encephalitis virus (TBEV) and yellow fever virus (YFV) (Mukhopadhyay et al., 2005). Some flaviviruses can cause encephalitis and other neurological manifestations, including WNV and JEV, while some tend to cause vascular leakage and hemorrhagic disease, including DENV and YFV (King et al., 2012; Barrows et al., 2018). Moreover, ZIKV has also been proved to be related to the development of Guillain-Barré syndrome in adults and severe fetal microcephaly (Culshaw et al., 2018).

Flavivirus infection is a global threat and is an endemic or epidemic in almost every tropical country. Flavivirus outbreaks still occur even the morbidity and mortality declined by using various vaccines, highlighting challenges in executing effective ways to control the epidemic (Campbell et al., 2011). To date, no specific commercial drugs against flaviviruses are available, so there is an urgent unmet need for new agents that can be used for prophylactic or therapeutic intervention in combating flavivirus infections. Recently, relevant kinds of literature have reported several compounds which have anti-flavivirus activities, such as ivermectin (Kok, 2016), manidipine (Wang et al., 2017), and chlorpromazine (Nawa et al., 2003). These studies underscore the value of developing novel uses for existing drugs, in addition to the discovery of new inhibitors against diseases caused by flavivirus infections.

Dehydroepiandrosterone (3β -hydroxyandrost-5-en-17-one, DHEA), a precursor of sex steroids, is one of the most plentiful steroids in human blood, a precursor of sex steroids (Hayashi et al., 2000). The peripheral levels of DHEA gradually decline with age (Barrett-Connor et al., 1986). The concentration of DHEA is exceptionally high in the brain tissue, since the neurons and astrocytes can synthesize DHEA (Zwain and Yen, 1999). DHEA has been proved to have chemoprotective effects against a series of diseases: diabetes, obesity, atherosclerosis, and cancer (Regelson et al., 2019). In addition, DHEA related hormones have been proved to exert antiviral effects on JEV, influenza virus, herpes simplex virus (HSV), vesicular stomatitis virus (VSV), human immunodeficiency virus (HIV), and Junin virus (JUNV) (Loria et al., 1988; Mulder et al., 1992; Chang et al., 2005; Acosta et al., 2008; Barrows et al., 2018). Therefore, the assessment of the antiviral activity of DHEA structurally related compounds can be used to pursue the effective treatment of viral infections. Many analogs have experimented with as antiviral agents *in vitro* and *in vivo* (Diallo et al., 2000; Torres et al., 2012).

Based on the highly potential antiviral activity of DHEA derivatives (Acosta et al., 2008; Romanutti et al., 2009; Torres et al., 2012), a series of novel steroidal derivatives were constructed using pharmacophore hybridization, and it was supposed that introduction of dihydrazone active unit would increase the interaction sites of steroidal molecules (Figure 1). Moreover, assess whether the structural changes of DHEA would lead to improving antiviral properties, the antiviral activity of a series of steroidal derivatives based on DHEA scaffold against JEV, ZIKV, and DENV type 2 (DENV-2) infections both *in vitro* and *in vivo* was thoroughly investigated. The identified drugs in this study provide novel potential treatment protocols for flavivirus diseases.

MATERIALS AND METHODS

Cell Cultures and Viruses

African green monkey kidney (Vero), Helen Lane (Hela), baby hamster kidney (BHK-21), and Human neuroblastoma (SHSY-5Y) cells were cultured and maintained in Dulbecco modified Eagle medium (DMEM; Sigma) supplemented with 10% fetal bovine serum (FBS; Gibco), 100 U/ml penicillin, and 100 mg/ml

streptomycin sulfate at 37°C in the 5% CO₂. The JEV P3 strain was stored in our laboratory. China Center for Type Culture Collection (CCTCC) kindly provided the DENV type-2 strain and ZIKV H/PF/2013 strain.

Chemicals and Reagents

All starting materials and reagents were supplied from commercial suppliers and used without further purification unless otherwise specified. All target steroidal molecules were efficiently synthesized in our laboratory according to the procedures described in our previous report (Ke et al., 2013). The physicochemical properties and the structures were elucidated by their corresponding NMR and ESI-MS comparison with the data in the literature. The substituents and structural formulae of target steroidal derivatives are indicated in Table 1. A stock solution was prepared in dimethyl sulfoxide (DMSO) with a concentration of 10 mM for storage and usage.

Screening of Potential Anti-flavivirus Compounds

A series of DHEA derivatives were stored as 10 mM stock solutions in DMSO for storage and usage. Cells were infected with JEV (1 MOI). One hour later, the supernatant was removed, and the 10 μ M DHEA derivatives or DMSO were added to the cells for additional 23 h. The antiviral effects of DHEA derivatives were determined by plaque assay. The compounds showing an inhibition ratio of > 90% were considered as candidates of subsequent experiments. The percentage of viral titer inhibition is the viral titer of the DMSO + JEV group minus the viral titer of the derivatives + JEV group and then divided by the viral titer of the DMSO + JEV group.

Japanese Encephalitis Virus Infection and Drug Administration

Adult 6-week-old C57BL/6 mice were purchased from the Laboratory Animal Center of Huazhong Agricultural University, Wuhan, China. Mice were randomly assigned into 4 groups: control group (DMSO; $n = 10$); only AV1004-treated group (AV1004; $n = 10$); JEV and DMSO-treated group (JEV; $n = 10$); JEV- and AV1004-treated group (JEV + AV1004; $n = 10$). Mice belonging to the JEV + DMSO and JEV + AV1004 groups were intraperitoneally injected with 10^5 PFU of the JEV P3 strain in 100 μ l of DMEM. The compound stock solution was prepared in DMSO with a concentration of 10 mM for usage. The infected mice were given oral compound AV1004 at 35 mg/kg of body weight or DMSO for 23 consecutive days. The experimental animal protocols were approved by The Scientific Ethics Committee of Huazhong Agriculture University (HZAUMO-2021-0003).

Cell Viability Assay

Using the Cell Titer-Glo® One Solution Assay kit (Promega) to detect the viability of cells. The quantification of luminescence signals was calculated based on the reported method (Chen et al., 2018).

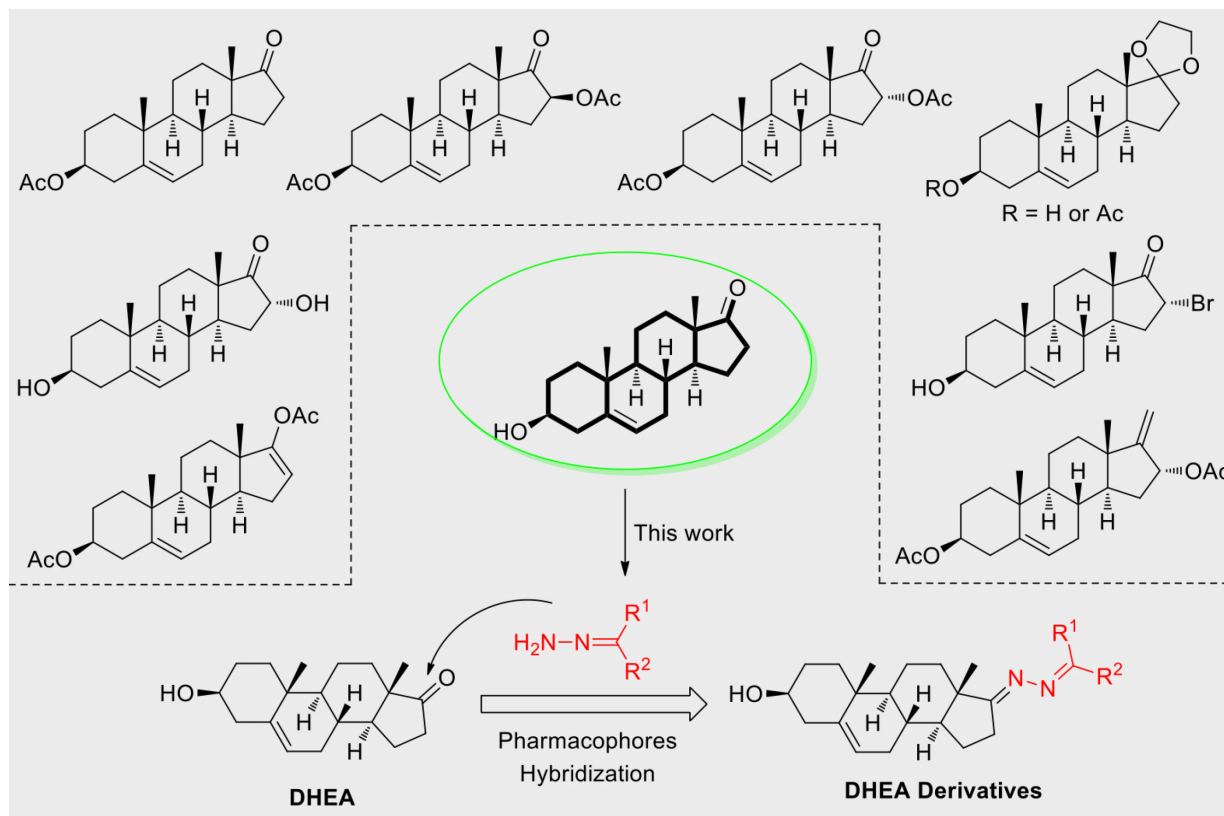


FIGURE 1 | Derivatives design based on DHEA scaffold.

Plaque Assay

Cell supernatants or cell lysates harvested at 12, 24, 36, and 48 h, were serially diluted in DMEM, then inoculated onto monolayers cells at 37°C for 1.5 h. Subsequently, the supernatants were removed, the cells were washed three times with serum-free DMEM and incubated with sodium carboxymethyl cellulose (Sigma) containing medium supplemented with 3% FBS. The cells were fixed with 10% formaldehyde and stained with crystal violet solution on day 4 post-incubation. Count the visible plaques and calculate the virus titer.

Immunofluorescence Assay

Vero cells were infected with JEV and treated with different concentrations of compounds or DMSO. Cells were fixed at multiple time points with 4% formaldehyde for 10 min then washed with PBS. Afterward, cells were blocked with 10% bovine serum albumin (BSA) in PBS for 1 h. Later, cells were incubated with JEV E mAb 4B4 for 3 h. After washing with PBS, cells were stained with a second antibody (Alexa Fluor 488) for 30 min. Cell nuclei were stained with DAPI. The staining results were observed under an fluorescence microscope (Zeiss).

Western Blotting

Cells were harvested and incubated in lysis buffer (Beyotime Biotechnology, Shanghai, China) for 15 min with ice-cold

water, then the supernatants were collected after centrifuging at 12,000 rpm for 10 min at 4°C. Using the BCA protein assay kit (Thermo Fisher Scientific, Waltham, MA, United States) to determine the protein concentration. Proteins were separated by SDS-PAGE and diverted to a nitrocellulose membrane using a Mini Trans-Blot Cell (Bio-Rad Laboratories). The membrane was incubated with the JEV E mAb 4B4 or JEV NS5 mAb 2A5 as requested, and signals were explored using ECL reagents (Thermo Fisher Scientific).

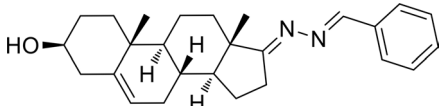
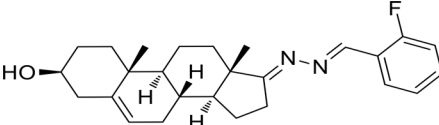
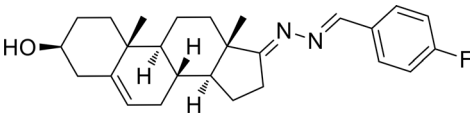
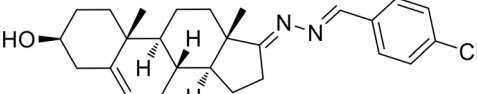
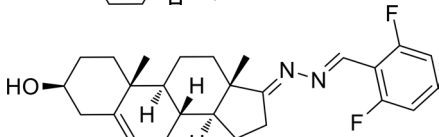
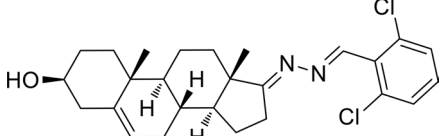
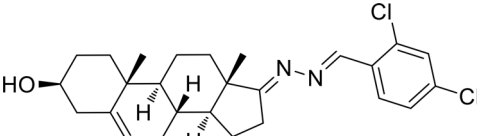
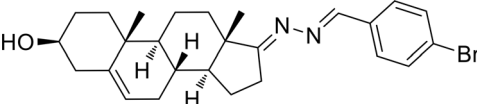
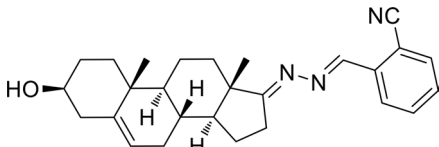
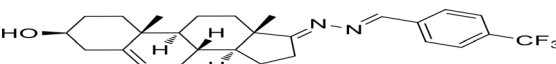
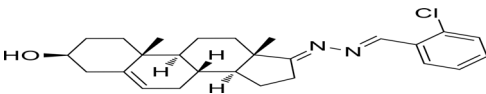
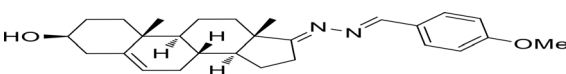
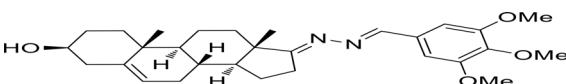
RNA Extraction and Quantitative Real-Time PCR

Total cellular RNA was obtained using TRIzol Reagent (Invitrogen), and reverse transcription of RNA was performed with the ABscript II cDNA First Strand Synthesis kit (ABclonal). qRT-PCR was performed using SYBR Green First qPCR Mix (ABclonal) and the QuantStudio 6 Flex PCR system (Applied Biosystems). The primers are listed in **Table 2**.

Time-of-Addition Assay

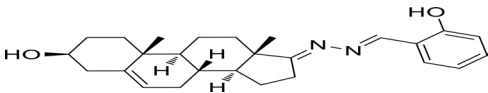
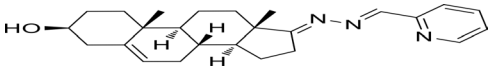
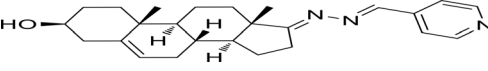
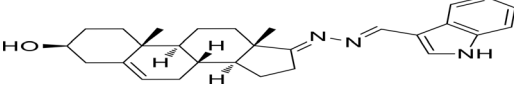
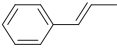
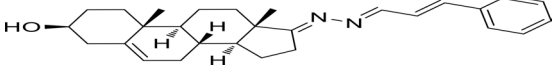
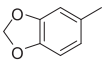
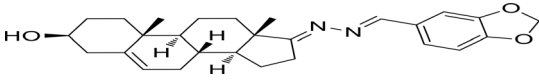
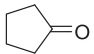
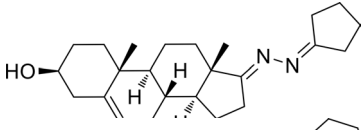
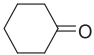
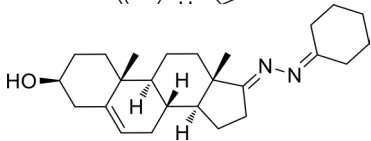
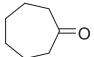
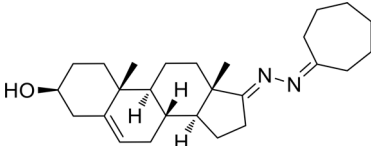
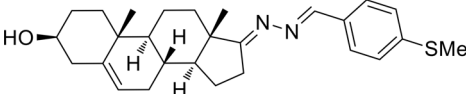
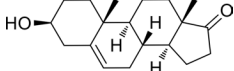
To determine which stage of the JEV life cycle was inhibited by each treatment, BHK-21 cells were treated with JEV (1 MOI) for 1 h (0 to 1 h). The test compounds were incubated with the cells or virus for 1 h pre-infection (−1 to 0 h), co-infection (0 to 1 h), and post-infection (1 to 24 h). At 24 h post-infection, the titer of

TABLE 1 | Synthetic analogs of DHEA.

Sample No.	Compd. No.	R ¹	R ²	Structure
1	HAAS-AV1001	Ph	H	
2	HAAS-AV1002	2-F-Ph	H	
3	HAAS-AV1003	4-F-Ph	H	
4	HAAS-AV1004	4-Cl-Ph	H	
5	HAAS-AV1005	2,6-F ₂ -Ph	H	
6	HAAS-AV1006	2,6-Cl ₂ -Ph	H	
7	HAAS-AV1007	2,4-Cl ₂ -Ph	H	
8	HAAS-AV1008	4-Br-Ph	H	
9	HAAS-AV1009	2-CN-Ph	H	
10	HAAS-AV1010	4-CF ₃ -Ph	H	
11	HAAS-AV1011	2-Cl-Ph	H	
12	HAAS-AV1012	4-MeO-Ph	H	
13	HAAS-AV1013	3,4,5-(MeO) ₃ -Ph	H	

(Continued)

TABLE 1 | (Continued)

Sample No.	Compd. No.	R ¹	R ²	Structure
14	HAAS-AV1014	2-OH-Ph	H	
15	HAAS-AV1015	2-Py	H	
16	HAAS-AV1016	4-Py	H	
17	HAAS-AV1017	Indole-3-yl	H	
18	HAAS-AV1018		H	
19	HAAS-AV1019		H	
20	HAAS-AV1020			
21	HAAS-AV1021			
22	HAAS-AV1022			
23	HAAS-AV1023	4-MeS-Ph	H	
24	HAAS-AV1024	DHEA		

supernatant was determined by plaque assay. The cell lysates were immunoblotted to detect the viral protein expression level.

Hematoxylin and Eosin Staining, Immunohistochemistry Assay

Ketamine-xylazine (0.1 ml per 10 g of body weight) was used to anesthesia the treated mice. Brain tissues were collected then embedded in paraffin for coronal sections. The sections were used for H&E staining and Immunohistochemistry (IHC) assay. For IHC, the antibodies ionized calcium-binding adapter molecule 1 (IBA-1) (Wako) and glial fibrillary acidic protein (GFAP) have been used in our previous studies (Chen et al., 2018). Using

ImagePro Plus software to analyze the number of positive cells for each antibody to obtain the comprehensive option density index.

Japanese Encephalitis Virus Replicon Assay

To ensure the compound's effectiveness in JEV replication, the JEV replicon cDNA clone in which the structural genes were replaced with the Renilla luciferase (Rluc) gene was employed to quantitatively evaluate the inhibitory effects (Li et al., 2014). *In vitro* transcripts were synthesized from linearized JEV replicon using a T7 mMessage mMachine kit (Invitrogen). Transfection of *in vitro* transcripts into Hela cells. At the indicated times

TABLE 2 | Primers used for qRT-PCR.

Primer Name	Sequence 5'-3'
m(β-actin-F	CACTGCCGCATCCTCTTCTCTCCC
m(β-actin-R	CAATAGTGATGACCTGGCCGT
mIL-1(β-F	AACCTGCTGGTGTGTGACGTTT
mIL-1(β-R	CAGCACGAGGCTTTTTTGTGT
mIL-6-F	AATGAGGAGACTTGCTGCTGGT
mIL-6-R	GCAGGAACCTGGATCAGGACT
mCCL-2-F	CGGCGAGATCAGAACCTACAAC
mCCL-2-R	GGCACTGTCACACTGGTCACTC
mCCL-5-F	TGCCACGTCGAAGGAGTATTTT
mCCL-5-R	AACCCACTTCTTCTCTGGGTTG
hβ-actin-F	AGCGGGAATCGTGCGTGAC
hβ-actin-R	GGAAGGAAGGCTGGAAGAGTG
JEV-F	GGCTCTTATCACGTTCTTCAAGTTT
JEV-R	TGCTTTCCATCGGCCCYAAAA
ZIKV-F	TAAACGGGGTTGTGACGGCTC
ZIKV-R	ACCTGACGAGTGCTTCTTTG
DENV-F	CTGAACGCGAGAGAAACCG
DENV-R	GTATCCCTGCTGTTGGTGGG

h, human; m, mouse; F, Forward; R, Reverse.

post-transfection, using the Rluc assay system (Promega) to measure the luciferase activity.

Statistical Analysis

All experiments were performed at least three times under similar conditions. Analyses were conducted using GraphPad Prism Software (version 8). Results were expressed as the mean ± standard error of the mean (SEM). Statistical differences were determined using the two-way analysis of variance (ANOVA) with subsequent Student’s test, or the Student *t*-test, or the Log-rank (Mantel-Cox) test. *P* < 0.05.

RESULTS

Screening of Potential Anti-flavivirus Compounds From Dehydroepiandrosterone and Its Derivatives

The antiviral abilities of DHEA and its derivatives against JEV were examined by inhibition of virus-induced cytopathogenicity effects (CPEs) in BHK-21. Among the 23 molecules, we found that 10 derivatives inhibited JEV infection by more than 90%. However, the inhibition rate of DHEA (AV1024) on JEV replication was only 50%. This result was consistent with that reported in the previous article (Chang et al., 2005). And the three compounds, AV1003, AV1004, and AV1017, showed the strongest antiviral effects were selected for the following experiments (Figure 2A). The luminescence-based viability assay was used to evaluate the cytotoxic effects of the three derivatives in Vero cells. The 50% cytotoxic concentration (CC₅₀) of derivatives, were identified as 383.1 μM (AV1003), 51.64 μM (AV1004) and 51.30 μM (AV1017), respectively (Figure 2B).

The highest non-toxic concentration of AV1003, AV1004, and AV1017 (20 μM) was used for subsequent experiments.

Dehydroepiandrosterone Derivatives Inhibit the Propagation of Japanese Encephalitis Virus *in vitro*

To verify the antiviral effect of AV1003, AV1004, and AV1017 against JEV, several *in vitro* experiments were carried out. The antiviral activity of AV1003, AV1004, and AV1017 against the flaviviruses was examined by plaque assay. The JEV infected Vero cells were immediately incubated in media containing different non-cytotoxic concentrations of DHEA derivatives. Virus yield was quantified at 24 h.p.i and compared to untreated virus-infected cultures. Virus multiplication was observed with a dose-dependent inhibition in all three derivatives-treated cultures by plaque assay and Western blot (Figures 3A,B). The 50% inhibitory concentration (IC₅₀) of AV1003, AV1004, and AV1017 were determined to be 2.537, 2.537, and 1.458 μM against JEV, respectively (Figure 3A). The levels of viral proteins have been quantified and normalized to GAPDH by using Image J software (Figure 3B), which showed that the higher the derivative concentration, the lower the viral protein expression. The CC₅₀ and IC₅₀ values were used to derive the selectivity index (SI) value for each compound (Table 3). At the highest non-cytotoxic concentration, the compound’s inhibitory effect on different MOIs of virus and time points was determined. It was found that the three compounds still have strong antiviral activity even at a higher MOI of 10 (Figure 3C). As showed by plaque assay, the production of infectious viral particles in the compounds treated infected cells reduced more than 2-log at 24, 36, and 48 h post-infection (Figure 3D). Based on immunofluorescence analysis, the JEV-E protein expression was significant inhibited by the three compounds (Figure 3E). These results indicate that these compounds have a strong anti-JEV effect.

The Antiviral Effects of Dehydroepiandrosterone Derivatives Is Cell Type-Independent

To investigate whether the compound-induced anti-JEV effect is influenced by cell type, the effect of highest non-toxic concentration of compounds on JEV replication in Hela, BHK-21 and SHSY-5Y cells was examined (Figure 4). We examined the cytotoxicity of hits by luminescence-based cell viability assay. Among the three derivatives, compound AV1017 containing an indole unit showed the potent cytotoxicity for cell lines, so we detected the antiviral effect of 5 μM compounds on Hela cells and 10 μM compounds on SHSY-5Y cells. The results of different concentrations of each compound on the production of infectious progeny were assessed. At 24 h.p.i., supernatants of infected cell cultures were harvested and titrated by plaque assays. The dose-dependent inhibitory effect of AV1003, AV1004, and AV1017 was recapitulated in JEV-infected Hela, BHK-21 and SHSY-5Y cells (Figure 4B), albeit at a decreased potency relative to drug treatment on JEV-infected Vero cells.

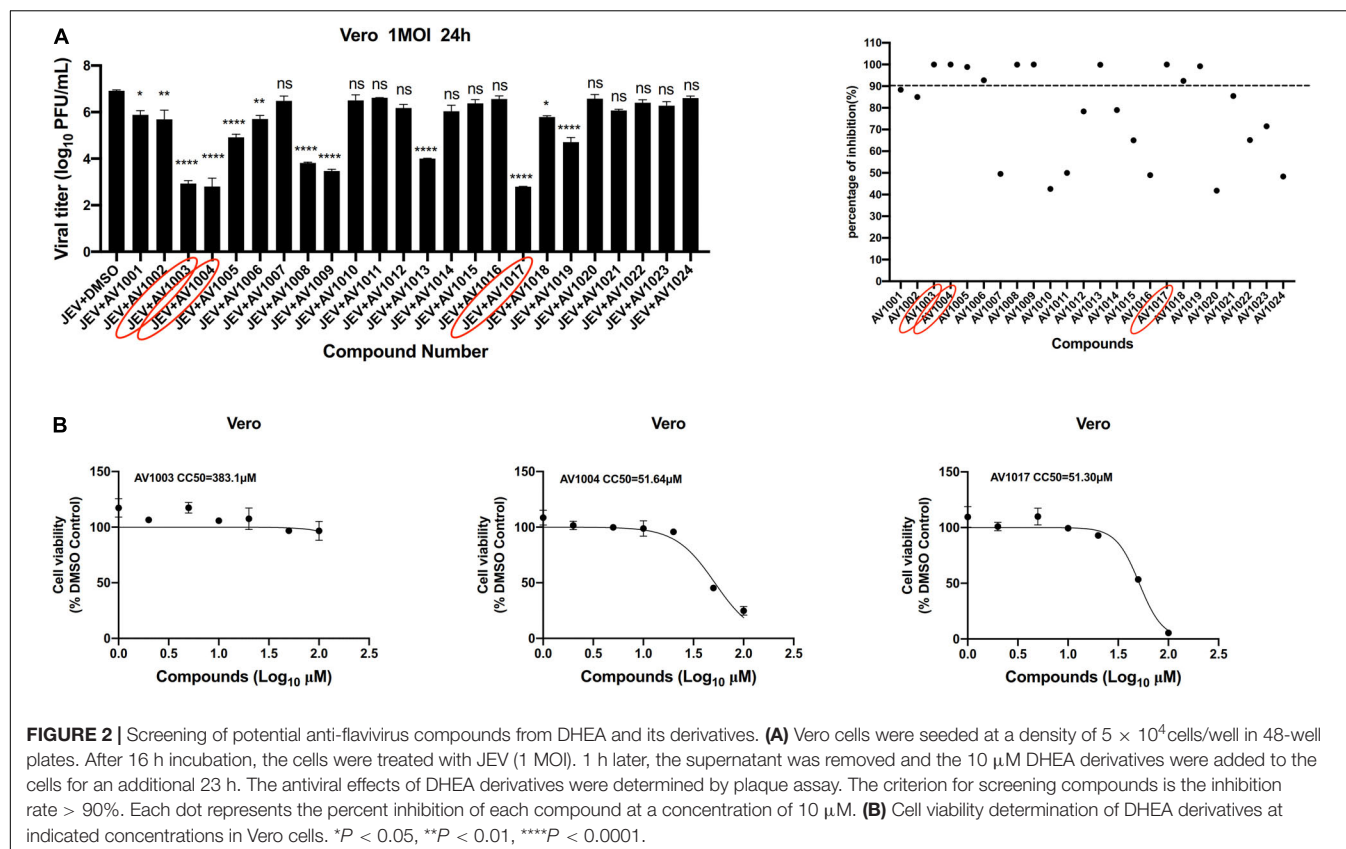


FIGURE 2 | Screening of potential anti-flavivirus compounds from DHEA and its derivatives. **(A)** Vero cells were seeded at a density of 5×10^4 cells/well in 48-well plates. After 16 h incubation, the cells were treated with JEV (1 MOI). 1 h later, the supernatant was removed and the 10 μ M DHEA derivatives were added to the cells for an additional 23 h. The antiviral effects of DHEA derivatives were determined by plaque assay. The criterion for screening compounds is the inhibition rate > 90%. Each dot represents the percent inhibition of each compound at a concentration of 10 μ M. **(B)** Cell viability determination of DHEA derivatives at indicated concentrations in Vero cells. * $P < 0.05$, ** $P < 0.01$, **** $P < 0.0001$.

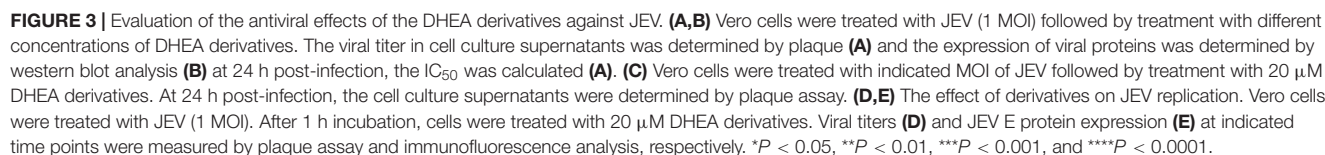
Dehydroepiandrosterone Derivatives Inhibit the Replication of Zika Virus and Dengue Virus *in vitro*

The antiviral ability of compounds against other flaviviruses such as DENV and ZIKV was investigated. Similar to JEV, DHEA derivatives significantly inhibit the replication of ZIKV (Figures 5A–C) and DENV (Figures 5D–F) in Vero cells at different time points. A drug-dose-dependent manner was proved by plaque and qRT-PCR assay. Among the three DHEA derivatives, AV1017 and AV1004 showed the most potent antiviral effect on ZIKV and DENV, respectively (Figures 5A,D). Subsequently, the antiviral efficacy of compounds against ZIKV (1 MOI) and DENV (1 MOI) in Vero cells was measured at multiple time points. According to Figure 5B, the derivatives exert an antiviral effect against ZIKV infection after 12 h. AV1004 and AV1017 have more substantial inhibitory effects on ZIKV. In Figure 5E, when DENV infected cells for 12 h, no virus particles were detected in the compound treatment groups, and the virus titer gradually increased over time. The results indicated that the replication of ZIKV and DENV was inhibited by compounds at indicated time points. The derivatives have a more substantial inhibitory effect on the early stage of DENV infection (Figures 5B,C,E,F). In addition, the infectivity of ZIKV and DENV on Vero cells were different, which may also be considered as a possible reason for affecting the early steps of DENV and ZIKV life cycle differentially. These data indicated that compounds exert broad-spectrum anti-flavivirus activity.

Dehydroepiandrosterone Derivatives Inhibit Flavivirus Multiplication After Viral Entry and Before Genomic Replication

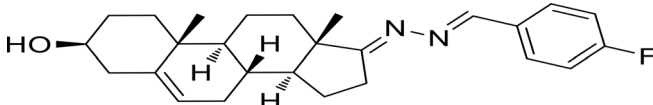
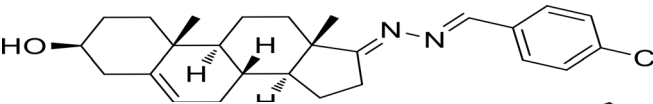
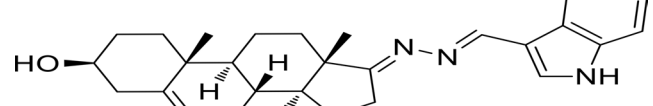
To delineate at which stage in virus life cycle compounds work, whether compounds impede a pre-infection or post-entry stage was determined. Cultured Vero cells were subjected to a time-of-addition assay: pre-infection, co-infection and post-infection (Figure 6A). The levels of viral proteins quantification have been done by using Image J software (Figure 6C), which showed that treatment of compounds post-infection reduced the viral particles production and viral protein expression to the most significant degree than treatment of compounds pre-infection and co-infection. Nonetheless, according to the plaques and western blot results, these effects were found less significant upon pre-infection and co-infection of compounds with the virus (Figures 6B,C). These results indicated that the derivatives mainly exert an inhibitory effect after viral infection.

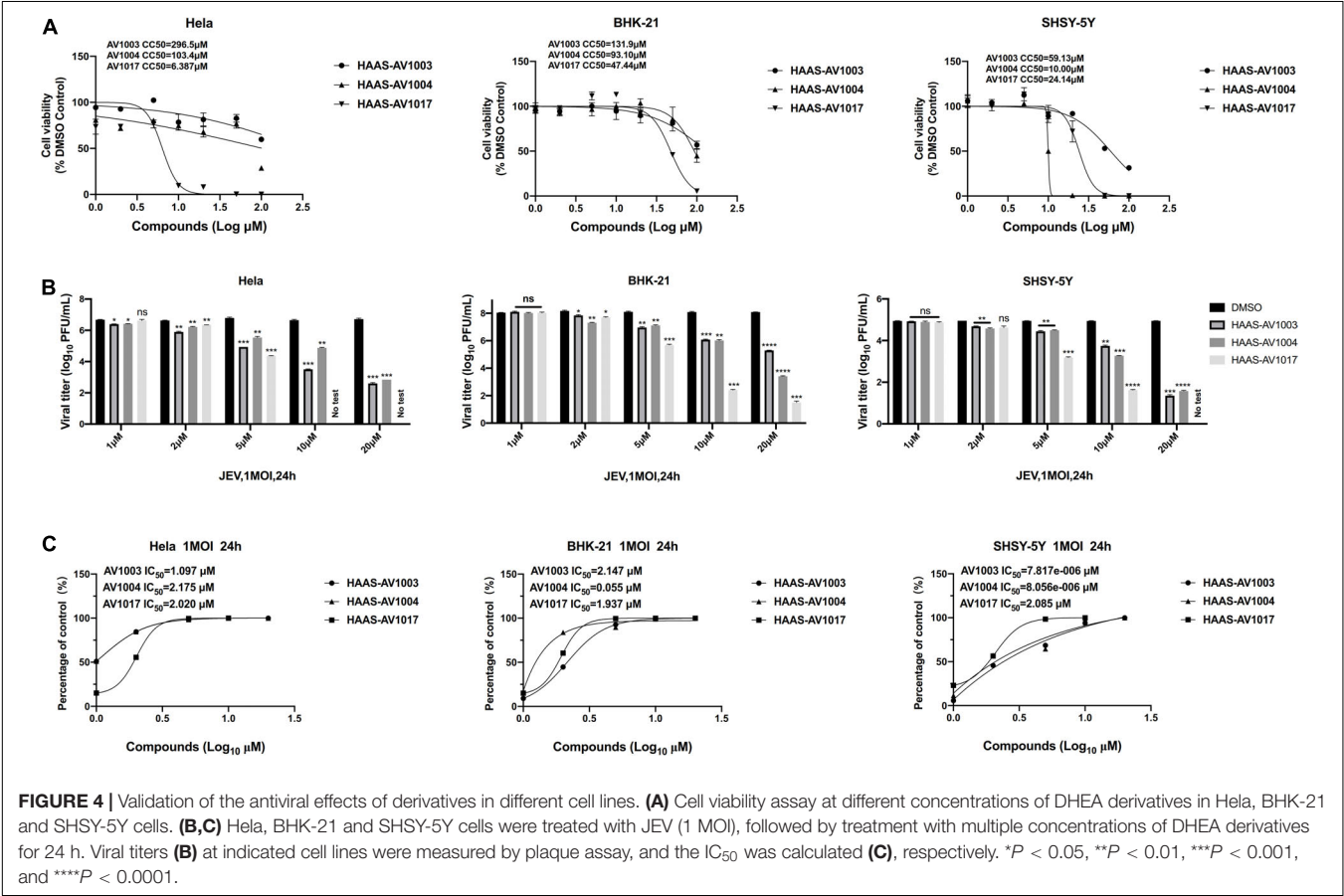
The effect of compounds on cellular adsorption and entry phases of the virus life cycle was verified. To detect the effect of compounds on the attachment step, after 1 h incubation with JEV (5 MOI) + DMSO or JEV (5 MOI) + AV1003, AV1004, and AV1017 at 4°C, the cells were washed with PBS to remove the unattached virus. The amounts of viruses attached to the cell surface were measured by plaque assay. No difference between JEV + AV1003/AV1004 and the JEV + DMSO group was shown. However, the virus titer of the JEV + AV1017 treatment group



plaque assay. Similar to the attachment results, viral titers of JEV + AV1003/AV1004 showed no significant difference, while JEV + AV1017 viral titer was lower than that of JEV + DMSO group viral (**Figure 6E**). These findings suggested that AV1003 and AV1004 do not disrupt the cellular adsorption and entry ability of the virus, but AV1017 affects both adsorption and invasion stages of the virus.

TABLE 3 | CC₅₀, IC₅₀, and SI values of derivatives on Vero cells, derived from data obtained from the cell viability and dose-dependent inhibition assays, respectively.

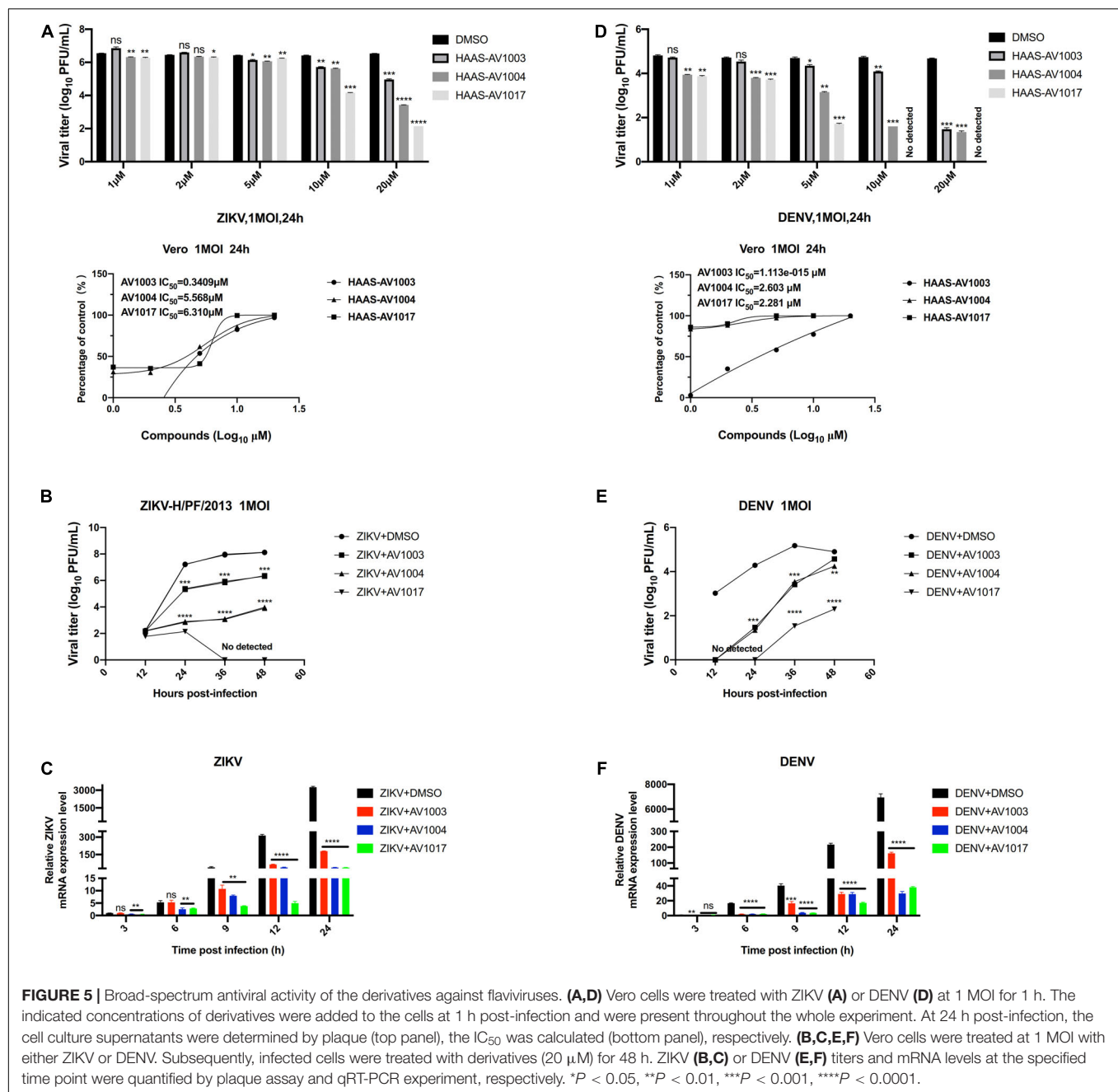
Sample No.	Compd. No.	Structure	IC ₅₀ (μM)	CC ₅₀ (μM)	SI
3	HAAS-AV1003		2.537	383.1	>151
4	HAAS-AV1004		2.537	51.64	>20.35
17	HAAS-AV1017		1.458	51.30	>35.19



To clarify at which stage of the virus infection the derivatives work, JEV-infected cell supernatants from the control (DMSO) and treatment (compounds 20 μM) groups were subjected to plaque assay and RT-qPCR at different time points. The plaque-forming unit (**Figure 7A**) and intracellular mRNA levels (**Figure 7B**) showed significant differences between the control and treatment groups. To determine whether the derivatives could inhibit flavivirus genomic replication, Hela cells were transfected with the JEV replicon followed by treatment with

the derivatives. However, there was no significant change in the luciferase signal and mRNA levels at 24 h post-transfection (**Figure 7C**), suggesting that the derivatives could not inhibit the genomic replication of JEV. These results indicated that the antiviral activity of derivatives against JEV infection occurs after viral entry and before genomic replication.

Cycloheximide (CHX) is a compound that has an inhibitory effect on protein biosynthesis in eukaryotes, and it is a product of *Streptomyces griseus*. It hinders the translation process by



interfering with the translocation step in the protein synthesis process. In biopharmaceutical research, cycloheximide is often used to inhibit protein synthesis in eukaryotic cells *in vitro* (Ramanathan et al., 2020). Afterward, an additional time course assay was performed with JEV and three derivatives in the presence or absence of CHX. Besides, we performed the cycloheximide experiment using the JEV replication system. Vero cells were treated with JEV (Figure 7D left panel) or Hela cells were transfected with the JEV replicon (Figure 7D right panel), and treated with the derivatives or the derivatives + CHX. Upon treatment of CHX, the RNA levels and the luciferase signal of the JEV + AV1003, AV1004, and AV1017 groups were still lower

than that of the DMSO group (Figure 7D). Taken together, these results demonstrated that the three compounds play the antiviral role against JEV infection after virus entry and before genomic translation.

AV1004 Reduce the Lethality of Japanese Encephalitis Virus Infected Mice

Given the best performance of AV1004 on inhibiting JEV, ZIKV and DENV propagation, it was selected to evaluate the therapeutic effect on JEV infected mice. JEV- or mock-infected mice were treated with AV1004 or DMSO at 35 mg/kg

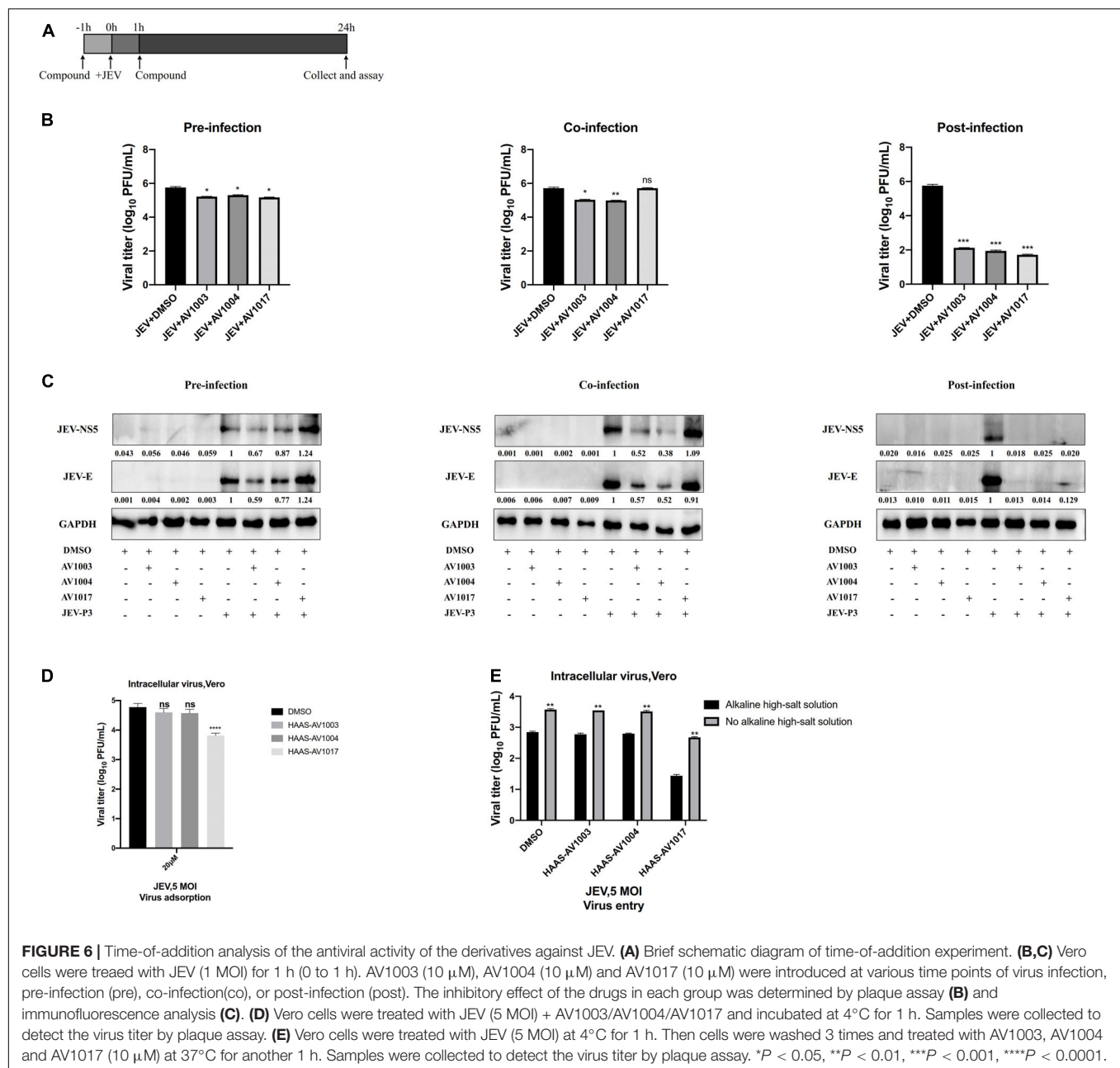


FIGURE 6 | Time-of-addition analysis of the antiviral activity of the derivatives against JEV. **(A)** Brief schematic diagram of time-of-addition experiment. **(B,C)** Vero cells were treated with JEV (1 MOI) for 1 h (0 to 1 h). AV1003 (10 μ M), AV1004 (10 μ M) and AV1017 (10 μ M) were introduced at various time points of virus infection, pre-infection (pre), co-infection (co), or post-infection (post). The inhibitory effect of the drugs in each group was determined by plaque assay **(B)** and immunofluorescence analysis **(C)**. **(D)** Vero cells were treated with JEV (5 MOI) + AV1003/AV1004/AV1017 and incubated at 4°C for 1 h. Samples were collected to detect the virus titer by plaque assay. **(E)** Vero cells were treated with JEV (5 MOI) at 4°C for 1 h. Then cells were washed 3 times and treated with AV1003, AV1004 and AV1017 (10 μ M) at 37°C for another 1 h. Samples were collected to detect the virus titer by plaque assay. * P < 0.05, ** P < 0.01, *** P < 0.001, **** P < 0.0001.

of body weight for 23 consecutive days. The *in vivo* results showed that all mice survived in the AV1004- or DMSO-treated group throughout the entire observation period. JEV-infected mice treated with DMSO or AV1004, mortality displayed on day 6 post-infection. On day 13 post-infection, the mortality rate was 90% in the DMSO-treated mice. In contrast, the survival rate of AV1004 protected mice was 40% throughout the entire 23-day period of observation (Figure 8A). To substantiate the effect of AV1004 on clinical symptoms, we scored the behavioral signs of mice in all the experimental groups. Compared to the DMSO-treated group, the AV1004-treated group improved the behavioral signs of JEV-infected mice. No obvious clinical symptoms were found of non-infected mice

in AV1004 and DMSO control groups during the observation period (Figure 8B). These results indicated that the AV1004 could reduce mortality caused by JEV infection.

AV1004 Reduce the Viral Load and Inflammatory Response in Brain Tissue of Japanese Encephalitis Virus Infected Mice

Mice were sacrificed on days 5 and 23 post-infection. Tissue samples were collected and processed for the subsequent experiments. The viral loads in infected mice brain tissues were measured by plaque assay. Compared to the

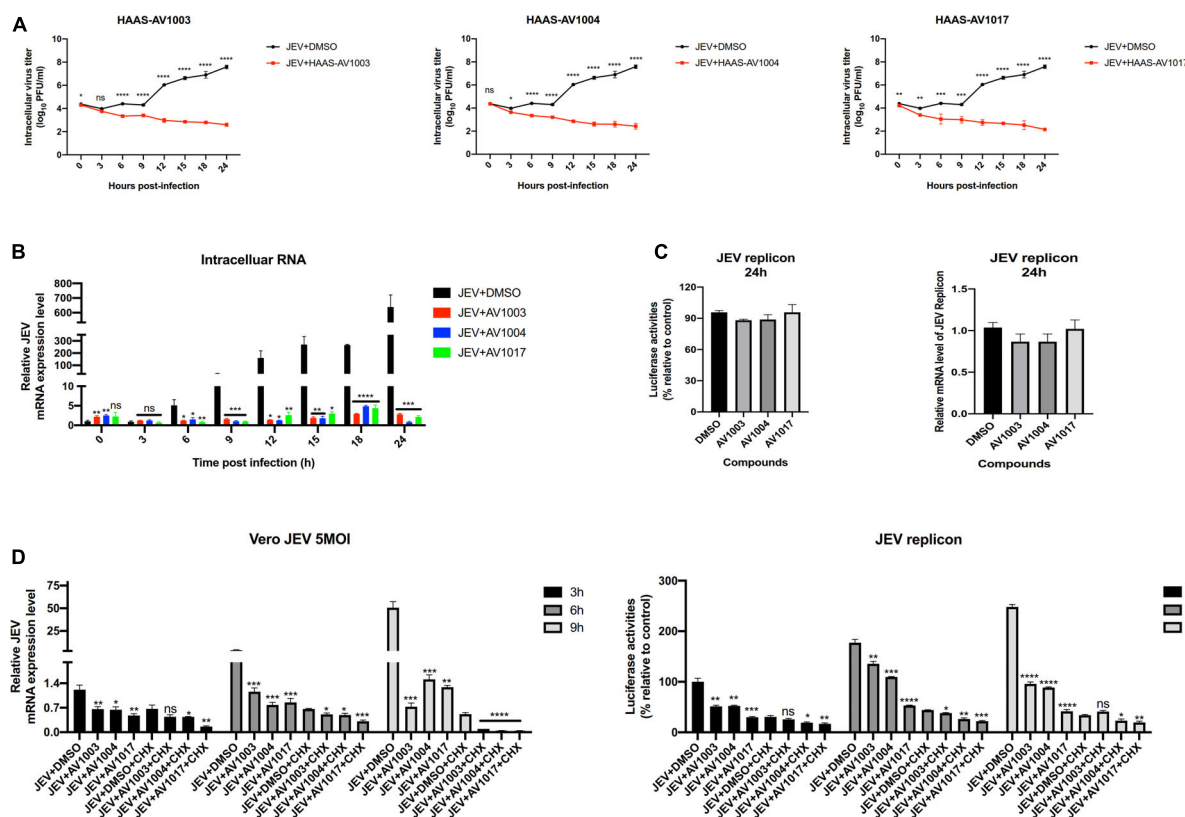


FIGURE 7 | DHEA derivatives play an inhibitory role in the early stage of viral infection. **(A,B)** Vero cells were treated with JEV (5 MOI) for 1 h followed by derivatives (20 μ M) or DMSO treatment. Cells were subjected to one freeze-thaw cycle to liberate cell-associated viruses at the indicated time points post-infection. Intracellular **(A)** virus titer was determined by plaque assay. And the JEV mRNAs levels **(B)** at specified time points were quantified by the qRT-PCR experiment. **(C)** Hela cells transfected with the JEV replicon were treated with derivatives at 10 μ M, luciferase activities and mRNAs levels were determined at 24 h. **(D)** Vero cells were treated with JEV (5 MOI) or Hela cells transfected with the JEV replicon followed by treatment with 20 μ M of DHEA derivatives and 100 μ g/ml of CHX. The mRNAs levels and luciferase activities at specified time points were quantified. * $P < 0.05$, ** $P < 0.01$, *** $P < 0.001$, and **** $P < 0.0001$.

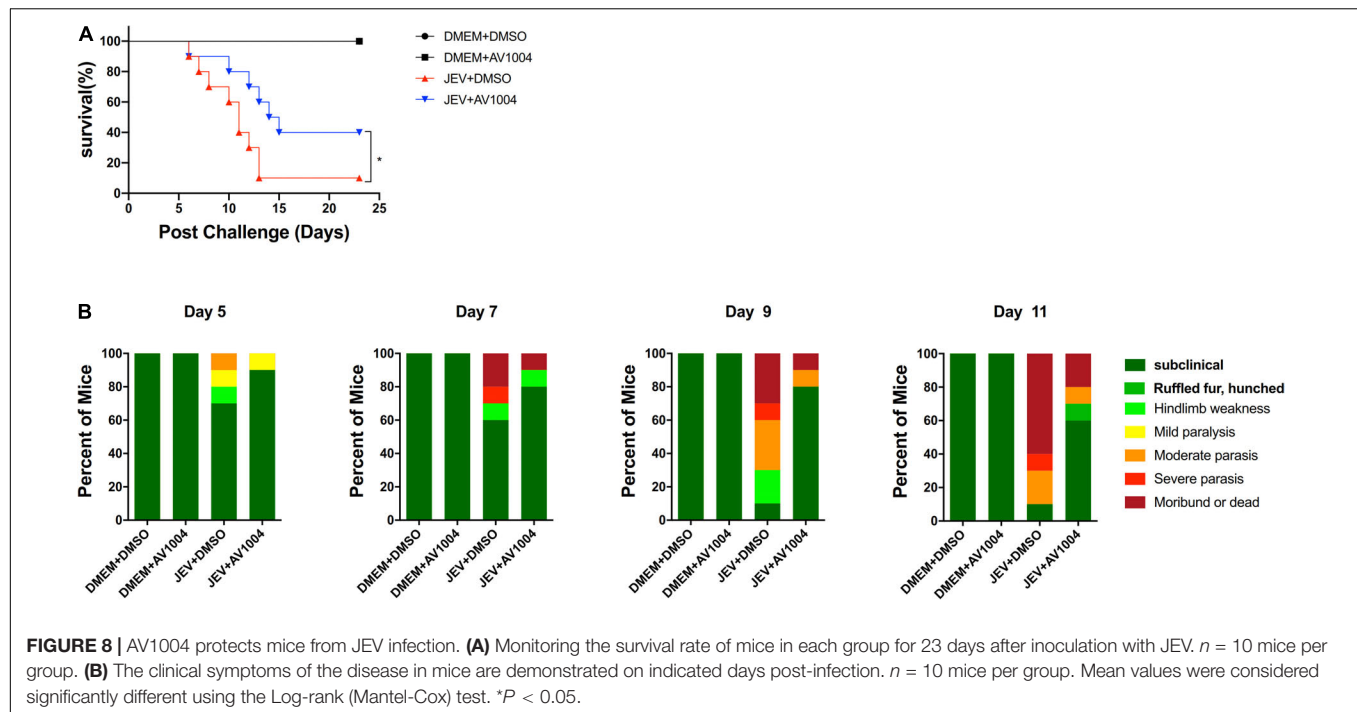
JEV-infected + DMSO-treated group, brain homogenates prepared on day 5 post-infection from JEV-infected + AV1004-treated mice, viral titers were reduced significantly (**Figure 9A**). On day 23 post-infection, all the survivals were recovered, no virus was detected in those mice. To assess the role of A1004 in attenuating the JEV induced massive inflammatory response in brain tissue. H&E, IHC staining and quantification of proinflammatory cytokines analysis were conducted on day 5 post-infection collected brain samples. The histopathological changes of the cerebrum in JEV-infected mice showed perivascular cuffing and meningitis, but these indicators of encephalitis were declined in JEV-infected + AV1004 treated mice (**Figure 9B**). To investigate the effect of AV1004 treatment on JEV-induced gliosis, IHC staining was performed by using the antibodies which can recognize the microglia marker protein IBA-1 and the astrocyte marker protein GFAP. The results suggested that AV1004 reduces reactive astrogliosis and microgliosis in infected mice. Furthermore, the expression of proinflammatory cytokines, such as *Il-1* β , *Il-6*, *Ccl2*, and *Ccl5* were measured by RT-qPCR assay. A significant reduction of RNA levels of proinflammatory cytokines was observed upon treatment of AV1004 was observed (**Figure 9C**). These results

indicate that A1004 has a potential therapeutic effect on reducing inflammation mediated by JEV.

DISCUSSION

The annual incidence of flavivirus infections in humans has reached millions of cases, no specific anti-flavivirus therapy has been developed yet (Campbell et al., 2011; Diamond and Pierson, 2015; Weaver et al., 2016). The increasing flavivirus infections worldwide highlight the urgent need for novel antiviral drugs. In accordance with the analysis of chemical structures of known drugs, it becomes feasible to design and synthesize novel drug derivatives, making the starting point of modern drug discovery. Considering the low cost, short cycles, and high benefits, the transformation of natural products is conducive to the construction of a significant number of molecular libraries for activity screening, thereby facilitating the development of high potential antiviral agents.

Dehydroepiandrosterone (DHEA) is an intermediate in testosterone biosynthesis and a typical steroid and sex hormone precursor, which can affect the formation of fat, regulate NADPH,



interfere with the production of interleukins and interferons, and bind endothelial cell membrane receptors (Berdanier et al., 1993; Labrie et al., 2003). DHEA has been characterized as an antiviral compound by previous studies as well as a potential therapeutic drug for specific viruses, for instance, HIV, JUNV, HSV, HCV, etc. (Loria et al., 1988; Mulder et al., 1992; Acosta et al., 2008; Barrows et al., 2018). To discover novel molecules as potential antiviral agents against flaviviruses, a series of steroidal derivatives based on DHEA scaffold were designed and synthesized in the present study. With the DHEA scaffold serving as the core structure, various aryl-hydrazone pharmacophores were integrated into the steroidal structure from the perspective of structure-activity relationships. The transformation was carried out at 17 positions of DHEA, with the resulting steroidal derivatives displaying more vital anti-flavivirus ability in comparison to that of DHEA. Therefore, it is of great practical significance to introduce this series of compounds as potential flavivirus inhibitors. We accordingly examined the antiviral and cytotoxic effects of DHEA and 23 synthetic derivatives using Vero cells. In this study, we found three-hit compounds and SI index greater than 30, which exert inhibitory effects on flavivirus. Among the three derivatives, compounds AV1003 and AV1004 were less toxic to different cells, with CC_{50} values higher than 100 μ M.

The time-of-drug additional assay revealed that AV1003, AV1004, and AV1017 worked more efficiently at post-infection. The effectiveness of AV1003, AV1004, and AV1017 against flavivirus infections was determined, respectively, at different time points (24, 36, and 48 h.p.i.) according to their ability to lower viral titers and impede virus spread from infected cells to neighboring cells. During a flavivirus life cycle, the viral particle is internalized by receptor-mediated endocytosis, and upon endosome acidification, conformational changes in

the E protein leads to membrane fusion (Modis et al., 2004; Nayak et al., 2009). The early stages of the flavivirus life cycle include binding, entry into the cells, uncoating, translation, and RNA replication (Ramanathan et al., 2020). Among the three derivatives, AV1017 affects both adsorption and invasion stages of the virus in Vero cells. The AV1017 provides a foundation for the development of JEV entry inhibitors. Recently, some relevant researches about inhibitors of JEV entry were reported. Berbamine, a bisbenzylisoquinoline alkaloid that is isolated from herbs. It's an effective anti-JEV agent, acting as a calcium channel or signaling inhibitor to prevent JEV entry (Huang et al., 2021). The sulfated polysaccharides "Carrageenan," a linear sulfated polysaccharide is extracted from red edible seaweeds, inhibits the early stages of JEV infection (Nor Rashid et al., 2020). As known that each replication cycle of flavivirus takes about 16 h (Mukherjee et al., 2011), our study suggests that AV1003/1004 can inhibit virus propagation at early steps after viral entry and before genomic replication. There are multiple endocytic pathways for JEV to be internalized from the host cell's plasma membrane to the endosomal compartment, which largely depends on the type of infected cells (Mayor and Pagano, 2007). The classical clathrin-dependent pathway was observed in BHK-21 (Liu et al., 2017), Vero (Nawa et al., 2003; Kalia et al., 2013), and PK15 (Yang et al., 2013). The non-classical clathrin-independent pathway was observed in the human neuroblastoma SK-N-SH (Xu et al., 2016), and mouse neuroblastoma Neuro-2a (Kalia et al., 2013). Considering the variations mentioned above, it is essential to investigate the main endocytic pathway for JEV to enter human brain neurons, peripheral human monocytes and macrophages/DCs, which may play an essential role in neuroinvasion.

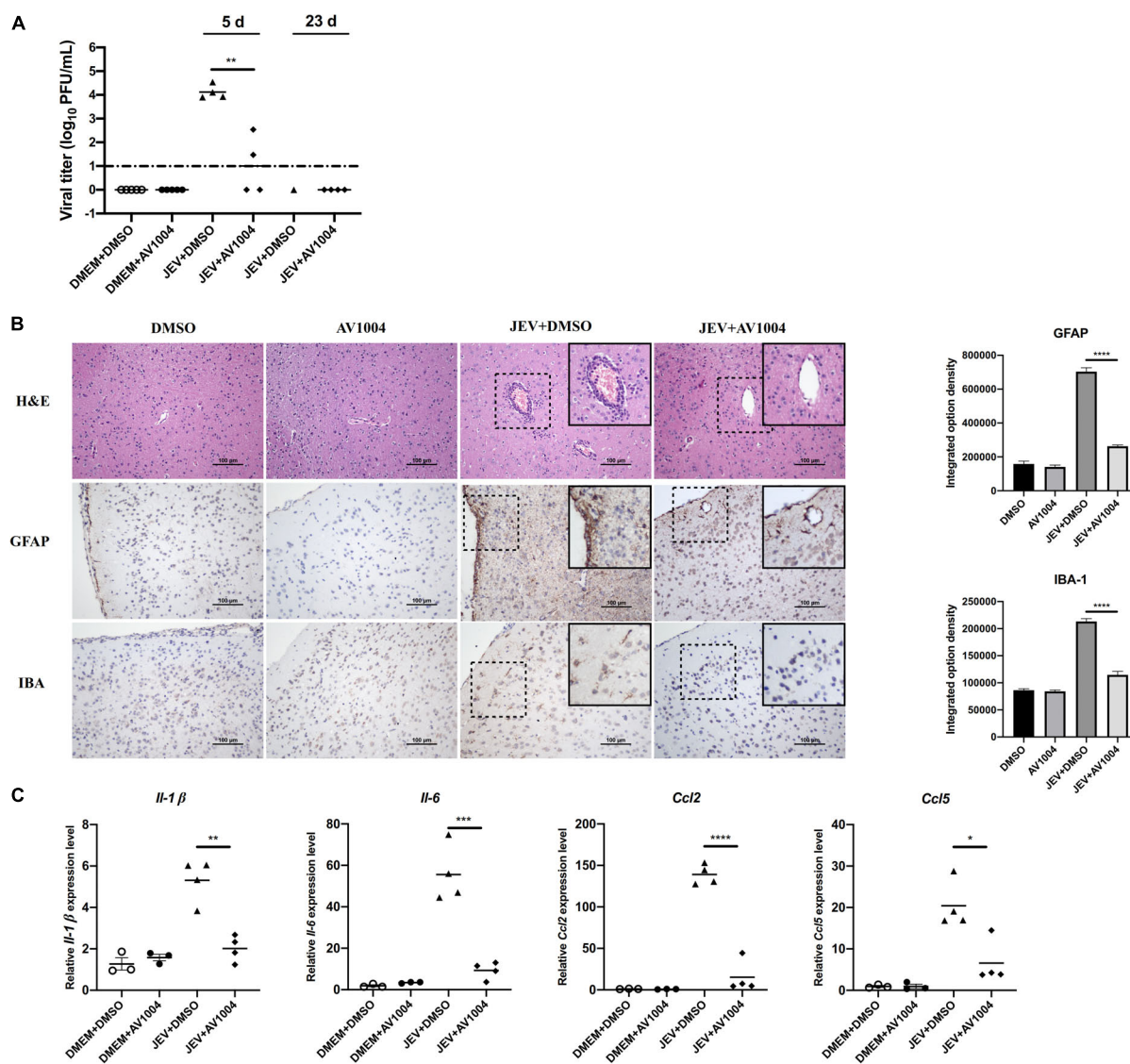


FIGURE 9 | AV1004 reduces the JEV-induced neuroinflammatory response *in vivo*. **(A)** Viral titers in the mouse brain tissue on days 5 and 23 post-infection were determined by plaque assay. Each data point represents one mouse. **(B)** IHC and H&E staining to observe the activation of glial cells and pathological changes. Black box visualization indicates activated glial cells and perivascular cuffing. Scale bar, 100 μ m. Integrated optical density analysis was performed to quantify the results of immunohistochemical staining. Data represent mean \pm SEM of 3 sections from 3 mice from each group. **(C)** The mRNA expression levels of inflammatory cytokines (*Il-1 β* , *Il-6*, *Ccl2* and *Ccl5*) in brain tissue lysates were quantified by qRT-PCR. Each data point represents one mouse. * $P < 0.05$, ** $P < 0.01$, *** $P < 0.001$, and **** $P < 0.0001$.

However, the molecular mechanism by which DHEA derivatives inhibit viruses remains unclear. The observed antiviral action of these derivatives may be associated with the host-signaling machinery. Therefore, the host factors had been already known to facilitate viral replication will provide clues for identifying the targets of those compounds. Recently, several reports suggest the role of a host signaling molecule that plays a vital role in virus replication post-invasion and at the time of genome replication. For instance, research proves that the targeted inhibitory effect of the virus on Dihydroorotate dehydrogenase (DHODH) can block the synthesis of new pyrimidines and cause DNA synthesis obstacles,

thereby effectively inhibiting the transcription and replication of viral RNA in host cells (Liu et al., 2000). The ubiquitin-proteasome system (UPS) was also involved in JEV entry, especially in the post-attachment step, which was before the initial translation of viral genomic RNA (Wang et al., 2016). The virus-host cell membrane fusion is a unique event in several flaviviruses (JEV and YFV) which was proved by the biochemical assays combined with live-cell imaging and single-particle tracking. The fusion precedes the microtubule-mediated viral nucleocapsid/genome released into the cytoplasm (Nour et al., 2013). Besides, a recent study demonstrated that during the entry of DENV, the viral genome releasing or nucleocapsid

uncoating is hampered by inhibiting ubiquitination (Byk et al., 2016). Transitional endoplasmic reticulum 94 (TER94) plays an essential role in viral uncoating by interacting with ZIKV capsid and trafficking it for proteasomal degradation (Gestuevo et al., 2021). Therefore, further research is needed to determine the exact role of DHEA derivatives post-entry of JEV and other flaviviruses in the host cells.

Meanwhile, the efficacy and toxicity of AV1004 were monitored in mice. AV1004 showed effective antiviral effect with favorable biocompatibility. It was observed that treated with AV1004 inhibited viral replication in JEV infected mice as well as alleviated manifestations of encephalitis in mouse brain tissues. This offers strong evidence that AV1004 is a potential therapeutic drug against JEV infection. The revamp of the DHEA structure also offers new insights for developing effective drugs against viral infections.

In conclusion, our *in vitro* and *in vivo* experimental findings demonstrate that DHEA derivatives could inhibit flaviviruses propagation. AV1004 exhibits significant antiviral activity against JEV infection within the period between viral entry and genomic replication. AV1004 protects mice from JEV-induced lethality and attenuates the histological manifestations of JEV through reduced viral loads and histopathological damage in the brain tissue. AV1004 is a potential treatment option for inhibiting multiple flaviviruses infections. In addition, this study suggests DHEA derivatives may provide a promising molecule framework basis for the further design and synthesis of potential antiviral drugs.

DATA AVAILABILITY STATEMENT

The original contributions presented in the study are included in the article/supplementary material, further inquiries can be directed to the corresponding author/s.

REFERENCES

- Acosta, E. G., Bruttomesso, A. C., Bisceglia, J. A., Wachsmann, M. B., Galagovsky, L. R., and Castilla, V. (2008). Dehydroepiandrosterone, epiandrosterone and synthetic derivatives inhibit Junin virus replication in vitro. *Virus Res.* 135, 203–212. doi: 10.1016/j.virusres.2008.03.014
- Barrett-Connor, E., Khaw, K. T., and Yen, S. S. (1986). A prospective study of dehydroepiandrosterone sulfate, mortality, and cardiovascular disease. *N. Engl. J. Med.* 315, 1519–1524. doi: 10.1056/nejm198612113152405
- Barrows, N. J., Campos, R. K., Liao, K. C., Prasanth, K. R., Soto-Acosta, R., Yeh, S. C., et al. (2018). Biochemistry and molecular biology of flaviviruses. *Chem Rev.* 118, 4448–4482. doi: 10.1021/acs.chemrev.7b00719
- Berdanier, C. D., Parente, J. A. Jr., and McIntosh, M. K. (1993). Is dehydroepiandrosterone an antiobesity agent? *FASEB J.* 7, 414–419. doi: 10.1096/fasebj.7.5.8462783
- Byk, L. A., Iglesias, N. G., De Maio, F. A., Gebhard, L. G., Rossi, M., and Gamarnik, A. V. (2016). Dengue Virus Genome Uncoating Requires Ubiquitination. *mBio* 7:e00804-16. doi: 10.1128/mBio.00804-16
- Campbell, G. L., Hills, S. L., Fischer, M., Jacobson, J. A., Hoke, C. H., Hombach, J. M., et al. (2011). Estimated global incidence of Japanese encephalitis: a systematic review. *Bull. World Health Organ.* 89, 766–874. doi: 10.2471/blt.10.085233

ETHICS STATEMENT

The animal study was reviewed and approved by The Scientific Ethic Committee of Huazhong Agriculture University (HZAUMO-2021-0003). Written informed consent was obtained from the owners for the participation of their animals in this study.

AUTHOR CONTRIBUTIONS

LZ, DZ, and JY contributed to the conception and design of the study. LZ organized the database, performed the statistical analysis, and wrote the first draft of the manuscript. LZ, ML, SK, and JY wrote the sections of the manuscript. All authors contributed to manuscript revision, read, and approved the submitted version.

FUNDING

This work was supported by the National Key Research and Development Program of China (2017YFD0501803 and 2016YFD0500407), National Natural Science Foundation of China (31825025, 32022082, 32030107, and 32002268), Fundamental Research Funds for the Central Universities (2662018QD025), Natural Science Foundation of Hubei Province (2019CFA010), and China Postdoctoral Science Foundation (2019M662677).

ACKNOWLEDGMENTS

We would like to thank China Center for Type Culture Collection for kindly providing the DENV type-2 strain and the ZIKV H/PF/2013 strain.

- Chang, C. C., Ou, Y. C., Raung, S. L., and Chen, C. J. (2005). Antiviral effect of dehydroepiandrosterone on Japanese encephalitis virus infection. *J. Gen. Virol.* 86(Pt 9), 2513–2523. doi: 10.1099/vir.0.81123-0
- Chen, Z., Wang, X., Ashraf, U., Zheng, B., Ye, J., Zhou, D., et al. (2018). Activation of neuronal N-methyl-D-aspartate receptor plays a pivotal role in Japanese encephalitis virus-induced neuronal cell damage. *J. Neuroinflammation* 15:238. doi: 10.1186/s12974-018-1280-8
- Culshaw, A., Mongkolsapaya, J., and Screaton, G. (2018). The immunology of Zika Virus. *F1000Research* 7:203. doi: 10.12688/f1000research.12271.1
- Diallo, K., Loemba, H., Oliveira, M., Mavoungou, D. D., and Wainberg, M. A. (2000). Inhibition of human immunodeficiency virus type-1 (HIV-1) replication by immunor (IM28), a new analog of dehydroepiandrosterone. *Nucleosides Nucleotides Nucleic Acids* 19, 2019–2024. doi: 10.1080/15257770008045475
- Diamond, M. S., and Pierson, T. C. (2015). Molecular insight into dengue virus pathogenesis and its implications for disease control. *Cell* 162, 488–492. doi: 10.1016/j.cell.2015.07.005
- Fernandez-Garcia, M. D., Mazzon, M., Jacobs, M., and Amara, A. (2009). Pathogenesis of flavivirus infections: using and abusing the host cell. *Cell Host Microbe* 5, 318–328. doi: 10.1016/j.chom.2009.04.001
- Gestuevo, R. J., Royle, J., Donald, C. L., Lamont, D. J., Hutchinson, E. C., Merits, A., et al. (2021). Analysis of Zika virus capsid-Aedes aegypti mosquito interactome

- reveals pro-viral host factors critical for establishing infection. *Nat. Commun.* 12:2766. doi: 10.1038/s41467-021-22966-8
- Gubler, D. J. (2007). Flaviviruses. *Fields Virol.* 5, 1153–1252.
- Hayashi, T., Esaki, T., Muto, E., Kano, H., Asai, Y., Thakur, N. K., et al. (2000). Dehydroepiandrosterone retards atherosclerosis formation through its conversion to estrogen: the possible role of nitric oxide. *Arterioscler. Thromb. Vasc. Biol.* 20, 782–792. doi: 10.1161/01.atv.20.3.782
- Huang, L., Li, H., Ye, Z., Xu, Q., Fu, Q., Sun, W., et al. (2021). Berbamine inhibits Japanese encephalitis virus (JEV) infection by compromising TPRMLs-mediated endolysosomal trafficking of low-density lipoprotein receptor (LDLR). *Emerg. Microbes Infect.* 10, 1257–1271. doi: 10.1080/22221751.2021.1941276
- Kalia, M., Khasa, R., Sharma, M., Nain, M., and Vrat, S. (2013). Japanese encephalitis virus infects neuronal cells through a clathrin-independent endocytic mechanism. *J. Virol.* 87, 148–162. doi: 10.1128/jvi.01399-12
- Ke, S., Wei, Y., Shi, L., Yang, Q., and Yang, Z. (2013). Synthesis of novel steroid derivatives derived from dehydroepiandrosterone as potential anticancer agents. *Anticancer Agents Med. Chem.* 13, 1291–1298. doi: 10.2174/18715206113139990323
- King, A. M., Adams, M. J., Carstens, E. B., and Lefkowitz, E. J. (2012). “Virus taxonomy,” in *Ninth Report of the International Committee on Taxonomy of Viruses*, eds J. K. Jancovich, V. G. Chinchir, A. Hyatt, T. Miyazaki, T. Williams, and Q. Y. Zhang (San Diego, CA: Elsevier Academic Press), 486–487.
- Kok, W. M. (2016). New developments in flavivirus drug discovery. *Expert Opin. Drug Discov.* 11, 433–445. doi: 10.1517/17460441.2016.1160887
- Labrie, F., Luu-The, V., Labrie, C., Bélanger, A., Simard, J., Lin, S. X., et al. (2003). Endocrine and intracrine sources of androgens in women: inhibition of breast cancer and other roles of androgens and their precursor dehydroepiandrosterone. *Endocr. Rev.* 24, 152–182. doi: 10.1210/er.2001-0031
- Li, X. D., Li, X. F., Ye, H. Q., Deng, C. L., Ye, Q., Shan, C., et al. (2014). Recovery of a chemically synthesized Japanese encephalitis virus reveals two critical adaptive mutations in NS2B and NS4A. *J. Gen. Virol.* 95(Pt 4), 806–815. doi: 10.1099/vir.0.061838-0
- Liu, C. C., Zhang, Y. N., Li, Z. Y., Hou, J. X., Zhou, J., Kan, L., et al. (2017). Rab5 and Rab11 are required for clathrin-dependent endocytosis of Japanese encephalitis virus in BHK-21 cells. *J. Virol.* 91, e1113–e1117. doi: 10.1128/jvi.01113-17
- Liu, S., Neidhardt, E. A., Grossman, T. H., Ocain, T., and Clardy, J. (2000). Structures of human dihydroorotate dehydrogenase in complex with antiproliferative agents. *Structure* 8, 25–33. doi: 10.1016/s0969-2126(00)00077-0
- Loria, R. M., Inge, T. H., Cook, S. S., Szakal, A. K., and Regelson, W. (1988). Protection against acute lethal viral infections with the native steroid dehydroepiandrosterone (DHEA). *J. Med. Virol.* 26, 301–314. doi: 10.1002/jmv.1890260310
- Mayor, S., and Pagano, R. E. (2007). Pathways of clathrin-independent endocytosis. *Nat. Rev. Mol. Cell Biol.* 8, 603–612. doi: 10.1038/nrm2216
- Modis, Y., Ogata, S., Clements, D., and Harrison, S. C. (2004). Structure of the dengue virus envelope protein after membrane fusion. *Nature* 427, 313–319. doi: 10.1038/nature02165
- Mukherjee, S., Lin, T. Y., Dowd, K. A., Manhart, C. J., and Pierson, T. C. (2011). The infectivity of prM-containing partially mature West Nile virus does not require the activity of cellular furin-like proteases. *J. Virol.* 85, 12067–12072. doi: 10.1128/jvi.05559-11
- Mukhopadhyay, S., Kuhn, R. J., and Rossmann, M. G. (2005). A structural perspective of the flavivirus life cycle. *Nat. Rev. Microbiol.* 3, 13–22. doi: 10.1038/nrmicro1067
- Mulder, J. W., Frissen, P. H., Krijnen, P., Endert, E., de Wolf, F., Goudsmit, J., et al. (1992). Dehydroepiandrosterone as predictor for progression to AIDS in asymptomatic human immunodeficiency virus-infected men. *J. Infect. Dis.* 165, 413–418. doi: 10.1093/infdis/165.3.413
- Nawa, M., Takasaki, T., Yamada, K. I., Kurane, I., and Akatsuka, T. (2003). Interference in Japanese encephalitis virus infection of Vero cells by a cationic amphiphilic drug, chlorpromazine. *J. Gen. Virol.* 84(Pt 7), 1737–1741. doi: 10.1099/vir.0.18883-0
- Nayak, V., Dessau, M., Kucera, K., Anthony, K., Ledizet, M., and Modis, Y. (2009). Crystal structure of dengue virus type 1 envelope protein in the postfusion conformation and its implications for membrane fusion. *J. Virol.* 83, 4338–4344. doi: 10.1128/jvi.02574-08
- Nor Rashid, N., Yusof, R., and Rothan, H. A. (2020). Antiviral and virucidal activities of sulphated polysaccharides against Japanese encephalitis virus. *Trop. Biomed.* 37, 713–721. doi: 10.47665/tb.37.3.713
- Nour, A. M., Li, Y., Wolenski, J., and Modis, Y. (2013). Viral membrane fusion and nucleocapsid delivery into the cytoplasm are distinct events in some flaviviruses. *PLoS Pathog.* 9:e1003585. doi: 10.1371/journal.ppat.1003585
- Ramanathan, H. N., Zhang, S., Douam, F., Mar, K. B., Chang, J., Yang, P. L., et al. (2020). A sensitive yellow fever virus entry reporter identifies valosin-containing protein (VCP/p97) as an essential host factor for flavivirus uncoating. *mBio* 11:e00467-20. doi: 10.1128/mBio.00467-20
- Regelson, W., Kalimi, M., and Loria, R. (2019). “DHEA: some thoughts as to its biologic and clinical action,” in *The Biologic Role of Dehydroepiandrosterone (DHEA)*, eds M. Y. Kalimi, W. Regelson, and W. de Gruyter (Berlin: De Gruyter), 405–446.
- Romanutti, C., Bruttomesso, A. C., Castilla, V., Biscaglia, J. A., Galagovsky, L. R., and Wachsmann, M. B. (2009). In vitro antiviral activity of dehydroepiandrosterone and its synthetic derivatives against vesicular stomatitis virus. *Vet. J.* 182, 327–335. doi: 10.1016/j.tvjl.2008.06.015
- Torres, N. I., Castilla, V., Bruttomesso, A. C., Eiras, J., Galagovsky, L. R., and Wachsmann, M. B. (2012). In vitro antiviral activity of dehydroepiandrosterone, 17 synthetic analogs and ERK modulators against herpes simplex virus type 1. *Antiviral Res.* 95, 37–48. doi: 10.1016/j.antiviral.2012.05.002
- Wang, S., Liu, H., Zu, X., Liu, Y., Chen, L., Zhu, X., et al. (2016). The ubiquitin-proteasome system is essential for the productive entry of Japanese encephalitis virus. *Virology* 498, 116–127. doi: 10.1016/j.virol.2016.08.013
- Wang, S., Liu, Y., Guo, J., Wang, P., Zhang, L., Xiao, G., et al. (2017). Screening of FDA-approved drugs for inhibitors of Japanese encephalitis virus infection. *J. Virol.* 91:e01055-17. doi: 10.1128/jvi.01055-17
- Weaver, S. C., Costa, F., Garcia-Blanco, M. A., Ko, A. I., Ribeiro, G. S., Saade, G., et al. (2016). Zika virus: history, emergence, biology, and prospects for control. *Antiviral Res.* 130, 69–80. doi: 10.1016/j.antiviral.2016.03.010
- Xu, Q., Cao, M., Song, H., Chen, S., Qian, X., Zhao, P., et al. (2016). Caveolin-1-mediated Japanese encephalitis virus entry requires a two-step regulation of actin reorganization. *Future Microbiol.* 11, 1227–1248. doi: 10.2217/fmb-2016-0002
- Yang, S., He, M., Liu, X., Li, X., Fan, B., and Zhao, S. (2013). Japanese encephalitis virus infects porcine kidney epithelial PK15 cells via clathrin- and cholesterol-dependent endocytosis. *Virol. J.* 10:258. doi: 10.1186/1743-422x-10-258
- Zwain, I. H., and Yen, S. S. (1999). Dehydroepiandrosterone: biosynthesis and metabolism in the brain. *Endocrinology* 140, 880–887. doi: 10.1210/endo.140.2.6528

Conflict of Interest: The authors declare that the research was conducted in the absence of any commercial or financial relationships that could be construed as a potential conflict of interest.

Publisher's Note: All claims expressed in this article are solely those of the authors and do not necessarily represent those of their affiliated organizations, or those of the publisher, the editors and the reviewers. Any product that may be evaluated in this article, or claim that may be made by its manufacturer, is not guaranteed or endorsed by the publisher.

Copyright © 2021 Zhang, Zhou, Li, Zhu, Imran, Duan, Cao, Ke and Ye. This is an open-access article distributed under the terms of the Creative Commons Attribution License (CC BY). The use, distribution or reproduction in other forums is permitted, provided the original author(s) and the copyright owner(s) are credited and that the original publication in this journal is cited, in accordance with accepted academic practice. No use, distribution or reproduction is permitted which does not comply with these terms.



The 5' and 3' Untranslated Regions of the *Japanese Encephalitis Virus* (JEV): Molecular Genetics and Higher Order Structures

Hong Liu^{1,2*}, Jun Zhang^{1†}, Yuzhen Niu¹ and Guodong Liang^{3*}

¹ Shandong Provincial Research Center for Bioinformatic Engineering and Technique, School of Life Sciences and Medicine, Shandong University of Technology, Zibo, China, ² Zibo Key Laboratory of Precise Gene Detection, Zibo, China, ³ State Key Laboratory of Infectious Disease Prevention and Control, National Institute for Viral Disease Control and Prevention, Chinese Center for Disease Control and Prevention, Beijing, China

OPEN ACCESS

Edited by:

Han Xia,

Key Laboratory of Special Pathogens and Biosafety, Wuhan Institute of Virology, Chinese Academy of Sciences (CAS), China

Reviewed by:

Margo A. Brinton,

Georgia State University, United States

Adriano de Bernardi Schneider, University of California, San Diego, United States

*Correspondence:

Hong Liu

liuhongseminar@hotmail.com

Guodong Liang

gdliang@hotmail.com

[†]These authors have contributed equally to this work

Specialty section:

This article was submitted to

Virology,

a section of the journal

Frontiers in Microbiology

Received: 24 June 2021

Accepted: 22 September 2021

Published: 28 October 2021

Citation:

Liu H, Zhang J, Niu Y and Liang G (2021) The 5' and 3' Untranslated Regions of the *Japanese Encephalitis Virus* (JEV): Molecular Genetics and Higher Order Structures. *Front. Microbiol.* 12:730045. doi: 10.3389/fmicb.2021.730045

The untranslated region (UTRs) of viral genome are important for viral replication and immune modulation. *Japanese encephalitis virus* (JEV) is the most significant cause of epidemic encephalitis worldwide. However, little is known regarding the characterization of the JEV UTRs. Here, systematic analyses of the UTRs of JEVs isolated from a variety of hosts worldwide spanning about 80 years were made. All the important *cis*-acting elements and structures were compared with other mosquito-borne *Flaviviruses* [*West Nile virus* (WNV), *Yellow fever virus* (YFV), *Zika virus* (ZIKV), *Dengue virus* (DENV)] and annotated in detail in the UTRs of different JEV genotypes. Our findings identified the JEV-specific structure and the sequence motif with unique JEV feature. (i) The 3' dbsHP was identified as a small hairpin located in the DB region in the 3' UTR of JEV, with the structure highly conserved among the JEV genotypes. (ii) The spacer sequence UARs of JEV consist of four discrete spacer sequences, whereas the UARs of other mosquito-borne *Flaviviruses* are continuous sequences. In addition, repetitive elements have been discovered in the UTRs of mosquito-borne *Flaviviruses*. The lengths, locations, and numbers of the repetitive elements of JEV also differed from other *Flaviviruses* (WNV, YFV, ZIKV, DENV). A 300 nt-length region located at the beginning of the 3' UTR exhibited significant genotypic specificity. This study lays the basis for future research on the relationships between the JEV specific structures and elements in the UTRs, and their important biological function.

Keywords: *Japanese encephalitis virus*, *Flavivirus*, secondary structure, 5'untranslated region, 3'untranslated region

INTRODUCTION

Flaviviruses are enveloped viruses with 11 kb, positive-sense single-stranded RNA genome containing highly structured 5' and 3' untranslated region (UTRs) between which lies a single open reading frame (ORF) encoding three structural proteins (C-prM-E) and seven non-structural (NS) proteins (NS1, NS2A, NS2B, NS3, NS4A, NS4B, NS5) (Sumiyoshi et al., 1987; Liu and Qin, 2020). The NS proteins interact with certain cellular factors to form the viral replicase complex that directs the replication of the genomic RNA

(Lindenbach et al., 2007; Garcia-Blanco et al., 2016; Wang et al., 2017; Sanford et al., 2019). The genome cyclizes so that a single minus strand can be synthesized with stem loop A (SLA) functioning to recruit the RNA dependent RNA polymerase (RdRp). The minus strand in the resulting double-strand serves as a template for multiple reinitiations of genome RNAs (Westaway et al., 2003; Lindenbach et al., 2007). Within the 5' UTR, there are several conserved stem-loop (SL) structures. These include (i) SLA, which serves as a viral polymerase binding site (Filomatori et al., 2006); and (ii) Stem-loop B (SLB), which contains the upstream of AUG region (5' UAR) (Alvarez et al., 2005) and 5'-UAR-flanking stem (UFS) (Liu et al., 2016) are involved in long-range RNA-RNA interactions and genome replication. The capsid-coding region hairpin (cHP) element lies within the coding region and aids in start codon recognition and viral replication (Clyde et al., 2008). The 5' UAR along with 5' downstream AUG region (DAR) (Friebe et al., 2011) and the 5' cyclization sequence (5' cCS) (Villordo and Gamarnik, 2009; Gebhard et al., 2011) cause genome circularization by hybridizing with their counterparts in the 3' UTR (i.e., 3' UAR, 3' DAR, and 3' cCS) (Hahn et al., 1987; Hodge et al., 2019). Besides the viral genome cyclization-related sequences, 3' UTR has a panel of stem-loop structures that halt XRN1 exoribonuclease digestion. This results in the synthesis of sets of subgenomic flaviviral RNA (sfRNA) (Pijlman et al., 2008) which are associated with viral pathogenicity, host adaption, and immune evasion and immune evasion (Moon et al., 2012; Chapman et al., 2014; Filomatori et al., 2017).

The 5' and 3'UTRs of the *Flavivirus* have been shown to be crucial for virus replication, immune regulation and pathogenicity (Brinton et al., 1986; Moon et al., 2012; Chang et al., 2013; Kieft et al., 2015). However, the studies of *cis*-acting elements in the UTRs have been mainly focused on *Dengue virus* (DENV), *Yellow fever virus* (YFV), *West Nile virus* (WNV), *Tick-borne encephalitis virus* (TBEV), and *Zika virus* (ZIKV) (Zeng et al., 2020). Although *Japanese encephalitis virus* (JEV) is arguably the most significant pathogen causing viral encephalitis within the *Flaviviruses*, few studies have been conducted to explore the functions and features of JEV UTRs. As a result, little is known about the primary and higher-order structures of JEV. Whether all of the functional important *cis*-acting elements that exist in the JEV UTRs share some features with the other *Flaviviruses* or whether JEV has some specific features has yet to be understood. It is largely unknown what the accurate locations and the sequence features of these important elements in JEV UTRs are.

Japanese encephalitis virus have evolved into five genetically different lineages in nature, diverged in the chronological order of GV, GIV, GIII, GII, and GI (Gao et al., 2015). JEV was initially isolated from viral encephalitis patients in 1935 in Japan and subsequently this strain was identified to be JEV GIII (Lewis et al., 1947). GIII has been the predominant genotype causing human and animal diseases in JE endemic areas until the late 20th century. In recent years, most JEV strains isolated from mosquito vectors, pigs, and humans in Asia belong to GI, thus replacing GIII as the dominant genotype in the Asian continent (Pan et al., 2011). GII primarily circulates in southeast Asia

and northern Australia (Williams et al., 2000; Schuh et al., 2010), whereas GIV and GV are mainly confined to the tropical regions of Southeast Asia (Li et al., 2011; Kuwata et al., 2020; Woo et al., 2020). Both the inactivated vaccine (Nakayama) and the attenuated live vaccine (SA14-14-2) currently used for JE vaccination are derived from GIII (Ni et al., 1994; Halstead and Jacobsen, 2008; Erlanger et al., 2009). However, a growing number of reports suggest that these vaccines do not provide complete protection against GI and GV virus strains (Cao et al., 2016; Hegde and Gore, 2017). Collectively, these reports suggest that viral evolution, transmission ability, pathogenicity, and immunogenicity differ among JEV genotypes. Previous JEV studies were mainly focused on the protein-coding sequences, neglecting the study of the UTRs region. The differences in the UTRs among the JEV genotypes are poorly understood. In this study, a comprehensive study of 160 JEV strains including 67 isolates sequenced in our lab was conducted on the JEV UTRs. The results will assist our understanding of the role of UTRs in the transcription, replication and pathogenicity of JEV.

MATERIALS AND METHODS

The Japanese Encephalitis Virus Untranslated Regions Data Analysis Pipeline

The following analyses were carried out in this work to investigate the primary sequence and secondary structural similarity and differences between representative *Flaviviruses* (WNV, YFV, ZIKV, DENV) and within the five genotypes of JEV UTRs. First, the JEV whole-genome sequence dataset was constructed, including 67 strains sequenced in our lab and 97 strains obtained from the NCBI database. Sequence inclusion criteria are described in the dataset construction section. The whole JEV genome dataset was then split into three parts to form the 5'UTR, ORF, and 3'UTR gene datasets. Meanwhile, the UTRs sequences of the representative *Flaviviruses* (WNV, YFV, ZIKV, DENV) were also downloaded as reference sequences for *cis*-acting element annotation and repeat sequences analysis. The general sequence feature analysis, primary sequence analysis, and higher-level structure analysis were performed using the JEV UTRs sequence datasets. The primary sequence analysis entailed sequence similarity, nucleotide composition, and repeat sequence analysis. The higher-level structural analysis comprised of the secondary structure and *cis*-acting elements annotation. Through these analyses, some genotypic sequence or structure features could be identified amongst the five JEV genotypes, if any. Such regions would then be selected for phylogenetic analysis. The software used in the analyses is listed in the flow chart of the JEV UTRs data analysis pipeline (Figure 1). The **Supplementary Data 2** contains the detailed parameter settings utilized in each software as well as the analysis scripts. The datasets, sequence alignments, and the software used in the current study are available from the corresponding authors upon request.

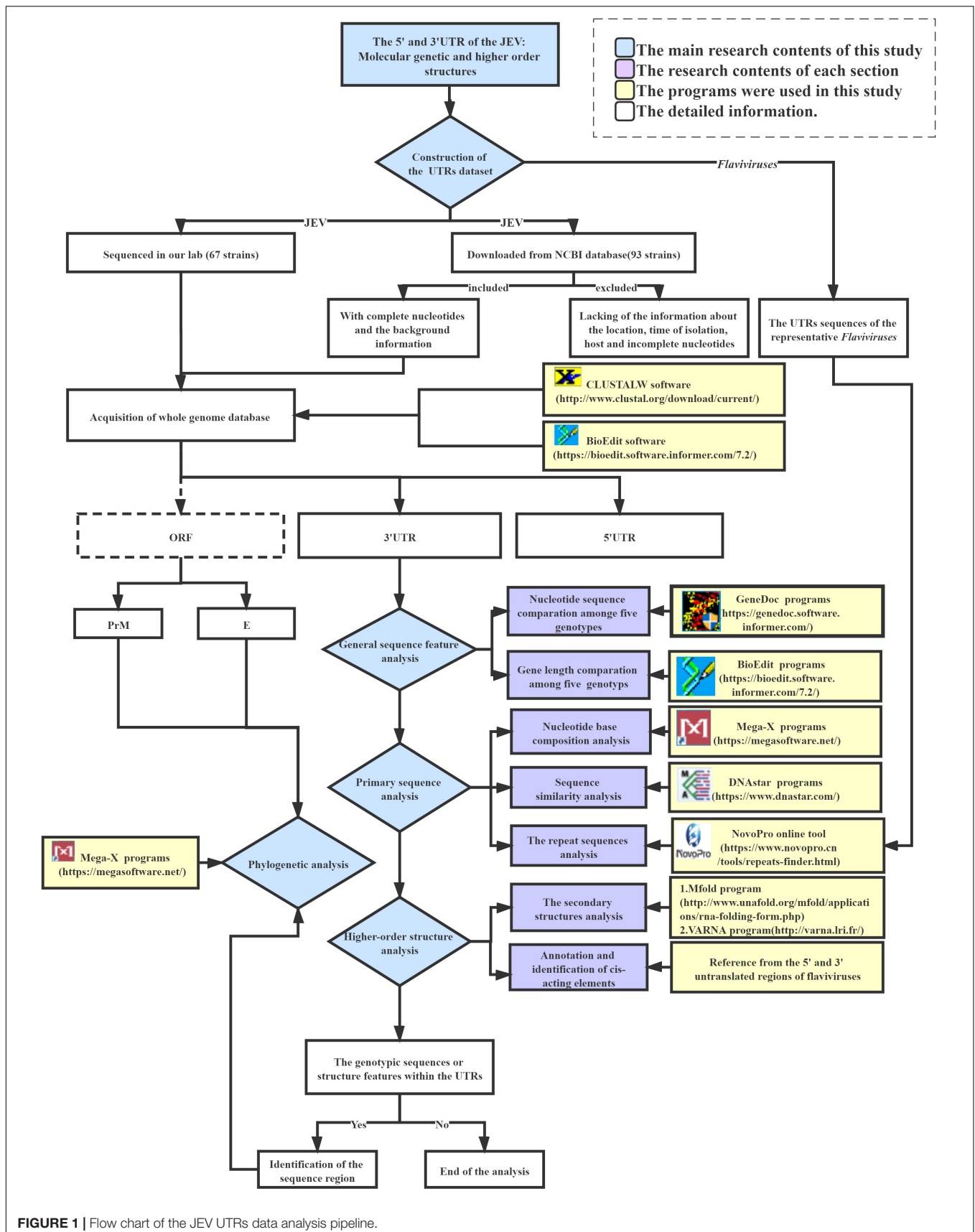


FIGURE 1 | Flow chart of the JEV UTRs data analysis pipeline.

The Japanese Encephalitis Virus Untranslated Regions Datasets Construction

In order to understand the sequence and structural features of the UTRs of JEV, the nucleotide sequences of the 5' and 3'UTRs of JEVs were downloaded from GenBank as of January 2020. The complete UTRs sequences with clear background information including location, data, origin (vector or host) were selected, we excluded all missing at least one of the three metadata.

The Japanese Encephalitis Virus Untranslated Regions' Sequence Analysis

The sequence analysis of the UTRs of the 160 JEV strains was conducted to explore the genetic features among the different JEV genotypes. First, CLUSTALW software (Thompson et al., 1997) was used to align the nucleotide sequences of the UTRs of JEV. The BioEdit and GeneDoc software were then used to perform sequence editing and nucleotide difference analysis in UTRs. The MegAlign incorporated in DNASTar software (Burland, 2000) was used to compute the sequence distance between different strains to generate the similarity matrix. The Mega-X program (Kumar et al., 2018) was used to analyze the base composition of the nucleotide sequences of the JEV UTRs. A scatter plot was then generated with ggplot2 package in RStudio¹ to show the proportion of bases (A, U, G, C) of each strain in different genotypes. The statistical analyses were conducted using SPSS software.

The Repeat Sequences Analysis of Japanese Encephalitis Virus and Representative Mosquito-Borne Flaviviruses

The UTR sequence alignments were generated using the CLUSTALW software. The GenDoc program was subsequently employed to extract the consensus sequences from the alignments. To determine whether there are repetitive sequences located in the UTRs of representative arboviral *Flaviviruses* (WNV, YFV, ZIKV, DENV) were also downloaded from GenBank for analysis. The NovoPro online tool that is based on the k-mer algorithm (Lerat, 2010) was used to search repeat sequences in the viral UTRs sequences. The core number setting of the minimum repeat sequence followed three principles: (1) The repetitive sequence unit should be obtained; (2) The longest repetitive sequence should be obtained; (3) There should be no overlap between two or more repetitive sequence units. Based on the three principles, 5 and 8 were the best minimum repeat sequence core numbers for the 5' and 3' UTRs, respectively. The IBS 1.0.3 software (Liu et al., 2015) was used for results visualization.

Higher-Order Structure Analysis of the Untranslated Regions of Japanese Encephalitis Virus

Prediction of the JEV UTR secondary structure was done using the Mfold software v 3.6 (Zuker, 2003). The parameters used included a folding temperature of 37°C, an ionic condition of 1M NaCl with no divalent ions, and a 5% suboptimality. The upper bound of the number of computed folding and the maximum upper bound of the total number of single-stranded bases allowed in a bulge or interior loop were set at 25. The other parameters were set at default, and the initial ΔG was selected as the smallest structure to obtain the Vienna format file. The representative *Flaviviruses*' (WNV and YFV) genome sequences with confirmed UTR secondary structures were used as references to validate the parameter settings. Taken the representative *Flaviviruses* as reference, a 50 nt-length sequence located after the start codon within the ORF that forms secondary structures, which are essential for genome cyclization, was also included in the present analysis. The VARNA program (Darty et al., 2009) was finally used for visualization of the UTR secondary structure.

The Phylogenetic Analysis Based on the Japanese Encephalitis Virus Untranslated Regions

According to results of sequence alignment of 3'UTRs, it is clear that the 3' variable region (VR) of JEV 3'UTR, which comprises 300 nt, exhibits clear genotype-specific features. Thus, this region was selected to conduct the phylogenetic analysis. Phylogenetic analyses based on the 5' and 3'UTRs, as well as on the 3'VR sequences, were all performed using both Maximum Likelihood (ML) and Neighbor-Joining (NJ) methods within MEGAX software. The best-fit substitution model of each dataset was estimated using ModelFinder (Kalyaanamoorthy et al., 2017) incorporated in the PhyloSuite software (Zhang et al., 2020). In order to verify the consistency of the phylogenetic trees generated using different gene regions, the phylogenetic tree were also generated using ORF, preM and E gene sequences. The topology of the phylogenetic trees based on the different gene datasets were compared using the Robinson–Foulds (RF) metric (Robinson and Foulds, 1981; Smith, 2020) to validate the accuracy of JEV genotyping based on the VR sequences. The ML and NJ trees were constructed with 1000 bootstrap replicates.

RESULTS

The Japanese Encephalitis Virus Untranslated Regions Datasets Construction

After removing the sequence with insufficient background information and incomplete nucleotides, the sequences of 93 JEV strains were selected, together with the sequences of 67 strains from our lab, to form a final whole-genome sequence dataset containing 160 JEV strains. Then the JEV whole-genome sequence dataset was split into three parts to form the 5'

¹<https://rstudio.com>

UTR, ORF, and 3' UTR gene datasets. The 160 JEV strains are representing the samples isolated from kinds of mosquitoes ($n = 82$) with *Culex tritaeniorhynchus* as the major species ($n = 46$), midges ($n = 2$), bats ($n = 6$), pigs ($n = 29$), horses ($n = 2$), and humans ($n = 38$). The isolation dates ranged from 1935 to 2018. The isolation sites including China ($n = 121$), Japan ($n = 17$), India ($n = 7$), South Korea ($n = 4$), South Korea ($n = 2$), Vietnam ($n = 1$), Laos ($n = 1$), Australia ($n = 1$), Angola ($n = 1$), Indonesia ($n = 1$), Malaysia ($n = 1$), Singapore ($n = 1$), and Philippines ($n = 1$). The geographical distribution extends from latitude 15°S to latitude 45°N. The 160 strains of JEV belong to five genotypes: GI ($n = 78$), GII ($n = 1$), GIII ($n = 77$), GIV ($n = 1$), and GV ($n = 3$) (detailed information in **Supplementary Table 1**).

The Sequence Analyses of the Japanese Encephalitis Virus Untranslated Regions

Both of the 5' and 3' UTRs sequences were compared and analyzed using CLUSTALW and GenDoc software. It is found that the length of the 5' UTR region of JEV is 95 nt (only GI is 96 nt). The 5' UTRs are more conserved compared with the 3' UTRs. There are nucleotide differences that exist in both the 5' and 3' UTRs among the different genotypes (**Tables 1–3** and **Supplementary Table 1**). The 3'UTR ranges in length from 557 to 596 nt, and the nucleotide sequence of the 3'UTRs is more variable than that of the 5'UTRs. There is a 300 nt-length region, starting from the stop codon, that is the most variable and exhibits a clear genotype specificity (**Tables 1, 3**). In JEV and other arboviral *Flaviviruses*, the 5'UTR initiates with an adenine (A) that is immediately connected with the 5'cap structure ($m^7G_{ppp}A_{mp}N$) and terminates with the CU. However, we identified that four out of 160 JEV strains were not terminated with CU.

The Nucleotide Similarity and Composition of the Japanese Encephalitis Virus Untranslated Regions

The nucleotide similarity analysis for the 5' and 3'UTRs of 160 JEV strains isolated from different vectors, hosts and locations during 1938–2018 revealed that the 5'UTRs exhibit a nucleotide similarity ranges from 84.5 to 100%, with an average similarity of $\mu = 97.62$. The nucleotide similarity of GI and GIII are 90.7–100% and 95.9–100%, respectively. The 3'UTRs exhibit nucleotide similarity ranges from 79.3% to 100%, with a $\mu = 94.47\%$. The nucleotide similarity of GI and GIII are 95.5–100% and 88.6–100%, respectively. The detailed similarity of the 5' and 3'UTRs for each JEV genotype are presented (**Tables 1, 4**). The JEV 5'UTRs are rich in AT (A + T content reaches 62%), and the 3'UTRs are rich in GC dinucleotides (A + T content is 47%) (**Figure 2** and **Table 1**).

The Repeat Sequences in the Japanese Encephalitis Virus Untranslated Regions

The repeat sequences in the JEV UTRs were analyzed using the NovoPro online tool and IBS 1.0.3 software. We found that both the JEV 5' and 3'UTRs consist of different numbers of repeat sequence elements. The numbers, locations and nucleotide

sequence composition of the repeat units of the 5' and 3'UTRs are different among the five JEV genotypes. The detailed information is shown in **Figure 3** and **Table 1**.

The Repeat Sequences in Representative Mosquito-Borne Flaviviruses

The repeat sequences identification in representative mosquito-borne *Flaviviruses* including WNV, YFV, ZIKV, and DENV were conducted using the NovoPro online tool and IBS 1.0.3 software. The results showed that the repeat sequence elements exist in the 5' and 3'UTRs of all the analyzed arboviral *Flaviviruses*. There are clearly differences in the length, number, position, and nucleotide sequence composition among the different arboviral *Flaviviruses*. The detailed information is shown in **Figure 4**.

The Secondary Structures and Important Functional Sequences in the Japanese Encephalitis Virus 5' Termini

As shown in **Figure 5** and **Table 1**, the 5'UTRs consist of two stem-loop structures termed SLA and SLB. Within the SLB lies the UAR and the UFS. There are three elements sited after the ATG start codon within the capsid-coding region, termed the DAR, the CHP and the 5'cCS. Except for GIV, the secondary structures of the JEV 5'UTR are conserved among the five JEV genotypes. The 5'UTRs start with an adenine (A) connecting to the 5' cap structure ($m^7G_{ppp}A_{mp}A$), directly linked to the SLA. SLA has a conserved structure with a length of about 70 nucleotides. GIV has a unique secondary structure in that instead of a direct connection between the 5' cap and SLA, a U-rich sequence is inserted. Furthermore, the morphology of SLA of GIV differs from those of other genotypes.

SLB sits closest to the SLA, and contains UFS and 5'UAR. The SLB starting sequence (5'-GUUUUU-3') and the sequence within the coding region (4 nucleotides behind the start codon, 5'-AAAAAC-3') are reversely complementary, which form a stem of 6 base pairs in length, termed the 5'UAR-flanking stem (UFS) (**Figure 5**). An 11 nt-length bulge structure is connected to the JEV UFS structure (stem), which includes both the 6 nt-length 5'UTR sequence and the 5 nt-length sequence from the start codon of the capsid protein-coding sequence (5'-ATGAC-3'). Among all the medically important arboviral *Flaviviruses* (DENV 1-4, YFV, ZIKA, WNV, TBEV), only DENV 4 and ZIKV have this bulge structure, but it lacks an ATG start codon. This structural feature is unique in the JEV 5' termini. The UAR sequence is located within the top loop of SLB, and the size and nucleotide composition of the top loop structures are different among the five JEV genotypes.

There is a clear difference that exists in the loop structure in JEV GI, due to the adenine insertion at position 92, as well as a mutation (93 T > C), resulting in the top loop structure change of SLB. The UARs of JEV are not continuous sequences but consists of four interspaced sequences (Denoted by yellow dashed lines in **Figure 5**). When compared to other mosquito-borne *Flaviviruses* (WNV, YFV, ZIKV, DENV), which have continuous UARs, the feature of JEV sequence is unique. We defined the JEV's UARs as spacer sequence UAR. The 5' DAR is located downstream of

TABLE 1 | Primary sequence and secondary structure elements analysis of the JEV's UTRs.

UTR		5'UTR					3'UTR				
Genotypes		I	II	III	IV	V	I	II	III	IV	V
Primary sequence	Length (nt)	96	95	95	95	95	565–571	570	557–583	584	586–591
	Similarity	90.7–100% (μ = 98.31%)	—	95.9–100% (μ = 99.36%)	—	99–100% (μ = 99.34%)	95.5–100% (μ = 98.71%)	—	88.6–100% (μ = 97.83%)	—	94.9–100% (μ = 96.6%)
	Nucleotide composition	A = 32.38%	A = 31.58%	A = 31.58%	A = 29.47%	A = 32.63%	A = 28.12%	A = 29.3%	A = 29.17%	A = 29.28%	A = 30.72%
		G = 24.00%	G = 24.21%	G = 24.20%	G = 24.21%	G = 24.21%	G = 29.65%	G = 28.95%	G = 29.03%	G = 28.42%	G = 28.51%
		T = 31.14%	T = 32.63%	T = 32.66%	T = 33.68%	T = 31.93%	T = 18.32%	T = 18.25%	T = 18.51%	T = 18.15%	T = 18.83%
		C = 12.50%	C = 11.58%	C = 11.57%	C = 12.63%	C = 11.23%	C = 23.92%	C = 23.51%	C = 23.42%	C = 24.14%	C = 21.95%
Secondary structure (Location and length)		A > T > G > C	T > A > G > C	T > A > G > C	T > A > G > C	A > T > G > C	G > A > C > T	A > G > C > T	A > G > C > T	A > G > C > T	A > G > C > T
	Repeat sequences (number)	5	4	4	3	4	5	4	5	5	4
	SLA	5–71 (67 nt)	5–71 (67 nt)	5–71 (67 nt)	11–73 (63 nt)	5–71 (67 nt)	na	na	na	na	na
	SLB	73–109 (37 nt)	73–108 (36 nt)	73–108 (36 nt)	85–95 (11 nt)	73–108 (36 nt)	na	na	na	na	na
	5'UAR	79–103 (13 nt)	79–102 (14 nt)	79–102 (15 nt)	79–102 (13 nt)	79–102 (12 nt)	na	na	na	na	na
	UFS	73–109 (12 nt)	73–108 (12 nt)	73–108 (12 nt)	—	73–108 (12 nt)	na	na	na	na	na
Domain1	cHP	116–135 (20 nt)	115–134 (20 nt)	115–134 (20 nt)	115–134 (20 nt)	115–134 (20 nt)	na	na	na	na	na
	5'DAR	109–113 (5 nt)	108–112 (5 nt)	108–112 (5 nt)	108–112 (5 nt)	108–112 (5 nt)	na	na	na	na	na
	5'cCS	137–147 (11 nt)	136–146 (11 nt)	136–146 (11 nt)	136–146 (11 nt)	136–146 (11 nt)	na	na	na	na	na
	VVR	na	na	na	na	na	1–48 (48 nt)	1–49 (49 nt)	1–62 (62 nt)	1–62 (62 nt)	1–74 (74 nt)
	xrRNA1	na	na	na	na	na	54–128 (75 nt)	55–129 (75 nt)	68–142 (75 nt)	68–142 (75 nt)	80–154 (75 nt)
	3'vrSL	na	na	na	na	na	136–208 (73 nt)	137–209 (73nt)	150–222 (73 nt)	150–222 (73 nt)	162–234 (73 nt)
	xrRNA2	na	na	na	na	na	123–278 (67 nt)	214–280 (67 nt)	227–293 (67 nt)	228–293 (66 nt)	238–302 (65 nt)

(Continued)

TABLE 1 | (Continued)

UTR		5'UTR					3'UTR				
Genotypes		I	II	III	IV	V	I	II	III	IV	V
Domain2	PK1	na	na	na	na	na	83–87 107–111 (3 nt)	84–88 108–112 (3 nt)	97–101 121–125 (3 nt)	97–101 121–125 (3 nt)	109–113 133–137 (3 nt)
	PK2	na	na	na	na	na	240–242 261–263 (3 nt)	241–243 262–264 (3 nt)	254–256 275–277 (3nt)	254–256 275–277 (3 nt)	263–265 284–286 (3 nt)
	3'vrCS1	na	na	na	na	na	154–179 (26 nt)	155–180 (26 nt)	168–193 (26 nt)	168–193 (26 nt)	180–205 (26 nt)
	DB1	na	na	na	na	na	300–370 (71 nt)	301–371 (71 nt)	314–384 (71 nt)	314–384 (71 nt)	323–393 (71 nt)
	DB2	na	na	na	na	na	381–448 (68 nt)	382–449 (68 nt)	395–462 (68 nt)	395–462 (68 nt)	402–469 (68 nt)
	PK3	na	na	na	na	na	322–328 449–455 (7 nt)	323–329 450–456 (7 nt)	336–342 463–469 (7 nt)	336–342 463–469 (7 nt)	345–351 450–456 (7 nt)
	PK4	na	na	na	na	na	403–407 459–463 (5 nt)	404–408 459–463 (5 nt)	417–421 472–475 (5 nt)	417–421 472–476 (5 nt)	424–428 480–484 (5 nt)
	3'dbRCS	na	na	na	na	na	341–367 419–445 (27 nt)	342–368 420–446 (27 nt)	355–381 433–459 (27 nt)	355–381 433–459 (27 nt)	364–390 440–466 (27 nt)
	3'dbCS2	na	na	na	na	na	381–391 (11 nt)	382–392 (11 nt)	395–405 (11 nt)	395–405 (11 nt)	402–412 (11 nt)
	3'dbsHP	na	na	na	na	na	450–464 (15nt)	451–464 (14 nt)	464–477 (14 nt)	464–477 (14 nt)	471–485 (15 nt)
	3'cCS	na	na	na	na	na	460–470 (11 nt)	460–470 (11 nt)	473–483 (11 nt)	473–483 (11 nt)	481–491 (11 nt)
	3'sHP	na	na	na	na	na	473–489 (17 nt)	473–489 (17 nt)	486–502 (17 nt)	486–502 (17 nt)	494–510 (17 nt)
	3'DAR	na	na	na	na	na	473–478 (5 nt)	473–478 (5 nt)	486–491 (5 nt)	486–491 (5 nt)	494–498 (5 nt)
	3'UAR	na	na	na	na	na	481–504 (13 nt)	481–504 (14 nt)	495–417 (15 nt)	495–417 (13 nt)	502–525 (12 nt)
	3'SL	na	na	na	na	na	490–573 (84 nt)	490–573 (84 nt)	503–586 (84 nt)	503–586 (85 nt)	511–594 (84 nt)

| : Non-contiguous nucleic acid sequence; | : non-contiguous complementary nucleic acid sequence; NA: Not available. The results of nucleotide similarity and base composition were all within genotypes. SLA, stem loop A; SLB, stem loop B; UFS, 5'-UAR-flanking stem; 5'UAR, 5' upstream AUG region; 5'DAR, 5' downstream AUG region; cHP, capsid-coding region hairpin; 5'cCS, 5'cyclization sequence; VR, variable region; xrRNA, the exoribonuclease XRN1 resistant RNA; PK, pseudoknot; 3'vrCS1, the 3'UTR variable region conserved sequences 1; 3'dbRCS, the 3'UTR dumbbell structure repeated conserved sequences; 3'dbCS2, the 3'UTR dumbbell structure conserved sequences 2; 3'dbsHP, the 3'UTR DB region small hairpin; 3'cCS, 3'cyclization sequence; 3'DAR, 3' downstream AUG region; 3'UAR, 3'upstream AUG region upstream AUG region; 3'sHP, the 3'UTR short hairpin; 3'SL, the 3'UTR stem loop.

TABLE 2 | The nucleotide differences within the 5'UTRs between five JEV genotypes.

No.	Positions of mutation	Standard Strain	Genotypes				
		Nakayama	I	II	III	IV	V
1	28	G					A(3/3)
2	37	C		T(1/1)		T(1/1)	
3	44	A				G(1/1)	
4	45	A					G(3/3)
5	50	A				C(1/1)	
6	79	T				C(1/1)	
7	83	G				A(1/1)	
8	92	–	A(76/78)				
9	93	T	C(77/78)	C(1/1)			A(3/3)

A, adenine; G, guanine; C, cytosine; T, thymine. "–" indicates missing nucleotides. I–V indicate genotype I to genotype V of JEVs. In parentheses, each denominator indicates the total number of the JEV strains of each genotype while the numerators indicate the number of the mutated JEV strains.

SLB, within the linker of SLB and cHP (Denoted by red dashed lines in **Figure 5**). It is conserved among JEV genotypes. The cHP contains a CG-rich stem and an A-rich top loop. The cHP's loop structure of GI is larger than GIII. The 5' cCS is an 11nt long conserved sequence motif within JEV genotypes and is located downstream the cHP. (5' cCS: 5'-TCA ATATGCTG-3'). Except for JEV GIV, the cCS sequences of the other four JEV genotypes differ only in the position of the starting codon. The JEV GIV's cCS sequence is 5'-TCTATATGCTG-3', located 39 nt downstream of the ATG start site. There is a mutation (A > T) at the third position within the cCS sequence (**Figure 5**).

The Secondary Structures and Important Functional Sequences in the Japanese Encephalitis Virus 3'UTR

We found the 3'UTR of JEV consists of three domains, termed domain I, II, III (**Figure 6**). Domain I comprised approximately 300 nt, which is immediately downstream of the stop codon, and is highly variable and termed the variable region (VR). The VR contains a very high variable region (VVR) and three stem-loop stem structures. The VVR ranges from 48 to 74 nt in length and is enriched in AU dinucleotides. The secondary structures of the VVR of the different JEV genotypes are significantly different (**Figure 6**). There are two SL structures that are resistant to host 5'-3' exoribonuclease (XRN1) activity, termed xrRNA1 and xrRNA2, which are conserved in the secondary structure of the five JEV genotypes. In xrRNA1, a three-nucleotide spacer sequence (5'-C-G-G-3') located in the long-arm top loop pairs with a reverse complementary spacer sequence (5'-C-C-G-3') that lies in the stem structure to form the pseudoknot (PK) PK1 (**Figure 6**, labeled with black dashed line). In xrRNA2, a three-nucleotide sequence (5'-GCU-3') located in the long-arm top loop pairs with a 3-nucleotide sequence (5'-AGC-3') that lies in the linear sequences between the SL structures to form PK2. The xrRNA1 and xrRNA2 structures of JEV are separated by a long SL structure, which is 73 nt in length. The structure is moderately conserved in the different JEV genotypes, and we named it the 3'UTR variable region stem loop (3'vrSL). There is a 25 nt-length conserved sequence, termed the 3'UTR variable

region conserved sequences 1(3'vrCSL), which lies at the top loop of the 3'vrSL. A short SL structure with a length of approximately 11 nt is located after the xrRNA2 structure. The stem structures of the short SL structure are highly conserved in the five JEV genotypes, whereas the loop sequences are divergent. For genotypes I–III, the loop sequences are conserved (5'-GUUGA-3'), and for GIV and GV, the sequences are 5'-CAUGA-3' and 5'-GAAAA-3', respectively (**Figure 6**). Domain II consists of two dumbbell structures (DB1, DB2) and a 15 nt-length small hairpin structure. These structures are highly conserved among the five JEV genotypes. After searching the 3'UTRs of other mosquito-borne *Flavivirus* (WNV, YFV, ZIKV, and DENV), it is found that the 15 nt-length small hairpin structure could only be identified in the DB region in 3'UTRs of JEV. Thus, we named it the 3'UTR DB region small hairpin (3'dbsHP). The long-arm top loop of DB1 (5'-GAUGCAA-3') pairs with a reverse complementary sequence (5'-UUGCAUC-3'), which lies in the 3'dbsHP, to form PK3. The long-arm top loop of DB2 (5'-GCUGU-3') pairs with a reverse complementary sequence (5'-ACAGC-3') in the 3'dbsHP to form PK4 (**Figure 6**). The two PKs serve to further stabilize the DB structures. Besides the PKs located in the 3'dbsHP, partial sequences of 3'cCS sequence (5'-CAG CAU AUU GA-3') overlaps the 3'dbsHP (**Figure 6**, bright pink dashed box). In the internal loop and the short arm structure of both DB1 and DB2, there are 27 nt-length repeated conserved sequences (-AAGGACUAGAGGUUUAGAGGA GACCCG-), designated the 3'UTR dumbbell structure repeated conserved sequences (3'dbRCS).

Domain III is considered to be highly conserved across the *Flaviviruses* and is also known as a highly conserved region (HCR). However, we found that there are structural differences that exist in the JEV genotypes. Domain III is approximately 100 nt in length, consisting of a hairpin named the 3'UTR short hairpin (3'sHP) and a long terminal SL structure termed the 3'UTR stem loop (3'SL). The 3'SL structures are almost identical among GI to GIII. However, the shapes of the 3'SL structures of GIV and GV differ from those of GI to GIII (**Figure 6**). The sequence (5'-CCUGG-3') that lies in the stem of 3'sHP is 3'DAR. In the 3'SL structure, the 3'UAR, which consist of four discrete spacer sequences, that complement the 5' UAR (**Figure 6**).

TABLE 3 | The nucleotide differences within the 3'UTRs between JEV genotypes.

No.	Position of mutation	Standard strain	Genotypes					
		Nakayama	I	II	III	IV	V	
1	1–13	-					Muar/Tengah AGAACTCTTGAAA	XZ0934 -AAACTTTTGGTA*
2	24	G	-	-		A	A	A
3	25–26	GT	-	AT			TA	TA
4	28	G				A	T	T
5	36	A					G	—*
6	14–17	TGTG	-	-			ACAA	ATGA*
7	27	A					G	G
8	30–31	AA	GG				GT	GC*
9	33	A	T	T	G		A	—*
10	35	A					T	—*
11	37	A	G	G			T	T
12	38	C	T	T		T	T	T
13	39	C		T	T	G	T	T
14	41	-					G	T*
15	45–47	AAA	GTG	GTA				
16	50	A				G	G	G
17	54	A	G	G		G		
18	56	-	G					
19	59	G	A	A		A	A	A
20	61	G				T	A	A
21	62	A					T	T
22	67	G					T	T
23	68–69	TA	-	-	CA	TG	-	-
24	71	G		A		A	A	A
25	72	C					G	A*
26	75	A	G					
27	76	T					G	G
28	78	G					A	G*
29	88–89	AG					GA	GA
30	91–93	AAA				GTT	GCG	GTA*
31	96–97	CT					TC	TC
32	108–109	TA					AG	TG*
33	113	G	A				A	A
34	133	T					C	C
35	139	T					C	C
36	172	A	G			G	C	C
37	179	G	G	G	G	G	A	A
38	180	A	G				G	G
39	207	T	C			A	A	A
40	219	C					T	T
41	222	T	C	C				
42	226	A				T	G	G
43	231	A		G		G	G	G
44	238–240	AAC					G-T	G-T
45	251–252	AA					G-	G-
46	253	A	T			T	-	-
47	254–256	TTT	TCT		TAT	CTT	TAA	CAA*
48	265	C					T	T
49	271	G				A	A	A
50	279	G					A	A

(Continued)

TABLE 3 | (Continued)

No.	Position of mutation	Standard strain	Genotypes				
			I	II	III	IV	V
51	285–286	CG				TA	TA
52	294	A					G
53	302	T					C
54	307	T					A
55	309	C	A	A		A	A
56	318–320	TTG				AAA	ATG*
57	338	G				A	A
58	343	G				A	A
59	348	G	A				
60	360	C				T	T
61	361	G	T				
62	365	T				C	C
63	400–401	AC				–	–
64	404	C				G	G
65	407	C	T	T		G	A*
66	419	G				A	A
67	421	C				T	T
68	423–424	CC				CT	TT
69	438	G				A	A
70	440–441	AG		AA		GA	GA
71	487	–	A			A	A
72	508	A				T	T
73	515	G				A	A
74	528	C				A	A
75	550	T				A	A

A, adenine; G, guanine; C, cytosine; and T, thymine. “–” indicates missing nucleotides.

I–V indicate genotype I to genotype V of JEVs. * Indicates in this site the mutation were equal within the strain XZ0934, Muar and Tengah.

TABLE 4 | The average nucleotide similarity of the JEVs' UTRs.

	Between different genotypes (%)					Within each genotype (%)	
	I	II	III	IV	V	5'UTR	3'UTR
I	*	97.06	96.75	90.93	94.72	98.31	98.71
II	94.48	*	97.63	93.80	96.23	99.36	97.83
III	91.88	92.69	*	93.55	96.27	100	100
IV	86.45	87.40	89.44	*	91.07	100	100
V	81.50	81.67	82.25	80.70	*	99.34	96.6

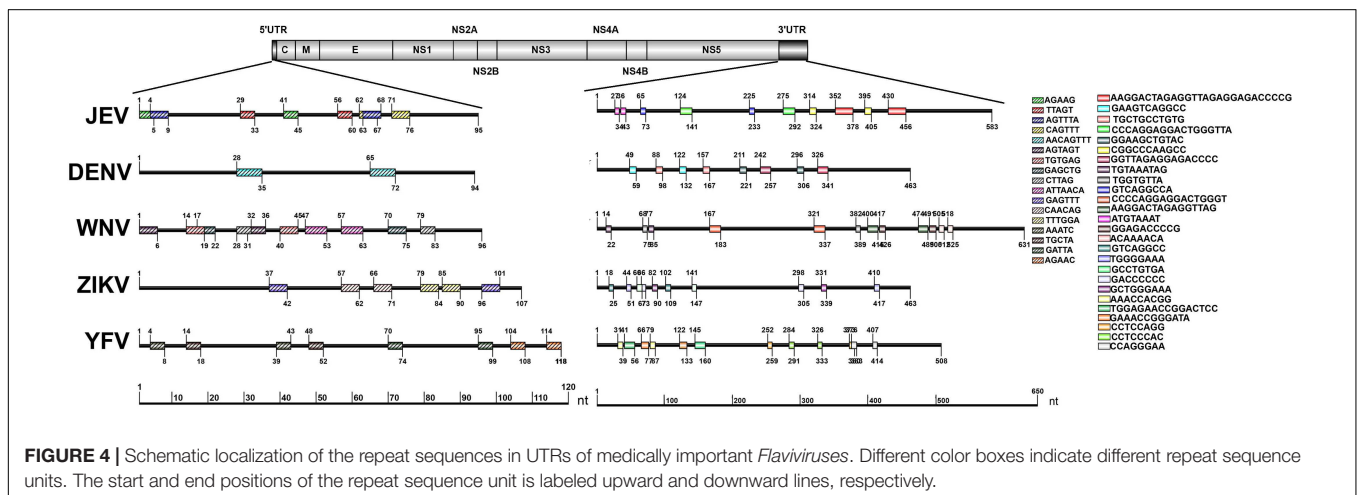
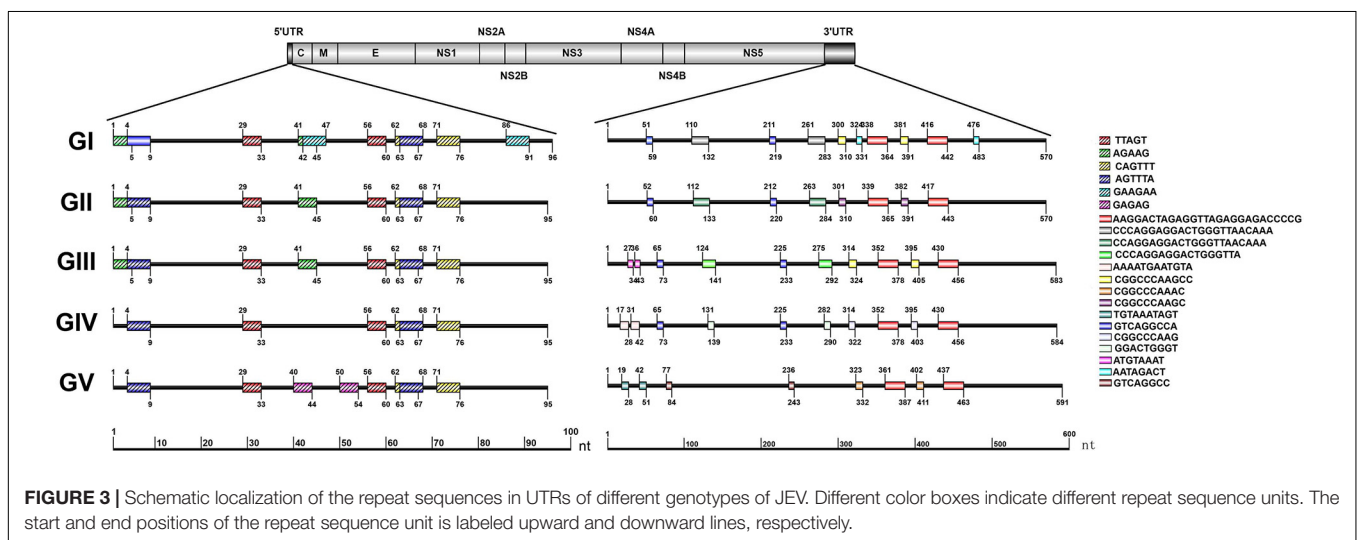
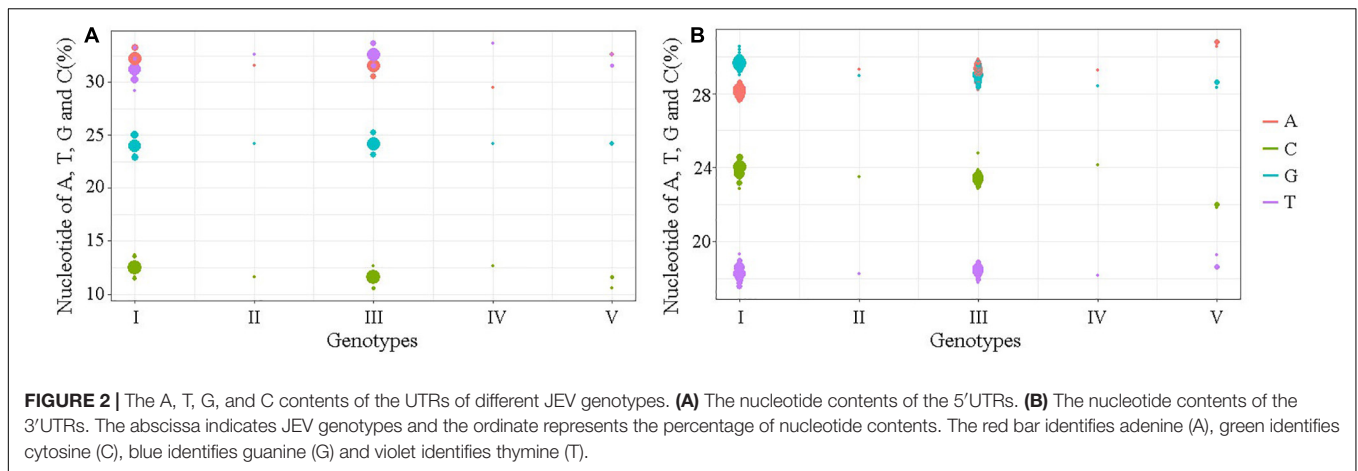
The average nucleotide similarity of 5'UTR is shown in the upper right corner and the value of 3'UTR is in the lower left corner.

* indicates identical.

Sequence Feature Information-Guided Japanese Encephalitis Virus Genome Typing

Prior to generate the NJ phylogenetic tree, the average evolutionary divergence over all sequence pairs was computed. The average divergence values for 5'UTR, 3'UTR, and 3'VR are 0.09 ± 0.01 , 0.07 ± 0.01 , and 0.04 ± 0.01 , respectively. The results proves the datasets are suitable for generating distance based phylogenetic trees. The ModelFinder program was used to select the best-fit nucleotide substitution model

based on the Bayesian information criterion (BIC) before generating the ML tree. The best-fit models for the 3'VR, PrM, E and the ORF gene datasets were GTR + G4, GTR + G4, GTR + I + G4, GTR + F + I + G4, respectively. The phylogenetic analyses showed that the JEV isolates can be clustered into five genotypes based on the JEV 3'UTR's VR gene sequences using both ML and NJ methods. The normalized RF values of the 3'VR tree vs. the ORF, E, and preE trees were 0.29, 0.31, and 0.34, respectively. Further analysis revealed that the main branches of the different phylogenetic trees were identical (**Figure 7**).



DISCUSSION

This study provides comprehensive and detailed information of the sequence features and the exact sequence composition,

position and distribution of the *Flavivirus*-conserved *cis*-acting elements in the JEV UTRs. The 5' and 3' terminal structures of JEV share the general characteristics of *Flaviviruses*, the reported structures and *cis*-acting elements of other *Flaviviruses* are all

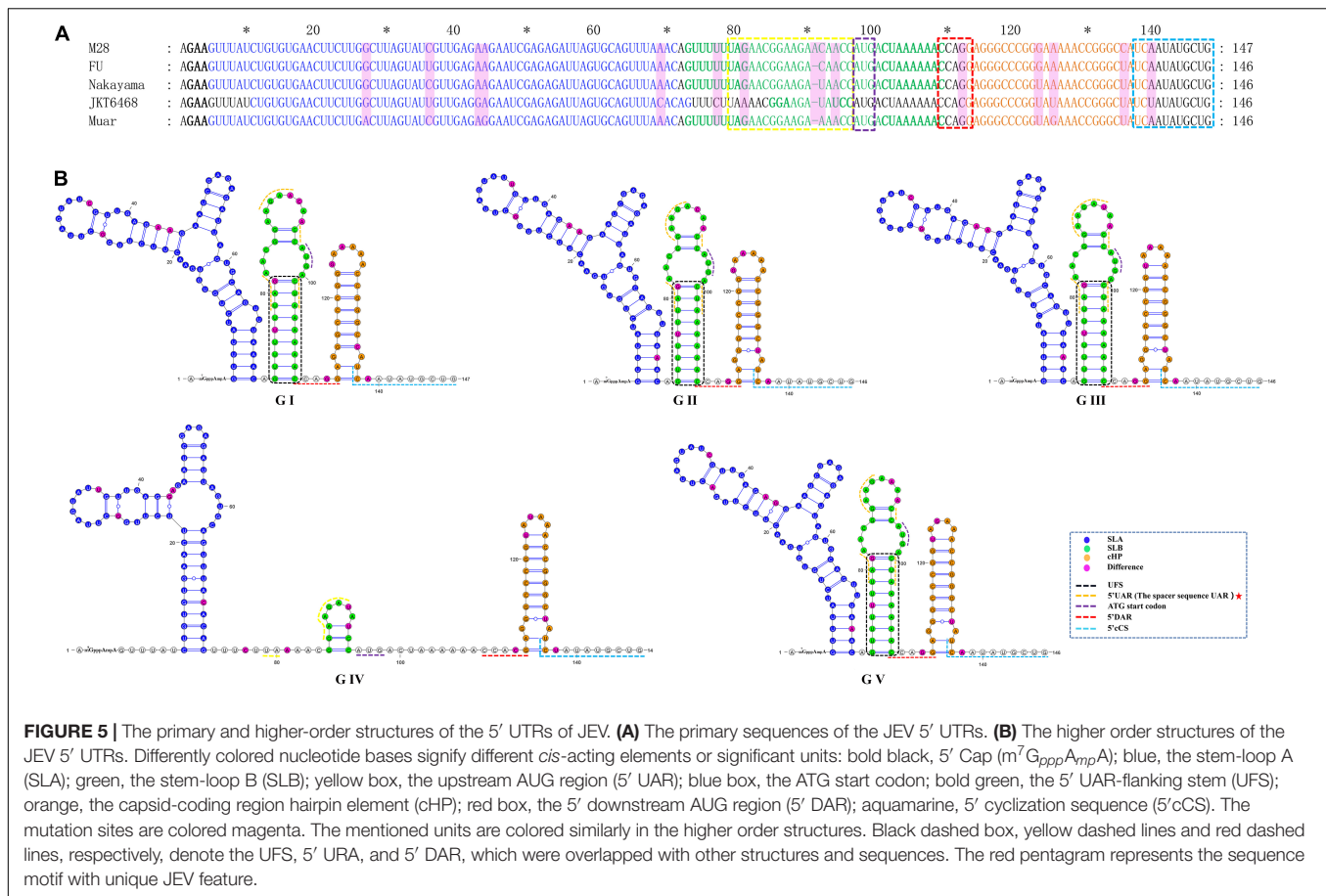


FIGURE 5 | The primary and higher-order structures of the 5' UTRs of JEV. **(A)** The primary sequences of the JEV 5' UTRs. **(B)** The higher order structures of the JEV 5' UTRs. Differently colored nucleotide bases signify different *cis*-acting elements or significant units: bold black, 5' Cap ($m^7G_{ppp}A_{mp}A$); blue, the stem-loop A (SLA); green, the stem-loop B (SLB); yellow box, the upstream AUG region (5' UAR); blue box, the ATG start codon; bold green, the 5' UAR-flanking stem (UFS); orange, the capsid-coding region hairpin element (cHP); red box, the 5' downstream AUG region (5' DAR); aquamarine, 5' cyclization sequence (5'cCS). The mutation sites are colored magenta. The mentioned units are colored similarly in the higher order structures. Black dashed box, yellow dashed lines and red dashed lines, respectively, denote the UFS, 5' UAR, and 5' DAR, which were overlapped with other structures and sequences. The red pentagram represents the sequence motif with unique JEV feature.

existed in the UTRs of JEV. The structure and *cis*-acting elements' sequence comparison with other mosquito-borne *Flaviviruses* (WNV, YFV, ZIKV, DENV) demonstrated the existence of a JEV-specific structure and a sequence motif with a unique feature of JEV UTRs. (i) The 3' dbHP, which is a small hair-pin structure located in the DB region within the 3' UTR. The 3' dbHP is highly conserved among five JEV genotypes and contains three functional important sequences (PK3, PK4, and 3' cCS) that involved in DB structure maintaining and viral genome cyclization. (ii) The spacer sequence UARs. The UARs of JEV consist of four discrete spacer sequences whereas the UARs of other mosquito-borne *Flaviviruses* (WNV, YFV, ZIKV, DENV) are continuous sequences. During viral RNA syntheses, the 5'UAR hybridizes with 3'UAR to form a complementary pairing structure that aids viral genome cyclization. The molecular dynamics and the function of the segmented UARs in JEV genome cyclization remain unclear. Given the importance of JEV, it is worth exploring the molecular functions of the unique structure and *cis*-acting element existent in the UTRs.

Our findings demonstrated that repeated sequences are found not only in the UTR of JEV but also in those of the other medically important mosquito-borne *Flaviviruses*, including WNV, YFV, ZIKV, and DENV. However, these repeated sequences differ in nucleotide composition, length and position among the different viruses. These results indicate

that the UTRs of *Flaviviruses* contain repeated sequences, but these sequences are not consistently conserved across species. Although repeated sequences are present in the UTRs of GI-V JEV, their lengths, distances between sequences, distributions in the UTR, distances between the repeated sequences and the initiation (termination) codons differ among the genotypes. Despite differences in host origin, regional distribution and isolation time, the length and position of the repeated sequences are highly conserved within the same JEV genotype. Therefore, these repeated sequences are important molecular markers for distinguishing JEV genotypes. The interaction between the conserved regions of the viral sequence and binding proteins is a long-term evolutionary interaction between the virus and the host cell. Even minor mutations in the nucleotide sequence can affect the binding affinity of the interacting proteins (Jin, 2001). *In vitro* experiments have demonstrated that removal of all repeat sequences from *Alphaviruses* maintains their viabilities but reduces their titers (Jin, 2001). However, the decrease in virus titer significantly varied among the different host cells (Zhai et al., 2008). This suggests that the repeated sequences can directly affect the replication efficiency of the virus and play varying roles in different host cells, demonstrating a significant host specificity. The latest research reveals that the repeated conserved sequences in the 3'UTR are involved in subgenomic flaviviral RNA production and viral

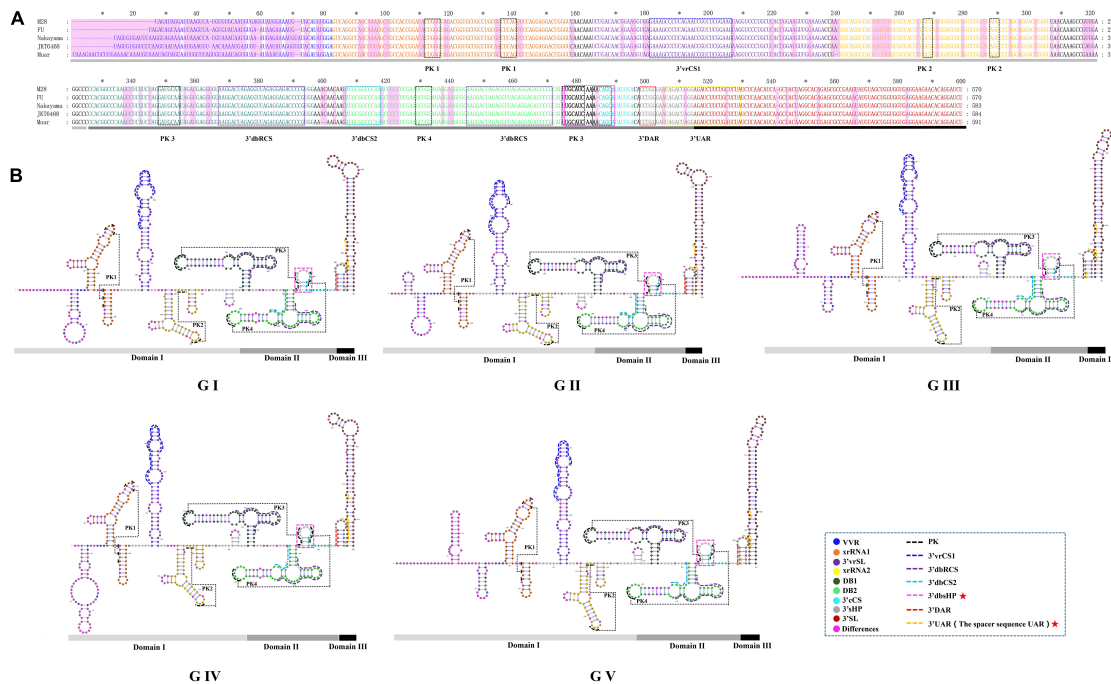


FIGURE 6 | The primary and higher order structures of the 3'UTRs of JEV. **(A)** The primary sequences of the JEV 3'UTRs. **(B)** The higher order structures of the JEV 3'UTRs. Differently colored nucleotide bases signify different structures, *cis*-acting elements or significant sequence motifs: blue, the very variable region (VVR); orange, the exoribonuclease resistant RNA (xrRNA1); purple, the 3'UTR variable region stem loop (3'vrSL); light yellow, the exoribonuclease resistant RNA (xrRNA2); dark green, dumbbell structure 1 (DB1); light green, dumbbell structure 2 (DB2); bold (black and aquamarine), the 3'UTR DB region small hairpin (3'dbSHP); aquamarine, 3'cyclization sequence (3'cCS); gray, the 3'UTR short hairpin (3'sHP); brick red, the 3'UTR stem loop (3'SL). The *cis*-acting elements or sequence motifs which were overlapped with other structures were labeled with different colored dashed line box: black, pseudoknot PK; blue, the 3'UTR variable region conserved sequences 1 (3'vrCS1); purple, the 3'UTR dumbbell structure repeated conserved sequences (3'dbRCS); light blue, the 3'UTR dumbbell structure conserved sequences 2 (3'dbCS2); bright pink, the 3'UTR DB region small hairpin (3'dbSHP); red, the 3'downstream AUG region (3'DAR); yellow, the 3' upstream AUG region (3'UAR). The magenta blocks represent the differences within five JEV genotypes. The Domain I, II, and III are indicated with light gray, dark gray and black bars, respectively. The mentioned units are labeled similarly in the higher order structures. The red pentagram represents the JEV specific structure or sequence motifs.

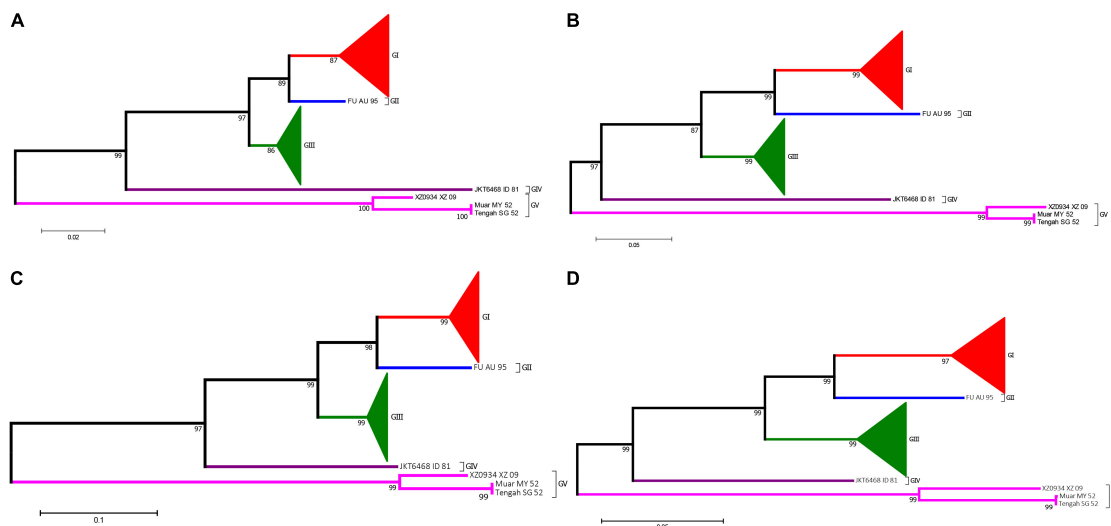


FIGURE 7 | Phylogenetic analysis of JEV. **(A)** The phylogenetic tree based on the sequences (1–300 nt) of domain I (VR) within the 3'UTRs of JEV. **(B)** The phylogenetic tree based on the PrM gene of JEVs. **(C)** The phylogenetic tree based on the E gene of JEVs. **(D)** The phylogenetic tree based on the ORF gene of JEVs. Red, blue, green, purple and violet were used to mark genotype I, II, III, IV, and V of JEV, respectively. The triangles were used to condense strains of the same genotypes.

virulence, indicating the importance of the repeated sequences for *Flaviviruses* (Zhang et al., 2020). JEV has the longest repeated sequences compared with other *Flaviviruses*, indicating that the use of long repeated sequences for completing the virus lifecycle is unique to JEV. These repeated sequences might play an important role in the successful viral replication and transmission. Nonetheless, further studies will be required to confirm the influence of these repeated sequences on viral biological functions.

In the present study, we find that the 3'UTRs are more divergent than the 5'UTRs in both the primary sequence and the higher-order structures of JEV. The JEV 3'UTR consists of three domains. Domain I is considered to be the most variable region within the 3'UTRs among all the arthropod-borne *Flaviviruses*, and thus this region has been termed the variable region (VR) (Proutski et al., 1997; Ng et al., 2017). In our study, it was also demonstrated that domain I is the most variable region within JEV and that this 300 nt-length region exhibits obvious genotype-specific features.

Currently, JEV can be classified into five genotypes (GI to GV), and the distribution, host range and pathogenesis among the five genotypes are quite different (Wang and Liang, 2015; Gao et al., 2019). In particular, JEV has already spread from its traditional endemic region in Asia to Europe (Platonov et al., 2012; Ravanini et al., 2012), and JEV-infected patients have even been identified in Africa (Simon-Loriere et al., 2017). Therefore, identification of the JEV genotype has an important significance for the prevention and treatment of JE. The current methods for JEV genotyping are all based on the protein-coding region sequences, such as the E or the PrM gene (Chen et al., 1990, 1992; Solomon et al., 2003; Wang et al., 2007). Our study demonstrated that the JEV 3'UTR VR region exhibits a strong genotype-specific and that this specificity does not change with the isolation time, distribution or the host (vector). Therefore, this 300 nt-long nucleotide sequence is ideal for JEV genotyping. The phylogenetic analysis results, based on the complete ORF genome sequence (10,300 nt), the E gene (1500 nt), the PrM gene (500 nt) and the 3'UTR conserved sequence (300 nt) using different phylogenetic algorithms, generated consistent results (Figure 6), which further suggests that the VR region sequence within the 3'UTR is an ideal sequence marker for JEV genotyping. Whether the VR region sequences of other *Flaviviruses* also exhibit genotype-specific features and could have been used for genome typing needs further evaluation.

Our study compared the sequence and predicted structural differences in the 5' and 3' UTRs of 160 JEV strains isolated over an 80-year period. GI and GIII are the most widespread genotypes of JEV and cause human viral encephalitis and animal

diseases (Zheng et al., 2012). All the previously reported GI and GIII strains were included and analyzed to systematically compare them and identify any nucleotide changes attributed to time, host, vector, and geographical distribution. We revealed nucleotide differences in the 5' and 3' UTR associated with genotype but not isolation time, host, vector, or geographical distribution. The imbalance in sequence information across the JEV genotypes in the JEV sequence dataset is because only a few JEV strains belonging to GII, GIV, and GV (Williams et al., 2000; Li et al., 2011; Woo et al., 2020) have been isolated in nature. Enhanced surveillance of JEV in nature to obtain sufficient genomic sequence information of different JEV genotypes to improve the understanding of its comprehensive genetic characteristics is highly recommended.

DATA AVAILABILITY STATEMENT

The original contributions presented in the study are included in the article/**Supplementary Material**, further inquiries can be directed to the corresponding author/s.

AUTHOR CONTRIBUTIONS

HL and GL carried out the study design and contributed to the revision of the manuscript. HL, JZ, and YN performed the experiment and data analysis. GL and HL wrote the manuscript. All authors read and approved the final manuscript.

FUNDING

This work was supported by grants from the National Natural Science Foundation of China (81301479, 81290342), a Development Grant of the State Key Laboratory of Infectious Disease Prevention and Control (2014SKLID103 and 2018SKLID309), the Key R&D projects in Zibo city (2020kj100011), and the Natural Science Foundation of Shandong Province, China (ZR2013HQ008). The funders had no role in study design, data collection and analysis, decision to publish, or preparation of the manuscript.

SUPPLEMENTARY MATERIAL

The Supplementary Material for this article can be found online at: <https://www.frontiersin.org/articles/10.3389/fmicb.2021.730045/full#supplementary-material>

REFERENCES

- Alvarez, D. E., Lodeiro, M. F., Luduena, S. J., Pietrasanta, L. I., and Gamarnik, A. V. (2005). Long-range RNA-RNA interactions circularize the dengue virus genome. *J. Virol.* 79, 6631–6643. doi: 10.1128/JVI.79.11.6631-6643.2005
- Brinton, M. A., Fernandez, A. V., and Disposito, J. H. (1986). The 3'-nucleotides of flavivirus genomic RNA form a conserved secondary structure. *Virology* 153, 113–121. doi: 10.1016/0042-6822(86)90012-7
- Burland, T. G. (2000). DNASTAR's Lasergene sequence analysis software. *Methods Mol. Biol.* 132, 71–91. doi: 10.1385/1-59259-192-2:71
- Cao, L., Fu, S., Gao, X., Li, M., Cui, S., Li, X., et al. (2016). Low protective efficacy of the current Japanese encephalitis vaccine against the emerging Genotype 5 Japanese encephalitis virus. *PLoS Negl. Trop. Dis.* 10:e0004686. doi: 10.1371/journal.pntd.0004686
- Chang, R. Y., Hsu, T. W., Chen, Y. L., Liu, S. F., Tsai, Y. J., Lin, Y. T., et al. (2013). Japanese encephalitis virus non-coding RNA inhibits activation of interferon by

- blocking nuclear translocation of interferon regulatory factor 3. *Vet. Microbiol.* 166, 11–21. doi: 10.1016/j.vetmic.2013.04.026
- Chapman, E. G., Moon, S. L., Wilusz, J., and Kieft, J. S. (2014). RNA structures that resist degradation by Xrn1 produce a pathogenic Dengue virus RNA. *Elife* 3:e01892. doi: 10.7554/eLife.01892.021
- Chen, W. R., Rico-Hesse, R., and Tesh, R. B. (1992). A new genotype of Japanese encephalitis virus from Indonesia. *Am. J. Trop. Med. Hyg.* 47, 61–69. doi: 10.4269/ajtmh.1992.47.61
- Chen, W. R., Tesh, R. B., and Rico-Hesse, R. (1990). Genetic variation of Japanese encephalitis virus in nature. *J. Gen. Virol.* 71, 2915–2922. doi: 10.1099/0022-1317-71-12-2915
- Clyde, K., Barrera, J., and Harris, E. (2008). The capsid-coding region hairpin element (cHP) is a critical determinant of dengue virus and West Nile virus RNA synthesis. *Virology* 379, 314–323. doi: 10.1016/j.virol.2008.06.034
- Darty, K., Denise, A., and Ponty, Y. (2009). VARNAs: interactive drawing and editing of the RNA secondary structure. *Bioinformatics* 25, 1974–1975. doi: 10.1093/bioinformatics/btp250
- Erlanger, T. E., Weiss, S., Keiser, J., Utzinger, J., and Wiedenmayer, K. (2009). Past, present, and future of Japanese encephalitis. *Emerg. Infect. Dis.* 15, 1–7. doi: 10.3201/eid1501.080311
- Filomatori, C. V., Carballada, J. M., Villordo, S. M., Aguirre, S., Pallares, H. M., Maestre, A. M., et al. (2017). Dengue virus genomic variation associated with mosquito adaptation defines the pattern of viral non-coding RNAs and fitness in human cells. *PLoS Pathog.* 13:e1006265. doi: 10.1371/journal.ppat.1006265
- Filomatori, C. V., Lodeiro, M. F., Alvarez, D. E., Samsa, M. M., Pietrasanta, L., and Gamarnik, A. V. (2006). A 5' RNA element promotes dengue virus RNA synthesis on a circular genome. *Genes Dev.* 20, 2238–2249. doi: 10.1101/gad.1444206
- Friebe, P., Shi, P. Y., and Harris, E. (2011). The 5' and 3' downstream AUG region elements are required for mosquito-borne flavivirus RNA replication. *J. Virol.* 85, 1900–1905. doi: 10.1128/JVI.02037-10
- Gao, X., Liu, H., Li, M., Fu, S., and Liang, G. (2015). Insights into the evolutionary history of Japanese encephalitis virus (JEV) based on whole-genome sequences comprising the five genotypes. *Virol. J.* 12:43. doi: 10.1186/s12985-015-0270-z
- Gao, X., Liu, H., Li, X., Fu, S., Cao, L., Shao, N., et al. (2019). Changing geographic distribution of Japanese Encephalitis virus Genotypes, 1935–2017. *Vector Borne Zoonotic Dis.* 19, 35–44. doi: 10.1089/vbz.2018.2291
- Garcia-Blanco, M. A., Vasudevan, S. G., Bradrick, S. S., and Nicchitta, C. (2016). Flavivirus RNA transactions from viral entry to genome replication. *Antivir. Res.* 134, 244–249. doi: 10.1016/j.antiviral.2016.09.010
- Gebhard, L. G., Filomatori, C. V., and Gamarnik, A. V. (2011). Functional RNA elements in the dengue virus genome. *Viruses* 3, 1739–1756. doi: 10.3390/v3091739
- Hahn, C. S., Hahn, Y. S., Rice, C. M., Lee, E., Dalgarno, L., Strauss, E. G., et al. (1987). Conserved elements in the 3' untranslated region of flavivirus RNAs and potential cyclization sequences. *J. Mol. Biol.* 198, 33–41. doi: 10.1016/0022-2836(87)90455-4
- Halstead, S. B., and Jacobsen, J. (2008). “Japanese Encephalitis vaccines,” in *Vaccines*, 5th Edn, eds S. A. Plotkin, W. A. Orenstein, and P. A. Offit (Amsterdam: Elsevier).
- Hegde, N. R., and Gore, M. M. (2017). Japanese encephalitis vaccines: immunogenicity, protective efficacy, effectiveness, and impact on the burden of disease. *Hum. Vaccin. Immunother.* 13, 1–18. doi: 10.1080/21645515.2017.1285472
- Hodge, K., Kamkaew, M., Pisitkun, T., and Chimnarong, S. (2019). Flavours of Flaviviral RNA structure: towards an integrated view of RNA function from translation through Encapsidation. *Bioessays* 41:e1900003. doi: 10.1002/bies.201900003
- Jin, Q. (2001). *Medical & Molecular Virology*. Beijing: Science Press.
- Kalyaanamoorthy, S., Minh, B. Q., Wong, T. K., von Haeseler, A., and Jermini, L. S. (2017). ModelFinder: fast model selection for accurate phylogenetic estimates. *Nat. Methods* 14, 587–589. doi: 10.1038/nmeth.4285
- Kieft, J. S., Rabe, J. L., and Chapman, E. G. (2015). New hypotheses derived from the structure of a flaviviral Xrn1-resistant RNA: conservation, folding, and host adaptation. *RNA Biol.* 12, 1169–1177. doi: 10.1080/15476286.2015.1094599
- Kumar, S., Stecher, G., Li, M., Knyaz, C., and Tamura, K. (2018). MEGA X: molecular evolutionary genetics analysis across computing platforms. *Mol. Biol. Evol.* 35, 1547–1549. doi: 10.1093/molbev/msy096
- Kuwata, R., Torii, S., Shimoda, H., Supriyono, S., Phichitraslip, T., Prasertsincharoen, N., et al. (2020). Distribution of Japanese Encephalitis virus, Japan and Southeast Asia, 2016–2018. *Emerg. Infect. Dis.* 26, 125–128. doi: 10.3201/eid2601.190235
- Lerat, E. (2010). Identifying repeats and transposable elements in sequenced genomes: how to find your way through the dense forest of programs. *Heredity* 104, 520–533. doi: 10.1038/hdy.2009.165
- Lewis, L., Taylor, H. G., Sorem, M. B., Norcross, J. W., and Kindsvatter, V. H. (1947). Japanese B encephalitis: clinical observations in an outbreak on okinawa shima. *Arch. Neurol. Psychiatry* 57, 430–463. doi: 10.1001/archneurpsyc.1947.02300270048004
- Li, M. H., Fu, S. H., Chen, W. X., Wang, H. Y., Guo, Y. H., Liu, Q. Y., et al. (2011). Genotype v Japanese encephalitis virus is emerging. *PLoS Negl. Trop. Dis.* 5:e1231. doi: 10.1371/journal.pntd.0001231
- Lindenbach, B. D., Thiel, H. J., and Rice, C. M. (2007). “Flaviviridae: the viruses and their replication,” in *Fields Virology*, 5th Edn, eds D. M. Knipe and P. M. Howley (Philadelphia, PA: Lippincott Williams & Wilkins).
- Liu, W., Xie, Y., Ma, J., Luo, X., Nie, P., Zuo, Z., et al. (2015). IBS: an illustrator for the presentation and visualization of biological sequences. *Bioinformatics* 31, 3359–3361. doi: 10.1093/bioinformatics/btv362
- Liu, Z. Y., and Qin, C. F. (2020). Structure and function of cis-acting RNA elements of flavivirus. *Rev. Med. Virol.* 30:e2092. doi: 10.1002/rmv.2092
- Liu, Z. Y., Li, X. F., Jiang, T., Deng, Y. Q., Ye, Q., Zhao, H., et al. (2016). Viral RNA switch mediates the dynamic control of flavivirus replicase recruitment by genome cyclization. *Elife* 5:e17636. doi: 10.7554/eLife.17636.044
- Moon, S. L., Anderson, J. R., Kumagai, Y., Wilusz, C. J., Akira, S., Khromykh, A. A., et al. (2012). A noncoding RNA produced by arthropod-borne flaviviruses inhibits the cellular exoribonuclease XRN1 and alters host mRNA stability. *RNA* 18, 2029–2040. doi: 10.1261/rna.034330.112
- Ng, W. C., Soto-Acosta, R., Bradrick, S. S., Garcia-Blanco, M. A., and Ooi, E. E. (2017). The 5' and 3' untranslated regions of the flaviviral genome. *Viruses* 9:137. doi: 10.3390/v9060137
- Ni, H., Burns, N. J., Chang, G. J., Zhang, M. J., Wills, M. R., Trent, D. W., et al. (1994). Comparison of nucleotide and deduced amino acid sequence of the 5' non-coding region and structural protein genes of the wild-type Japanese encephalitis virus strain SA14 and its attenuated vaccine derivatives. *J. Gen. Virol.* 75(Pt 6), 1505–1510. doi: 10.1099/0022-1317-75-6-1505
- Pan, X. L., Liu, H., Wang, H. Y., Fu, S. H., Liu, H. Z., Zhang, H. L., et al. (2011). Emergence of genotype I of Japanese encephalitis virus as the dominant genotype in Asia. *J. Virol.* 85, 9847–9853. doi: 10.1128/JVI.00825-11
- Pijlman, G. P., Funk, A., Kondratieva, N., Leung, J., Torres, S., van der, et al. (2008). A highly structured, nuclease-resistant, noncoding RNA produced by flaviviruses is required for pathogenicity. *Cell Host Microbe* 4, 579–591. doi: 10.1016/j.chom.2008.10.007
- Platonov, A., Rossi, G., Karan, L., Mironov, K., Busani, L., and Rezza, G. (2012). Does the Japanese encephalitis virus (JEV) represent a threat for human health in Europe? detection of JEV RNA sequences in birds collected in Italy. *Euro. Surveill.* 17:20241. doi: 10.2807/ese.17.32.20241-en
- Proutski, V., Gould, E. A., and Holmes, E. C. (1997). Secondary structure of the 3' untranslated region of flaviviruses: similarities and differences. *Nucleic Acids Res.* 25, 1194–1202. doi: 10.1093/nar/25.6.1194
- Ravanini, P., Huhtamo, E., Ilaria, V., Crobu, M. G., Nicosia, A. M., Servino, L., et al. (2012). Japanese encephalitis virus RNA detected in Culex pipiens mosquitoes in Italy. *Euro. Surveill.* 17:20221. doi: 10.2807/ese.17.28.20221-en
- Robinson, D. F., and Foulds, L. R. (1981). Comparison of phylogenetic trees. *Math. Biosci.* 53, 131–147. doi: 10.1016/0025-5564(81)90043-2
- Sanford, T. J., Mears, H. V., Fajardo, T., Locker, N., and Sweeney, T. R. (2019). Circularization of flavivirus genomic RNA inhibits de novo translation initiation. *Nucleic Acids Res.* 47, 9789–9802. doi: 10.1093/nar/gkz686
- Schuh, A. J., Li, L., Tesh, R. B., Innis, B. L., and Barrett, A. D. (2010). Genetic characterization of early isolates of Japanese encephalitis virus: genotype II has been circulating since at least 1951. *J. Gen. Virol.* 91(Pt 1), 95–102. doi: 10.1099/vir.0.013631-0
- Simon-Loriere, E., Faye, O., Prot, M., Casademont, I., Fall, G., Fernandez-Garcia, M. D., et al. (2017). Autochthonous Japanese Encephalitis with yellow fever coinfection in Africa. *N. Engl. J. Med.* 376, 1483–1485. doi: 10.1056/NEJMc1701600

- Smith, M. R. (2020). Information theoretic generalized robinson-foulds metrics for comparing phylogenetic trees. *Bioinformatics* 36, 5007–5013. doi: 10.1093/bioinformatics/btaa614
- Solomon, T., Ni, H., Beasley, D. W., Ekkelenkamp, M., Cardoso, M. J., and Barrett, A. D. (2003). Origin and evolution of Japanese encephalitis virus in southeast Asia. *J. Virol.* 77, 3091–3098. doi: 10.1128/JVI.77.5.3091-3098.2003
- Sumiyoshi, H., Mori, C., Fuke, I., Morita, K., Kuhara, S., Kondou, J., et al. (1987). Complete nucleotide sequence of the Japanese encephalitis virus genome RNA. *Virology* 161, 497–510. doi: 10.1016/0042-6822(87)90144-9
- Thompson, J. D., Gibson, T. J., Plewniak, F., Jeanmougin, F., and Higgins, D. G. (1997). The CLUSTAL_X windows interface: flexible strategies for multiple sequence alignment aided by quality analysis tools. *Nucleic Acids Res.* 25, 4876–4882. doi: 10.1093/nar/25.24.4876
- Villordo, S. M., and Gamarnik, A. V. (2009). Genome cyclization as strategy for flavivirus RNA replication. *Virus Res.* 139, 230–239. doi: 10.1016/j.virusres.2008.07.016
- Wang, H. Y., Takasaki, T., Fu, S. H., Sun, X. H., Zhang, H. L., Wang, Z. X., et al. (2007). Molecular epidemiological analysis of Japanese encephalitis virus in China. *J. Gen. Virol.* 88, 885–894. doi: 10.1099/vir.0.82185-0
- Wang, H., and Liang, G. (2015). Epidemiology of Japanese encephalitis: past, present, and future prospects. *Ther. Clin. Risk Manag.* 11, 435–448. doi: 10.2147/TCRM.S51168
- Wang, H., Han, M., Qi, J., Hilgenfeld, R., Luo, T., Shi, Y., et al. (2017). Crystal structure of the C-terminal fragment of NS1 protein from yellow fever virus. *Sci. China Life Sci.* 60, 1403–1406. doi: 10.1007/s11427-017-9238-8
- Westaway, E. G., Mackenzie, J. M., and Khromykh, A. A. (2003). Kunjin RNA replication and applications of Kunjin replicons. *Adv. Virus Res.* 59, 99–140. doi: 10.1016/S0065-3527(03)59004-2
- Williams, D. T., Wang, L. F., Daniels, P. W., and Mackenzie, J. S. (2000). Molecular characterization of the first Australian isolate of Japanese encephalitis virus, the FU strain. *J. Gen. Virol.* 81(Pt 10), 2471–2480. doi: 10.1099/0022-1317-81-10-2471
- Woo, J. H., Jeong, Y. E., Jo, J. E., Shim, S. M., Ryou, J., Kim, K. C., et al. (2020). Genetic characterization of Japanese encephalitis virus Genotype 5 isolated from patient, South Korea, 2015. *Emerg. Infect. Dis.* 26, 1002–1006. doi: 10.3201/eid2605.190977
- Zeng, M., Duan, Y., Zhang, W., Wang, M., Jia, R., Zhu, D., et al. (2020). Universal RNA secondary structure insight into Mosquito-Borne Flavivirus (MBFV) cis-Acting RNA biology. *Front. Microbiol.* 11:473. doi: 10.3389/fmicb.2020.00473
- Zhai, Y. G., Wang, H. Y., Sun, X. H., Fu, S. H., Wang, H. Q., Attoui, H., et al. (2008). Complete sequence characterization of isolates of Getah virus (genus Alphavirus, family Togaviridae) from China. *J. Gen. Virol.* 89, 1446–1456. doi: 10.1099/vir.0.83607-0
- Zhang, Q. Y., Li, X. F., Niu, X., Li, N., Wang, H. J., Deng, C. L., et al. (2020). Short Direct Repeats in the 3' untranslated region are involved in Subgenomic Flaviviral RNA Production. *J. Virol.* 94:e1175-19. doi: 10.1128/JVI.01175-19
- Zheng, Y., Li, M., Wang, H., and Liang, G. (2012). Japanese encephalitis and Japanese encephalitis virus in mainland China. *Rev. Med. Virol.* 22, 301–322. doi: 10.1002/rmv.1710
- Zuker, M. (2003). Mfold web server for nucleic acid folding and hybridization prediction. *Nucleic Acids Res.* 31, 3406–3415. doi: 10.1093/nar/gkg595

Conflict of Interest: The authors declare that the research was conducted in the absence of any commercial or financial relationships that could be construed as a potential conflict of interest.

Publisher's Note: All claims expressed in this article are solely those of the authors and do not necessarily represent those of their affiliated organizations, or those of the publisher, the editors and the reviewers. Any product that may be evaluated in this article, or claim that may be made by its manufacturer, is not guaranteed or endorsed by the publisher.

Copyright © 2021 Liu, Zhang, Niu and Liang. This is an open-access article distributed under the terms of the Creative Commons Attribution License (CC BY). The use, distribution or reproduction in other forums is permitted, provided the original author(s) and the copyright owner(s) are credited and that the original publication in this journal is cited, in accordance with accepted academic practice. No use, distribution or reproduction is permitted which does not comply with these terms.



Peptide OPTX-1 From *Ornithodoros papillipes* Tick Inhibits the pS273R Protease of African Swine Fever Virus

Jingjing Wang^{1,2†}, Mengyao Ji^{2†}, Bingqian Yuan^{3†}, Anna Luo^{2†}, Zhenyuan Jiang^{2,4}, Tengyu Zhu^{2,4}, Yang Liu^{2,4}, Peter Muiruri Kamau², Lin Jin^{2,4*} and Ren Lai^{1,2,3,4*}

¹School of Life Sciences, University of Science and Technology of China, Hefei, China, ²Key Laboratory of Animal Models and Human Disease Mechanisms of Chinese Academy of Sciences/Key Laboratory of Bioactive Peptides of Yunnan Province, KIZ-CUHK Joint Laboratory of Bioresources and Molecular Research in Common Diseases, National Resource Center for Non-Human Primates, Kunming Primate Research Center, National Research Facility for Phenotypic & Genetic Analysis of Model Animals (Primate Facility), Sino-African Joint Research Center, and Engineering Laboratory of Peptides, Kunming Institute of Zoology, Chinese Academy of Sciences, Kunming, China, ³School of Life Sciences, Tianjin University, Tianjin, China, ⁴Kunming College of Life Science, University of Chinese Academy of Sciences, Kunming, China

OPEN ACCESS

Edited by:

Na Jia,
Beijing Institute of Microbiology
and Epidemiology, China

Reviewed by:

Geng Meng,
China Agricultural University,
China
Liang Jiang,
Southwest University,
China

*Correspondence:

Lin Jin
jinlin@mail.kiz.ac.cn
Ren Lai
rlai@mail.kiz.ac.cn

[†]These authors have contributed
equally to this work

Specialty section:

This article was submitted to
Virology,
a section of the journal
Frontiers in Microbiology

Received: 16 September 2021

Accepted: 12 November 2021

Published: 03 December 2021

Citation:

Wang J, Ji M, Yuan B, Luo A,
Jiang Z, Zhu T, Liu Y, Kamau PM,
Jin L and Lai R (2021) Peptide
OPTX-1 From *Ornithodoros papillipes*
Tick Inhibits the pS273R Protease of
African Swine Fever Virus.
Front. Microbiol. 12:778309.
doi: 10.3389/fmicb.2021.778309

African swine fever virus (ASFV) is a large double-stranded DNA virus and causes high mortality in swine. ASFV can be transmitted by biological vectors, including soft ticks in genus *Ornithodoros* but not hard ticks. However, the underlying mechanisms evolved in the vectorial capacity of soft ticks are not well-understood. Here, we found that a defensin-like peptide toxin OPTX-1 identified from *Ornithodoros papillipes* inhibits the enzyme activity of the ASFV pS273R protease with a $K_i = 0.821 \pm 0.526 \mu\text{M}$ and shows inhibitory activity on the replication of ASFV. The analogs of OPTX-1 from hard ticks show more inhibitory efficient on pS273R protease. Considering that ticks are blood-sucking animals, we tested the effects of OPTX-1 and its analogs on the coagulation system. At last, top 3D structures represented surface analyses of the binding sites of pS273R with different inhibitors that were obtained by molecular docking based on known structural information. In summary, our study provides evidence that different inhibitory efficiencies between soft tick-derived OPTX-1 and hard tick-derived defensin-like peptides may determine the vector and reservoir competence of ticks.

Keywords: *Ornithodoros papillipes*, African swine fever virus, soft ticks, pS273R protease, vector

INTRODUCTION

African swine fever virus (ASFV), which causes a highly contagious and hemorrhagic disease of swine with a 100% mortality rate, is the only known DNA arbovirus and can be transmitted by *Ornithodoros* soft ticks (Kleiboeker et al., 1998). As a vector, soft ticks have ability to acquire and support replication of ASFV (Burrage, 2013; Ribeiro et al., 2015; Pereira de Oliveira et al., 2019). The viral titer and persistence were tested on the soft tick and virus combination, which highlights the vector and reservoir competence of *Ornithodoros* ticks for ASFV (Pereira De Oliveira et al., 2020). However, it was reported that even though viral DNA can be detected

in many hard ticks, hard ticks are unlikely to be vectors of ASFV given the lack of virus replication (de Carvalho Ferreira et al., 2014). So far, the underlying mechanisms evolved in the contrasting vectorial capacity between hard ticks and soft ticks are not well-understood. Thus, it is essential to further investigate the interaction between ASFV and ticks.

Defensins are important host defense peptides (HDPs) found in vertebrates, invertebrates, and plants. They are important endogenous antimicrobial factors to combat invading pathogens and have therapeutic potential for infectious disease (Rothan et al., 2014; Boto et al., 2018; Bruzzoni-Giovanelli et al., 2018; Zhao et al., 2018). For example, a defensin-like antiviral peptide BmKDFsin4 from the scorpion *Mesobuthus martensii* Karsch has been reported to inhibit hepatitis B virus replication (Zeng et al., 2016). An1a, an antiviral peptide from the venom of the *Alopecosa nagpaga* spider, has shown potent inhibitory activities targeting the NS2B–NS3 protease of DENV2 and ZIKV (Ji et al., 2019). Several antiviral peptides from ticks have also been identified (Talactac et al., 2017).

As a large DNA virus, ASFV capsid comprises 8,280 major capsid protein p72 and 60 penton protein copies (Liu et al., 2019). It is known that some polyprotein precursors cleaved by viral proteinases can yield structural proteins. pS273R is a specific SUMO-1 cysteine protease that catalyzes the maturation of the pp220 and pp62 polyprotein precursors into core-shell proteins (Li et al., 2020a). The proteolytic processes are important for the core maturation and infectivity of ASFV (Alejo et al., 2003). The approaches in describing the 3D structure of pS273R protease are very helpful in the development of anti-viral agents against ASFV (Li et al., 2020a; Liu et al., 2021). Moreover, in this study, the reported high-resolution structural basis of ASFV and pS273R is useful in understanding the vectorial capacity between hard ticks and soft ticks. Herein, we have found that the peptide toxin OPTX-1 identified from *Ornithodoros papillipes* inhibits the enzyme activity of the pS273R protease with a $K_i = 0.821 \pm 0.526 \mu\text{M}$. Interestingly, we also found that the analogs of OPTX-1 from hard ticks show more inhibitory efficiency on pS273R protease. The molecular docking results show that OPTX-1 interacts with pS273R mainly through the active site in the core domain. Given the lack of effective treatments against ASFV, our results may also provide insights into anti-ASFV drugs development from natural origin.

MATERIALS AND METHODS

Cell Lines and Viruses

PAM cells were prepared from a healthy 2-month-old pig (Huang et al., 2020). Lungs were removed from euthanized pigs, and then the bronchoalveolar lavage was performed. The collected PAMs were washed and cultivated in RPMI-1640 supplemented with 10% FBS, 0.1 mM MEM non-essential amino acids, 1 mM sodium pyruvate, 100 U/ml penicillin, and 100 $\mu\text{g}/\text{ml}$ streptomycin in 5% CO_2 at 37°C.

Vero cells (African green monkey kidney epithelial cell line) were obtained from Kunming Cell Bank, Kunming Institute of Zoology, Chinese Academy of Science. Vero cells were

cultured in DMEM medium (Gibco, Waltham, MA, USA) supplemented with 10% fetal bovine serum (FBS), 100 U/ml penicillin, and 100 $\mu\text{g}/\text{ml}$ streptomycin in 5% CO_2 at 37°C.

Protein Production

The codon-optimized cDNA of ASFV pS273R protease was synthesized (TsingKe Biotech, Co., Ltd., Beijing, China) as previously reported (Li et al., 2020a). The full-length pS273R protease was cloned into the pET-28b (Novagen) vector, and the sequence accuracy was verified. The recombinant plasmid of ASFV pS273R protease was transformed into *Escherichia coli* strain BL21(DE3) (TransGen Biotech, Beijing, China) and overexpressed. Protein expression was induced by 0.5 mM IPTG (isopropyl- β -D-thiogalactopyranoside) and further purified on a Ni-NTA column. SDS-PAGE analysis revealed >98% purity of the final purified recombinant protein.

Peptide Synthesis and Refolding

Peptides were synthesized by GL Biochem (Shanghai) Ltd. (Shanghai, China) and analyzed by reversed-phase high-performance liquid chromatography (RP-HPLC) and mass spectrometry to confirm their purity greater than 98%. The linear reduced peptide was dissolved in 0.1 M Tris-HCl and 0.1 M sodium chloride buffer (pH 8.0) at a final concentration of 30 μM glutathione containing 0.1 mM reduced glutathione and 0.5 mM oxidized glutathione at 25°C for 24 h. Oxidized and folded peptides were fractionated by analytical C_{18} RP-HPLC using a linear acetonitrile gradient, and the purity was detected by MALDI-TOF-MS (Luo et al., 2018).

Protease Inhibition Assay

To test if the peptides inhibited pS273R protease activity, assays were conducted in 96-well black microplates utilizing Bz-Nle-Gly-Gly-Arg-AMC (GL Biochem Ltd., Shanghai, China) as a substrate (Andres et al., 2001). Monitoring was initiated, and the fluorescence of each well was recorded every 30 s using an excitation of 360 nm and emission of 460 nm on a FlexStation microplate reader (Molecular Devices, Sunnyvale, CA, USA). Results were determined as relative fluorescence units (RFU). Curves were generated using the GraphPad Prism 6 software (Version 6.01, GraphPad Software, Inc., San Diego, CA, 2012, USA).

The effects of peptides on thrombin (T4393, Sigma-Aldrich, USA) were determined as described previously (Tang et al., 2020). Substrates for thrombin (β -Ala-Gly-Arg-pNA diacetate, T3068) were purchased from Sigma-Aldrich (USA). The rate of protease hydrolyzate was monitored continuously at 405 nm from 20 to 60 min. The inhibition constant K_i was determined according to the reported methods.

ASFV Infection and Quantification

For virus infection, PAM cells were infected with ASFV SY18 strain (GenBank: MH766894) at 0.1 MOI with or without OPTX-1 administration for 48 h in a biosafety facility. The total DNA were extracted with TIANamp Genomic DNA Kits (DP304-03, Tiangen, Beijing, China). qRT-PCR was performed on the StepOnePlus Real-Time PCR Systems (Thermo Fisher Scientific,

Waltham, MA, USA), and the primer sequences are p72-F (TTAGGTACTGTAACGCAGCA) and p72-R (ATGGCATCAGGAGGAGC; Li et al., 2020b). Swine *Actb* gene (ACTB-F, ACCTTCTACAATGAGCTGCG and ACTB-R, CTGGATGGCTACGTACATGG) was used as a reference gene for relative quantification.

Blood Coagulation Assays

Blood coagulation assays were performed according to our previous study (Luan et al., 2017). Healthy human plasma was collected from the Kunming Blood Center, and blood was prepared by mixing a 1:9 volume of trisodium citrate (0.13 M) and blood, with plasma then obtained by centrifugation at 3,000 rpm for 20 min at 4°C. Twenty microliter of platelet-poor plasma (PPP) collected from healthy human subjects was dispensed into round-bottomed 96-well plates, and then the testing sample which was dissolved in 80 µl of HEPES buffer (with 0.15 M NaCl, pH 7.4) was added to the plates. After incubation for 10 min at room temperature, 50 µl of 0.025 M calcium chloride (CaCl₂) was added to the plates, and the clotting time was recorded. Clotting time was calculated by measuring the time to half maximal increase in absorbance. All the analyses were monitored by a microplate spectrophotometer (BioTek Instrument, Inc., Winooski, VT, USA) at the absorbance of 650 nm.

Cell Viability Assay

Cell viability was evaluated by conventional 3-(4,5-dimethyl-2-thiazolyl)-2,5-diphenyl-2H-tetrazolium bromide (MTT) reduction assays in 96-well plates. After a 24 h treatment by testing sample, MTT was added to each well to a final concentration of 0.5 mg/ml and incubated at 37°C for 4 h. The MTT solution was then removed, and dimethyl sulfoxide (DMSO) was added to solubilize the MTT-formazan crystals in living cells. The absorbance of the resulting solution was measured at 570 nm.

Molecular Docking

The Modeller v9.18 software was used to construct a model of three tick defensins, OPTX-1, persulcatusin, and longicin by homology modeling and then used ZDOCK v3.0.2 software to perform molecular docking (Pierce et al., 2014; Webb and Sali, 2021).

Statistical Analysis

Figures were generated using the GraphPad Prism 6 software (Version 6.01, GraphPad Software, Inc., San Diego, CA, 2012, USA). Data are given as mean ± SEM. Statistical analysis was performed using two-tailed Student *t* test. Value of *p* ≤ 0.05 was considered significant.

RESULTS

Refolding of OPTX-1 and Hard Tick-Derived Defensins

Synthesized peptides were oxidized and folded before use. As shown in Figure 1A and Supplementary Figure 1, peptides

were fractionated by analytical C₁₈ RP-HPLC using a linear acetonitrile gradient, and the purity was further confirmed by MALDI-TOF-MS (Supplementary Figure 2). The observed molecular mass of refolded OPTX-1 was 4166.6 Da by using a positive ion and linear mode. Considering that the sequence contains six cysteine residues, which likely form three intramolecular disulfide bridges, it is corresponded with the predicted molecular mass. As shown in Figure 1B, OPTX-1 exhibited both sequence identities and diversities of other known hard tick-derived defensin-like peptides.

OPTX-1 Inhibits the Activity of pS273R and the Replication of ASFV

The pS273R protease is essential for ASFV replication and maturation. It has been regarded as an important antiviral target (Li et al., 2020a). The docking model of the peptides–pS273R complex indicated that the active site of pS273R core domain may directly interact with OPTX-1 and other hard tick-derived defensins by forming several hydrogen bonds and/or hydrophobic bonds (Figure 2A and Supplementary Figure 3A). The Lineweaver–Burk plot shows that OPTX-1 is a competitive inhibitor of the pS273R protease, and the *K_i* value was determined as 0.821 ± 0.526 µM by the method of Dixon (Figure 2B). The hard tick-derived defensins were also demonstrated to be competitive inhibitors of the pS273R

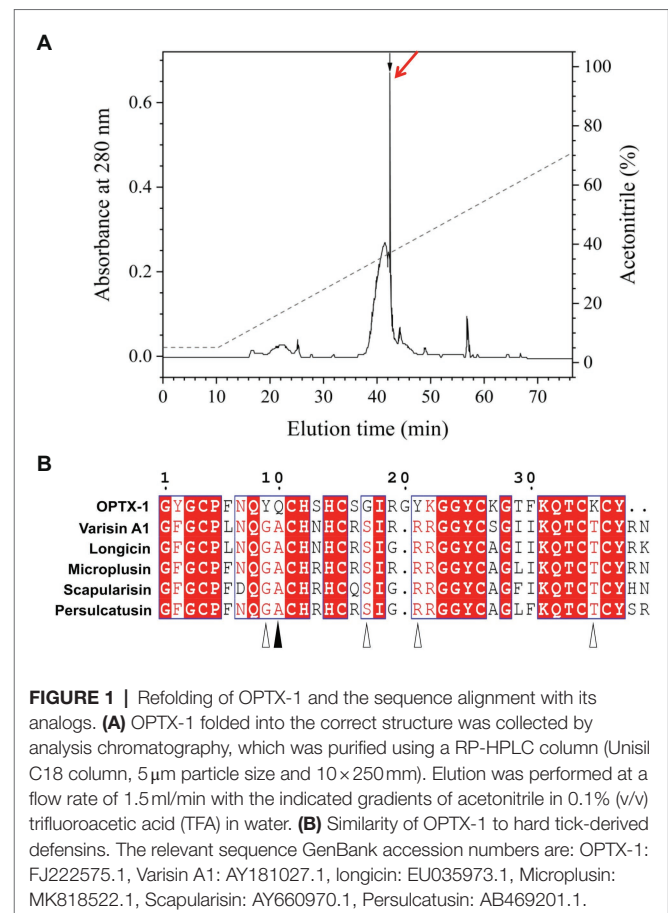


FIGURE 1 | Refolding of OPTX-1 and the sequence alignment with its analogs. **(A)** OPTX-1 folded into the correct structure was collected by analysis chromatography, which was purified using a RP-HPLC column (Unisil C18 column, 5 µm particle size and 10 × 250 mm). Elution was performed at a flow rate of 1.5 ml/min with the indicated gradients of acetonitrile in 0.1% (v/v) trifluoroacetic acid (TFA) in water. **(B)** Similarity of OPTX-1 to hard tick-derived defensins. The relevant sequence GenBank accession numbers are: OPTX-1: FJ222575.1, Varisin A1: AY181027.1, longicin: EU035973.1, Microplusin: MK818522.1, Scapularisin: AY660970.1, Persulcatusin: AB469201.1.

protease with much more remarkable inhibitory effect (**Supplementary Figure 3B**). To determine the anti-ASFV activity of OPTX-1, we analyzed the replication of ASFV by qRT-PCR at 48-h post-infection. In line with the observations, we found that OPTX-1 inhibited ASFV infection in PAM cells at the concentration 5 μ M and 10 μ M (**Figure 2C**). The results indicated that OPTX-1 is a competitive inhibitor of pS273R protease of ASFV by interacting with its active site and hence inhibits the replication of ASFV.

OPTX-1 Shows Inhibitory Effects on Coagulation System

Ticks are obligate blood-feeding arthropod vectors and are responsible for highly prevalent tick-borne diseases (TBDs) worldwide. It is reasonable to speculate that the tick-derived peptides possess anticoagulant activity. As shown in **Figure 3A**, OPTX-1 and other hard tick-derived defensins show anticoagulant effects in plasma-based coagulation assays except scapularisin. Further investigation demonstrated that the activity of thrombin was inhibited by OPTX-1 (**Figure 3B**). These data suggest that OPTX-1 and hard tick-derived defensins may be conducive to blood feeding of ticks by inhibiting the host coagulation system.

OPTX-1 Has Relative Low Cytotoxicity

ASF currently has no effective pharmacological treatment. As competitive inhibitors of pS273R protease of ASFV, OPTX-1 and its analogs are expected to provide peptide precursor molecules for the development of therapeutic drugs for ASF, for further evaluation, cytotoxicity was assessed by using the MTT test. As shown in **Figure 4A**, OPTX-1 showed less cytotoxicity on Vero cells than other defensins. The cytotoxicity of OPTX-1 on PAM cell was more significant than on Vero cells (**Figure 4B**). Taken together, these data suggest that OPTX-1 as well as hard tick-derived defensins has relative low cytotoxicities and might be good template for anti-ASF drug design.

DISCUSSION

ASFV affects domestic and wild members of the Suidae family, leading to a wide range of symptoms from chronic or persistent infection to acute hemorrhagic fever, and inflicts up to 100% mortality (Gallardo et al., 2015). The main routes for disease transmission are direct contact between susceptible and sick animals or their fluids or excretions, and indirect contact through contaminated feed, pork meat, people, vehicles, or

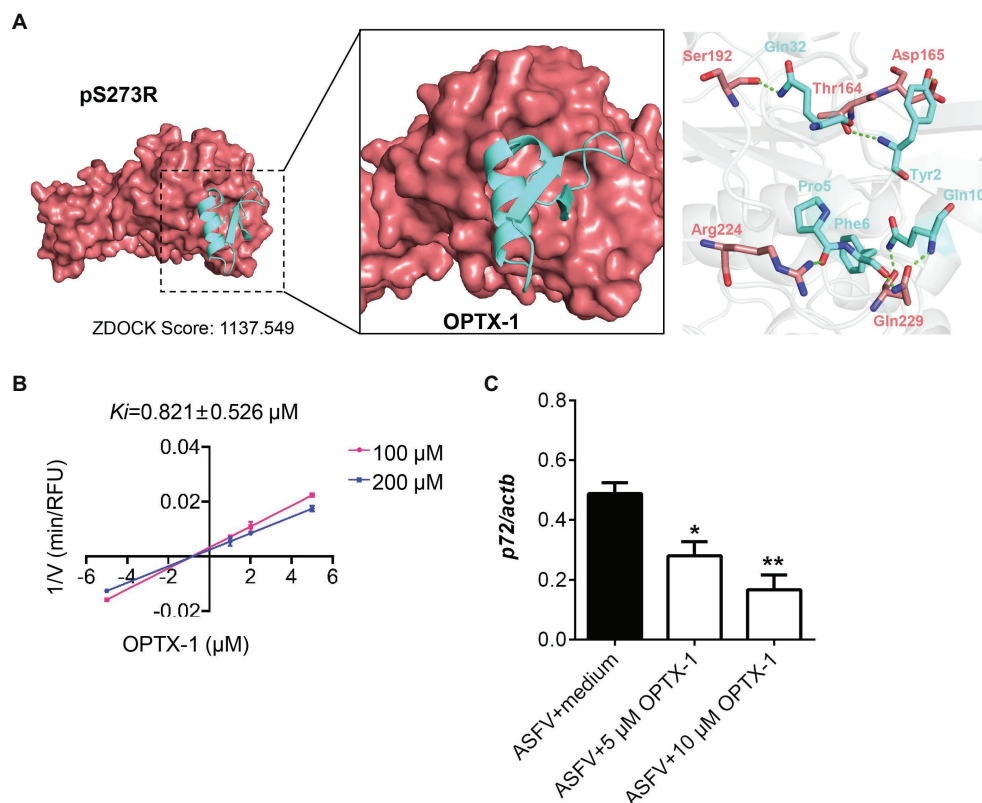
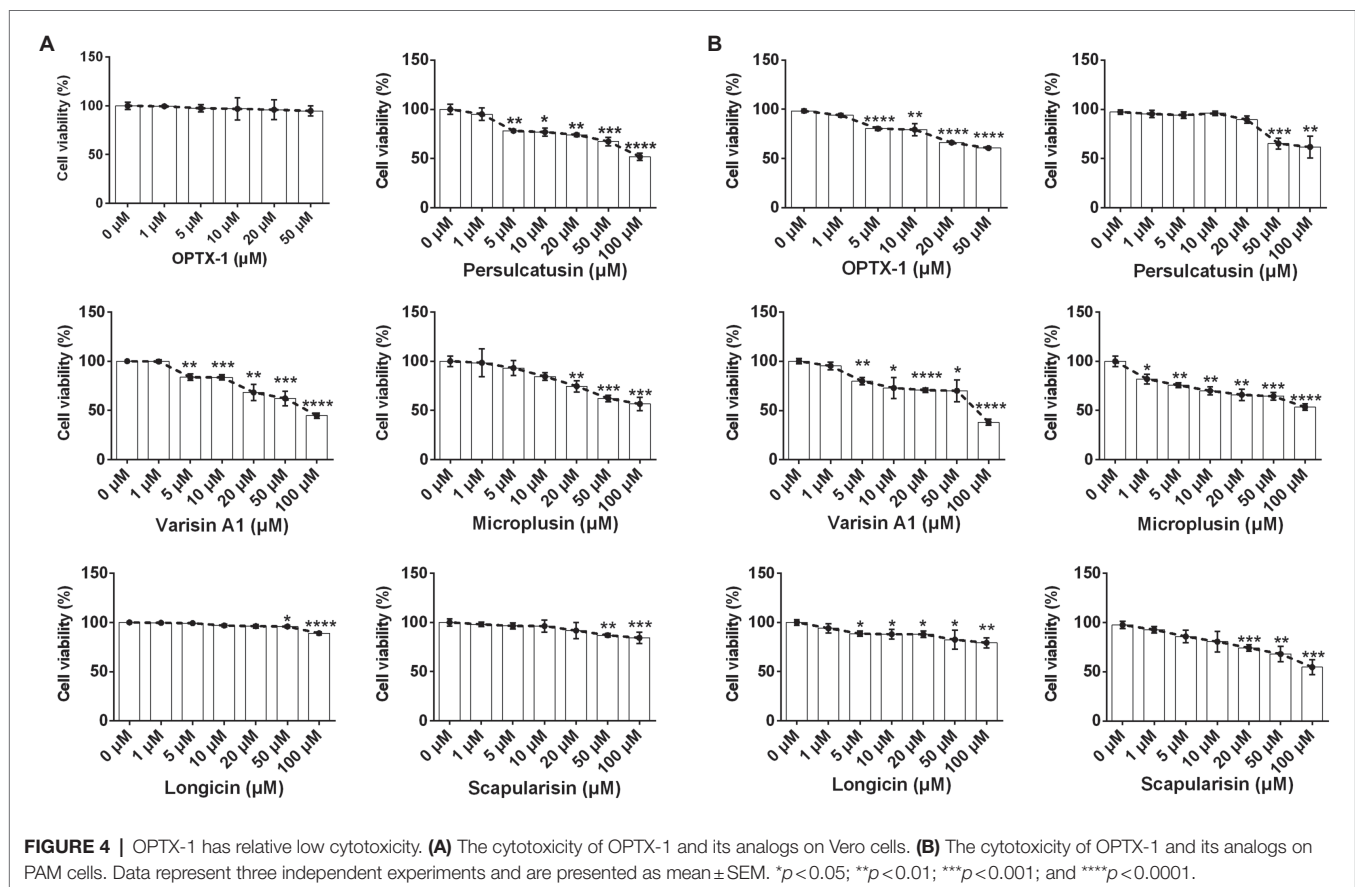
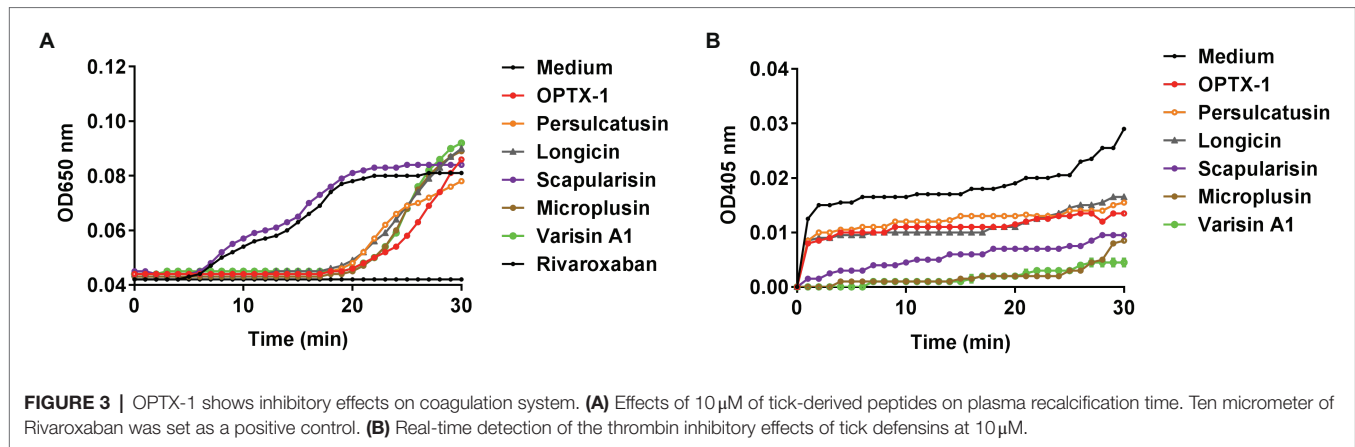


FIGURE 2 | OPTX-1 inhibits the activity of pS273R and the replication of ASFV. **(A)** Molecular docking between OPTX-1 and pS273R. The residues are shown as stick models. The hydrogen bonds are shown as dashed green lines. **(B)** The Lineweaver-Burk plot shows that OPTX-1 is a competitive inhibitor of the pS273R protease, and the K_i value was determined by the method of Dixon. V is the reaction rate. **(C)** OPTX-1 inhibits the replication of ASFV in PAM cells at 48 hpi. Data represent three independent experiments in **A, B** and two independent experiments in **C**. * $p < 0.05$ and ** $p < 0.01$.



fomites (Mur et al., 2012; Dee et al., 2019). Until now, there are no effective drugs and vaccines for ASF. In 2018, the ASFV has been spread to China and other Asian countries. Other than the direct contact transmission, another possible way of the spread of ASFV is vectorial transmissions by some species of *Ornithodoros* soft ticks. We assumed that the vectorial efficiencies of ticks are depended on the successful but limited replication of ASFV.

As a crucial SUMO-1-specific protease of ASFV, pS273R represents an attractive therapeutic target (Li et al., 2020a).

This study implicated that tick defensins which inhibit the pS273R protease of ASFV may play an important role in vector borne transmission. The cleavage of polyproteins by viral encoded proteases is a common strategy (Yost and Marcotrigiano, 2013). The polyprotein precursors pp220 and pp62 expressed by ASFV have cleavage sites of the consensus sequence Gly-Gly-Xaa, which can be processed by the pS273R (Alejo et al., 2003). In this study, we have found that OPTX-1 is a competitive inhibitor of pS273R protease of ASFV and inhibits the replication of ASFV *in vitro*.

The docking model indicated that the active site of pS273R core domain directly interacts with the peptides mainly through the hydrogen bonds. The cysteine protease activity of pS273R can be abolished by mutation of the predicted catalytic histidine and cysteine residues or inhibited by sulfhydryl-blocking reagents (Andres et al., 2001; Alejo et al., 2003). However, the sequence similarity of the defensins included in this study indicates that some amino acid residues are distinguished markedly between soft tick (Tyr9, Gln10, Gly17, Tyr21, and Lys35) and hard tick (Gly9, Ala10, Ser17, Arg21, and Thr35) origin. In particular, the Gln10 of OPTX-1 is the estimated key sites which may form hydrogen bonds with Gln229 of pS273R. The Lineweaver–Burk plot shows that tick defensins are competitive inhibitors of the pS273R protease. As we all know, ticks are blood-feeding arthropods. Tick-derived peptides may possess anticoagulant activity. We found that OPTX-1 and other hard tick-derived defensins show anticoagulant and thrombin inhibitory effects except scapularisin. These findings indicate that the effects of tick defensins on pS273R protease and coagulant system are relatively independent. Thus, further investigations are needed to fully elucidate the underlying biological functions and mechanisms of tick defensin-like peptides.

Defensins are known major immunoregulatory components of ticks that have been shown to provide protection against gram-negative and gram-positive bacteria, fungi, viruses and protozoan parasites (Taute et al., 2015; Wang et al., 2015; Yada et al., 2018). Functional mature defensins are cationic peptides with molecular mass up to 4 kDa, containing six cysteine residues that form characteristic intra-molecular disulfide bridges (Chrudimska et al., 2010). Considering that the ASFV assembly process is strictly depended on the correct spatial and temporal maturation of the pp220 and pp62 polyproteins, tick defensins may limit the replication of ASFV by inhibiting the pS273R. Inhibitors of pS273R protease of ASFV are expected to be potential therapeutic drugs for ASF. As OPTX-1 and hard tick-derived defensins have relative low cytotoxicities, they might provide valuable structural information for further anti-ASF small molecular inhibitor drug development targeting pS273R. Previous experimental studies showed that some species of *Ornithodoros* soft ticks can be orally infected, maintained and transmitted ASFV vertically (transstadially and transovarially) among ticks, and horizontally to naive pigs. Several studies emphasized that vector competence was not only related to the tick but also to the ASFV strain. Thus, it is necessary to test the inhibitory effects on pS273R protease as well as the virus replications of tick defensins with different ASFV variants.

REFERENCES

- Alejo, A., Andres, G., and Salas, M. L. (2003). African swine fever virus proteinase is essential for core maturation and infectivity. *J. Virol.* 77, 5571–5577. doi: 10.1128/JVI.77.10.5571-5577.2003
- Andres, G., Alejo, A., Simon-Mateo, C., and Salas, M. L. (2001). African swine fever virus protease, a new viral member of the SUMO-1-specific protease family. *J. Biol. Chem.* 276, 780–787. doi: 10.1074/jbc.M006844200
- Boto, A., Perez de la Lastra, J. M., and Gonzalez, C. C. (2018). The road from host-Defense peptides to a new generation of antimicrobial drugs. *Molecules* 23:311. doi: 10.3390/molecules23020311

DATA AVAILABILITY STATEMENT

The raw data supporting the conclusions of this article will be made available by the authors, without undue reservation.

AUTHOR CONTRIBUTIONS

JW, MJ, BY, AL, ZJ, TZ, and YL conducted the experiments. RL and LJ designed the experiments and provided guidance for the research. LJ analyzed the data and wrote the paper. PK revised the manuscript. All authors contributed to the article and approved the submitted version.

FUNDING

This work was supported by the African Swine Fever Research Emergency program of the Chinese Academy of Sciences (CAS) (KJZD-SW-L06-02). LJ is partly supported by the National Natural Science Foundation of China (NSFC) grant (31900331 and 32070444), Science and Technology Department of Yunnan Province (202001AW070019), Chinese Academy of Sciences “Light of West China” program and Youth Innovation Promotion Association (2019378). RL is partly supported by the NSFC grant (3193001521761142002), the CAS grants (XDB31000000, SAJC202103, KFJ-PTXM-28SAJC201606, and KGFZD-135-17-011), and Yunnan Province grant (2019-YT-053, 202002AA 100007, and 2019ZF003).

ACKNOWLEDGMENTS

The authors would like to thank Zongjie Li (Shanghai Veterinary Research Institute, Chinese Academy of Agricultural Science) for the help in ASFV assays and all members of the African Swine Fever Research Emergency program of the CAS (KJZD-SW-L06) for their advices and help.

SUPPLEMENTARY MATERIAL

The Supplementary Material for this article can be found online at: <https://www.frontiersin.org/articles/10.3389/fmicb.2021.778309/full#supplementary-material>

- Bruzzoni-Giovanelli, H., Alezra, V., Wolff, N., Dong, C. Z., Tuffery, P., and Rebollo, A. (2018). Interfering peptides targeting protein-protein interactions: the next generation of drugs? *Drug Discov. Today* 23, 272–285. doi: 10.1016/j.drudis.2017.10.016
- Burrage, T. G. (2013). African swine fever virus infection in *Ornithodoros* ticks. *Virus Res.* 173, 131–139. doi: 10.1016/j.virusres.2012.10.010
- Chrudimska, T., Chrudimsky, T., Golovchenko, M., Rudenko, N., and Grubhoffer, L. (2010). New defensins from hard and soft ticks: similarities, differences, and phylogenetic analyses. *Vet. Parasitol.* 167, 298–303. doi: 10.1016/j.vetpar.2009.09.032
- de Carvalho Ferreira, H. C., Tudela Zuquete, S., Wijnveld, M., Weesendorp, E., Jongejans, F., Stegeman, A., et al. (2014). No evidence of African swine

- fever virus replication in hard ticks. *Ticks Tick Borne Dis.* 5, 582–589. doi: 10.1016/j.ttbdis.2013.12.012
- Dee, S. A., Bauermann, F. V., Niederwerder, M. C., Singrey, A., Clement, T., de Lima, M., et al. (2019). Correction: survival of viral pathogens in animal feed ingredients under transboundary shipping models. *PLoS One* 14:e0214529. doi: 10.1371/journal.pone.0214529
- Gallardo, M. C., Reoyo, A. T., Fernandez-Pinero, J., Iglesias, I., Munoz, M. J., and Arias, M. L. (2015). African swine fever: a global view of the current challenge. *Porc. Health Manag.* 1:21. doi: 10.1186/s40813-015-0013-y
- Huang, C., Zhu, J., Wang, L., Chu, A., Yin, Y., Vali, K., et al. (2020). Cryptotanshinone protects porcine alveolar macrophages from infection with porcine reproductive and respiratory syndrome virus. *Antivir. Res.* 183:104937. doi: 10.1016/j.antiviral.2020.104937
- Ji, M., Zhu, T., Xing, M., Luan, N., Mwangi, J., Yan, X., et al. (2019). An antiviral peptide from *Alopecosa nagpaga* spider targets NS2B-NS3 protease of Flaviviruses. *Toxins* 11:584. doi: 10.3390/toxins11100584
- Kleiboeker, S. B., Burrage, T. G., Scoles, G. A., Fish, D., and Rock, D. L. (1998). African swine fever virus infection in the argasid host, *Ornithodoros porcinus porcinus*. *J. Virol.* 72, 1711–1724. doi: 10.1128/JVI.72.3.1711-1724.1998
- Li, G., Liu, X., Yang, M., Zhang, G., Wang, Z., Guo, K., et al. (2020a). Crystal structure of African swine fever virus pS273R protease and implications for inhibitor design. *J. Virol.* 94:e02125–19. doi: 10.1128/JVI.02125-19
- Li, Z., Wei, J., Di, D., Wang, X., Li, C., Li, B., et al. (2020b). Rapid and accurate detection of African swine fever virus by DNA endonuclease-targeted CRISPR trans reporter assay. *Acta Biochim. Biophys. Sin.* 52, 1413–1419. doi: 10.1093/abbs/gmaa135
- Liu, B., Cui, Y., Lu, G., Wei, S., Yang, Z., Du, F., et al. (2021). Small molecule inhibitor E-64 exhibiting the activity against African swine fever virus pS273R. *Bioorg. Med. Chem.* 35:116055. doi: 10.1016/j.bmc.2021.116055
- Liu, S., Luo, Y., Wang, Y., Li, S., Zhao, Z., Bi, Y., et al. (2019). Cryo-EM structure of the African swine fever virus. *Cell Host Microbe* 26, 836.e833–843.e833. doi: 10.1016/j.chom.2019.11.004
- Luan, N., Zhou, C., Li, P., Ombati, R., Yan, X., Mo, G., et al. (2017). Joannsin, a novel Kunitz-type FXa inhibitor from the venom of *Prospirobolus joannsi*. *Thromb. Haemost.* 117, 1031–1039. doi: 10.1160/TH16-11-0829
- Luo, L., Li, B., Wang, S., Wu, F., Wang, X., Liang, P., et al. (2018). Centipedes subdue giant prey by blocking KCNQ channels. *Proc. Natl. Acad. Sci. U. S. A.* 115, 1646–1651. doi: 10.1073/pnas.1714760115
- Mur, L., Martinez-Lopez, B., and Sanchez-Vizcaino, J. M. (2012). Risk of African swine fever introduction into the European Union through transport-associated routes: returning trucks and waste from international ships and planes. *BMC Vet. Res.* 8:149. doi: 10.1186/1746-6148-8-149
- Pereira De Oliveira, R., Hutet, E., Lancelot, R., Paboeuf, F., Duhayon, M., Boinas, F., et al. (2020). Differential vector competence of *Ornithodoros* soft ticks for African swine fever virus: what if it involves more than just crossing organic barriers in ticks? *Parasit. Vectors* 13:618. doi: 10.1186/s13071-020-04497-1
- Pereira de Oliveira, R., Hutet, E., Paboeuf, F., Duhayon, M., Boinas, F., Perez de Leon, A., et al. (2019). Comparative vector competence of the Afrotropical soft tick *Ornithodoros moubata* and Palearctic species, *O. erraticus* and *O. verrucosus*, for African swine fever virus strains circulating in Eurasia. *PLoS One* 14:e0225657. doi: 10.1371/journal.pone.0225657
- Pierce, B. G., Wiehe, K., Hwang, H., Kim, B. H., Vreven, T., and Weng, Z. (2014). ZDOCK server: interactive docking prediction of protein-protein complexes and symmetric multimers. *Bioinformatics* 30, 1771–1773. doi: 10.1093/bioinformatics/btu097
- Ribeiro, R., Otte, J., Madeira, S., Hutchings, G. H., and Boinas, F. (2015). Experimental infection of *Ornithodoros erraticus* sensu stricto with two Portuguese African swine fever virus strains. Study of factors involved in the dynamics of infection in ticks. *PLoS One* 10:e0137718. doi: 10.1371/journal.pone.0137718
- Rothan, H. A., Bahrani, H., Rahman, N. A., and Yusof, R. (2014). Identification of natural antimicrobial agents to treat dengue infection: in vitro analysis of laticin peptide activity against dengue virus. *BMC Microbiol.* 14:140. doi: 10.1186/1471-2180-14-140
- Talactac, M. R., Yada, Y., Yoshii, K., Hernandez, E. P., Kusakisako, K., Maeda, H., et al. (2017). Characterization and antiviral activity of a newly identified defensin-like peptide, HEdefensin, in the hard tick *Haemaphysalis longicornis*. *Dev. Comp. Immunol.* 68, 98–107. doi: 10.1016/j.dci.2016.11.013
- Tang, X., Zhang, Z., Fang, M., Han, Y., Wang, G., Wang, S., et al. (2020). Transferrin plays a central role in coagulation balance by interacting with clotting factors. *Cell Res.* 30, 119–132. doi: 10.1038/s41422-019-0260-6
- Taute, H., Bester, M. J., Neitz, A. W., and Gaspar, A. R. (2015). Investigation into the mechanism of action of the antimicrobial peptides Os and Os-C derived from a tick defensin. *Peptides* 71, 179–187. doi: 10.1016/j.peptides.2015.07.017
- Wang, J., Bian, G., Pan, W., Feng, T., and Dai, J. (2015). Molecular characterization of a defensin gene from a hard tick, *Dermacentor silvarum*. *Parasit. Vectors* 8:25. doi: 10.1186/s13071-014-0625-0
- Webb, B., and Sali, A. (2021). Protein structure Modeling with MODELLER. *Methods Mol. Biol.* 2199, 239–255. doi: 10.1007/978-1-0716-0892-0_14
- Yada, Y., Talactac, M. R., Kusakisako, K., Hernandez, E. P., Galay, R. L., Andoh, M., et al. (2018). Hemolymph defensin from the hard tick *Haemaphysalis longicornis* attacks gram-positive bacteria. *J. Invertebr. Pathol.* 156, 14–18. doi: 10.1016/j.jip.2018.07.005
- Yost, S. A., and Marcotrigiano, J. (2013). Viral precursor polyproteins: keys of regulation from replication to maturation. *Curr. Opin. Virol.* 3, 137–142. doi: 10.1016/j.coviro.2013.03.009
- Zeng, Z., Zhang, Q., Hong, W., Xie, Y., Liu, Y., Li, W., et al. (2016). A scorpion Defensin BmKDFsin4 inhibits hepatitis B virus replication in vitro. *Toxins* 8:124. doi: 10.3390/toxins8050124
- Zhao, P., Xue, Y., Gao, W., Li, J., Zu, X., Fu, D., et al. (2018). Actinobacteria-derived peptide antibiotics since 2000. *Peptides* 103, 48–59. doi: 10.1016/j.peptides.2018.03.011

Conflict of Interest: The authors declare that the research was conducted in the absence of any commercial or financial relationships that could be construed as a potential conflict of interest.

Publisher's Note: All claims expressed in this article are solely those of the authors and do not necessarily represent those of their affiliated organizations, or those of the publisher, the editors and the reviewers. Any product that may be evaluated in this article, or claim that may be made by its manufacturer, is not guaranteed or endorsed by the publisher.

Copyright © 2021 Wang, Ji, Yuan, Luo, Jiang, Zhu, Liu, Kamau, Jin and Lai. This is an open-access article distributed under the terms of the Creative Commons Attribution License (CC BY). The use, distribution or reproduction in other forums is permitted, provided the original author(s) and the copyright owner(s) are credited and that the original publication in this journal is cited, in accordance with accepted academic practice. No use, distribution or reproduction is permitted which does not comply with these terms.



Recent Advances in Bunyavirus Reverse Genetics Research: Systems Development, Applications, and Future Perspectives

Fuli Ren^{1,2,3}, Shu Shen^{2,3}, Qiongya Wang¹, Gang Wei¹, Chaolin Huang^{1*}, Hualin Wang^{2,3*}, Yun-Jia Ning^{2,3*}, Ding-Yu Zhang^{1*} and Fei Deng^{2,3*}

OPEN ACCESS

Edited by:

Felix Rey,
Institut Pasteur, France

Reviewed by:

Olivier Escaffre,
University of Texas Medical Branch at
Galveston, United States
Chunsheng Dong,
Soochow University, China

*Correspondence:

Chaolin Huang
88071718@qq.com
Hualin Wang
h.wang@wh.iov.cn
Yun-Jia Ning
nyj@wh.iov.cn
Ding-Yu Zhang
zhangdy63@hotmail.com
Fei Deng
df@wh.iov.cn

Specialty section:

This article was submitted to
Virology,
a section of the journal
Frontiers in Microbiology

Received: 07 September 2021

Accepted: 03 November 2021

Published: 07 December 2021

Citation:

Ren F, Shen S, Wang Q, Wei G,
Huang C, Wang H, Ning Y-J, Zhang
D-Y and Deng F (2021) Recent
Advances in Bunyavirus Reverse
Genetics Research: Systems
Development, Applications, and
Future Perspectives.
Front. Microbiol. 12:771934.
doi: 10.3389/fmicb.2021.771934

¹Research Center for Translational Medicine, Wuhan Jinyintan Hospital, Wuhan, China, ²State Key Laboratory of Virology, Wuhan Institute of Virology, Chinese Academy of Sciences, Wuhan, China, ³National Virus Resource Center, Wuhan Institute of Virology, Chinese Academy of Sciences, Wuhan, China

Bunyaviruses are members of the *Bunyavirales* order, which is the largest group of RNA viruses, comprising 12 families, including a large group of emerging and re-emerging viruses. These viruses can infect a wide variety of species worldwide, such as arthropods, protozoans, plants, animals, and humans, and pose substantial threats to the public. In view of the fact that a better understanding of the life cycle of a highly pathogenic virus is often a precondition for developing vaccines and antivirals, it is urgent to develop powerful tools to unravel the molecular basis of the pathogenesis. However, biosafety level –3 or even –4 containment laboratory is considered as a necessary condition for working with a number of bunyaviruses, which has hampered various studies. Reverse genetics systems, including minigenome (MG), infectious virus-like particle (iVLP), and infectious full-length clone (IFLC) systems, are capable of recapitulating some or all steps of the viral replication cycle; among these, the MG and iVLP systems have been very convenient and effective tools, allowing researchers to manipulate the genome segments of pathogenic viruses at lower biocontainment to investigate the viral genome transcription, replication, virus entry, and budding. The IFLC system is generally developed based on the MG or iVLP systems, which have facilitated the generation of recombinant infectious viruses. The MG, iVLP, and IFLC systems have been successfully developed for some important bunyaviruses and have been widely employed as powerful tools to investigate the viral replication cycle, virus–host interactions, virus pathogenesis, and virus evolutionary process. The majority of bunyaviruses is generally enveloped negative-strand RNA viruses with two to six genome segments, of which the viruses with bipartite and tripartite genome segments have mostly been characterized. This review aimed to summarize current knowledge on reverse genetic studies of representative bunyaviruses causing severe diseases in humans and animals, which will contribute to the better understanding of the bunyavirus replication cycle and provide some hints for developing designed antivirals.

Keywords: bunyavirus, reverse genetics, minigenome, iVLP, infectious full-length clone system

INTRODUCTION

As the handling of many infectious and highly pathogenic members of the order Bunyvirales is restricted to occurring in a laboratory with a biosafety level –3, or even –4, many studies focused on different aspects of the viral life cycle and pathogenesis have been hampered. Reverse genetics systems established up to now, such as the minigenome (MG), infectious virus-like particles (iVLP), and infectious full-length clone (IFLC) systems, have been efficient tools for researchers to conduct some important experiments at lower biocontainment than at level 3 or 4. Among these experimental systems constructed for bunyaviruses, MG and iVLP systems are used to model their partial life cycle, which enables the dissection of virus invasion (a process the virus enter the host cells), viral genome replication, transcription, ribonucleoprotein assembly, virion packaging, and budding processes. The IFLC system is used to rescue recombinant viruses, which has made it possible to manipulate viral genomes at the RNA/DNA molecular level. These established reverse genetics systems have exerted great potential to help us to better understand the bunyaviruses and to develop antivirals and vaccines.

Over the past few decades, reverse genetics technology has revolutionized the field of RNA virology, which has made it possible to manipulate RNA viral genomes and rescue genome analogs (referring to minigenome RNA in generally), infectious iVLP, and recombinant viruses from cDNA clones. Here, we summarize the already established MG, iVLP, and IFLC systems for bunyaviruses causing severe diseases in humans and animals. These bunyaviruses are mostly distributed in the families *Arenaviridae*, *Hantaviridae*, *Nairoviridae*, *Peribunyaviridae*, and *Phenuiviridae* (as shown in **Table 1**). Among members of these families, the viral genome of viruses belonging to *Hantaviridae*, *Nairoviridae*, *Peribunyaviridae*, and *Phenuiviridae* generally consists of three genome segments denoted as large (L), medium (M), and small (S), while the viral genome of viruses in *Arenaviridae* is mainly composed of two segments, i.e., L and S segments. These established systems suggest that the reverse genetics technology has been widely developed for bunyaviruses and widely used by researchers to dissect all aspects of the viral life cycle.

This review provides an overview of the current status of reverse genetic studies on important bi- and trisegmented emerging and re-emerging bunyaviruses, recent advances in the applications of these systems. Furthermore, we also discuss the limitations of the currently established systems for bunyaviruses and unsolved problems that urgently need to be addressed.

CLASSIFICATION AND GENOME ORGANIZATION OF BUNYAVIRALES

Bunyvirales is a newly proposed order consisting of related viruses distributed among 12 families: *Arenaviridae*, *Cruliviridae*, *Filoviridae*, *Hantaviridae*, *Leishbuviridae*, *Myopoviridae*,

Nairoviridae, *Peribunyaviridae*, *Phasmaviridae*, *Phenuiviridae*, *Tospoviridae*, and *Wupedeviridae* proposed by the International Committee on Taxonomy of Viruses, of which the viral genome is composed of linear, segmented, single-stranded, negative-sense, or ambisense RNA genomes; this order is now comprised of 48 genera and over 383 species (Abudurexiti et al., 2019; Kuhn et al., 2020). Among the 12 families in the *Bunyvirales* order, *Arenaviridae*, *Hantaviridae*, *Nairoviridae*, *Peribunyaviridae*, and *Phenuiviridae* contain lots of important pathogens that are able to cause severe diseases in humans and animals with a worldwide geographical distribution.

Viruses from the family *Arenaviridae*, *Hantaviridae*, *Nairoviridae*, *Peribunyaviridae*, and *Phenuiviridae* are comprised of a variety of widely known representative pathogenic viruses, such as the Lassa virus (LASV, *Arenaviridae* family), which is endemic across large regions within Western Africa and is estimated to infect hundreds of thousands of individuals annually (Cai et al., 2020b). Hantaan virus (HTNV, *Hantaviridae* family) is found predominantly in Europe and Asia (Brocato and Hooper, 2019). Crimean-Congo hemorrhagic fever virus (CCHFV, *Nairoviridae* family) can infect human host primarily through infected ticks or by contact with infected hosts or their body fluids and tissues (Serretiello et al., 2020). Bunyamwera virus (BUNV, *Peribunyaviridae* family), which causes disease in livestock animals, avian species, and humans, is considered the prototype of the bunyavirus as it is the most characterized to date (Dutuze et al., 2018). Rift Valley fever virus (RVFV, *Phenuiviridae* family), which is found in Sub-Saharan Africa, is associated with disease in camels, cattle, goats, and sheep but also causes severe morbidity and mortality in humans (Paweska, 2015; Noronha and Wilson, 2017).

Bunyaviruses are mostly spherical virion with a lipid bilayer envelope containing segmented negative-sense or ambisense single-stranded RNA. For the majority in the five families discussed, the virus genomes comprise tripartite segments, except for some members in *Arenaviridae*, whose genomes consist of bipartite segments. For the majority of arenaviruses, the genome is generally comprised of bipartite segments denoted as L and S, of which the S encodes glycoprotein precursor (GP) and the nucleocapsid protein (N) in an ambisense arrangement, and L codes for the RNA-dependent RNA polymerase (RdRp) and a zinc-binding protein (Z) for some members in the genera *Mammarenavirus* and *Reptarenavirus* (as shown in **Figure 1A**). It has been demonstrated that the matrix Z-protein of virus from the genus *Mammarenavirus* species participates in the formation of infectious viral particles and viral budding during the life cycle (Perez et al., 2003; Pontremoli et al., 2019). As shown in **Figure 1B**, a typical three-segmented bunyavirus contains tripartite genome segments, and the genomic RNA segments are named according to their relative sizes, which are termed L, M, and S. L and S code for, respectively, RdRp and nucleoprotein (N), which participates in genome replication and transcription. S generally also encodes the nonstructural protein NSs, which participates in virus immune escape. M codes for a single-polyprotein precursor (GP), from which two surface GPs, such as Gn (or G2) and Gc (or G1), are produced by host cell proteases (Guardado-Calvo and Rey, 2017). In a few cases, an additional nonstructural

TABLE 1 | Summary of the established reverse genetics systems for *Bunyavirales*.

Virus	Genus	Family	Endemic area	Established systems	References
Lassa virus (LASV)	<i>Mammarenavirus</i>	<i>Arenaviridae</i>	Western Africa	T7- and pol-I-driven MG, IFLC systems	Cai et al., 2018, 2020a
Lymphocytic choriomeningitis Mammarenavirus (LCMV)			Americas, Africa, Asia, and Europe	T7-driven MG, IFLC systems	Lee et al., 2000; Cheng et al., 2015
Tacaribe virus (TCRV)			America	pol-I-driven MG, IFLC systems	Ye et al., 2020
Lujo virus (LJV)			South Africa	T7-driven MG, IFLC systems	Bergeron et al., 2012
Junin virus (JUNV)			Argentina	pol-I-driven MG, IFLC systems	Emonet et al., 2011
Pichinde virus (PICV)			Guinea	T7-driven MG, IFLC system	Lan et al., 2009
Machupo virus (MACV)			South America	pol-I-driven MG, IFLC systems	Patterson et al., 2014
Bunyamwera virus (BUNV)	<i>Orthobunyavirus</i>	<i>Peribunyaviridae</i>	Africa	T7- and pol-I-driven MG, iVLP and IFLC systems	Weber et al., 2001; Shi et al., 2006; Mazel-Sanchez and Elliott, 2012
Shuni virus (SHUV)			South Africa	T7-driven IFLC system	Oymans et al., 2020
Akabane virus (AKAV)			Africa, Australia, and Asia	T7- and pol-I-driven IFLC system	Takenaka-Uerna et al., 2015, 2016
LaCrosse virus (LACV)			North America	T7-driven MG, iVLP and IFLC systems	Blakqori and Weber, 2005; Klemm et al., 2013
Schmallenberg virus (SBV)			Europe	T7-driven IFLC system	Elliott et al., 2013; Varela et al., 2013
Cache Valley virus (CVV)			America	T7-driven MG and IFLC system	Dunlop et al., 2018
Kairi virus (KRIV)			America	T7-driven MG and IFLC systems	Dunlop et al., 2018
Oropouche virus (OROV)			Central and South America	T7-driven IFLC system	Tilston-Lunel et al., 2015
Hantaan virus (HTNV)	<i>Orthohantavirus</i>	<i>Hantaviridae</i>	Asia, Europe, and America	T7- and pol-I-driven MG system	Flick et al., 2003; Zhang et al., 2008
Andes virus (ANDV)			South America	T7-driven MG system	Brown et al., 2012
SFTS bandavirus (SFTSV)	<i>Bandavirus</i>	<i>Phenuiviridae</i>	East Asia	T7- and pol-I-driven MG, iVLP and IFLC systems	Brennan et al., 2015, 2017; Rezelj et al., 2019; Ren et al., 2020
Heartland virus (HRTV)			America	T7- and pol-I-driven MG, iVLP system	Rezelj et al., 2019; Ren et al., 2020
Uukuniemi Virus (UUKV)	<i>Phlebovirus</i>	<i>Phenuiviridae</i>	Europe, Asia	T7 and pol-I-driven MG, iVLP and IFLC systems	Flick and Pettersson, 2001; Flick et al., 2004; Overby et al., 2006; Rezelj et al., 2015
Rift Valley fever virus (RVFV)			Africa	T7- and pol-I-driven MG, iVLP and IFLC systems	Ikegami et al., 2006; Habjan et al., 2008, 2009; Smith et al., 2018; Jerome et al., 2019
Arumowot virus (AMTV)			Africa	T7-driven IFLC system	Hallam et al., 2019
Crimean-Congo hemorrhagic fever virus (CCHFV)	<i>Orthonairovirus</i>	<i>Nairoviridae</i>	Asia, Europe and Africa	T7-driven MG, iVLP and IFLC systems	Bergeron et al., 2015; Welch et al., 2020
Hazara virus (HAZV)			Pakistan	T7-driven MG and IFLC system	Fuller et al., 2019; Matsumoto et al., 2019
Tomato spotted wilt virus (TSWV)	<i>Orthotospovirus</i>	<i>Tospoviridae</i>	Australia, India and America	CUP1promoter-driven MG system	Ishibashi et al., 2017

protein NSm is also encoded by M. Some members of the genus *Orthobunyavirus* (BUNV for instance) and *Phlebovirus* (RVFV for instance) encode the NSm protein as part of a precursor with the glycoproteins, whereas NSm of virus from the genus *Orthotospovirus* (tomato spotted wilt virus for instance) is translated from a subgenomic messenger RNA (mRNA) in an ambisense manner (Guu et al., 2012).

VIRAL REPLICATION CYCLE AND REVERSE GENETICS SYSTEMS OF BUNYAVIRUSES

Genomes of bunyaviruses are comprised of linear single-stranded negative-sense RNA, and the viral genomic RNA segments always contain untranslated regions (UTRs) on both the 5'

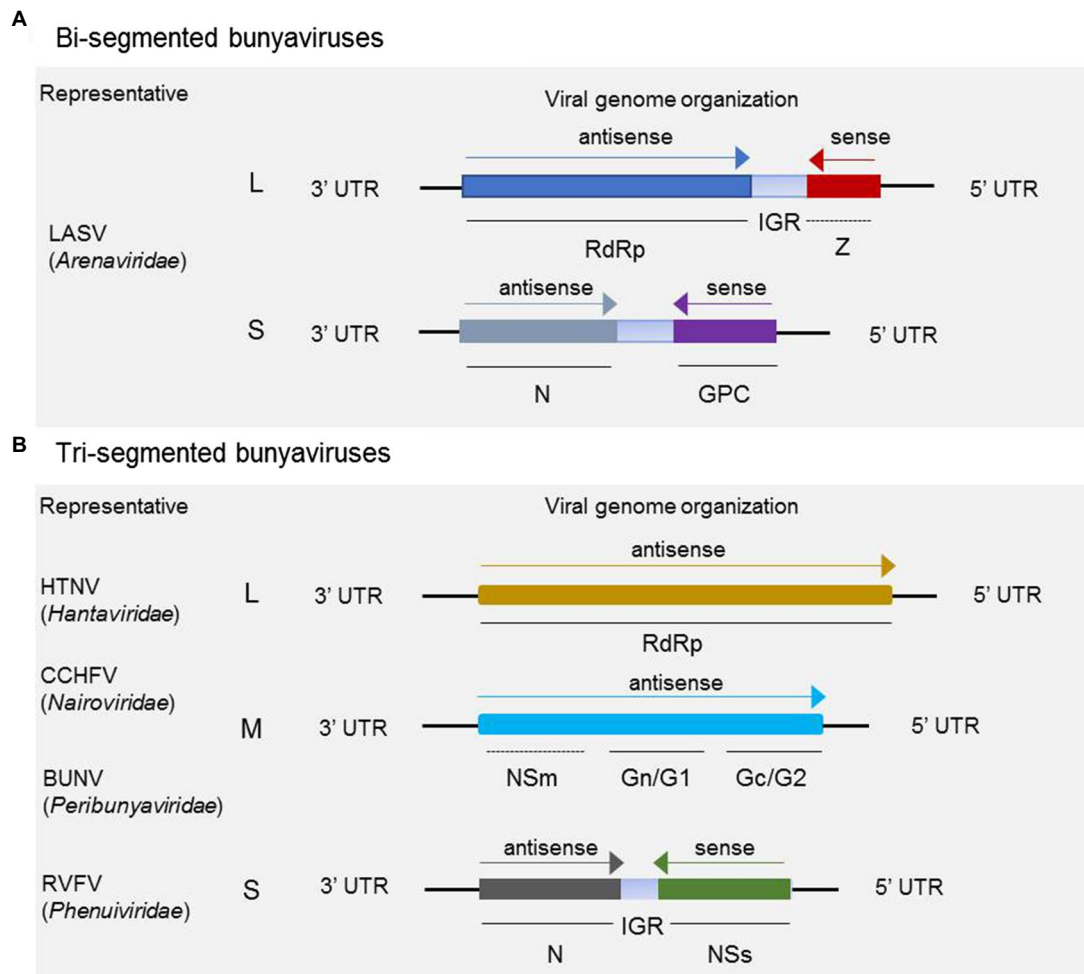


FIGURE 1 | Schematic of genome organization and coding strategies of bisegmented and trisegmented bunyaviruses. For bisegmented bunyaviruses, in Lassa arenavirus (LASV), for example, the L and S are generally ambisense segments, of which the L codes for RdRp and a zinc-binding protein (Z), and S codes for glycoprotein precursor (GP) and nucleoprotein (N). The Z protein is only encoded by some members in *Mammarenavirus* and *Reptarenavirus* **(A)**; **(B)** for trisegmented bunyaviruses, such as Hantaan virus (HTNV), Crimean-Congo hemorrhagic fever virus (CCHFV), Bunyamwera virus (BUNV), and Rift Valley fever virus (RVFV), the viral genome consists of L, M, and S, of which the L codes for RdRp and M mainly codes for glycoprotein Gn (or G1) and Gc (or G2). For CCHFV, BUNV, RVFV, and several other members not shown here, the M segment also encodes NSm besides the glycoproteins. It should be noted that the NSm encoding gene of CCHFV and BUNV is both located between the encoding genes of Gn and Gc, which is different from the schematic shown for RVFV. The S segment adopts an ambisense coding strategy to encode nonstructural protein NSs and nucleoprotein N.

and 3' ends that are denoted as 5' UTR and 3' UTR, which play important roles in the virus life cycle by promoting transcription, replication, and encapsidation of the viral genome. Bunyaviruses replicate exclusively in the host cell cytoplasm, with maturation and budding occurring in the Golgi apparatus, and are released *via* cellular export pathways (Hoenen et al., 2011). The viral genomic and antigenomic RNAs are always encapsidated by N and associated with RdRp to form ribonucleoprotein (RNP) complexes both within the host cell and in the virion. These RNP particles are able to serve as functional templates to synthesize positive-sense mRNA and progeny virus genome RNA with the assist of the viral polymerase (Sun et al., 2018). The bunyaviruses enter a host cell through a glycoprotein-mediated virus binding process. Once this process

is finished, the viral genomic RNAs will undergo an uncoating process to initiate the transcription to generate mRNA and the intermediate products cRNA with the assist of some specific viral proteins (Guu et al., 2012; Ferron et al., 2017; Sun et al., 2018). Initiation of transcription of the viral mRNAs is primed by short sequences derived from the 5' end of host mRNAs through a so-called cap-snatching mechanism (Simons and Pettersson, 1991). The mRNA can serve as a template for viral protein synthesis, such as RdRp, Gn (or G2), Gc (or G1), NSm, N, and NSs; and the cRNA coated by N can recruit RdRp to form functional cRNPs, which can serve as templates to synthesize progeny vRNAs. Similarly, after the recruitment and encapsidation, the progeny vRNPs are formed and can be packaged by glycoprotein into progeny virus. Meanwhile,

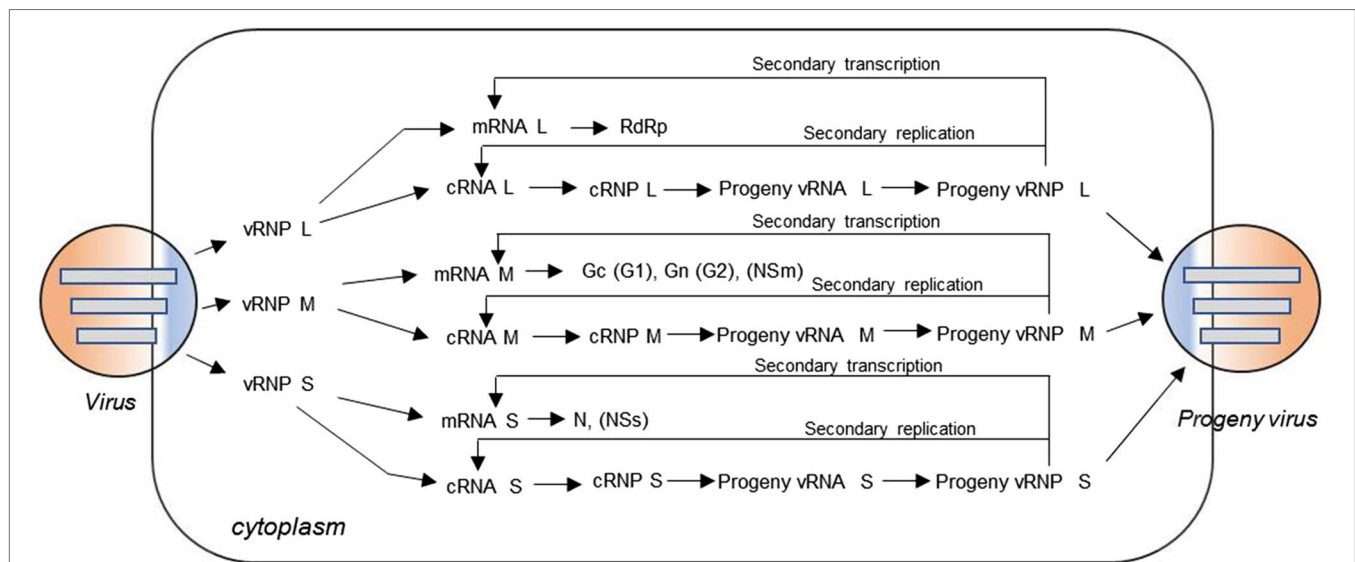


FIGURE 2 | Virus replication cycle of typical three-segmented bunyaviruses in the cytoplasm. The viral genomic RNA is always encapsidated by N protein and associated with L protein to form ribonucleoprotein (RNP) complexes in the virion. After virus entry, uncoating occurs and the genomic RNAs with some specific viral proteins can be used to initiate transcription of positive-sense messenger RNA (mRNA) and the intermediate product cRNA. The mRNA can serve as a template for viral protein synthesis, such as L protein, Gc (or G1), Gn (or G2), NSm, N, and NSs; and the cRNA coated by N can recruit L protein to form functional cRNPs, which can serve as templates to synthesize progeny vRNAs. Similarly, after recruitment and encapsidation, the progeny vRNPs are formed and then packaged by glycoprotein into progeny viruses. Meanwhile, the nascent vRNP can also be used as templates to synthesize cRNA and mRNA through the so-called secondary replication and secondary transcription.

the progeny vRNPs can also be used as templates to synthesize mRNA and cRNA *via* so-called secondary transcription and secondary replication. The replication cycle for a typical trisegmented bunyavirus is shown in **Figure 2**, and there are very few differences for a bisegmented bunyavirus.

According to the viral replication cycle and the initial transcripts of the cDNA clones, two categories of reverse genetics systems can be constructed for negative-strand RNA bunyaviruses, including sense (–) and antisense (+) MG, iVLP, and IFLC systems, of which the initial transcripts are genomic RNA (vRNA) and antigenomic RNA (cRNA), respectively. It is theoretically possible that both (+) and (–) systems can successfully model the partial or entire virus replication cycle. It has been demonstrated that the sense (+) and antisense (–) reverse genetics systems of Uukuniemi virus (UUKV) show no obviously different efficiencies in rescuing MG RNAs and the recombinant virus (Flick and Pettersson, 2001; Flick et al., 2004; Overby et al., 2006; Rezeli et al., 2015).

CURRENT STATUS OF REVERSE GENETICS RESEARCH ON BUNYAVIRUSES

Currently, the definition of reverse genetics is not just used exclusively to describe the generation or rescue of replication competent viruses from cDNA clones; a broader definition consisting of the generation and subsequent replication and

transcription of full-length virus RNA genomes or truncated genome analogs from cDNA clones has been widely recognized by researchers (Hoenen et al., 2011). According to the broader definition, the reverse genetics systems constructed for bunyaviruses mainly consist of MG (or minireplicons), iVLP [or transcription and replication competent virus-like particles (trVLPs)], and IFLC systems. The reverse genetic systems developed for segmented bunyaviruses mainly rely on the production of viral transcripts from transfected plasmids by either bacteriophage T7 RNA polymerase or cellular RNA polymerase I (pol-I; Walpita and Flick, 2005). In a T7 RNA polymerase-driven reverse genetics system, the viral transcripts are produced in the cytoplasm, whereas RNA pol-I is a cellular protein that synthesizes unmodified RNA species with defined terminal sequences in the nuclei of transfected cells. Moreover, it has been reported that the 5'-triphosphate group of T7 pol transcripts strongly activates the antiviral interferon system *via* the intracellular RNA receptor RIG-I (Hornung et al., 2006). However, it has been demonstrated that the T7- and pol-I-driven reverse genetics systems are equally efficient in rescuing MG RNAs and recombinant virus for trisegmented RVFV (Habjan et al., 2008) and bisegmented lymphocytic choriomeningitis mammarenavirus (LCMV; Flatz et al., 2006; Sanchez and de la Torre, 2006).

For a typical three-segmented bunyavirus, schematic organization of reverse genetics systems, including MG, iVLP, and IFLC systems, can be seen in **Figure 3**. Briefly, RdRp, N, and Gn/Gc proteins are provided in trans form from Pol-II or T7-driven expression plasmids or from the helper virus

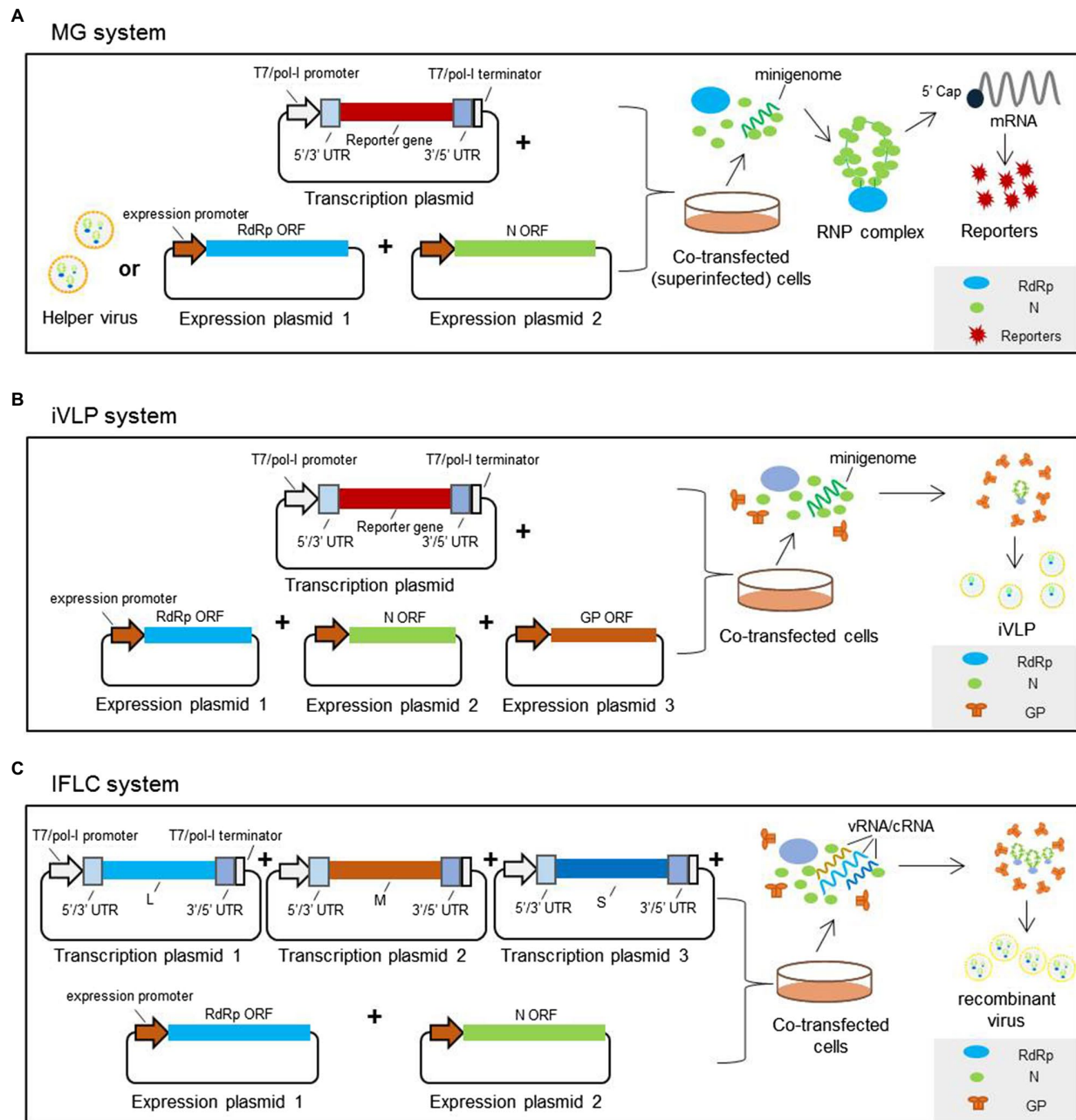


FIGURE 3 | Reverse genetics systems established for typical three-segmented bunyaviruses. **(A)** Minigenome system based on plasmid transfection mainly consisting of expression plasmids encoding RdRp, N, and T7 or pol-I-driven transcription plasmid to express virus-like genome or antigenome RNA. The transcription plasmids are constructed by inserting the reporter-encoding gene flanked by viral UTRs into a T7 or pol-I promoter-driven vector in sense or antisense orientation. The expression plasmids are constructed by inserting the RdRp- or N-encoding gene into an expression vector. While in a minigenome system with helper virus, the RdRp and N are provided by the authentic wild-type virus instead of the expression plasmids. After co-transfection of the plasmid mix, the functional RNP complexes can form, leading to the expression of reporter proteins. **(B)** The infectious virus-like particle system is constructed based on the minigenome system, in which Gn/Gc proteins are also provided in trans form from expression plasmids to package the functional RNP complexes to form iVLPs. **(C)** In an IFLC system, after the cells are co-transfected with plasmids to express full-length antigenomic or genomic L, M, and S and plasmids to express RdRp and N, the functional L-, M-, and S-RNP complexes form. The RNP particles are then packaged by glycoproteins to generate infectious recombinant viruses.

and the genomic or antigenomic RNA segments, which are generated from a T7 or pol-I-driven expression plasmid. The MG system is mainly comprised of two expression plasmids to encode RdRp and N, and one transcription plasmid to

express virus-like genome or antigenome RNA (as shown in **Figure 3A**). For the iVLP system, the expression plasmid encoding glycoprotein Gn/Gc is added to generate iVLPs based on the MG system (as shown in **Figure 3B**). For the IFLC

system, expression plasmids encoding viral RdRp, NP, and sometimes Gn/Gc are also included, and transcription plasmids to express viral genomic or antigenomic L, M, and S are co-transfected into targeted cells to generate infectious recombinant viruses (as shown in **Figure 3C**). However, in BSR-T7/5 cells, the recombinant BUNV can be generated by transfecting just three antigenomic plasmids under the control of the T7 promoter, though these antigenomic plasmids provide low levels of supporting proteins (Lowen et al., 2004).

The segmented nature of the bunyavirus genome potentially contributes to easy reassortment between two genetically related viruses when they co-infect the same host cell (Briese et al., 2013). To evaluate the genome reassortment potential and model the evolutionary process between closely related bunyaviruses, the so-called combinatory MG and iVLP systems based on traditional MG and iVLP systems have been developed for several important bunyaviruses, such as severe fever with thrombocytopenia syndrome virus (SFTSV), Heartland virus (HRTV; Rezelj et al., 2019; Ren et al., 2020), Oropouche virus (OROV), Schmallenberg virus (SBV; Tilston-Lunel et al., 2017), Cache Valley virus (CVV), and Kairi virus (KRIV; Dunlop et al., 2018). The combinatorial MG or iVLP system is generally comprised of the RdRp and N from the same virus (virus A for instance), the vRNA/cRNA-MG from a closely related virus (virus B for instance), and the glycoprotein (omitted from the MG system) from virus A or B. Results of our previous studies have revealed that the RdRp and N of SFTSV and HRTV cannot cross-recognize each other in a murine pol-I-driven MG system though the NP of SFTSV and another novel *Banyangvirus* Guertu virus (GTV) can efficiently substitute for each other to form functional RNP complex (Shen et al., 2018). However, Dunn et al. have reported that the BUNV RdRp can also transcribe the MG-RNA in concert with the N proteins of closely related bunyaviruses, such as Batai virus, CVV, Maguari virus, Main Drain virus, and Northway virus, which prove that bunyavirus RdRp sometimes can also interact with the N from another virus.

DEVELOPMENT AND APPLICATION OF REVERSE GENETIC SYSTEMS FOR BUNYAVIRUSES

Minigenome Reporter Systems

MGs or minireplicons are virus-like genome segments (or genome analogs) that contain the *cis*-acting elements required for replication and transcription, but in which some or all of the viral protein-coding regions have been replaced with genes encoding reporter proteins, such as enhanced green fluorescent protein (*EGFP*), chloramphenicol acetyltransferase, or luciferase. Viral proteins, such as RdRp and N, required for the replication and transcription of MG, are provided in trans form to drive expression of the encoded reporter protein, and viral proteins can be provided *via* either a co-infecting helper virus or by expression plasmids. MG systems are generally used as model systems for virus genome transcription and replication, and

are frequently, although not always, generated as precursors to the development of IFLC systems.

It is incontestable that a breakthrough came when Palese et al. established the first MG system for the modification of a negative-sense segmented RNA virus, influenza A virus, in 1989 (Luytjes et al., 1989). However, the reliance on helper virus infection restricted its applications. For negative-sense RNA viruses, the first established plasmid-based MG system was pioneered by Pattnaik and Wertz et al., who established a replication system to study the structure–function relationships between viral proteins and RNA replication (Pattnaik and Wertz, 1990, 1991). For bunyaviruses, the first established MG system based on the T7 promoter and BUNV S segment was established by Dunn et al. (1995); thereafter, MG systems have been advancing rapidly and widely applied by researchers to investigate the transcription, replication, and pathogenesis of bunyaviruses.

The MG system has been mainly used to examine the *cis*- and *trans*-acting factors involved in bunyavirus replication and transcription (Barr et al., 2003; Ikegami et al., 2005), defining the minimal *cis*- and *trans*-acting factors required for viral replication (Barr et al., 2003), mapping critical residues of the viral promoter (Flick et al., 2004; Zhao et al., 2013), exploring the packaging (Kohl et al., 2006), revealing the pathogenic mechanism (Ruiz-Jarabo et al., 2003; Shao et al., 2018), and identifying novel antiviral compounds (Rathbun et al., 2015) without requiring the use of live forms of bunyaviruses. For example, Flick et al. created the first pol-I-driven MG system of HTNV (Hantaviridae) in 2003, which provided powerful tools for studying the functions of essential genes or proteins of hantavirus (Flick et al., 2003). The first pol-I promoter-based cRNA and vRNA MG systems of CCHFV (family Nairoviridae) were constructed with a helper virus in 2003, and this is also the first reported reverse genetics system for nairoviruses. Then, Bergeron et al. developed a more efficient CCHFV helper virus-independent MG system based on S, M, and L segments for the analysis of virus RNA and protein features involved in CCHFV replication. Using these systems, they revealed that UTRs of CCHFV L, M, and S were similar in support of replication of the respective MGs, and the ovarian tumor protease activity from the L protein was dispensable for virus RNA replication (Bergeron et al., 2010). The first reported MG system of the prototype bunyavirus BUNV (*Peribunyaviridae*) was pioneered by Dunn et al. in 1995, and they performed a wide-scale mutagenic analysis of viral N to examine the effects of different N mutants on viral RNA transcription and replication using the T7-driven MG system (Dunn et al., 1995). Over the next several years, T7-driven MG systems have been developed for many other viruses from the genus *Peribunyaviridae*, such as Shuni virus (SHUV), AKAV, LACV, SBV, CVV, KRIV, and OROV (as shown in **Table 1**), and these systems have been widely used to study the viral replication cycle. For viruses from the genus *Phenuiviridae*, the first successfully constructed MG system was reported in 1995 for RVFV based on the classical T7-vaccinia virus (T7-VV) system, where it was proven that viral N and L are absolutely required and sufficient to reconstitute the

transcriptase activity (Lopez et al., 1995). Thereafter, T7- and/or pol-I-driven MG systems have been successively developed for UUKV, SFTSV, and HRTV (see **Table 1**).

Infectious Virus-Like Particle System

MG system has been used to model the replication and transcription process of the viral life cycle, but it cannot mimic other steps, such as virus entry, budding, and packaging. Therefore, the iVLP or trVLP system has been developed to generate single-cycle infection particles. As this system can model a complete single infectious cycle of bunyavirus, it has become a very effective tool to further our understanding of every aspect of the virus life cycle.

Currently, a variety of iVLP systems have been developed for bunyaviruses, such as BUNV, RVFV, UUKV, CCHFV, and SFTSV, which belong to *Peribunyaviridae*, *Nairoviridae*, and *Phenuiviridae*, respectively. The first iVLP system was successfully constructed for BUNV (*Orthobunyavirus*) by Shi et al., (2006), which was used to investigate the role of the nonstructural protein NSm in virus assembly and morphogenesis (Shi et al., 2006). Using an iVLP assay, Feng et al. revealed that interferon-stimulated genes 20 (ISG20) can strongly inhibit gene expression from all three viral segments of BUNV in a recent study (Feng et al., 2018). An iVLP system for UUKV (*Phlebovirus*) was also constructed in 2006, and the authors reported that the RNP complexes are incorporated into iVLPs but are not required for the generation of particles. Morphological analysis of these particles by electron microscopy revealed that iVLPs, either with or without MGs, display a surface morphology indistinguishable from that of the authentic UUKV and that they bud into Golgi vesicles in the same way as UUKV does (Overby et al., 2006). In the case of RVFV (*Phlebovirus*), Habjan et al. developed an iVLP system and revealed that a human interferon-induced protein, MxA, inhibits both primary and secondary transcriptions of RVFV (Habjan et al., 2009). Based on the previous results, the authors further evaluated the potential of RVFV iVLPs being developed as a vaccine candidate and found that the RVFV iVLPs were highly immunogenic and conferred protection against RVFV infection in mice without exhibiting any side effects (Naslund et al., 2009). For CCHFV (*Orthonairovirus*), a so-called transcription and entry-competent virus-like particle (tc-VLP) system first developed in 2014, the authors revealed that the endonuclease domain of CCHFV L protein is located around amino acid D693 using this system (Devignot et al., 2015). Furthermore, the immunogenicity and protection were also investigated using the CCHFV tc-VLP as a vaccine candidate in an interferon alpha receptor knockout mouse model, and the results showed that mice vaccinated with a specific DNA vaccine combined with the tc-VLP were fully protected (Hinkula et al., 2017). In a recent study, the authors revealed the important role of CCHFV GP38 and NSm on CCHFV particle production and infectivity using the tc-VLP system (Freitas et al., 2020). An iVLP system of SFTSV (*Bandavirus*) based on the M segment was developed by Rezeli et al. in 2019 and revealed the reassortment potential of SFTSV and the closely related bandaviruses and phleboviruses (Rezeli et al., 2019).

Besides the classical reverse genetics systems, the so-called combinatorial MG and iVLP systems that contain viral components derived from closely related viruses were also established. Recently, Rezeli and Ren et al., respectively, developed T7- and pol-I-driven combinatorial MG and iVLP systems to study the *Bandavirus* (SFTSV, HRTV, and GTV) and *Phlebovirus* (RVFV and UUKV) genome reassortment potential (Rezeli et al., 2019; Ren et al., 2020). Similarly, other studies have also investigated the genome reassortment among orthobunyaviruses using combinatorial MG and iVLP systems, such as for OROV, SBV, and others within the Simbu serogroup (Tilston-Lunel et al., 2017). Since then, the reassortment potential of CVV and KRIV has also been evaluated (Dunlop et al., 2018). These combinatorial systems are excellent tools for researchers to assess the viral genome reassortment potential through evaluating the compatibility of viral components coming from closely related bunyaviruses without too much emphasis on the biosafety risk caused by co-infection. Meanwhile, they also have been used to identify the factors that affect the genome reassortment potential between different members of *Bunyavirales*.

Infectious Full-Length Clone System

The IFLC system generally consists of expression plasmids encoding RdRp and N, and transcription plasmids based on cellular pol-I or T7 promoter expressing all viral genome segments; this system has always been used to generate infectious wild type or recombinant viruses and has tremendous potential in studying the virus replication cycle in its entirety. Today, IFLC systems for many members in the families of *Arenaviridae*, *Hantaviridae*, *Nairoviridae*, *Peribunyaviridae*, and *Phenuiviridae* have been successfully developed and widely applied to study various aspects of bunyaviruses.

Bridgen and Elliott made an important breakthrough in 1996 by successfully rescuing infectious BUNV entirely from cloned cDNAs under the control of T7 promoter. However, the procedure, including infection with a recombinant virus that expresses T7 RNA polymerase, transfection with three helper plasmids to express all of the BUNV proteins, and a second transfection with a mixture of plasmids to generate full-length antigenome viral RNAs, was cumbersome and the efficiency of generating infectious viruses was rather low (Bridgen and Elliott, 1996). With the IFLC system, they generated mutant BUNV without expressing NSs (nonstructural protein) and then revealed that although the NSs of BUNV are not essential for virus growth in tissue culture or mice, it has several functions in the virus life cycle and contributes to viral pathogenesis (Bridgen et al., 2001). As the complicated procedure and low rescue efficiency limit its application, Lowen et al. then improved the IFLC system of BUNV by replacing the recombinant virus with BSR-T7/5 cell lines to express T7 RNA polymerase. Then, the recombinant BUNV can be efficiently recovered following transfection with a mixture of plasmids, including two helper-protein (RdRp and N) expression plasmids and three ribozyme plasmids expressing L, M, and S antigenome RNAs. Interestingly, the BUNV can also be recovered following transfection with just three ribozyme plasmids without the need for separate helper-protein expression plasmids, which

may be ascribed to the positive-sense transcripts generated by T7 RNA polymerase appearing to act as both messenger and antigenome RNA (Lowen et al., 2004). From then on, the five or three plasmids rescue system based on promoter T7 or pol-I has been widely used to generate wild type and recombinant bunyaviruses (see **Table 1**).

The IFLC system has been applied to facilitate the development of novel recombinant viruses for many pathogenic members of the families *Arenaviridae*, *Hantaviridae*, *Nairoviridae*, *Peribunyaviridae*, and *Phenuiviridae*, and the recombinant virus has been used to study the viral life cycle and develop vaccine candidates. A variety of approaches based on reverse genetics has been undertaken to use recombinant viruses to rapidly generate live-attenuated vaccine candidates and the strategies have been reviewed elsewhere (Tercero and Makino, 2020). Therefore, here, we just highlight the applications of IFLC systems by providing several representative examples. For the prototypic arenavirus LCMV, a live-attenuated vaccine candidate was developed in 2015 based on the presence of the noncoding intergenic region of the S genome segment in both L and S segments using IFLC systems (Iwasaki et al., 2015). The same strategy was recently utilized by others to develop a safe and effective recombinant virus vaccine candidate for LASV, which is a pathogenic arenavirus that causes Lassa fever with high morbidity and lethality, and there is no approved LASV vaccine currently available (Cai et al., 2020a). Based on the reverse genetics systems, Cai et al. also generated a recombinant LASV expressing a codon-deoptimized GP gene, which also has the potential to be developed as an excellent live-attenuated vaccine candidate (Cai et al., 2020b). For another high-pathogenic bunyavirus RVFV (genus *Phlebovirus*, family *Phenuiviridae*), the classical live-attenuated vaccine candidates, including recombinant virus with genome segment rearrangement (Wichgers Schreur et al., 2014) and single-cycle replicable virus (Murakami et al., 2014), were also successfully generated based on the IFLC system. These studies suggest that the IFLC systems can be used as excellent tools to rapidly develop vaccine candidates for emerging bunyaviruses, as long as a proper strategy is adopted.

Meanwhile, the rescued recombinant bunyaviruses with reporters can also be used as powerful tools to allow high-throughput screening for host factors affecting virus replication and antiviral drugs. Taking the prototype bunyavirus BUNV as an example, using a recombinant BUNV with expressing *EGFP*, the authors screened a library of more than 350 human ISGs for the effects on virus replication, and IFITM3 and IRF1 were identified as modest inhibitors of BUNV replication (Schoggins et al., 2014). Then, they increased the library size to 488 unique ISGs and found that the antiviral exonuclease ISG20 had broad-spectrum antiviral activity against multiple bunyaviruses, including BUNV, HRTV, SFTSV, and SBV (Feng et al., 2018). For most bunyaviruses, nonstructural proteins generally act as pathogenicity and virulence factors and a lot of IFLC systems have also been used to study the NSs or NSm of bunyaviruses, such as BUNV (Bridgen et al., 2001; Weber et al., 2002), UUKV (Rezelj et al., 2015), SFTSV (Brennan et al., 2017), RVFV (Bird et al., 2008, 2011), and SHUV (Oymans et al., 2020).

CURRENT LIMITATIONS AND FUTURE PERSPECTIVES

It is undisputed that the above studies on MG, iVLP, and IFLC systems highlight the importance of reverse genetics in improving our understanding of negative RNA viruses at the molecular level. Indeed, the established reverse genetics systems for bunyaviruses have been powerful tools for researchers to study bunyaviruses and develop antiviral countermeasures. However, in many situations, cautionary notes need to be introduced in interpreting the data obtained using reverse genetics approaches since there are many differences between modeling systems and the authentic viral replication cycle.

The reverse genetics systems based on plasmid transfection express the naked MG/viral RNA *via* T7 or cellular pol-I promoter and the naked RNAs must undergo artificial encapsidation by N that is also expressed by transfected plasmid. As there is no strictly equivalent process during virus infection, there may be many factors affecting the activity of reverse genetics systems rather than virus replication. For example, it has been reported previously that the NSs protein of both BUNV and RVFV decrease MG-encoded activity through inhibiting the viral polymerase (Weber et al., 2001; Brennan et al., 2011). In contrast, other studies have shown that expression of the RVFV NSs protein in a MG system enhances RNA replication and transcription, as measured by an increase in reporter gene activity (Ikegami et al., 2005). Interestingly, the NSs proteins of both BUNV and RVFV have been reported to be able to promote virus replication through counteracting the host antiviral responses during infection (Weber et al., 2002; Billecocq et al., 2004). These results suggest that conflicting data may be produced using different experimental systems, especially when the MG or iVLP system is used to conduct similar studies. When dealing with these problems, the different details between plasmid transfection-based reverse genetics systems and authentic virus infection should be taken into account. The IFLC systems based on transfection can be used to generate nascent wild type or recombinant viruses that can perform all the basic steps of the authentic viral replication cycle. It seems that there are very few limitations when dissecting the virus life cycle with the IFLC systems, as long as mutations introduced into the virus genome do not render the virus replicative incompetent. However, if the recombinant virus cannot be generated because of introduced mutations, it will be hard to determine which specific step of the viral replication cycle was interrupted without using the MG or iVLP system.

Although the reverse genetics systems have been successfully constructed for an increasing number of emerging bunyaviruses and have been used to dissect the viral life cycle, many questions remain to be answered in the future. For the MG and iVLP systems, it remains uncertain how the viral N selectively recognizes the foreign part of the MG RNAs despite there being huge differences between viral and reporter genes. It has been demonstrated that RdRp and N can recognize the heterologous MG RNAs to form functional RNP complexes and these combinatorial RNPs can also be packaged by heterologous glycoprotein (Rezelj et al., 2019; Ren et al., 2020), of which the molecular mechanisms also wait to

be revealed through utilizing reverse genetics systems. Moreover, in the case of bunyavirus packaging, it also remains to be elucidated whether the progeny virions package viral segments intricately in a selective manner or in a random packaging manner. Based on better understanding of the common characteristics of bunyaviruses, the bivalent or polyvalent vaccines against closely related emerging bunyaviruses may be rapidly generated in future, which will provide us with timely and effective protection when faced with an outbreak of a pathogenic bunyavirus.

CONCLUSION

The advent of reverse genetics technology has greatly facilitated our understanding of the life cycle of negative viruses, including the largest group of RNA viruses, bunyaviruses. This review focused mainly on members of the families *Arenaviridae*, *Hantaviridae*, *Nairoviridae*, *Peribunyaviridae*, and *Phenuiviridae*, which are comprised of a large group of important pathogens infecting humans and animals and posing a threat to global health, food, and economy. The majority of the bunyaviruses is restricted to be handled in containment conditions, which has stunted the better understanding of the viral life cycle and the development of antivirals.

The reverse genetics system provides a powerful platform, allowing researchers to work with highly pathogenic viruses at a lower biocontainment level than normally required. Here, we not only summarized the already developed reverse genetics systems, including MG, iVLP, and IFLC, for important bunyaviruses but also provided a brief overview of the wide applications of these systems and future perspectives. These exciting research results can provide a foundation to fully

exploit the potential of these reverse genetics systems and develop reverse genetics systems for other novel segmented negative-stranded RNA viruses.

AUTHOR CONTRIBUTIONS

FD, D-YZ, HW, Y-JN, CH, and FR conceived and designed the review and wrote the manuscript. QW and GW assisted with reference collection. FR and SS wrote and proofread the original manuscript. All authors contributed to the article and approved the submitted version.

FUNDING

This work was funded by the National Major Scientific and Technological Special Project for “Significant New Drugs Development” (2020ZX09201-001), the National Natural Science Foundation of China (U20A20135), the National Program on Key Research Project of China (2018YFE0200402), the Innovation Team Project of Hubei Provincial Health Commission (WJ2019C003), the Special Project of Hubei Science and Technology Innovation Platform (2020DFE018), and the Biological Resources Programme, Chinese Academy of Sciences (KFJ-BRP-017-74).

ACKNOWLEDGMENTS

We extend our greatest thanks to the core facility and technical support of Wuhan Institute of Virology and the financial support of the Research Center for Translational Medicine, Wuhan Jinyintan Hospital.

REFERENCES

- Abudurexiti, A., Adkins, S., Alioto, D., Alkhovsky, S. V., Avsic-Zupanc, T., Ballinger, M. J., et al. (2019). Taxonomy of the order Bunyavirales: update 2019. *Arch. Virol.* 164, 1949–1965. doi: 10.1007/s00705-019-04253-6
- Barr, J. N., Elliott, R. M., Dunn, E. F., and Wertz, G. W. (2003). Segment-specific terminal sequences of Bunyamwera bunyavirus regulate genome replication. *Virology* 311, 326–338. doi: 10.1016/s0042-6822(03)00130-2
- Bergeron, E., Albarino, C. G., Khristova, M. L., and Nichol, S. T. (2010). Crimean-Congo hemorrhagic fever virus-encoded ovarian tumor protease activity is dispensable for virus RNA polymerase function. *J. Virol.* 84, 216–226. doi: 10.1128/JVI.01859-09
- Bergeron, E., Chakrabarti, A. K., Bird, B. H., Dodd, K. A., McMullan, L. K., Spiropoulou, C. F., et al. (2012). Reverse genetics recovery of Lujo virus and role of virus RNA secondary structures in efficient virus growth. *J. Virol.* 86, 10759–10765. doi: 10.1128/JVI.01144-12
- Bergeron, E., Zivcec, M., Chakrabarti, A. K., Nichol, S. T., Albarino, C. G., and Spiropoulou, C. F. (2015). Recovery of recombinant Crimean Congo hemorrhagic fever virus reveals a function for non-structural glycoproteins cleavage by Furin. *PLoS Pathog.* 11:e1004879. doi: 10.1371/journal.ppat.1004879
- Billecocq, A., Spiegel, M., Vialat, P., Kohl, A., Weber, F., Bouloy, M., et al. (2004). NSs protein of Rift Valley fever virus blocks interferon production by inhibiting host gene transcription. *J. Virol.* 78, 9798–9806. doi: 10.1128/JVI.78.18.9798-9806.2004
- Bird, B. H., Albarino, C. G., Hartman, A. L., Erickson, B. R., Ksiazek, T. G., and Nichol, S. T. (2008). Rift valley fever virus lacking the NSs and NSm genes is highly attenuated, confers protective immunity from virulent virus challenge, and allows for differential identification of infected and vaccinated animals. *J. Virol.* 82, 2681–2691. doi: 10.1128/Jvi.02501-07
- Bird, B. H., Maartens, L. H., Campbell, S., Erasmus, B. J., Erickson, B. R., Dodd, K. A., et al. (2011). Rift Valley fever virus vaccine lacking the NSs and NSm genes is safe, Nonteratogenic, and confers protection from Viremia, pyrexia, and abortion following challenge in adult and pregnant sheep. *J. Virol.* 85, 12901–12909. doi: 10.1128/Jvi.06046-11
- Blakqori, G., and Weber, F. (2005). Efficient cDNA-based rescue of La Crosse bunyaviruses expressing or lacking the nonstructural protein NSs. *J. Virol.* 79, 10420–10428. doi: 10.1128/JVI.79.16.10420-10428.2005
- Brennan, B., Li, P., and Elliott, R. M. (2011). Generation and characterization of a recombinant Rift Valley fever virus expressing a V5 epitope-tagged RNA-dependent RNA polymerase. *J. Gen. Virol.* 92, 2906–2913. doi: 10.1099/vir.0.036749-0
- Brennan, B., Li, P., Zhang, S., Li, A., Liang, M., Li, D., et al. (2015). Reverse genetics system for severe fever with thrombocytopenia syndrome virus. *J. Virol.* 89, 3026–3037. doi: 10.1128/JVI.03432-14
- Brennan, B., Rezelj, V. V., and Elliott, R. M. (2017). Mapping of transcription termination within the S segment of SFTS Phlebovirus facilitated generation of NSs Deletant viruses. *J. Virol.* 91:e00743-17. doi: 10.1128/JVI.00743-17
- Bridgen, A., and Elliott, R. M. (1996). Rescue of a segmented negative-strand RNA virus entirely from cloned complementary DNAs. *Proc. Natl. Acad. Sci. U. S. A.* 93, 15400–15404. doi: 10.1073/pnas.93.26.15400
- Bridgen, A., Weber, F., Fazakerley, J. K., and Elliott, R. M. (2001). Bunyamwera bunyavirus nonstructural protein NSs is a nonessential gene product that

- contributes to viral pathogenesis. *Proc. Natl. Acad. Sci. U. S. A.* 98, 664–669. doi: 10.1073/pnas.98.2.664
- Briese, T., Calisher, C. H., and Higgs, S. (2013). Viruses of the family Bunyaviridae: are all available isolates reassortants? *Virology* 446, 207–216. doi: 10.1016/j.virol.2013.07.030
- Brocato, R. L., and Hooper, J. W. (2019). Progress on the prevention and treatment of hantavirus disease. *Viruses* 11, 610. doi: 10.3390/v11070610
- Brown, K. S., Ebihara, H., and Feldmann, H. (2012). Development of a minigenome system for Andes virus, a New World hantavirus. *Arch. Virol.* 157, 2227–2233. doi: 10.1007/s00705-012-1401-0
- Cai, Y. Y., Iwasaki, M., Beitzel, B. F., Yu, S. Q., Postnikova, E. N., Cubitt, B., et al. (2018). Recombinant Lassa virus expressing green fluorescent protein as a tool for high-throughput drug screens and neutralizing antibody assays. *Viruses* 10:655. doi: 10.3390/v10110655
- Cai, Y., Iwasaki, M., Motooka, D., Liu, D. X., Yu, S., Cooper, K., et al. (2020a). A Lassa virus live-attenuated vaccine candidate based on rearrangement of the Intergenic region. *mBio* 11:e00186-20. doi: 10.1128/mBio.00186-20
- Cai, Y., Ye, C., Cheng, B., Nogales, A., Iwasaki, M., Yu, S., et al. (2020b). A Lassa fever live-attenuated vaccine based on codon Deoptimization of the viral glycoprotein gene. *mBio* 11:e00039-20. doi: 10.1128/mBio.00039-20
- Cheng, B. Y., Ortiz-Riano, E., de la Torre, J. C., and Martinez-Sobrido, L. (2015). Arenavirus genome rearrangement for the development of live attenuated vaccines. *J. Virol.* 89, 7373–7384. doi: 10.1128/JVI.00307-15
- Devignot, S., Bergeron, E., Nichol, S., Mirazimi, A., and Weber, F. (2015). A virus-like particle system identifies the endonuclease domain of Crimean-Congo hemorrhagic fever virus. *J. Virol.* 89, 5957–5967. doi: 10.1128/JVI.03691-14
- Dunlop, J. I., Szemiel, A. M., Navarro, A., Wilkie, G. S., Tong, L., Modha, S., et al. (2018). Development of reverse genetics systems and investigation of host response antagonism and reassortment potential for Cache Valley and Kairi viruses, two emerging orthobunyaviruses of the Americas. *PLoS Negl. Trop. Dis.* 12:e0006884. doi: 10.1371/journal.pntd.0006884
- Dunn, E. F., Pritlove, D. C., Jin, H., and Elliott, R. M. (1995). Transcription of a recombinant bunyavirus RNA template by transiently expressed bunyavirus proteins. *Virology* 211, 133–143. doi: 10.1006/viro.1995.1386
- Dutuze, M. F., Nzayirambaho, M., Mores, C. N., and Christofferson, R. C. (2018). A review of Bunyamwera, Batai, and Ngari viruses: understudied Orthobunyaviruses With potential one health implications. *Front. Vet. Sci.* 5:69. doi: 10.3389/fvets.2018.00069
- Elliott, R. M., Blakqori, G., van Knippenberg, I. C., Koudriakova, E., Li, P., McLees, A., et al. (2013). Establishment of a reverse genetics system for Schmallenberg virus, a newly emerged orthobunyavirus in Europe. *J. Gen. Virol.* 94, 851–859. doi: 10.1099/vir.0.049981-0
- Emonet, S. F., Seregin, A. V., Yun, N. E., Poussard, A. L., Walker, A. G., de la Torre, J. C., et al. (2011). Rescue from cloned cDNAs and in vivo characterization of recombinant pathogenic Romero and live-attenuated candid #1 strains of Junin virus, the causative agent of Argentine hemorrhagic fever disease. *J. Virol.* 85, 1473–1483. doi: 10.1128/JVI.02102-10
- Feng, J., Wickenhagen, A., Turnbull, M. L., Rezeli, V. V., Kreher, F., Tilston-Lunel, N. L., et al. (2018). Interferon-stimulated gene (ISG)-expression screening reveals the specific Antiviral activity of ISG20. *J. Virol.* 92, e02140–e02117. doi: 10.1128/JVI.02140-17
- Ferron, F., Weber, F., de la Torre, J. C., and Reguera, J. (2017). Transcription and replication mechanisms of Bunyaviridae and Arenaviridae L proteins. *Viruses* 9, 234, 118–134. doi: 10.1016/j.virusres.2017.01.018
- Flatz, L., Bergthaler, A., de la Torre, J. C., and Pinschewer, D. D. (2006). Recovery of an arenavirus entirely from RNA polymerase I/II-driven cDNA. *Proc. Natl. Acad. Sci. U. S. A.* 103, 4663–4668. doi: 10.1073/pnas.0600652103
- Flick, K., Hooper, J. W., Schmaljohn, C. S., Pettersson, R. F., Feldmann, H., and Flick, R. (2003). Rescue of Hantaan virus minigenomes. *Virology* 306, 219–224. doi: 10.1016/s0042-6822(02)00070-3
- Flick, K., Katz, A., Overby, A., Feldmann, H., Pettersson, R. F., and Flick, R. (2004). Functional analysis of the noncoding regions of the Uukuniemi virus (Bunyaviridae) RNA segments. *J. Virol.* 78, 11726–11738. doi: 10.1128/JVI.78.21.11726-11738.2004
- Flick, R., and Pettersson, R. F. (2001). Reverse genetics system for Uukuniemi virus (Bunyaviridae): RNA polymerase I-catalyzed expression of chimeric viral RNAs. *J. Virol.* 75, 1643–1655. doi: 10.1128/JVI.75.4.1643-1655.2001
- Freitas, N., Enguehard, M., Denolly, S., Levy, C., Neveu, G., Lerolle, S., et al. (2020). The interplays between Crimean-Congo hemorrhagic fever virus (CCHFV) M segment-encoded accessory proteins and structural proteins promote virus assembly and infectivity. *PLoS Pathog.* 16:e1008850. doi: 10.1371/journal.ppat.1008850
- Fuller, J., Surtees, R. A., Slack, G. S., Mankouri, J., Hewson, R., and Barr, J. N. (2019). Rescue of Infectious Recombinant Hazara Nairovirus from cDNA reveals the Nucleocapsid protein DQVD Caspase cleavage motif performs an essential role other than cleavage. *J. Virol.* 93:e00616-19. doi: 10.1128/JVI.00616-19
- Guardado-Calvo, P., and Rey, F. A. (2017). The envelope proteins of the Bunyavirales. *Adv. Virus Res.* 98, 83–118. doi: 10.1016/bs.aivir.2017.02.002
- Guu, T. S., Zheng, W., and Tao, Y. J. (2012). Bunyavirus: structure and replication. *Adv. Exp. Med. Biol.* 726, 245–266. doi: 10.1007/978-1-4614-0980-9_11
- Habjan, M., Penski, N., Spiegel, M., and Weber, F. (2008). T7 RNA polymerase-dependent and -independent systems for cDNA-based rescue of Rift Valley fever virus. *J. Gen. Virol.* 89, 2157–2166. doi: 10.1099/vir.0.2008/002097-0
- Habjan, M., Penski, N., Wagner, V., Spiegel, M., Overby, A. K., Kochs, G., et al. (2009). Efficient production of Rift Valley fever virus-like particles: The antiviral protein MxA can inhibit primary transcription of bunyaviruses. *Virology* 385, 400–408. doi: 10.1016/j.virol.2008.12.011
- Hallam, H. J., Lokugamage, N., and Ikegami, T. (2019). Rescue of infectious Arumowot virus from cloned cDNA: posttranslational degradation of Arumowot virus NSs protein in human cells. *PLoS Negl. Trop. Dis.* 13:e0007904. doi: 10.1371/journal.pntd.0007904
- Hinkula, J., Devignot, S., Akerstrom, S., Karlberg, H., Watrang, E., Bereczky, S., et al. (2017). Immunization with DNA plasmids coding for Crimean-Congo hemorrhagic fever virus capsid and envelope proteins and/or virus-like particles induces protection and survival in challenged mice. *J. Virol.* 91:e02076-16. doi: 10.1128/JVI.02076-16
- Hoenen, T., Groseth, A., de Kok-Mercado, F., Kuhn, J. H., and Wahl-Jensen, V. (2011). Minigenomes, transcription and replication competent virus-like particles and beyond: reverse genetics systems for filoviruses and other negative stranded hemorrhagic fever viruses. *Antivir. Res.* 91, 195–208. doi: 10.1016/j.antiviral.2011.06.003
- Hornung, V., Ellegast, J., Kim, S., Brzozka, K., Jung, A., Kato, H., et al. (2006). 5'-triphosphate RNA is the ligand for RIG-I. *Science* 314, 994–997. doi: 10.1126/science.1132505
- Ikegami, T., Peters, C. J., and Makino, S. (2005). Rift Valley fever virus nonstructural protein NSs promotes viral RNA replication and transcription in a minigenome system. *J. Virol.* 79, 5606–5615. doi: 10.1128/Jvi.79.9.5606-5615.2005
- Ikegami, T., Won, S., Peters, C. J., and Makino, S. (2006). Rescue of infectious rift valley fever virus entirely from cDNA, analysis of virus lacking the NSs gene, and expression of a foreign gene. *J. Virol.* 80, 2933–2940. doi: 10.1128/JVI.80.6.2933-2940.2006
- Ishibashi, K., Matsumoto-Yokoyama, E., and Ishikawa, M. (2017). A tomato spotted wilt virus S RNA-based replicon system in yeast. *Sci. Rep.* 7, 12647. doi: 10.1038/s41598-017-12687-8
- Iwasaki, M., Ngo, N., Cubitt, B., Teijaro, J. R., and de la Torre, J. C. (2015). General molecular strategy for development of Arenavirus live-attenuated vaccines. *J. Virol.* 89, 12166–12177. doi: 10.1128/JVI.02075-15
- Jerome, H., Rudolf, M., Lelke, M., Pahlmann, M., Busch, C., Bockholt, S., et al. (2019). Rift Valley fever virus minigenome system for investigating the role of L protein residues in viral transcription and replication. *J. Gen. Virol.* 100, 1093–1098. doi: 10.1099/jgv.0.001281
- Klemm, C., Reguera, J., Cusack, S., Zielecki, F., Kochs, G., and Weber, F. (2013). Systems to establish bunyavirus genome replication in the absence of transcription. *J. Virol.* 87, 8205–8212. doi: 10.1128/JVI.00371-13
- Kohl, A., Lowen, A. C., Leonard, V. H. J., and Elliott, R. M. (2006). Genetic elements regulating packaging of the Bunyamwera orthobunyavirus genome. *J. Gen. Virol.* 87, 177–187. doi: 10.1099/vir.0.81227-0
- Kuhn, J. H., Adkins, S., Alioto, D., Alkhovsky, S. V., Amarasinghe, G. K., Anthony, S. J., et al. (2020). 2020 taxonomic update for phylum Negarnaviricota (Riboviria: Orthornavirae), including the large orders Bunyavirales and Mononegavirales. *Arch. Virol.* 165, 3023–3072. doi: 10.1007/s00705-020-04731-2
- Lan, S., McLay Schelde, L., Wang, J., Kumar, N., Ly, H., and Liang, Y. (2009). Development of infectious clones for virulent and avirulent pichinde viruses:

- a model virus to study arenavirus-induced hemorrhagic fevers. *J. Virol.* 83, 6357–6362. doi: 10.1128/JVI.00019-09
- Lee, K. J., Novella, I. S., Teng, M. N., Oldstone, M. B., and de La Torre, J. C. (2000). NP and L proteins of lymphocytic choriomeningitis virus (LCMV) are sufficient for efficient transcription and replication of LCMV genomic RNA analogs. *J. Virol.* 74, 3470–3477. doi: 10.1128/jvi.74.8.3470-3477.2000
- Lopez, N., Muller, R., Prehaud, C., and Bouloy, M. (1995). The L-protein of Rift-Valley fever virus can rescue viral Ribonucleoproteins and transcribe synthetic genome-Like RNA molecules. *J. Virol.* 69, 3972–3979. doi: 10.1128/Jvi.69.7.3972-3979.1995
- Lowen, A. C., Noonan, C., McLees, A., and Elliott, R. M. (2004). Efficient bunyavirus rescue from cloned cDNA. *Virology* 330, 493–500. doi: 10.1016/j.virol.2004.10.009
- Luytjens, W., Krystal, M., Enami, M., Parvin, J. D., and Palese, P. (1989). Amplification, expression, and packaging of foreign gene by influenza virus. *Cell* 59, 1107–1113. doi: 10.1016/0092-8674(89)90766-6
- Matsumoto, Y., Ohta, K., Kolakofsky, D., and Nishio, M. (2019). A Minigenome study of Hazara Nairovirus genomic promoters. *J. Virol.* 93, e02118–e02118. doi: 10.1128/JVI.02118-18
- Mazel-Sanchez, B., and Elliott, R. M. (2012). Attenuation of bunyamwera orthobunyavirus replication by targeted mutagenesis of genomic untranslated regions and creation of viable viruses with minimal genome segments. *J. Virol.* 86, 13672–13678. doi: 10.1128/JVI.02253-12
- Murakami, S., Terasaki, K., Ramirez, S. I., Morrill, J. C., and Makino, S. (2014). Development of a novel, single-cycle replicable rift valley fever vaccine. *PLoS Negl. Trop. Dis.* 8:e2746. doi: 10.1371/journal.pntd.0002746
- Naslund, J., Lagerqvist, N., Habjan, M., Lundkvist, A., Evander, M., Ahlm, C., et al. (2009). Vaccination with virus-like particles protects mice from lethal infection of Rift Valley fever virus. *Virology* 385, 409–415. doi: 10.1016/j.virol.2008.12.012
- Noronha, L. E., and Wilson, W. C. (2017). Comparison of two zoonotic viruses from the order Bunyavirales. *Curr. Opin. Virol.* 27, 36–41. doi: 10.1016/j.coviro.2017.10.007
- Overby, A. K., Popov, V., Neve, E. P., and Pettersson, R. F. (2006). Generation and analysis of infectious virus-like particles of uukuniemi virus (bunyaviridae): a useful system for studying bunyaviral packaging and budding. *J. Virol.* 80, 10428–10435. doi: 10.1128/JVI.01362-06
- Oymans, J., Wichgers Schreur, P. J., van Oort, S., Vloet, R., Venter, M., Pijlman, G. P., et al. (2020). Reverse genetics system for Shuni virus, an emerging Orthobunyavirus with zoonotic potential. *Viruses* 12, 455. doi: 10.3390/v12040455
- Patterson, M., Seregin, A., Huang, C., Kolokoltsova, O., Smith, J., Miller, M., et al. (2014). Rescue of a recombinant Machupo virus from cloned cDNAs and in vivo characterization in interferon (alpha/beta/gamma) receptor double knockout mice. *J. Virol.* 88, 1914–1923. doi: 10.1128/JVI.02925-13
- Pattnaik, A. K., and Wertz, G. W. (1990). Replication and amplification of defective interfering particle RNAs of vesicular stomatitis virus in cells expressing viral proteins from vectors containing cloned cDNAs. *J. Virol.* 64, 2948–2957. doi: 10.1128/JVI.64.6.2948-2957.1990
- Pattnaik, A. K., and Wertz, G. W. (1991). Cells that express all five proteins of vesicular stomatitis virus from cloned cDNAs support replication, assembly, and budding of defective interfering particles. *Proc. Natl. Acad. Sci. U. S. A.* 88, 1379–1383. doi: 10.1073/pnas.88.4.1379
- Paweska, J. T. (2015). Rift Valley fever. *Rev. Sci. Tech.* 34, 375–389. doi: 10.20506/rst.34.2.2364
- Perez, M., Craven, R. C., and de la Torre, J. C. (2003). The small RING finger protein Z drives arenavirus budding: implications for antiviral strategies. *Proc. Natl. Acad. Sci. U. S. A.* 100, 12978–12983. doi: 10.1073/pnas.2133782100
- Pontremoli, C., Forni, D., and Sironi, M. (2019). Arenavirus genomics: novel insights into viral diversity, origin, and evolution. *Curr. Opin. Virol.* 34, 18–28. doi: 10.1016/j.coviro.2018.11.001
- Rathbun, J. Y., Droniou, M. E., Damoiseaux, R., Haworth, K. G., Henley, J. E., Exline, C. M., et al. (2015). Novel Arenavirus entry inhibitors discovered by using a Minigenome rescue system for high-throughput drug screening. *J. Virol.* 89, 8428–8443. doi: 10.1128/jvi.00997-15
- Ren, F., Zhou, M., Deng, F., Wang, H., and Ning, Y. J. (2020). Combinatorial Minigenome Systems for Emerging Banyangviruses Reveal Viral Reassortment Potential and Importance of a protruding nucleotide in genome "panhandle" for promoter activity and Reassortment. *Front. Microbiol.* 11:599. doi: 10.3389/fmicb.2020.00599
- Rezelj, V. V., Mottram, T. J., Hughes, J., Elliott, R. M., Kohl, A., and Brennan, B. (2019). M segment-based Minigenomes and virus-Like particle assays as an approach to assess the potential of tick-borne Phlebovirus genome Reassortment. *J. Virol.* 93:e02068-18. doi: 10.1128/JVI.02068-18
- Rezelj, V. V., Overby, A. K., and Elliott, R. M. (2015). Generation of mutant Uukuniemi viruses lacking the nonstructural protein NSs by reverse genetics indicates that NSs is a weak interferon antagonist. *J. Virol.* 89, 4849–4856. doi: 10.1128/JVI.03511-14
- Ruiz-Jarabo, C. M., Ly, C., Domingo, E., and de la Torre, J. C. (2003). Lethal mutagenesis of the prototypic arenavirus lymphocytic choriomeningitis virus (LCMV). *Virology* 308, 37–47. doi: 10.1016/s0042-6822(02)00046-6
- Sanchez, A. B., and de la Torre, J. C. (2006). Rescue of the prototypic Arenavirus LCMV entirely from plasmid. *Virology* 350, 370–380. doi: 10.1016/j.virol.2006.01.012
- Schoggins, J. W., MacDuff, D. A., Imanaka, N., Gainey, M. D., Shrestha, B., Eitson, J. L., et al. (2014). Pan-viral specificity of IFN-induced genes reveals new roles for cGAS in innate immunity. *Nature* 505, 691–695. doi: 10.1038/nature12862
- Serrettiello, E., Astorri, R., Chianese, A., Stelitano, D., Zannella, C., Folliero, V., et al. (2020). The emerging tick-borne Crimean-Congo haemorrhagic fever virus: A narrative review. *Travel Med. Infect. Dis.* 37:101871. doi: 10.1016/j.tmaid.2020.101871
- Shao, J., Liang, Y., and Ly, H. (2018). Roles of Arenavirus Z protein in mediating Virion budding, viral transcription-inhibition and interferon-Beta suppression. *Methods Mol. Biol.* 1604, 217–227. doi: 10.1007/978-1-4939-6981-4_16
- Shen, S., Duan, X., Wang, B., Zhu, L., Zhang, Y., Zhang, J., et al. (2018). A novel tick-borne phlebovirus, closely related to severe fever with thrombocytopenia syndrome virus and heartland virus, is a potential pathogen. *Emerg. Microbes Infect.* 7:95. doi: 10.1038/s41426-018-0093-2
- Shi, X., Kohl, A., Leonard, V. H., Li, P., McLees, A., and Elliott, R. M. (2006). Requirement of the N-terminal region of orthobunyavirus nonstructural protein NSm for virus assembly and morphogenesis. *J. Virol.* 80, 8089–8099. doi: 10.1128/JVI.00579-06
- Simons, J. F., and Pettersson, R. F. (1991). Host-derived 5' ends and overlapping complementary 3' ends of the two mRNAs transcribed from the ambisense S segment of Uukuniemi virus. *J. Virol.* 65, 4741–4748. doi: 10.1128/JVI.65.9.4741-4748.1991
- Smith, D. R., Johnston, S. C., Piper, A., Botto, M., Donnelly, G., Shamblin, J., et al. (2018). Attenuation and efficacy of live-attenuated Rift Valley fever virus vaccine candidates in non-human primates. *PLoS Negl. Trop. Dis.* 12:e0006474. doi: 10.1371/journal.pntd.0006474
- Sun, Y., Li, J., Gao, G. F., Tien, P., and Liu, W. (2018). Bunyavirales ribonucleoproteins: the viral replication and transcription machinery. *Crit. Rev. Microbiol.* 44, 522–540. doi: 10.1080/1040841X.2018.1446901
- Takenaka-Uema, A., Murata, Y., Gen, F., Ishihara-Saeki, Y., Watanabe, K., Uchida, K., et al. (2015). Generation of a recombinant Akabane virus expressing enhanced green fluorescent protein. *J. Virol.* 89, 9477–9484. doi: 10.1128/JVI.00681-15
- Takenaka-Uema, A., Sugiura, K., Bangphoomi, N., Shioda, C., Uchida, K., Kato, K., et al. (2016). Development of an improved reverse genetics system for Akabane bunyavirus. *J. Virol. Methods* 232, 16–20. doi: 10.1016/j.jviromet.2015.12.014
- Tercero, B., and Makino, S. (2020). Reverse genetics approaches for the development of bunyavirus vaccines. *Curr. Opin. Virol.* 44, 16–25. doi: 10.1016/j.coviro.2020.05.004
- Tilston-Lunel, N. L., Acrani, G. O., Randall, R. E., and Elliott, R. M. (2015). Generation of recombinant Oropouche viruses lacking the nonstructural protein NSm or NSs. *J. Virol.* 90, 2616–2627. doi: 10.1128/JVI.02849-15
- Tilston-Lunel, N. L., Shi, X. H., Elliott, R. M., and Acrani, G. O. (2017). The potential for Reassortment between Oropouche and Schmallenberg Orthobunyaviruses. *Viruses* 9:220. doi: 10.3390/v9080220
- Varela, M., Schnettler, E., Caporale, M., Murgia, C., Barry, G., McFarlane, M., et al. (2013). Schmallenberg virus pathogenesis, tropism and interaction with the innate immune system of the host. *PLoS Pathog.* 9:e1003133. doi: 10.1371/journal.ppat.1003133

- Walpita, P., and Flick, R. (2005). Reverse genetics of negative-stranded RNA viruses: a global perspective. *FEMS Microbiol. Lett.* 244, 9–18. doi: 10.1016/j.femsle.2005.01.046
- Weber, F., Bridgen, A., Fazakerley, J. K., Streitenfeld, H., Kessler, N., Randall, R. E., et al. (2002). Bunyamwera bunyavirus nonstructural protein NSs counteracts the induction of alpha/beta interferon. *J. Virol.* 76, 7949–7955. doi: 10.1128/Jvi.76.16.7949-7955.2002
- Weber, F., Dunn, E. F., Bridgen, A., and Elliott, R. M. (2001). The Bunyamwera virus nonstructural protein NSs inhibits viral RNA synthesis in a minireplicon system. *Virology* 281, 67–74. doi: 10.1006/viro.2000.0774
- Welch, S. R., Scholte, F. E. M., Spengler, J. R., Ritter, J. M., Coleman-McCray, J. D., Harmon, J. R., et al. (2020). The Crimean-Congo hemorrhagic fever virus NSm protein is dispensable for growth In vitro and disease in Ifnar(–/–) mice. *Microorganisms* 8:775. doi: 10.3390/microorganisms8050775
- Wichgers Schreur, P. J., Oreshkova, N., Moormann, R. J., and Kortekaas, J. (2014). Creation of Rift Valley fever viruses with four-segmented genomes reveals flexibility in bunyavirus genome packaging. *J. Virol.* 88, 10883–10893. doi: 10.1128/JVI.00961-14
- Ye, C., de la Torre, J. C., and Martinez-Sobrido, L. (2020). Development of reverse genetics for the prototype New World Mammarenavirus Tacaribe virus. *J. Virol.* 94:e01014-20. doi: 10.1128/JVI.01014-20
- Zhang, Y., Li, X. H., Jiang, H., Huang, C. X., Wang, P. Z., Mou, D. L., et al. (2008). Expression of L protein of Hantaan virus 84FLi strain and its application for recovery of minigenomes. *APMIS* 116, 1089–1090. doi: 10.1111/j.1600-0463.2008.01011.x
- Zhao, J. R., Xia, H., Zhang, Y. J., Yin, S. Y., Zhang, Z., Tang, S., et al. (2013). Mini-genome rescue of Crimean-Congo hemorrhagic fever virus and research into the evolutionary patterns of its untranslated regions. *Virus Res.* 177, 22–34. doi: 10.1016/j.virusres.2013.07.005

Conflict of Interest: The authors declare that the review was conducted in the absence of any commercial or financial relationships that could be construed as a potential conflict of interest.

Publisher's Note: All claims expressed in this article are solely those of the authors and do not necessarily represent those of their affiliated organizations, or those of the publisher, the editors and the reviewers. Any product that may be evaluated in this article, or claim that may be made by its manufacturer, is not guaranteed or endorsed by the publisher.

Copyright © 2021 Ren, Shen, Wang, Wei, Huang, Wang, Ning, Zhang and Deng. This is an open-access article distributed under the terms of the Creative Commons Attribution License (CC BY). The use, distribution or reproduction in other forums is permitted, provided the original author(s) and the copyright owner(s) are credited and that the original publication in this journal is cited, in accordance with accepted academic practice. No use, distribution or reproduction is permitted which does not comply with these terms.



Co-circulation of *Orthobunyaviruses* and Rift Valley Fever Virus in Mauritania, 2015

Nicole Cichon¹, Yahya Barry², Franziska Stoeck¹, Abdellah Diambar², Aliou Ba², Ute Ziegler¹, Melanie Rissmann^{1,3}, Jana Schulz^{1,4}, Mohamed L. Haki², Dirk Höper⁵, Baba A. Doumbia⁶, Mohamed Y. Bah⁶, Martin H. Groschup¹ and Martin Eiden^{1*}

¹Institute of Novel and Emerging Infectious Diseases, Friedrich-Loeffler-Institut, Greifswald-Insel Riems, Germany, ²Office National de Recherche et de Développement de l'Élevage (ONARDEL), Nouakchott, Mauritania, ³Department of Viroscience, Erasmus Medical Center, Rotterdam, Netherlands, ⁴Institute of Epidemiology, Friedrich-Loeffler-Institut, Greifswald-Insel Riems, Germany, ⁵Institute of Diagnostic Virology, Friedrich-Loeffler-Institut, Greifswald-Insel Riems, Germany, ⁶Ministère du Développement Rural, Nouakchott, Mauritania

OPEN ACCESS

Edited by:

Ali Zohaib,
Islamia University, Pakistan

Reviewed by:

David Safronetz,
Public Health Agency of Canada
(PHAC), Canada
Laurent Dacheux,
Institut Pasteur, France

*Correspondence:

Martin Eiden
martin.eiden@fli.de

Specialty section:

This article was submitted to
Virology,
a section of the journal
Frontiers in Microbiology

Received: 30 August 2021

Accepted: 26 October 2021

Published: 24 December 2021

Citation:

Cichon N, Barry Y, Stoeck F,
Diambar A, Ba A, Ziegler U,
Rissmann M, Schulz J, Haki ML,
Höper D, Doumbia BA, Bah MY,
Groschup MH and Eiden M (2021)
Co-circulation of *Orthobunyaviruses*
and Rift Valley Fever Virus in
Mauritania, 2015.
Front. Microbiol. 12:766977.
doi: 10.3389/fmicb.2021.766977

Ngari virus (NRIV) has been mostly detected during concurrent outbreaks of Rift Valley fever virus (RVFV). NRIV is grouped in the genus *Orthobunyavirus* within the *Bunyaviridae* family and RVFV in the genus *Phlebovirus* in the family *Phenuiviridae*. Both are zoonotic arboviruses and can induce hemorrhagic fever displaying the same clinical picture in humans and small ruminants. To investigate if NRIV and its parental viruses, Bunyamwera virus (BUNV) and Batai virus (BATV), played a role during the Mauritanian RVF outbreak in 2015/16, we analyzed serum samples of sheep and goats from central and southern regions in Mauritania by quantitative real-time RT-PCR, serum neutralization test (SNT) and ELISA. 41 of 458 samples exhibited neutralizing reactivity against NRIV, nine against BATV and three against BUNV. Moreover, complete virus genomes from BUNV could be recovered from two sheep as well as two NRIV isolates from a goat and a sheep. No RVFV-derived viral RNA was detected, but 81 seropositive animals including 22 IgM-positive individuals were found. Of these specimens, 61 samples revealed antibodies against RVFV and at least against one of the three orthobunyaviruses. An indirect ELISA based on NRIV/BATV and BUNV derived Gc protein was established as complement to SNT, which showed high performance regarding NRIV, but decreased sensitivity and specificity regarding BATV and BUNV. Moreover, we observed high cross-reactivity among NRIV and BATV serological assays. Taken together, the data indicate the co-circulation of at least BUNV and NRIV in the Mauritanian sheep and goat populations.

Keywords: NRIV, BUNV, BATV, RVFV, Mauritania, co-circulation

INTRODUCTION

Ngari virus (NRIV), Bunyamwera virus (BUNV) and Batai virus (BATV) are members of the Bunyamwera serogroup in the genus *Orthobunyavirus* of the family *Peribunyaviridae*. They are characterized by a tri-segmented (S-, M- and L-segment) enveloped negative-stranded RNA genome. The S-segment encodes the NP and NSs proteins, the M-segment encodes

the two glycoproteins Gn and Gc and the NSm protein, and the L-segment codes for the RNA-dependent RNA-polymerase (Elliott, 2014). Sequence analysis showed that NRIV is a natural reassortant resulting from co-infection of BUNV and BATV, as NRIV possesses the M-segment of BATV combined with the S- and L-segments of BUNV (Briese et al., 2006). This reassortment probably led to an increased virulence, which is associated with hemorrhagic fever in humans and ruminants (Dutuze et al., 2018). In contrast, infection with BATV or BUNV is reported to cause only mild flu-like disease in humans (Dutuze et al., 2018). Susceptible vertebrate hosts for BUNV and BATV are ruminants, horses and birds (Hubálek et al., 2014). The BATV strain Chittoor in India caused mild unspecific disease in sheep and goats (Singh and Pavri, 1966), whereas in Europe no disease association in ruminants was described yet, although a high seroprevalence has been determined in Central German goats, sheep and cattle (Ziegler et al., 2018; Cichon et al., 2021). Nevertheless, a German captive harbour seal, which died from encephalitis, tested positive for BATV infection (Jo et al., 2018). In North America, the BUNV strain Cache Valley virus is associated with congenital abnormalities in sheep and other ruminants (Chung et al., 1990; Edwards, 1994). Moreover, in Argentina, BUNV was determined as a causative agent for fatal encephalitis and abortion in horses (Tauro et al., 2015). Likewise, NRIV, BATV and BUNV are transmitted by mosquitoes (Dutuze et al., 2018). For transmission of BUNV, *Aedes aegypti* might be the primary vector (Odhiambo et al., 2014). Additionally, in Argentina, BUNV was isolated from *Ochloretatus scapularis* (Tauro et al., 2015). Infection studies revealed that *Anopheles gambiae* Giles is a competent vector for both, BUNV and NRIV (Odhiambo et al., 2014). Furthermore, NRIV was isolated from various mosquito species in Senegal such as *Aedes argenteopunctatus*, *A. minutus*, *A. vexans*, *A. mcintoshi*, *A. simpsoni*, *A. vittatus*, *A. neoaffricanus*, *Anopheles coustani*, *A. pretoriensis*, *A. pharoensis*, *A. mascarensis*, *Culex bitaeniorhynchus*, *C. tritaeniorhynchus*, *C. antennatus*, and *C. poicilipes* (Zeller et al., 1996). European mosquito species transmitting BATV are *Anopheles maculipennis s.l.*, *A. claviger*, *Coquillettidia richiardii*, *Culex pipiens*, *Ochlerotatus punctor*, *O. communis*, and *Aedes vexans* (Hubálek et al., 2014). Recently, NRIV was detected in ticks [species: *Amblyomma variegatum*, *Rhipicephalus geigy*, and *Rhipicephalus (Boophilus) spp.*] collected from cattle in Guinea (Makenov et al., 2021).

So far, NRIV was isolated only from sub-Saharan Africa, whereas BATV is distributed almost worldwide. Its distribution ranges from Malaysia towards Asian Russia and India and in Europe from Scandinavia towards Italy and Romania (Dutuze et al., 2018). In Africa, the virus was described as Ilesha virus in Sudan, Cameroon, Nigeria, Uganda, and Central African Republic (Hubálek et al., 2014; Dutuze et al., 2018), detected in Mauritania (Gonzalez, 1988) and most recently in Rwanda (Dutuze et al., 2020). BUNV was primarily isolated in several sub-Saharan African countries, such as Uganda, Tanzania, Mozambique, Nigeria, Guinea, South Africa, Democratic Republic of Congo, Senegal, Guinea, Ivory Coast, Nigeria, Cameroon, Central African Republic, Kenya, Uganda,

South Africa, Madagascar, and Rwanda (Dutuze et al., 2018, 2020). Moreover, strains of BUNV have been discovered in North America towards Mexico and Argentina (Dutuze et al., 2018). However, the distribution of these viruses might be underestimated since diagnostic capabilities available for orthobunyaviruses in general are limited and the diagnostic approach was primarily based on clinical presentation (Dutuze et al., 2018). Hence, three outbreaks of NRIV were first mistaken for more common aetiologies of hemorrhagic fever, but afterwards were identified as NRIV outbreak. This happened in Sudan in 1988, when an outbreak of hemorrhagic fever was clinically diagnosed as malaria, but subsequently two isolates of NRIV were found and IgM antibodies against NRIV were detected in 7% of patients (Briese et al., 2006). Likewise, NRIV has been isolated twice during concurrent Rift Valley fever (RVF) outbreaks, in Kenya and Somalia in 1997–1998 and in Mauritania in 2010 (Bowen et al., 2001; Eiden et al., 2014). Rift Valley fever virus (RVFV), a member of the *Phenuiviridae* family in the genus *Phlebovirus*, is a zoonotic mosquito-borne virus of major concern throughout Africa (from Egypt towards South Africa) and even emerged in the Arabian Peninsula in 2000 (Linthicum et al., 2016). Clinical symptoms of an infection with RVFV closely resemble the symptoms caused by NRIV infection: in mild cases human patients show flu-like febrile illness, whereas in 1–2% the infection can develop into severe hemorrhagic fever, encephalitis, and retinitis (Chevalier, 2013). RVFV and NRIV not only present many similarities in their clinical manifestations, but as well share the same ecological distribution, and co-circulate within the same vector and vertebrate host ranges (Dutuze et al., 2018). Outbreaks of RVF characteristically coincide with episodes of unusually heavy rains and extensive flooding in areas normally arid, which were also observed in Sudan in 1988 and Somalia/Kenya in 1997–1998 during the NRIV outbreaks (Briese et al., 2006). Heavy rainfall and consecutive flooding induce mass hatching of *Aedes* species from infected eggs and subsequently of *Culex* species, which then infect humans and ruminants (Linthicum et al., 2016).

In 2015/16, Mauritania experienced the most recent outbreak of RVF, affecting sheep and goats (OIE) as well as humans (Boushab et al., 2016). To investigate the prevalence of RVFV and possible co-infection with NRIV, BATV, and BUNV in the small ruminant population, 492 serum samples of goats and sheep were collected in 2015 in southwestern Mauritania and analyzed by quantitative real-time RT-PCR (qRT-PCR), serum neutralization tests (SNT) specific for each virus, and commercial enzyme-linked immunosorbent assays (ELISA). Additionally, we implemented ELISAs based on the glycoprotein Gc of each NRIV, BATV, and BUNV.

MATERIALS AND METHODS

Sample Collection and Workflow

A total number of 492 apparently healthy sheep and goats were sampled in eight different governorates of Mauritania (Inchiri, Hodh Ech Chargui, Tagant, Assaba, Trarza, Guidimakha,

TABLE 1 | Samples ordered by species and region.

Region	Species	No of samples	Age	Date of sample collection
Inchiri	goat	50	1–5	February 2015
	sheep	29	1–4	November 2015
Chargui	goat	41	1–10	July 2015
	sheep	40	1–5	July 2015
Gharbi	sheep	81	1–7	August 2015
	not available (NA)	4	not available (NA)	October 2015
Tagant	goat	54	1–3	September + October 2015
	sheep	5	not available (NA)	October 2015
Assaba	goat	28	1–6	September 2015
	sheep	32	1–5	October 2015
Trarza	goat	12	1–4	October 2015
	sheep	19	1–3	October 2015
Guidimakha	goat	40	1–4	September 2015
	sheep	34	1–4	September 2015
Brakna	goat	9	3–6	September 2015
	sheep	13	3–5	September 2015
	not available (NA)	1	not available (NA)	September 2015

Brakna, Hodh El Gharbi) in 2015 (Table 1). Serum samples were kept frozen at -20°C for further investigations. After transportation to Germany, all samples were first analyzed for viral RNA with qRT-PCR. For serological testing, the sera were inactivated with 1:1 phosphate-buffered saline (PBS) Tween at 56°C for 30 min. For detection of antibodies against NRIV, BATV, and BUNV, samples were subjected to SNTs and additionally to indirect Glycoprotein Gc-based ELISA. The serological investigation for RVFV-specific antibodies was performed with a competition ELISA (IDvet, Grabels, France) followed by SNT (Rissmann et al., 2017b). Samples with positive and inconclusive results in the ELISAs, were further tested with the RVF IDvet IgM capture ELISA (IDvet, Grabels, France). In case of divergent results in the ELISA and SNT, a final assessment was performed with an adapted commercial immunofluorescence assay (IIFA; Euroimmun, Lübeck, Germany). The complete workflow is seen in Figure 1.

Quantitative Real-Time RT-PCR

RNA isolation was performed using the Nucleo[®]Mag VET Kit (Macherey-Nagel, Düren, Germany) according to the manufacturer's instructions. The samples were processed in a pool of five samples. As internal extraction control, MS2 bacteriophage was added to each serum pool before the extraction process. Control RNA detection was performed with primers MS2F (5'-CTC TGA GAG CGG CTC TAT TGG T-3') and MS2R (5'-GTT CCC TAC AAC GAG CCT AAA TTC-3') and MS2P (HEX-TCAGACACGCGGTCCGCTATAACGA-BHQ1; Ninove et al., 2011). The qRT-PCR for RVFV was carried out according to an adapted multiplex qRT-PCR protocol (Wernike et al., 2015) using the AgPath-ID[™] One-Step RT-PCR Kit (Applied Biosystems, Foster City, United States). The protocol

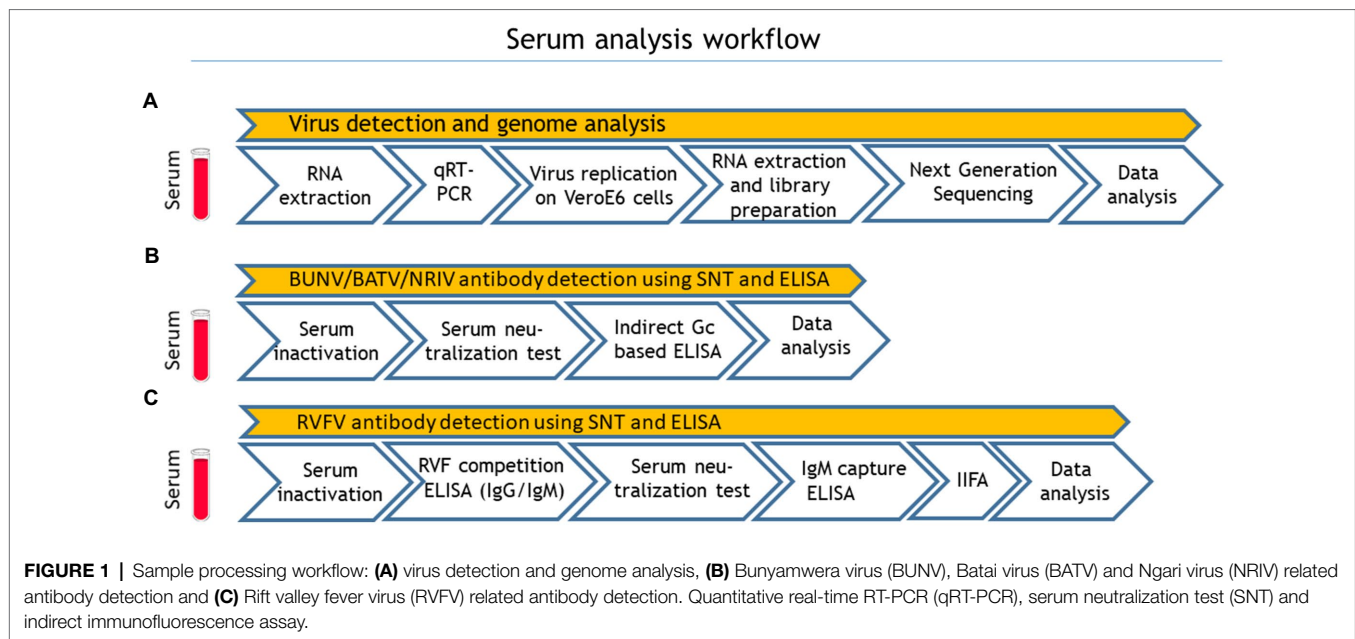
allows the simultaneous detection of RVFV, foot and mouth disease virus (FMDV) and NRIV/BUNV, and uses the following primers: RVF-forw (5'-TGA AAA TTC CTG AGA CAC ATG G-3'), RVF-rev (5'-CTT CCT TGC ATC TGA TG-3') and RVFV probe (FAM-CAATGTAAGGGGCTGTGTGGACTTGTG-BHQ1) for RVFV, FMD-IRES-4.1F (5'-TAA CAW GGA CCC RCS GGG CC-3'), FMD-IRES-4R (5'-TGA AGG GCA TCC TTA GCC TG-3') and FMD-IRES probe (Texas Red-CAT GTG TGC AAY CCC AGC ACR G-BHQ2) for FMDV. For detection of NRIV/BUNV S-segment, novel primers/probes were used: Bunyam_F (5'-GCT GGA AGA TTA CTG TAT ATA C-3'), Bunyam_R (5'-CAA GGA ATC CAC TGA GGC GGT G-3') and Bunyam_P (HEX-AAC AAC CCA GTT CCT GAC GAT GGT C-BHQ2). The final concentrations in the used AgPath-ID[™] One-Step RT-PCR Kit (Applied Biosystems, Foster City, United States) were $0.4\text{ }\mu\text{M}$ for primer and $0.08\text{ }\mu\text{M}$ for the probe, respectively. For each reaction, $2.5\text{ }\mu\text{l}$ of RNA, 5 pmol of both forward and reverse primer and 0.625 pmol of the probe were used in a total volume of $12.5\text{ }\mu\text{l}$. PCR reaction condition was used as follows: 48°C for 10 min, 95°C for 10 min and 44 cycles at 95°C for 15 s, and 60°C for 45 s. Finally, a qRT-PCR assay in a total volume of $12.5\text{ }\mu\text{l}$ targeting the BATV S-segment (Jöst et al., 2011) was performed.

Phylogenetic Analysis

Phylogenetic analysis of full-length sequences was done with Geneious Tree Builder using Neighbor-Joining analysis and genetic distances were calculated using the Tamura-Nei Method. Bootstrap values >80 are displayed at nodes. A sequence of a La Crosse virus, Human/78 strain (accession number: AF528165-167) was used as outgroup to root the tree. Sequence alignments were performed with Clustal W.

Sequencing

Vero E6 cells (CRL-1586, Collection of Cell Lines in Veterinary Medicine, Friedrich-Loeffler-Institut, Germany) were inoculated with $100\text{ }\mu\text{l}$ PCR positive serum samples and assayed for virus replication and cytopathic effects (CPE). After appearance of CPE after 3–4 days, viral RNA was extracted from the supernatant and subjected to a next-generation sequencing workflow (Wylezich et al., 2018). All assembly and mapping analyses were conducted with the 454/Roche Genome Sequencer FLX software suite v3.0 (Roche, Mannheim, Germany) leading to three final datasets (lib02232-lib02234). As part of the assemblies and mappings, adapter and quality trimming were performed using the available adapter sequences' default software settings. First, a partial dataset (25,000 reads) of lib02232 was assembled and the genome segments identified in the obtained contigs. For quality control, the sequences were visually inspected for base qualities and the ORFs were detected using emboss getorf (Rice et al., 2000). Subsequently, the sequences were analyzed using blast (Altschul et al., 1990) with the suitable NCBI nt (for nucleotide sequence analyses) and nr (for amino acid sequence analyses) databases. Afterwards, the quality checked sequences of lib02232 were used to map the full datasets along



these to obtain the three segment sequences of lib02232 (total number of reads 2.228.328, after trimming 2.230.666, matching reads 519.568, resulting average depth approx. 24.900), lib02233 (total 617.530, trimmed 617.664, mapped 270.410, avg. depth 6,500) and lib02234 (total 570.042, trimmed 570.434, mapped 325.364, avg. depth 7,700), which were again quality checked as described. The obtained full-length recovered genome sequences of BUNV (accession no. MT731755 - MT731757) and NRIV (accession Nr. MT747972 - MT747974 and MT747975 - MT747977) were submitted to GenBank.

Serum Neutralization Test

The SNT for detecting BATV neutralizing antibodies was performed using BATV strain 53.2 (acc. no. HQ455790, kindly provided by J. Schmidt-Chanasit, BNITM Hamburg, Germany) as already described by Seidowski et al. (2010) and Ziegler et al. (2018). Modifications were made using Vero E6 cells (CRL-1586) and applying an incubation time of 6 days. Similarly, the SNTs for detecting NRIV and BUNV neutralizing antibodies were performed using a Mauritanian NRIV strain (accession nos. KJ716848–716850) and BUNV ATCC® VR87™ (kindly provided by J. Schmidt-Chanasit, BNITM Hamburg, Germany). Briefly, a virus concentration of 100 TCID₅₀/well was added to each sample running in duplicate at a starting serum dilution of 1:10. Cytopathic effects were seen 4–6 days post infection. The SNT for detecting RVFV neutralizing antibodies was performed as described in the OIE Terrestrial Manual 2014 (OIE, 2020). Briefly, 100 TCID₅₀ of RVFV (MP-12 vaccine strain) were added to serial two-fold diluted sera and 3 × 10⁵ Vero 76 cells/ml (Collection of Cell Lines in Veterinary Medicine, Friedrich-Loeffler-Institut, Germany) were added to each well. Plates were incubated at 37°C, 5% CO₂ for 6 days. The neutralizing antibody titer of the samples was defined as the 50% neutralization dose (ND₅₀). Positive results for neutralizing antibodies were

confirmed when the ND₅₀ was 10 or higher. Positive serum controls were obtained from a sheep immunised with inactivated NRIV virus, a goat immunised with inactivated BUNV virus and a rabbit immunised with inactivated BATV. Negative control serum was derived from an untreated goat.

Recombinant Glycoprotein Gc

Synthetic genes encompassing the domains GI and GII of the glycoprotein Gc were produced by Eurofins (Munich, Germany) based on a partial BATV sequence (acc. no. HQ455791, nucleotide position 601–1,650), the corresponding NRIV sequence (acc. no. KJ716849, position 1,552–2,505) and a BUNV sequence (acc. no. M11852, position 1,479–2,534). The corresponding protein sequences were aligned using CLUSTALW within the geneious® software platform (Auckland, New Zealand). The alignment is depicted in **Supplementary Figure S1**. All three sequences were optimized for expression in *E. coli*. The sequence codes for putative domains I and II of glycoprotein Gc and were cloned into *E. coli* expression vector pET21a using 5' *Bam*HI and 3' *Xho*I restrictions sites and expressed in BL21-Lys cells. Expression of the recombinant proteins and purification by nickel chelating agarose were carried out under denaturing conditions as described previously (Jäckel et al., 2013a). Finally, the proteins were dialyzed against 0.05 M carbonate-bicarbonate buffer pH 9.6 and checked in SDS-PAGE and Coomassie-staining.

Indirect (NRIV/BATV/BUNV) ELISA

For serological testing by ELISA, the collected serum samples were inactivated with 1:1 PBS Tween at 56°C for 30 min. The three indirect in-house ELISAs were based on a partial recombinant glycoprotein Gc of either NRIV or BATV or BUNV which were used for coating immunoplates in a dilution of 2 µg/ml in 0.05 M carbonate-bicarbonate buffer pH 9.6

(100 µl diluted antigen per well). Protocol parameters, dilutions, optimal reagent concentrations and the selection of immunoplates were determined by standard checkerboard titration and choosing the combination with the highest difference in the optical density (OD value) between positive and negative controls. After incubation of the coated immunoplates at 4°C overnight, plates were washed three times with 300 µl washing buffer, containing PBS pH 7.2 and 0.1% Tween 20. After blocking with 200 µl/well 10% skim milk powder (DIFCO™) diluted in PBS for 1 h at 37°C in a moist chamber, ruminant field sera diluted 1:20 for NRIV ELISA and 1:10 for BATV and BUNV ELISA in PBS containing 2% skim milk were added in duplicate to the plates. As positive control, polyclonal hyperimmune sheep serum were diluted 1:20 for NRIV ELISA and 1:10 for BATV and BUNV ELISA, respectively. A volume of 100 µl of each sample and control was added to the plates. After incubation at 37°C for 1 h in a moist chamber, plates were again washed three times with washing buffer. A volume of 100 µl per well of horseradish peroxidase conjugated Protein G (Calbiochem, San Diego, CA) diluted 1:5000 in dilution buffer was then added to the plates and incubated again for 1 h, as described before. After a final washing step, 100 µl per well of 2,20-azinodiethylbenzothiazoline sulfonic acid substrate (ABTS, Roche, Mannheim, Germany) was added and plates were incubated for 30 min at room temperature in the dark. The reaction was stopped by adding 1% sodium dodecyl sulphate and OD value was determined at 405 nm. In case of BUNV ELISA, blocking milk and dilution buffer of IDvet were used following the same protocol as described above. The results were expressed as percentage of the positive control serum (PP value) using the following formula: (mean OD of duplicate test serum/median OD of duplicate positive control) *100. Cut-off value, sensitivity and specificity of the indirect ELISAs were determined in correlation to the corresponding SNT results using the receiver operating characteristic analysis (ROC analysis) with regard to the criterion “Maximization of sensitivity and specificity.” Finally, to determine the accordance between the SNTs and the ELISAs among each other, the kappa coefficient was calculated.

IDvet RVF Competition ELISA and IDvet RVF IgM Capture ELISA

All samples were analyzed in the commercial ID Screen® RVFV competition multispecies ELISA (IDvet, Grabels, France) according to the manufacturer's instructions. Both IgG and IgM antibodies are detected indistinguishably. Samples that gave positive or inconclusive results in the competition ELISA, were further tested with the ID Screen® Rift Valley Fever IgM capture ELISA (IDvet, Grabels, France) according to the manufacturer's description.

Indirect Immunofluorescence

Samples that gave divergent results in ELISAs and SNT were further analyzed with a RVFV in-house IIFA according to a previously published protocol (Jäckel et al., 2013b) using the commercial RVFV immunofluorescence slides from Euroimmun

TABLE 2 | Summary of results from multiplex qRT-PCR (detecting NRIV, BATV, and BUNV) and sequencing.

Sample ID	Species	Region	CT Multiplex	CT Singleplex	Sequencing
			(BUNV S)	(BUNV S)	
MR 393/15 SR	goat	Trarza	no CT	34.69	NRIV
MR 410/15 SR	sheep	Guidimakha	32.33	32.04	
MR 411/15 SR	sheep	Guidimakha	26.96	26.72	NRIV
MR 471/15 SR	sheep	Brakna	28.86	28.82	
MR 478/15 SR	sheep	Brakna	27.19	26.85	BUNV
MR 479/15 SR	sheep	Brakna	30.51	30.21	
MR 487/15 SR	sheep	Brakna	27.4	25.05	BUNV
MR 492/15 SR	goat	Brakna	no CT	34.47	
MR 495/15 SR	sheep	Brakna	30.48	28.16	
MR 496/15 SR	sheep	Brakna	33.98	31.21	

(Lübeck, Germany). The detection of antibodies was realized with species-specific Cy3 labelled secondary antibodies (donkey anti-sheep, donkey anti-goat) from dianova (Hamburg, Germany), in a 1:200 dilution.

Statistical Analysis

The estimated prevalence and 95% confidence intervals (95% CI) were calculated using the calculation tool of EpiTools.¹ Calculations for ROC-analysis were performed using the software (R Core Team, 2020) and the R package OptimalCutpoints (Lopez-Raton et al., 2014).

RESULTS

Among the 492 serum samples tested consecutively for NRIV, BUNV, BATV and RVFV by qRT-PCR assays, 10 samples were tested positive for BUNV/NRIV-derived RNA. Subsequent sequencing revealed two NRIV isolates and two BUNV isolates (Table 2). The positive serum samples originated from one goat and three sheep from Trarza, Guidimakha and Brakna governorates. No RVFV or BATV genome was detected (Table 2).

From four animals, full-length genome sequences of the S-, M-, and L-segments were recovered. Phylogenetic analysis of complete genomes revealed that two isolates clustered to NRIV and two isolates to the BUNV group (Figure 2). NRIV was isolated from one goat of the Trarza region and from a sheep of the Guidimakha region. Both isolates show high similarity among each other with 4 (99,6% sequence identity), 32 (99,8% sequence identity) and 31 (99,5% sequence identity) nucleotide differences corresponding to S-, M-, and L-segment. In addition, they exhibited high similarity to a NRIV isolate recovered from a goat of the Adrar region in 2010. BUNV was isolated from two sheep of the Brakna region. The sequences were identical, indicating the co-infection of two individuals from one flock with the same isolate. The strain showed highest similarity to isolates from Kenya (43 nucleotide differences),

¹<https://epitools.ausvet.com.au/ciproportion>

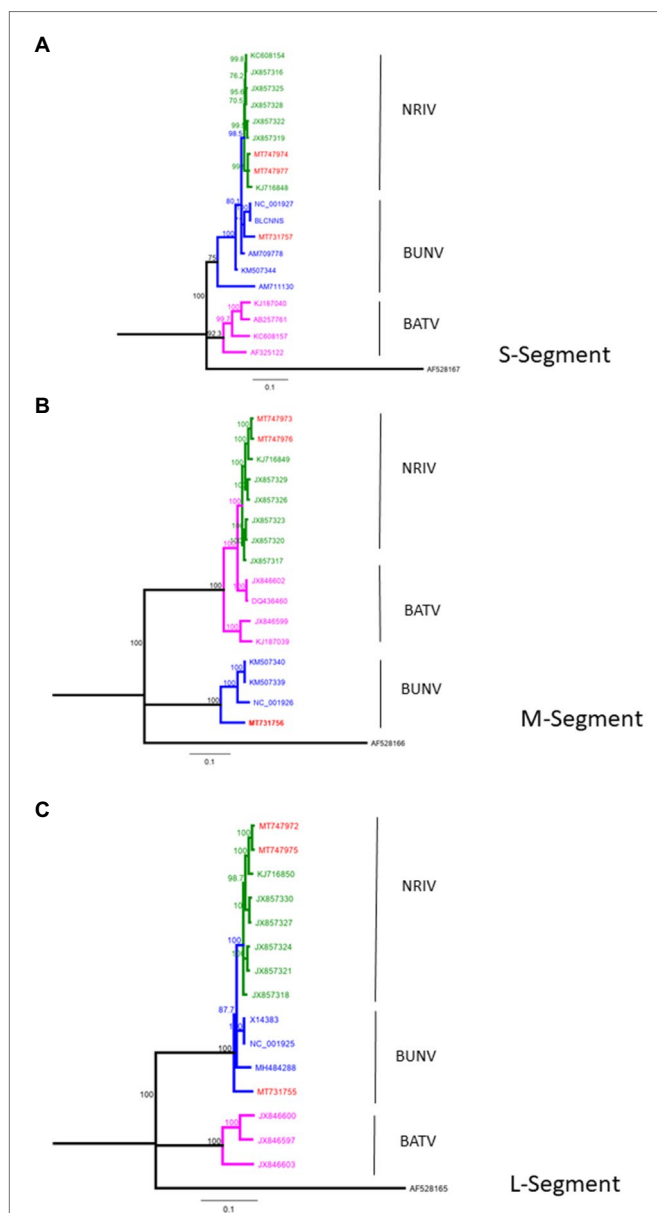


FIGURE 2 | Phylogeny of complete BUNV, BATV and NRIV sequences for (A) small (S)-Segment, (B) medium (M)-Segment and (C) large (L)-Segment compared with sequences obtained from goat and sheep in Mauritania from 2015 (red lines). Green lines indicate NRIV related, blue lines BUNV related and purple lines BATV related sequences. The tree was constructed by Neighbor-Joining analysis and genetic distances were calculated using the Tamura-Nei Method. The scale bar indicates the number of nucleotide substitutions per site. Numbers before the nodes denote bootstrap values $\geq 80\%$. The tree was rooted to the sequence of La Crosse virus, Human/78 strain (accession number: AF528165-167).

from Dakar (161 nucleotide differences) and the BUNV prototype (279 nucleotide differences) regarding S-, M- and L-segments.

The detection of antibodies directed against all three viruses was determined by screening the samples consecutively by NRIV-, BATV- and BUNV-derived SNTs. Due to low sample volume, only 458 out of 492 sera could

be comprehensively analyzed in SNTs and indirect ELISAs. Sera showing a ND_{50} higher than 1:30 were retested to determine the endpoint values. Different neutralizing antibodies detected simultaneously in one sample were considered specific if individual ND_{50} was four times higher compared to the other(s). Within the meaning of that definition, in 41 out of 458 samples NRIV-specific antibodies were detected, leading to a total prevalence of 8.95% (Table 3). BATV-specific antibodies were found in nine samples (prevalence of 1.97%), and BUNV-specific antibodies in only three samples (prevalence of 0.66%). In 97 sera, similar antibody titers against NRIV and BATV were found (prevalence of 21.18%), whereas only one sample was positive for NRIV as well as BUNV antibodies and another one for BATV as well as BUNV antibodies corresponding to a prevalence of 0.22%. Finally, 62 sera were tested positive in all three SNTs leading to a prevalence of 13.54%. Interestingly, the NRIV-positive samples showed the highest values with antibody titers up to 1:2560. In BATV-based SNT, only one sample reached a titer of up to 1:960. Regarding BUNV-specific SNT, the titer did not exceed 1:40, but mostly ranged between 1:10 and 1:20. The geographical distribution of seropositive samples is displayed in Figure 3. To further analyze the antibodies, they were tested in an indirect ELISA for reactivity against glycoprotein Gc of NRIV, BATV or BUNV, which are the main targets for virus neutralisation. The resulting OD values were compared with the results of the homologous SNT, which is used as reference and gold standard. Goat and sheep samples were evaluated separately by ROC analysis to determine specificity and sensitivity (Figure 4). All individual values are compiled in the Supplementary Table.

The NRIV Gc-based ELISA displayed a specificity of 93.75 and 77.61% for goats and sheep, respectively, and a corresponding sensitivity of 86 and 79.46%. BATV Gc-based ELISA exhibited a specificity of 83.21% (goat) and 78.38% (sheep), and a sensitivity of 84.69 and 89.8%, respectively. In the case of the BUNV Gc-based ELISA, significantly lower values for specificity (72.86 and 59.77%) and sensitivity (48.65 and 73.33%) were found. Using the calculated cut-offs, the NRIV Gc-based ELISA detected 13 positive samples, the BATV Gc-based ELISA 24 seropositive specimens and the BUNV-based ELISA 37 positive samples. 92 specimens showed reactivity in all three ELISAs, whereas 87 samples were positive in the NRIV/BATV-based ELISAs. 15 samples showed reactivity against NRIV and BUNV Gc and 14 samples reactivity against BUNV/BATV Gc.

The degree of accordance between the serological assays of the three viruses was calculated by the kappa coefficient. Between SNT specific for NRIV and SNT specific for BATV for both goat- and sheep-derived samples, the coefficient revealed an almost perfect agreement ($\kappa=0.90$, value of $p < 2.2e-16$, 95% CI 0.84–0.96, and $\kappa=0.86$, value of $p < 2.2e-16$, 95% CI 0.80–0.93). Between NRIV Gc-based ELISA and BATV Gc-based ELISA (for goat and sheep) the kappa coefficient showed a substantial agreement ($\kappa=0.73$, value of $p < 2.2e-16$, 95% CI 0.64–0.82, and $\kappa=0.71$, value of $p < 2.2e-16$, 95% CI 0.62–0.80). In contrast, the comparison

TABLE 3 | Serological analysis of the Mauritanian serum samples using SNT.

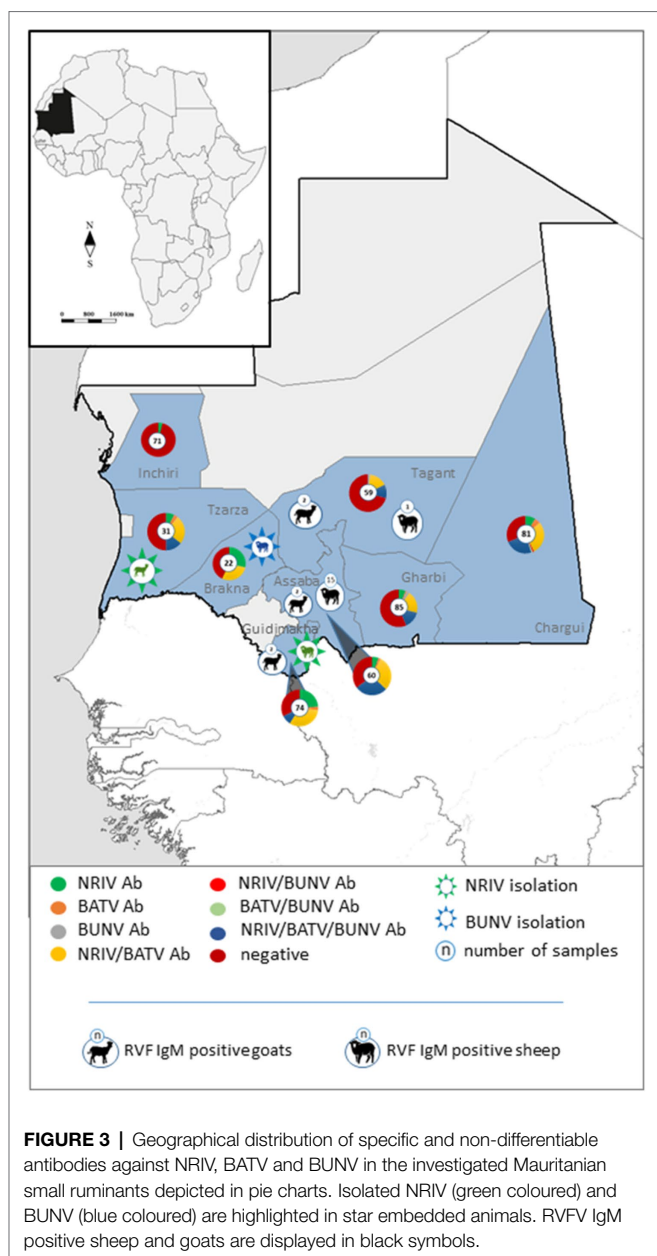
(A) NRIV SNT positive							
Species/Region	No of samples	Goat	Sheep	Not available (NA)	Total	Prevalence (%)	95% CI
Inchiri	77	2	1	0	3	3.9	1.3–10.8
Chargui	80	1	5	1	7	8.8	4.3–17.0
Gharbi	83	0	5	0	5	6.0	2.6–13.3
Tagant	51	0	0	0	0	0.0	0.0–7.0
Assaba	54	3	0	0	3	5.6	1.9–15.1
Trarza	28	1	1	0	2	7.1	2–22.7
Guidimaka	71	11	6	0	17	23.9	15.5–35.0
Brakna	14	2	2	0	4	28.6	11.7–54.7
total	458	20	20	1	41	9.0	6.7–11.9
(B) BATV SNT positive							
Inchiri	77	0	0	0	0	0.0	0.0–4.8
Chargui	80	2	2	0	4	5.0	2.0–12.1
Gharbi	83	0	0	1	1	1.2	0.2–6.5
Tagant	51	0	0	0	0	0.0	0.0–7.0
Assaba	54	1	0	0	1	1.9	0.3–9.8
Trarza	28	0	1	0	1	3.6	0.6–17.7
Guidimaka	71	2	0	0	2	2.8	0.8–9.7
Brakna	14	0	0	0	0	0.0	0.0–21.5
total	458	5	3	1	9	2.0	1.0–3.7
(C) BUNV SNT positive							
Inchiri	77	0	0	0	0	0.0	0.0–4.8
Chargui	80	0	0	0	0	0.0	0.0–4.6
Gharbi	83	0	2	0	2	2.4	0.7–8.3
Tagant	51	1	0	0	1	2.0	0.4–10.3
Assaba	54	0	0	0	0	0.0	0.0–6.6
Trarza	28	0	0	0	0	0.0	0.0–12.1
Guidimaka	71	0	0	0	0	0.0	0.0–5.1
Brakna	14	0	0	0	0	0.0	0.0–21.5
total	458	1	2	0	3	0.7	0.2–1.9
(D) RVFV SNT positive							
Inchiri	77	1	3	0	4	5.2	2.0–12.6
Chargui	80	1	0	0	1	1.3	0.2–6.8
Gharbi	83	0	11	2	13	15.7	9.4–25.0
Tagant	51	14	1	0	15	29.4	18.7–43.0
Assaba	54	9	20	0	29	53.7	40.6–66.3
Trarza	28	4	0	0	4	14.3	5.1–31.5
Guidimaka	71	6	3	0	9	12.7	6.8–22.4
Brakna	14	3	3	0	6	42.9	21.4–67.4
total	458	38	41	2	81	17.7	14.5–21.4

(A) NRIV, **(B)** BATV, **(C)** BUNV, and **(D)** RVFV specific antibodies.

of BUNV Gc ELISA or specific SNT only showed fair to moderate agreement with BATV and NRIV serological tests (data not shown).

Finally, all samples were analyzed for antibodies against RVFV with a commercial species independent ELISA which revealed 84 antibody positive samples. All positive sera were verified by the SNT, which confirmed seropositivity in 81 cases (**Table 3**). Hence, 81 out of 458 sera were determined antibody positive for RVFV corresponding to a prevalence of 17.69% (**Table 3**). Highest antibody titer were found in the regions Tagant, Assaba, and Brakna (29.41, 53.7, and

42.86%, respectively). Since the competition ELISA does not distinguish between IgG and IgM antibodies, all seropositive samples were tested by the IDvet IgM capture ELISA. Hereby, 22 samples revealed RVFV IgM antibodies resulting in a prevalence of 4.80%, of which 16 samples were collected in Assaba alone. Interestingly, of these samples only 4 were exclusively positive for RVF IgM, but the remaining IgM positive were found in BATV/NRIV positive individuals. The distribution of RVFV IgM positive and NRIV and BUNV positive samples is shown in **Figure 2**.



DISCUSSION

A co-infection of the ruminant population with RVFV and NRIV was already described in Kenya and Somalia in 1997–1998 (Bowen et al., 2001) and in Mauritania in 2010 (Eiden et al., 2014). In Kenya, 23% of the hemorrhagic fever cases were diagnosed as infected with RVFV and 27% as infected with NRIV (Bowen et al., 2001). In Mauritania, the RVF outbreak caused 63 human infections (El Mamy et al., 2011) and 57 infected small ruminants out of 93 tested animals (Jäckel et al., 2013b). Moreover, Dutuze et al. observed the co-circulation of RVFV with BUNV and BATV in the ruminant population in Rwanda (Dutuze et al., 2020). In Mauritania, the most recent RVF outbreak started in

September 2020 in Assaba, Tagant, Brakna, Trarza, Hodh El Gharbi and Hodh Ech Chargui and affected camels, small ruminants and cattle. Moreover, 25 human deaths have been reported (World Health Organization, 2020). Five years earlier, 31 human patients were infected in the same region, some of whom were suffering from hemorrhagic and neurologic manifestations (Boushab et al., 2016). Furthermore, in three regions in southern Mauritania (Brakna, Tagant, and Assaba) a total of 19 infected sheep and goats were detected and stamped out as part of outbreak control (OIE). In these three and in additional five regions (Brakna, Tagant, Assaba, Tasiast in Inchiri region) Hodh Ech Chargui, Trarza, Guidimakha, and Hodh El Gharbi, our project partners collected 492 samples of sheep and goats before and at the beginning of the outbreak in the year of 2015. The serum samples were investigated comprehensively for RVFV and the orthobunyaviruses NRIV, BATV, and BUNV to determine if these viruses were co-circulating in Mauritania again.

Viral RVFV RNA was not detected, but 17.69% of the investigated animals showed IgG/IgM antibodies. In comparison, in 2012/13 during an inter-epidemic phase, Rissmann et al. reported a much lower prevalence of 3.8% in 497 investigated small ruminants in Mauritania (Rissmann et al., 2017a). Thus, we observed a clear increase in the overall RVFV antibody prevalence in the small ruminant population in the year of 2015. If the regions are viewed separately, the tested animals from Brakna, Tagant, and Assaba developed the highest antibody titers (29.41, 53.70, and 42.86%, respectively). These were the exact three regions affected by the RVF outbreak in OIE (2020). The OIE reported the first RVFV positive case in Assaba in mid October (OIE). At the same time, we collected serum samples of 32 sheep, of which 16 samples showed RVFV-specific IgM antibodies, underlining the circulation of the virus in Assaba. The goat samples from Assaba were taken 1 month earlier and tested positive for IgM antibodies in only one case. Likewise, in the other investigated regions, only few IgM-positive animals were detected. Therefore, the overall prevalence of IgM antibodies was just 4.80%. As already mentioned, viral RVFV RNA was not detected, but the molecular analysis indicated the presence of NRIV RNA in 10 samples collected in Brakna, Trarza, and Guidimakha. The subsequent sequencing revealed two positive samples for NRIV and two positive samples for BUNV from one goat and three sheep.

Both NRIV- and both BUNV-positive samples were negative for RVFV RNA as well as for RVFV-specific antibodies. However, a total of 61 NRIV, BATV and/or BUNV seropositive samples also revealed antibodies against RVFV, indicating a co-circulation of these viruses in the animal population in Mauritania. Since the RVFV sequence is highly divergent from the deduced orthobunyavirus sequences, cross-reactivity is highly unlikely but needs to be substantiated.

The serological investigation for orthobunyaviruses revealed NRIV-specific antibodies in 41 out of 458 tested samples corresponding to a prevalence of 8.95%, BATV-specific

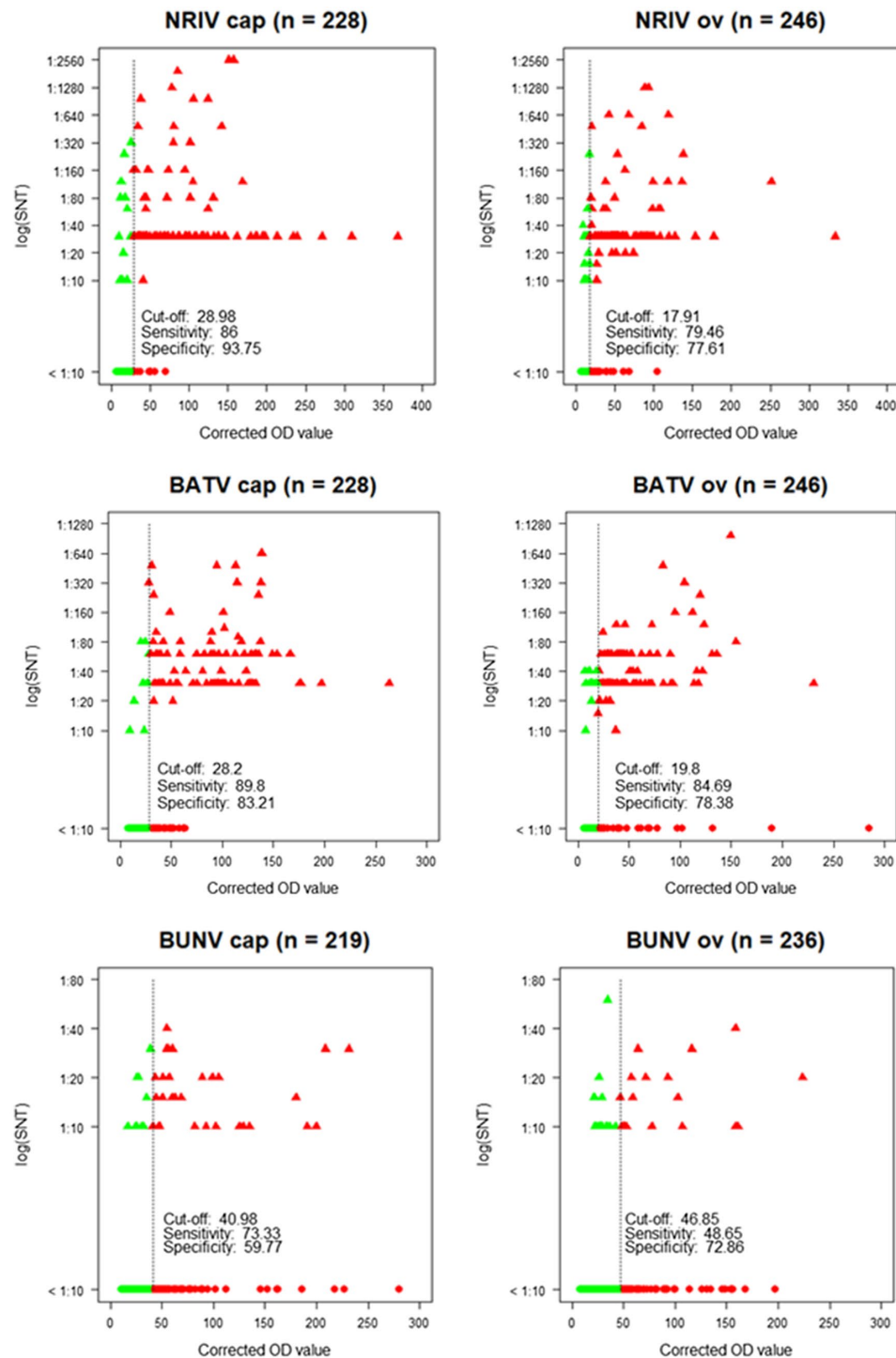


FIGURE 4 | Corrected OD values of the ELISA in relation to neutralization titers [log (SNT)] of the SNT showing cut-off, sensitivity and specificity for each species (cap = goat, ov = sheep) and each virus. Green dots: SNT and ELISA negative samples. Green triangles: SNT positive, but ELISA negative samples. Red triangles: SNT and ELISA positive samples. Red dots: SNT negative, but ELISA positive samples.

antibodies in nine samples leading to a prevalence of 1.97%, and BUNV-specific antibodies in only three sera (prevalence of 0.66%). However, the results need to be interpreted carefully, since for a large part of seropositive samples an

unambiguous determination was not possible. In a total of 161 samples, the SNT of at least two viruses detected neutralizing antibodies. In most cases, the SNT based on NRIV and the SNT based on BATV showed undistinguishable

high antibody titers (97 samples corresponding to a prevalence of 21.18%). The percentage of NRIV neutralizing antibodies against BATV and NRIV in each individual sample is shown in **Supplementary Figure S2** and indicates the high number of double-positive samples. The high cross-reactivity between NRIV and BATV induced antibodies is based on high sequence identity of NRIV and BATV derived Gc proteins. Alignment of three Gc protein (Domains I and II, **Supplementary Figure S1**) showed 89.5% sequence identity between BATV and NRIV, but only 45.1% and 46.1% with BUNV glycoprotein. For this reason, the specificity was selected *via* a cut-off with a fourfold higher activity compared to the other two viruses in order to be able to reliably determine a virus-specific reactivity. Factor 4 was taken from previous flavivirus studies in which flaviviruses (particularly from the same serocomplex) can be identified by determining the virus with the highest neutralizing capacity and at least a fourfold difference in titer (Yeh et al., 2012). A total of 62 samples were positive in all three SNTs (prevalence of 13.54%). Thereby, the antibody titer in the BUNV-specific SNT did not exceed a titer of 1:40, but mostly ranged between 1:10 and 1:20. In contrast, in BATV- and NRIV-based SNTs, the antibody titer reached up to 1:1280 or even 1:2560. Apparently, BUNV is less immunogenic and induces a less neutralizing activity. At least, BUNV cross-reacts less with NRIV and BATV than the latter among themselves. A limited cross-reaction between BUNV and BATV was already described by Hunt and Calisher, who investigated the antigenic relationship of 23 strains of Bunyamwera serogroup viruses by plaque reduction neutralization test (Hunt and Calisher, 1979). A further indication for a low neutralizing activity of BUNV is that twice as many samples were positive in the BUNV Gc-based ELISA than in the BUNV SNT (158 ELISA-positive and 67 SNT-positive samples). This also explains the low sensitivity and specificity of the ELISA calculated in correlation to the SNT (48.65% for sheep and 73.33% for goats, and 72.86% for sheep and 59.77% for goats, respectively). The low prevalence of BUNV-seropositive animals determined by the SNT is surprising since we proved the presence of BUNV in the animal population by isolating the virus from two sheep, and therefore expected to detect a stronger immune response in the investigated animals. Similar to the SNT, the ELISAs do not allow an unambiguous differentiation between NRIV, BATV, and BUNV for each sample. Of 458 samples, 87 samples were equally positive in the NRIV Gc-based ELISA and the ELISA based on BATV Gc, whereas a total of 37 samples exhibited antibodies against only one of the viruses. The strong agreement of NRIV- and BATV-based SNTs and ELISAs is confirmed by the kappa coefficient, which for the SNT is $\kappa=0.90$ (for goats) and $\kappa=0.86$ (for sheep), and for the ELISA $\kappa=0.73$ (for goats) and $\kappa=0.71$ (for sheep). The high cross-reactivity among the serological tests impedes the determination of whether only one of the viruses has induced the antibody response or a co-infection is present. Neutralizing antibodies are induced by the surface glycoproteins which are encoded by M-segment of the virus

(Briese et al., 2006). The M-segment of NRIV closely resembles that of BATV, showing only 11 and 5% differences in nucleotide or deduced amino acid sequence, respectively. This limited divergence is mainly observed in the N-terminal portion of Gc around the conserved potential trypsin cleavage site (Briese et al., 2006). Thus, the specific differentiation between NRIV and BATV antibodies by Gc ELISA or SNT is not possible, but the strong accordance among the assays offers the advantage to use the BATV SNT instead of the NRIV SNT and hereby enables to work in a lower biosafety containment facility.

Overall, we could demonstrate that NRIV and BUNV were co-circulating in Mauritania during the RVF outbreak in 2015/16. Prevalence studies for NRIV, BATV and BUNV are complicated by high cross-reactivity, especially between NRIV and BATV serological assays. Future attempts might consider establishing tests that are based on the nucleoprotein NP to distinguish BATV and NRIV induced antibodies to finally attain a clear serological differentiation of infections by NRIV, BATV and BUNV.

DATA AVAILABILITY STATEMENT

The datasets presented in this study can be found in online repositories. The names of the repository/repositories and accession number(s) can be found in the article/**Supplementary Material**.

ETHICS STATEMENT

Ethical review and approval were not required for the animal study because the samples were taken by Office National de Recherche et de Développement de l'Élevage (ONARDEL) in order to fulfill its governmental mandate to conduct livestock animal monitoring and surveillance programs for veterinary and zoonotic pathogens following all relevant national as well as international regulations and according to fundamental ethical principles. Written informed consent for participation was not obtained from the owners.

AUTHOR CONTRIBUTIONS

NC: methodology, practical implementation, data curation and validation, writing of the first draft. YB: conceptualization, practical implementation, data curation. FS: methodology, practical implementation, data curation and validation writing (review and editing). AD: local project implementation. AB: on-site methodology implementation, data curation. UZ, MR, JS, DH: methodology, practical implementation, data curation and validation. MLH: local supervision of project administration. BAD, MYB: resources, project administration. MHG: conceptualization, design of the research strategy and overall supervision of its implementation, data interpretation, funding acquisition and professional project administration, writing. ME: conceptualization, design of the research strategy,

methodology, data curation and validation, writing. All authors contributed to the article and approved the submitted version.

FUNDING

This work was funded by the German Office for Foreign Affairs (German Partnership Program for Biosecurity, OR12-370-43 BIOS Subsahara). All funding sources were raised by MG. The funders had no role in study design, data collection and analysis, decision to publish, or preparation of the manuscript.

ACKNOWLEDGMENTS

BATV strain 53.2 was kindly provided by J. Schmidt-Chanasit (BNITM Hamburg, Germany). We kindly acknowledge the

excellent technical assistance of Birke Lange, Katja Wittig, and Cornelia Steffen (Institute of Novel and Emerging Infectious Disease, Friedrich-Loeffler-Institut, Greifswald, Germany).

SUPPLEMENTARY MATERIAL

The Supplementary Material for this article can be found online at: <https://www.frontiersin.org/articles/10.3389/fmicb.2021.766977/full#supplementary-material>

Supplementary Figure S1 | Alignment of glycoprotein Gc sequences (domains GI and II) of BATV, NRIV and BUNV. Homologous amino acids are marked in color. Alignment is performed with ClustalW.

Supplementary Figure S2 | The percentage of NRIV neutralizing antibodies against BATV and NRIV in each individual positive sample. The proportion of NRIV neutralizing antibodies in each sample is indicated in blue and that of BATV neutralizing antibodies in red.

REFERENCES

- Altschul, S. F., Gish, W., Miller, W., Myers, E. W., and Lipman, D. J. (1990). Basic local alignment search tool. *J. Mol. Biol.* 215, 403–410. doi: 10.1016/S0022-2836(05)80360-2
- Boushab, B. M., Fall-Malick, F. Z., Ould Baba, S. E., Ould Salem, M. L., Belizaire, M. R., Ledib, H., et al. (2016). Severe Human Illness Caused by Rift Valley Fever Virus in Mauritania, 2015. *Open Forum Infect. Dis.* 3:ofw200. doi: 10.1093/ofid/ofw200
- Bowen, M. D., Trappier, S. G., Sanchez, A. J., Meyer, R. F., Goldsmith, C. S., Zaki, S. R., et al. (2001). A reassortant bunyavirus isolated from acute hemorrhagic fever cases in Kenya and Somalia. *Virology* 291, 185–190. doi: 10.1006/viro.2001.1201
- Briese, T., Bird, B., Kapoor, V., Nichol, S. T., and Lipkin, W. I. (2006). Batai and Ngari viruses: M segment reassortment and association with severe febrile disease outbreaks in East Africa. *J. Virol.* 80, 5627–5630. doi: 10.1128/JVI.02448-05
- Chevalier, V. (2013). Relevance of Rift Valley fever to public health in the European Union. *Clin. Microbiol. Infect.* 19, 705–708. doi: 10.1111/1469-0691.12163
- Chung, S. I., Livingston, C. W. Jr., Edwards, J. F., Crandell, R. W., Shope, R. E., Shelton, M. J., et al. (1990). Evidence that Cache Valley virus induces congenital malformations in sheep. *Vet. Microbiol.* 21, 297–307. doi: 10.1016/0378-1135(90)90001-C
- Cichon, N., Eiden, M., Schulz, J., Günther, A., Wysocki, P., Holicki, C. M., et al. (2021). Serological and molecular investigation of Batai virus infections in ruminants from the state of Saxony-Anhalt, Germany, 2018. *Viruses* 13:370. doi: 10.3390/v13030370
- Dutuze, M. F., Ingabire, A., Gafarasi, I., Uwituze, S., Nzayirambaho, M., and Christofferson, R. C. (2020). Identification of Bunyamwera and possible other Orthobunyavirus infections and disease in cattle during a Rift Valley fever outbreak in Rwanda in 2018. *Am. J. Trop. Med. Hyg.* 103, 183–189. doi: 10.4269/ajtmh.19-0596
- Dutuze, M. F., Nzayirambaho, M., Mores, C. N., and Christofferson, R. C. (2018). A review of Bunyamwera, Batai, and Ngari viruses: understudied Orthobunyaviruses With potential one health implications. *Front. Vet. Sci.* 5:69. doi: 10.3389/fvets.2018.00069
- Edwards, J. F. (1994). Cache Valley virus. *Vet. Clin. North Am. Food Anim. Pract.* 10, 515–524. doi: 10.1016/s0749-0720(15)30536-3
- Eiden, M., Vina-Rodriguez, A., El Mamy, B. O., Isselmou, K., Ziegler, U., Höper, D., et al. (2014). Ngari virus in goats during Rift Valley fever outbreak, Mauritania, 2010. *Emerg. Infect. Dis.* 20, 2174–2176. doi: 10.3201/eid2012.140787
- El Mamy, A. B., Baba, M. O., Barry, Y., Isselmou, K., Dia, M. L., El Kory, M. O., et al. (2011). Unexpected Rift Valley fever outbreak, northern Mauritania. *Emerg. Infect. Dis.* 17, 1894–1896. doi: 10.3201/eid1710.110397
- Elliott, R. M. (2014). Orthobunyaviruses: recent genetic and structural insights. *Nat. Rev. Microbiol.* 12, 673–685. doi: 10.1038/nrmicro3332
- Gonzalez, J. P. (1988). Activités du laboratoire d'écologie virale. *Rapp. sur la fonct. tech. de l'Institut Pasteur de Dakar*. 89, 100–118.
- Hubálek, Z., Rudolf, I., and Nowotny, N. (2014). Arboviruses pathogenic for domestic and wild animals. *Adv. Virus Res.* 89, 201–275. doi: 10.1016/B978-0-12-800172-1.00005-7
- Hunt, A. R., and Calisher, C. H. (1979). Relationships of bunyamwera group viruses by neutralization. *Am. J. Trop. Med. Hyg.* 28, 740–749. doi: 10.4269/ajtmh.1979.28.740
- Jäckel, S., Eiden, M., Balkema-Buschmann, A., Ziller, M., van Vuren, P. J., Paweska, J. T., et al. (2013a). A novel indirect ELISA based on glycoprotein Gn for the detection of IgG antibodies against Rift Valley fever virus in small ruminants. *Res. Vet. Sci.* 95, 725–730. doi: 10.1016/j.rvsc.2013.04.015
- Jäckel, S., Eiden, M., El Mamy, B. O., Isselmou, K., Vina-Rodriguez, A., Dombia, B., et al. (2013b). Molecular and serological studies on the Rift Valley fever outbreak in Mauritania in 2010. *Transbound. Emerg. Dis.* 60(Suppl. 2), 31–39. doi: 10.1111/tbed.12142
- Jo, W. K., Pfankuche, V. M., Lehmbecker, A., Martina, B., Rubio-Garcia, A., Becker, S., et al. (2018). Association of Batai Virus Infection and Encephalitis in harbor seals, Germany, 2016. *Emerg. Infect. Dis.* 24, 1691–1695. doi: 10.3201/eid2409.171829
- Jöst, H., Bialonski, A., Schmetz, C., Günther, S., Becker, N., and Schmidt-Chanasit, J. (2011). Isolation and phylogenetic analysis of Batai virus, Germany. *Am. J. Trop. Med. Hyg.* 84, 241–243. doi: 10.4269/ajtmh.2011.10-0483
- Linthicum, K. J., Britch, S. C., and Anyamba, A. (2016). Rift Valley fever: An emerging mosquito-borne disease. *Annu. Rev. Entomol.* 61, 395–415. doi: 10.1146/annurev-ento-010715-023819
- Lopez-Raton, M., Rodriguez-Alvarez, M. X., Cadarso Suarez, C., and Gude Sampedro, F. (2014). OptimalCutpoints: an R package for selecting optimal Cutpoints in diagnostic tests. *J. Stat. Softw.* 61, 1–36. doi: 10.18637/jss.v061.i08
- Makenov, M. T., Toure, A. H., Bayandin, R. B., Gladysheva, A. V., Shipovalov, A. V., Boumbaly, S., et al. (2021). Ngari virus (Orthobunyavirus, Peribunyaviridae) in ixodid ticks collected from cattle in Guinea. *Acta Trop.* 214:105790. doi: 10.1016/j.actatropica.2020.105790
- Ninove, L., Nougaiere, A., Gazin, C., Thirion, L., Delogu, I., Zandotti, C., et al. (2011). RNA and DNA bacteriophages as molecular diagnosis controls in clinical virology: a comprehensive study of more than 45,000 routine PCR tests. *PLoS One* 6:e16142. doi: 10.1371/journal.pone.0016142
- Odhiambo, C., Venter, M., Chepkorir, E., Mbaika, S., Lutomia, J., Swanepoel, R., et al. (2014). Vector competence of selected mosquito species in Kenya for Ngari and Bunyamwera viruses. *J. Med. Entomol.* 51, 1248–1253. doi: 10.1603/ME14063
- OIE (2020) Available at: <https://www.oie.int/en/what-we-do/standards/codes-and-manuals/terrestrial-manual-online-access/>

- R Core Team (2020). A Language and Environment for Statistical Computing. R Foundation for Statistical Computing, Vienna, Austria. Available at: <https://www.R-project.org/>
- Rice, P., Longden, I., and Bleasby, A. (2000). EMBOSS: the European molecular biology open software suite. *Trends Genet.* 16, 276–277. doi: 10.1016/S0168-9525(00)00204-2
- Rissmann, M., Eiden, M., El Mamy, B. O., Isselmou, K., Doumbia, B., Ziegler, U., et al. (2017a). Serological and genomic evidence of Rift Valley fever virus during inter-epidemic periods in Mauritania. *Epidemiol. Infect.* 145, 1058–1068. doi: 10.1017/S0950268816003022
- Rissmann, M., Eiden, M., Wade, A., Poueme, R., Abdoukadi, S., Unger, H., et al. (2017b). Evidence for enzootic circulation of Rift Valley fever virus among livestock in Cameroon. *Acta Trop.* 172, 7–13. doi: 10.1016/j.actatropica.2017.04.001
- Seidowski, D., Ziegler, U., von Rönn, J. A., Müller, K., Hüppop, K., Müller, T., et al. (2010). West Nile virus monitoring of migratory and resident birds in Germany. *Vector Borne Zoonotic Dis.* 10, 639–647. doi: 10.1089/vbz.2009.0236
- Singh, K. R., and Pavri, K. M. (1966). Isolation of Chittoor virus from mosquitoes and demonstration of serological conversions in sera of domestic animals at Manjri, Poona, India. *Indian J. Med. Res.* 54, 220–224.
- Tauro, L. B., Rivarola, M. E., Lucca, E., Mariño, B., Mazzini, R., Cardoso, J. F., et al. (2015). First isolation of Bunyamwera virus (Bunyaviridae family) from horses with neurological disease and an abortion in Argentina. *Vet. J.* 206, 111–114. doi: 10.1016/j.tvjl.2015.06.013
- Wernike, K., Hoffmann, B., and Beer, M. (2015). Simultaneous detection of five notifiable viral diseases of cattle by single-tube multiplex real-time RT-PCR. *J. Virol. Methods* 217, 28–35. doi: 10.1016/j.jviromet.2015.02.023
- World Health Organization (2020). Rift valley fever – Mauritania. Available at: <https://www.who.int/emergencies/disease-outbreak-news/item/rift-valley-fever-mauritania>
- Wylezich, C., Papa, A., Beer, M., and Höper, D. (2018). A versatile sample processing workflow for metagenomic pathogen detection. *Sci. Rep.* 8:13108. doi: 10.1038/s41598-018-31496-1
- Yeh, J. Y., Lee, J. H., Park, J. Y., Seo, H. J., Moon, J. S., Cho, I. S., et al. (2012). A diagnostic algorithm to serologically differentiate West Nile virus from Japanese encephalitis virus infections and its validation in field surveillance of poultry and horses. *Vector Borne Zoonotic Dis.* 12, 372–379. doi: 10.1089/vbz.2011.0709
- Zeller, H. G., Diallo, M., Angel, G., Traoré-Lamizana, M., Thonnon, J., Digoutte, J. P., et al. (1996). Le virus Ngari (Bunyaviridae: Bunyavirus). Premiers isolements chez l'homme au Sénégal, nouveaux vecteurs culicidiens, le point sur son épidémiologie [Ngari virus (Bunyaviridae: Bunyavirus). First isolation from humans in Senegal, new mosquito vectors, its epidemiology]. *Bull. Soc. Pathol. Exot.* 89, 12–16.
- Ziegler, U., Groschup, M. H., Wysocki, P., Press, F., Gehrmann, B., Fast, C., et al. (2018). Seroprevalence of Batai virus in ruminants from East Germany. *Vet. Microbiol.* 227, 97–102. doi: 10.1016/j.vetmic.2018.10.029

Conflict of Interest: The authors declare that the research was conducted in the absence of any commercial or financial relationships that could be construed as a potential conflict of interest.

Publisher's Note: All claims expressed in this article are solely those of the authors and do not necessarily represent those of their affiliated organizations, or those of the publisher, the editors and the reviewers. Any product that may be evaluated in this article, or claim that may be made by its manufacturer, is not guaranteed or endorsed by the publisher.

Copyright © 2021 Cichon, Barry, Stoek, Diambar, Ba, Ziegler, Rissmann, Schulz, Haki, Höper, Doumbia, Bah, Groschup and Eiden. This is an open-access article distributed under the terms of the Creative Commons Attribution License (CC BY). The use, distribution or reproduction in other forums is permitted, provided the original author(s) and the copyright owner(s) are credited and that the original publication in this journal is cited, in accordance with accepted academic practice. No use, distribution or reproduction is permitted which does not comply with these terms.



Virome and Blood Meal-Associated Host Responses in *Ixodes persulcatus* Naturally Fed on Patients

Liang-Jing Li¹, Nian-Zhi Ning¹, Yuan-Chun Zheng², Yan-Li Chu², Xiao-Ming Cui¹, Ming-Zhu Zhang¹, Wen-Bin Guo¹, Ran Wei^{1,3}, Hong-Bo Liu^{1,4}, Yi Sun¹, Jin-Ling Ye², Bao-Gui Jiang¹, Ting-Ting Yuan^{1,5}, Jie Li¹, Cai Bian², Lesley Bell-Sakyi⁶, Hui Wang¹, Jia-Fu Jiang¹, Ju-Liang Song², Wu-Chun Cao¹, Tommy Tsan-Yuk Lam^{7,8}, Xue-Bing Ni^{7*} and Na Jia^{1*}

¹ State Key Laboratory of Pathogen and Biosecurity, Beijing Institute of Microbiology and Epidemiology, Beijing, China, ² Mudanjiang Forestry Central Hospital, Mudanjiang, China, ³ The Affiliated Hospital of Shandong University of Traditional Chinese Medicine, Jinan, China, ⁴ Chinese PLA Center for Disease Control and Prevention, Beijing, China, ⁵ Shanghai Institute for Emerging and Re-emerging Infectious Diseases, Shanghai Public Health Clinical Center, Shanghai, China, ⁶ Department of Infection Biology and Microbiomes, Institute of Infection, Veterinary, and Ecological Sciences, University of Liverpool, Liverpool, United Kingdom, ⁷ State Key Laboratory of Emerging Infectious Diseases and Centre of Influenza Research, School of Public Health, The University of Hong Kong, Pok Fu Lam, Hong Kong SAR, China, ⁸ Joint Institute of Virology (SU/HKU), Shantou University, Shantou, China

OPEN ACCESS

Edited by:

Erna Geessien Kroon,
Federal University of Minas Gerais,
Brazil

Reviewed by:

Sara Louise Cosby,
Queen's University Belfast,
United Kingdom
Emmanuel Hernandez,
Kitasato University, Japan

*Correspondence:

Xue-Bing Ni
nixuebing72@163.com
Na Jia
jjana79_41@hotmail.com

Specialty section:

This article was submitted to
Virology,
a section of the journal
Frontiers in Microbiology

Received: 22 June 2021

Accepted: 20 December 2021

Published: 17 February 2022

Citation:

Li L-J, Ning N-Z, Zheng Y-C,
Chu Y-L, Cui X-M, Zhang M-Z,
Guo W-B, Wei R, Liu H-B, Sun Y,
Ye J-L, Jiang B-G, Yuan T-T, Li J,
Bian C, Bell-Sakyi L, Wang H,
Jiang J-F, Song J-L, Cao W-C,
Tsan-Yuk Lam T, Ni X-B and Jia N
(2022) Virome and Blood
Meal-Associated Host Responses
in *Ixodes persulcatus* Naturally Fed on
Patients. *Front. Microbiol.* 12:728996.
doi: 10.3389/fmicb.2021.728996

The long-lasting co-evolution of ticks with pathogens results in mutual adaptation. Blood-feeding is one of the critical physiological behaviors that have been associated with the tick microbiome; however, most knowledge was gained through the study of laboratory-reared ticks. Here we detached *Ixodes persulcatus* ticks at different stages of blood-feeding from human patients and performed high-throughput transcriptomic analysis on them to identify their virome and genes differentially expressed between flat and fully fed ticks. We also traced bloodmeal sources of those ticks and identified bats and three other potential mammalian hosts, highlighting the public health significance. We found Jingmen tick virus and 13 putative new viruses belonging to 11 viral families, three of which even exhibited high genetic divergence from viruses previously reported in the same tick species from the same geographic region. Furthermore, differential expression analysis suggested a downregulation of antioxidant genes in the fully fed *I. persulcatus* ticks, which might be related to bloodmeal-related redox homeostasis. Our work highlights the significance of active surveillance of tick viromes and suggests a role of reactive oxygen species (ROS) in modulating changes in the microbiome during blood-feeding.

Keywords: ticks, bloodmeal, virome, reactive oxygen species, patients, Jingmen tick virus

INTRODUCTION

Zoonotic pathogens, which reside in animal reservoir species and may spill over into the human population, are emerging at an unprecedented rate (Jones et al., 2008; Shi et al., 2016). Vectors exacerbate and complicate zoonotic disease transmission. Ticks are obligate blood-feeding vectors that parasitize a wide range of animals, including reptiles, birds, and mammals. As a result of their feeding on blood, these arthropods are versatile vectors transmitting a plethora of pathogenic

agents, including viruses, bacteria, helminths, and protozoa (de la Fuente et al., 2008; Jia et al., 2020). Blood-feeding is a key physiological process providing essential nutrients for ticks, mainly dietary hemoglobin which is acquired as an exogenous source of heme and thereby sequestered by vitellins in the developing oocytes (Perner et al., 2016). The blood-feeding strategy of ticks provides an ideal system for pathogen transmission, benefiting from their multiple bloodmeals on different hosts to accomplish their complete life cycle and their relatively long-lasting attachment to hosts for several days or weeks (Nava et al., 2009).

Screening of a fed tick detached from a patient is important to evaluate the risk to human health; however, most questions related to this natural, field-collected feeding tick are unsolved. Firstly, identification of the host species on which the tick fed during its previous parasitic stage is imperative to predict the risk of pathogen transmission; however, there are only limited reports of tracing the host species of tick blood meals (Allan et al., 2010; Önder et al., 2013). Secondly, the vector-borne virome has been increasingly highlighted in identifying new pathogens; however, the virome is only available for about 10 tick species (Tokarz et al., 2014, 2018; Pettersson et al., 2017; Harvey et al., 2019; Meng et al., 2019; Vandegrift and Kapoor, 2019) among over 800 tick species worldwide (Jongejan and Uilenberg, 2004). Thirdly, studies have demonstrated that the host bloodmeal can significantly influence the tick microbiome in various ways, which may fundamentally impact the transmission of zoonotic pathogens in these natural systems (Hawlena et al., 2013; Zhang et al., 2014; Rynkiewicz et al., 2015; Swei and Kwan, 2017; Charrier et al., 2018; Zolnik et al., 2018). However, most blood-feeding ticks in previous studies were reared under laboratory conditions, whereas field-collected ticks were rarely analyzed.

To fill the knowledge gaps mentioned above, we detached *Ixodes persulcatus* at different blood-feeding stages from patients and carried out a transcriptomic analysis. The hard tick *I. persulcatus* is widely distributed in Northern China and is most commonly responsible for tick-borne diseases in humans in this region (Cao et al., 2000, 2003). *Ixodes persulcatus* transmits a various disease-causing bacteria, including genera *Borrelia*, *Rickettsia*, *Anaplasma*, *Francisella*, *Coxiella*, and *Ehrlichia*. We aimed to identify the possible animal hosts on which the ticks had fed during the previous parasitic stage, elucidate the virome of detached ticks using transcriptomic approaches, and explore blood meal-related tick responses. Our study may help to identify new biotic drivers indicating new strategies to control ticks and the pathogens they transmit.

MATERIALS AND METHODS

Tick Collection

Ticks feeding on patients who sought treatment at Mudanjiang Forestry Central Hospital in Heilongjiang Province, China, were collected between May and August 2016. The study was approved by the ethics committee of the hospital (Mudanjiang Forest Central Hospital 2011-03) in accordance with the medical research regulations of China. The species and developmental

stage were identified by an entomologist (Yi Sun). Adult *I. persulcatus* ticks were included in the study, and the species was later confirmed by analyzing sequences of the mitochondrial cytochrome *c* oxidase subunit I gene. We further divided the feeding ticks into three groups: flat (ticks that had imbibed small amounts of blood and had not started to enlarge), partially fed (ticks that had begun to enlarge but were not fully engorged), and fully fed (ticks that had fully engorged and were almost ready to detach). All samples were captured alive and thoroughly surface-sterilized (two successive washes in 70% ethanol for 30 s each) before storage at -80°C for DNA/RNA extraction.

Sample Preparation and Sequencing

Extraction of total DNA and RNA from ticks was performed using the AllPrep DNA/RNA Mini Kit (Qiagen, Valencia, CA, United States) with modifications. Briefly, ticks were homogenized in RLT solution under liquid nitrogen. The homogenate was then incubated at 55°C for 10 min with proteinase K (Qiagen) and centrifuged for 30 s at $15,000 \times g$. The homogenized lysate was transferred to an AllPrep DNA spin column and centrifuged for 30 s at $8,000 \times g$. The AllPrep DNA spin column was used for later DNA purification, and the flow-through was used for RNA purification as per the manufacturer's instructions. Ten ticks were pooled together to extract RNA/DNA, and each group comprised three pools.

The extracted RNA was used for transcriptome sequencing (RNA-seq) after RNA quantification and quality checking. The rRNA was removed using Ribo-Zero Gold rRNA removal reagents (human/mouse/rat) (Illumina). Then, the sequencing library was prepared following the Illumina standard protocol. Paired-end (2×150 bp) sequencing of the RNA library was performed on an Illumina HiSeq 4000 platform at Novogene Tech (Beijing, China).

Discovery and Assembly of Viral Genomes

RNA sequencing reads were *de novo* assembled using the Trinity program (Grabherr et al., 2011). Assembled contigs were subject to BLASTx against all non-redundant (nr) database downloaded from GenBank, and the threshold *E* value was set to $1e-5$. Putative viral contigs were further merged by high-identity overlaps using the SeqMan program of Lasergene package v7.1 (DNASTAR, Madison, WI, United States). Original reads were aligned to the contigs again using Bowtie2 (Langmead and Salzberg, 2012) to complete the remaining gaps, and the assembly was verified in the Integrated Genomics Viewer (Thorvaldsdóttir et al., 2013).

Phylogenetic Analyses

The highly conserved RNA-dependent RNA polymerase (RdRp) gene was used to construct family-level phylogenies comprising the viruses that were highly divergent. Predicted viral proteins of the RdRp genes in this study were aligned with reference proteins of the same viral families using the E-INS-i algorithm in MAFFT version 7 (Katoh and Standley, 2013). Ambiguously aligned regions were removed using TrimAl (Capella-Gutiérrez et al., 2009). The WAG + Γ model was identified as the best-fit

amino acid substitution model using Prot-Test 3.4 (Darriba et al., 2011), which was used for maximum likelihood (ML) phylogeny reconstruction with bootstrap tests (1,000 replicates) in PhyML version 3.0 (Guindon and Gascuel, 2003). The ML trees were visualized with FigTree v1.4.2.

Differential Expression Analysis

A single *de novo* assembly across all samples was generated using Trinity (Grabherr et al., 2011), then reads from each sample were separately aligned back to the single Trinity assembly for downstream analyses of the differential expression of transcripts. Transcript abundance containing RNA-Seq fragment counts for each transcript (or gene) across each sample was estimated using the alignment-based abundance estimation method RSEM (Li et al., 2009). The trimmed mean of M-values normalization method (TMM) were subsequently used to normalize the transcript abundance. Differentially expressed (DE) transcripts or genes were identified by Fisher's exact test running "edge" R packages (Robinson et al., 2010; McCarthy et al., 2012), and then those transcripts or genes that had *p*-values of at most 5×10^{-2} and were at least 2^{1.5}-fold differentially expressed were extracted to generate a sample correlation matrix heatmap and a DE gene vs. samples heatmap using Trinity downstream analysis script. The DE genes shown in the heatmap were grouped into gene clusters with similar expression patterns by

cutting the hierarchically clustered gene tree at 60% from the tip. The functional annotations of the DE transcripts or genes were performed using Trinotate (Bryant et al., 2017) based on Pfam database. We classified these annotated transcripts or genes based on the COG database using eggNOG mapper (Huerta-Cepas et al., 2017).

RESULTS

Identification of Bloodmeal Source in Adult *Ixodes persulcatus*

A total of 90 feeding adult *I. persulcatus* ticks were collected from patients. We sequenced nine pools of ticks (10 ticks/pool) by transcriptomic survey. Pools TG1, TG2, and TG13 comprised flat ticks; pools TG3, TG4, and TG14 comprised partially fed ticks; and pools TG5, TG6, and TG15 comprised fully fed ticks. We analyzed *cox1* genes from RNA-seq data to identify the source of previous bloodmeals of *I. persulcatus* and found five mammal host sources, namely, *Tonatia saurophila*, *Mus musculus*, *Ovis aries*, *Sus scrofa*, and *Homo sapiens* (Figure 1). The host *cox1* gene sequences assembled in the study had over 98.5% identity to the respective reference sequences (Supplementary Table 1). The most abundant *cox1* sequence was from *Homo sapiens*, accounting for 1,570 reads across all samples. Intriguingly, one

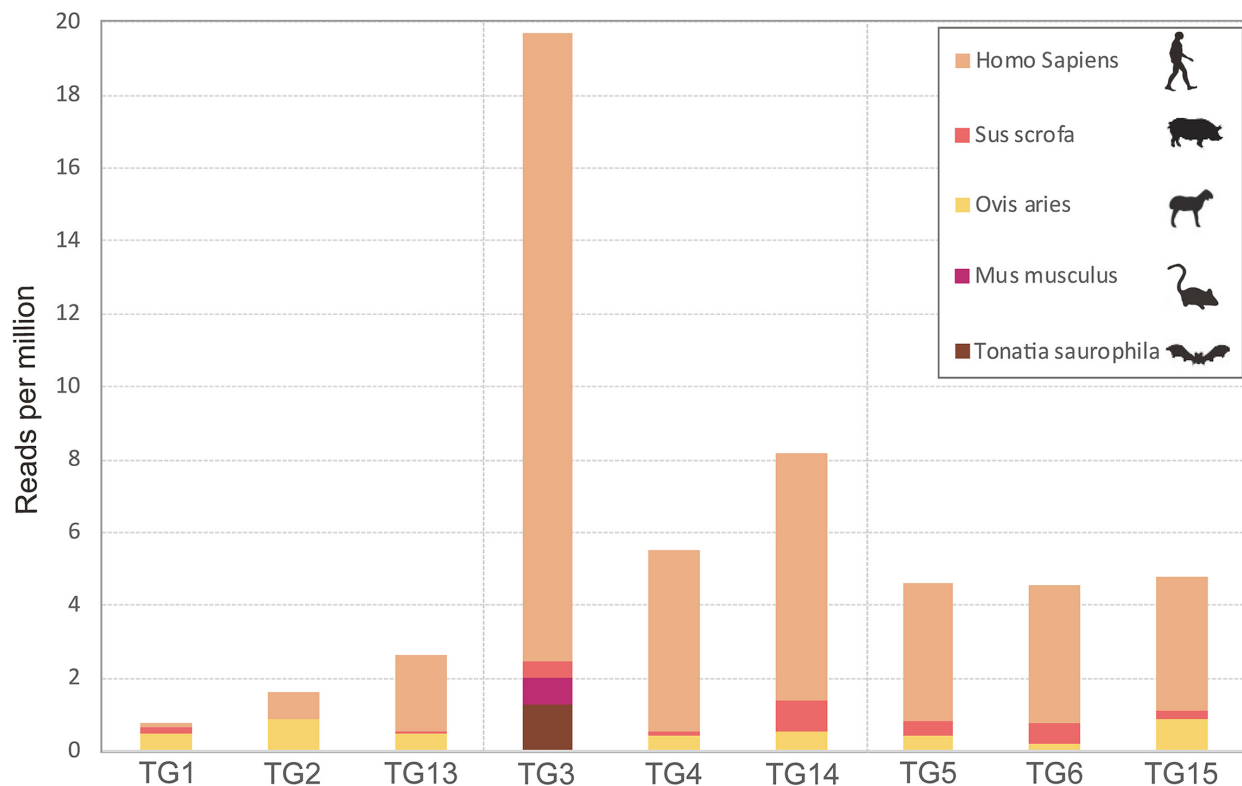


FIGURE 1 | Expression levels of the cytochrome c oxidase subunit I gene of various host species revealed by RNAseq analysis of pools of *Ixodes persulcatus* ticks removed from human patients at Mudanjiang Forestry Central Hospital in Heilongjiang Province, China. Ticks were divided into three groups each comprising three pools of ten ticks: flat (pools TG1, TG2, and TG13), partially fed (pools TG3, TG4, and TG14), and fully fed (pools TG5, TG6, and TG15).

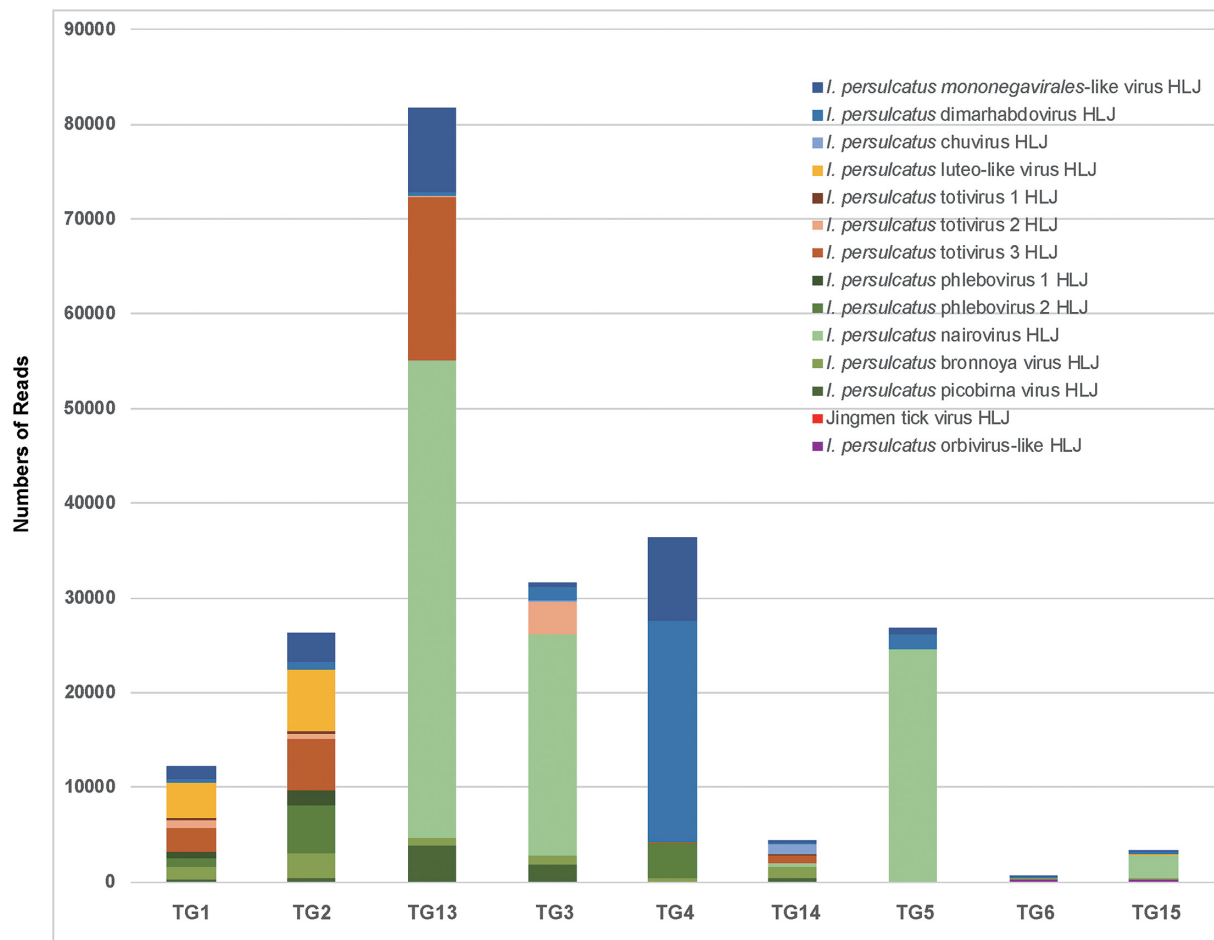


FIGURE 2 | Detection by RNAseq of known and novel viruses in pools of *I. persulcatus* ticks removed from human patients at Mudanjiang Forestry Central Hospital in Heilongjiang Province, China. Levels of abundance of Jingmen tick virus and 13 newly discovered viruses in flat (pools TG1, TG2, and TG13), partially fed (pools TG3, TG4, and TG14), and fully fed (pools TG5, TG6, and TG15) ticks.

bat species, *Tonatia saurophila*, was detected with a read count of 48 in one of the partially fed tick pools (Figure 1 and Supplementary Table 1).

Ixodes persulcatus Tick Virome

We performed nine RNA-seq runs on each of the nine pools of *I. persulcatus* ticks, generating 72 GB of total sequence data. Among the nine resultant RNA-seq libraries, library TG13 (flat ticks) had the most abundant viral reads, followed by library TG4 (partially fed ticks), while libraries TG6 and TG15 (fully fed ticks) had the fewest viral reads (Figure 2). Through a BLASTx search with the assembled genome sequences, we discovered 14 known or novel viruses belonging to 11 viral families (Table 1). All of which had fully or almost fully intact genomes with undisrupted reading frames. These included, with proposed names of new viruses in brackets, one *Mononegavirales*-like virus (*I. persulcatus mononegavirales*-like virus HLJ), one novel chuvirus (*I. persulcatus chuvirus* HLJ), one novel rhabdovirus (*I. persulcatus dimarhabdovirus* HLJ), three distant relatives of *Totiviridae* (*I. persulcatus totivirus 1* HLJ, *I. persulcatus*

totivirus 2 HLJ and *I. persulcatus totivirus 3* HLJ), one novel *Partitiviridae* (*I. persulcatus picobirna virus* HLJ), one novel orbivirus (*I. persulcatus orbivirus*-like HLJ), one *Luteoviridae*-like virus (*I. persulcatus luteo-like virus* HLJ), four distant relatives of *Bunyavirales* (*I. persulcatus phlebovirus 1* HLJ, *I. persulcatus phlebovirus 2* HLJ, *I. persulcatus nairovirus* HLJ, *I. persulcatus bronnoya virus* HLJ), and Jingmen tick virus (JMTV). Reads from *I. persulcatus nairovirus* HLJ were most abundant, followed by reads from *I. persulcatus dimarhabdovirus* HLJ (Figure 2). These viruses shared 36–99% amino acid identities compared with previously reported viruses, and the query coverage varied from around 30 to 90% (Table 1).

We identified three viruses in the *Mononegavirales*. Among them, *I. persulcatus mononegavirales*-like virus HLJ was closely related to deer tick *mononegavirales*-like virus, which had been previously reported in Heilongjiang Province, China (Meng et al., 2019; Figure 3A). *Ixodes persulcatus dimarhabdovirus* HLJ clustered with Long Island tick rhabdovirus and formed a monophyletic clade with other rhabdoviruses (Figure 3A). *Ixodes persulcatus chuvirus* HLJ had 83% amino acid

TABLE 1 | Summary of the viruses discovered by RNAseq in *Ixodes persulcatus* ticks removed from human patients at Mudanjiang Forestry Central Hospital in Heilongjiang Province, China.

Proposed name	Length	Closest Blastx hit	Identity %	Query Coverage %	Abundance (reads count)
<i>Ixodes persulcatus</i> mononegavirales-like virus HLJ	10,865	Deer tick mononegavirales-like virus RNA-dependent RNA polymerase gene	97.64	36	23,431
<i>Ixodes persulcatus</i> phlebovirus 1 HLJ	6,696	Blacklegged tick phlebovirus 3 L gene	74.66	97	2,156
<i>Ixodes persulcatus</i> phlebovirus 2 HLJ	6,715	Norway phlebovirus 1 L gene	87.28	98	9,687
<i>Ixodes persulcatus</i> picobirna virus	1,639	Norway partiti-like virus 1 RNA-dependent RNA-polymerase	93.82	91	6,825
<i>Ixodes persulcatus</i> totivirus 3 HLJ	5,615	Hubei toti-like virus 24 hypothetical protein 2	36.97	42	26,215
<i>Ixodes persulcatus</i> bronnoya virus HLJ	9,320	Bronnoya virus RNA-dependent RNA-polymerase	38.85	88	7,756
<i>Ixodes persulcatus</i> totivirus 1 HLJ	2,682	Lonestar tick totivirus polymerase	39.8	98	672
<i>Ixodes persulcatus</i> luteo-like virus HLJ	2,646	Norway luteo-like virus 2 RNA-dependent RNA-polymerase	93.6	89	10,215
<i>Ixodes persulcatus</i> dimarhabdovirus HLJ	10,365	Norway mononegavirus 1 RNA-dependent RNA-polymerase	49.46	61	28,533
<i>Ixodes persulcatus</i> totivirus 2 HLJ	8,914	Lonestar tick totivirus polymerase	39.96	31	4,857
<i>Ixodes persulcatus</i> nairovirus HLJ	14,779	Beiji nairovirus RNA-dependent RNA polymerase	99.43	85	101,149
<i>Ixodes persulcatus</i> orbivirus-like HLJ	4,017	Skunk River virus VP1 gene	40.26	94	560
Jingmen tick virus HLJ	2,313	Jingmen tick virus NS5-like protein gene	92.6	99	84
<i>Ixodes persulcatus</i> chuvirus HLJ	11,440	Blacklegged tick chuvirus 2 L gene	83.07	57	1,229

similarity with blacklegged tick chuvirus-2 but only 57% coverage of the L segment sequence. We obtained the nearly complete genomes of these three viruses. The genome of *I. persulcatus* mononegavirales-like virus HLJ, *I. persulcatus* dimarhabdovirus HLJ, and *I. persulcatus* chuvirus HLJ were 10,865, 10,365, and 11,440 nucleotides (nt) long, and all encoded four predicted ORFs.

Three distant relatives of *Totiviridae* (*I. persulcatus* totivirus 1 HLJ, *I. persulcatus* totivirus 2 HLJ, *I. persulcatus* totivirus 3 HLJ) had extremely low amino acid identity (37–40%) with previously described viruses. Their RdRp sequences were highly divergent from the existing clades and fell into the unclassified groups on the phylogenetic tree (Figure 3C). This indicates the distinct phylogenetic position of these newly identified viruses from the currently known viruses.

Three members of the *Bunyavirales*, *I. persulcatus* phlebovirus 1 HLJ, *I. persulcatus* phlebovirus 2 HLJ, and *I. persulcatus* nairovirus HLJ showed high amino acid identities of 75, 87, and 99% with previously reported blacklegged tick phlebovirus 3, Norway phlebovirus 1, and Beiji nairovirus, respectively, based on the RdRp gene. The fourth member of the *Bunyavirales*, *I. persulcatus* bronnoya virus HLJ exhibited 38% amino acid identity with Bronnoya virus (88% sequence coverage of RdRp gene). The phylogenetic tree of *Bunyavirales* indicated that the two phleboviruses and the nairovirus clustered with previously reported Chinese strains and formed well-supported

monophyletic groups closely related to the “classic” phleboviruses and nairoviruses (Figure 3D). It is suggested that they may share a single common ancestor for this gene. The newly discovered Bronnoya virus RdRp sequence clustered with the previously reported Bronnoya virus.

Ixodes persulcatus luteo-like virus HLJ, *I. persulcatus* picobirna virus HLJ, and JMTV found in this study exhibited 87, 94, and 99% amino acid identities to previously reported viruses with, respectively, 98, 91, and 93% sequence coverage (Figures 3B,E,F).

Ixodes persulcatus orbivirus-like HLJ revealed 40% amino acid similarity across 94% of the VP1 gene sequence of the orbivirus Skunk River virus (MK100569.1), and it showed a phylogenetic position distinct from other orbiviruses in the phylogenetic tree (Figure 3G).

Bloodmeal-Associated Differential Gene Expression Analyses

We next detected the differential expression responses of ticks at two different stages of feeding: flat (pools TG1, TG2, and TG13) and fully fed (pools TG5, TG6, and TG15) to investigate the effect of the bloodmeal. We first generated a single Trinity assembly across all pools and then calculated the abundance separately for each pool. The subsequent differential expression analysis showed that a total of 1,302 genes were differently expressed ($p < 0.05$, $\log_{2}FC > 1.5$). Most of the

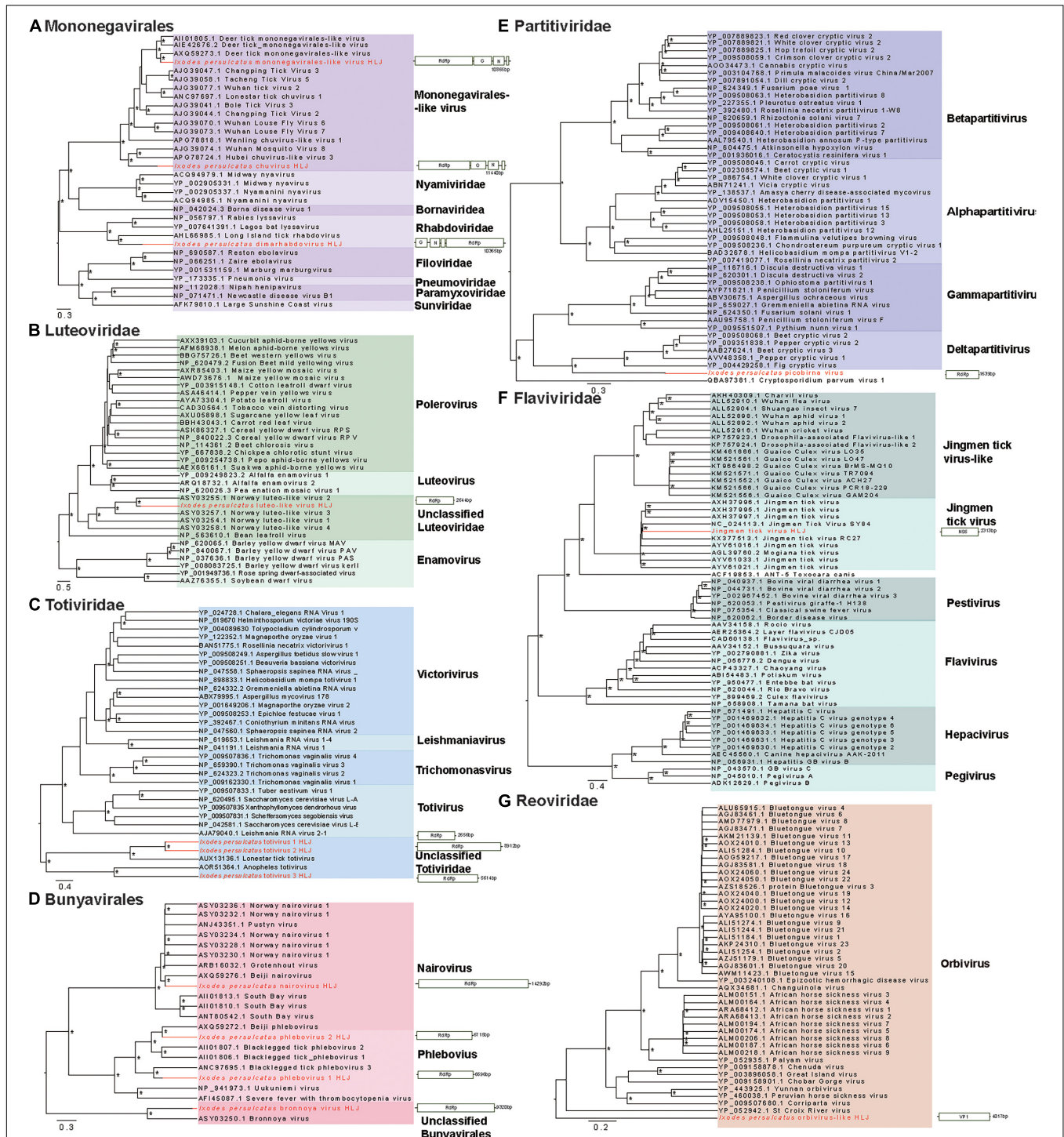
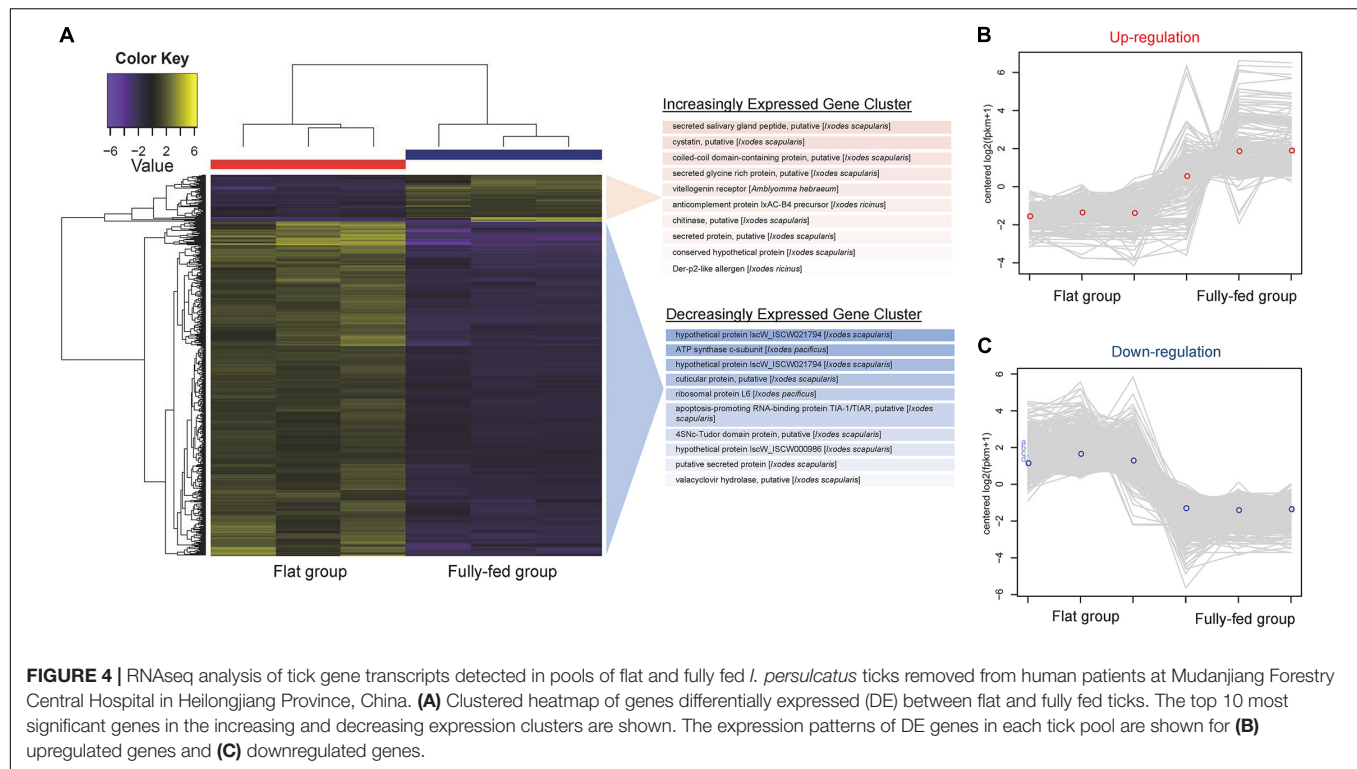


FIGURE 3 | Phylogenetic trees of the RNA-dependent RNA polymerase (RdRp) gene-based on representative amino acid sequences and schematic genome structures of 14 viruses detected in *I. persulcatus* ticks removed from human patients at Mudanjiang Forestry Central Hospital in Heilongjiang Province, China.

(A) Mononegavirales; (B) Luteoviridae; (C) Totiviridae; (D) Bunyavirales; (E) Partitiviridae; (F) Flaviviridae; and (G) Reoviridae. Support values above 0.7 are indicated by asterisk. The trees were mid-point rooted.

DE genes were negatively correlated (**Supplementary Figure 1**). As shown in **Figure 4A**, most of the DE genes (71.4%) were downregulated in fully fed ticks; of these, ATP synthase c-subunit,

a putative cuticular protein, ribosomal protein L6, and the putative apoptosis-promoting RNA-binding protein TIA-1/TIAR were the most downregulated (**Supplementary Table 2**). The



gene encoding a putative secreted salivary gland peptide was most upregulated at engorgement, followed by a putative cystatin, putative coiled-coil domain-containing protein, and putative secreted glycine-rich protein (Supplementary Table 2). One antimicrobial peptide, lysozyme, was downregulated in fully fed ticks (Supplementary Table 3).

All DE genes shown in the heatmap (Figure 4A) were grouped into clusters of genes with similar expression patterns. A total of 251 transcripts were clustered in the upregulation category (Figure 4B), while 930 transcripts were clustered in the downregulation category (Figure 4C). According to the taxonomy classification based on the COG database, 18.7% of DE genes in the upregulated category were related to post-translational modification, protein turnover, and chaperones, and 12.7% of upregulated DE genes displayed functions of translation, ribosomal structure, and biogenesis (Supplementary Figure 2A). Most of the DE genes in the downregulated category were related to functions of nucleotide transport and metabolism (18.2%) and cytoskeleton (18.3%) (Supplementary Figure 2B).

Reactive Oxygen Species

Reactive Oxygen Species (ROS) produced by the mosquito midgut play a role in maintenance of redox homeostasis (Citelli et al., 2007; Hernandez et al., 2019), and previous literatures also suggested that the balance between positive and negative aspects of ROS in ticks should be carefully maintained (Hernandez et al., 2019). To achieve redox homeostasis, the ticks have a complex anti-oxidant system composed of enzymes such as glutathione peroxidase, glutathione-S transferase, and so on (Hernandez et al., 2018, 2020; Kusakisako et al., 2018, 2020). We found that

antioxidant genes including glutathione peroxidase, glutathione S-transferase, peroxidase, peroxiredoxin, and protein kinase C were all downregulated in the fully fed ticks compared with the flat ticks (Supplementary Table 3).

DISCUSSION

Blood-feeding is an essential behavior for ticks, and its role is far beyond that of providing nutrition and energy for molting, development, and vitellogenesis. Its requirement for transmission of tick-borne pathogens is another important function. The present study is the first report on the virome of ticks fed on patients who sought medical attention in a sentinel hospital in northeastern China. Using unbiased high-throughput sequencing platforms, we found that five mammalian species had served as hosts for *I. persulcatus*, including a bat. We also identified Jingmen tick virus and 13 new viruses belonging to 11 viral families. A downregulation of antioxidant genes associated with blood intake was observed in the fed ticks, which might be correlated with maintenance of the redox homeostasis.

It is important to identify the sources of *I. persulcatus* bloodmeals to aid in assessing the risk to patients of tick-borne disease transmission. Bats are some of the most notorious natural reservoir/hosts for many fatal viruses, such as Ebola virus, SARS virus, and SARS-CoV-2 virus (Calisher et al., 2006; Zhou et al., 2020). We found that some *I. persulcatus* ticks feeding on humans may have previously imbibed bat blood, highlighting the need for alertness on this tick species for its role in transmitting novel pathogens from bats to humans.

Various host *cox1* genes were identified in our data, namely mouse, bat, sheep, wild boar, and human, indicating the high risk of interspecies transmission of tick-borne pathogens. Previous studies have developed DNA barcoding (Kent, 2009; Allan et al., 2010; Gariepy et al., 2012) or proteome profiling (Önder et al., 2013) techniques to identify sources of tick blood meals. However, the host identification success was limited due to the heavily degraded remnants of blood. We used the RNA-seq platform to identify the origin of the host bloodmeals of the pooled samples; however, the sensitivity and specificity of this approach should be further evaluated.

We found 14 viruses, belonging to 11 viral families, and most of them showed quite low similarity and query coverage compared with previously found viruses. Meng et al. found five species of viruses, including JMTV, in the same geographic area (Pettersson et al., 2017). We have previously reported that JMTV was pathogenic to humans (Jia et al., 2019), and the known range of this virus has rapidly expanded to cover Africa, South America, the Caribbean, and Europe (Temmam et al., 2019). We will extend our vigilance to other new viruses found in this study for their potential pathogenicity in humans, as these viruses were found in ticks directly detached from human patients. However, whether *I. persulcatus* is the vector of these viruses remains to be explored. In addition, the possibility of the new viruses being endogenous virus elements (Bell-Sakyi and Attoui, 2016) is very low because all the viruses were found to have fully or almost fully intact genomes, without disrupted reading frames.

Reactive oxygen species level seems to be a typical association with the maintenance of redox homeostasis in hematophagous arthropods, such as ticks (Lara et al., 2005; Citelli et al., 2007) and mosquitoes (Cirimotich et al., 2011; Oliveira et al., 2011). However, ticks might have developed different mechanisms to control ROS level compared with mosquitoes. For example, ticks have a different pathway for heme biosynthesis and require the acquisition of exogenous heme (Perner et al., 2016). Due to their feeding physiology, ticks are exposed to elevated amount of ROS. The ingestion of host blood containing pro-oxidant molecules, such as heme, could catalyze the production of ROS (Graça-Souza et al., 2006). Aside from blood-feeding, many cellular processes and enzyme activity could result in ROS production and eventually increase oxidative stress levels (Hernandez et al., 2019). Recently, carbohydrate metabolic compensation and peroxiredoxin production were reported to be necessary to maintain the redox balance in ticks (Kusakisako et al., 2016; Della Noce et al., 2019). It has been proposed that tick microbiome would be influenced by oxidative stress (Narasimhan and Fikrig, 2015), and different AMP would have different inhibitory consequence on microbial growth (Saito et al., 2009; Zhang et al., 2015). These immune responses in ticks may work together and eventually influence the viral and bacterial composition of a specific host blood meal through a complicated pathway.

On the other hand, the redox situation may indirectly affect pathogen transmission by changing its balance with other microflora in the ticks as suggested in mosquitoes (Cirimotich et al., 2011). We noticed that the gene encoding reeler domain-containing gut protein was significantly upregulated in the fully

fed ticks (**Supplementary Table 3**). A protein of *Ixodes scapularis* with a Reeler domain (PIXR) was induced upon feeding and upregulated in *Borrelia burgdorferi*-infected *I. scapularis* tick guts. PIXR might influence the tick gut microbiome composition by regulating the ability of gram-positive bacteria to form biofilms in the gut when the tick takes a blood meal (Narasimhan et al., 2017). These alterations may influence *B. burgdorferi* entering the tick gut in multiple ways (Zhang et al., 2015). We identified that the gene encoding a protein similar to PIXR was upregulated in the fully fed *I. persulcatus* ticks; however, its role in the transmission of *Borrelia* and other tick-borne pathogens deserves further study.

We noted several limitations as follows: The interpretation of differential gene expression between the flat and fully fed ticks might be over-cautious because we used pooled samples with a relatively limited sample size. Using laboratory-reared ticks from a single colony can decrease the bias caused by individual tick differences; however, this study examined bloodmeal-induced gene regulation and virome in ticks originating from the field and feeding on human patients. We thereby gained valuable information on the risks to patients from tick-borne viruses, at the expense of likely uniformity in response to blood-feeding amongst the studied ticks. We suggest that further research with more field and laboratory-derived samples, and experiments from proteomics and functional genomics perspectives, could be performed to verify our findings.

DATA AVAILABILITY STATEMENT

The datasets presented in this study can be found in online repositories. The names of the repository/repositories and accession number(s) can be found below: <https://www.ncbi.nlm.nih.gov/>, PRJNA639641.

ETHICS STATEMENT

The studies involving human participants were reviewed and approved by Mudanjiang Forest Central Hospital 2011-03. The patients/participants provided their written informed consent to participate in this study.

AUTHOR CONTRIBUTIONS

All authors contributed to the manuscript and approved the submitted version.

FUNDING

This study was supported by Natural Science Foundation of China (81773492) and the State Key Research Development Program of China (2019YFC1200202). LB-S was funded by the United Kingdom Biotechnology and Biological Sciences Research Council grant BB/P024270/1.

ACKNOWLEDGMENTS

We thank all the staff in the tick-borne disease department in Mudanjiang Forestry Central Hospital for their help with sample collections.

SUPPLEMENTARY MATERIAL

The Supplementary Material for this article can be found online at: <https://www.frontiersin.org/articles/10.3389/fmicb.2021.728996/full#supplementary-material>

REFERENCES

- Allan, B. F., Goessling, L. S., Storch, G. A., and Thach, R. E. (2010). Blood meal analysis to identify reservoir hosts for *Amblyomma americanum* ticks. *Emerg. Infect. Dis.* 16, 433–440. doi: 10.3201/eid1603.090911
- Bell-Sakyi, L., and Attoui, H. (2016). Virus Discovery Using Tick Cell Lines. *Evol. Bioinform. Online* 12, 31–34. doi: 10.4137/EBO.S39675
- Bryant, D. M., Johnson, K., DiTommaso, T., Tickle, T., Couger, M. B., Payzin-Dogru, D., et al. (2017). A tissue-mapped axolotl de novo transcriptome enables identification of limb regeneration factors. *Cell Rep.* 18, 762–776. doi: 10.1016/j.celrep.2016.12.063
- Calisher, C. H., Childs, J. E., Field, H. E., Holmes, K. V., and Schountz, T. (2006). Bats: important reservoir hosts of emerging viruses. *Clin. Microbiol. Rev.* 19, 531–545. doi: 10.1128/CMR.00017-06
- Cao, W. C., Zhao, Q. M., Zhang, P. H., Dumler, J. S., Zhang, X. T., Fang, L. Q., et al. (2000). Granulocytic Ehrlichiae in *Ixodes persulcatus* ticks from an area in China where Lyme disease is endemic. *J. Clin. Microbiol.* 38, 4208–4210. doi: 10.1128/JCM.38.11.4208-4210.2000
- Cao, W. C., Zhao, Q. M., Zhang, P. H., Yang, H., Wu, X. M., Wen, B. H., et al. (2003). Prevalence of *Anaplasma phagocytophila* and *Borrelia burgdorferi* in *Ixodes persulcatus* ticks from northeastern China. *Am. J. Trop. Med. Hyg.* 68, 547–550. doi: 10.4269/ajtmh.2003.68.547
- Capella-Gutiérrez, S., Silla-Martínez, J. M., and Gabaldón, T. (2009). trimAl: a tool for automated alignment trimming in large-scale phylogenetic analyses. *Bioinformatics* 25, 1972–1973. doi: 10.1093/bioinformatics/bt p348
- Charrier, N. P., Couton, M., Voordouw, M. J., Rais, O., Durand-Hermouet, A., Hervet, C., et al. (2018). Whole body transcriptomes and new insights into the biology of the tick *Ixodes ricinus*. *Parasit. Vectors* 11:364. doi: 10.1186/s13071-018-2932-3
- Cirimotich, C. M., Dong, Y., Clayton, A. M., Sandiford, S. L., Souza-Neto, J. A., Mulenga, M., et al. (2011). Natural microbe-mediated refractoriness to *Plasmodium* infection in *Anopheles gambiae*. *Science* 332, 855–858. doi: 10.1126/science.1201618
- Citelli, M., Lara, F. A., da Silva Vaz, I. Jr., and Oliveira, P. L. (2007). Oxidative stress impairs heme detoxification in the midgut of the cattle tick, *Rhipicephalus* (Boophilus) microplus. *Mol. Biochem. Parasitol.* 151, 81–88. doi: 10.1016/j.molbiopara.2006.10.008
- Darriba, D., Taboada, G. L., Doallo, R., and Posada, D. (2011). ProtTest 3: fast selection of best-fit models of protein evolution. *Bioinformatics* 27, 1164–1165. doi: 10.1093/bioinformatics/btr088
- de la Fuente, J., Estrada-Pena, A., Venzal, J. M., Kocan, K. M., and Sonenshine, D. E. (2008). Overview: ticks as vectors of pathogens that cause disease in humans and animals. *Front. Biosci.* 13, 6938–6946. doi: 10.2741/3200
- Della Noce, B., Carvalho Uhl, M. V., Machado, J., Walthero, C. F., de Abreu, L. A., da Silva, R. M., et al. (2019). Carbohydrate Metabolic Compensation Coupled to High tolerance to oxidative stress in ticks. *Sci. Rep.* 9:4753. doi: 10.1038/s41598-019-41036-0
- Garipey, T. D., Lindsay, R., Ogden, N., and Gregory, T. R. (2012). Identifying the last supper: utility of the DNA barcode library for bloodmeal identification in ticks. *Mol. Ecol. Resour.* 12, 646–652. doi: 10.1111/j.1755-0998.2012.03140.x
- Grabherr, M. G., Haas, B. J., Yassour, M., Levin, J. Z., Thompson, D. A., Amit, I., et al. (2011). Full-length transcriptome assembly from RNA-Seq data without a reference genome. *Nat. Biotechnol.* 29, 644–652. doi: 10.1038/nbt.1883
- Graça-Souza, A. V., Maya-Monteiro, C., Paiva-Silva, G. O., Braz, G. R., Paes, M. C., Sorgine, M. H., et al. (2006). Adaptations against heme toxicity in blood-feeding arthropods. *Insect Biochem. Mol. Biol.* 36, 322–335. doi: 10.1016/j.ibmb.2006.01.009
- Guindon, S., and Gascuel, O. (2003). A simple, fast, and accurate algorithm to estimate large phylogenies by maximum likelihood. *Syst. Biol.* 52, 696–704. doi: 10.1080/10635150390235520
- Harvey, E., Rose, K., Eden, J. S., Lo, N., Abeyasuriya, T., Shi, M., et al. (2019). Extensive diversity of RNA viruses in Australian ticks. *J. Virol.* 93, e01358–18. doi: 10.1128/JVI.01358-18
- Hawlana, H., Rynkiewicz, E., Toh, E., Alfred, A., Durden, L. A., Hastriter, M. W., et al. (2013). The arthropod, but not the vertebrate host or its environment, dictates bacterial community composition of fleas and ticks. *ISME J.* 7, 221–223. doi: 10.1038/ismej.2012.71
- Hernandez, E. P., Kusakisako, K., Talactac, M. R., Galay, R. L., Hatta, T., Matsuo, T., et al. (2018). Characterization and expression analysis of a newly identified glutathione S-transferase of the hard tick *Haemaphysalis longicornis* during blood-feeding. *Parasit. Vectors* 11:91. doi: 10.1186/s13071-018-2667-1
- Hernandez, E. P., Shimazaki, K., Niihara, H., Umemiya-Shirafuji, R., Fujisaki, K., and Tanaka, T. (2020). Expression analysis of glutathione S-transferases and ferritins during the embryogenesis of the tick *Haemaphysalis longicornis*. *Heliyon* 6:e03644. doi: 10.1016/j.heliyon.2020.e03644
- Hernandez, E. P., Talactac, M. R., Fujisaki, K., and Tanaka, T. (2019). The case for oxidative stress molecule involvement in the tick-pathogen interactions - an omics approach. *Dev. Comp. Immunol.* 100:103409. doi: 10.1016/j.dci.2019.103409
- Huerta-Cepas, J., Forslund, K., Coelho, L. P., Szklarczyk, D., Jensen, L. J., von Mering, C., et al. (2017). Fast genome-wide functional annotation through orthology assignment by eggNOG-mapper. *Mol. Biol. Evol.* 34, 2115–2122. doi: 10.1093/molbev/msx148
- Jia, N., Liu, H. B., Ni, X. B., Bell-Sakyi, L., Zheng, Y. C., Song, J. L., et al. (2019). Emergence of human infection with Jingmen tick virus in China: a retrospective study. *EBioMedicine* 43, 317–324. doi: 10.1016/j.ebiom.2019.04.004
- Jia, N., Wang, J., Shi, W., Du, L., Sun, Y., Zhan, W., et al. (2020). Large-Scale Comparative Analyses of Tick Genomes Elucidate Their Genetic Diversity and Vector Capacities. *Cell* 182, 1328–1340.e13. doi: 10.1016/j.cell.2020.07.023
- Jones, K. E., Patel, N. G., Levy, M. A., Storeygard, A., Balk, D., Gittleman, J. L., et al. (2008). Global trends in emerging infectious diseases. *Nature* 451, 990–993. doi: 10.1038/nature06536
- Jongejan, F., and Uilenberg, G. (2004). The global importance of ticks. *Parasitology* 129, S3–S14. doi: 10.1017/s0031182004005967
- Katoh, K., and Standley, D. M. (2013). MAFFT multiple sequence alignment software version 7: improvements in performance and usability. *Mol. Biol. Evol.* 30, 772–780. doi: 10.1093/molbev/mst010
- Kent, R. J. (2009). Molecular methods for arthropod bloodmeal identification and applications to ecological and vector-borne disease studies. *Mol. Ecol. Resour.* 9, 4–18. doi: 10.1111/j.1755-0998.2008.02469.x
- Kusakisako, K., Galay, R. L., Umemiya-Shirafuji, R., Hernandez, E. P., Maeda, H., Talactac, M. R., et al. (2016). 2-Cys peroxiredoxin is required in successful

- blood-feeding, reproduction, and antioxidant response in the hard tick *Haemaphysalis longicornis*. *Parasit. Vectors* 9:457. doi: 10.1186/s13071-016-1748-2
- Kusakisako, K., Hernandez, E. P., Talactac, M. R., Yoshii, K., Umemiya-Shirafuji, R., Fujisaki, K., et al. (2018). Peroxiredoxins are important for the regulation of hydrogen peroxide concentrations in ticks and tick cell line. *Ticks Tick Borne Dis.* 9, 872–881. doi: 10.1016/j.ttbdis.2018.03.016
- Kusakisako, K., Morokuma, H., Talactac, M. R., Hernandez, E. P., Yoshii, K., and Tanaka, T. A. (2020). Peroxiredoxin From the *Haemaphysalis longicornis* Tick Affects Langat Virus Replication in a Hamster Cell Line. *Front. Cell. Infect. Microbiol.* 10:7. doi: 10.3389/fcimb.2020.00007
- Langmead, B., and Salzberg, S. L. (2012). Fast gapped-read alignment with Bowtie 2. *Nat. Methods* 9, 357–359. doi: 10.1038/nmeth.1923
- Lara, F. A., Lins, U., Bechara, G. H., and Oliveira, P. L. (2005). Tracing heme in a living cell: hemoglobin degradation and heme traffic in digest cells of the cattle tick *Boophilus microplus*. *J. Exp. Biol.* 208, 3093–3101. doi: 10.1242/jeb.01749
- Li, B., Ruotti, V., Stewart, R. M., Thomson, J. A., and Dewey, C. N. (2009). RNA-Seq gene expression estimation with read mapping uncertainty. *Bioinformatics* 26, 493–500. doi: 10.1093/bioinformatics/btp692
- McCarthy, D. J., Chen, Y., and Smyth, G. K. (2012). Differential expression analysis of multifactor RNA-Seq experiments with respect to biological variation. *Nucleic Acids Res.* 40, 4288–4297. doi: 10.1093/nar/gks042
- Meng, F., Ding, M., Tan, Z., Zhao, Z., Xu, L., Wu, J., et al. (2019). Virome analysis of tick-borne viruses in Heilongjiang Province, China. *Ticks Tick-Borne Dis.* 10, 412–420. doi: 10.1016/j.ttbdis.2018.12.002
- Narasimhan, S., and Fikrig, E. (2015). Tick microbiome: the force within. *Trends Parasitol.* 31, 315–323. doi: 10.1016/j.pt.2015.03.010
- Narasimhan, S., Schuijt, T. J., Abraham, N. M., Rajeevan, N., Coumou, J., Graham, M., et al. (2017). Modulation of the tick gut milieu by a secreted tick protein favors *Borrelia burgdorferi* colonization. *Nat. Commun.* 8:184. doi: 10.1038/s41467-017-00208-0
- Nava, S., Guglielmoni, A. A., and Mangold, A. J. (2009). An overview of systematics and evolution of ticks. *Front. Biosci.* 14, 2857–2877. doi: 10.2741/3418
- Oliveira, J. H., Gonçalves, R. L., Lara, F. A., Dias, F. A., Gandara, A. C., Menna-Barreto, R. F., et al. (2011). Blood meal-derived heme decreases ROS levels in the midgut of *Aedes aegypti* and allows proliferation of intestinal microbiota. *PLoS Pathog.* 7:e1001320. doi: 10.1371/journal.ppat.1001320
- Önder, Ö., Shao, W., Kemps, B. D., Lam, H., and Brisson, D. (2013). Identifying sources of tick blood meals using unidentified tandem mass spectral libraries. *Nat. Commun.* 4:1746. doi: 10.1038/ncomms2730
- Perner, J., Sobotka, R., Sima, R., Konvickova, J., Sojka, D., Oliveira, P. L., et al. (2016). Acquisition of exogenous haem is essential for tick reproduction. *Elife* 5:e12318. doi: 10.7554/eLife.12318
- Pettersson, J. H., Shi, M., Bohlin, J., Eldholm, V., Brynildsrud, O. B., Paulsen, K. M., et al. (2017). Characterizing the virome of *Ixodes ricinus* ticks from northern Europe. *Sci. Rep.* 7:10870. doi: 10.1038/s41598-017-11439-y
- Robinson, M. D., McCarthy, D. J., and Smyth, G. K. (2010). edgeR: a Bioconductor package for differential expression analysis of digital gene expression data. *Bioinformatics* 26, 139–140. doi: 10.1093/bioinformatics/btp616
- Rynkiewicz, E. C., Hemmerich, C., Rusch, D. B., Fuqua, C., and Clay, K. (2015). Concordance of bacterial communities of two tick species and blood of their shared rodent host. *Mol. Ecol.* 24, 2566–2579. doi: 10.1111/mec.13187
- Saito, Y., Konnai, S., Yamada, S., Imamura, S., Nishikado, H., Ito, T., et al. (2009). Identification and characterization of antimicrobial peptide, defensin, in the taiga tick, *Ixodes persulcatus*. *Insect Mol. Biol.* 18, 531–539. doi: 10.1111/j.1365-2583.2009.00897.x
- Shi, M., Lin, X. D., Tian, J. H., Chen, L. J., Chen, X., and Li, C. X. (2016). Redefining the invertebrate RNA virosphere. *Nature* 540, 539–543. doi: 10.1038/nature20167
- Swei, A., and Kwan, J. Y. (2017). Tick microbiome and pathogen acquisition altered by host blood meal. *ISME J.* 11, 813–816. doi: 10.1038/ismej.2016.152
- Temmam, S., Bigot, T., Chrétien, D., Gondard, M., Pérot, P., Pommelet, V., et al. (2019). Insights into the Host Range, Genetic Diversity, and Geographical Distribution of Jingmenviruses. *mSphere* 4, e00645–19. doi: 10.1128/mSphere.00645-19
- Thorvaldsdóttir, H., Robinson, J. T., and Mesirov, J. P. (2013). Integrative Genomics Viewer (IGV): high-performance genomics data visualization and exploration. *Brief. Bioinform.* 14, 178–192. doi: 10.1093/bib/bbs017
- Tokarz, R., Sameroff, S., Tagliaferro, T., Jain, K., Williams, S. H., Cucura, D. M., et al. (2018). Identification of novel viruses in *Amblyomma americanum*, *Dermacentor variabilis*, and *Ixodes scapularis* ticks. *mSphere* 3, e00614–17.
- Tokarz, R., Williams, S. H., Sameroff, S., Sanchez Leon, M., Jain, K., and Lipkin, W. I. (2014). Virome analysis of *Amblyomma americanum*, *Dermacentor variabilis*, and *Ixodes scapularis* ticks reveals novel highly divergent vertebrate and invertebrate viruses. *J. Virol.* 88, 11480–11492. doi: 10.1128/JVI.01858-14
- Vandegrift, K. A.-O., and Kapoor, A. A.-O. (2019). The Ecology of New Constituents of the Tick Virome and Their Relevance to Public Health. *Viruses* 11:529. doi: 10.3390/v11060529
- Zhang, H., Yang, S., Gong, H., Cao, J., Zhou, Y., and Zhou, J. (2015). Functional analysis of a novel cysteine-rich antimicrobial peptide from the salivary glands of the tick *Rhipicephalus haemaphysaloides*. *Parasitol. Res.* 114, 3855–3863. doi: 10.1007/s00436-015-4615-8
- Zhang, X. C., Yang, Z. N., Lu, B., Ma, X. F., Zhang, C. X., and Xu, H. J. (2014). The composition and transmission of microbiome in hard tick, *Ixodes persulcatus*, during blood meal. *Ticks Tick-Borne Dis.* 5, 864–870. doi: 10.1016/j.ttbdis.2014.07.009
- Zhou, P., Yang, X. L., Wang, X. G., Hu, B., Zhang, L., Zhang, W., et al. (2020). A pneumonia outbreak associated with a new coronavirus of probable bat origin. *Nature* 579, 270–273.
- Zolnik, C. P., Falco, R. C., Daniels, T. J., and Kolokotronis, S. O. (2018). Transient influence of blood meal and natural environment on blacklegged tick bacterial communities. *Ticks Tick-Borne Dis.* 9, 563–572. doi: 10.1016/j.ttbdis.2018.01.007

Conflict of Interest: The authors declare that the research was conducted in the absence of any commercial or financial relationships that could be construed as a potential conflict of interest.

Publisher's Note: All claims expressed in this article are solely those of the authors and do not necessarily represent those of their affiliated organizations, or those of the publisher, the editors and the reviewers. Any product that may be evaluated in this article, or claim that may be made by its manufacturer, is not guaranteed or endorsed by the publisher.

Copyright © 2022 Li, Ning, Zheng, Chu, Cui, Zhang, Guo, Wei, Liu, Sun, Ye, Jiang, Yuan, Li, Bian, Bell-Sakyi, Wang, Jiang, Song, Cao, Tsan-Yuk Lam, Ni and Jia. This is an open-access article distributed under the terms of the Creative Commons Attribution License (CC BY). The use, distribution or reproduction in other forums is permitted, provided the original author(s) and the copyright owner(s) are credited and that the original publication in this journal is cited, in accordance with accepted academic practice. No use, distribution or reproduction is permitted which does not comply with these terms.



Dissecting the Species-Specific Virome in *Culicoides* of Thrace

Konstantinos Konstantinidis^{1†}, Maria Bampali^{1†}, Michael de Courcy Williams¹, Nikolas Dovrolis¹, Elisavet Gatzidou¹, Pavlos Papazilakis², Andreas Nearchou³, Stavroula Veletza¹ and Ioannis Karakasiliotis^{1*}

¹ Department of Medicine, Laboratory of Biology, Democritus University of Thrace, Alexandroupolis, Greece, ² Evrofarma S.A., Didymoteicho, Greece, ³ Geotechno Ygeionomiki O.E, Xanthi, Greece

OPEN ACCESS

Edited by:

Na Jia,
Beijing Institute of Microbiology
and Epidemiology, China

Reviewed by:

Gabriel Luz Wallau,
Aggeu Magalhães Institute (IAM),
Brazil
Laurent Dacheux,
Institut Pasteur, France
Aiping Wu,
Chinese Academy of Medical
Sciences, China

*Correspondence:

Ioannis Karakasiliotis
ioakarak@med.duth.gr

[†] These authors have contributed
equally to this work

Specialty section:

This article was submitted to
Virology,
a section of the journal
Frontiers in Microbiology

Received: 26 October 2021

Accepted: 31 January 2022

Published: 07 March 2022

Citation:

Konstantinidis K, Bampali M,
de Courcy Williams M, Dovrolis N,
Gatzidou E, Papazilakis P,
Nearchou A, Veletza S and
Karakasiliotis I (2022) Dissecting
the Species-Specific Virome
in *Culicoides* of Thrace.
Front. Microbiol. 13:802577.
doi: 10.3389/fmicb.2022.802577

Biting midges (*Culicoides*) are vectors of arboviruses of both veterinary and medical importance. The surge of emerging and reemerging vector-borne diseases and their expansion in geographical areas affected by climate change has increased the importance of understanding their capacity to contribute to novel and emerging infectious diseases. The study of *Culicoides* virome is the first step in the assessment of this potential. In this study, we analyzed the RNA virome of 10 *Culicoides* species within the geographical area of Thrace in the southeastern part of Europe, a crossing point between Asia and Europe and important path of various arboviruses, utilizing the Ion Torrent next-generation sequencing (NGS) platform and a custom bioinformatics pipeline based on TRINITY assembler and alignment algorithms. The analysis of the RNA virome of 10 *Culicoides* species resulted in the identification of the genomic signatures of 14 novel RNA viruses, including three fully assembled viruses and four segmented viruses with at least one segment fully assembled, most of which were significantly divergent from previously identified related viruses from the *Solemoviridae*, *Phasmaviridae*, *Phenuiviridae*, *Reoviridae*, *Chuviridae*, *Partitiviridae*, *Orthomyxoviridae*, *Rhabdoviridae*, and *Flaviviridae* families. Each *Culicoides* species carried a species-specific set of viruses, some of which are related to viruses from other insect vectors in the same area, contributing to the idea of a virus-carrier web within the ecosystem. The identified viruses not only expand our current knowledge on the virome of *Culicoides* but also set the basis of the genetic diversity of such viruses in the area of southeastern Europe. Furthermore, our study highlights that such metagenomic approaches should include as many species as possible of the local virus-carrier web that interact and share the virome of a geographical area.

Keywords: *Culicoides*, arboviruses, emerging infectious diseases, vectors, virome analysis, metagenomics, Thrace, Greece

INTRODUCTION

Analyses of arthropod-borne viruses (arboviruses) have spurred the interest of the scientific community. Epidemics caused by yellow fever virus (Cracknell Daniels et al., 2021), Zika virus (Estévez-Herrera et al., 2021), dengue virus (Mayer et al., 2017), West Nile virus (Petersen, 2019), Rift Valley virus (Gregor et al., 2021), chikungunya virus (Mayer et al., 2017), equine encephalitis

virus (Lecollinet et al., 2020), lumpy skin disease virus (Klement et al., 2020), and bluetongue virus (BTV) (Saminathan et al., 2020) have constituted a great burden on public health and animal husbandry worldwide over the past few years. Climate change, inducing variations in rainfall, humidity, and wind patterns (Whitehorn and Yacoub, 2019), accompanied by globalization and urbanization phenomena, the alteration of natural habitats, and agricultural structures (Miles et al., 2019), all can affect arthropod reproduction, development, distribution, and feeding behavior. Parallel changes in arthropod ecology may dramatically influence arthropod-borne virus proliferation and transmission.

Among arthropod vectors that include mainly mosquitoes (Culicidae), ticks (Ixodidae), sand flies (Psychodidae, Phlebotominae), black flies (Simuliidae), and biting midges (Ceratopogonidae), the biting midges have received less attention regarding their ability to host or carry viruses, despite the fact that they are the most abundant hematophagous insects worldwide (Sick et al., 2019). The genus *Culicoides* encompasses the most important virus vectors in the family Ceratopogonidae and consists of more than 1,300 identified species (Borkent and Dominiak, 2020) flourishing between moderate climate areas to the tropics. *Culicoides* females feed on vertebrates, with preferences either toward a single species or a wide range of animals (Scholtz, 2018). Most *Culicoides* present crepuscular and nocturnal activity, whereas a few are active mostly during the day time. While they fly mostly in close proximity to their breeding and feeding sites, strong winds may carry them for hundreds of miles affecting their epidemiological importance.

Culicoides are of both medical and veterinary importance not only because of their numerical abundance and severity of biting activity but because they carry, either actively or mechanically, a wide range of pathogens, including bacteria, viruses, protozoa, and nematodes (Borkent, 2004; Žiegytė et al., 2021). *Culicoides* species are well known for their role in the emergence and spread of Schmallenberg virus (Rasmussen et al., 2012) (SBV) and BTV (Saminathan et al., 2020), mainly affecting ruminants (cattle, sheep, goats, etc.), and the emergence of Oropouche virus (Sakkas et al., 2018) (OROV) responsible for the Oropouche fever in humans. Most of the viruses transmitted by *Culicoides* are members of the Reoviridae [BTV, epizootic hemorrhagic disease virus, and African horse sickness virus (AHSV)], Rhabdoviridae (bovine ephemeral fever virus), and Peribunyaviridae family [SBV, OROV, and Akabane virus (AKAV)] (Elbers et al., 2015). The geographical distribution of these viruses correlates with the distribution of the respective vector species (Sick et al., 2019). Changes in climate conditions and intensified trade (Elbers et al., 2015) have assisted in the geographic spread of vectors into regions previously naive to viruses such as BTV (Purse et al., 2008) and SBV (Endalew et al., 2019).

An important aspect in the ecology of the viruses vectored by arthropods such as *Culicoides* is the vector specificity and competence. Viruses such as BTV are vectored by multiple species in a specific area (Foxi et al., 2016; Duan et al., 2021). Virus adaptation may determine vector specificity and competence (van Gennip et al., 2019). On the other hand, several *Culicoides* species host or carry multiple viruses. *Culicoides imicola* is a

known vector for AKAV, BTV, AHSV, and equine encephalosis virus (Leta et al., 2019), whereas *Culicoides brevitarsis* in Australia presents a similarly wide vector capacity (Tay et al., 2016). The interactions among multiple hosts and viruses in a specific region form a rather complicated network, the elucidation of which necessitates using holistic approaches in the identification of novel virus–host relationships.

Identification of novel viruses in known vectors has been especially highlighted during the coronavirus pandemic as the virus most related to SARS-CoV-2 (severe acute respiratory syndrome coronavirus 2) was identified in virome screenings in bats several years before its emergence in the same geographic area (Menachery et al., 2015; Corman et al., 2018; Morens et al., 2020). Despite the importance of *Culicoides* as vectors, very few studies have been done regarding the analysis of their virome (Temmam et al., 2015, 2016; Modha et al., 2019; Kobayashi et al., 2020; Liu et al., 2020). Metagenomic approaches have successfully yielded various novel and previously known viruses in analyses of single species of *Culicoides impunctatus* populations in Scotland (Modha et al., 2019), *C. imicola* in Senegal (Temmam et al., 2016), and *Culicoides arakawae* in Japan (Kobayashi et al., 2020). On the other hand, mixed populations of *Culicoides* species have been screened for viruses in efforts directed toward developing a more global understanding of the *Culicoides* virome (Temmam et al., 2015; Liu et al., 2020).

During the emergence of a new vector-borne disease, it is important to link the pathogen to its corresponding vector species, in order to promptly access the relevant epidemiological parameters and apply control measures. This is especially important in *Culicoides* as most species have distinct ecological and ethological characteristics, and control measures may vary greatly. Furthermore, biological control using the identified viruses against a certain *Culicoides* species may also be considered a possibility. In the context of this study, a holistic approach is attempted by simultaneously identifying the virome of 10 field-collected *Culicoides* species present in the geographic area of Thrace, Greece, at the southeastern part of Europe, an important path of various arboviruses between the continents of Asia and Europe. In contrast to previous attempts that analyzed either one species or mixtures of species of a taxon (Temmam et al., 2015, 2016; Modha et al., 2019; Kobayashi et al., 2020; Liu et al., 2020), our approach aimed to dissect the local *Culicoides* virome of Thrace and attribute a species-specific virome to all the identified species of *Culicoides* in the area during a collection period. Our methodology was based on the total RNA sequencing of 10 single-species pools followed by a custom bioinformatics pipeline, aiming to investigate, assemble, and phylogenetically characterize the virome of the examined *Culicoides* samples.

RESULTS

The identification of the virome of 10 *Culicoides* species was conducted upon 10 separate pools of *Culicoides* biting midges, which were field-collected from various sites in Thrace, Greece (**Supplementary Figure 1**), using Centers for Disease Control and Prevention (CDC) light traps. After sorting individuals

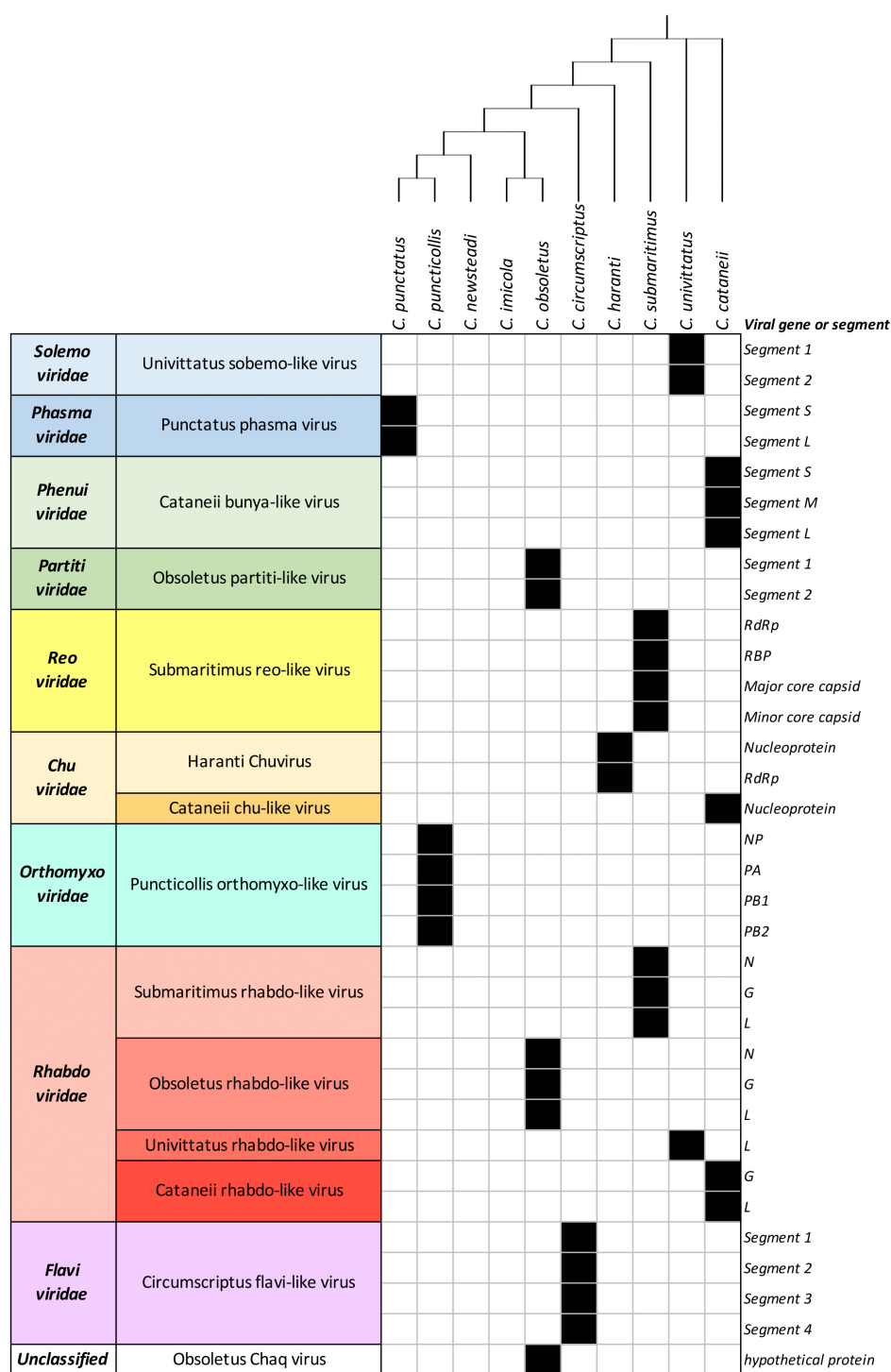


FIGURE 1 | List of detected viruses within *Culicoides* samples. Black filled squares indicate presence of the corresponding viral genes or segments.

by morphological identification, with subsequent validation of identifications using DNA barcoding, we analyzed the total RNA virome of 10 *Culicoides* single-species homogenous pools of 10 individuals each. All field-collected *Culicoides* samples underwent a total RNA-Seq protocol based on the

Ion Torrent sequencing platform followed by three repetitive assembly runs of the output next-generation sequencing (NGS) data due to the stochastic nature of TRINITY assembler program. The results of Ion torrent sequencing and TRINITY assembly are summarized in **Supplementary Tables 1, 2.**

We were able to identify and assemble 14 RNA viruses (**Supplementary Tables 3, 4**), all of which were novel virus species to only limited phylogenetic relationship to previously known viruses. In total, all 10 *Culicoides* species showcased a wide range of viruses, which corresponded to 9 viral families: *Solemoviridae*, *Phasmaviridae*, *Phenuiviridae*, *Reoviridae*, *Chuviridae*, *Partitiviridae*, *Orthomyxoviridae*, *Rhabdoviridae*, *Flaviviridae*, and one marked as unclassified at the family level (**Figure 1**).

All of the examined *Culicoides* species presented a diverse profile among the detected viruses, with *Culicoides obsoletus* and *Culicoides cataneii* being the most potent carriers in our study, carrying three different viruses each. *Culicoides submaritimus* and *Culicoides univittatus* harbored two different viruses each, whereas the majority of the tested field-collected samples (*Culicoides puncticollis*, *Culicoides punctatus*, *Culicoides circumscriptus*, *Culicoides haranti*) possessed a single virus species each. Notably, *Culicoides newsteadi* and *C. imicola* did not yield any viral sequences in the context of this study, despite both being notorious virus vectors. The virome of each *Culicoides* sample is described analytically per examined species in the following paragraphs.

Culicoides punctatus

C. punctatus harbored a *punctatus* phasma virus, member of the *Phasmaviridae* viral family, which was also partially assembled. Members of the family *Phasmaviridae* typically comprise three diverse genomic segments, namely, the nucleocapsid (segment S), glycoprotein (segment M), and RdRp (segment L) (**Figure 2**). However, the M segment could not be detected here, whereas the rest of the segments were recovered successfully from the examined samples of *C. punctatus*. The assembled N segment of *punctatus* phasma virus returned the nucleocapsid protein of Wuhan mosquito virus 1 (YP_009305133.1) as best overall BLASTp hit, whereas the assembled L segment matched the corresponding RdRp of *Aedes phasmavirus* (QOI91399.1) after a BLASTp search.

Culicoides submaritimus

Two viruses were detected within *C. submaritimus* belonging to the families *Reoviridae* and *Rhabdoviridae*, namely, *submaritimus* reo-like virus and *submaritimus* rhabdo-like virus, respectively. Four segments of *submaritimus* reo-like virus were successfully identified, constituting the RNA-dependent RNA-polymerase (RdRp), the RNA-binding protein (RBP), the major core capsid, and the minor core capsid (**Figure 3**). Only the latter was assembled completely, whereas the rest of the segments exhibited minor fragmentation. The RdRp segment of *submaritimus* reo-like virus showed the highest identity to the putative RdRp of Atrato reo-like virus (QHA33828). Similarly, the RBP and major core capsid segments of *submaritimus* reo-like virus matched the corresponding RBP (QHA33825) and major core capsid (QHA33826) segments of the aforementioned Atrato reo-like virus. The fully assembled minor core capsid segment of *submaritimus* reo-like virus displayed the highest coverage and aa identity compared with the rest of the detected

segments, returning the minor core capsid of Hubei reo-like virus 11 (APG79054) as top BLASTp hit.

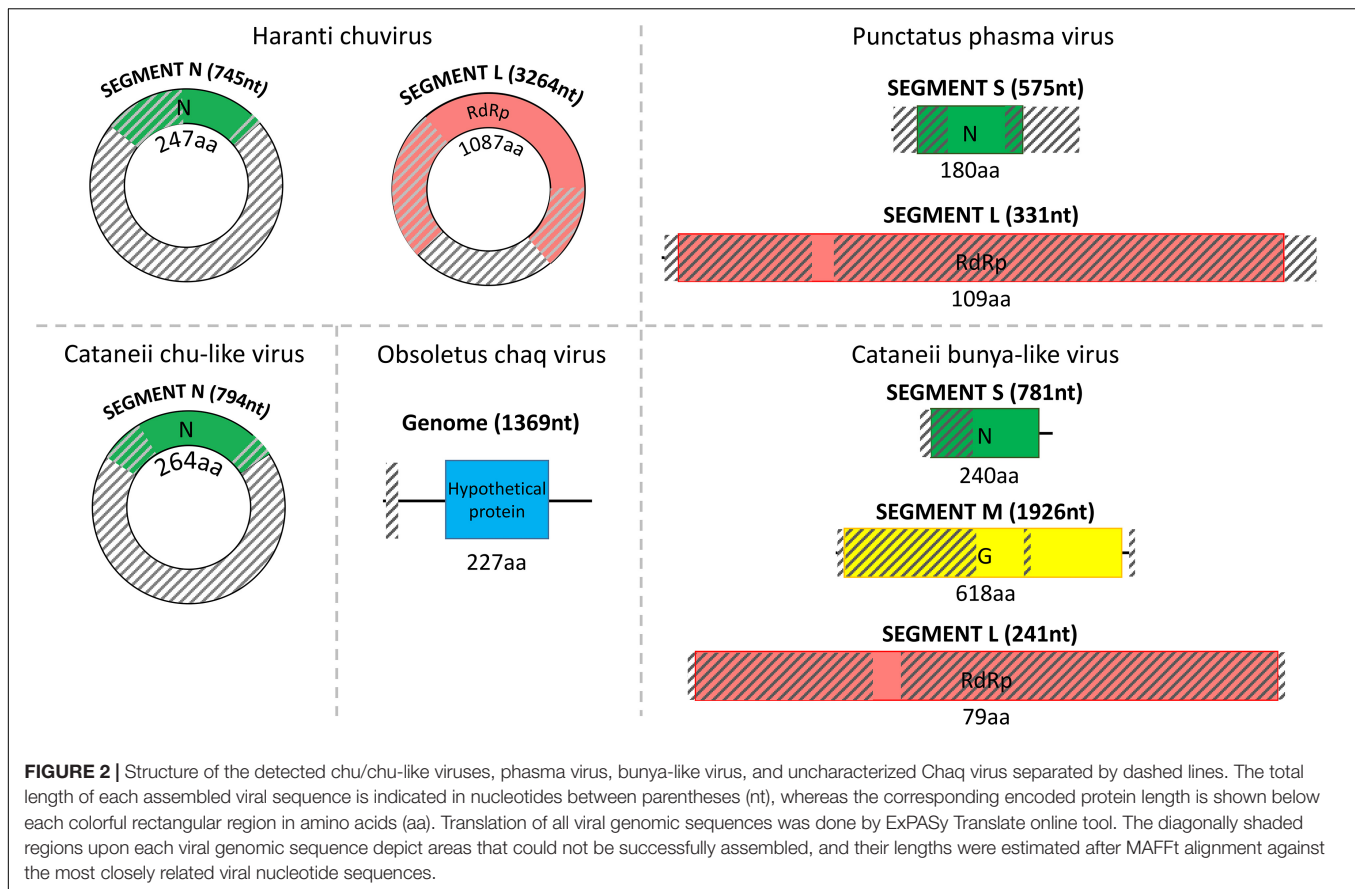
Moreover, *submaritimus* rhabdo-like virus was retrieved with its nearly complete nucleoprotein (N protein), as well as the partially assembled glycoprotein (G protein) and RdRp (L protein), whereas matrix and phosphoprotein transcripts could not be recovered (**Figure 4**). The best BLASTp match of *submaritimus* rhabdo-like virus nucleoprotein (NP) was the hypothetical protein of Wuhan mosquito virus 9 (QW97821.1). Glycoprotein of *submaritimus* rhabdo-like virus BLASTp aligned against the glycoprotein of Sanxia Water Strider Virus 5 (YP_009289351.1), whereas the assembled RdRp yielded the RNA-dependent RNA polymerase of Guadeloupe *Culex* rhabdovirus (QEM39120.1) as top BLASTp hit.

Culicoides puncticollis

Only 1 virus was obtained from *C. puncticollis* species, which carried a *puncticollis* orthomyxo-like virus, member of the *Orthomyxoviridae* viral family, consisting of four partially assembled genomic segments, specifically one NP and three discrete polymerases (PA, PB1, PB2) (**Figure 3**). Despite the small length of the assembled *puncticollis* orthomyxo-like virus NP segment, BLASTp reported the nucleocapsid protein of Jingshan fly virus 1 (APG77879.1) as best match. The assembled PA segment was highly similar to the PA polymerase of *Aedes alboannulatus* orthomyxo-like virus (ASA47422.1). The remaining PB1 and PB2 polymerases matched PB1 of Wuhan mosquito virus 3 (AJG39091.1) and PB2 of *A. alboannulatus* orthomyxo-like virus (ASA47421.1), respectively.

Culicoides univittatus

Field-collected samples of *C. univittatus* showed the species was infected with two different viruses, a *univittatus* sobemo-like virus and a *univittatus* rhabdo-like virus, belonging to the families *Solemoviridae* and *Rhabdoviridae*, respectively. *Solemoviridae* and sobemo-like viruses typically consist of two discrete genomic segments, each one encoding two proteins (**Figure 3**). Similarly, in this study, the first segment of *univittatus* sobemo-like virus encoded two separate proteins. The protein encoded first in this segment was identified as a putative protein, similar to the hypothetical protein of *Vespa velutina* RNA virus 3 (ATY36114.1) after a BLASTp search, whereas the second protein product of the same segment showed the highest identity to the RdRp of Atrato sobemo-like virus 1 (QHA33896.1). Nevertheless, the second segment of *univittatus* sobemo-like virus encoded only one protein noted as capsid. The assembled capsid of *univittatus* sobemo-like virus was closely related to the putative coat protein of Atrato sobemo-like virus 2 (QHA33889.1) according to BLASTp results. *Univittatus* rhabdo-like virus was also detected and recovered successfully from *C. univittatus*. However, it was assembled only partially as most of its genes were missing except for the encoded RdRp (**Figure 4**). The assembled RdRp of *univittatus* rhabdo-like virus showed the highest identity to the RNA-dependent RNA polymerase of *Culex pseudovishnui* rhabdo-like virus (BBQ04832.1) via BLASTp.



Culicoides obsoletus

C. obsoletus was one of the most potent virus carriers of the examined species, carrying two viruses belonging to *Partitiviridae* and *Rhabdoviridae* families and one unclassified virus. Obsoletus partiti-like virus, obsoletus rhabdo-like virus, and an unclassified obsoletus Chaq virus were detected within the field-collected samples of *C. obsoletus*. Like all partitiviruses, obsoletus partiti-like virus had a bipartite genome, with each segment encoding the RdRp and capsid proteins of the virus, respectively, which were both assembled successfully (Figure 3). The RdRp segment of obsoletus partiti-like virus yielded the corresponding RdRp of Hubei diptera virus 17 (YP_009337870.1) as top BLASTp hit, whereas the assembled capsid segment BLASTp matched the putative capsid protein of Atrato partiti-like virus 2 (QHA33903.1). A rhabdo-like virus (obsoletus rhabdo-like virus) was also identified in this study, possessing monopartite linear genomic structure and sequentially transcribing the NP, phosphoprotein, matrix, glycoprotein, and RdRp genes as usual for members of the family *Rhabdoviridae*. Three of the transcribed genes were almost fully assembled, but the phosphoprotein and matrix genes could not be retrieved (Figure 4). The NP of obsoletus rhabdo-like virus showed the highest identity to the putative NP of *Culex* rhabdo-like virus (AXQ04770.1), whereas BLASTp of the assembled glycoprotein returned the glycoprotein of Ohlsdorf virus (ATG83561.1) as a top hit. The RdRp of obsoletus rhabdo-like

virus BLASTp matched the polymerase-associated protein of Ohlsdorf virus (ATG83562.1). Notably, *C. obsoletus* carried an unclassified obsoletus Chaq virus, whose closest relative was the corresponding ORF of Chaq-like virus (QMI58124.1) after BLASTp search (Figure 2).

Culicoides cataneii

Similarly, *C. cataneii* harbored three viruses, namely, *cataneii* bunya-like virus, *cataneii* chu-like virus, and *cataneii* rhabdo-like virus, which are members of the families *Phenuiviridae*, *Chuviridae*, and *Rhabdoviridae*, respectively. The *cataneii* bunya-like virus was successfully recovered from the field-collected samples of *C. cataneii*, but its genomic segments were only partially assembled. The *cataneii* bunya-like virus consisted of three separate segments, encoding the corresponding nucleocapsid (segment S), glycoprotein (segment M), and RdRp (segment L) proteins (Figure 2). The assembled segment S of *cataneii* bunya-like virus yielded the nucleocapsid of *Austropotamobius* brown spot virus (QCO84581.1) as top BLASTp hit, whereas the assembled glycoprotein BLASTp matched the glycoprotein of Dar es Salaam virus TZ-189 (QDF82061.1). A BLASTp of the RdRp of *cataneii* bunya-like virus returned the L protein of Blacklegged tick phlebovirus 1 (ANT80544.1) as top hit. A member of the recently described family *Chuviridae*, *cataneii* chu-like virus was detected in this study, but only the NP gene of which could be assembled partially

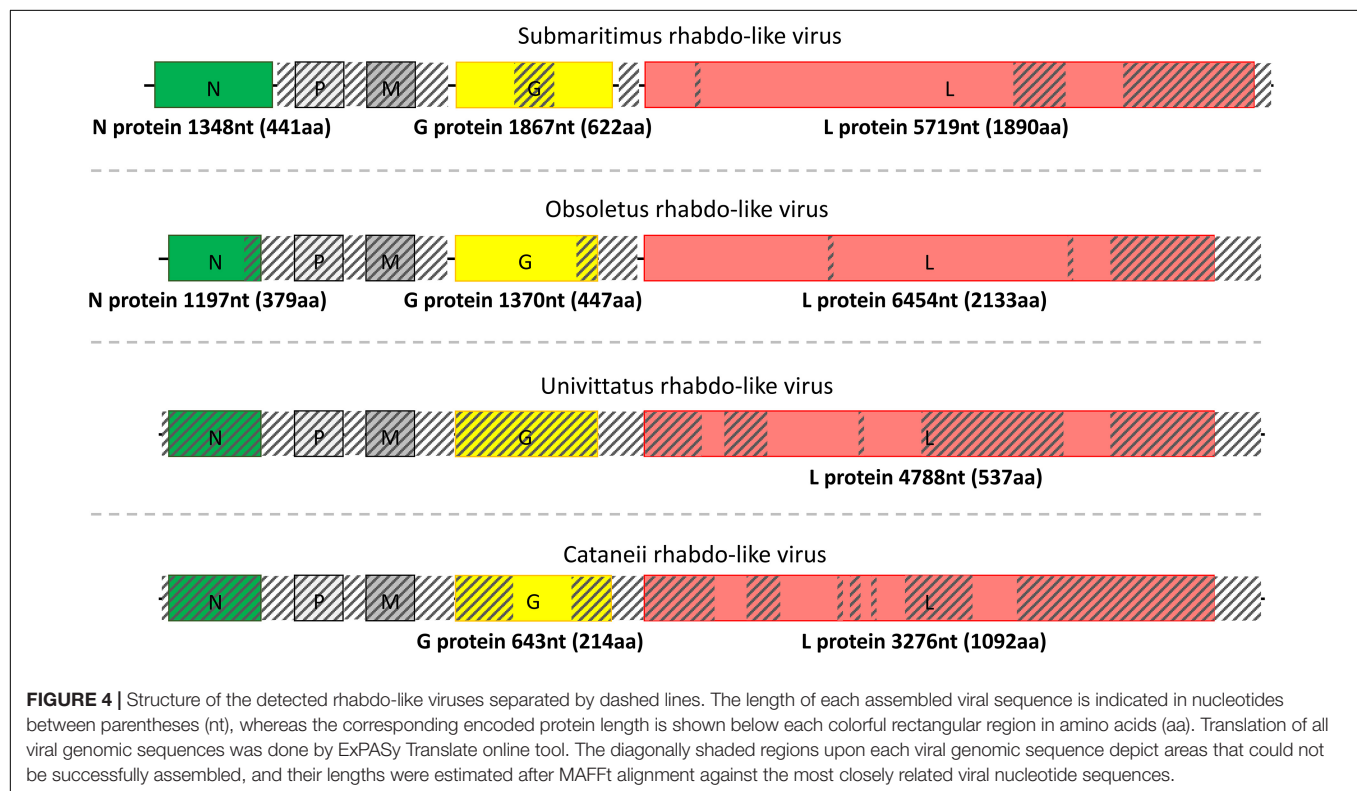
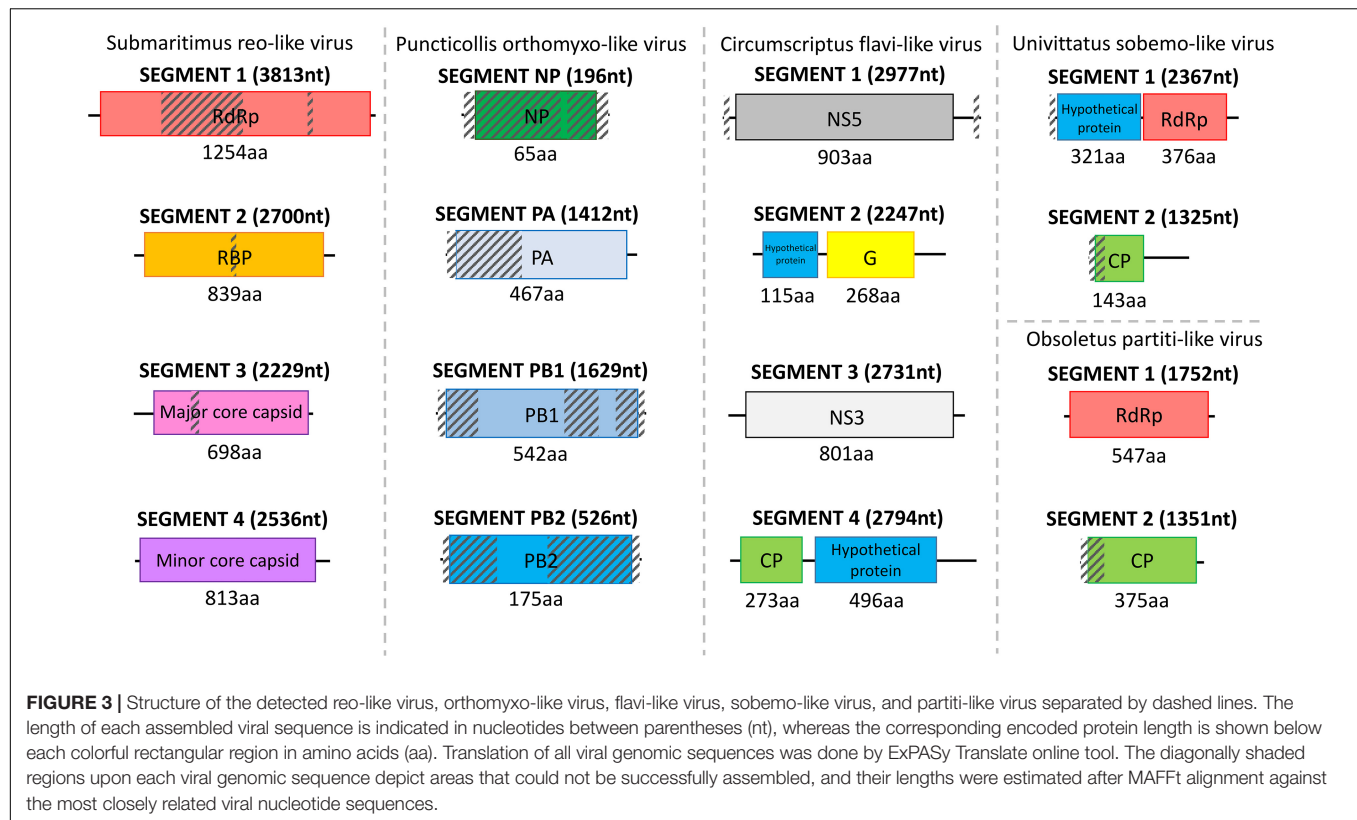


(Figure 2). The NP of *cataneii* chu-like virus BLASTp aligned against the putative NP of Atrato chu-like virus 1 (QHA33915.1). Another member of the family *Rhabdoviridae* was found within *C. cataneii*, named *cataneii* rhabdo-like virus. The glycoprotein and RdRp genes of *cataneii* rhabdo-like virus were recovered successfully and assembled partially, whereas the rest of the viral genes could not be retrieved (Figure 4). The glycoprotein of Riverside virus 1 (YP_009552819.1) BLASTp matched the *cataneii* rhabdo-like virus glycoprotein. The large protein (RdRp) of Riverside virus 1 (AMJ52373.1) was the top BLASTp hit of *cataneii* rhabdo-like virus RdRp.

Culicoides circumscriptus

Interestingly, *C. circumscriptus* carried *circumscriptus* flavi-like virus, which resembled members of the family *Flaviviridae*. Although *circumscriptus* flavi-like virus characteristics have not been described fully, six viral genes were recovered successfully and assembled completely from the field-collected samples of *C. circumscriptus* (Figure 3). Notably, both the fully assembled sequences for capsid and glycoprotein encoded an extra protein product, in one case after and in the other case before these transcribed genes. More specifically, the assembled capsid of *circumscriptus* flavi-like virus showed the highest identity to the putative capsid protein of Wuhan aphid virus 2 (QDF44112.1), whereas the protein product following capsid transcription BLASTp matched the hypothetical protein of Wuhan aphid virus 1 (BBV14760.1). Similarly, an extra protein product was found before glycoprotein transcription highly similar to the hypothetical protein of Wuhan aphid virus 1 (YP_009179380.1), whereas the main glycoprotein product itself was closer to the putative glycoprotein of Wuhan aphid virus 2 (QDF44110.1) via BLASTp searches. The remaining two assembled genes displayed high similarities with the corresponding NS3 and NS5 transcribed genes of flavi-like viruses. The NS3 of *circumscriptus* flavi-like virus retrieved NS3-like protein of soybean thrips virus 4 (QPZ88419.1) as the top BLASTp hit. Furthermore, its assembled NS5 showed the highest identity to the NS5-like protein of Wuhan aphid virus 1 (QPZ88370.1).

Culicoides haranti

C. haranti also presented interesting findings in the tested field-collected samples as they harbored haranti chuvirus, a member of the recently described family *Chuviridae*. With little prior knowledge regarding the genomic structure and other characteristics of this viral family, two genes of haranti chuvirus were recovered successfully but assembled only partially (Figure 2). The assembled NP of haranti chuvirus BLASTp matched the nucleocapsid protein of Coleopteran chu-related virus (QMP82322.1). Lastly, the RdRp of haranti chuvirus showed the highest identity to the RNA-dependent RNA polymerase of Hubei chuvirus-like virus 3 (YP_009337089.1).

Phylogenetic Analysis of Novel Viruses

An assessment of the phylogeny of the identified new viruses revealed both local and global links with viruses of other

invertebrates but also vertebrates. Univittatus sobemo-like virus belonged to a cluster of viruses identified mainly in insects such as mosquitoes (Figure 5). Within the same cluster, a related virus in *Culex theileri* had been identified before in the area of Thrace (Thassos sobemo-like virus) (Figure 5). The only vertebrate virus in the cluster was an uncharacterized *Sobemovirus* identified in the bird *Abrornis inornate* (*Solemoviridae* sp. QJI53819.1) (Figure 5). Punctatus phasma virus was clustered within the characterized genus of *Orthophasmaviruses* containing the related Carapha virus identified in *C. arakawae* in Shinjuku, Tokyo, Japan (Figure 5). Interestingly, a distinct subgroup that comprised mostly mosquito viruses within the genus contained Makri bunya-like virus identified in *Aedes albopictus* by our group in the same region (deposited in NCBI GenBank, QRD99886.1) (Figure 5). Another member of the order of *Bunyavirales*, *cataneii* bunya-like virus clustered together with other members of the *Phenuiviridae* family and very close to a cluster containing important human phleboviruses such as Chandiru virus and Maldonado virus (Figure 6). Submaritimus reo-like virus was very similar to other unclassified insect reoviruses closely related to *Phytoreovirus* genus of plant viruses within the *Sedoreovirinae* subfamily (Figure 7). Four *Culicoides* species harbored a rhabdo-like virus of the *Alpharhabdovirinae* subfamily. Submaritimus rhabdo-like virus formed a branch between *Sigmavirus* and *Merhavirus* cluster as exemplified by *Bactrocera dorsalis* sigmavirus and Merida virus, respectively (Figure 5). Univittatus rhabdo-like virus was mostly related to the *Merhavirus* cluster and interestingly related to another virus (Evros rhabdovirus 2) identified in the same region in *Anopheles algeriensis* mosquitoes (Figure 5). Obsoletus rhabdo-like virus and *cataneii* rhabdo-like virus formed their own cluster between Merhaviruses and Ohlshaviruses (Figure 5). Obsoletus partiti-like virus was clustered only with unclassified Partitiviruses, intriguingly, in a subcluster that contained previously identified Partitiviruses of mosquitoes (*Culiseta longiareolata* and *Coquillettidia richiardii*) in the same area (Figure 5). Haranti chuvirus and *cataneii* chu-like virus were both clustered closely within the novel *Chuviridae* family (Figure 6). Puncticollis orthomyxo-like virus was clustered with Sanxia water strider virus 3 and other Orthomyxoviruses belonging to the *Quaranjavirus* genus (Figure 6). Circumscriptus flavi-like virus was closely related to insect-specific viruses but phylogenetically distant from human flaviviruses such as yellow fever virus and Saint Louis encephalitis virus (Figure 6). Obsoletus Chaq virus was another virus within an unclassified family of Chaq viruses that have been proposed to be satellite viruses of other viruses (Shi et al., 2018). Didymoteicho Chaq virus detected in *C. richiardii* mosquitoes in the area of Thrace was also closely related to Obsoletus Chaq virus (Figure 7).

In terms of phylogeography, the viruses identified in this study did not cluster according to area, country, or continent. Although in some cases such as in *Solemoviridae*, *Rhabdoviridae*, *Phasmaviridae*, and *Partitiviridae* families, the novel viruses reported in this study were closely related to viruses previously identified in mosquitoes in the area of Thrace, Greece.



MATERIALS AND METHODS

Culicoides Collection and Identification

Adult *Culicoides* were field-collected using CDC light traps with Photo Cell and Air Gate (BioQuip Products, Inc., United States) (Supplementary Table 5). Collection points spanned across the areas of Eastern Macedonia and Thrace in Greece (Supplementary Figure 1) during a period of intensified *Culicoides* activity; April–October 2019. Post collection, the samples were stored and delivered on dry ice. *Culicoides* specimens were examined over a bed of crushed ice to maintain their condition at all times, both during sample sorting and during species identification. Good-quality intact individuals were stored at -80°C prior to RNA and DNA extraction. Female *Culicoides* were identified using external morphological features (Mathieu et al., 2012).

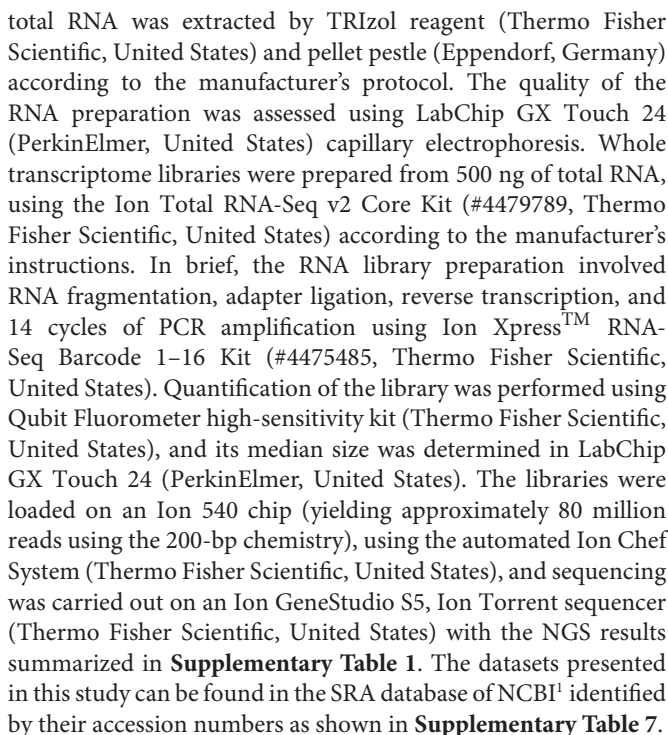
Species Identification Through Cytochrome C Oxidase Subunit 1 Barcoding

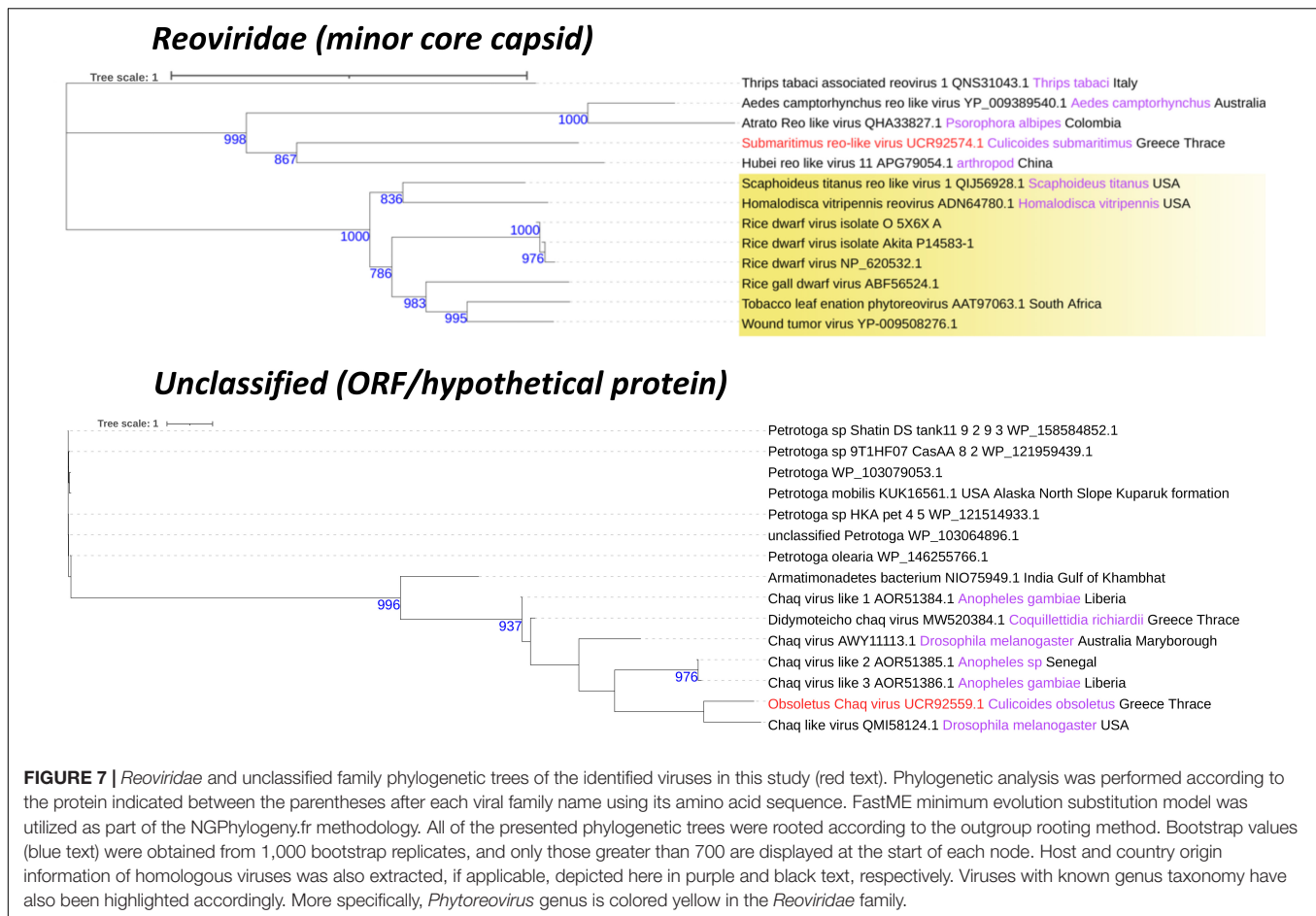
Culicoides were homogenized using pellet pestle (Eppendorf, Germany), and total RNA was extracted by TRIzol reagent (Thermo Fisher Scientific, United States) according to the manufacturer's protocol. As verification of the morphological identification, DNA barcoding was done using standard cytochrome c oxidase subunit 1 (COI) polymerase chain

reaction (PCR) and Sanger sequencing. One microgram of the RNA extract was reverse-transcribed at 42°C for 60 min, using M-MLV reverse transcriptase (Promega, United States) according to the manufacturer and COI_R primer (5'-AAAAATTTTAAATTCAGTTGGAACAGC-3'). Universal primers COI_F (5'-GGATTGTGAAATGATTGATTCCTT-3') and COI_R were used to amplify a 600-bp PCR product. The PCR reaction mixture contained $0.25 \times$ GC buffer, 1.5 mM MgCl_2 , 1 mM dNTPs mix, 0.2 μM of each primer, 1.5 U KAPA Taq DNA polymerase (Kapa Biosystems, United States), and 1 μL of cDNA. The thermal profile of the PCR included 40 cycles of denaturation at 95°C for 30 s, annealing at 50°C for 45 s, and elongation at 65°C for 1 min, and a final elongation step at 65°C for 7 min. PCR products were purified using the NucleoSpin Gel and PCR Clean-up purification kit (Macherey-Nagel, Germany). Sanger sequencing was performed on the PCR product, and the resulting sequence was analyzed using the Barcode of Life Data System V4 platform (Ratnasingham and Hebert, 2007) and tested vs. local COI sequences submitted in the NCBI Genbank database (Supplementary Table 6).

Total RNA Next-Generation Sequencing

Culicoides biting midges were separated into homogenous single-species pools of 10 well-preserved individuals each, from various collection sites within the Thrace region (two individuals from every area presented in Supplementary Figure 1), and





aiming to maximize viral genome assembly efficiency. Lastly, alignment algorithms [Burrows-Wheeler Aligner (Li and Durbin, 2009), MAFFT (Katoh et al., 2002)] and Integrated Genomics Viewer (Robinson et al., 2011) program were utilized in order to fine tune and validate the assembled viral sequences before submitting them to the NCBI GenBank database. All assembled viral sequences of this study can be accessed online by their accession numbers (MZ771201- MZ771234) (**Supplementary Table 3**).

Phylogenetic Analysis

For the phylogenetic analysis of *Culicoides* species, the COI sequences of the respective species (**Supplementary Table 5**) were input to the NGPhylogeny.fr website (Lemoine et al., 2019) running a custom workflow with successive stages of multiple-sequence alignment by MAFFT (Katoh, 2002), alignment refinement by BMGE (Criscuolo and Gribaldo, 2010), and phylogenetic reconstruction via FastME substitution model (Lefort et al., 2015), based on balanced minimum evolution for 1,000 bootstrap cycles and, finally, graphical representation of the inferred tree through Newick Display. Tree was exported to iTol (Letunic and Bork, 2019). *Culicoides* phylogeny was verified by previously constructed phylogenetic trees (Morag et al., 2012; Augot et al., 2017).

For the phylogenetic analysis of the assembled viruses, the amino acid sequence of the RNA-dependent RNA polymerase or RdRp (also characterized as segment L or L protein) was used for the construction of the phylogenetic trees. In case the RdRp segment was not assembled, nucleocapsid (segment S or N) or glycoprotein (segment M or G) amino acid sequence was used. The length of the input sequence varied, depending on the length of the assembled contigs. The respective virus amino acid sequence obtained from ExPASy Translate online tool (Gasteiger et al., 2003) according to the standard genetic code was input to BLASTp against the nr protein sequence database of NCBI, and hits with not less than 25% coverage and 30% identity were selected. Host and geographic origin data were extracted through the NCBI tool *Entrez-direct* (Kans, 2021) by using a custom in-house bash script (available in github).² All previously selected sequences were fed to the NGPhylogeny.fr website (Lemoine et al., 2019) for the elucidation of phylogenetic relationships, running a custom workflow with successive stages of multiple sequence alignment by MAFFT (Katoh, 2002); alignment refinement by BMGE (Criscuolo and Gribaldo, 2010); phylogenetic reconstruction via FastME substitution model (Lefort et al., 2015), based on balanced minimum evolution for

²https://github.com/konskons11/konskons11/blob/NCBI_HOST-COUNTRY_DATA/NCBI_VIRUS_data.sh

1,000 bootstrap cycles; and finally, graphical representation of the inferred trees through Newick Display. Trees were rooted using the outgroup rooting method and were exported to iTol (Letunic and Bork, 2019).

DISCUSSION

The recurrent outbreaks of BTV (Foxi et al., 2016; Saminathan et al., 2020; Duan et al., 2021), the discovery of SBV in Europe (Carpenter et al., 2013; Endalew et al., 2019), and the wide distribution of OROV in Southern America (McGregor et al., 2021) have highlighted the importance of understanding *Culicoides* ecology and biology. As climate change alters vector ecology and distribution, vector-borne pathogens find new paths in naive territories (Purse et al., 2008). Despite the great economic (Gethmann et al., 2020) and public health impact of the viruses vectored by *Culicoides*, knowledge relating the ecology and epidemiology of *Culicoides*-specific viruses is lagging behind that of viruses transmitted by other major arthropod vectors. Analysis of the virome in insect vectors, such as mosquitoes, has given clues on their ability to harbor a large variety of viruses (Cook et al., 2013; Huhtamo et al., 2014; Atoni et al., 2019). Such endeavors have revealed the potential of vectors to harbor viruses closely related to human pathogens such as flaviviruses (Cook et al., 2013; Huhtamo et al., 2014; Atoni et al., 2019). Either transmitted to another animal species or as being insect-specific, hundreds of novel arboviruses have been identified through RNA metagenomics (Öhlund et al., 2019a; Sanborn et al., 2019; Shi et al., 2019; Ramírez et al., 2020; de Almeida et al., 2021; Thannesberger et al., 2021). Although we know very little about these novel viruses their impact on vector competence in relation to previously known pathogenic arboviruses has been extensively studied (Öhlund et al., 2019b). It is believed that the insect core virome, a virome that shows relative stability between individuals of the same species (Shi et al., 2019), presents similarities to the human microbiome, which has been shown to affect the ability of pathogens to establish growth and induce disease. However, most of the reports have shown negative or inconclusive results on the effect of insect specific viruses on important human or animal pathogens (Kent et al., 2010; Bolling et al., 2012; Pereira et al., 2018; Talavera et al., 2018; Koh et al., 2021; Utarini et al., 2021). With mosquito vectors, coinfection with the insect-specific virus *Culex* flavivirus (Bolling et al., 2012; Talavera et al., 2018) did not alter competence in relation to Rift Valley fever phlebovirus and showed variable results with respect to vector competence for West Nile virus (Kent et al., 2010). Similarly, with mosquitoes of the genus *Aedes*, an infection with the insect specific Palm Creek virus did not affect competence of the same mosquitoes toward Zika and chikungunya virus (Koh et al., 2021). Although these observations confute the hypothesis, previous experiments on bacterial species that affect vector competence have shown considerable effect with *Wolbachia* species (Pereira et al., 2018; Utarini et al., 2021). As vector-borne diseases are soaring worldwide, there is an increased effort for the identification of vector competence altering agents for disease control. The continuous identification and

characterization process of novel viromes are essential for the isolation of competence altering viral agents but also for the understanding of emerging pathogen potential.

In our study, we aimed to identify novel viruses in field populations of a range of *Culicoides* species in the area of Thrace, northeast Greece, collected during the monitoring period April–October 2019. This region is of great zoogeographic importance as it bridges three distinct biogeographic realms, and it constitutes an area that is a major route of various animal and human pathogens from Asia to Europe [e.g., BTV (Purse et al., 2008), lumpy skin disease virus (Tasioudi et al., 2016), sheep pox virus (Mangana et al., 2008), *Plasmodium vivax* (Danis et al., 2013), and West Nile virus (Erdem et al., 2014)], the majority of which are vector-borne pathogens. An RNA-seq-based methodology for the metagenomic analysis of transcriptomes of all *Culicoides* species collected in the region of Thrace in 2019 was used to elucidate their core virome in a holistic but also species-specific approach for this period. From the morphological evaluation of the collected samples, the individuals were divided into 10 species. Aiming to identify the core virome of these species that has been shown before to be stable in other vectors such as mosquitoes (Shi et al., 2019, 2020), we processed 10 well-preserved (dry ice) specimens from each species as a homogenous pool.

Using the Ion Total RNA-Seq v2 Core Kit for total RNA sequencing and the Ion Torrent S5 sequencer, we prepared libraries of pools of 10 representative individuals for each species. After TRINITY assembly of all possible contigs, we identified sequences belonging to 14 distinct and novel viruses, members of the *Solemoviridae*, *Phasmaviridae*, *Phenuiviridae*, *Partitiviridae*, *Reoviridae*, *Chuviridae*, *Rhabdoviridae*, and *Flaviviridae*, as well as sequences of a virus similar to the unclassified Chaq virus. Interestingly, every virus was identified in only one *Culicoides* species, whereas several species of biting midges harbored multiple viruses, in line with the notion of a species-specific virome that has been described before for mosquitoes (Shi et al., 2019). However, more individuals are required for thorough identification of the virome of each species as several viruses may be less abundant or are present in low viral load. Previous reports on virus metagenomics of *Culicoides* showed a similar composition in terms of viral families, although the reports either focused on a single species (Modha et al., 2019) or the genus as a whole (Liu et al., 2020) (i.e., pools of different species).

Partial (8) and near-complete or complete (6) genomes corresponding to species of the *Solemoviridae*, *Phasmaviridae*, *Phenuiviridae*, *Partitiviridae*, *Reoviridae*, *Chuviridae*, *Rhabdoviridae*, and *Flaviviridae* virus families were identified (Figures 2–4). The phylogenetic analysis of these viruses gave insights into their relationships with other previously identified viruses in the area but also worldwide. Most of the viruses identified in the virome of *Culicoides* biting midges from Thrace clustered together with previously identified—mostly arthropod-specific, viruses identified in aphids, flies (including mosquitoes), and ticks. Although viruses from mosquitoes seem to populate most of the phylogenetic clusters, the bias resulting from the extensive virome analysis in mosquitoes should be taken into consideration. Viruses similar to puncticolis othomyxo-like

virus have been identified before only in mosquito species of the genera *Culex* (Batson et al., 2021) and *Aedes* (Shi et al., 2017; Batson et al., 2021; **Figure 6**). Obsoletus rhabdo-like virus, submaritimus rhabdo-like virus, *cataneii* rhabdo-like virus, and univittatus rhabdo-like virus formed a cluster that encompassed mainly similar viruses detected in mosquito species of the genera *Anopheles*, *Aedes* (including *Ochlerotatus* subgenus) (Reuter et al., 2016; Shahhosseini et al., 2017), and *Culex* (Coffey et al., 2014; Hang et al., 2016; Sadeghi et al., 2018; Öncü et al., 2018; Faizah et al., 2020; Batson et al., 2021; **Figure 5**). The aforementioned *Rhabdoviruses* were phylogenetically related to *Sigmavirus*, *Ohlsrhavirus*, and *Merhavirus* genera coclustering with Evros rhabdovirus 2 and Merida-like virus (Ergünay et al., 2017) identified in the Greek and Turkish part of Thrace region, respectively. Similarly, *cataneii* chu-like virus was related to viruses found previously infecting mosquito species of the genera *Culiseta* (API61889.1) and *Coquillettidia* (QHA33915.1) (**Figure 6**). Interestingly, obsoletus partiti-like virus, similar to arthropod viruses from China (Shi et al., 2016), Colombia, and Liberia, clustered together with two viruses identified previously by our group in the mosquito species *C. longiareolata* (QRD99865.1) and *C. richiardii* (QRD99905.1) in Thrace (**Figure 5**). Similarly, univittatus sobemo-like virus was related to Thassos sobemo-like virus identified in *C. theileri* in the same region, although more closely related to *V. velutina* RNA virus 2 identified in the Belgium (Garigliany et al., 2017; **Figure 5**). This co-occurrence of similar viruses in different vector groups highlights the possibility of interactions occurring among different arbovirus vector species in the area. A recent extensive analysis of *Culicoides* and mosquitoes assessed the potential virome interactions between the two taxa in China (Liu et al., 2020). Comparative analysis highlights the fact that there is a web of viruses and carriers in the ecosystem where hosts/carriers exchange viruses, which eventually evolve to adapt among host species. Occasionally some viruses may “leak” out of the web, infecting vertebrates occurring in close proximity with the vectors.

As very few studies have been conducted on *Culicoides* virome, it is not surprising that only Carapha virus identified in *C. arakawae* in Japan (Kobayashi et al., 2020) was related to a virus from this study (*punctatus* phasma virus) (**Figure 5**). To be noted, *C. arakawae* and *C. punctatus* were phylogenetically distant within the genus (Morag et al., 2012). Often, insect-specific viruses are closely related to viruses detected or isolated in plants and fungi (Vasilakis and Tesh, 2015; Franco et al., 2021). Hypotheses that attempt to explain such an observation include a central role of the insects in a “one-health” concept of vector-borne diseases of both plants and animals (Dietzgen et al., 2016) or contamination of insect samples with fungi (Cook et al., 2013; Chandler et al., 2015). Studies that include virome characterization after a cell culture on insect cells may support or confute the above hypotheses (Pyke et al., 2021). Submaritimus reo-like virus fell into the same phylogenetic clade with three other insect viruses, namely, *Aedes camptorynhus* reo-like virus, Atrato reo-like virus and Hubei reo-like virus. This cluster formed a distant phylogenetic clade to viruses of the genus *Phytoreovirus* of *Reoviridae* that infect plants such

as rice and tobacco as reported previously (Shi et al., 2017; **Figure 7**).

Members of the uncharacterized group of Chaq viruses and the recently described *Chuviridae* family were identified in three *Culicoides* species, namely, obsoletus Chaq virus, haranti chuvirus, and *cataneii* chu-like virus. Chaq viruses were proposed to be satellite viruses of other viruses, as in its initial identification, Chaq virus contigs were always present together with Galbut virus during viral metagenomics (Shi et al., 2018). In our study, we did not identify any contigs corresponding to Galbut virus or any other related viruses. *Chuviridae* is a family of arthropod viruses often found only in metagenomic studies with variable genomic structure (Dezordi et al., 2020). The close proximity of haranti chuvirus and *cataneii* chu-like virus with Wuchang cockroach virus 3 within the phylogenetic tree and their distance from Tacheng tick virus 5 and Bole tick virus 3 favored a segmented genome structure depiction (type II) as proposed by Li et al. (2015; **Figure 6**). Moreover, chuviruses have been linked to endogenous viral elements (EVEs) that include either small or larger fragments of insect-specific viruses incorporated into insect genomes (Aguiar et al., 2015; Dezordi et al., 2020). It is possible that viruses represented by a partial fragment or a single segment may actually be EVEs as even sequences of well-established viral families such as *Flaviviridae* have been shown to form EVEs (Lequime and Lambrechts, 2017). However, it should be noted that the vast majority of viruses identified in this study comprised either large contigs or multiple segments (**Figures 2–4**).

Some of the most important vector-borne viruses that infect humans and animals are members of the family *Flaviviridae*. The family is divided into distinct clusters that contain either vertebrate or invertebrate-specific viruses (de Oliveira Ribeiro et al., 2021). A flavivirus that clustered together with invertebrate-specific viruses was identified in *C. circumscriptus*. In our study, only one virus clustered together with non-arthropod viruses. A bunyavirus similar to *cataneii* bunya-like virus in the past had been identified in the fecal virome of otters in Spain (Bodewes et al., 2014; **Figure 6**). Within the same tree of *Phlebovirus* (*Phenuiviridae*, *Bunyavirales*), *cataneii* bunya-like virus was closer to a group of viruses from aphids (Zhang et al., 2019), whereas a neighboring cluster contained important human *Phlebovirus* such as Chandiru virus (Palacios et al., 2011) and Maldonado virus (Palacios et al., 2011; **Figure 6**). The possibility that these viruses are transferred to vertebrates or have the potential to underscores the importance of metagenomic approaches that link viruses with specific species in the same habitat. These data provide an important component in the development of risk assessments of the new pathogens occurring and could be used to screen co-occurring mammal and avian species that act as hosts for blood feeding vectors and the viruses they harbor.

Our work follows a new global approach in the study of *Culicoides* virome, assigning viruses to specific species occurring naturally within the same geographical area. The new viruses identified help us understand the web of virus–host/carrier interactions at the ecosystem level in Thrace. Finally, our study provides a database useful for the wider geographical

area of southeastern Europe in the analysis of vector and virus distributions and risk assessment analyses for emerging infectious diseases.

DATA AVAILABILITY STATEMENT

The datasets presented in this study can be found in online repositories. The names of the repository/repositories and accession number(s) can be found below: <https://www.ncbi.nlm.nih.gov/>, SRR15194102, SRR15194673, SRR15194737, SRR15194761, SRR15194763, SRR15194765, SRR15194766, SRR15194470, SRR15194764, and SRR15194762.

AUTHOR CONTRIBUTIONS

IK designed the study. IK and SV obtained funding for the project. AN and PP conducted fieldwork and collected samples. MC performed morphological species identification. KK, MB,

and EG performed experiments. KK and ND performed the analysis. KK, MB, and IK wrote the manuscript with input from all authors. All authors contributed to the article and approved the submitted version.

FUNDING

This research has been co-financed by the European Union and Greek national funds through the Operational Program Competitiveness, Entrepreneurship and Innovation, under the call RESEARCH—CREATE—INNOVATE (project code:T1EDK-5000).

SUPPLEMENTARY MATERIAL

The Supplementary Material for this article can be found online at: <https://www.frontiersin.org/articles/10.3389/fmicb.2022.802577/full#supplementary-material>

REFERENCES

- Aguiar, E. R. G. R., Olmo, R. P., Paro, S., Ferreira, F. V., de Faria, I. J., da, S., et al. (2015). Sequence-Independent Characterization of Viruses Based on the Pattern of Viral Small RNAs Produced by the Host. *Nucleic Acids Res.* 43, 6191–6206. doi: 10.1093/nar/gkv587
- Altschul, S. F., Gish, W., Miller, W., Myers, E. W., and Lipman, D. J. (1990). Basic Local Alignment Search Tool. *J. Mol. Biol.* 215, 403–410. doi: 10.1016/S0022-2836(05)80360-2
- Atoni, E., Zhao, L., Karungu, S., Obanda, V., Agwanda, B., Xia, H., et al. (2019). The Discovery and Global Distribution of Novel Mosquito-Associated Viruses in the Last Decade (2007–2017). *Rev. Med. Virol.* 29:e2079. doi: 10.1002/rmv.2079
- Augot, D., Mathieu, B., Hadj-Henni, L., Barriel, V., Mena, S. Z., Smolis, S., et al. (2017). Molecular Phylogeny of 42 Species of *Culicoides* (Diptera, Ceratopogonidae) from Three Continents. *Parasite* 24:23. doi: 10.1051/parasite/2017020
- Batson, J., Dudas, G., Haas-Stapleton, E., Kistler, A. L., Li, L. M., Logan, P., et al. (2021). Single Mosquito Metatranscriptomics Identifies Vectors, Emerging Pathogens and Reservoirs in One Assay. *eLife* 10:e68353. doi: 10.7554/eLife.68353
- Bodewes, R., Ruiz-Gonzalez, A., Schapendonk, C. M., van den Brand, J. M., Osterhaus, A. D., and Smits, S. L. (2014). Viral Metagenomic Analysis of Feces of Wild Small Carnivores. *Virol. J.* 11:89. doi: 10.1186/1743-422X-11-89
- Bolling, B. G., Olea-Popelka, F. J., Eisen, L., Moore, C. G., and Blair, C. D. (2012). Transmission Dynamics of an Insect-Specific Flavivirus in a Naturally Infected *Culex pipiens* Laboratory Colony and Effects of Co-Infection on Vector Competence for West Nile Virus. *Virology* 427, 90–97. doi: 10.1016/j.virol.2012.02.016
- Borkent, A. (2004). “10. The Biting Midges, the Ceratopogonidae (Diptera),” *Biology of Disease Vectors. 2nd Edition* in ed W. C. Marquardt, (Burlington: Elsevier Academic Press).
- Borkent, A., and Dominiak, P. (2020). Catalog of the Biting Midges of the World (Diptera: Ceratopogonidae). *Zootaxa* 4787, 1–377. doi: 10.11646/zootaxa.4787.1.1
- Carpenter, S., Groschup, M. H., Garros, C., Felipe-Bauer, M. L., and Purse, B. V. (2013). *Culicoides* Biting Midges, Arboviruses and Public Health in Europe. *Antiviral Res.* 100, 102–113. doi: 10.1016/j.antiviral.2013.07.020
- Chandler, J. A., Liu, R. M., and Bennett, S. N. (2015). RNA Shotgun Metagenomic Sequencing of Northern California (USA) Mosquitoes Uncovers Viruses, Bacteria, and Fungi. *Front. Microbiol.* 6:185. doi: 10.3389/fmicb.2015.00185
- Coffey, L. L., Page, B. L., Greninger, A. L., Herring, B. L., Russell, R. C., Doggett, S. L., et al. (2014). Enhanced Arbovirus Surveillance with Deep Sequencing: Identification of Novel Rhabdoviruses and Bunyaviruses in Australian Mosquitoes. *Virology* 448:10.1016/j.virol.2013.09.026. doi: 10.1016/j.virol.2013.09.026
- Cook, S., Chung, B. Y.-W., Bass, D., Moureau, G., Tang, S., McAlister, E., et al. (2013). Novel Virus Discovery and Genome Reconstruction from Field RNA Samples Reveals Highly Divergent Viruses in Dipteran Hosts. *PLoS One* 8:e80720. doi: 10.1371/journal.pone.0080720
- Corman, V. M., Muth, D., Niemeyer, D., and Drosten, C. (2018). Hosts and Sources of Endemic Human Coronaviruses. *Adv. Virus Res.* 100, 163–188. doi: 10.1016/b.s.aivir.2018.01.001
- Cracknell Daniels, B., Gaythorpe, K., Imai, N., and Dorigatti, I. (2021). Yellow Fever in Asia—a Risk Analysis. *J. Travel Med.* 28:taab015. doi: 10.1093/jtm/taab015
- Crisuolo, A., and Gribaldo, S. (2010). BMGE (Block Mapping and Gathering with Entropy): A New Software for Selection of Phylogenetic Informative Regions from Multiple Sequence Alignments. *BMC Evol. Biol.* 10:210. doi: 10.1186/1471-2148-10-210
- Danis, K., Lenglet, A., Tseroni, M., Baka, A., Tsiordas, S., and Bonovas, S. (2013). Malaria in Greece: Historical and Current Reflections on a Re-Emerging Vector Borne Disease. *Travel Med. Infect. Dis.* 11, 8–14. doi: 10.1016/j.tmaid.2013.01.001
- de Almeida, J. P., Aguiar, E. R., Armache, J. N., Olmo, R. P., and Marques, J. T. (2021). The Virome of Vector Mosquitoes. *Curr. Opin. Virol.* 49, 7–12. doi: 10.1016/j.coviro.2021.04.002
- de Oliveira Ribeiro, G., da Costa, A. C., Gill, D. E., Ribeiro, E. S. D., Rego, M. O., da, S., et al. (2021). Guapiaçu Virus, a New Insect-Specific Flavivirus Isolated from Two Species of *Aedes* Mosquitoes from Brazil. *Sci. Rep.* 11:4674. doi: 10.1038/s41598-021-83879-6
- Dezordi, F. Z., Vasconcelos, C. R., dos, S., Rezende, A. M., and Wallau, G. L. (2020). In and Outs of *Chuviridae* Endogenous Viral Elements: Origin of a Potentially New Retrovirus and Signature of Ancient and Ongoing Arms Race in Mosquito Genomes. *Front. Genet.* 11:1291. doi: 10.3389/fgene.2020.542437
- Dietzen, R. G., Mann, K. S., and Johnson, K. N. (2016). Plant Virus–Insect Vector Interactions: Current and Potential Future Research Directions. *Viruses* 8:303. doi: 10.3390/v8110303
- Duan, Y. L., Li, L., Bellis, G., Yang, Z. X., and Li, H. C. (2021). Detection of Bluetongue Virus in *Culicoides* Spp. in Southern Yunnan Province, China. *Parasit. Vectors* 14:68. doi: 10.1186/s13071-020-04518-z

- Elbers, A. R. W., Koenraadt, C. J. M., and Meiswinkel, R. (2015). Mosquitoes and *Culicoides* Biting Midges: Vector Range and the Influence of Climate Change. *Rev. Sci. Tech. Int. Off. Epizoot.* 34, 123–137. doi: 10.20506/rst.34.1.2349
- Endalew, A. D., Faburay, B., Wilson, W. C., and Richt, J. A. (2019). Schmallenberg Disease—A Newly Emerged *Culicoides*-Borne Viral Disease of Ruminants. *Viruses* 11:1605. doi: 10.3390/v11111065
- Erdem, H., Ergunay, K., Yilmaz, A., Naz, H., Akata, F., Inan, A. S., et al. (2014). Emergence and Co-Infections of West Nile Virus and Toscana Virus in Eastern Thrace, Turkey. *Clin. Microbiol. Infect.* 20, 319–325. doi: 10.1111/1469-0691.12310
- Ergünay, K., Brinkmann, A., Litzba, N., Günay, F., Kar, S., Öter, K., et al. (2017). A Novel Rhabdovirus, Related to Merida Virus, in Field-Collected Mosquitoes from Anatolia and Thrace. *Arch. Virol.* 162, 1903–1911. doi: 10.1007/s00705-017-3314-4
- Estévez-Herrera, J., Pérez-Yanes, S., Cabrera-Rodríguez, R., Márquez-Arce, D., Trujillo-González, R., Machado, J.-D., et al. (2021). Zika Virus Pathogenesis: A Battle for Immune Evasion. *Vaccines* 9:294. doi: 10.3390/vaccines9030294
- Faizah, A. N., Kobayashi, D., and Isawa, H. (2020). Deciphering the Virome of *Culex vishnui* Subgroup Mosquitoes, the Major Vectors of Japanese Encephalitis, in Japan. *Viruses* 12:264. doi: 10.3390/v12030264
- Foxi, C., Delrio, G., Falchi, G., Marche, M. G., Satta, G., and Ruii, L. (2016). Role of Different *Culicoides* Vectors (Diptera: Ceratopogonidae) in Bluetongue Virus Transmission and Overwintering in Sardinia (Italy). *Parasit. Vect.* 9:440. doi: 10.1186/s13071-016-1733-9
- Franco, F. P., Tüler, A. C., Gallan, D. Z., Gonçalves, F. G., Favaris, A. P., Peñaflor, M. F. G. V., et al. (2021). Fungal Phytopathogen Modulates Plant and Insect Responses to Promote Its Dissemination. *ISME J.* 15, 3522–3533. doi: 10.1038/s41396-021-01010-z
- Gargliany, M., Taminiau, B., El Agrebi, N., Cadar, D., Gilliaux, G., Hue, M., et al. (2017). Moku Virus in Invasive Asian Hornets, Belgium, 2016. *Emerg. Infect. Dis.* 23, 2109–2112. doi: 10.3201/eid2312.171080
- Gasteiger, E., Gattiker, A., Hoogland, C., Ivanyi, I., Appel, R. D., and Bairoch, A. (2003). ExPASy: The Proteomics Server for in-Depth Protein Knowledge and Analysis. *Nucleic Acids Res.* 31, 3784–3788. doi: 10.1093/nar/gkg563
- Gethmann, J., Probst, C., and Conraths, F. J. (2020). Economic Impact of a Bluetongue Serotype 8 Epidemic in Germany. *Front. Vet. Sci.* 7:65. doi: 10.3389/fvets.2020.00065
- Grabherr, M. G., Haas, B. J., Yassour, M., Levin, J. Z., Thompson, D. A., Amit, I., et al. (2011). Trinity: Reconstructing a Full-Length Transcriptome without a Genome from RNA-Seq Data. *Nat. Biotechnol.* 29, 644–652. doi: 10.1038/nbt.1883
- Gregor, K. M., Michaely, L. M., Gutjahr, B., Rissmann, M., Keller, M., Dornbusch, S., et al. (2021). Rift Valley Fever Virus Detection in Susceptible Hosts with Special Emphasis in Insects. *Sci. Rep.* 11:9822. doi: 10.1038/s41598-021-89226-z
- Hang, J., Klein, T. A., Kim, H.-C., Yang, Y., Jima, D. D., Richardson, J. H., et al. (2016). Genome Sequences of Five Arboviruses in Field-Captured Mosquitoes in a Unique Rural Environment of South Korea. *Genome Announc.* 4, e1644–e1615. doi: 10.1128/genomeA.01644-15
- Huang, X., and Madan, A. (1999). CAP3: A DNA Sequence Assembly Program. *Genome Res.* 9, 868–877. doi: 10.1101/gr.9.9.868
- Huhtamo, E., Cook, S., Moureau, G., Uzcátegui, N. Y., Sironen, T., Kuivanen, S., et al. (2014). Novel Flaviviruses from Mosquitoes: Mosquito-Specific Evolutionary Lineages within the Phylogenetic Group of Mosquito-Borne Flaviviruses. *Virology* 46, 320–329. doi: 10.1016/j.virol.2014.07.015
- Kans, J. (2021). *Entrez Direct: E-Utilities on the Unix Command Line*. Maryland, US: National Center for Biotechnology Information.
- Katoh, K., Misawa, K., Kuma, K., and Miyata, T. (2002). MAFFT: a novel method for rapid multiple sequence alignment based on fast Fourier transform. *Nucleic Acids Res.* 30, 3059–3066. doi: 10.1093/nar/gkf436
- Katoh, K. M. A. F. F. T. (2002). A Novel Method for Rapid Multiple Sequence Alignment Based on Fast Fourier Transform. *Nucleic Acids Res.* 30, 3059–3066.
- Kent, R. J., Crabtree, M. B., and Miller, B. R. (2010). Transmission of West Nile Virus by *Culex Quinquefasciatus* Say Infected with *Culex Flavivirus* Izabal. *PLoS Negl. Trop. Dis.* 4:e671. doi: 10.1371/journal.pntd.0000671
- Klement, E., Broglia, A., Antoniou, S.-E., Tsiamadis, V., Plevraki, E., Petrović, T., et al. (2020). Neethling Vaccine Proved Highly Effective in Controlling Lumpy Skin Disease Epidemics in the Balkans. *Prev. Vet. Med.* 181:104595. doi: 10.1016/j.prevetmed.2018.12.001
- Kobayashi, D., Murota, K., Faizah, A. N., Amoa-Bosompem, M., Higa, Y., Hayashi, T., et al. (2020). Virome Analysis of Hematophagous Chironomidae Flies (Diptera: Ceratopogonidae and Simuliidae) Collected in Tokyo Japan. *衛生動物* 71, 225–243. doi: 10.7601/mez.71.225
- Koh, C., Henrion-Lacritick, A., Frangeul, L., and Saleh, M.-C. (2021). Interactions of the Insect-Specific Palm Creek Virus with Zika and Chikungunya Viruses in *Aedes Mosquitoes*. *Microorganisms* 9:1652. doi: 10.3390/microorganisms9081652
- Lecollinet, S., Pronost, S., Couplier, M., Beck, C., Gonzalez, G., Leblond, A., et al. (2020). Viral Equine Encephalitis, a Growing Threat to the Horse Population in Europe? *Viruses* 12:23. doi: 10.3390/v12010023
- Lefort, V., Desper, R., and Gascuel, O. (2015). FastME 2.0: A Comprehensive, Accurate, and Fast Distance-Based Phylogeny Inference Program. *Mol. Biol. Evol.* 32:2798. doi: 10.1093/molbev/msv150
- Lemoine, F., Correia, D., Lefort, V., Doppelt-Azeroual, O., Mareuil, F., Cohen-Boulakia, S., et al. (2019). NGPhylogeny.Fr: New Generation Phylogenetic Services for Non-Specialists. *Nucleic Acids Res.* 47, W260–W265. doi: 10.1093/nar/gkz303
- Lequime, S., and Lambrechts, L. (2017). Discovery of Flavivirus-Derived Endogenous Viral Elements in *Anopheles Mosquito* Genomes Supports the Existence of *Anopheles*-Associated Insect-Specific Flaviviruses. *Virus Evol.* 3:vev035. doi: 10.1093/ve/vev035
- Leta, S., Fetene, E., Mulatu, T., Amenu, K., Jaleta, M. B., Beyene, T. J., et al. (2019). Updating the Global Occurrence of *Culicoides Imicola*, a Vector for Emerging Viral Diseases. *Sci. Data* 6:185. doi: 10.1038/s41597-019-0197-0
- Letunic, I., and Bork, P. (2019). Interactive Tree Of Life (ITOL) v4: Recent Updates and New Developments. *Nucleic Acids Res.* 47, W256–W259. doi: 10.1093/nar/gkz239
- Li, C.-X., Shi, M., Tian, J.-H., Lin, X.-D., Kang, Y.-J., Chen, L.-J., et al. (2015). Unprecedented Genomic Diversity of RNA Viruses in Arthropods Reveals the Ancestry of Negative-Sense RNA Viruses. *eLife* 4:e05378. doi: 10.7554/eLife.05378
- Li, H., and Durbin, R. (2009). Fast and accurate short read alignment with Burrows–Wheeler transform. *Bioinformatics* 25, 1754–1760. doi: 10.1093/bioinformatics/btp324
- Liu, L., Shen, Q., Li, N., He, Y., Han, N., Wang, X., et al. (2020). Comparative Viromes of *Culicoides* and Mosquitoes Reveal Their Consistency and Diversity in Viral Profiles. *Brief. Bioinform.* 22:bbaa323. doi: 10.1093/bib/bbaa323
- Mangana, O., Kottaridi, C., and Nomikou, K. (2008). The Epidemiology of Sheep Pox in Greece from 1987 to 2007. *Rev. Sci. Tech. Int. Off. Epizoot.* 27, 899–905. doi: 10.20506/rst.27.3.1845
- Mathieu, B., Cêtre-Sossah, C., Garros, C., Chavernac, D., Balenghien, T., Carpenter, S., et al. (2012). Development and Validation of IIKC: An Interactive Identification Key for *Culicoides* (Diptera: Ceratopogonidae) Females from the Western Palaearctic Region. *Parasit. Vectors* 5:137. doi: 10.1186/1756-3305-5-137
- Mayer, S. V., Tesh, R. B., and Vasilakis, N. (2017). The Emergence of Arthropod-Borne Viral Diseases: A Global Prospective on Dengue, Chikungunya and Zika Fevers. *Acta Trop.* 166, 155–163. doi: 10.1016/j.actatropica.2016.11.020
- McGregor, B. L., Connelly, C. R., and Kenney, J. L. (2021). Infection, Dissemination, and Transmission Potential of North American *Culex Quinquefasciatus*, *Culex Tarsalis*, and *Culicoides Sonorensis* for Oropouche Virus. *Viruses* 13:226. doi: 10.3390/v13020226
- Menachery, V. D., Yount, B. L., Debink, K., Agnihothram, S., Gralinski, L. E., and Plante, J. A. (2015). A SARS-like Cluster of Circulating Bat Coronaviruses Shows Potential for Human Emergence. *Nat. Med.* 21, 1508–1513. doi: 10.1038/nm.3985
- Miles, L. S., Breitbart, S. T., Wagner, H. H., and Johnson, M. T. J. (2019). Urbanization Shapes the Ecology and Evolution of Plant-Arthropod Herbivore Interactions. *Front. Ecol. Evol.* 7:310. doi: 10.3389/fevo.2019.00310
- Modha, S., Hughes, J., Bianco, G., Ferguson, H. M., Helm, B., Tong, L., et al. (2019). Metaviromics Reveals Unknown Viral Diversity in the Biting Midge *Culicoides Impunctatus*. *Viruses* 11:865. doi: 10.3390/v11090865
- Morag, N., Saroya, Y., Braverman, Y., Klement, E., and Gottlieb, Y. (2012). Molecular Identification, Phylogenetic Status, and Geographic Distribution of

- Culicoides Oxystoma* (Diptera: Ceratopogonidae) in Israel. *PLoS One* 7:e33610. doi: 10.1371/journal.pone.0033610
- Morens, D. M., Breman, J. G., Calisher, C. H., Doherty, P. C., Hahn, B. H., Keusch, G. T., et al. (2020). The Origin of COVID-19 and Why It Matters. *Am. J. Trop. Med. Hyg.* 103, 955–959. doi: 10.4269/ajtmh.20-0849
- Öhlund, P., Hayer, J., Lundén, H., Hesson, J. C., and Blomström, A.-L. (2019a). Viromics Reveal a Number of Novel RNA Viruses in Swedish Mosquitoes. *Viruses* 11:E1027. doi: 10.3390/v11111027
- Öhlund, P., Lundén, H., and Blomström, A.-L. (2019b). Insect-Specific Virus Evolution and Potential Effects on Vector Competence. *Virus Genes* 55, 127–137. doi: 10.1007/s11262-018-01629-9
- Öncü, C., Brinkmann, A., Günay, F., Kar, S., Öter, K., Sarıkaya, Y., et al. (2018). West Nile virus, *Anopheles flavivirus*, a novel flavivirus as well as Merida-like rhabdovirus Turkey in field-collected mosquitoes from Thrace and Anatolia. *Infect Genet Evol.* 57, 36–45. doi: 10.1016/j.meegid.2017.11.003
- Palacios, G., Tesh, R., Travassos da Rosa, A., Savji, N., Sze, W., Jain, K., et al. (2011). Characterization of the Candiru Antigenic Complex (Bunyaviridae: Phlebovirus), a Highly Diverse and Reassorting Group of Viruses Affecting Humans in Tropical America. *J. Virol.* 85, 3811–3820. doi: 10.1128/JVI.02275-10
- Pereira, T. N., Rocha, M. N., Sucupira, P. H. F., Carvalho, F. D., and Moreira, L. A. (2018). Wolbachia Significantly Impacts the Vector Competence of *Aedes Aegypti* for Mayaro Virus. *Sci. Rep.* 8:6889. doi: 10.1038/s41598-018-25236-8
- Petersen, L. R. (2019). Epidemiology of West Nile Virus in the United States: Implications for Arbovirology and Public Health. *J. Med. Entomol.* 56, 1456–1462. doi: 10.1093/jme/tjz085
- Purse, B., Brown, H., Harrup, L., Mertens, P., and Rogers, D. (2008). Invasion of Bluetongue and Other Orbivirus Infections into Europe: The Role of Biological and Climatic Processes. *Rev. Sci. Tech. Int. Off. Epizoot.* 27, 427–442. doi: 10.20506/rst.27.2.1801
- Pyke, A. T., Shivas, M. A., Darbro, J. M., Onn, M. B., Johnson, P. H., Crunkhorn, A., et al. (2021). Uncovering the Genetic Diversity within the *Aedes Notoscriptus* Virome and Isolation of New Viruses from This Highly Urbanised and Invasive Mosquito. *Virus Evol.* 7:veab082. doi: 10.1093/ve/veab082
- Ramírez, A. L., Colmant, A. M. G., Warrilow, D., Huang, B., Pyke, A. T., McMahon, J. L., et al. (2020). Metagenomic Analysis of the Virome of Mosquito Excreta. *mSphere* 5, e587–e520. doi: 10.1128/mSphere.00587-20
- Rasmussen, L. D., Kristensen, B., Kirkeby, C., Rasmussen, T. B., Belsham, G. J., Bødker, R., et al. (2012). Culicoids as Vectors of Schmallenberg Virus. *Emerg. Infect. Dis.* 18, 1204–1206. doi: 10.3201/eid1807.120385
- Ratnasingham, S., and Hebert, P. B. O. L. D. (2007). The Barcode of Life Data System (Www.Barcodinglife.org). *Mol. Ecol. Notes* 7, 355–364. doi: 10.1111/j.1471-8286.2007.01678.x
- Reuter, G., Boros, Á., Pál, J., Kapusinszky, B., Delwart, E., and Pankovics, P. (2016). Detection and genome analysis of a novel (dima)rhabdovirus (Riverside virus) from *Ochlerotatus* sp. mosquitoes in Central Europe. *Infect Genet Evol.* 39, 336–341. doi: 10.1016/j.meegid.2016.02.016
- Robinson, J. T., Thorvaldsdóttir, H., Winckler, W., Guttman, M., Lander, E. S., Getz, G., et al. (2011). Integrative Genomics Viewer. *Nat. Biotechnol.* 29, 24–26. doi: 10.1038/nbt.1754
- Sadeghi, M., Altan, E., Deng, X., Barker, C. M., Fang, Y., Coffey, L. L., et al. (2018). Virome of ampgt; 12 thousand *Culex* mosquitoes from throughout California. *Virology* 523, 74–88. doi: 10.1016/j.virol.2018.07.029
- Sakkas, H., Bozidis, P., Franks, A., and Papadopoulou, C. (2018). Oropouche Fever: A Review. *Viruses* 10:175. doi: 10.3390/v10040175
- Saminathan, M., Singh, K. P., Khorajiya, J. H., Dinesh, M., Vineetha, S., Maity, M., et al. (2020). An Updated Review on Bluetongue Virus: Epidemiology, Pathobiology, and Advances in Diagnosis and Control with Special Reference to India. *Vet. Q.* 40, 258–321. doi: 10.1080/01652176.2020.1831708
- Sanborn, M. A., Klein, T. A., Kim, H.-C., Fung, C. K., Figueroa, K. L., Yang, Y., et al. (2019). Metagenomic Analysis Reveals Three Novel and Prevalent Mosquito Viruses from a Single Pool of *Aedes Vexans* Nipponii Collected in the Republic of Korea. *Viruses* 11:E222. doi: 10.3390/v11030222
- Scholtz, C. H. (2018). Manual of Afrotropical Diptera, Vol. 1. Introductory Chapters and Keys to Diptera Families / Manual of Afrotropical Diptera, Vol. 2. Nematocorous Diptera and Lower Brachycera. *Trans. R. Soc. South Afr.* 73, 209–210. doi: 10.1080/0035919X.2018.1449770
- Shahhosseini, N., Lühken, R., Jöst, H., Jansen, S., Börstler, J., Rieger, T., et al. (2017). Detection and characterization of a novel rhabdovirus in *Aedes cantans* mosquitoes and evidence for a mosquito-associated new genus in the family Rhabdoviridae. *Infect Genet Evol.* 55, 260–268. doi: 10.1016/j.meegid.2017.09.026
- Shi, C., Beller, L., Deboutte, W., Yinda, K. C., Delang, L., Vega-Rúa, A., et al. (2019). Stable Distinct Core Eukaryotic Viromes in Different Mosquito Species from Guadeloupe, Using Single Mosquito Viral Metagenomics. *Microbiome* 7:121. doi: 10.1186/s40168-019-0734-2
- Shi, C., Zhao, L., Atoni, E., Zeng, W., Hu, X., Matthijnsens, J., et al. (2020). Stability of the Virome in Lab- and Field-Collected *Aedes Albopictus* Mosquitoes across Different Developmental Stages and Possible Core Viruses in the Publicly Available Virome Data of *Aedes* Mosquitoes. *mSystems* 5, e640–e620. doi: 10.1128/mSystems.00640-20
- Shi, M., Lin, X.-D., Tian, J.-H., Chen, L.-J., Chen, X., Li, C.-X., et al. (2016). Redefining the Invertebrate RNA Virosphere. *Nature* 540, 539–543. doi: 10.1038/nature20167
- Shi, M., Neville, P., Nicholson, J., Eden, J.-S., Imrie, A., and Holmes, E. C. (2017). High-Resolution Metatranscriptomics Reveals the Ecological Dynamics of Mosquito-Associated RNA Viruses in Western Australia. *J. Virol.* 91, e680–e617. doi: 10.1128/JVI.00680-17
- Shi, M., White, V. L., Schlub, T., Eden, J.-S., Hoffmann, A. A., and Holmes, E. C. (2018). No Detectable Effect of Wolbachia WMe1 on the Prevalence and Abundance of the RNA Virome of *Drosophila Melanogaster*. *Proc. R. Soc. B Biol. Sci.* 285:20181165. doi: 10.1098/rspb.2018.1165
- Sick, F., Beer, M., Kampen, H., and Wernike, K. (2019). *Culicoides* Biting Midges—Underestimated Vectors for Arboviruses of Public Health and Veterinary Importance. *Viruses* 11:376. doi: 10.3390/v11040376
- Talavera, S., Birnberg, L., Nuñez, A. I., Muñoz-Muñoz, F., Vázquez, A., and Busquets, N. (2018). *Culex* Flavivirus Infection in a *Culex Pipiens* Mosquito Colony and Its Effects on Vector Competence for Rift Valley Fever Phlebovirus. *Parasit. Vect.* 11:310. doi: 10.1186/s13071-018-2887-4
- Tasioudi, K. E., Antoniou, S. E., Iliadou, P., Sachpatzidis, A., Plevraki, E., Agianniotaki, E. I., et al. (2016). Emergence of Lumpy Skin Disease in Greece, 2015. *Transbound. Emerg. Dis.* 63, 260–265. doi: 10.1111/tbed.12497
- Tay, W. T., Kerr, P. J., and Jermini, L. S. (2016). Population Genetic Structure and Potential Incursion Pathways of the Bluetongue Virus Vector *Culicoides Brevitarsis* (Diptera: Ceratopogonidae) in Australia. *PLoS One* 11:e0146699. doi: 10.1371/journal.pone.0146699
- Temmam, S., Monteil-Bouchard, S., Robert, C., Baudoin, J.-P., Sambou, M., Aubadie-Ladrix, M., et al. (2016). Characterization of Viral Communities of Biting Midges and Identification of Novel Thogotovirus Species and Rhabdovirus Genus. *Viruses* 8:77. doi: 10.3390/v8030077
- Temmam, S., Monteil-Bouchard, S., Sambou, M., Aubadie-Ladrix, M., Azza, S., and Decloquement, P. (2015). Faustovirus-Like Asfarvirus in Hematophagous Biting Midges and Their Vertebrate Hosts. *Front. Microbiol.* 6:1406. doi: 10.3389/fmicb.2015.01406
- Thannesberger, J., Rascovan, N., Eisenmann, A., Klymiuk, I., Zitzra, C., Fuehrer, H. P., et al. (2021). Viral Metagenomics Reveals the Presence of Novel Zika Virus Variants in *Aedes* Mosquitoes from Barbados. *Parasit. Vect.* 14:343. doi: 10.1186/s13071-021-04840-0
- Utarini, A., Indriani, C., Ahmad, R. A., Tantowijoyo, W., Arguni, E., Ansari, M. R., et al. (2021). Efficacy of Wolbachia-Infected Mosquito Deployments for the Control of Dengue. *N. Engl. J. Med.* 384, 2177–2186. doi: 10.1056/NEJMoa2030243
- van Gennip, R. G. P., Drolet, B. S., Roza Lopez, P., Roost, A. J. C., Boonstra, J., and van Rijn, P. A. (2019). Vector Competence Is Strongly Affected by a Small Deletion or Point Mutations in Bluetongue Virus. *Parasit. Vect.* 12:470. doi: 10.1186/s13071-019-3722-2
- Vasilakis, N., and Tesh, R. B. (2015). Insect-Specific Viruses and Their Potential Impact on Arbovirus Transmission. *Curr. Opin. Virol.* 15, 69–74. doi: 10.1016/j.coviro.2015.08.007
- Whitehorn, J., and Yacoub, S. (2019). Global Warming and Arboviral Infections. *Clin. Med.* 19, 149–152. doi: 10.7861/clinmedicine.19-2-149
- Zhang, W., Wu, T., Guo, M., Chang, T., Yang, L., Tan, Y., et al. (2019). Characterization of a New Bunyavirus and Its Derived Small RNAs in the Brown

Citrus Aphid, *Aphis Citricidus*. *Virus Genes* 55, 557–561. doi: 10.1007/s11262-019-01667-x

Žiegytė, R., Platonova, E., Kinderis, E., Mukhin, A., Palinauskas, V., and Bernotienė, R. (2021). *Culicoides* Biting Midges Involved in Transmission of Haemoproteids. *Parasit. Vect.* 14:27. doi: 10.1186/s13071-020-04516-1

Conflict of Interest: PP was employed by the company Evrofarma S.A. AN was employed by the company Geotechno Ygeionomiki O.E.

The remaining authors declare that the research was conducted in the absence of any commercial or financial relationships that could be construed as a potential conflict of interest.

Publisher's Note: All claims expressed in this article are solely those of the authors and do not necessarily represent those of their affiliated organizations, or those of the publisher, the editors and the reviewers. Any product that may be evaluated in this article, or claim that may be made by its manufacturer, is not guaranteed or endorsed by the publisher.

Copyright © 2022 Konstantinidis, Bampali, de Courcy Williams, Dovrolis, Gatzidou, Papazilakis, Nearchou, Veletza and Karakasiliotis. This is an open-access article distributed under the terms of the Creative Commons Attribution License (CC BY). The use, distribution or reproduction in other forums is permitted, provided the original author(s) and the copyright owner(s) are credited and that the original publication in this journal is cited, in accordance with accepted academic practice. No use, distribution or reproduction is permitted which does not comply with these terms.



SUMOylation Is Essential for Dengue Virus Replication and Transmission in the Mosquito *Aedes aegypti*

Shih-Che Weng and Shin-Hong Shiao*

Department of Tropical Medicine and Parasitology, College of Medicine, National Taiwan University, Taipei, Taiwan

OPEN ACCESS

Edited by:

Shu Shen,
Wuhan Institute of Virology (CAS),
China

Reviewed by:

Youichi Suzuki,
Osaka Medical and Pharmaceutical
University, Japan
Vinod R. M. T. Balasubramaniam,
Monash University Malaysia, Malaysia
Julien Pompon,
Institut de Recherche Pour le
Développement (IRD), France

*Correspondence:

Shin-Hong Shiao
shshiao@ntu.edu.tw

Specialty section:

This article was submitted to
Virology,
a section of the journal
Frontiers in Microbiology

Received: 25 October 2021

Accepted: 04 April 2022

Published: 27 April 2022

Citation:

Weng S-C and Shiao S-H (2022)
SUMOylation Is Essential for Dengue
Virus Replication and Transmission
in the Mosquito *Aedes aegypti*.
Front. Microbiol. 13:801284.
doi: 10.3389/fmicb.2022.801284

Small ubiquitin-like modifier (SUMO) is a reversible post-translational protein modifier. Protein SUMOylation regulates a wide variety of cellular processes and is important for controlling virus replication. Earlier studies suggest that dengue virus envelope protein interacts with Ubc9, the sole E2-conjugating enzyme required for protein SUMOylation in mammalian cells. However, little is known about the effect of protein SUMOylation on dengue virus replication in the major dengue vector, *Aedes aegypti*. Thus, in this study, we investigated the impact of protein SUMOylation on dengue virus replication in *A. aegypti*. The transcription of *A. aegypti* Ubc9 was significantly increased in the midgut after a normal blood meal. Silencing AaUbc9 resulted in significant inhibition of dengue virus NS1 protein production, viral genome transcription, and reduced viral titer in the mosquito saliva. In addition, we showed that dengue virus E proteins and prM proteins were SUMOylated post-infection. The amino acid residues K51 and K241 of dengue virus E protein were essential for protein SUMOylation. Taken together, our results reveal that protein SUMOylation contributes to dengue virus replication and transmission in the mosquito *A. aegypti*. This study introduces the possibility that protein SUMOylation is beneficial for virus replication and facilitates virus transmission from the mosquito.

Keywords: *Aedes aegypti* (mosquito), dengue virus (DENV), envelop protein, SUMOylation, Ubc9

INTRODUCTION

Dengue virus infection causes several disease manifestations, ranging from dengue fever (DF) to life-threatening dengue hemorrhagic fever/dengue shock syndrome (DHF/DSS) (Wellekens et al., 2020; Roy and Bhattacharjee, 2021; Sharp et al., 2021). DF is one of the most significant arthropod-borne viral diseases, and is caused by four serotypes of DENV (Wilder-Smith et al., 2019; Roy and Bhattacharjee, 2021; Sharp et al., 2021). DENV is a positive-sense single-stranded RNA virus that belongs to the *Flaviviridae* family and is transmitted to humans primarily through the bites of infected mosquitoes of *Aedes* spp. (Wilder-Smith et al., 2019; Roy and Bhattacharjee, 2021; Sharp et al., 2021). Current studies indicate that more than 390 million DENV infections are reported worldwide annually (Bhatt et al., 2013; Shepard et al., 2016; Stanaway et al., 2016; Cattarino et al., 2020).

Transmission of DENV occurs via female *Aedes* mosquitoes, primarily *Aedes aegypti*, and, to a lesser extent, *Aedes albopictus*. Generally, the mosquitoes acquire the virus while taking a blood meal from an infected person (Wellekens et al., 2020; Roy and Bhattacharjee, 2021; Sharp et al., 2021). Within the mosquito, DENV initially infects and replicates in the mosquito midgut epithelial

cells. Five to seven days post-infection (dpi), DENV disseminates to other tissues of the mosquito via the hemolymph. Upon arriving at the mosquito's salivary gland, the virus undergoes further replication and becomes primed for transmission to another host (Salazar et al., 2007; Mukherjee et al., 2019).

Protein posttranslational modifications (PTMs) play essential roles in many cellular processes (Khoury et al., 2011; Silva et al., 2013; Loboda et al., 2019). Target proteins can be modified by adding small molecules (phosphorylation, glycosylation, acetylation, and methylation) and small proteins (ubiquitination, SUMOylation, and neddylation) (Khoury et al., 2011; Silva et al., 2013; Loboda et al., 2019). SUMOylation, as a PTM, is essential for various biological functions including cell growth, cell migration, cellular response to stress, and tumorigenesis (Yang et al., 2017; Loboda et al., 2019; Chang and Yeh, 2020). SUMO modification is well conserved between various species, including *Homo sapiens*, *Drosophila melanogaster*, and *Saccharomyces cerevisiae* (Epps and Tanda, 1998; Fraser et al., 2000; Apionishev et al., 2001; Hayashi et al., 2002; Li et al., 2021). Covalent linkages between lysine residues of target proteins and SUMO proteins are regulated by the hierarchical action of E1 SUMO activating enzyme complex SAE1/2, the E2 conjugating enzyme Ubc9, and E3 SUMO ligases, while deconjugation is performed by SUMO-specific proteases (Johnson, 2004; Loboda et al., 2019; Chang and Yeh, 2020; Li et al., 2021).

Changes in protein SUMOylation may occur following heat shock, DNA damage, proteasome inhibition, and other cellular stimuli, such as viral infection (Wimmer and Schreiner, 2015; Yang et al., 2017; Chang and Yeh, 2020; Li et al., 2021). During infection and replication, viruses manipulate the SUMOylation process to ensure viral persistence within the host (Varadaraj et al., 2014; Wimmer and Schreiner, 2015; Loboda et al., 2019; El Motiam et al., 2020). Multiple depletion studies have implicated components of the SUMOylation pathway in viral survival, pathogenesis, and host immunity (Chiu et al., 2007; Brown et al., 2016; Conn et al., 2016; Su et al., 2016; Guo et al., 2017; Feng et al., 2018; Zhu et al., 2019; Stokes et al., 2020).

Previous studies have shown that most eukaryotic organisms express both SUMO1 and a SUMO2/3 paralog. Insects, however, do not possess a SUMO1 paralog, and the SUMO2/3 paralogs lack the SUMO consensus motif (SCM) (Choy et al., 2013; Urena et al., 2016). This suggests that insect SUMO mechanisms lack the ability to efficiently form poly-SUMO chains without the presence of an E3 ligase, indicating an extra degree of regulation in insects. Additionally, studies have shown that *D. melanogaster* SUMO (DmSUMO) is not able to form poly-SUMO chains due to the lack of a SCM (Urena et al., 2016). A study of *A. aegypti* SUMO (AaSUMO) pathways showed poly-SUMO chains form more efficiently in the presence of an *A. aegypti* Protein Inhibitor of Activated STAT (AaPIAS). Depletion of AaSUMO, AaUbc9, or AaPIAS in *A. aegypti* cell lines resulted in a small but consistent significant increase in Zika virus (ZIKV) replication (Stokes et al., 2020). However, the *in vivo* roles of protein SUMOylation in regulating viral replication in the mosquito *A. aegypti* are yet to be elucidated.

Here, we demonstrate that protein SUMOylation is essential for dengue virus replication and transmission in the mosquito

A. aegypti. Silencing of AaUbc9 resulted in significant inhibition of dengue virus replication in the mosquito. Moreover, we showed that dengue virus envelop (E) protein and pre-membrane (prM) protein were SUMOylated. Finally, our results revealed that amino acid residues K51 and K241 of dengue virus E protein are required for protein SUMOylation. Our findings reveal how viruses manipulate the SUMOylation process, as well as provide new targets for potential antiviral therapies.

MATERIALS AND METHODS

Mosquitoes

Mosquitoes (*Ae. aegypti* UGAL/Rockefeller strain) were kept at 28°C and 70% relative humidity under a 12 h: 12 h light-dark cycle as previously described (Sri-In et al., 2019). Hatched larvae were transferred to plastic containers with sufficient water and fed yeast extract daily. Pupae were collected and transferred to a plastic container in an insect dorm. Emerged mosquitoes were fed using cotton balls soaked in 10% sucrose solution. Female mosquitoes were used for our experiments at 3–5 days post-eclosion (PE). The sucrose-soaked cotton balls were removed at least 12 h before blood-feeding. Female mosquitoes were permitted to blood-feed on an anesthetized Institute of Cancer research, ICR strain mouse for 15–30 min. ICR strain mice were anesthetized via an intraperitoneal injection of avertin at a dose of 0.2 ml/10 g. All animal procedures and experimental protocols were approved by an AAALAC-accredited facility and the Committee on the Ethics of Animal Experiments of the National Taiwan University College of Medicine (IACUC approval No: 20200210).

Cell Culture and Virus

Aedes albopictus C6/36 and *Ae. aegypti* CCL-125 cell lines were cultured in Dulbecco's Modified Eagle's Medium (DMEM) and Mitsuhashi and Maramorosch Insect Medium (MM) in a 1:1 ratio containing 2% heat-inactivated fetal bovine serum and 1% penicillin-streptomycin solution. For virus production, C6/36 cells were infected with the DENV serotype 2 (DENV2) strain 16681 at a multiplicity of infection of 0.01. The culture supernatant was harvested on day 7 post-infection and stored at –80°C. To determine the viral titer, the virus stock was subjected to examination using a plaque assay, as previously described (Sri-In et al., 2019). Approximately 1.0×10^7 PFUs/mL DENV2 were used to infect the mosquitoes. For Ubc9 inhibitor (2-D08) assay, *Aedes aegypti* CCL-125 cells infected with DENV2 16681 strain at MOI of 1 for 2 h. Cells were incubated with 2-D08 before, simultaneously, or after DENV2 infection for 2 h. Intracellular DENV NS1 protein was measured by cell-based enzyme-linked immunoassay (ELISA).

Oral Infection of Mosquitoes and Mosquito Saliva Collection

Infection of mosquitoes was achieved through an infectious blood meal via folded Parafilm-M. After starvation through sugar deprivation for 24 h, female mosquitoes were subsequently

provided an infectious blood meal prepared by mixing 200 μ l of mouse whole blood, 50 μ l of 1 mM ATP, and 250 μ l of DENV2 16681 strain (2.5×10^6 PFU in 250 μ l). After the blood feeding, each mosquito was examined on a stereo microscope to determine whether it had taken a full meal. Mosquitoes were kept at 28°C and 70% relative humidity under a 12 h:12 h light-dark cycle as previously described (Sri-In et al., 2019, 2020). To collect saliva, female mosquitoes were starved for 24 h prior to saliva collection. On the day of saliva collection, the feeding solution [ATP-containing phosphate-buffered saline (PBS)] was wrapped in stretched Parafilm-M membrane and put on the top of a container covered with nylon mesh, allowing mosquitoes to feed on the meal. The mosquito saliva-containing solution was removed from the membrane and transferred to a microtube and centrifuged at $12,000 \times g$ for 1 min at 4°C. The protein concentration of mosquito saliva was measured using Bradford protein assays (Sri-In et al., 2019, 2020).

RNA Extraction and Reverse Transcription

The whole bodies of 3–5 mosquitoes were collected in 1.5-ml tubes containing 0.5 ml of TRIzol (Invitrogen, Carlsbad, CA, United States). Tissue was homogenized using a rotor-stator homogenizer at room temperature for 5 min and centrifuged at $15,890 \times g$ for 10 min at 4°C. After centrifugation, the supernatant was transferred to a new micro-tube containing 0.1 ml of chloroform (J. T. Baker) and mixed thoroughly at room temperature for 3 min. Samples were then centrifuged at $15,890 \times g$ for 15 min at 4°C, and the supernatant was transferred carefully to a new micro-tube containing 0.25 ml of isopropanol (J. T. Baker). Samples were gently mixed and stored at –80°C for 30 min. After precipitation, the samples were again centrifuged at $15,890 \times g$ for 30 min at 4°C. The supernatant was discarded, and 0.5 ml of 75% ethanol (Taiwan Burnett International Co., Ltd, Taipei, Taiwan) was used to wash the RNA pellet. All resulting samples were centrifuged at $15,890 \times g$ for 5 min at 4°C, and the supernatant was discarded. Finally, the RNA pellet was dried in a laminar flow hood and dissolved in DEPC-H₂O. After Baseline-ZEROTM DNase (Epicenter, Madison, WI, United States) treatment, the RNA sample was stored at –80°C. The RNA concentration was quantified using a spectrophotometer (Nanodrop 2000, Thermo Fisher Scientific, Waltham, MA, United States), and the sample was diluted with DEPC-H₂O to a concentration of 1 μ g/ μ l. The RNA samples were reverse-transcribed to cDNA using a High-Capacity cDNA Reverse Transcription Kit (Applied Biosystems, Waltham, MA, United States). The cDNA samples were stored at –20°C for further use. Gene expression was analyzed via real-time quantitative polymerase chain reaction (RT-qPCR). The ribosomal protein S7 gene was used as an internal control.

Real-Time Quantitative PCR

The SYBR Green dye binding system was used for RT-qPCR in this study. SYBR Green binds the minor groove of DNA, and the target gene expression was quantified by detecting the resulting fluorescence signal. The cDNA sample was quantified using a

KAPA SYBR FAST Universal qPCR kit (KAPA), via the qPCR primers (S7: 5'-TCAGTGTACAAGAAGCTGACCGGA-3'/5'-TTCCGCGCGCGCTCACTTATTAGATT-3'; DENV:5'-GAAGACATTGACTGYTGGTGCAA-3'/5'-CGATGTTTCCACGCCCTTC-3'). The PCR protocol consisted of initial denaturation at 95°C for 3 min, followed by 40 cycles of 3 s at 94°C and 40 s at 60°C. Fluorescence readings were measured at 72°C after each cycle. The target gene signal was detected and analyzed using the ABI 7900HT Fast Real-Time PCR System, and relative quantification results were normalized using the ribosomal protein S7 gene as an internal control.

Double-Stranded RNA Preparation

RNA interference (RNAi) primers were designed using the E-RNAi webservice¹. The T7 promoter sequence (5'-TAATACGACTCACTATAGGG-3') was incorporated into all forward and reverse RNAi primers. The target gene fragment was amplified using Ex Taq DNA Polymerase (Takara, Kusatsu-shi, Japan). Fragments were amplified and cloned into a pCR 2.1-TOPO vector at 23°C for 30 min using a TOPO TA Cloning Kit (Invitrogen, Carlsbad CA, United States). The constructed plasmid was transformed into HIT-DH5 α competent cells. Plasmids from positive colonies were purified using a FarvoPrepTM Plasmid DNA Extraction Mini Kit (Favorgen, Taipei, Taiwan) and sequenced to confirm that the cDNA was in frame.

The plasmid was digested by a restriction enzyme, and fragments were separated using 1% agarose gel. Target fragments were isolated and purified from the gel using a FarvoPrepTM GEL/PCR Purification Kit (Favorgen, Taipei, Taiwan). The fragments were then amplified using Ex Taq DNA Polymerase and purified using a FarvoPrepTM GEL/PCR Purification Kit. The purified PCR product was used as the template to synthesize Double-Stranded RNA (dsRNA) *in vitro* using a T7-ScribeTM Transcription Kit (Epicenter, Madison, WI, United States). The reaction was performed at 37°C for 4–12 h. A solution of 95 μ l of DEPC-H₂O and ammonium acetate (stop solution) was added to stop the reaction, and the supernatant was transferred into a new Eppendorf tube containing 150 μ l of a phenol/chloroform (Amresco) solution. Samples were centrifuged at $15,890 \times g$ for 5 min, at 4°C, and the supernatant was transferred to a new Eppendorf tube containing 150 μ l of chloroform. After centrifugation at $15,890 \times g$ for 5 min at 4°C, the supernatant was transferred to a new Eppendorf tube containing 110 μ l of isopropanol. Samples were gently mixed and stored at –80°C for 30 min. Finally, each sample was centrifuged at $15,890 \times g$ for 30 min at 4°C. The dsRNA pellets were dried in a laminar flow hood and dissolved in DEPC-H₂O. The dsRNA was diluted to a final concentration of 5 μ g/ μ l. Between day 3 and 5 PE, female mosquitoes were injected with 280 nl of dsRNA (5 μ g/ μ l) using a Nanoject II AutoNanoliter Injector (Drummond Scientific, Broomall, PA, United States). dsRNA against LacZ was used as the control dsRNA (dsLacZ) (Sri-In et al., 2019). Silencing efficiency was confirmed by collecting the total RNA of mosquitoes 3 days post-injection for RT-PCR.

¹<http://www.dkfz.de/signaling/e-rnai3/>

Western Blot Analysis

The whole bodies of three to five mosquitoes or the tissues of 30–50 mosquitoes were collected in 1.5-ml tubes containing 100 μ l of protein lysis buffer [50 mM Tris (pH 7.4), 1% IGEPAL, 0.25% sodium deoxycholate, 150 mM NaCl, 1 mM EDTA, 1 mM phenylmethyl-sulfonylfluoride, 1X protease inhibitor mixture, 1X phosphatase inhibitor mixture, and 10 mM *N*-ethylmaleimide (Sigma-Aldrich, St. Louis, MO, United States)] and homogenized using a rotor-stator homogenizer. Each homogenized sample was centrifuged at $15,890 \times g$ for 30 min at 4°C, and the supernatant was transferred to a QIAshredderTM column (Qiagen, Hilden, Germany). The eluted samples were collected and transferred to new Eppendorf tubes at –80°C. The protein concentration was quantified using the Bradford method and Bio-Rad Protein Assay Dye Reagent (Bio-Rad Laboratories, Inc, Hercules, CA, United States). Each protein sample was mixed with the same volume of sample buffer Laemmli 2 \times Concentrate (Sigma-Aldrich, St. Louis, MO, United States) and adjusted to the same volume with 1 \times sample buffer. To denature proteins for electrophoresis, protein samples were incubated at 65°C for 15 min. The protein samples (40 μ g) were subjected to SDS-PAGE and blotted onto a PVDF membrane (Pall Corporation, New York, NY, United States) for 1.5 h. The membranes were blocked with 1% bovine serum albumin (BSA) in 1 \times phosphate-buffered saline containing 0.4% Tween 20 (PBST) at room temperature for 1 h. Afterward, the membranes were incubated in PBST containing primary antibody overnight at 4°C. The antibodies used in this study were: mouse anti-SUMO antibody (Developmental Studies Hybridoma Bank, SUMO-2 8A2, 1/100), mouse anti-NS1 antibody (Yao-Hong Biotechnology, Taipei, Taiwan, YH0023, 1/10000), mouse anti-E antibody (Yao-Hong Biotechnology, Taipei, Taiwan, YH0026, 1/10000), mouse anti-prM antibody (from Dr. Kao-Jean Huang at the Development Center for Biotechnology, Taipei, Taiwan, 1/100), and rabbit anti-GAPDH antibody (GeneTex, Irvine CA, United States, GTX100118, 1/10000). Membranes were washed in PBST and incubated with secondary antibody [HRP-conjugated anti-mouse IgG (Abcam, Cambridge, United Kingdom, ab6728), or HRP-conjugated anti-rabbit IgG (GeneTex, Irvine CA, United States, GTX213110)] in PBST at room temperature for 1 h. Finally, membranes were washed in PBST and developed using WesternBrightTM Peroxide and ECL (Advansta Inc. San Jose, CA, United States) as the substrate for horseradish peroxidase following the manufacturer's instructions.

Cell-Based Enzyme-Linked Immunoassay

The whole bodies and saliva of AaUbc9-silenced or dsLacZ-treated mosquitoes were collected in 100 μ l of serum-free medium and stored at –80°C. C6/36 cells were seeded in a 96-well tissue culture plate and incubated at 28°C overnight. The homogenized suspensions of infectious mosquitoes were centrifuged at $18,928 \times g$ for 30 min and kept on ice. The cell monolayers were washed with phosphate-buffered saline (PBS), and 50 μ l of 10-fold serial dilutions of infectious mosquito suspensions were applied to the cells for 2 h. After virus

absorption, each well was covered with 100 μ l of culture medium, and the plates were incubated at 28°C for 4 days.

Cells were then fixed with 4% paraformaldehyde for 30 min at 4°C, washed four times with PBS, and treated with 0.1% Triton X-100 at room temperature for 1 h. The cells were subsequently incubated with blocking buffer (1% BSA, 0.5% Triton X-100 in PBS) at room temperature for 1 h. The blocking buffer was then substituted with 50 μ l/well of a 1:1000 dilution of mouse monoclonal anti-NS1 IgG (Yao-Hong Biotechnology, Taipei, Taiwan) at 4°C overnight. After another four PBS washes, the cells were incubated with 30 μ l/well of 1:500 dilution of HRP-conjugated anti-mouse IgG (Abcam, Cambridge, United Kingdom, ab6728) at room temperature. Two hours post antibody incubation, the cells were gently washed four times with PBS, followed by addition of 100 μ l/well of 3,3',5,5'-tetramethylbenzidine (TMB) substrate for HRP activity detection. The substrate reaction was inhibited using an equal volume of 1 N HCl. After reaction inhibition, the soluble yellow product that developed was read using a microtiter plate reader at a wavelength of 450 nm (Tan et al., 2014).

For cell viability assay, the 96-well tissue culture plates were stained with crystal violet staining solution (1% crystal violet in 75% ethanol) at room temperature for 30 min. After being washed four times in a stream of tap water, the plates were air-dried at room temperature. The stained cells were lysed in 1% SDS and measured the optical density of each well at 570 nm. Setting the OD570 of non-stimulated cells to 100%, and determine the percentage of 2-D08 treated cells that are viable by comparing the OD570 values of 2-D08 treated cells with the OD570 values of the non-stimulated cells (Feoktistova et al., 2016).

Detection of Proteins SUMOylated *in vivo*

To identify targets of protein SUMOylation, we used a protocol applicable to a wide range of species (including *Homo sapiens* and *Mus musculus*, and other vertebrates such as *Gallus gallus*, *Xenopus laevis*, *Danio rerio*, and *D. melanogaster*) and applied it to SUMOylated protein identification in mosquitoes (Barysch et al., 2014). Briefly, the whole bodies of ten DENV2 infected mosquitoes were collected in 1.5-ml Eppendorf tubes containing 100 μ l of 1X lysis buffer [1X PBS, 1% SDS, 5 mM EDTA, 1 mM phenylmethyl-sulfonylfluoride, 1X protease inhibitor mixture, 1X phosphatase inhibitor mixture, and 10 mM *N*-ethylmaleimide (Sigma-Aldrich, St. Louis, MO, United States)]. The solution was homogenized using a rotor-stator homogenizer and the resulting lysate was incubated at 65°C for 15 min. The lysate was then diluted with 900 μ l of cold RIPA dilution buffer [1X PBS, 5 mM EDTA, 1 mM phenylmethyl-sulfonylfluoride, 1X protease inhibitor mixture, 1X phosphatase inhibitor mixture, and 10 μ l of 10 mM *N*-ethylmaleimide (Sigma-Aldrich, St. Louis, MO, United States)] in a 10-fold dilution. The diluted lysate was centrifuged at $15,890 \times g$ for 30 min at 4°C, and the supernatant was transferred to a QIAshredderTM column (Qiagen, Hilden, Germany). The eluted samples were collected and transferred to new Eppendorf tubes that were stored at –80°C. The protein concentration was quantified using the Bradford method and Bio-Rad Protein Assay Dye Reagent (Bio-Rad Laboratories, Inc, Hercules, CA, United

States). Protein concentrations higher than 10 $\mu\text{g}/\mu\text{l}$ were used as input material. We combined 1 ml of input material with antibody (1 μl of mouse anti-E, 100 μl of mouse anti-prM, 1 μl of mouse anti-NS1, or 100 μl of mouse anti-SUMO) and 10 μl of protein G-agarose beads, and incubated with gentle agitation at 4°C overnight. The following day, the antibody-coupled beads were centrifuged at $700 \times g$ for 5 min at 4°C and the supernatant was removed. The antibody-coupled beads were washed three times in 1 ml of RIPA buffer with centrifugation after each wash at $700 \times g$ and at 4°C for 5 min. The protein was eluted by adding 50 μl of 2X Laemmli sample buffer (Sigma-Aldrich, St. Louis, MO, United States) before incubation at 65°C for 15 min. Western blot was performed on the eluted samples to detect SUMO-modified proteins.

Detection of Proteins SUMOylated *in vitro*

An *in vitro* SUMOylation assay kit (Abcam, Cambridge, United Kingdom, ab139470) was used to generate SUMOylated proteins *in vitro* via covalent isopeptide linkage of the c-terminus of SUMO protein to specific lysine residues on the target protein through the SUMOylation enzyme cascade. Target proteins (DENV2 or Zika virus), SUMO protein, SUMOylation enzyme (E1 and E2 of protein SUMOylation), SUMOylation buffer, and Mg-ATP were combined as per Abcam SUMOylation kit protocol and incubated at 37°C for 2 h to generate the SUMOylated product *in vitro*. A western blot was used to detect viral protein SUMOylation in the reaction mixture via antibodies against E protein, prM protein, and NS1 protein. The reaction mixture, omitting Mg-ATP cofactors (required for E1 activation), was used as a negative control.

RESULTS

Protein SUMOylation Plays an Essential Role in Dengue Virus Replication in the Mosquito

To investigate the roles of protein SUMOylation in virus replication in *A. aegypti*, we used a reverse genetic approach by introducing double-stranded RNA of AaUbc9 (dsAaUbc9) into the mosquito to silence AaUbc9 expression. Three-day-old female mosquitoes were injected with dsRNA of LacZ (dsLacZ) or dsAaUbc9 3 days prior to an infectious blood-feeding with DENV2 (10^7 pfu/ml). Total RNA from the midgut, fat body, ovary, and salivary gland from individual female mosquitoes was collected 10 days post-infection. The expression of the DENV2 viral genome was quantified by RT-qPCR. Our results showed that in response to the depletion of AaUbc9, the expression of the viral genome was inhibited in the mosquito midgut, ovary, and salivary gland at 10 days post infection (**Figure 1A**). Next, we examined the effect of AaUbc9 silencing on viral protein production in mosquitoes. Female mosquitoes were injected with dsLacZ or dsAaUbc9 at 3 days prior to DENV2 virus infection by thoracic injection (200 pfu/mosquito). Total protein was collected at 5 and 7 days

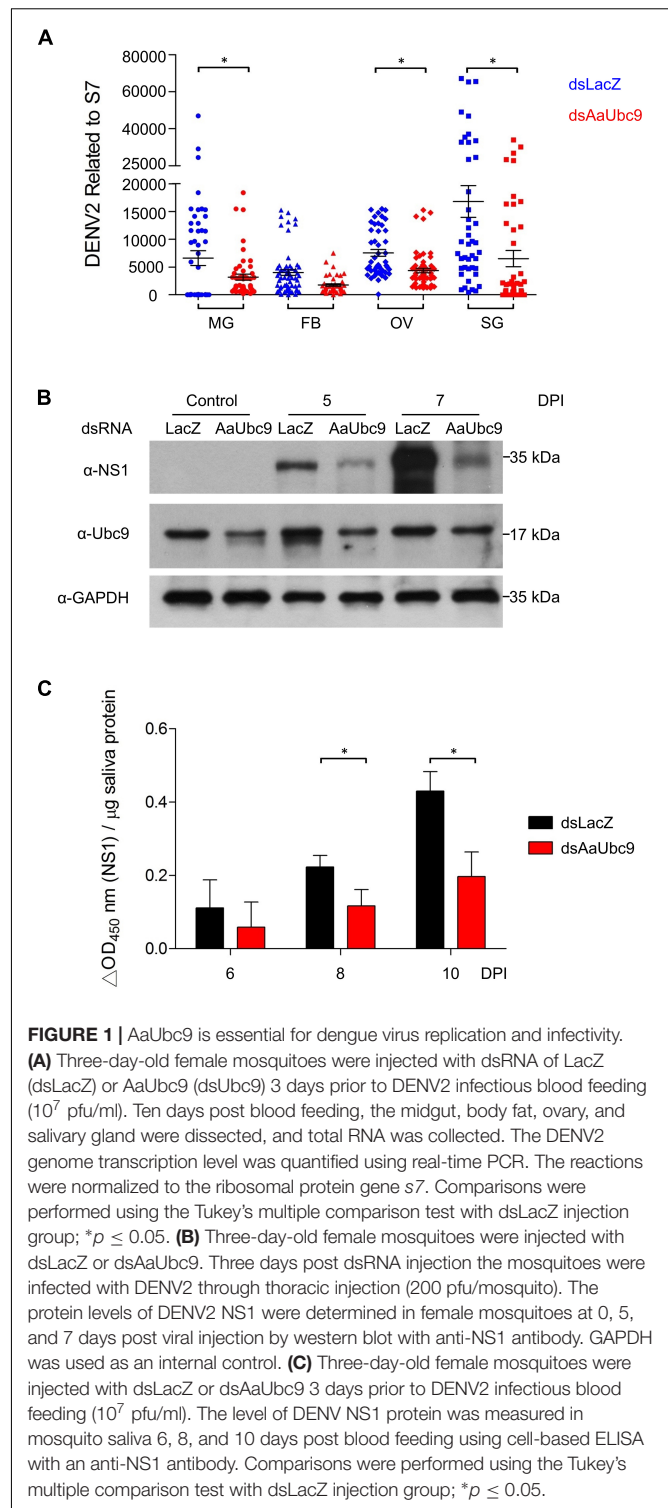


FIGURE 1 | AaUbc9 is essential for dengue virus replication and infectivity. **(A)** Three-day-old female mosquitoes were injected with dsRNA of LacZ (dsLacZ) or AaUbc9 (dsAaUbc9) 3 days prior to DENV2 infectious blood feeding (10^7 pfu/ml). Ten days post blood feeding, the midgut, body fat, ovary, and salivary gland were dissected, and total RNA was collected. The DENV2 genome transcription level was quantified using real-time PCR. The reactions were normalized to the ribosomal protein gene s7. Comparisons were performed using the Tukey's multiple comparison test with dsLacZ injection group; $*p \leq 0.05$. **(B)** Three-day-old female mosquitoes were injected with dsLacZ or dsAaUbc9. Three days post dsRNA injection the mosquitoes were infected with DENV2 through thoracic injection (200 pfu/mosquito). The protein levels of DENV2 NS1 were determined in female mosquitoes at 0, 5, and 7 days post viral injection by western blot with anti-NS1 antibody. GAPDH was used as an internal control. **(C)** Three-day-old female mosquitoes were injected with dsLacZ or dsAaUbc9 3 days prior to DENV2 infectious blood feeding (10^7 pfu/ml). The level of DENV NS1 protein was measured in mosquito saliva 6, 8, and 10 days post blood feeding using cell-based ELISA with an anti-NS1 antibody. Comparisons were performed using the Tukey's multiple comparison test with dsLacZ injection group; $*p \leq 0.05$.

post-infection and the production of DENV2 virus NS1 protein was analyzed by western blot using an anti-NS1 antibody. The production of NS1 protein was inhibited by AaUbc9 silencing in mosquitoes (**Figure 1B**). The anti-Ubc9 antibody was used to validate the silencing of Ubc9 in mosquitoes. To

further investigate the effect of protein SUMOylation on virus transmission, female mosquitoes were injected with dsLacZ or dsAaUbc9 3 days prior to DENV2 infection *per os* (10^7 pfu/ml). Mosquito saliva was collected at 6, 8, and 10 days post-infection and the expression of infectious virus particles in saliva was determined by cell-based ELISA with an anti-NS1 antibody. The silencing of AaUbc9 significantly inhibited the expression of infectious virus particles in the saliva of mosquitoes (Figure 1C). Taken together, our results suggest that AaUbc9 regulates dengue virus replication and transmission in the mosquito *A. aegypti*.

Ubc9 Inhibitor Blocks Viral Protein Production Post Virus Entry

Next, we made use of a Ubc9 inhibitor (2-D08) to investigate the interaction between protein SUMOylation and viral protein production. The cytotoxicity of Ubc9 inhibitor (2-D08) in *A. aegypti* CCL-125 cells were examined by cell viability assay (Supplementary Figure 1). The expression of DENV2 NS1 protein was analyzed by cell-based ELISA using an anti-NS1 antibody. Briefly, *A. aegypti* CCL-125 cells were treated with Ubc9 inhibitor at a variety of concentrations either before, simultaneously, or after DENV2 infection at a multiplicity of infection (MOI) of 1. Viral protein production was determined using a microtiter plate reader utilizing a mouse monoclonal anti-NS1 antibody followed by an HRP-conjugated anti-mouse antibody. Our data revealed that viral protein production was inhibited in response to the reduced AaUbc9 activity (Figure 2). It is worth noting that AaUbc9-mediated viral protein suppression is regulated at a stage post viral entry.

Protein SUMOylation Pathway Is Activated After Virus Infection in the Mosquito

When the mosquito take an infectious blood meal, the DENV first infects the epithelial cells of midgut. Five to seven days post-infection, DENV disseminates to other tissues of the mosquito via the hemolymph (Salazar et al., 2007; Mukherjee et al., 2019). To examine protein SUMOylation in the mosquito in response to dengue virus infection, total protein from mosquito midgut and salivary gland was collected at 6, 8, and 10 days post DENV2 infection. The expression of SUMO and NS1 proteins were determined by western blot analysis using anti-SUMO and anti-NS1 antibodies, respectively. Our results showed that protein SUMOylation was strongly activated at 8 and 10 days in midgut and salivary gland post DENV2 infection (Figure 3).

These results suggest that protein SUMOylation is induced after an infectious blood meal in the mosquito.

Dengue Virus Envelope Protein and Pre-membrane Protein Are Potential Targets of Protein SUMOylation

To further understand how SUMOylation influence DENV infection, it was necessary to identify specific target proteins by performing *in vivo* and *in vitro* protein SUMOylation assays. For the *in vivo* protein SUMOylation assay, we collected whole

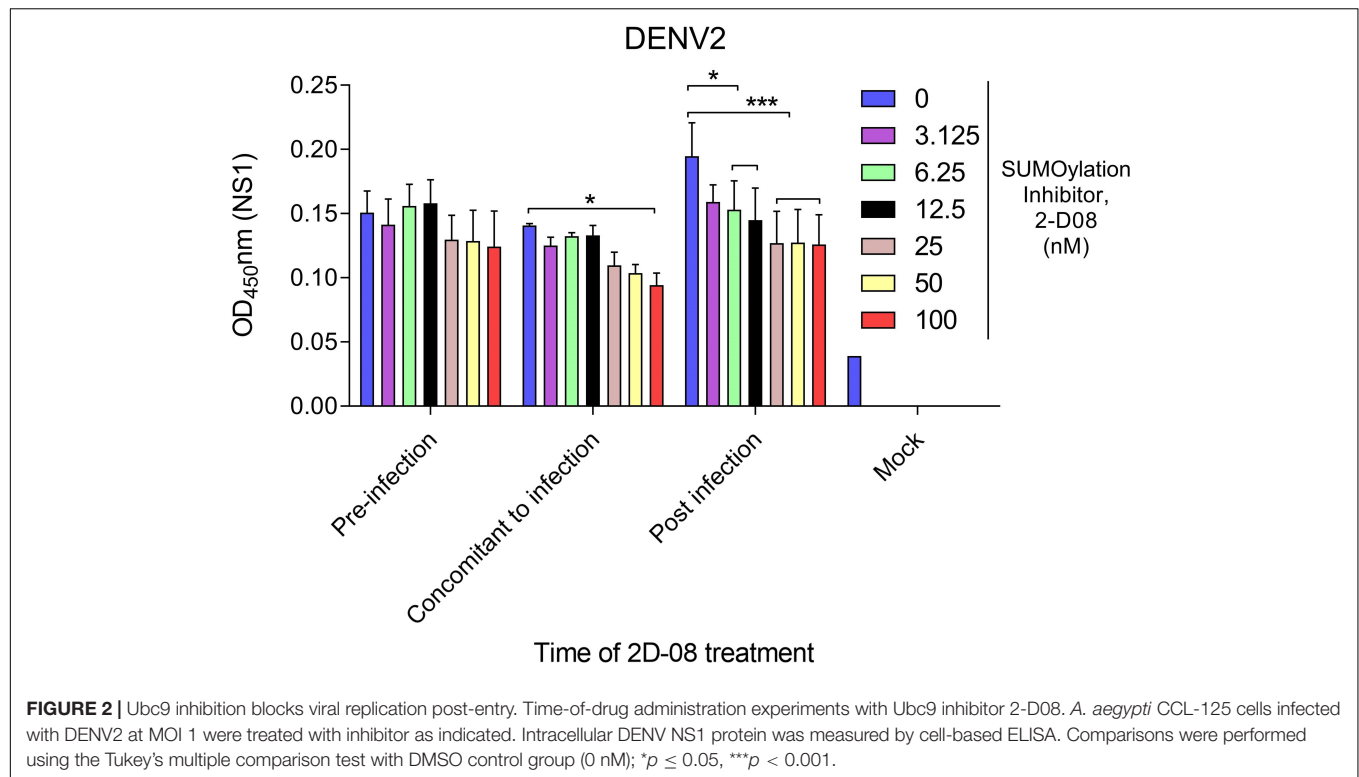
body protein from DENV2-infected mosquitoes. Input protein concentrations of at least $10 \mu\text{g}/\mu\text{l}$ were denatured and used in the immunoprecipitation reactions. The resultant data indicated dengue virus E and prM were potential target proteins for SUMOylation (Figures 4A,B).

To verify this observation, we proceeded with an *in vitro* protein SUMOylation analysis. It has been previously demonstrated that SUMO modification occurs through an ATP-dependent enzymatic cascade. The E1 enzyme, as an integral protein in this process, covalently links SUMO proteins through cysteine at the active site (Johnson, 2004; Chang and Yeh, 2020). Understanding this, we collected the medium from C6/36 cells infected with DENV2 or ZIKV. SUMO protein and SUMOylation enzymes (E1 and E2) were mixed with DENV- or ZIKV-containing medium and incubated to generate SUMOylated products *in vitro*. The reaction mixture was analyzed via western blot to examine SUMOylation of viral proteins (Figure 4C). The same reaction without ATP served as a negative control. In concert with our *in vivo* studies, this data suggests that the envelope proteins and pre-membrane proteins, but not non-structural protein 1 (NS1), of DENV2 and ZIKV are potential targets for protein SUMOylation.

Dengue Virus Envelope Protein SUMOylation Is Essential for Virus Particle Production

To investigate and elucidate the role of dengue virus E protein SUMOylation in virus replication in mosquitoes, we blocked protein SUMOylation via site-directed mutagenesis. A previous study showed that the N-terminus of DENV2 non-structural protein 5 (NS5) was SUMOylated, leading to increased viral protein stability. However, the modification sites were unknown (Su et al., 2016). In contrast, other findings suggested that dengue virus E protein residues K51 and K241 are required for interaction with Ubc9 in mammalian cells, and that this interaction is essential for dengue virus E protein SUMOylation (Chiu et al., 2007). To investigate this issue, we constructed a plasmid containing the linear fusion of mosquito SUMO-E1 (AaAos1 and AaUba2), SUMO-E2 (AaUbc9), SUMO protein, and target protein variants (wild type and K51/241R mutant of DENV2 envelope protein), with transcription being controlled by a T7 promoter (Figure 5A). Prior to *in vivo* experimentation, SUMOylation was established in *Escherichia coli*. After protein synthesis induction with IPTG, the bacterial pellet was collected and analyzed by western blot to determine DENV2 E SUMOylation. Our results showed that the high molecular weight form of DENV2 E was only observed in samples with the wild type envelope protein but not those with the K51/241R mutant (Figure 5C). This indicates that the DENV2 envelope protein can be SUMOylated, and the amino acid residues K51 and K241 of dengue virus E protein are essential for protein SUMOylation.

We next performed site-directed mutagenesis to generate wild type and K51/241R mutant envelope protein containing pseudovirus particles. A plasmid containing the structural proteins [capsid (C), envelope (E), and membrane (M) proteins]



of DENV2 strain 16681 was linked to the actin promoter of *D. melanogaster* (Figure 5B). The structural proteins of the DENV2 were expressed in the *A. aegypti* cell line CCL-125, leading to pseudoviral particle secretion. The supernatant of the transfected CCL-125 culture medium was collected and examined by western blot analysis. Secretion of E and prM proteins was suppressed in the K51/241R mutant expressing cells (Figure 5D, secretory protein), suggesting the inhibition of viral structural proteins secretion. The cellular protein of transfected CCL-125 from wild type and K51/241R mutant cells was then collected and examined by western blot analysis. Our results showed that the production of E and prM proteins from K51/241R mutants were inhibited (Figure 5D, cellular protein). Interestingly, the transcriptional expression of DENV2E protein in wild type and K51/241R mutant remained equal (Figure 5D, cellular RNA), suggesting the inhibition of E and prM proteins production from K51/241R mutant is transcription independent. Taken together, our results indicate that envelope protein SUMOylation is essential for viral structural proteins secretion, a critical step for virus transmission.

DISCUSSION

SUMO modification is known to be well-conserved between species; including *H. sapiens*, *D. melanogaster*, and *S. cerevisiae* (Epps and Tanda, 1998; Fraser et al., 2000; Apionishev et al., 2001; Hayashi et al., 2002; Urena et al., 2016; Li et al., 2021). Bioinformatic analysis of the amino acid sequence and tertiary structure of SUMO proteins, E2 conjugating enzyme

(Ubc9), and SUMOylation activating heterodimer (SAE1/2) has demonstrated these high conservation rates (Stokes et al., 2020; Li et al., 2021). Interestingly, while previous studies show most eukaryotic organisms express both a SUMO1 and SUMO2/3 paralog, insects do not possess a SUMO1 paralog, and the insect SUMO2/3 paralogs lack the SCM (Choy et al., 2013; Urena et al., 2016). DmSUMO, as an example of this phenomenon, lacks a SCM and is thus unable to form poly-SUMO chains (Urena et al., 2016). This suggests that insect SUMO cannot efficiently form poly-SUMO chains without the presence of an E3 ligase. Although the amino acid sequence and predicted tertiary structure of AaSUMO is well conserved in *H. sapiens* SUMO3 (HsSUMO3), the lack of SCM in the N-terminus suggests that the biochemical function of AaSUMO is more similar to that of HsSUMO1 than HsSUMO3 (Stokes et al., 2020).

Poly-SUMO chain formation is important for many cellular processes across a range of species (Epps and Tanda, 1998; Fraser et al., 2000; Apionishev et al., 2001; Hayashi et al., 2002; Stokes et al., 2020). Regarding *A. aegypti*, AaSUMO can form poly-SUMO chains efficiently when in the presence of an AaPIAS (Stokes et al., 2020). The highly conserved formation of poly-SUMO chains across species, as well as the formation of SUMO conjugated proteins in *A. aegypti* (Figure 3), indicates that protein SUMOylation likely serves an important biological function in the mosquito *A. aegypti*.

Many studies have implicated components of the SUMOylation pathway in regulating viral survival, pathogenesis, and host immunity (Brown et al., 2016; Conn et al., 2016; Su et al., 2016; Feng et al., 2018; Stokes et al., 2020). It remains difficult to determine if a phenotype is directly or indirectly linked to

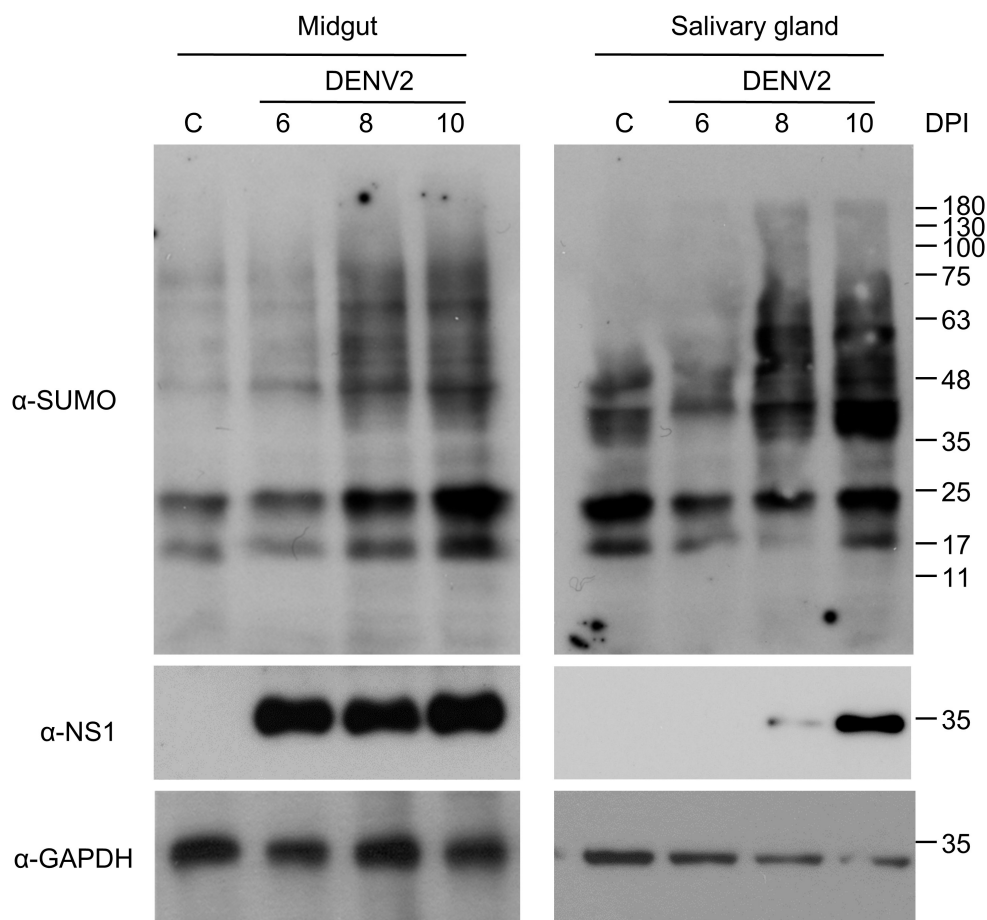


FIGURE 3 | Protein SUMOylation is activated after a blood meal in the midgut of mosquitoes. Three-day-old female mosquitoes were fed with DENV2 infectious blood meal (10^7 pfu/ml). At 6, 8, or 10 days post blood feeding the midgut and salivary gland were dissected, and the protein levels of SUMO and DENV2 NS1 protein were analyzed by western blot with anti-SUMO or anti-NS1 antibodies. GAPDH was used as an internal control.

the SUMOylation pathway because current studies are not able to distinguish between different targets of SUMO modification (Lyst and Stancheva, 2007). To further investigate the effect of protein SUMOylation on virus replication in mosquitoes and examine the interaction between protein SUMOylation and dengue virus replication, we utilized dsRNA to silence the expression of the SUMO-conjugating enzyme AaUbc9. Our data showed that production of the DENV genome, viral proteins, and infectious virus particles were inhibited in response to silencing AaUbc9 (**Figure 1**). Moreover, we showed that a Ubc9 inhibitor blocked virus production post viral entry (**Figure 2**). Taken together, our results indicate that AaUbc9 plays a key role in dengue virus replication in the mosquito.

In a previous study, depletion of AaSUMO, AaUbc9, or AaPIAS *in vitro* resulted in a small but consistent increase in ZIKV replication (Stokes et al., 2020). The authors proposed that this could be due to the modification of viral NS5 proteins or immune-related proteins, which normally function to suppress ZIKV replication. It remains difficult to distinguish the function of protein SUMOylation in mosquitoes, especially as they may be virus-specific in certain mosquito cell types or tissues. In

addition, it is difficult to determine if a phenotype is directly or indirectly linked to the SUMOylation pathway. Therefore, we aimed to determine the target proteins of SUMOylation in mosquitoes post DENV infection.

Previously, dengue virus E and NS5 proteins have been identified as potential targets for protein SUMOylation in mammalian cells (Chiu et al., 2007; Su et al., 2016). Although specific lysine residues were not identified, DENV SUMO modification was noted at the N-terminus of NS5, increasing protein stability. Consequently, it was hypothesized that SUMO “floats” around the N-terminus of the protein and can modify any available lysine residues (Su et al., 2016). In this study, our data indicate that dengue virus E and prM proteins, but not NS1, are potential target proteins of SUMOylation. Paralleling this, ZIKV E and prM proteins were also identified as potential targets of SUMOylation (**Figure 4**).

A range of viral structural proteins are known to be SUMO modified, including HIV-1 p6 protein (Gurer et al., 2005), dengue virus E protein (Chiu et al., 2007), and coronavirus nucleocapsid protein (Li et al., 2005, 2006). A previous study demonstrated that dengue virus E protein interacts with Ubc9

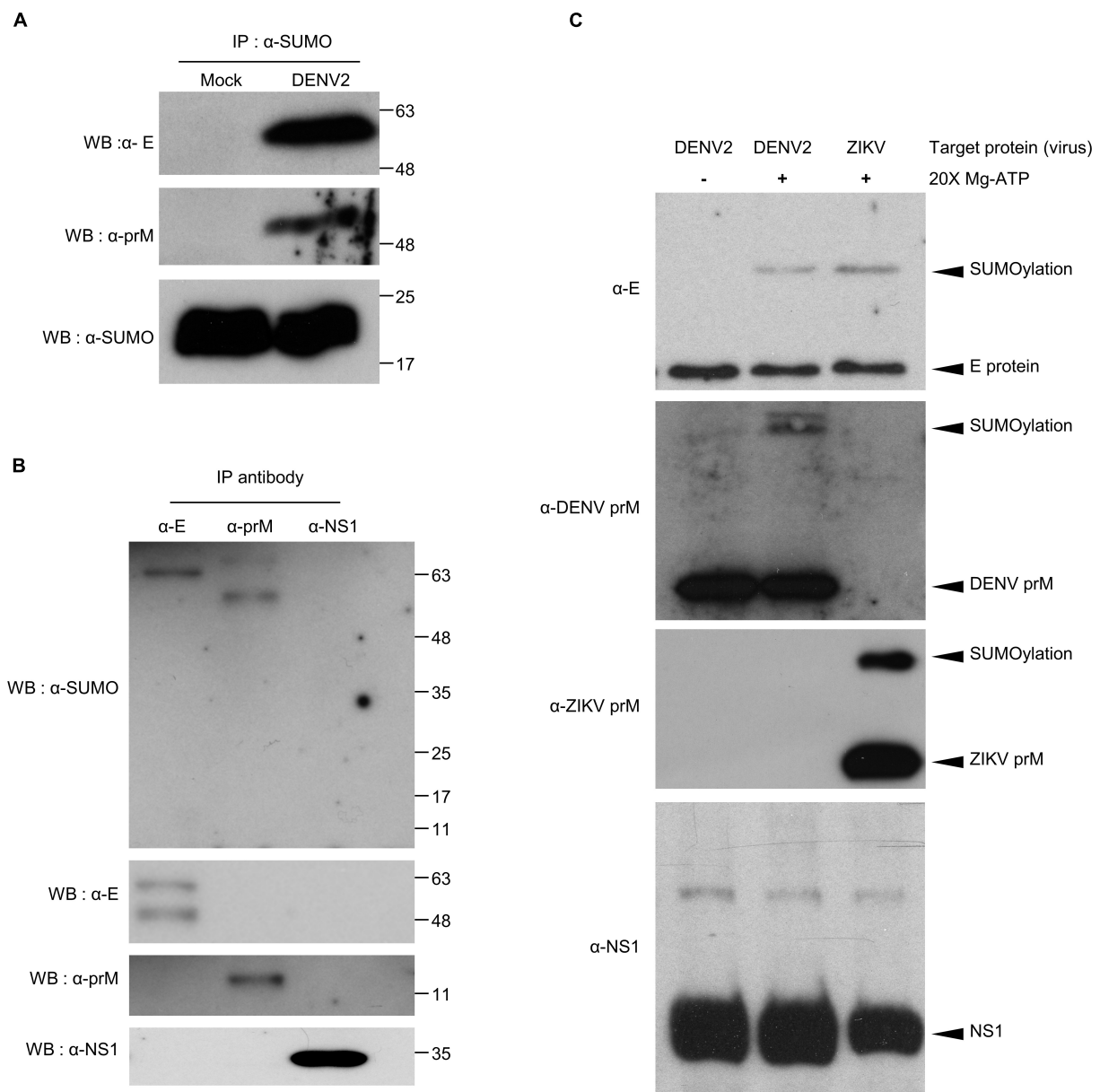


FIGURE 4 | Covalent modification of DENV2 and ZIKV E and prM proteins by SUMO protein in virus-infected mosquitoes. **(A,B)** Seven days post virus injection (2000 pfu/mosquito), mosquito whole body cell lysate was collected and incubated at 65°C for 15 min. The denatured proteins were immunoprecipitated using antibodies specific to SUMO protein **(A)** and DENV proteins E, prM, and NS1 **(B)**. The immunoprecipitation products were analyzed via western blot with anti-SUMO, anti-E, anti-prM, and anti-NS1 antibodies. **(C)** *In vitro* SUMOylation assay of DENV proteins, E, prM, and NS1. The medium from DENV infected C6/36 cells was collected and examined via our *in vitro* SUMOylation assay. We used a western blot to probe the reaction mixture with anti-E, anti-prM, and anti-NS1 antibodies. A reaction without ATP was used as a negative control.

through residues K51 and K241 in mammalian cells, and that this interaction plays a key role in dengue virus E protein SUMOylation (Chiu et al., 2007). To investigate this issue in mosquitoes, we developed an *in vitro* SUMOylation system in *E. coli*. Our results showed that dengue virus E protein is a target protein for protein SUMOylation, and residues K51 and K241 of the protein are crucial for protein SUMOylation in mosquitoes (Figure 5C). We further performed

site-directed mutagenesis to generate wild type and K51/241R mutant envelope protein containing pseudovirus particles. Our results showed that E and prM proteins secretion and protein production were inhibited from K51/241R mutant (Figure 5D, secretory and cellular protein), which are important for viral transmission. However, the transcriptional expression of DENV2 E protein in wild type and K51/241R mutant remained equal (Figure 5D, cellular RNA), suggesting the inhibition of E and

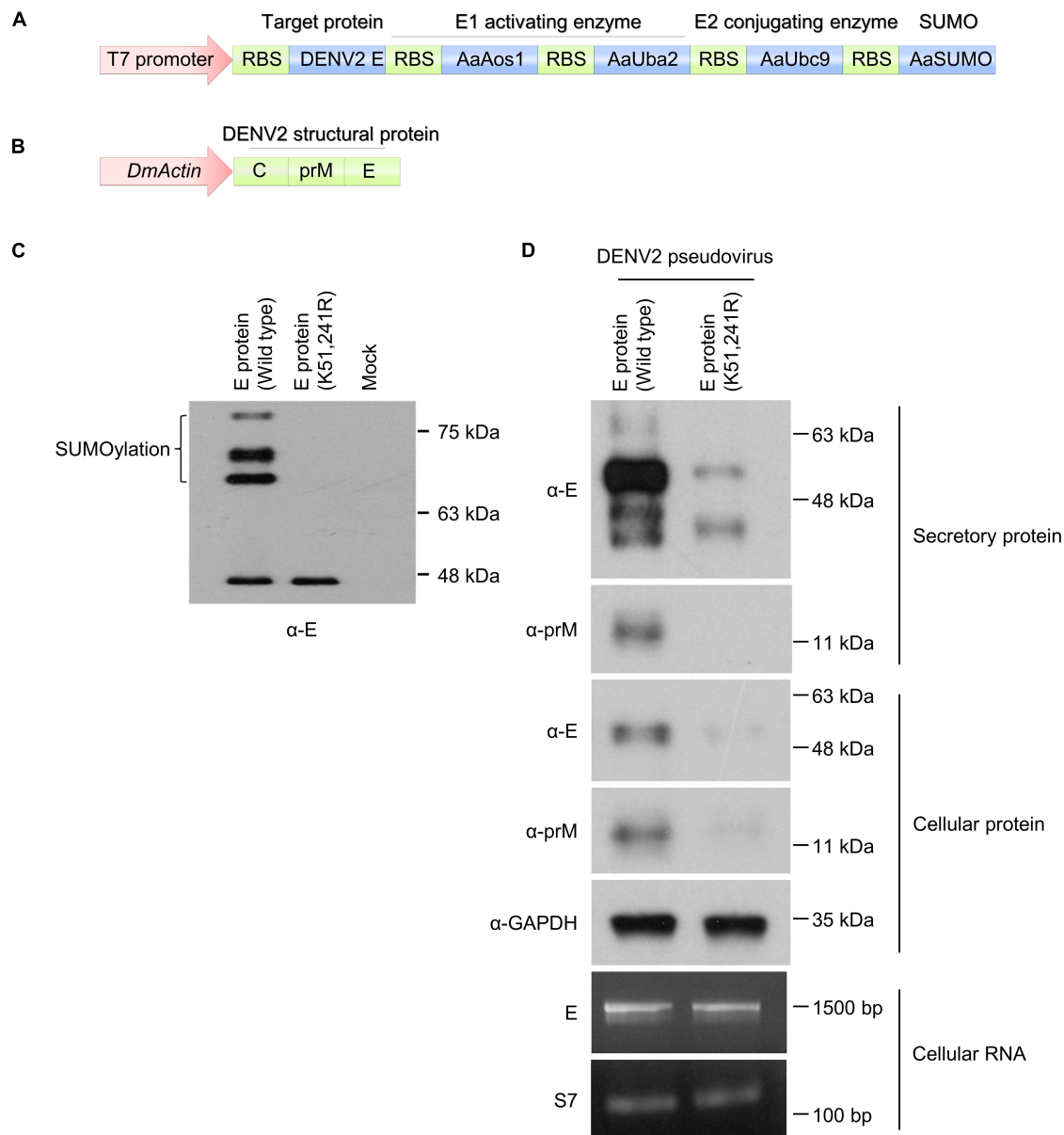


FIGURE 5 | DENV2 envelope protein SUMOylation is essential for viral particle production in mosquito cells. **(A)** A plasmid encoding the linear fusion of mosquito SUMO-E1 (AaAos1 and AaUba2), SUMO-E2 (AaUbc9), SUMO protein, and target protein (wild type or K51/241R mutant of DENV2E). **(B)** A plasmid encoding the linear fusion of DENV2 prM and E proteins linked to an actin 5C promoter. **(C)** The plasmid depicted in A was transformed into *E. coli* BL21 (DE3) and protein expression was induced with 1 mM IPTG at 25°C. Four hours post protein transcription induction, the bacterial lysate was analyzed by western blot using anti-E antibody. **(D)** The plasmid described in B was transfected into CCL-125 cells. Four days post transfection the secretory virus-like particles, cellular protein lysate, and cellular RNA were collected and analyzed by western blot and RT-PCR.

prM proteins production from K51/241R mutant is transcription independent. Additionally, in the pseudovirus system, the coding sequences of wild type and K51/241R mutant are both linked to the actin promoter of *D. melanogaster*. Therefore, the regulation of wild type and K51/241R mutant protein expression remained equal. These results raise the possibility that the inhibition of E and prM proteins production from K51/241R mutant are due to the regulation of protein stability.

In conclusion, we demonstrated that protein SUMOylation is essential for dengue virus replication and transmission in the mosquito *A. aegypti*. Silencing of AaUbc9 resulted in significant inhibition of dengue virus replication in the mosquito. Moreover, we showed that dengue virus E and prM proteins were SUMOylated. Finally, our results revealed that amino acid residues K51 and K241 of dengue virus E protein are essential for protein SUMOylation. Our findings

elucidate how the protein SUMOylation process manipulate virus replication, as well as provide new targets for potential antiviral therapies.

DATA AVAILABILITY STATEMENT

The original contributions presented in the study are included in the article/**Supplementary Material**, further inquiries can be directed to the corresponding author/s.

ETHICS STATEMENT

The animal study was reviewed and approved by AAALAC-accredited facility and the Committee on the Ethics of Animal Experiments of the National Taiwan University College of Medicine (IACUC approval No: 20200210).

AUTHOR CONTRIBUTIONS

S-CW and S-HS contributed to conception and design of the study, performed the experiments and statistical analysis, and

wrote the manuscript. Both authors contributed to manuscript revision, read, and approved the submitted version.

FUNDING

This work was supported by the Ministry of Science and Technology (Taiwan) MOST 109-2320-B-002-062-MY3 and MOST 109-2327-B-400-004 to S-HS. The anti-prM antibody was a gift from Kao-Jean Huang at the Development Center for Biotechnology, Taipei, Taiwan.

SUPPLEMENTARY MATERIAL

The Supplementary Material for this article can be found online at: <https://www.frontiersin.org/articles/10.3389/fmicb.2022.801284/full#supplementary-material>

Supplementary Figure 1 | Cytotoxic effect of Ubc9 inhibitor (2-D08) in *A. aegypti* CCL-125 cells. *A. aegypti* CCL-125 cells were incubated with culture medium containing Ubc9 inhibitor (2-D08) as indicated for 2 days. Attached cells were measured by cell viability assay.

REFERENCES

- Apionishev, S., Malhotra, D., Raghavachari, S., Tanda, S., and Rasooly, R. S. (2001). The Drosophila UBC9 homologue lesswright mediates the disjunction of homologues in meiosis I. *Genes Cells* 6, 215–224. doi: 10.1046/j.1365-2443.2001.00413.x
- Barysch, S. V., Dittner, C., Flotho, A., Becker, J., and Melchior, F. (2014). Identification and analysis of endogenous SUMO1 and SUMO2/3 targets in mammalian cells and tissues using monoclonal antibodies. *Nat. Protoc.* 9, 896–909. doi: 10.1038/nprot.2014.053
- Bhatt, S., Gething, P. W., Brady, O. J., Messina, J. P., Farlow, A. W., Moyes, C. L., et al. (2013). The global distribution and burden of dengue. *Nature* 496, 504–507. doi: 10.1038/nature12060
- Brown, J. R., Conn, K. L., Wasson, P., Charman, M., Tong, L., Grant, K., et al. (2016). SUMO ligase protein inhibitor of activated STAT1 (PIAS1) is a constituent promyelocytic leukemia nuclear body protein that contributes to the intrinsic antiviral immune response to herpes simplex virus 1. *J. Virol.* 90, 5939–5952. doi: 10.1128/JVI.00426-16
- Cattarino, L., Rodriguez-Barraquer, I., Imai, N., Cummings, D. A. T., and Ferguson, N. M. (2020). Mapping global variation in dengue transmission intensity. *Sci. Transl. Med.* 12:eaax4144. doi: 10.1126/scitranslmed.aax4144
- Chang, H. M., and Yeh, E. T. H. (2020). SUMO: from bench to bedside. *Physiol. Rev.* 100, 1599–1619. doi: 10.1152/physrev.00025.2019
- Chiu, M. W., Shih, H. M., Yang, T. H., and Yang, Y. L. (2007). The type 2 dengue virus envelope protein interacts with small ubiquitin-like modifier-1 (SUMO-1) conjugating enzyme 9 (Ubc9). *J. Biomed. Sci.* 14, 429–444. doi: 10.1007/s11373-007-9151-9
- Choy, A., Severo, M. S., Sun, R., Girke, T., Gillespie, J. J., and Pedra, J. H. (2013). Decoding the ubiquitin-mediated pathway of arthropod disease vectors. *PLoS One* 8:e78077. doi: 10.1371/journal.pone.0078077
- Conn, K. L., Wasson, P., McFarlane, S., Tong, L., Brown, J. R., Grant, K. G., et al. (2016). Novel role for protein inhibitor of activated STAT 4 (PIAS4) in the restriction of herpes simplex virus 1 by the cellular intrinsic antiviral immune response. *J. Virol.* 90, 4807–4826. doi: 10.1128/JVI.03055-15
- El Motiam, A., Vidal, S., Seoane, R., Bouzaher, Y. H., Gonzalez-Santamaria, J., and Rivas, C. (2020). SUMO and cytoplasmic RNA viruses: from enemies to best friends. *Adv. Exp. Med. Biol.* 1233, 263–277. doi: 10.1007/978-3-030-38266-7_11
- Epps, J. L., and Tanda, S. (1998). The Drosophila semushi mutation blocks nuclear import of bicoid during embryogenesis. *Curr. Biol.* 8, 1277–1280. doi: 10.1016/s0960-9822(07)00538-6
- Feng, T., Deng, L., Lu, X., Pan, W., Wu, Q., and Dai, J. (2018). Ubiquitin-conjugating enzyme UBE2J1 negatively modulates interferon pathway and promotes RNA virus infection. *Virol. J.* 15:132. doi: 10.1186/s12985-018-1040-5
- Feoktistova, M., Geserick, P., and Leverkus, M. (2016). Crystal violet assay for determining viability of cultured cells. *Cold Spring Harb. Protoc.* 2016:rot087379. doi: 10.1101/pdb.prot087379
- Fraser, A. G., Kamath, R. S., Zipperlen, P., Martinez-Campos, M., Sohrmann, M., and Ahringer, J. (2000). Functional genomic analysis of *C. elegans* chromosome I by systematic RNA interference. *Nature* 408, 325–330. doi: 10.1038/35042517
- Guo, J., Chen, D., Gao, X., Hu, X., Zhou, Y., Wu, C., et al. (2017). Protein inhibitor of activated STAT2 restricts HCV replication by modulating viral proteins degradation. *Viruses* 9:285. doi: 10.3390/v9100285
- Gurer, C., Berthou, L., and Luban, J. (2005). Covalent modification of human immunodeficiency virus type 1 p6 by SUMO-1. *J. Virol.* 79, 910–917. doi: 10.1128/JVI.79.2.910-917.2005
- Hayashi, T., Seki, M., Maeda, D., Wang, W., Kawabe, Y., Seki, T., et al. (2002). Ubc9 is essential for viability of higher eukaryotic cells. *Exp. Cell Res.* 280, 212–221. doi: 10.1006/excr.2002.5634
- Johnson, E. S. (2004). Protein modification by SUMO. *Annu. Rev. Biochem.* 73, 355–382. doi: 10.1146/annurev.biochem.73.011303.074118
- Khoury, G. A., Baliban, R. C., and Floudas, C. A. (2011). Proteome-wide post-translational modification statistics: frequency analysis and curation of the swiss-prot database. *Sci. Rep.* 1:90. doi: 10.1038/srep00090
- Li, F. Q., Xiao, H., Tam, J. P., and Liu, D. X. (2005). Sumoylation of the nucleocapsid protein of severe acute respiratory syndrome coronavirus. *FEBS Lett.* 579, 2387–2396. doi: 10.1016/j.febslet.2005.03.039
- Li, P., Jing, H., Wang, Y., Yuan, L., Xiao, H., and Zheng, Q. (2021). SUMO modification in apoptosis. *J. Mol. Histol.* 52, 1–10. doi: 10.1007/s10735-020-09924-2
- Li, Q., Xiao, H., Tam, J. P., and Liu, D. X. (2006). Sumoylation of the nucleocapsid protein of severe acute respiratory syndrome coronavirus by interaction with Ubc9. *Adv. Exp. Med. Biol.* 581, 121–126. doi: 10.1007/978-0-387-33012-9_21
- Loboda, A. P., Soond, S. M., Piacentini, M., and Barlev, N. A. (2019). Lysine-specific post-translational modifications of proteins in the life cycle of viruses. *Cell Cycle* 18, 1995–2005. doi: 10.1080/15384101.2019.1639305

- Lyst, M. J., and Stancheva, I. (2007). A role for SUMO modification in transcriptional repression and activation. *Biochem. Soc. Trans.* 35(Pt 6), 1389–1392. doi: 10.1042/BST0351389
- Mukherjee, D., Das, S., Begum, F., Mal, S., and Ray, U. (2019). The mosquito immune system and the life of dengue virus: what we know and do not know. *Pathogens* 8:77. doi: 10.3390/pathogens8020077
- Roy, S. K., and Bhattacharjee, S. (2021). Dengue virus: epidemiology, biology and disease aetiology. *Can. J. Microbiol.* 67, 687–702. doi: 10.1139/cjm-2020-0572
- Salazar, M. I., Richardson, J. H., Sanchez-Vargas, I., Olson, K. E., and Beaty, B. J. (2007). Dengue virus type 2: replication and tropisms in orally infected *Aedes aegypti* mosquitoes. *BMC Microbiol.* 7:9. doi: 10.1186/1471-2180-7-9
- Sharp, T. M., Anderson, K. B., Katzelnick, L. C., Clapham, H., Johansson, M. A., Morrison, A. C., et al. (2021). Knowledge gaps in the epidemiology of severe dengue impede vaccine evaluation. *Lancet Infect. Dis.* 22, E42–E51. doi: 10.1016/S1473-3099(20)30871-9
- Shepard, D. S., Undurraga, E. A., Halasa, Y. A., and Stanaway, J. D. (2016). The global economic burden of dengue: a systematic analysis. *Lancet Infect. Dis.* 16, 935–941. doi: 10.1016/S1473-3099(16)00146-8
- Silva, A. M. N., Vitorino, R., Domingues, M. R. M., Spickett, C. M., and Domingues, P. (2013). Post-translational modifications and mass spectrometry detection. *Free Radic. Biol. Med.* 65, 925–941. doi: 10.1016/j.freeradbiomed.2013.08.184
- Sri-In, C., Weng, S. C., Chen, W. Y., Wu-Hsieh, B. A., Tu, W. C., and Shiao, S. H. (2019). A salivary protein of *Aedes aegypti* promotes dengue-2 virus replication and transmission. *Insect Biochem. Mol. Biol.* 111:103181. doi: 10.1016/j.ibmb.2019.103181
- Sri-In, C., Weng, S. C., Shiao, S. H., and Tu, W. C. (2020). A simplified method for blood feeding, oral infection, and saliva collection of the dengue vector mosquitoes. *PLoS One* 15:e0233618. doi: 10.1371/journal.pone.0233618
- Stanaway, J. D., Shepard, D. S., Undurraga, E. A., Halasa, Y. A., Coffeng, L. E., Brady, O. J., et al. (2016). The global burden of dengue: an analysis from the Global Burden of Disease Study 2013. *Lancet Infect. Dis.* 16, 712–723. doi: 10.1016/S1473-3099(16)00026-8
- Stokes, S., Almire, F., Tatham, M. H., McFarlane, S., Mertens, P., Pondeville, E., et al. (2020). The SUMOylation pathway suppresses arbovirus replication in *Aedes aegypti* cells. *PLoS Pathog.* 16:e1009134. doi: 10.1371/journal.ppat.1009134
- Su, C. I., Tseng, C. H., Yu, C. Y., and Lai, M. M. C. (2016). SUMO modification stabilizes dengue virus nonstructural protein 5 to support virus replication. *J. Virol.* 90, 4308–4319. doi: 10.1128/JVI.00223-16
- Tan, K. H., Ki, K. C., Watanabe, S., Vasudevan, S. G., and Krishnan, M. (2014). Cell-based flavivirus infection (CFI) assay for the evaluation of dengue antiviral candidates using high-content imaging. *Methods Mol. Biol.* 1138, 99–109. doi: 10.1007/978-1-4939-0348-1_7
- Urena, E., Pirone, L., Chafino, S., Perez, C., Sutherland, J. D., Lang, V., et al. (2016). Evolution of SUMO function and chain formation in insects. *Mol. Biol. Evol.* 33, 568–584. doi: 10.1093/molbev/msv242
- Varadaraj, A., Mattoscio, D., and Chiocca, S. (2014). SUMO Ubc9 enzyme as a viral target. *IUBMB Life* 66, 27–33. doi: 10.1002/iub.1240
- Wellekens, K., Bettrains, A., De Munter, P., and Peetermans, W. (2020). Dengue: current state one year before WHO 2010–2020 goals. *Acta Clin. Belg.* 77, 436–444. doi: 10.1080/17843286.2020.1837576
- Wilder-Smith, A., Ooi, E. E., Horstick, O., and Wills, B. (2019). Dengue. *Lancet* 393, 350–363. doi: 10.1016/S0140-6736(18)32560-1
- Wimmer, P., and Schreiner, S. (2015). Viral mimicry to usurp ubiquitin and SUMO host pathways. *Viruses* 7, 4854–4872. doi: 10.3390/v7092849
- Yang, Y., He, Y., Wang, X., Liang, Z., He, G., Zhang, P., et al. (2017). Protein SUMOylation modification and its associations with disease. *Open Biol.* 7:170167. doi: 10.1098/rsob.170167
- Zhu, Z., Chu, H., Wen, L., Yuan, S., Chik, K. K., Yuen, T. T., et al. (2019). Targeting SUMO modification of the non-structural protein 5 of zika virus as a host-targeting antiviral strategy. *Int. J. Mol. Sci.* 20:392. doi: 10.3390/ijms20020392

Conflict of Interest: The authors declare that the research was conducted in the absence of any commercial or financial relationships that could be construed as a potential conflict of interest.

Publisher's Note: All claims expressed in this article are solely those of the authors and do not necessarily represent those of their affiliated organizations, or those of the publisher, the editors and the reviewers. Any product that may be evaluated in this article, or claim that may be made by its manufacturer, is not guaranteed or endorsed by the publisher.

Copyright © 2022 Weng and Shiao. This is an open-access article distributed under the terms of the Creative Commons Attribution License (CC BY). The use, distribution or reproduction in other forums is permitted, provided the original author(s) and the copyright owner(s) are credited and that the original publication in this journal is cited, in accordance with accepted academic practice. No use, distribution or reproduction is permitted which does not comply with these terms.



Discovery of Tick-Borne Karshi Virus Implies Misinterpretation of the Tick-Borne Encephalitis Virus Seroprevalence in Northwest China

Yuan Bai^{1,2}, Yanfang Zhang¹, Zhengyuan Su¹, Shuang Tang¹, Jun Wang¹, Qiaoli Wu¹, Juan Yang¹, Abulimiti Moming¹, Yujiang Zhang³, Lesley Bell-Sakyi⁴, Surong Sun^{5*}, Shu Shen^{1*} and Fei Deng^{1*}

OPEN ACCESS

Edited by:

Mengji Cao,
Southwest University, China

Reviewed by:

Felfei Yin,
Hainan Medical University, China
Ali Zohaib,
Islamia University of Bahawalpur,
Pakistan

*Correspondence:

Surong Sun
sr_sun2005@163.com
Shu Shen
shenshu@wh.iov.cn
Fei Deng
df@wh.iov.cn

Specialty section:

This article was submitted to
Virology,
a section of the journal
Frontiers in Microbiology

Received: 09 February 2022

Accepted: 25 March 2022

Published: 03 May 2022

Citation:

Bai Y, Zhang Y, Su Z, Tang S, Wang J, Wu Q, Yang J, Moming A, Zhang Y, Bell-Sakyi L, Sun S, Shen S and Deng F (2022) Discovery of Tick-Borne Karshi Virus Implies Misinterpretation of the Tick-Borne Encephalitis Virus Seroprevalence in Northwest China. *Front. Microbiol.* 13:872067. doi: 10.3389/fmicb.2022.872067

¹ State Key Laboratory of Virology and National Virus Resource Centre, Wuhan Institute of Virology, Chinese Academy of Sciences, Wuhan, China, ² University of Chinese Academy of Sciences, Beijing, China, ³ Center for Disease Control and Prevention of Xinjiang Uygur Autonomous Region, Urumqi, China, ⁴ Department of Infection Biology and Microbiomes, Institute of Infection, Veterinary and Ecological Sciences, University of Liverpool, Liverpool, United Kingdom, ⁵ Xinjiang Key Laboratory of Biological Resources and Genetic Engineering, College of Life Science and Technology, Xinjiang University, Urumqi, China

Despite few human cases of tick-borne encephalitis virus (TBEV), high rates of TBEV seroprevalence were reported among humans and animals in Xinjiang Uygur Autonomous Region in Northwestern China. In this study, the Karshi virus (KSIV) was identified and isolated from *Hyalomma asiaticum* ticks in Xinjiang. It belongs to the genus *Flavivirus* of the family *Flaviviridae* and is closely related to TBEV. KSIV infects cell lines from humans, other mammals and ticks, and causes encephalitis in suckling mice. High minimum infection rates (4.96%) with KSIV were detected among tick groups. KSIV infections have occurred in sheep and marmots, resulting in antibody-positive rates of 2.43 and 2.56%, respectively. We further found that, of the KSIV antibody-positive serum samples from animals, 13.9% had TBEV exposure showing cross-reaction to KSIV, and 11.1% had KSIV infection resulting in cross-reaction to TBEV; 8.3% were likely to have co-exposure to both viruses (or may be infected with one of them and present cross-reactivity with the other). The results revealed a substantial KSIV prevalence among ticks in Xinjiang, indicating exposure of animals to KSIV and TBEV. The findings implied misinterpretation of the high rates of TBEV seroprevalence among humans and animals in previous studies. There is a need to develop detection methods to distinguish KSIV from TBEV and to perform an in-depth investigation of KSIV and TBEV prevalence and incidence in Northwestern China, which would enhance our preparation to provide medical treatment of emerging diseases caused by tick-borne viral pathogens such as KSIV.

Keywords: Karshi virus, tick-borne encephalitis virus, prevalence, serological correlation, cross-reaction

INTRODUCTION

Ticks are blood-sucking arthropods and vectors of viral pathogens causing diseases in animal hosts and humans. Located in the Northwest of China, Xinjiang Uygur Autonomous Region is the habitat of 49 tick species (Zhang et al., 2019), and is known as a natural focal point of tick-borne viral diseases, such as Crimean–Congo haemorrhagic fever and tick-borne encephalitis (CCHF and TBE, also known in China as Xinjiang Haemorrhagic Fever and Forest Encephalitis, respectively). The first record of a CCHF outbreak occurred in Bachu County of Xinjiang in 1965, resulting in a fatality rate of up to 50% (Papa et al., 2002). Since then, outbreaks and sporadic cases among the residents were reported from different areas of Xinjiang. Although no cases have been further reported after 2003, the causative agent, Crimean–Congo haemorrhagic fever virus, could be persistently detected and isolated from ticks collected in different locations there (Sun et al., 2009; Guo et al., 2017; Moming et al., 2018; Zhang et al., 2018). While there were very few cases of TBE disease diagnosed in Xinjiang, serological evidence revealed that the residents had tick-borne encephalitis virus (TBEV) exposure (Zhang et al., 2013). High positive rates of TBEV were detected from the ticks *Ixodes persulcatus* (minimum infection rate: 14.3–47.7%) and *Dermacentor silvarum* (minimum infection rate: 0.01–1.67%) in Xinjiang, where both Siberian and Far Eastern TBEV strains were isolated from these two tick species (Xie et al., 1991; Wang H. et al., 2015; Liu et al., 2016; Zhang G. et al., 2017). These studies showed substantial prevalence of Crimean–Congo haemorrhagic fever virus and TBEV, which posed persistent risks from virus transmission and infection to humans and animals in Northwestern China.

Novel tick-borne viruses (TBVs) have been discovered and isolated from ticks in Xinjiang in the recent decade. Guertu virus (GTV, belonging to the genus *Bandavirus* in the family *Phenuiviridae*) was isolated from *Dermacentor nuttalli* and was considered a potential pathogen, as evidenced by local people having neutralizing antibodies to this virus (Shen et al., 2018). Tamdy virus (TAMV, belonging to the genus *Orthonairovirus* in the family *Nairoviridae*) was detected and isolated from *Hyalomma asiaticum* in Xinjiang and might be related to a local disease outbreak among humans as early as 1997 (Moming et al., 2021). A variety of novel viruses was found in ticks by next-generation sequencing (Li et al., 2015); however, risks of their transmission from ticks to humans and other animals were unclear. Recently, one of these viruses identified by sequencing, Tacheng tick virus (TcTV-1), was identified as the causative agent of fever in a patient in Xinjiang (Liu et al., 2020). This raised concern about the medical significance of novel TBVs and suggested the urgent need to identify novel tick-borne viral pathogens and to perform further in-depth surveys on the prevalence and potential threats of TBVs in Xinjiang, China.

Tick-borne encephalitis virus is the representative virus of the “TBEV serocomplex” group in the genus *Flavivirus*, family *Flaviviridae*. This group is composed of the TBEV-related viruses transmitted by ticks, including the human disease-related pathogens TBEV, Omsk haemorrhagic fever virus, Powassan

virus and Kyasanur Forest disease virus, and zoonotic pathogens such as louping ill virus, Langat virus, and Royal Farm virus (Grard et al., 2007). Karshi virus (KSIV), which was firstly isolated from soft ticks from Uzbekistan in 1972 (Lvov et al., 1976), also belongs to this group and is genetically related to TBEV. However, its prevalence among ticks and pathogenicity for domestic animals and humans remained unclear.

In this study, KSIV was identified in and isolated from *Hy. asiaticum* ticks in Xinjiang, China. We characterized the etiological characteristics of KSIV and the pathogenesis in mice and evaluated its potential to infect humans and other animals by surveying KSIV prevalence among ticks and serological exposure in animals. Moreover, serological cross-reaction between KSIV and TBEV was demonstrated using laboratory-prepared polyclonal antibodies and serum samples from domestic and wild mammals. The results revealed a substantial prevalence of KSIV in ticks and the occurrence of KSIV infection among animals, which suggested the threat of KSIV spillover from ticks and animal hosts to humans. The serological cross-reactivity between these two viruses raised the need to develop detection methods to distinguish KSIV from TBEV, which would facilitate follow-up investigations of these two viruses and promote subsequent evaluation of the threat from KSIV infection to humans in Northwestern China.

MATERIALS AND METHODS

Viruses and Cell Lines

The detailed information regarding human, other mammal, tick and mosquito cell lines used in this study, and the TBEV strain NM-Tick-2020 used to investigate its serological correlation with KSIV, are described in **Supplementary Material**.

Tick Collection and Viral Metagenomics Analysis

Ticks were collected from vegetation at fourteen sites in cities and counties of Xinjiang during 2016–2017. Tick species were identified by PCR amplification of a partial sequence of the ribosome Internal Transcribed Spacer 2 (ITS2) and confirmed by Sanger sequencing as previously described (Ya et al., 2016). These ticks were grouped ($n = 50$ –100/group) according to species and sampling locations. Clarified homogenates of each tick group were prepared and inoculated into Kunming suckling mice (1–2 days old) by both intraperitoneal and intracranial routes as previously described (Deng et al., 2007). Diseased mice were sacrificed, and their brains were collected and preserved in glycerine at -80°C until further examination. Homogenates of the brain tissue from one diseased mouse randomly selected from a group were prepared and sub-packaged as described (Zhang Y. et al., 2017). Total RNA was purified from the brain homogenates (300 μL) and subsequently applied for next-generation sequencing (RNAseq) using the Illumina Hiseq 3000 platform according to the manufacturer's instructions (Illumina, San Diego, CA, United States). The sequencing data was subjected to quality control (FastaQC,

Trimmomatic), then the Trinity (Version 2.5) program was used for sequence assembly and splicing. BLASTn and BLASTx comparisons were performed to discover and annotate virus-related sequences.

Virus Isolation, Infection Assays, and One-Step Growth Curve Analyses

The KSIV-positive brain homogenates (200 μ L) from a diseased mouse were diluted and incubated with BHK-21 cells. Further subculture was performed for four generations as previously described (Zhang Y. et al., 2017). To obtain the 5' and 3' ends of the KSIV genomic sequence, rapid amplification of cDNA ends (RACE) was performed with specific primers using a SMARTer RACE cDNA Amplification Kit (Takara, Kusatsu, Japan). Virus infection in cells was examined by immunofluorescence assay (IFA; **Supplementary Material**), and plaque assay was performed as previously described (De Madrid and Porterfield, 1969). The KSIV particles were purified from cell culture supernatants and were visualized using a transmission electron microscope (TEM, Tecnai G2 20 TWIN, United States) as previously described (Zhang Y. et al., 2017). Sections of BHK-21 cells infected with KSIV were prepared and examined by TEM to visualize the intracellular distribution of KSIV (Moming et al., 2021).

The KSIV infection assays on human, other mammal, tick and mosquito cell lines were performed at a dose of 1 multiplicity of infection (MOI) unit per cell as previously described (Shen et al., 2018). IFAs were performed to examine KSIV infection in cells at 48 h post-infection (h p.i). KSIV growth properties were characterized by one-step growth curve analysis in SH-SY5Y, SW-13, and BHK-21 cells as previously described (Dai et al., 2018), and titers were determined by end-point dilution assays on BHK-21 cells.

Animal Experiments

To investigate KSIV pathogenesis, adult mice and suckling mice were inoculated with KSIV and monitored for signs of disease onset and changes in body weight as well as survival rates. Tissues were harvested from suckling mice after KSIV infection. A qRT-PCR was performed to quantify KSIV RNA copies in tissues. H&E staining, immunohistochemical assays and IFAs were performed on tissue sections to characterize KSIV infection in the brains of suckling mice. The processes of each assay are detailed in **Supplementary Material**.

Serological Tests for Karshi Virus Among Domestic and Wild Animals

Serum samples collected from sheep and small mammals in Xinjiang during 2006–2015 were archived in the National Virus Resource Center, Wuhan. IFAs were performed to determine the antibody response to KSIV among the samples. The IFA-positive sera were further verified by western blot using purified KSIV particles. The levels of antibody response to E protein domain III (E-DIII) of KSIV were measured by Luciferase Immunoprecipitation System (LIPS) assays. Neutralizing activity of the antibody-positive serum samples against KSIV was determined by virus

neutralization test (VNT). All the above methods are detailed in the **Supplementary Material**.

Analyses of Serological Cross-Reactivity Between Karshi Virus and Tick-Borne Encephalitis Virus

Immunofluorescence assay (IFAs) were carried out to determine the efficiencies of polyclonal antibodies, prepared in-house against KSIV E protein (α -KSIV-E) and TBEV E protein (α -TBEV-E), reacting to BHK-21 cells infected with each of the two viruses. Images were captured and reaction efficiency values were expressed as the percentage of Harmony High-Content Imaging and Analysis Software-defined (PerkinElmer, Inc., United States) fluorescence-labeled cells among the total number of cells in each test for each of the dilutions. The 50 and 90% detection efficiencies (DE_{50} and DE_{90}) of α -KSIV-E and α -TBEV-E in reaction to KSIV and TBEV antigens were calculated, respectively, using the least square fitting method in GraphPad Prism (Version 8).

Cross-neutralization between KSIV and TBEV was characterized by performing virus neutralization tests using KSIV- or TBEV- inoculated mouse serum. The neutralizing serum dilution was determined as an antibody titer that inhibited 50 and 90% of viral infection (VNT_{50} and VNT_{90}).

The serological reaction of field-collected KSIV antibody-positive serum samples to TBEV antigens were further investigated by IFAs, western blot, and LIPS as well as neutralization assays against TBEV. All the above-mentioned materials and methods are detailed in the **Supplementary Material**.

Sequencing, Bioinformatics, and Data Analysis

The complete genome sequence of KSIV strain WJQ-16209 [GenBank No: MH688511; China National GeneBank DataBase (CNCBdb) No: CNP0002450], and partial sequences representing other KSIV strains (GenBank Nos: OL699896–OL699904, MH688625, and MH688632) detected in ticks by RT-PCR were deposited in CNCBdb or GenBank. The data resulting from RNAseq of the brain homogenates from diseased mice were deposited in the CNCBdb (No: CNP0002610).¹

All sequence alignments were performed using MEGA X. The phylogenetic tree of flaviviruses was built based on the full-length nucleic acid sequence of the open reading frame (ORF) and the partial sequences (302 nucleotides, nt) of the NS5 protein sequence using the maximum likelihood method with a bootstrap value of 1,000. The alignment of E proteins of KSIV (KSIV-E) and TBEV (TBEV-E) was illustrated using ESPript 3.0² to predict the secondary structure of KSIV-E according to that of TBEV-E. The predicted three-dimensional (3D) structure of KSIV-E protein was constructed using I-TASSER (Zheng et al., 2021) and visualized using PymolTM (version 1.4.1). The significant

¹<http://db.cngb.org/cnsa/project/CNP0002610/reviewlink/>

²<https://esprict.ibcp.fr/ESPript/ESPript/>

difference of data between groups was calculated using Student's *t*-test.

Biosafety and Ethics

The *in vitro* and *in vivo* experiments involving KSIV were conducted in a Biosafety Level 2 (BSL-2) laboratory and an Animal Biosafety Level 2 (ABSL-2) laboratory, respectively, while the *in vitro* and *in vivo* experiments involving TBEV were conducted in BSL-3 and ABSL-3 laboratories, according to the Directory of Pathogenic Microorganisms Transmitted among Humans issued by the Chinese Ministry of Health.³ Animal experiments were approved by the ethics committee of Wuhan Institute of Virology, Chinese Academy of Sciences under the approval numbers WIVA33201901 and WIVA33202108.

RESULTS

Karshi Virus Was Identified in and Isolated From *Hyalomma* Ticks in Xinjiang, China

A total of 31,542 ticks were collected, including the species *Hyalomma detritum*, now reclassified as *Hyalomma scupense* (Apanaskevich et al., 2010; *n* = 326), *Hy. asiaticum* (*n* = 8,741) and *D. nuttalli* (*n* = 22,475). To isolate viruses from ticks, the clarified homogenates prepared from tick groups were inoculated into suckling mice, which were monitored for disease onset within 14 days after inoculation. One group of mice, which were inoculated with the homogenates from a group of *Hy. asiaticum* ticks (*n* = 400) collected from Wujiaqu City in 2016, developed clinical illness. Brains were harvested from diseased mice and homogenized for the second round of inoculation, during which illness among suckling mice was still noted, suggesting potential pathogen(s) might be isolated and could be effectively passaged among generations of suckling mice. Subsequently, a total number of non-redundant 92,253,190 reads were obtained by RNAseq from one diseased mouse brain in the second round of inoculation. The sequence comparison analysis showed that 37,872 reads were closely related to the flavivirus KSIV, which had never before been found in China. KSIV RNA present in the brain of the diseased mice was confirmed by RT-PCR on the rest of the homogenates (data not shown). The homogenate of this KSIV-positive brain sample was diluted and further incubated with BHK-21 cells. As suggested by the results of IFAs, KSIV was isolated and amplified after passages on BHK-21 cells, as increasing infection levels were observed in cells from the first passage (P1) to the fourth (P4) (Figure 1A). KSIV infection could also induce plaque formation in BHK-21 cells (Figure 1B). The TEM analysis showed that KSIV is an enveloped particle with a diameter of approximately 50 nm (Figure 1C). KSIV particles were mainly located in cytoplasmic vesicles of BHK-21 cells (Figure 1D). The full-length genomic sequence of a new KSIV strain (10,828 nt), which contains a polyprotein ORF (10,251 nt), was obtained by sequence assembly based on the

KSIV-related reads together with the result from RACE. This new strain clusters with three other KSIV strains reported from Central Asian countries (Supplementary Figure 1), and shares 85.7–86.9% nucleotide sequence identity and 94.5–95.1% amino acid similarity to them (Supplementary Table 1). It was therefore designated as strain WJQ16209 by following the year and location of tick sampling. As a member of the TBEV serocomplex group belonging to the genus *Flavivirus* in the family *Flaviviridae*, the polyprotein ORF of KSIV strain WJQ16209 has 69.7–71.7% amino acid and 67.1–67.9% nucleotide identity to those of other viruses in this group, with the highest to that of TBEV (67.9% for nucleotide and 71.1% for amino acid sequences) (Supplementary Table 1).

Human, Other Mammal, Tick, and Mosquito Cell Lines Had Different Levels of Susceptibility to Karshi Virus

As evidenced by the green fluorescent foci present in infected cells in IFAs at 48 h p.i (Figure 2A), KSIV can infect human cell lines, resulting in high efficiencies in neuroblastoma cells (SH-SY5Y), adrenocortical carcinoma cells (SW-13) and liver hepatocellular carcinoma cells (HepG2) and lower efficiency in HEK293 (embryonic kidney cells) and U-87 MG (malignant glioblastoma cells) (Figure 2A, upper panel). KSIV can infect other mammalian cell lines including Vero (monkey), MDOK (sheep), and DH82 (dog) (Figure 2A, middle panel). However, the infection efficiencies in these cells were lower than in BHK-21 (hamster), which had green fluorescence in almost all cells, while KSIV infection was not detected in the bovine cell line (MDBK) (Figure 2A, middle panel). Since KSIV was isolated from *Hy. asiaticum* ticks, its infection in tick cells was characterized using the HAE/CTVM9 (*Hyalomma anatolicum*) and IDE8 (*Ixodes scapularis*) cell lines. At 48 h p.i., green fluorescence was observed in IDE8 but not in HAE/CTVM9, suggesting that the cells from different tick species may have different susceptibility or infection efficiency to KSIV (Figure 2A, bottom panel). In addition, KSIV infection was not observed in the mosquito cell line C6/36 (Figure 2A, bottom panel).

Furthermore, KSIV could replicate efficiently to generate progeny viruses from SW-13, SH-SY5Y, and BHK-21 cells. The virus titer in culture supernatants reached a peak at 24 h p.i. for BHK-21 ($4.97 \pm 1.13 \times 10^8$ TCID₅₀/mL) and SW-13 ($2.42 \pm 1.42 \times 10^8$ TCID₅₀/mL), while the virus titer was increasing for SH-SY5Y ($2.20 \pm 0.22 \times 10^8$ TCID₅₀/mL) until 48 h p.i (Figure 2B).

Karshi Virus Causes Fatal Encephalitis in Suckling Mice

In an attempt to investigate KSIV pathogenesis, 6-week-old C57BL/6 mice were inoculated with KSIV. However, these mice did not subsequently display any sign of illness, nor any effect on body weight (data not shown). Then, 2- and 9-day-old suckling mice were inoculated with KSIV (Figure 3). The 2-day-old mice showed signs of neurological symptoms, such as drowsiness, stroke and paralysis 3 days after infection (D3), and death occurred on D7. The 9-day-old mice displayed onset of

³<http://www.nhc.gov.cn/wjw/gfxwj/201304/64601962954745c1929e814462d0746c.shtml>

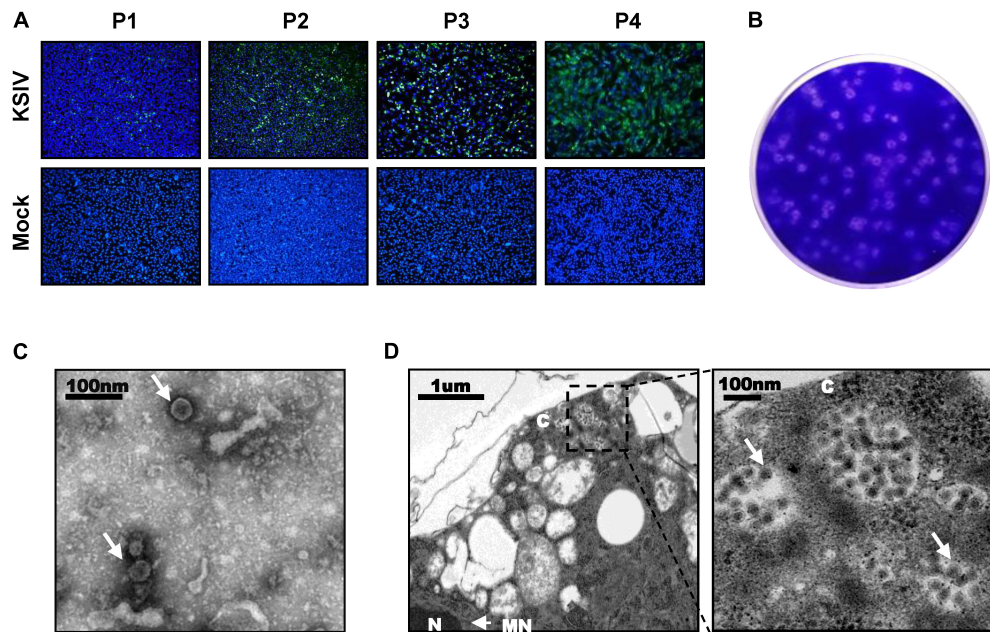


FIGURE 1 | Karshi virus (KSIV) isolation, characteristics and analysis of viral particles. **(A)** Immunofluorescence assays to survey KSIV isolation in BHK-21 cells. The images were taken from different passages showing KSIV proliferation. Cells were immunostained and green fluorescence indicates the cells infected by KSIV. P1, the first passage; P2, the second passage; P3, the third passage; P4, the fourth passage. **(B)** Plaque assay to verify KSIV isolation in BHK-21 cells with the P4 supernatants. Cells were stained with crystal violet to show plaques at 3 days post-infection. **(C)** TEM analysis of KSIV particles purified from supernatants harvested from BHK-21 cells infected with KSIV at 3 days post-infection. The clarified supernatants were subjected to ultracentrifugation. The fractions containing viral particles were harvested and used in negative-staining. **(D)** The image obtained by TEM shows that virus particles were located in the cytoplasm of infected BHK-21 cells. The enlarged area on the right shows groups of virus particles (arrow). N, nucleus; C, cytoplasm; NM, nuclear membrane.

illness from D5, and death occurred on D8. None of these mice survived the KSIV infection (**Figure 3A**), and their body weight decreased after onset of illness (**Figure 3B**).

Karshi virus infection in the mouse tissues was determined on D6 and D8. The 2-day-old mice had higher viral loads in all tested tissues than the 9-day-old mice (**Figures 3C,D**). For the 2-day-old mice, viral loads significantly decreased in the liver, spleen, and kidney from D6 to D8 ($p < 0.05$), while the decrease was not significant in the heart and lung (**Figure 3C**). In 9-day-old mice, viral loads significantly decreased in the liver, spleen, lung, and kidney from D6 to D8 ($p < 0.05$ or $p < 0.01$), while the decrease in the heart was not significant (**Figure 3D**). In contrast to the decreased viral loads in these tissues, a significant increase in virus load was observed in the brain from both 2- and 9-day-old mice ($p < 0.05$), suggesting KSIV proliferation in the brain of suckling mice (**Figures 3C,D**).

Pathological lesions in the brains of diseased suckling mice were characterized by H&E staining. The 2-day-old mice with KSIV infection developed herniation in a large area of the thalamus on D6 and D8, which showed severe tissue oedema, and nuclear pyknosis in neuronal nuclei. The 9-day-old mice also developed brain herniation in restricted regions of the thalamus on D8; however, they had slight brain tissue oedema and inflammatory infiltration (**Figure 3Ea**). The prosencephalon had severe brain tissue porosity, oedema, pyknosis, and necrosis of neuronal nuclei in 2-day-old mice on D6, and the lesion deteriorated further on D8. However, despite inflammatory cell

infiltration being observed in prosencephalon for the 9-day-old mice, the lesions seemed to be less severe than those in the 2-day-old mice (**Figure 3Eb**). In the hippocampus, inflammatory cell infiltration and necrosis of nerve cells were observed to be more severe in the 2-day-old mice than the 9-day-old mice, and the lesions further deteriorated from D6 to D8 (**Figure 3Ec**). Generally, the 2-day-old mice had more severe pathological changes due to KSIV infection in the thalamus, forebrain, and hippocampus of the brain than the 9-day-old mice. Furthermore, the results of IFA assays with the mouse brain sections revealed KSIV infection in several neurons in brain tissues of the 2- and 9-day-old mice on D8, suggesting that neurons are the targets of KSIV infection *in vivo* (**Figure 3F**).

Molecular Prevalence of Karshi Virus Among Ticks and Seroprevalence Among Animals in the Field Suggesting Karshi Virus Spillover From Ticks to Animal Hosts

KSIV prevalence was investigated among 363 groups of ticks, of which 18 groups were identified as KSIV RNA positive (the minimum infection rate was 4.96%) (**Table 1** and **Figure 4**). Two of the seven *Hy. detritum* tick groups from Fuhai County were positive for KSIV RNA, resulting in a high minimum infection rate of 28.57%. Among *Hy. asiaticum* ticks, KSIV RNA was detected in 10 (8.77%) of the 114 groups, of which the ticks

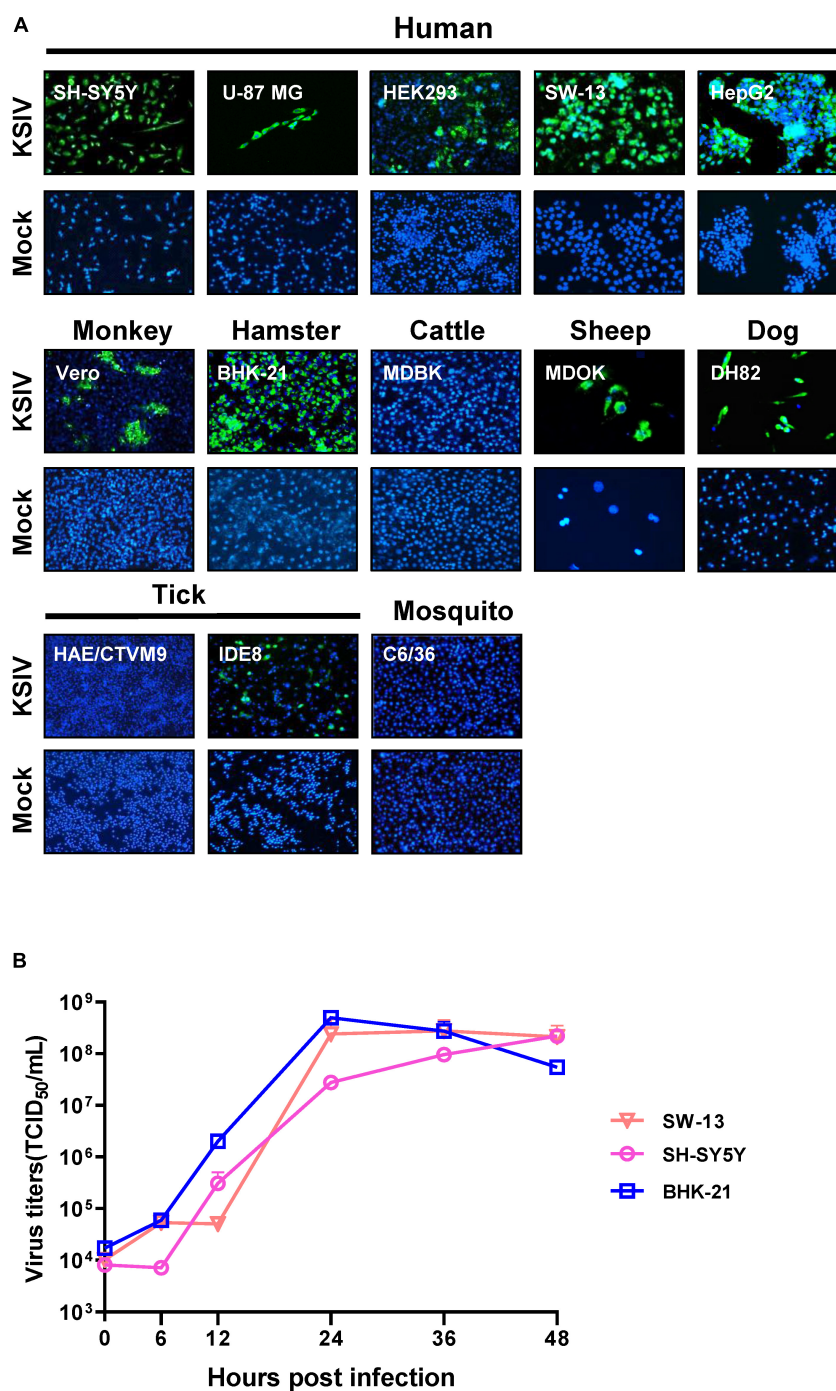


FIGURE 2 | The susceptibility of cell lines derived from different hosts to KSIV and viral one-step growth curve test. **(A)** Cell lines derived from humans (SH-SY5Y, U-87 MG, SW-13, HEK293 and HepG2), other mammals (Vero, BHK-21, MDBK, MDOK, and DH82), mosquito (C6/36) and ticks (HAE/CTVM9 and IDE8) were infected with KSIV at MOI of 1. The cells were cultured for 48 h and examined by immunofluorescence for KSIV E protein. KSIV infection was detected in all cell lines except MDBK, HAE/CTVM9 and C6/36. **(B)** The viral one-step growth curve in various cell lines. BHK-21 cells were infected with KSIV at an MOI of 5 and the supernatant for collected infection of cell lines of different species: human (SH-SY5Y, SW13) and hamster (BHK-21), virus titers were measured by end-point dilution assays.

from Luntai had the highest minimum infection rate (two groups, 22.22%), followed by those from Wujiaqu (three groups, 21.43%), Minfeng (two groups, 14.29%), Yuli (one group, 7.15%), and

North of Usu (two groups, 6.25%). In contrast, KSIV RNA was not detected among *Hy. asiaticum* ticks from Yutian, Karamay, Beitun, Mulei, or Fukang. Among *D. nuttalli* ticks, 6 of the 242

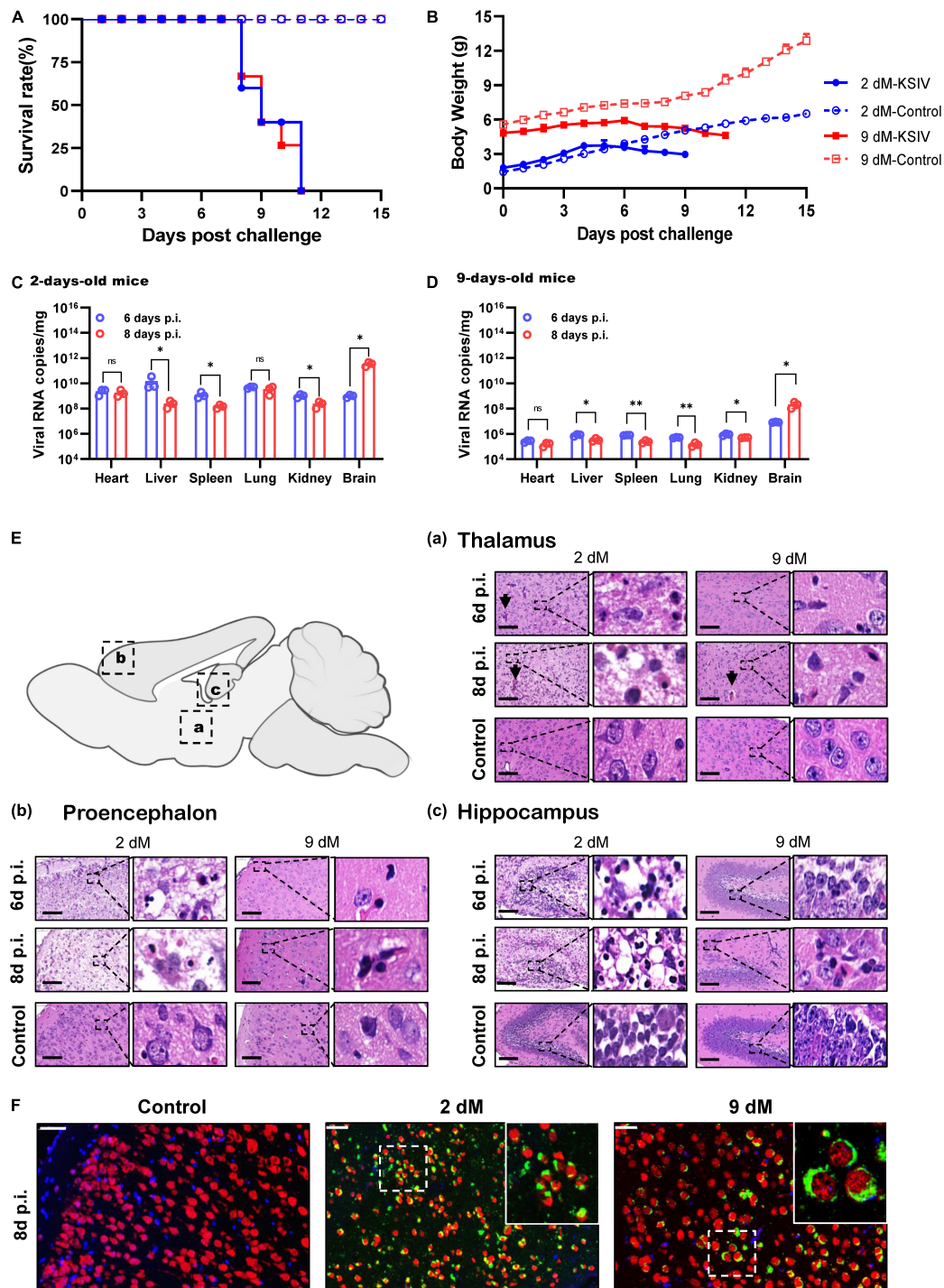


FIGURE 3 | The pathogenicity of KSV infection in 2- and 9-day-old suckling C57BL/6 mice. The 2- and 9-day-old suckling C57BL/6 mice (2- and 9-dM) were inoculated with KSV intracranially (1×10^4 PFU) and intraperitoneally (2×10^4 PFU) and monitored for clinical symptoms and mortality over 15 days. **(A)** Survival analysis of mice infected with KSV. **(B)** Bodyweight changes of mice infected with KSV. Mice were inoculated with KSV and different tissues were collected at 6- and 8-days post inoculation ($n = 3/\text{group}$) to enable comparisons of virus loads between the 2-day-old **(C)** and the 9-day-old **(D)** infected mice groups. For each time point, the measured values are the average of three mice. Error bars represent standard deviations. Data shown are pooled from three independent experiments. n.s. indicates no significant difference, $*p < 0.05$, $**p < 0.01$. **(E)** H&E staining of brains from 2- to 9-day-old KSV-infected and uninfected suckling mice. At 6- and 8-days post inoculation, mice were euthanized, and brains were H&E stained. Representative images of the brain from **(a)** thalamus, **(b)** prosencephalon, and **(c)** hippocampus. Scale bars represent 100 μm . The enlarged images of interest show details demonstrating inflammation and neuronal necrosis. **(F)** Double immunofluorescence staining was performed on mouse brain sections from 2- to 9-day-old mice 8 days after KSV infection, and on uninfected mice. The mature neurons were marked with red fluorescence (Alexa Fluor 555), KSV antigens were stained with green fluorescence (Alexa Fluor 488), and the nuclei were stained with Hoechst 33258.

groups (the minimum infection rate was 2.48%) were positive for KSIV RNA, including two groups from North of Jinghe (5.26%) and four groups from South of Usu (3.92%), while among the 102 groups from the South of Jinghe, KSIV was not detected (Table 1). The partial sequences of NS5 (302 nt) were used to construct a phylogenetic tree, which showed that all the KSIV sequences in Xinjiang clustered together with the new isolate KSIV-WJQ16209 (Supplementary Figure 2).

Subsequently, KSIV seroprevalence was investigated among domestic (sheep) and wild (marmot, great gerbil and long-tailed ground squirrel) animals (Table 2). Of the serum samples from 329 sheep, only eight (2.43%) samples were anti-KSIV antibody-positive as evidenced by IFA. However, these eight samples were not identified as positive either by western blot, which was performed using the linearized viral proteins from purified KSIV particles, or by LIPS assays, which were conducted using the KSIV E-DIII. This difference could have resulted from using different antigens or from different sensitivities in detecting antibodies by these methods. Nevertheless, one of the eight IFA-positive samples from sheep showed neutralizing activity against KSIV (0.54% of the total number of sheep tested), resulting in a neutralizing titer of 2^6 , which confirmed that KSIV infection had occurred among sheep in Qitai in 2014 (Table 2). Of the 1,098 serum samples tested from wild animals, 28 samples (2.56%) were antibody positive by IFA, among which 10 samples (0.91%) were confirmed as having antibody responses to linearized KSIV antigens by western blot and the E-DIII of KSIV by LIPS assays, respectively (Table 2). Furthermore, seven samples (0.64%) had neutralizing activity against KSIV with the titers ranging from 2^4 to 2^6 . All the 28 antibody-positive samples were derived from marmots, including 15 collected from Aheqi in 2006 and 13 from Wujiaqu in 2015 (Table 2), whereas none of the tested samples from great gerbil or long-tailed

ground squirrel were positive. The results demonstrated evidence of serological exposure to KSIV among marmots as early as 2006 in Xinjiang.

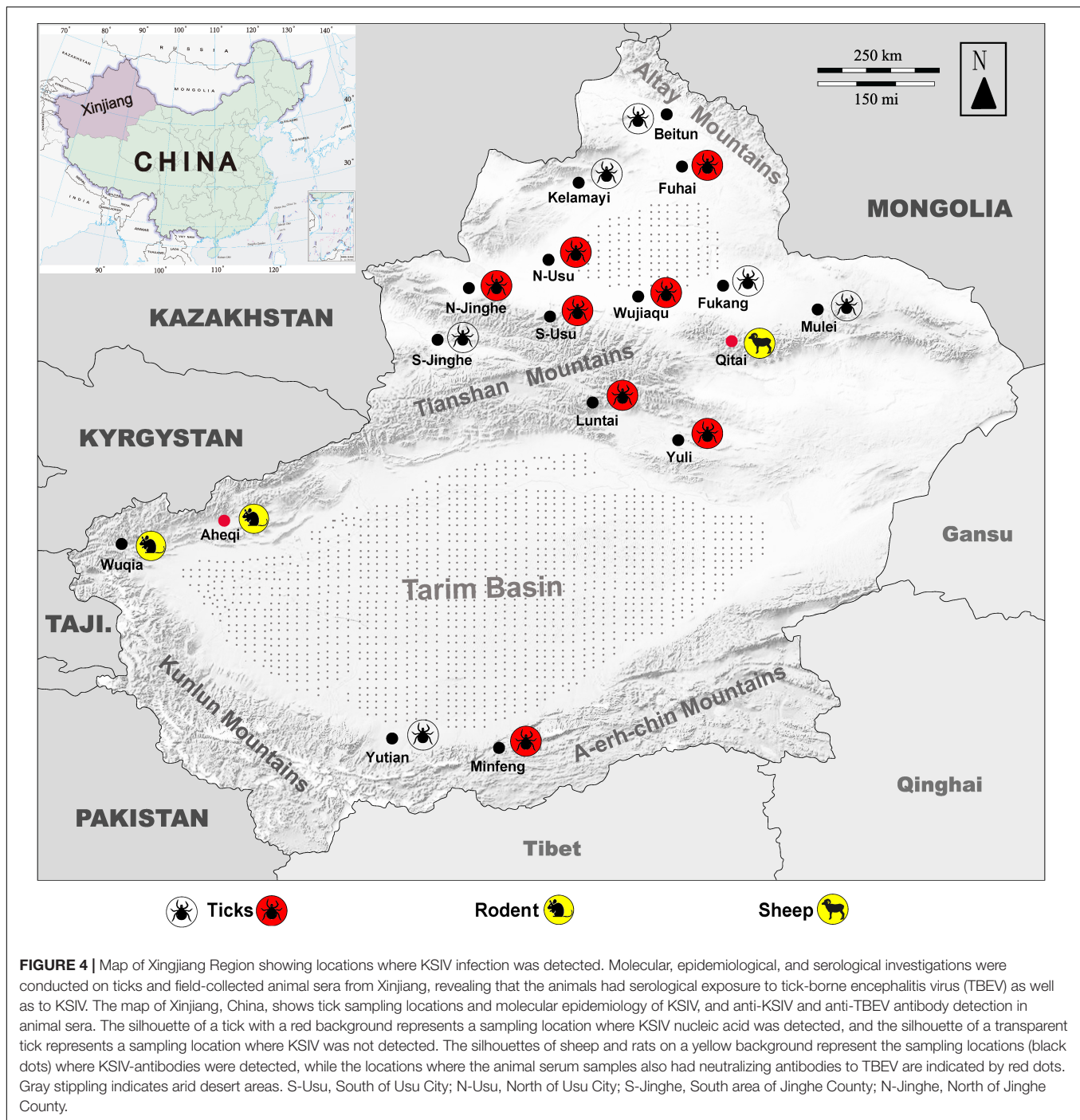
Karshi Virus Has Serological Cross-Reactivity With Tick-Borne Encephalitis Virus

The KSIV E protein (KSIV-E) shares 78.3% amino acid sequence identity with TBEV E protein (TBEV-E) (Supplementary Table 1). KSIV-E may have protein structural properties similar to TBEV-E according to the sequence alignment and structure prediction. Like TBEV-E, it has the conserved flavivirus fusion loop “DRGW” and could be divided into four functional domains I, II, III, and IV (Supplementary Figure 3A). It has six disulfide bridges linked by cysteines at conserved positions. The secondary structure of KSIV-E contains 31 β -sheets, 7 η -helices, and 7 α -helices, which is very similar to that of TBEV-E which contains 31 β -sheets, 7 η -helices, and 8 α -helices (Supplementary Figure 3B). Moreover, KSIV-E has a predicted 3D structure similar to that of TBEV (root mean square deviation: 0.225 Å) (Supplementary Figure 3C). All these findings suggested that KSIV-E and TBEV-E have a similar mode of function as well as protein antigenicity, further indicating that there may be a serological association between KSIV and TBEV.

As expected, the lab-prepared polyclonal antibody, α -KSIV-E, could efficiently recognize KSIV antigen, resulting in a DE_{50} of $11,116.7 \pm 116.8$ and DE_{90} of $6,175.7 \pm 421.8$, while its recognition of TBEV antigen was significantly reduced (DE_{50} : $4,578.0 \pm 847.8$, $p < 0.05$; DE_{90} : $1,787.3 \pm 828.0$, $p < 0.001$; Figure 5A). Moreover, antibody α -TBEV-E could recognize both TBEV and KSIV antigens, but with efficiency to KSIV (DE_{50} and DE_{90} : $2,314.7 \pm 115.0$ and $1,121.6 \pm 84.4$) significantly lower than

TABLE 1 | Prevalence of Karshi virus (KSIV) among groups of *Hyalomma detritum*, *Hyalomma asiaticum*, and *Dermacentor nuttalli* ticks collected from vegetation in Xinjiang.

Tick species	Location	Ticks (n)	Tick groups	KSIV RNA-positive groups	Minimum infection rate (%)
<i>Hyalomma detritum</i>	Fuhai County	326	7	2	28.57
Subtotal		326	7	2	28.57
<i>Hyalomma asiaticum</i>	Luntai County	750	9	2	22.22
	Wujiaqu City	1,102	14	3	21.43
	Minfeng County	1,500	14	2	14.29
	Yuli County	1,100	14	1	7.15
	North of Usu City	2,300	32	2	6.25
	Yutian County	103	2	0	0
	Karamay City	783	11	0	0
	Beitun County	70	1	0	0
	Mulei County	560	8	0	0
	Fukang City	473	9	0	0
Subtotal		8,741	114	10	8.77
<i>Dermacentor nuttalli</i>	North of Jinghe County	3,700	38	2	5.26
	South of Usu City	9,245	102	4	3.92
	South of Jinghe County	9,530	102	0	0
Subtotal		22,475	242	6	2.48
Total		31,542	363	18	4.96



to TBEV (DE_{50} and DE_{90} : $12,984.0 \pm 969.7$ and $6,373.7 \pm 522.2$) ($p < 0.001$; **Figure 5B**). Therefore, the anti-serum prepared in the lab against KSIV-E cross-reacted with TBEV, and vice versa, which confirmed the serological relationship between these two viruses.

The serological cross-reactivity between KSIV and TBEV was further demonstrated by determining neutralizing activities of the serum samples from KSIV- or TBEV-infected mice. The serum samples from KSIV-infected mice could effectively

neutralize KSIV, resulting in VNT_{50} of 130.1 ± 18.9 and VNT_{90} of 65.8 ± 10.9 . These serum samples could also neutralize TBEV infection, resulting in significantly reduced titers of VNT_{50} (15.8 ± 2.8) and VNT_{90} (10.64 ± 2.1) ($p < 0.001$; **Figures 5C,D**). This was similar to the serum samples from TBEV-infected mice, which could effectively neutralize TBEV ($VNT_{50} = 262.0 \pm 71.9$; $VNT_{90} = 104.0 \pm 22.4$) and could cross-neutralize KSIV with reduced efficiency ($VNT_{50} = 19.3 \pm 1.5$; $VNT_{90} = 12.3 \pm 1.1$) ($p < 0.05$; **Figures 5E,F**).

TABLE 2 | Seroprevalence of antibodies to KSIV among domestic and wild animals in Xinjiang.

Animal	Year	Location	Serum samples	Positive sample number and rates, <i>n</i> (%)			VNT number, rates and titer <i>n</i> , (%), (titer)
				IFA	WB	LIPS	
Domestic animals							
Sheep	2014	Qitai County	183	8 (4.37)	0	0	1 (0.54, 2 ⁴)
		Yuepuhu County	72	0	0	0	0
	2015	Shawan County	74	0	0	0	0
Subtotal			329	8 (2.43)	0	0	1 (0.30, 2 ⁴)
Wild animals							
Marmot	2006	Aheqi County	308	15 (4.87)	2 (0.65)	10 (3.3)	7 (0.23, 2 ⁴ –2 ⁶)
	2014	Wenquan County	61	0	0	0	0
	2015	Wuqia County	306	13 (4.25)	8 (2.61)	0	0
Great gerbil	2008	Hetian County	59	0	0	0	0
Long-tailed ground squirrel	2014	Yiwu County	364	0	0	0	0
Subtotal			1098	28 (2.56)	10 (0.91)	10 (0.91)	7 (0.64, 2 ⁴ –2 ⁶)
Total			1427	36 (2.52)	10 (0.07)	10 (0.07)	8 (0.06, 2 ⁴ –2 ⁶)

IFA, immunofluorescence assays; WB, western blot assays; LIPS, luciferase immunoprecipitation system detection assays; VNT, virus neutralization test assays.

Animals in Xinjiang Had Serological Exposure to Tick-Borne Encephalitis Virus as Well as to Karshi Virus

Based on the above results, we speculated that the KSIV-antibody-positive serum samples from animals might cross-react with TBEV. The thirty-six KSIV antibody-positive serum samples and three randomly selected negative serum samples were used to detect antibody reaction with TBEV by IFAs, western blot and LIPS assays as well as by virus neutralization assays to evaluate cross-neutralization of TBEV. The three KSIV-negative samples were still negative with TBEV (**Supplementary Figure 4**). Twenty-five (64.9%) of the 36 KSIV-antibody-positive samples had antibody responses to TBEV by IFA, among which 14 samples (38.9%) were confirmed as having antibody responses to linearized TBEV antigens by western blot and seven (19.4%) having a response to the E-DIII of TBEV by LIPS assays, respectively (**Table 3** and **Supplementary Figure 4**). Furthermore, eight (32%) of the twenty-five TBEV antibody-positive serum samples had neutralizing activity against TBEV, resulting in titers ranging from 2³ to 2⁸; these samples comprised four from marmot in Aheqi and four from sheep in Qitai (**Table 3** and **Supplementary Table 2**). These results indicated that infection with KSIV or TBEV, or with both viruses, could have occurred in these animals.

Based on the detailed results of detecting antibody reaction to TBEV among the 36 KSIV antibody-positive animal serum samples as listed in **Supplementary Table 2**, we proposed that at least five samples (one from marmot and four from sheep) were more likely to have been exposed to TBEV than to KSIV. First, regarding the neutralization activity against TBEV of the five samples, one (11–107) had a neutralizing titer to TBEV higher than to KSIV, and four (6–59, 7–334, 7–168, and 7–177) had neutralizing activity against TBEV but not against KSIV. Second, regarding the fold changes of the light units normalized to the cut-off value by LIPS, which represented the levels of an antibody reacting to E-DIII of the respective virus, three of the five samples

(6–59, 7–334, and 7–168) were antibody-positive for TBEV but negative for KSIV. One (11–107) had a two-fold higher level of antibody reaction to TBEV than to KSIV. One other sample (7–177) from the five did not show a response to TBEV E-D III, probably due to the limitation of LIPS assay to detect antibody specific to epitopes more than those in domain III. Nevertheless, its positive reaction to TBEV antigen by IFA and neutralization activity against TBEV still suggested this animal was previously exposed to TBEV. Moreover, we proposed that four other samples (three from marmot and one from sheep) were more likely to have exposure to KSIV rather than to TBEV, as they (11–260, 10–191, 10–264, and 6–132) had neutralization specifically against KSIV but not TBEV, and were antibody-positive to KSIV-E rather than to TBEV-E. Furthermore, three samples had neutralization activity against both viruses, including one sample (11–199) with higher neutralization titer to KSIV than to TBEV, and two others (11–189 and 10–258) showing identical neutralizing titers to both viruses. For the sample 11–199, although its reaction to KSIV and TBEV was negative by LIPS, its antibody responses to both viruses were confirmed by IFAs and western blot assays. Sample 11–189 showed an antibody response to TBEV slightly higher than to KSIV, while sample 10–258 had an antibody response to KSIV but not to TBEV by LIPS assays. Their serological reactions to KSIV and TBEV antigens were both confirmed by IFAs but not by western blot assays. Therefore, we speculated that these three samples were likely to have co-exposure to KSIV and TBEV, or that due to the close serological correlation between KSIV and TBEV, the two samples have an infection with one of the two viruses and showed effective antibody cross-reaction with the other.

DISCUSSION

Karshi virus was first isolated from *Ornithodoros papillipes* ticks collected in Uzbekistan in 1972 (Lvov et al., 1976), and subsequently from *Hy. asiaticum* ticks collected in the north of

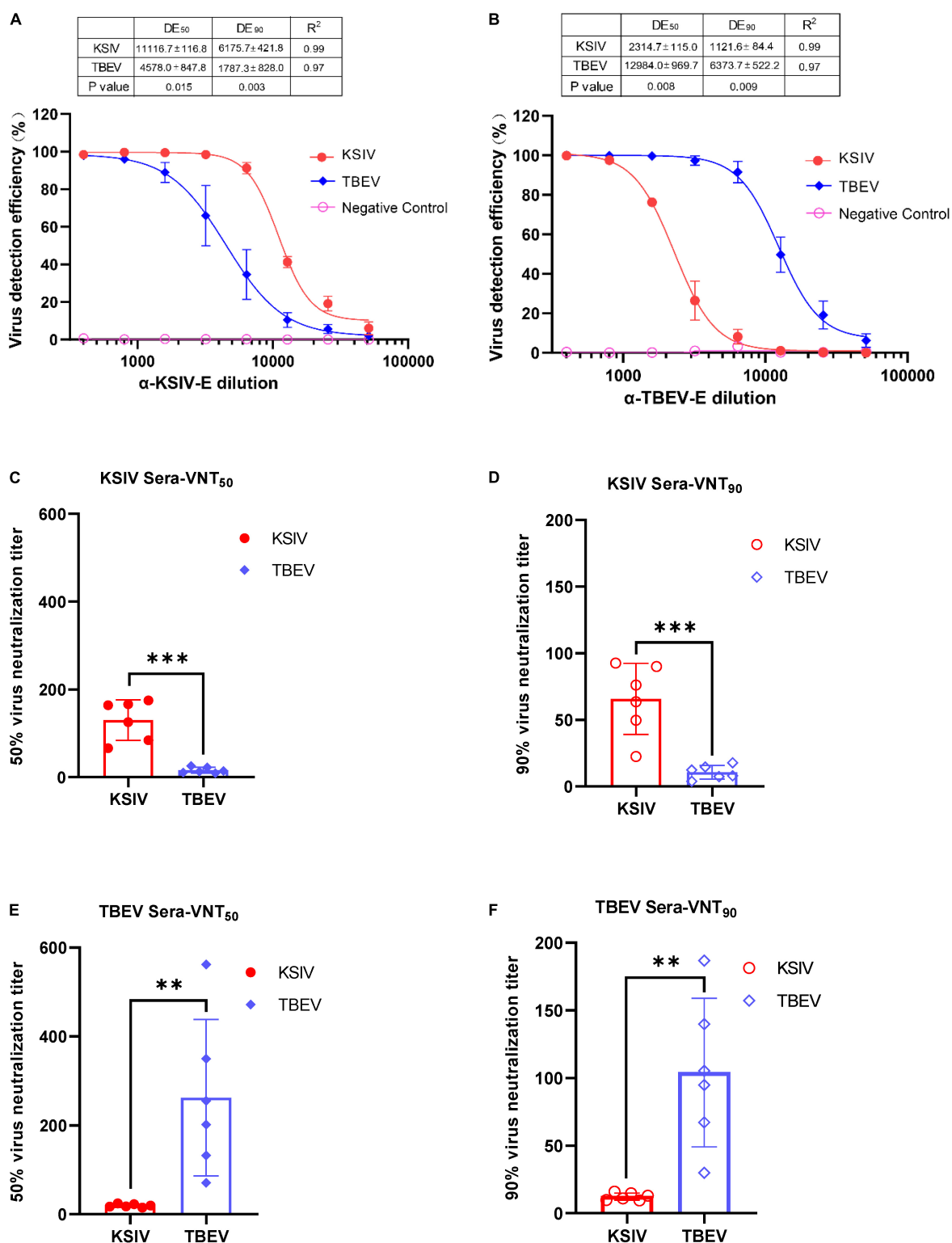


FIGURE 5 | Karshi virus has serological cross-reactivity with TBEV. The determination of KSIV and TBEV serological cross-reaction and neutralization was based on the immunofluorescence test. Percentages of KSIV-infected/TBEV-infected cells were obtained and normalized with the Operetta High-Content Imaging System (PerkinElmer). KSIV and TBEV serological cross-reaction test. The efficiencies of the lab-prepared polyclonal antibodies α -KSIV-E (**A**) and α -TBEV-E (**B**) reacting to the KSIV- and TBEV-infected cells were evaluated using GraphPad Prism software (Version 8) least square fitting method to determine the detection efficiency curve. The KSIV-infected mouse serum dilution was determined as an antibody titer that inhibited 50% (**C**) and 90% (**D**) of KSIV and TBEV infection. The TBEV-infected mouse serum dilution was determined as an antibody titer that inhibited 50% (**E**) and 90% (**F**) of KSIV and TBEV infection. The data were shown as means \pm SD. ** $p < 0.01$, *** $p < 0.001$.

TABLE 3 | Antibody response against tick-borne encephalitis virus among Karshi virus-IFA positive animal serum samples.

Species	Location	No.	Positive sample number and rates, n (%)			
			IFAs	WB	LIPS	By-Neutralization
Marmot	Wuqia County	13	10 (76.9)	9 (69.2)	1 (7.7)	0
	Aheqi County	15	9 (60.0)	3 (20.0)	3 (20.0)	4 (26.7)
Sheep	Qitai County	8	6 (75.0)	2 (25.0)	3 (37.5)	4 (50.0)
Total		36	25 (69.4)	14 (38.9)	7 (19.4)	8 (32.0)

IFA, immunofluorescence assays; WB, western blot assays; LIPS, luciferase immunoprecipitation system detection assays.

Central Asia (Alma-Ata region of the Kazakh Soviet Socialist Republic) in 1976 and from *Ornithodoros caniceps* collected in Turkmenistan in 1978 (Khutoretskaya et al., 1985). In the present study, a strain of KSIV was isolated from *Hy. asiaticum* ticks in Xinjiang, Northwestern China. Investigation of KSIV prevalence revealed that *Hy. detritum*, *Hy. asiaticum* and *D. nuttalli* ticks collected in Xinjiang could be the natural reservoirs of this virus, with the highest minimum infection rate (28.57%) among the *Hy. detritum* groups, followed by the *Hy. asiaticum* and *D. nuttalli* groups. Although the rates could be affected by geographically limited sampling of ticks, which was performed mostly around the Tianshan Mountainous regions, the resulting minimum infection rates of 4.96% in total still suggested the substantial prevalence of KSIV in Xinjiang, especially around the pasture and farming areas relying on irrigation from the Tianshan Mountains. Moreover, KSIV was proved to be transmitted by *Ornithodoros* ticks and was able to replicate in ixodid ticks in laboratory experiments (Lvov et al., 1976; Aristova et al., 1986; Turell et al., 2004). Our study showed that KSIV could infect the *I. scapularis* cell line IDE8; however, KSIV infection was not observed in the *Hy. anatolicum* cell line HAE/CTVM9. This could be because KSIV had different infection and replication efficiencies in the *Hyalomma* and *Ixodes* cells at the tested time point (48 h p.i.). In a comparative *in vitro* study, levels of infective TBEV particles produced between 24 and 48 h.p.i. increased in *Ixodes* spp. cell lines, but decreased in HAE/CTVM9 cultures (Růzek et al., 2008). Alternatively, the HAE/CTVM9 cells may have been unable to support production of KSIV E protein or were refractory to infection. The results of KSIV detection in *Hy. detritum*, *Hy. asiaticum*, and *D. nuttalli* ticks and KSIV infection in the *I. scapularis* cell line, together with previous studies on KSIV isolation, transmission, and replication in other tick species (Lvov et al., 1976; Khutoretskaya et al., 1985; Terskikh et al., 1989; L'Vov et al., 1994; Turell et al., 2004, 2008; Turell, 2015), suggested that multiple tick species may harbor KSIV, which indicated the importance of performing a survey on KSIV molecular prevalence among more tick species from wider geographic areas.

Tick-borne encephalitis virus is a notorious viral pathogen, which causes acute encephalitis accompanied by myelitis, and may be fatal to humans (Lindquist and Vapalahti, 2008). Experimental animals including rodents, dogs, horses, monkeys, cows, goats, and sheep were susceptible to TBEV infection (Nalca et al., 2003; Klaus et al., 2014). TBEV infection with European, Siberian, and Far Eastern subtypes resulted in mild to severe

symptoms in experimental animals, suggesting that different viral strains may have differential pathogenicity (Nalca et al., 2003). Nevertheless, these the experimental animals susceptible to TBEV exhibited neuronal damage, necrosis or encephalitis associated with inflammatory cell infiltration. Due to its close relationship to TBEV, KSIV may be an emerging tick-borne viral pathogen, which should be evaluated for its potential threats to infect different hosts. A previous study reported that KSIV could infect animals such as white mice, Syrian hamsters and green monkeys, but lacked details about the pathological lesions and responses of these animals (Terskikh et al., 1989). Moreover, it is unknown whether KSIV could infect and cause disease in humans. The current study showed that KSIV could infect cell lines derived from different tissues of humans and mammals including monkeys, hamsters, sheep, and dogs. The efficient replication of KSIV in the human kidney and neural cell lines, as well as the hamster cell line, suggested that KSIV has the potential to infect humans and other animals. We attempted to investigate KSIV pathogenesis in adult C57BL/6 mice in this study. Although these mice did not show any symptoms, detection of neutralizing antibody to KSIV in serum samples from these mice suggested the occurrence of transient infection and humoral immunity caused by KSIV infection. As expected, KSIV infection resulted in fatal disease in the suckling mice, which are supposed to have a naïve or developing immune system. Further investigation of KSIV infection in different species of experimental animals would promote our understanding of its pathogenesis and reveal whether its pathology is similar to that of TBEV infection.

Karshi virus RNA was detected in mouse tissues collected during the acute infection phase. While the viral loads decreased or were maintained in most tested tissues from D6 to D8 after KSIV infection, the viral load in the brain significantly increased. Moreover, severe lesions were observed in the thalamus, prosencephalon, and hippocampus of the mouse brain, and KSIV antigen expression was detected in the neurons. The results showed that KSIV could infect and replicate in the brain of mice with developing immune systems, and result in encephalitis, which suggested that KSIV is pathogenic by causing lesions in the brain and infecting neurons in the same way as TBEV. Investigation of serum samples from domestic and wild animals further revealed serological evidence of KSIV exposure among sheep from Qitai and marmots from Aheqi and Wuqia. This suggested that KSIV spillover had occurred to domestic and wild animals.

The serological correlation between KSIV and TBEV was confirmed by detecting the efficiency of laboratory-prepared KSIV antibodies in reacting with TBEV antigen and neutralizing TBEV infection, and vice versa. Therefore, we speculated that the KSIV antibody-positive animal serum samples identified in this study might include those having serological exposure to KSIV and showing cross-reaction to TBEV, and those having serological exposure to TBEV and also showing cross-reaction to KSIV. As expected, the serological tests with 36 KSIV antibody-positive animal serum samples confirmed that, at most, 25 samples had antibody responses to TBEV. By carefully analyzing the detailed results, we found that at least five among the 36 samples (13.9%) were more likely to have TBEV exposure and showed serological cross-reaction to KSIV. Four samples (11.1%) had infection with KSIV and showed cross-reaction to TBEV without cross-neutralization against TBEV. Three of the 36 sampled animals (8.3%) might have had co-exposure to both TBEV and KSIV or might have had an infection with one of these two viruses and showed strong cross-reactivity to the other. Our results suggested that both KSIV and TBEV infections have occurred among animals in Xinjiang.

Since the 1990s, the areas close to Tianshan Mountains and Altay Mountains have been considered epidemic foci of forest encephalitis in Northwestern China (Bi et al., 1997). High TBEV seroprevalence among humans and animals including marmots and sheep was also reported from there (Xie et al., 1991). The rate of TBEV seroprevalence in humans was 15.9% from 2011 to 2015, and in marmots from the Tianshan Mountains, this rate reached up to 75%, which is in contrast to the very few numbers of TBEV-infected human cases that occurred throughout the whole province (Men et al., 2021). Here, we presented the locations in a map to show where tick groups were detected positive for KSIV RNA, and where animals had positive antibody responses to KSIV and/or TBEV (Figure 4). While ticks collected from areas close to Tianshan Mountains (Usu, Jinghe, Wujiaqu, Luntai, and Yuli) as well as from Altay Mountains (Fuhai) and Kunlun Mountains (Minfeng) were KSIV-positive, a serological response to KSIV was detected among animals in the areas along Tianshan Mountains (Wuqia, Aheqi, and Qitai) where antibody response to TBEV in animals was also found (Figure 4). Therefore, according to the results of our study, we speculated that there could be a misinterpretation of the high TBEV seroprevalence. First, the rates may have included human cases and animals having KSIV infection or exposure due to the close serological relationship between these two viruses. Second, the regions of high KSIV prevalence among ticks, including the counties around Tianshan Mountains as well as Altay Mountains, merged with the natural foci of TBEV. Therefore, we suggest that it is necessary to perform follow-up surveys on both TBEV and KSIV by detecting viral RNA among human patients, domestic and wild animals and ticks, to further investigate in depth the substantial prevalence of both viruses among vectors and hosts. The results also raised the need to develop specific serological detection methods to distinguish KSIV infection from TBEV, which may promote understanding of the seroprevalence of KSIV and TBEV among humans and animals and further improve diagnosis and

therapeutic strategies regarding infectious diseases related to these two viruses.

Very few studies performed surveys of tick species parasitic on animals in Xinjiang; nevertheless, it was found that 45.4% of juvenile gray marmots in Shawan County from the Tianshan Mountains carried *I. persulcatus* (Xie et al., 1991), and that in Qitai County, the tick species carried by sheep included *Hy. asiaticum*, *D. nuttalli*, *Hy. anatolicum*, *Dermacentor pavlovsky*, and *Rhipicephalus sanguineus* (Wang Y. et al., 2015; Sheng et al., 2019; Li et al., 2020). These reports suggested that ticks, during their life cycles, had substantial contact with marmots and sheep, which indicated the potential for virus transmission between the tick vectors and animal hosts. In the present study, there were limitations on time and locations of sample collection, and the locations of KSIV-positive ticks were not consistent with those of KSIV antibody-positive animals, which may not accurately reflect the possibility of direct transmission of KSIV from ticks to animal hosts. Since we found serological evidence of the occurrence of KSIV exposure in marmots and sheep, further investigation of ticks and animal serum samples collected from the same locations in more regions in Northwestern China may further clarify the threat of KSIV transmission from ticks to animal hosts. One other limitation of the present study is that serological exposure of KSIV or KSIV infection incidence among humans were not characterized due to the lack of human samples. Nevertheless, our results of serological correlations between KSIV and TBEV, together with the previous reports on high TBEV seroprevalence among humans in Xinjiang, indicated that KSIV might be prevalent in the areas reporting TBEV antibody-positive humans.

In summary, this study isolated a new KSIV strain and reported the prevalence of KSIV among ticks in Xinjiang, Northwestern China. KSIV was able to infect various cell lines from humans, animals and ticks, caused encephalitis in experimental mice (with pathogenesis similar to TBEV) and had low seroprevalence among marmots and sheep. All these findings suggested that KSIV is a potential pathogen with the ability to spill over from ticks and animal hosts to humans. This study further evaluated the serological cross-reactivity between KSIV and TBEV and found that KSIV and TBEV infection have both occurred among animals, which indicated that there has been misinterpretation of the high seroprevalence of TBEV among humans and animals in Xinjiang. The results of this study have improved our knowledge of the etiology and epidemiology of tick-borne flavivirus pathogens in Xinjiang. Moreover, the findings suggested the necessity to perform an extensive investigation of KSIV prevalence and incidence in Northwestern China, which may enhance our preparation to provide medical care against emerging diseases caused by tick-borne viral pathogens such as KSIV.

DATA AVAILABILITY STATEMENT

The datasets presented in this study can be found in online repositories. The names of the repository/repositories and accession number(s) can be found below: <http://db.cngb.org/cnsa/project/CNP0002610/reviewlink/>, CNP0002610.

ETHICS STATEMENT

The animal study was reviewed and approved by the ethics committee of Wuhan Institute of Virology, Chinese Academy of Sciences.

AUTHOR CONTRIBUTIONS

YuZ, SSu, ZS, and AM collected the tick samples and performed the morphological classification of ticks. YaZ, ST, and SSh grouped the ticks and prepared the homogenates. AM extracted RNA from ticks. LB-S established the *Hyalomma* tick cells and provided suggestions on virus infection in tick cells. SSh performed the molecular classification of ticks and directed RNAseq analyses. JW and SSh analyzed the RNAseq data. SSu and YuZ collected the animal serum samples. FD and SSh conceived the study. YB conducted the experiments and analyzed the data. YB and SSh wrote the manuscript. SSu, SSh, LB-S, and FD reviewed and finalized the manuscript. All authors contributed to the article and approved the submitted version.

FUNDING

This work was supported by the National Key R&D Program of China (2021YFC2300900), the Key Deployment Projects of Chinese Academy of Sciences (KJZD-SW-L11), the Biological

Resources Program, Chinese Academy of Sciences (KFJ-BRP-017-74), the National Natural Science Foundation of China (81960369), the Science Research Key Project of Xinjiang Education Department (XJEDU2019I002), and the United Kingdom Biotechnology and Biological Sciences Research Council (BB/P024270/1).

ACKNOWLEDGMENTS

We thank the Core Facility and Technical Support facility of the Wuhan Institute of Virology for the technical assistance. We would like to thank Linfa Wang from Duke University and Peng Zhou from Wuhan Institute of Virology, Chinese Academy of Sciences, for providing the plasmids and the staff of the National Virus Resource Center for assisting with sample preservation and technical support. We would like to thank Feifei Yin and Bo Wang from Hainan Medical University for assisting with virus collection. We also thank the Tick Cell Biobank for providing the tick cell lines, and Ulrike Munderloh, University of Minnesota, for permission to use the IDE8 cell line.

SUPPLEMENTARY MATERIAL

The Supplementary Material for this article can be found online at: <https://www.frontiersin.org/articles/10.3389/fmicb.2022.872067/full#supplementary-material>

REFERENCES

- Apanaskevich, D. A., Filippova, N. A., and Horak, I. G. (2010). The genus *Hyalomma* Koch, 1844. x. redescription of all parasitic stages of *H. (Euhyalomma)* scupense Schulze, 1919 (= *H. detritum* Schulze) (Acari: Ixodidae) and notes on its biology. *Folia Parasitol.* 57, 69–78. doi: 10.14411/fp.2010.009
- Aristova, V. A., Gushchina, E. A., Gromashevskii, V. L., and Gushchin, B. V. (1986). Experimental infection of ixodid ticks with Karshi virus. *Parazitologiya* 20, 347–350.
- Bi, W., Deng, H., and Bu, X. (1997). Regionalisation of natural foci of forest encephalitis. *Shou Du Shi Fan Da Xue Xue Bao* 18, 100–107.
- Dai, S., Zhang, T., Zhang, Y., and Wang, H. (2018). Zika Virus Baculovirus-Expressed Virus-Like Particles Induce Neutralizing Antibodies in Mice. *Viol. Sin.* 33, 213–226. doi: 10.1007/s12250-018-0030-5
- De Madrid, A. T., and Porterfield, J. S. (1969). A simple micro-culture method for the study of group B arboviruses. *Bull. World Health Organ.* 40, 113–121.
- Deng, F., Wang, R., Fang, M., Jiang, Y., Xu, X., Wang, H., et al. (2007). Proteomics analysis of *Helicoverpa armigera* single nucleocapsid nucleopolyhedrovirus identified two new occlusion-derived virus-associated proteins, HA44 and HA100. *J. Virol.* 81, 9377–9385. doi: 10.1128/jvi.00632-07
- Grard, G., Moureau, G., Charrel, R. N., Lemasson, J. J., Gonzalez, J. P., Gallian, P., et al. (2007). Genetic characterization of tick-borne flaviviruses: new insights into evolution, pathogenetic determinants and taxonomy. *Virology* 361, 80–92. doi: 10.1016/j.virol.2006.09.015
- Guo, R., Shen, S., Zhang, Y., Shi, J., Su, Z., Liu, D., et al. (2017). A new strain of Crimean-Congo hemorrhagic fever virus isolated from Xinjiang, China. *Viol. Sin.* 32, 80–88. doi: 10.1007/s12250-016-3936-9
- Khutoretskaya, N. V., Aristova, V. A., Rogovaya, S. G., Lvov, D. K., Karimov, S. K., Skvortsova, T. M., et al. (1985). Experimental study of the reproduction of Karshi virus (*Togaviridae*, *flavivirus*) in some species of mosquitoes and ticks. *Acta Virol.* 29, 231–236.
- Klaus, C., Ziegler, U., Kalthoff, D., Hoffmann, B., and Beer, M. (2014). Tick-borne encephalitis virus (TBEV) - findings on cross reactivity and longevity of TBEV antibodies in animal sera. *BMC Vet. Res.* 10:78. doi: 10.1186/1746-6148-10-78
- Li, C., Shi, M., Tian, J., Lin, X., Kang, Y., Chen, L., et al. (2015). Unprecedented genomic diversity of RNA viruses in arthropods reveals the ancestry of negative-sense RNA viruses. *Elife* 4:5378. doi: 10.7554/eLife.05378
- Li, Y., Wen, X., Li, M., Moumouni, P. F. A., Galon, E. M., Guo, Q., et al. (2020). Molecular detection of tick-borne pathogens harbored by ticks collected from livestock in the Xinjiang Uygur Autonomous Region, China. *Ticks Tick Borne Dis.* 11:101478. doi: 10.1016/j.ttbdis.2020.101478
- Lindquist, L., and Vapalahti, O. (2008). Tick-borne encephalitis. *Lancet* 371, 1861–1871.
- Liu, R., Zhang, G., Liu, X., Li, Y., Zheng, Z., Sun, X., et al. (2016). Detection of the Siberian Tick-borne Encephalitis Virus in the Xinjiang Uygur Autonomous Region, northwestern China. *Bing Du Xue Bao* 32, 26–31.
- Liu, X., Zhang, X., Wang, Z., Dong, Z., Xie, S., Jiang, M., et al. (2020). A Tentative Tamdy Orthonairovirus Related to Febrile Illness in Northwestern China. *Clin. Infect. Dis.* 70, 2155–2160. doi: 10.1093/cid/ciz602
- Lvov, D. K., Neronov, V. M., Gromashevsky, V. L., Skvortsova, T. M., Berezina, L. K., Sidorova, G. A., et al. (1976). “Karshi” virus, a new flavivirus (*Togaviridae*) isolated from *Ornithodoros papillipes* (Birula, 1895) ticks in Uzbek S.S.R. *Arch. Virol.* 50, 29–36. doi: 10.1007/bf01317998
- L’Vov, D., Loginova, N. V., Lebedeva, G. A., Deriabina, P. G., Parygina, M. M., and Buunitskaia, O. B. (1994). Biological properties and antigenic interconnection between Tiuleniy and Karshi flaviviruses. *Vopr. Virusol.* 39, 205–208.
- Men, X., Du, H., Cai, X., Fu, L., and Zhu, Y. (2021). Meta analysis of TBEV prevalence in ticks and human populations in China. *Chin. J. Zoonoses* 37, 631–638. doi: 10.3969/j.issn.1002-2694.2021.00.104
- Moming, A., Shen, S., Fang, Y., Zhang, J., Zhang, Y., Tang, S., et al. (2021). Evidence of Human Exposure to Tamdy Virus, Northwest China. *Emerg. Infect. Dis.* 27, 3166–3170. doi: 10.3201/eid2712.203532

- Moming, A., Yue, X., Shen, S., Chang, C., Wang, C., Luo, T., et al. (2018). Prevalence and Phylogenetic Analysis of Crimean-Congo Hemorrhagic Fever Virus in Ticks from Different Ecosystems in Xinjiang, China. *Virol. Sin.* 33, 67–73. doi: 10.1007/s12250-018-0016-3
- Nalca, A., Fellows, P. F., and Whitehouse, C. A. (2003). Vaccines and animal models for arboviral encephalitis. *Antiviral. Res.* 60, 153–174. doi: 10.1016/j.antiviral.2003.08.001
- Papa, A., Ma, B., Kouidou, S., Tang, Q., Hang, C., and Antoniadis, A. (2002). Genetic characterization of the M RNA segment of Crimean Congo hemorrhagic fever virus strains, China. *Emerg. Infect. Dis.* 8, 50–53. doi: 10.3201/eid0801.010087
- Růžek, D., Bell-Sakyi, L., Kopecký, J., and Grubhoffer, L. (2008). Growth of tick-borne encephalitis virus (European subtype) in cell lines from vector and non-vector ticks. *Virus Res.* 137, 142–146. doi: 10.1016/j.virusres.2008.05.013
- Shen, S., Duan, X., Wang, B., Zhu, L., Zhang, Y., Zhang, J., et al. (2018). A novel tick-borne phlebovirus, closely related to severe fever with thrombocytopenia syndrome virus and Heartland virus, is a potential pathogen. *Emerg. Microbes Infect.* 7:95. doi: 10.1038/s41426-018-0093-2
- Sheng, J., Jiang, M., Yang, M., Bo, X., Zhao, S., Zhang, Y., et al. (2019). Tick distribution in border regions of Northwestern China. *Ticks Tick Borne Dis.* 10, 665–669. doi: 10.1016/j.ttbdis.2019.02.011
- Sun, S., Dai, X., Aishan, M., Wang, X., Meng, W., Feng, C., et al. (2009). Epidemiology and phylogenetic analysis of Crimean-Congo hemorrhagic fever viruses in Xinjiang, China. *J. Clin. Microbiol.* 47, 2536–2543. doi: 10.1128/jcm.00265-09
- Tersikh, I. I., Abramova, L. N., Savostina, N. S., Gromashevskii, V. L., and L'Vov, D. K. (1989). Results of infecting experimental animals and monkeys with Karshi virus. *Med. Parazitol.* 1998, 71–74.
- Turell, M. J. (2015). Experimental Transmission of Karshi (Mammalian Tick-Borne Flavivirus Group) Virus by *Ornithodoros* Ticks >2,900 Days after Initial Virus Exposure Supports the Role of Soft Ticks as a Long-Term Maintenance Mechanism for Certain Flaviviruses. *PLoS Negl. Trop. Dis.* 9:e0004012. doi: 10.1371/journal.pntd.0004012
- Turell, M. J., Mores, C. N., Lee, J. S., Paragas, J. J., Shermuhemedova, D., Endy, T. P., et al. (2004). Experimental transmission of Karshi and Langat (tick-borne encephalitis virus complex) viruses by *Ornithodoros* ticks (Acari: Argasidae). *J. Med. Entomol.* 41, 973–977. doi: 10.1603/0022-2585-41.5.973
- Turell, M. J., Whitehouse, C. A., Butler, A., Baldwin, C., Hottel, H., and Mores, C. N. (2008). Assay for and replication of Karshi (mammalian tick-borne flavivirus group) virus in mice. *Am. J. Trop. Med. Hyg.* 78, 344–347. doi: 10.4269/ajtmh.2008.78.344
- Wang, H., Yan, H., Sun, X., Liu, X., Zhao, Y., Zheng, Z., et al. (2015). The distribution, epidemiological characteristics and prevention and control measures of tick-borne encephalitis in Xinjiang. *Jie Fang Jun Yu Fang Yi Xue Za Zhi* 33, 709–710. doi: 10.13704/j.cnki.jyyx.2015.06.059
- Wang, Y., Mu, L., Zhang, K., Yang, M., Zhang, L., Du, J., et al. (2015). A broad-range survey of ticks from livestock in Northern Xinjiang: changes in tick distribution and the isolation of *Borrelia burgdorferi sensu stricto*. *Parasit. Vectors* 8:449. doi: 10.1186/s13071-015-1021-0
- Xie, X., Yu, X., Zhang, T., and Jiang, G. (1991). A survey report on the natural foci of Russian Spring Summer encephalitis in the mountainous areas of Tianshan and Altay mountains in Xinjiang. *Di Fang Bing Tong Bao* 6, 09–14.
- Ya, H., Shen, S., Su, Z., Deng, F., and Zhang, Y. (2016). Tick species and genetic variants analysis of tick gene in Hengduan Mountains, west Yunnan Province, China. *Chin. J. Zoonoses* 32, 865–870. doi: 10.3969/j.issn.1002-2694.2016.010.003
- Zhang, G., Liu, R., Sun, X., Zheng, Y., Liu, M., Zhao, Y., et al. (2013). Investigation on the endemic foci of tick-borne encephalitis virus in Xiaerxili Natural Reserve, Xinjiang. *Zhonghua Liu Xing Bing Xue Za Zhi* 34, 438–442. doi: 10.3760/cma.j.issn.0254-6450.2013.05.006
- Zhang, G., Sun, X., Liu, R., Zheng, Z., Liu, X., and Yin, X. (2017). Isolation of tick-borne encephalitis virus Far-eastern subtype and Siberian subtype in the China-Kazakhstan border area in Xinjiang. *Chin. J. Zoonoses* 33, 312–315. doi: 10.3969/j.issn.1002-2694.2017.04.004
- Zhang, Y. K., Zhang, X. Y., and Liu, J. Z. (2019). Ticks (Acari: Ixodoidea) in China: geographical distribution, host diversity, and specificity. *Arch. Insect Biochem. Physiol.* 102:e21544. doi: 10.1002/arch.21544
- Zhang, Y., Shen, S., Fang, Y., Liu, J., Su, Z., Liang, J., et al. (2018). Isolation, Characterization, and Phylogenetic Analysis of Two New Crimean-Congo Hemorrhagic Fever Virus Strains from the Northern Region of Xinjiang Province, China. *Virol. Sin.* 33, 74–86. doi: 10.1007/s12250-018-0020-7
- Zhang, Y., Shen, S., Shi, J., Su, Z., Li, M., Zhang, W., et al. (2017). Isolation, characterization, and phylogenetic analysis of three new severe fever with thrombocytopenia syndrome bunyavirus strains derived from Hubei Province, China. *Virol. Sin.* 32, 89–96. doi: 10.1007/s12250-017-3953-3
- Zheng, W., Zhang, C., Li, Y., Pearce, R., Bell, E. W., and Zhang, Y. (2021). Folding non-homologous proteins by coupling deep-learning contact maps with I-TASSER assembly simulations. *Cell Rep. Methods* 1:100014. doi: 10.1016/j.crmeth.2021.100014

Conflict of Interest: The authors declare that the research was conducted in the absence of any commercial or financial relationships that could be construed as a potential conflict of interest.

Publisher's Note: All claims expressed in this article are solely those of the authors and do not necessarily represent those of their affiliated organizations, or those of the publisher, the editors and the reviewers. Any product that may be evaluated in this article, or claim that may be made by its manufacturer, is not guaranteed or endorsed by the publisher.

Copyright © 2022 Bai, Zhang, Su, Tang, Wang, Wu, Yang, Moming, Zhang, Bell-Sakyi, Sun, Shen and Deng. This is an open-access article distributed under the terms of the Creative Commons Attribution License (CC BY). The use, distribution or reproduction in other forums is permitted, provided the original author(s) and the copyright owner(s) are credited and that the original publication in this journal is cited, in accordance with accepted academic practice. No use, distribution or reproduction is permitted which does not comply with these terms.



Potential Mechanisms of Transmission of Tick-Borne Viruses at the Virus-Tick Interface

Mahvish Maqbool¹, Muhammad Sohail Sajid^{1,2*}, Muhammad Saqib³, Faisal Rasheed Anjum^{2,4}, Muhammad Haleem Tayyab³, Hafiz Muhammad Rizwan⁵, Muhammad Imran Rashid⁶, Imaad Rashid³, Asif Iqbal⁷, Rao Muhammad Siddique⁷, Asim Shamim⁸, Muhammad Adeel Hassan⁹, Farhan Ahmad Atif^{10,11}, Abdul Razzaq¹², Muhammad Zeeshan¹, Kashif Hussain¹, Rana Hamid Ali Nisar¹, Akasha Tanveer¹, Sahar Younas¹, Kashif Kamran¹³ and Sajjad ur Rahman⁴

¹ Department of Parasitology, University of Agriculture, Faisalabad, Pakistan, ² Department of Epidemiology and Public Health, University of Agriculture, Faisalabad, Pakistan, ³ Department of Clinical Medicine and Surgery, University of Agriculture, Faisalabad, Pakistan, ⁴ Institute of Microbiology, University of Agriculture, Faisalabad, Pakistan, ⁵ Section of Parasitology, Department of Pathobiology, KBCMA College of Veterinary and Animal Sciences Narowal, Lahore, Pakistan, ⁶ Department of Parasitology, University of Veterinary and Animal Sciences, Lahore, Pakistan, ⁷ Section of Parasitology, Department of Pathobiology, Riphah College of Veterinary Sciences, Riphah International University, Lahore, Pakistan, ⁸ Department of Pathobiology, University of the Poonch Rawalakot, Rawalakot, Pakistan, ⁹ Department of Parasitology, Cholistan University of Veterinary and Animal Sciences, Bahawalpur, Pakistan, ¹⁰ Medicine Section, Department of Clinical Sciences, Collège of Veterinary and Animal Sciences, Jhang, Pakistan, ¹¹ University of Veterinary and Animal Sciences, Lahore, Pakistan, ¹² Agricultural Linkages Program, Pakistan Agriculture Research Council, Islamabad, Pakistan, ¹³ Department of Zoology, University of Balochistan, Quetta, Pakistan

OPEN ACCESS

Edited by:

Ali Zohaib,
Islamia University of
Bahawalpur, Pakistan

Reviewed by:

Khalid Mehmood,
Islamia University of
Bahawalpur, Pakistan

*Correspondence:

Muhammad Sohail Sajid
drsohailuaf@hotmail.com

Specialty section:

This article was submitted to
Virology,
a section of the journal
Frontiers in Microbiology

Received: 31 December 2021

Accepted: 18 March 2022

Published: 05 May 2022

Citation:

Maqbool M, Sajid MS, Saqib M, Anjum FR, Tayyab MH, Rizwan HM, Rashid MI, Rashid I, Iqbal A, Siddique RM, Shamim A, Hassan MA, Atif FA, Razzaq A, Zeeshan M, Hussain K, Nisar RHA, Tanveer A, Younas S, Kamran K and Rahman Su (2022) Potential Mechanisms of Transmission of Tick-Borne Viruses at the Virus-Tick Interface. *Front. Microbiol.* 13:846884. doi: 10.3389/fmicb.2022.846884

Ticks (Acari; Ixodidae) are the second most important vector for transmission of pathogens to humans, livestock, and wildlife. Ticks as vectors for viruses have been reported many times over the last 100 years. Tick-borne viruses (TBVs) belong to two orders (*Bunyavirales* and *Mononegavirales*) containing nine families (*Bunyaviridae*, *Rhabdoviridae*, *Asfarviridae*, *Orthomyxovirida*, *Reoviridae*, *Flaviviridae*, *Phenuviridae*, *Nyamiviridae*, and *Nairoviridae*). Among these TBVs, some are very pathogenic, causing huge mortality, and hence, deserve to be covered under the umbrella of one health. About 38 viral species are being transmitted by <10% of the tick species of the families *Ixodidae* and *Argasidae*. All TBVs are RNA viruses except for the African swine fever virus from the family *Asfarviridae*. Tick-borne viral diseases have also been classified as an emerging threat to public health and animals, especially in resource-poor communities of the developing world. Tick-host interaction plays an important role in the successful transmission of pathogens. The ticks' salivary glands are the main cellular machinery involved in the uptake, settlement, and multiplication of viruses, which are required for successful transmission into the final host. Furthermore, tick saliva also participates as an augmenting tool during the physiological process of transmission. Tick saliva is an important key element in the successful transmission of pathogens and contains different antimicrobial proteins, e.g., defensin, serine, proteases, and cement protein, which are key players in tick-virus interaction. While tick-virus interaction is a crucial factor in the propagation of tick-borne viral diseases, other factors (physiological, immunological, and gut flora) are also involved. Some immunological factors, e.g., toll-like receptors, scavenger receptors, Janus-kinase (JAK-STAT) pathway, and immunodeficiency (IMD)

pathway are involved in tick-virus interaction by helping in virus assembly and acting to increase transmission. Ticks also harbor some endogenous viruses as internal microbial faunas, which also play a significant role in tick-virus interaction. Studies focusing on tick saliva and its role in pathogen transmission, tick feeding, and control of ticks using functional genomics all point toward solutions to this emerging threat. Information regarding tick-virus interaction is somewhat lacking; however, this information is necessary for a complete understanding of transmission TBVs and their persistence in nature. This review encompasses insight into the ecology and vectorial capacity of tick vectors, as well as our current understanding of the predisposing, enabling, precipitating, and reinforcing factors that influence TBV epidemics. The review explores the cellular, biochemical, and immunological tools which ensure and augment successful evading of the ticks' defense systems and transmission of the viruses to the final hosts at the virus-vector interface. The role of functional genomics, proteomics, and metabolomics in profiling tick-virus interaction is also discussed. This review is an initial attempt to comprehensively elaborate on the epidemiological determinants of TBVs with a focus on intra-vector physiological processes involved in the successful execution of the docking, uptake, settlement, replication, and transmission processes of arboviruses. This adds valuable data to the existing bank of knowledge for global stakeholders, policymakers, and the scientific community working to devise appropriate strategies to control ticks and TBVs.

Keywords: ticks, immunity, tick-virus interaction, tick microbes, salivary glands

INTRODUCTION

Pests are causing damage to our lives. Several organisms act as vectors and transmit or cause diseases in the agriculture sector, humans, wildlife, and livestock. Ticks (Acari: Ixodida) are blood-sucking ectoparasites and act as vectors of pathogens infecting livestock, wildlife, and humans across the world (Bente et al., 2013; Pfäffle et al., 2013; Guglielmone et al., 2014; Monfared et al., 2015; de la Fuente et al., 2016; Sajid et al., 2017; Ghafar et al., 2020). Ticks and tick-borne diseases (hereafter abbreviated as TBDs) are known to decrease production below the genetic potential of livestock (Sajid et al., 2007). Ticks are ectoparasites of a wide range of mammals, reptiles, and birds (Karim et al., 2017). Even if not infected with tick-borne diseases (TBDs), ticks are responsible for direct damage to the skin and hides, cause allergy, irritation, and toxicosis, and can lead to decreased livestock productivity (Sajid et al., 2007). Over 80% of the world's cattle population is affected by tick-transmitted pathogens that cause diseases called TBDs (De Meneghi et al., 2016; Rodriguez-Vivas et al., 2018). They are one of the major management issues in Africa and the Americas, and are particularly important in Asia because of hot and humid climatic conditions (Moming et al., 2018; Rosà et al., 2018). The typical life cycle involving questing and infesting stages, host diversity, and inappropriate micro and macro-management lead to the successful settlement of these arthropod vectors (Soulsby, 1982). In some countries (e.g., Turkey), ticks have adapted themselves to wild animals, such as spur-thighed tortoises, which can act as reservoirs of

infestation for contiguous livestock populations (Uslu et al., 2019).

It is a proven fact that ticks act as biological vectors of a wide range of causative agents of protozoal (e.g., babesiosis and theileriosis), bacterial (ehrlichiosis, borreliosis, Rocky Mountain spotted fever, and Q fever), viral (e.g., Crimean Congo hemorrhagic fever, and Powassan), and rickettsial (e.g., anaplasmosis) diseases and Lyme disease (Dantas-Torres et al., 2012; McCoy et al., 2013; Pfäffle et al., 2013; Gharbi and Aziz Darghouth, 2014; Ghosh and Nagar, 2014; Guglielmone et al., 2014; Pantchev et al., 2015; Solano-Gallego et al., 2016; Rashid et al., 2019; Siddique et al., 2020). Ticks are known to infest a wide range of hosts, including humans, livestock, pets, and wildlife, and are considered the second most widely used vector for disease transmission among arthropods on the planet (again behind mosquitoes) (Monfared et al., 2015). Almost 898 tick species are recognized, belonging to three different families: Argasidae (soft ticks, 194 species), Nuttalliellidae (intermediate, 1 species), and Ixodidae (hard ticks, 703 species) (Latif et al., 2012). Among these, the Ixodidae is the most diverse, abundant, and dominant tick family from a One Health significance (Tsatsaris et al., 2016). The prevalence of tick-borne diseases (TBDs) has increased recently because of several biotic and abiotic factors (Estrada-Peña and de la Fuente, 2014, 2018; Estrada-Peña et al., 2017; Martina et al., 2017). Thus, ticks are among the major contributing factors to lowered production and mortality, and are the basic reason for economic losses in livestock around the globe (Grisi et al., 2014).

TICK-BORNE VIRUSES

Tick-borne viruses (TBVs), also known as tibo viruses, constitute various viruses that are transmitted successfully between two different environments. These are the host environment, the stable one, while the other is the opposite of stable, i.e., tick internal environment (Hubálek and Rudolf, 2012). Over time, the relationship between ticks and viruses has evolved. Consequently, the tick feeding cycle is synced with the viral life cycle, sculpting the evolution of tibo viruses (Sidorenko et al., 2021; Migné et al., 2022). Recent studies have illuminated the fact that tick cells undergo transcriptional changes while harboring viruses (Mansfield et al., 2017).

The history of TBVs links back to 1929, when the tick transmission of a flavivirus, the louping ill virus, accountable for encephalitis in sheep, was discovered (Bichaud et al., 2014; Shi et al., 2018). Later, in 1945, another TBV, the Crimean Congo virus, was confirmed in Soviet soldiers and local inhabitants of the Crimean Peninsula of the USSR (Zivcec et al., 2016). This led to a path for the subsequent discovery of heterogenous TBVs falling under two orders, *Bunyavirales* and *Mononegavirales*. These are divided into one DNA virus family (*Asfarviridae*) and eight RNA virus families (*Bunyaviridae*, *Rhabdoviridae*, *Orthomyxoviridae*, *Reoviridae*, *Flaviviridae*, *Phenuviridae*, *Nyamiviridae*, and *Nairoviridae*) (Nuttall, 2013).

In the last decade, there was an emergence or re-emergence of tick-borne encephalitis virus that jeopardized public and animal health. There have been reports of TBVs in new geographical locations, a rise in several specific diseases, e.g., Possowan virus

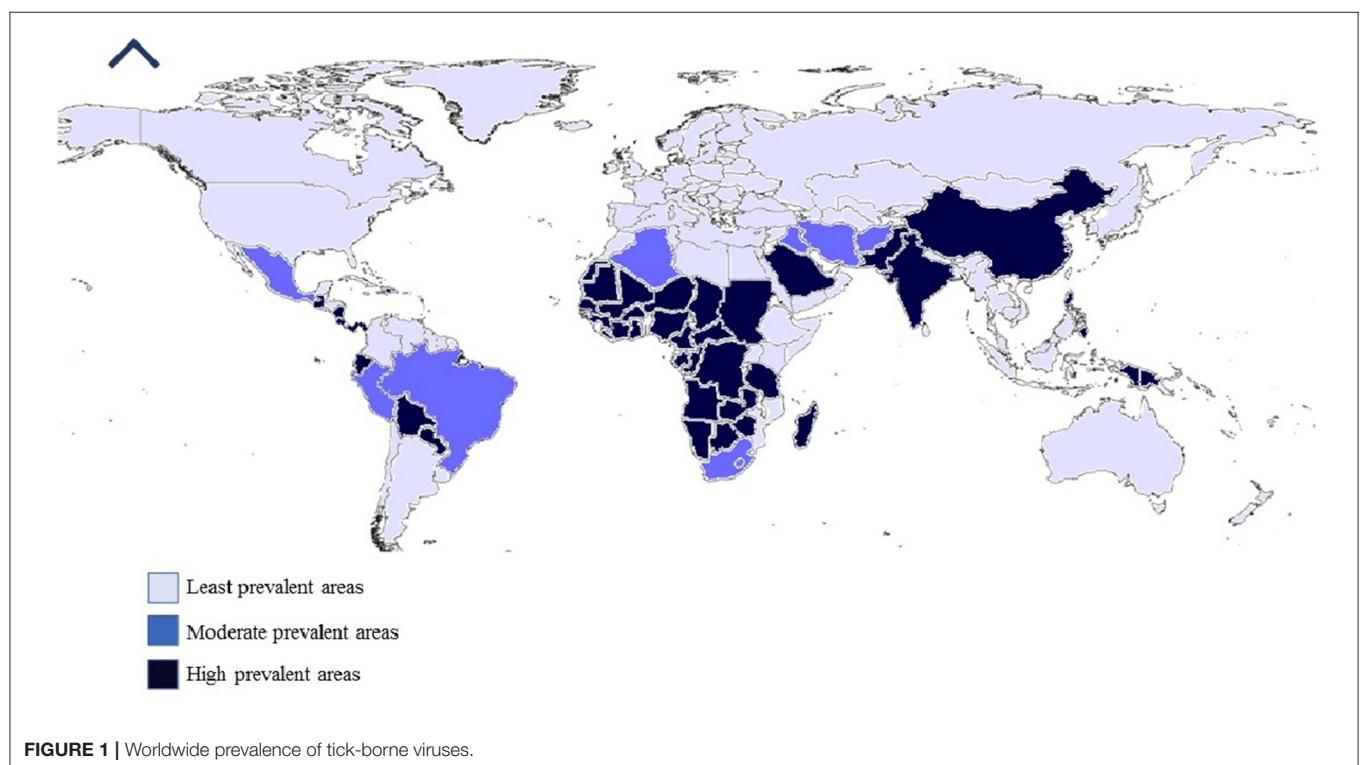
in America, and the occurrence of novel viruses, such as the Alkhurma virus, (a subtype of Kyasanur forest disease virus) (Burthe et al., 2020; Madani and Abuelzein, 2021; Yang et al., 2022), and deer tick virus (a subtype of POWV) (Hermance and Thangamani, 2018). These new viruses are placed in different families based on the latest molecular diagnostic techniques, resulting in major changes made in the families *Bunyaviridae* and *Rhabdoviridae* (Kazimírová et al., 2017) (Figure 1).

MORPHOLOGY OF TICK SALIVARY GLANDS

During tick-host interaction, host tissues (blood) and tick saliva pass through a common buccal canal. Tick saliva originates from branched and paired alveolar salivary glands, which are present anterolaterally and extend into the posterior sides of the body. From each salivary gland, a duct originates that enters a broad shallow tube, i.e., salivarium. This tube lies above the pharynx in the pharyngeal region valve and opens into the food canal at the anterior opening of the pharynx (Kemp and Tatchell, 1971).

ANATOMY OF TICK SALIVARY GLANDS OF IXODIDAE

Complex alveoli are present in the Ixodid ticks' salivary glands, which are variable in numbers in female and male ticks, i.e., three in females and four in males (Balashov, 1972; Krolak et al., 1982; Barker et al., 1984).



Type 1 Alveoli

The anterior region of the main salivary duct is attached with type 1 alveoli and may extend toward the posterior branches of the main duct. Type I alveoli contain granular cells.

Type 2 Alveoli

Morphologically, types 2 and 3 alveoli are similar, and type 2 contains six types of granular cells, i.e., a,b, C-C4, which form reactions during staining procedures (Binnington, 1978). The morphology of an alveolus undergoes remarkable changes after several days of tick feeding but a change in number has not been reported. Enlargement of nuclei and the cytoplasm occurs, which, in turn, causes an increase in the overall mass of the alveolus. Along with this, abluminal interstitial cell enlargement also occurs, which forms a basal labyrinth during the feeding procedure. The granular materials present in the salivary glands of unfed ticks in the early feeding stage are absent during their final feeding stages. In the case of *Ixodes (I.) holocyclus*, type 2 female alveoli contain only two granular cell types (Šimo et al., 2013).

Type 3 Alveoli

The most abundant type of alveoli in ticks' salivary glands are type 3 alveoli, which contain three granular cell types (d, e, and f), along with some granular cells. Type 3 alveoli are located in the posterior and peripheral regions of the glands (Binnington, 1978). The f cells of type 3 alveoli undergo cell transformation during the feeding process. The proliferation of cell plasma membrane occurs, and hypertrophy of abluminal interstitial cells and an increase in the number of mitochondria result in the formation of the basal labyrinth. Transformed f cells form a complex mass of plasma membranes and mitochondria, which is a common feature for fluid-transporting epithelia (Fawcett et al., 1986). An increase in the size of type 3 alveoli suggests that the transportation of the bulk of excreted fluid has taken place during the feeding process. In male ticks, the development of abluminal cells and f-cells occurs to a lesser degree than in female ticks (Coons and Lamoreaux, 1986). Only one common ad-luminal cell is present in types 2 and 3 cells that line the alveolus lumen in a web-like fashion (Labuda et al., 1993). In type 3 alveoli, the main function of ad-luminal cells is the same as that performed by myoepithelial cells, i.e., expansion of fluid-filled alveolus causing the ejection of fluid from the lumen to the salivary ducts and then outside the ducts (Kim et al., 2014).

Type 4 Alveoli

Type 4 alveoli are only present in males along with abluminal and ad-luminal cells (Binnington, 1978). Only one granular cell type is present in type 4 alveoli, i.e., which is filled with secretion granules during the feeding process (Fawcett et al., 1986).

ANATOMY OF TICK SALIVARY GLANDS OF ARGASIDAE

Argasids or soft ticks' salivary glands are less complex as compared to those of hard ticks and contain only two types of alveolar acini i.e., I and II (El Shoura, 1987). In soft ticks, coxal organs are involved in fluid secretion instead of salivary

glands, and the change in salivary gland morphology during feeding is minor as compared to Ixodidae (Kaufman and Sauer, 1982).

Type 1 Alveolar Acini

Type I alveolar acini are connected to the anterior region of the main salivary duct through short alveolar ducts. Cell types and ducts present in argasid type 1 alveoli are like Ixodid type 1 alveoli (El Shoura, 1987).

Type 2 Alveolar Acini

In the case of type 2 alveoli, three granular cells are present, i.e., a, b, and c. The fourth type of cell, d, is also reported in *Ornithodoros (O.) savignyi* (Mans et al., 2004). The lumen of alveoli leads to a chitinous alveolar duct, which lacks a complex valvular structure compared to ixodid alveoli (Roshdy and Coons, 1975). Canaliculi formation occurs in argasid ticks but not to the extent observed in type III alveoli of Ixodid ticks (El Shoura, 1987).

DEVELOPMENT AND DEGENERATION OF SALIVARY GLANDS

In newly hatched larvae, extremely small salivary glands are present, and only ducts are distinguishable. Few alveoli begin to develop in older Ixodid larvae, e.g., types 1, 2, and 3 alveoli are observed in larvae of *Haemaphysalis (Hae.) spinigera*. Type 4 alveoli are not distinguishable in larval stages (Ullah and Kaufman, 2014). The size of salivary glands enlarges during the larval feeding process, and when engorged larvae drop from the host, degeneration of salivary gland alveoli occurs. However, salivary ducts form branch ducts that terminate in small alveoli containing undifferentiated cells (Nodari et al., 2012). Salivary alveoli continue to increase in numbers and differentiate into types 1, 2, and 3 alveoli in nymphal stages, while fully differentiated types of salivary gland alveoli are present in molted adults (Esteves et al., 2017).

During tick feeding, a 25-fold increase in mass, protein content (stimulation of mRNA synthesis and new protein expression), and size of salivary glands takes place (Tirloni et al., 2017). Further development of salivary glands occurs after the mating process, and mRNA and protein synthesis rates become double during this phase. In mated rapid-feeding female ticks, higher ATPase, Na⁺, K⁺, and adenylate cyclase activities and fluid secretion rate are present (Yu et al., 2017). Different hemolymph-borne factors are involved in controlling these changes in salivary glands during feeding and mating phases, e.g., an applied juvenile hormone partially stimulates protein synthesis and ATPase, Na⁺- and K⁺- activity in *Amblyomma (A.) americanum* (Kim et al., 2016).

COMPOSITION AND FUNCTION OF TICK SALIVA

Saliva is mostly water-derived during the blood meal process and, as in the Ixodid group, most of the blood meal is taken during the last 12–24 h of feeding, so the excess amount of saliva is

produced during the final engorgement stage (Šimo et al., 2014). About 1-ml volume of saliva is secreted by large tick species (Koči et al., 2014). During blood feeding, extra water is secreted, so ions are balanced by secreting hypo-stomatic saliva containing 70% water and ions taken up during blood-feeding (Kim et al., 2017).

CEMENT

The secure attachment of ticks to the host body is due to cement proteins, which result in a prolonged feeding period (Suppan et al., 2018). In the case of soft ticks (fast feeder), adults, and nymphal stages penetrate deep into the skin of the host and make some strong unnecessary attachment, while in hard ticks, all slow Ixodid feeders use cement and enhance protein production to ensure secure attachment by enlarging tick-host association. Types 2 and 3 alveolus cells d and e are involved in cement production (Mans and Neitz, 2004). Cement protein contains some lipid and glycol proteins (Leal et al., 2018). A recent proteomic analysis of a cement cone has provided information regarding the presence of metalloproteases and serine protease inhibitors in *A. americanum* (Bullard et al., 2016). Cement proteins also have antigenic properties and contain a 90-kDa polypeptide in d and e cells of type 3 alveolus cells, and some of them can be considered potent anti-tick vaccine candidates (Suppan et al., 2018). When a tick attaches to the surface of the host, the cement protein forms a cement cone around tick mouthparts and allows for firm attachment to the host's skin and protection against the host's immune system. A cement cone is also involved in playing an antibacterial role (Suppan et al., 2018). Cement cone production is a specialty of the Ixodid group and differs in composition, size, and shape among the members of this group (Leal et al., 2018). Glycine-rich proteins, such as those found in cement cones, are normally biologically inert and non-immunogenic; however, the use of cement proteins as a vaccine protects mice from lethal tick-borne encephalitis virus. These glycine-rich proteins also play a role in tick embryo development (Suppan et al., 2018).

ENZYMES AND ENZYME INHIBITORS PRESENT IN TICK SALIVA

Tick saliva is a colorless, hypertonic, alkaline substance. Histochemical analysis of tick saliva has reported the presence of triacylglycerol, aminopeptidase, carboxylic ester hydrolases, and lipases (Bullard et al., 2016). Transcriptomic studies have revealed more than 500 different proteins and peptides further divided into different multigene groups, i.e., metalloproteases, lipocalins, Kunitz-domain proteins, some unique proteins found only in ticks, and some ancestral protein families that are present in Ixodid, argasid, and *Nutailella* (Mans et al., 2016). Esterases are also found in larvae of *B. microplus* causing a hypersensitivity reaction in cattle that are previously exposed to ticks; they hydrolyze cholesterol esters in the mast cell membrane, resulting in increased vascular permeability and release of

pharmacologically active compounds, i.e., hyaluronidase. The kininase present in tick saliva deactivates the action of bradykinin (a pain-causing mediator) at the feeding site and enhances the tick feeding process (Mulenga et al., 2013).

Members of the Ixodid group contain proteins that inhibit the production of proteolytic enzymes, i.e., plasmin, trypsin, porcine kallikrein, and chymotrypsin (Štibrániová et al., 2013). The metalloprotease proteins of ticks have been identified in saliva, ovary, and midgut, and play an important role in tick blood uptake, vitellogenesis, blood digestion, and innate immunity (Kotál et al., 2015a). Metalloproteases have been identified in diverse tick species, e.g., *A. maculatum*, *Rhipicephalus* (*R.*) *samguneus*, *I. scapularis*, *R. microplus*, *I. ricinus*, and *A. americanum* (Ali et al., 2015a,b; Chmelar et al., 2016a). Ticks contain several protease inhibitors that play a role in tick-host interactions (Chmelar et al., 2016b). Four major groups of protease inhibitors are present in ticks: trypsin inhibitors, serpins, and Kazal domain and Kunitz domain cysteine protease inhibitors (Parizi et al., 2018).

Serine protease inhibitors are involved in the production of antimicrobial peptides, digestion of blood, and innate immunity (Meekins et al., 2017). Serine protease inhibitors also bind with different protease and non-protease ligands, including maspin, nexin-1, kallistatin, and anti-chymotrypsin. Different tick species were screened for serine protease inhibitors and reported in *I. ricinus*, *D. variabilis*, *R. microplus*, *I. scapularis*, *A. variegatum*, *Hae. logicornis*, *A. americanum*, *R. appendiculatus*, and *A. hebraeum* (Kim et al., 2014). Characterization of some serine protease inhibitors has been conducted, and they were found to play a role in host defense mechanisms through pro-inflammatory cytokine production (Wikel, 2013; Valdés, 2014).

Another large group of tick protease inhibitors is that of cystatins, which modulate vertebrate biological processes, i.e., immunity, antigen presentation, phagocytosis, apoptosis, and hemoglobin digestion and regulation (Chmelar et al., 2016b). The cystatin group is further divided into four subgroups, i.e., types 1, 2, 3, and 4 cystatins (Kazimírová and Štibrániová, 2013). In ticks, types 1 and 2 cystatins are present, and type 1 was first isolated from *R. microplus* causing inhibition of vitelline by degrading the cystatin endopeptidase, and plays an immunomodulatory role (Schwarz et al., 2012). Different cystatins are reported on various tick species, i.e., *Hae. longicornis*, *A. americanum*, *I. ovatus*, *I. scapularis*, and *R. microplus*, and on a soft tick, *Orintodoros moubata* (Chmelar et al., 2017). Type 2 cystatins were characterized in *I. scapularis* and play an important role in the transmission of tick-borne pathogens by interfering with interferon-mediated immune responses and increasing the multiplication of tick-borne viruses in bone marrow dendritic cells (Chen et al., 2014). Various other cystatin forms are characterized by tick species, and interference with their actions results in the impaired feeding process, higher mortality, immunosuppressive effects, and block attachment, and are promising anti-tick vaccine candidates (Kotsyfakis et al., 2008; Chmelar et al., 2017).

PROSTAGLANDINS

Prostaglandins have been identified in tick saliva and possess anti-inflammatory, hyperemic, and immunosuppressive activities (Chmelar et al., 2012). Different forms of prostaglandins are identified in ticks' saliva, i.e., $F_{2\alpha}$, A_2/B_2 , prostacyclin (I_2), and D_2 ; among these, A_2/B_2 is considered to be derived from PGE2 because of the alkaline nature of tick saliva (Carvalho-Costa et al., 2015). Arachidonic acid and its derivatives act as precursors for salivary gland prostaglandins, e.g., endocannabinoids in *A. americanum*. Arachidonic acid is 8% of total fatty acids in partially fed tick salivary glands compared to the 2% in unfed ticks and increases more than any other fatty acid (Gao et al., 2016). Most vertebrates are capable of synthesizing arachidonic acid from linoleate by desaturation and elongation reactions, but in the case of ticks, females have the capability to synthesize degenerative fatty acids, but desaturation ability is lacking in ticks, and the stearoyl CoA desaturase gene is present in ticks. Phospholipase PLA_2 activity is related to arachidonic acid release. Dopamine was also found associated with an increase in free arachidonic acid by stimulating PLA_2 by the opening of voltage-dependent Ca^{2+} channel (Kannangara and Patel, 2018).

EXOSOMES AND KNOWN UNKNOWNNS

Tick saliva also contains some exosomes, i.e., microRNA (miRNA) in the Ixodid species, and is involved in change in exosomal origin (Díaz-Martín et al., 2015; Hackenberg et al., 2017; Rodriguez et al., 2018). A transcriptomics analysis revealed the presence of some known unknowns in tick saliva, e.g., in *D. andersoni*, 677 proteins are identified, and out of this, 80% are of unknown function (Mudenda et al., 2014). It is also probable that tick saliva also contains some unknown unknowns, which are likely to reveal further interesting information regarding the saliva of ticks.

THE FUNCTION OF TICK SALIVA IN CONTROLLING HOST RESPONSE

When a tick bites, it causes activation of coagulation factor XII and bradykinin release, which cause host pain sensation; however Ixodid ticks destroy the bradykinin by metalloprotease enzyme angiotensin-converting enzyme (ACE) (Chmelar et al., 2012). Two types of ACE have been identified in *A. maculatum* (Jelinski, 2016). Ticks also use lipid mediators (endocannabinoids) as an analgesic to hide their presence, and, along with this, other analgesic mediators are found: adenosine and miRNA (Hackenberg et al., 2017).

Vasoconstriction is another phenomenon that occurs during tick bite, and Ixodid ticks use prostaglandins and adenosine as counter agents against vasoconstriction (Chmelar et al., 2012). Other proteins involved in vasoconstriction are apyrase, serotonin-binding salivary proteins, histamine-binding proteins, and phenylalanine-rich peptides, which may modulate vascular permeability (Pekáriková et al., 2015).

Platelet aggregation and activation are controlled during tick bite, by the tick releasing, *via* the saliva, apyrases, thrombin inhibitors, arginine-glycine-aspartate motif, and serotonin binders, which break down the platelet activation agonist ADP, damage the cells, and, ultimately, neutralize the platelet aggregation agonist (Tang et al., 2015; Yun et al., 2016). After platelet plug formation, the secondary phase of hemostasis occurs, i.e., coagulation factor assembly, which leads to fibrin plug formation (Palta et al., 2014). Tick saliva contains serine protease inhibitors as anti-coagulants which target the thrombin and coagulation factor FXa (Blisnick et al., 2017) along with these Kunitz domains also contain thrombin inhibitors e.g., *O. moubata* contain ornithodorin, variegin in *A. variegatum*, Salp 14 in *I. scapularis* saliva, and ixonexin (tail peptide) in *I. scapularis* (Thompson et al., 2017; Assumpção et al., 2018). This multi-targeted approach by ticks allows for successful control of the coagulation process by interacting with the host coagulation cascade.

Mast cells containing pro-inflammatory compounds are present in abundance in host skin and act as the first line of defense against ticks (Wernersson and Pejler, 2014). When ticks attach to host skin, they activate mast cells, which results in degranulation, and the release of their contents into the extracellular environment, starting bioactive compound *de novo* synthesis. Ticks use lipocalins, Kunitz-type proteins, to control histamine, serotonin, and tryptase activity, stabilize mast cells, and prevent *de novo* synthesis (Schuijt et al., 2013). Sialostatin L targets IRF-4-dependent transcription in mast cells, resulting in interleukin-9 suppression (Klein et al., 2015). Pro-inflammatory cytokines (i.e., IL-1, IL-6, IL-8, and TNF) are produced by the host, and ticks inhibit these cytokines by capturing the ligand using cytokine binders called evasions, and about 265 evasions have been identified in different tick genera (Hayward et al., 2018). In *A. variegatum*, the salivary peptide amphiregulin inhibits cytokine production (Tian et al., 2016). The complement system is the main trigger for inflammation, and about 40 proteins take part in this phenomenon. During tick bite, the complement system is inhibited by the different complement inhibitors present in tick saliva that is produced during feeding and stored in the granular acini (Jore et al., 2016; Perner et al., 2018).

Ticks can control host immune responses by producing immunomodulators that target the host acquired and innate immune system (Kotál et al., 2015a; Wikel, 2018a). In *R. appendiculatus*, 64 TRP proteins cross-react with epitopes in tick midgut (Kotál et al., 2015b; Chmelar et al., 2016b). Dendritic cells are known as immune sentinels and sense danger and send information to other immune cells and contribute to both adaptive and innate immunities (Heath and Carbone, 2013; Austyn, 2017). In metastrongyloid Ixodid ticks, lipocalin proteins are available that target dendritic cells, e.g., japanin (Preston et al., 2013), while in prostrongyloid ticks, the sialostatin L group, cystatin protease inhibitors, are available for dendritic cell control, e.g., Salp 15 that inhibits $CD4^+$ T cell and dendritic cell activation (Carvalho-Costa et al., 2015; Kotál et al., 2015b; Tomás-Cortázar et al., 2017). Regulatory T cells are also controlled by Salp 15 by

the production of immunosuppressants, e.g., adenosine (Tomás-Cortázar et al., 2017). Salp 15 also affects the ability of B cells to produce antigen-specific antibodies, and direct inhibitors of B cells are also found in tick saliva, e.g., B cell inhibitory proteins in *I. ricinus* and B cell inhibitory factors in *Hyalomma* (*H.*) *asiaticum* (Páleníková et al., 2015).

Dynamic changes in salivary bioactive compound activity are correlated with host responses, cellular and chemical mediators, gluttony, and sex (Heinze et al., 2014). In adult *D. andersoni* females, it was found that within 2–5 days of the start of the feeding process, a total of 372 proteins can be identified, and among these, almost 140 were identified on day 2 and 165 on day 5 (Mudenda et al., 2014). Expression of saliva genes was recorded to be higher in female ticks than in males, which reflects the goals of feeding females to attain maximum blood meal size and increase egg production (De Castro et al., 2017). Transcriptomics studies have confirmed that salivary gene expression is variable as feeding progresses in *I. ricinus* females (Perner et al., 2018). For changes in saliva compositions, the term “sialome switching” is used. This change may be attributed to feeding environment changes, i.e., change in host type and host immune system (Karim and Ribeiro, 2015). Studies on saliva time regulation are limited; possibly, epigenetic regulation, chromatin remodeling, and histone modification are involved (Kotsyfakis et al., 2015; Cabezas-Cruz et al., 2016). Salivary gland acini granules are also involved in tick blood-feeding dynamism. Immunoglobulin binding proteins specific for males are stored in unfed *R. appendiculatus* male type IV acini, cement protein in type 3 acini in *D. variabilis*, and migration inhibitory factor (MIF) in *A. americanum* (Perner et al., 2018). This indicates that tick saliva is ready to start its action as soon as ticks attach and start feeding, and the contents of early salivary gland granules help to elucidate tick-host interaction at the feeding site and are early-stage targets for anti-tick vaccine development.

TRANSMISSION DYNAMICS OF VIRUSES IN TICKS

Vector-borne viruses (VBVs) exhibit biological transmission: they enter into the vector, infect, and replicate before reaching the vertebrate host. Following the entry of a virus into the midgut of ticks, it must escape from the midgut and reach the tick salivary glands from which it will be transmitted to the vertebrate host (Šimo et al., 2017). This is described as an extrinsic incubation period as the virus remains inside the vector. Movements of the virus within a vector (midgut to salivary glands) are life-threatening for viruses because of various potential barriers: midgut infection, midgut escape, salivary gland infection, and salivary glands escape (Kazimírová et al., 2017) (**Figures 2, 3**).

More precisely, at the cellular level, the virus may remain unable to cross the cell membrane for entry into the cytoplasm, or the virus may replicate inside the cell following entry but is incompetent to come out of the infected cell (Dou et al., 2018). The intrinsic ability of a tick to become infected, support replication, and ultimately, transmit a tick-borne virus is genetically determined and influenced by environmental

factors. Likewise, the ability of a tick-borne virus to infect, replicate, and be dispersed by a tick is both determined genetically and influenced by extrinsic factors. At one level, vector competence is determined through genotype-by-genotype interactions (Althouse and Hanley, 2015). In this sense, the outcome of infection depends on the interplay between the products of 2 genomes, the so-called virus–vector interactome. However, molecular interactions between tick-borne viruses and their tick vectors are yet to be explored. For example, we know little about the role of RNA interference (RNAi) in ticks and, in particular, whether it acts as an innate antiviral immune response modulating virus infection (Kurscheid et al., 2009; Kazimírová et al., 2017). Evidence in mosquitoes indicates that the RNAi pathway modulates arboviral infections, for example, by acting as a gatekeeper to the incoming viruses at the midgut, by minimizing the intensity of the viral infections, and reducing the spread of viruses from the midgut to secondary tissues (Khoo et al., 2010). It seems likely that a similar phenomenon occurs in ticks (Kazimírová et al., 2017).

MIDGUT INFECTION BARRIER

Evidence of a midgut infection barrier has been reported in experimental studies with *Rhipicephalus appendiculatus* and *Amblyomma variegatum*, two tick species that are adept vectors of the Thogoto virus but are not competent for the Dhori virus (Gondard et al., 2020). When larvae and nymphs were fed on virus-infected hamsters, the Thogotovirus settled and replicated within the ticks and was subsequently transmitted when the succeeding adults fed on uninfected hamsters. In contrast, both tick species were refractory to infection by the Dhori virus when they fed on hamsters infected with this virus, with infectivity in the engorged ticks disappearing in 2–6 days. However, when the Dhori virus was inoculated into the hemocoel of engorged nymphs, effectually bypassing the midgut, the virus survived transcardially and was transmitted during the feeding of infected ticks. Thus, the midgut of *R. appendiculatus* and *A. variegatum* appear to be a barrier to infection by the Dhori virus but not by the Thogoto virus. As the Thogoto virus and the Dhori virus are members of the same virus genus and have similar infection strategies, the most likely reason for the variation in vector-species specificity lies in the sequence diversity of viral surface glycoproteins (Gondard et al., 2020). If this is the case, specific surface receptors might be existing on the surface of tick midgut cells to which the Thogoto virus binds *via* its glycoprotein but are not recognized by the Dhori virus. Alternatively, the Thogoto virus might have evolved a mechanism for evading the defense mechanism of *R. appendiculatus* and *A. variegatum* that is efficient against the Dhori virus.

Studies on African swine fever virus have also demonstrated the importance of virus replication in the midgut for successful infection of its vector, *Ornithodoros porcinus* (Nuttall, 2019b). A Malawi strain of the virus failed to replicate successfully in midgut epithelial cells of ticks exposed orally to the virus, although the virus replicated successfully in other cell types.

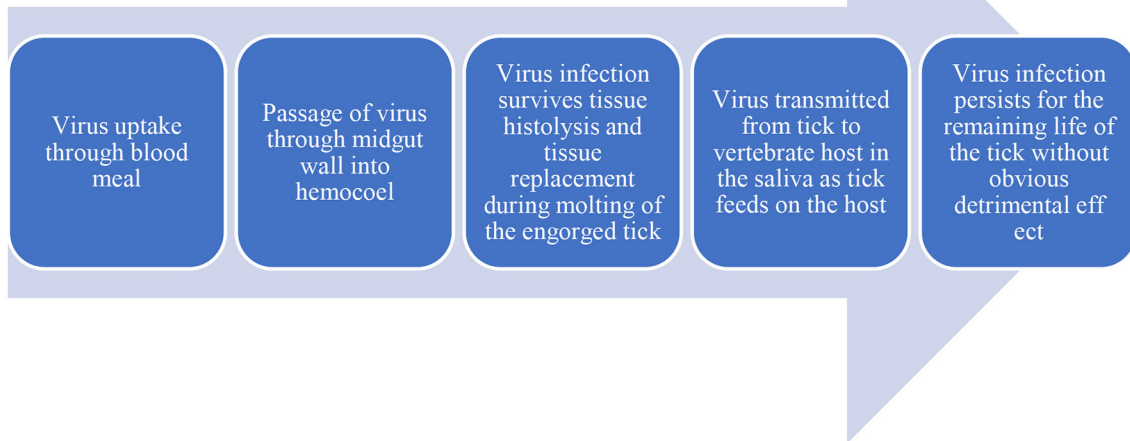


FIGURE 2 | Flowdiagram depicting the virus flow in Host and Vector.

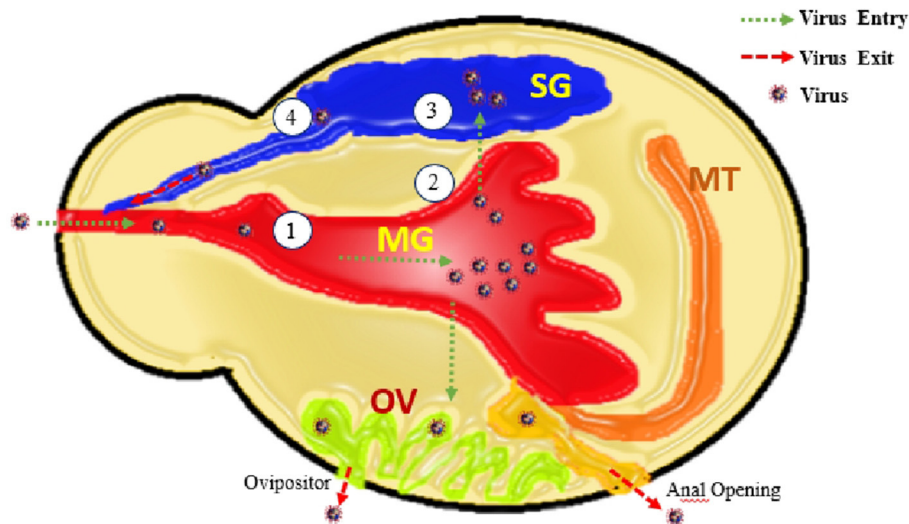


FIGURE 3 | Elaborating the entry of virus through mouth opening along with bleed meal into mid gut (MG), virus multiplication and transfer into ovaries (OV), Salivary glands (SG), and anal opening. From these routes virus shed with saliva, transovarial (with next progeny of ticks), and anus. Along with these four barriers 1. Entry of virus into MG-cell, 2. Exit of virus from midgut cells, 3. Entry of virus into SG-cells (acini), and 4. Exit of virus from MG-cells.

Moreover, a different virus strain was infected and replicated successfully under the same experimental conditions. The results suggest that missing or defective genes in the Malawi strain might account for the failure of the virus to replicate successfully in midgut epithelial cells, although why this should be the case for midgut cells and not appear for other cell types is a conundrum (Lledó et al., 2020). Compared with evidence of a midgut infection barrier based on experimental studies with the Dhori and Thogoto viruses, African swine fever virus data

suggest that there might be different types of midgut infection barriers in ticks (Rock, 2021).

One type of midgut barrier might be provided by the unusual way in which ticks digest their blood meal. Unlike insects, in which blood meal digestion is extracellular, ticks are heterophagous: intracellular digestion of blood meal takes place in midgut cells. Several insect-borne viruses depend on proteolytic conditions in the insect gut lumen to cleave a surface protein and expose the virus receptor that initiates infection of

the vector (Talactac et al., 2021). The absence of such proteolytic enzymes in tick lumen could provide a highly efficient barrier to infection by viruses that require cleavage of a surface virus protein to initiate infection. If the process of blood meal digestion in ticks is an efficacious barrier to virus infection, arboviruses that can infect ticks are likely to have evolved an outer surface structure that differs significantly from that of their genetic relatives that are not transmitted by ticks. There are some data to support this hypothesis: (i) striking size variations in outer surface proteins of midge-transmitted arboviruses relative to the tick-transmitted arbovirus Broadhaven virus (Nuttall, 2013) and (ii) similarly pronounced differences in surface glycoproteins of influenza viruses relative to their tick-borne relatives (Shi et al., 2018).

However, the three-dimensional structures of the flavivirus that envelope proteins of tick-borne and mosquito-borne flaviviruses appear similar, although this similarity might reflect the common fusion role of this protein after entry into cells (Lemasson et al., 2021). One factor in the infection process that is usually overlooked is the state of a virus within the blood meal of its vector, whether as an extracellular virion (virus particle) or as an infected cell that may potentially be imbibed in the infected blood meal of a feeding tick. If a cellular rather than an extracellular viral inoculum is more effective in establishing infection in the tick vector, this might in part explain the efficiency of non-viremic transmission. Besides the state of a virus in the blood meal (whether “free” or within host cells), the timing of virus uptake also might be a critical factor in determining whether a virus infects a tick. This is because, like hematophagous insects, ticks produce a peritrophic membrane or glycocalyx on the apical surface of the midgut epithelium some hours after the commencement of feeding (Bhowmick and Han, 2020). The chitin-enriched covering potentially presents a formidable barrier to the infection of midgut epithelial cells by viruses. Studies on mosquitoes have shown that virions ingested in the viremic blood meal acquired from chickens infected with western equine encephalitis virus concentrate adjacent to the midgut epithelium. In contrast, when ticks fed on an artificial blood meal containing the virus, the disseminated virus was observed throughout the midgut lumen (Talactac et al., 2021). It waits to be revealed whether such concentration of virions occurs in the tick midgut and/or whether ingestion of infected cells rather than “free” virions helps the virus overcome the barrier presented by the peritrophic membrane. This suggests that viruses are unable to survive if they do not exit the midgut.

MIDGUT ESCAPE BARRIER

The evidence of a midgut escape barrier in ticks is based on comparative studies on infection of *R. appendiculatus* nymphs infected with the Dhori virus or the Dugbe virus. The Dhori virus can survive for <4 days in *R. appendiculatus* nymphs following vector feeding on an infected host. The Dugbe virus can survive for at least 21 days after vector meal ingestion but remains unable to survive during molting and has no transmission through adult ticks. Following virus inoculation directly into the hemocoel,

just like the Dhori virus, the Dugbe virus replicates and is transmitted by *R. appendiculatus*; explaining that, there are no barriers for the Dugbe virus to infect the salivary glands of *R. appendiculatus* as for the Dhori virus (Kazimírová et al., 2017; Nuttall, 2019a). The variation in survival dynamics recommends that *R. appendiculatus* reveals a midgut infection barrier to the Dhori virus and a midgut escape barrier to the Dugbe virus. However, the nature of the midgut escape barrier is unknown.

DISSEMINATION BARRIER

Once a tick-borne virus has escaped from the tick midgut, it presumably passes through the hemocoel, where tissues and organs are immersed in hemolymph, the transport medium for hormones, nutrients, and immune effector molecules. To migrate to the salivary glands while hiding from the tick's immune system, viruses, such as tick-borne encephalitis virus, African swine fever virus, and Dugbe virus, infect tick hemocytes (Talactac et al., 2021). An alternative route of dissemination is *via* the nervous system. However, although the Thogoto virus was recognized in the neural cortex of the synganglion, it was not apparent in nerve fibers, suggesting that dissemination through tick vector occurs *via* the hemolymph rather than a neural route (Grabowski et al., 2018). A dissemination barrier might exist in mosquitoes in which a virus is restricted to abdominal fat body cells, which play a role in insect immune responses (Lee et al., 2019). Their presence in ticks has not been described.

SALIVARY GLAND INFECTION BARRIER

After reaching the salivary glands, a virus faces barriers like those of the midgut: (i) cell infection and replication and (ii) virus release. Although there are some records of virus detection in saliva, little is known about this critical stage of tick-borne virus transmission (Nuttall, 2019a). Experimental studies with the Thogoto virus and *Amblyomma variegatum* indicate that infection of the salivary glands might not be a precondition for transmission (Gondard et al., 2020); extracellular virus inoculated into the hemocoel was detected shortly afterward in the saliva of ticks. The result was consistent with previous observations that the transmission of Thogoto virus occurred within 24 h of tick attachment to a host, even though virus infection of the salivary glands was not detected until 7 days after feeding commenced. The mechanism of virus transfer from the hemocoel to saliva is unknown. Some proteins found in the hemocoel (e.g., host immunoglobulins) appear to be excreted in tick saliva even though tick salivary glands exclude smaller molecules, such as polyethylene and inulin (Brzezinski, 2019). If tick-borne viruses can pass from the hemocoel into saliva without requiring infection of the salivary glands, salivary gland infection and escape barriers as described for the mosquito-borne transmission of insect-borne arboviruses might not exist in ticks. More importantly, there might be processes by which tick-borne viruses can be transmitted rapidly to the vertebrate host, presenting a greater epidemiological risk to humans.

Interestingly, Thogoto virus-infected ticks secreted less saliva than uninfected ticks or ticks inoculated with the virus into the hemocoel (Nuttall, 2019a). Possibly, virus infection had a deleterious impact on the fluid secretory process. Alternatively, the virus might have stimulated a more vigorous secretion in infected ticks, which would result in lower saliva volumes collected during experimentation. The latter hypothesis is consistent with observations that the tick-borne encephalitis virus stimulates the aggressiveness of its tick vector, *Ixodes persulcatus* (Morozova et al., 2020).

SALIVARY GLAND ESCAPE BARRIER

Once a tick-borne virus has passed into the infected tick's hemocoel and survived molting, there might be a mechanism where the virus can pass into the saliva without having to overcome barriers to infection of the salivary glands. However, evidence of infection of tick salivary glands has been reported for several tick-borne viruses. For example, Dugbe virus infection was detected in discrete cells of type 3 salivary gland acini (Kramer and Tavakoli, 2021). A virus infecting the salivary glands has to be released into the salivary ducts to be transmitted in saliva. Little is known of the mechanisms of release of salivary proteins into saliva, let alone viruses. Similarly, the impact of the physicochemical properties of saliva on tick-borne viruses is unknown. There is no evidence that salivary proteins interact directly with virions, as reported for the tick-borne bacterium *Borrelia burgdorferi*. However, if tick saliva has a pH value in the range of 9–9.5, as some studies have indicated, the alkalinity of saliva could have a profound effect on the conformation of virions in tick saliva. For example, the icosahedral outer surface of the tick-borne encephalitis virus is steady in a limited pH range and opens when exposed to either acidic or alkaline circumstances (Šimo et al., 2017).

TRANS-STADIAL SURVIVAL

After engorgement, immature ticks undergo ecdysis, and histolytic enzymes and tissue replacement create a potentially hostile environment for viruses. For example, the salivary glands undergo reabsorption and restoration during molting. Thus, an essential feature of a tick-borne virus is its ability to survive the molting period for the virus to be transmitted from its tick vector to a vertebrate host. Virus replication dynamics in ticks might indicate these changing environmental conditions (i.e., a fall in infectious virus titer followed by an increase in titer as a virus infects and replicates in replacement tissues) (Nazar et al., 2013; Yoshii, 2019; Migné et al., 2022). However, the replication of some viruses (e.g., Langat in *I. ricinus* and Thogoto virus in *R. appendiculatus*) does not follow these dynamics (Godsey et al., 2021; Hart and Thangamani, 2021). The conflicting results may be explained by various cell and tissue tropisms of tick-borne viruses in their tick vectors. For example, the Thogoto virus establishes infection in the synganglion, where presumably it is safe from the processes of tissue replacement (Nuttall, 2013, 2019b; Morozova et al., 2020).

Because the salivary glands experience reabsorption and rejuvenation during molting, salivary gland infection is expected to be a relatively late event in virus dissemination in tick vectors following the uptake of an infective blood meal. The actual timing of infection of the salivary glands appears to vary. Tick-borne encephalitis virus and Powassan virus infect tick salivary glands before the commencement of feeding; seemingly, they can be transmitted to the vertebrate of the host as soon as fluid secretion occurs (Morozova et al., 2020). In contrast, the Thogoto virus and the Dugbe virus amass in the salivary glands following the commencement of feeding (Nuttall, 2013), although in ticks infected in the earlier stage, the Thogoto virus is found in the salivary glands before blood-feeding (Nuttall, 2019a).

HORIZONTAL TRANSMISSION BY TICKS

The principal route of transmission for tick-borne viruses is horizontal, from an infected tick to an uninfected definitive host and from an infected host to an uninfected tick. Classically, horizontal transmission from vertebrate to tick was suggested to depend on the level of viremia (virus circulating in the blood). It is now recognized that tick-borne viruses can be transmitted effectively even when an infectious virus is not detectable in the blood (Turell, 2020).

VIREMIC TRANSMISSION

Arboviruses have been defined as “viruses that are maintained in nature principally, or to an important extent, through biological transmission between susceptible vertebrate hosts by hematophagous arthropods or through transovarial and possibly venereal transmission in arthropods: the viruses multiply and produce viremia in the vertebrates, multiply in the tissues of arthropods, and are passed on to new vertebrates by the bites of arthropods after a period of extrinsic incubation.” A crucial point in the WHO definition of an arbovirus is the production of viremia. In animals (including humans) infected by the bite of a tick infected with tick-borne encephalitis virus, the virus replicates first in the skin site of tick feeding and in lymph nodes that drain the site. Neutrophils, monocytes/macrophages, and Langerhans cells attracted to the tick feeding site become infected (Hermance and Thangamani, 2018). Viremia develops when a virus is carried *via* the lymphatics to the thoracic duct and into the bloodstream. Primary viremia seeds are extraneural tissues that support further virus replication and shedding of the virus into circulation. In studies on mosquito-borne viruses, the threshold level of viremia was defined as the lowest amount of virus capable of causing an infection in around 1 to 5% of the vector population feeding on the viraemic host (Holding et al., 2020). Thus, the lower the infection level, the smaller the infective dose of virus required to infect the vector and, hence, the greater the likelihood of infection of the vector in nature. However, it was assumed that vertebrates in which an arbovirus induced a level of viremia that was below the threshold (or undetectable) were not hosts of the virus and did not contribute to the cycle of transmission (Nuttall, 2019a).

Experiments designed to evaluate host susceptibility to arbovirus infection routinely involved needle-and-syringe inoculation with the virus and subsequent assays of blood or other tissues for infectivity by intracerebral inoculation of suckling mice or plaque titration in cell cultures. For example, investigations of the infection threshold of *I. ricinus* for louping ill virus in which ticks were fed on domestic chicks inoculated with the virus indicated that viraemic titers of 4.7 and 3.7 log₁₀ infectious units/ml blood were required to establish infections in larvae and nymphs, respectively. This agreed with the threshold of 3.9 log₁₀ infectious units/ml blood for nymphs fed on viraemic sheep. Based on this experimental approach of needle-and-syringe inoculation with virus and sampling for threshold levels of viremia, mountain hares (*Lepus timidus*) were considered not to play a significant role in the transmission cycle of louping ill virus (Reid, 2019; Clark et al., 2020). However, subsequent studies have shown that mountain hares play a critical role in the maintenance of the louping ill virus in nature (Holding et al., 2020).

NON-VIREMIC (CO-FEEDING) TRANSMISSION

The original concept of an arbovirus requiring threshold levels of virus infectivity in the blood for infection to be transmitted to an arthropod vector feeding on an viremic host has now been updated. The first challenges to the role of viremic arbovirus transmission were reported in experimental studies involving the Thogoto virus and tick-borne encephalitis virus (Morozova et al., 2020). Following the feeding of infected and uninfected ticks (adults and nymphs) on susceptible hosts, most uninfected nymphs were infected during co-feeding without viremia (Brault et al., 2018). Another study was performed on non-viremic transmission of tick-borne encephalitis virus during co-feeding of virus-infected and non-virus-infected ticks on a non-viraemic host. The virus-free ticks were found positive while co-feeding (Morozova et al., 2020).

The original demonstration of non-viremic transmission using unnatural laboratory hosts has been corroborated by studies using natural host species. For example, infected and uninfected *I. ricinus* co-feeding on field mice (*Apodemus flavicollis* and *A. agrarius*) and bank voles (*Myodes glareolus*) demonstrated efficient transmission in the absence of viremia or at comparatively low viremia levels. In contrast, pine voles (*Pitymys subterraneus*), which developed high levels of viremia, produced only a few infected ticks (Nuttall, 2019b). Similar results were observed for louping ill virus and uninfected wild-caught hares (*Lepus timidus*). Uninfected *I. ricinus* nymphs became infected with the virus when co-feeding with infected ticks, while the hares showed only low or undetectable levels of viremia (Brault et al., 2018). Evidence of non-viremic or efficient co-feeding transmission has now been recorded for at least 8 different tick-borne viruses. Further evidence of non-viremic transmission has been provided by studies using hosts' immunity to the virus. For example, natural rodent hosts (bank voles and field mice) of tick-borne

encephalitis virus were immunized with the virus, either *via* subcutaneous syringe inoculation with a virus or by an infective tick bite.

Considering host immune status, it was found that there is a significant reduction in transmission efficiency in virus-immune relative to non-immune hosts, the evidence indicates that immunity to a tick-borne virus does not necessarily mean that an immune host is a dead-end for the virus, as is generally assumed. A 5-year survey on small mammals trapped in western Slovakia revealed a 15% neutralizing antibody prevalence for tick-borne encephalitis virus. The antibody prevalence varied seasonally and according to species (Bournez et al., 2020).

In addition to acquired immunity to tick-borne viruses, vertebrate hosts may also develop resistance to tick infestation, which can impair virus transmission (Nuttall, 2013). Immunity to ticks might explain field mice's greater efficiency than bank voles in supporting tick-borne virus transmission among co-feeding ticks (Brault et al., 2018). Further studies are considered necessary to illustrate the effect of host immune status to ticks on the transmission of tick-borne viruses. In non-viremic transmission, a virus is more likely to be ingested in the blood meal as infected cells than as extracellular virions (virus particles). An infected cell provides a bolus inoculum that might contain tens or even thousands of virions, depending on virus genotype (and its cell tropism), cell type, and stage of virus replication in the infected cell. Infected cells should be a more successful means of infection than extracellular virions in the blood meal, not only because they are likely to provide a larger dose of an infective virus but also because of the heterophagic way ticks digest their blood meal. Thus, the uptake of infected cells during co-feeding transmission might contribute to the efficiency of non-viremic relative to viremic transmission, in which the blood meal contains extracellular virions.

SALIVA-ASSISTED TRANSMISSION

Non-viremic transmission between infected and uninfected ticks during co-feeding on the same host can be replicated empirically *via* needle-and-syringe inoculation if tick saliva or salivary gland extracts are included in the virus inoculum. This phenomenon has been named "saliva-assisted transmission" (Šimo et al., 2017). The first evidence that salivary gland constituents promote virus transmission was reported for the Thogoto virus and tick-borne encephalitis virus (Nuttall, 2019a). For example, syringe inoculation experiments using the Thogoto virus mixed with salivary gland extract generated from uninfected ticks resulted in a 10-times higher number of infected nymphs as compared to the numbers infected while feeding on a host inoculated with the virus. As with non-viremic virus transmission between co-feeding infected and uninfected ticks, none of the inoculated animals showed detectable viremia (Brault et al., 2018).

Augmentation of virus transmission was observed only with an inoculum mixed with salivary gland extract of infected ticks and was not observed with salivary glands from unfed ticks or with extracts from any other tick organ. Similar direct evidence of saliva-assisted transmission has been reported for

the Lyme disease spirochetes *Borrelia afzelii*, *B. burgdorferi sensu stricto*, and *B. lusitaniae*, and for *Francisellatularensis* (Sprygin et al., 2019). The recognition of a saliva protein of *I. scapularis*, Salp15, that promotes the transmission of *B. burgdorferi sensu stricto* enabled the direct demonstration of saliva-assisted transmission *via* co-inoculation of mice with the recombinant Salp15 protein and the spirochete and by use of the RNAi technique. Comparable evidence of saliva components that promote virus transmission is lacking, although many candidates have been considered (Nuttall, 2019b). One of the most promising attribute of the tick-borne encephalitis virus is that it is the dendritic cell modulator (Fialová et al., 2010).

VERTICAL TRANSMISSION BY TICKS

Various tick-borne viruses are transferred vertically from parents to offspring. This ability is found in all virus families and occurs in a range of both Argasid and Ixodid tick species. However, the percentage of infection in offspring (larvae) from mothers as transovarial transmission was <5 percent (Raney et al., 2022). Therefore, the prevalence rate *via* vertical transmission is considered too low to maintain tick-borne viruses without the amplifying effect of horizontal transmission (Turell, 2020). However, larvae show a highly non-random distribution on their hosts, and individuals from an egg batch quests together. Even if only a few larvae from an egg batch are infected transovarially, the infection rate might be enhanced as a result of non-viremic transmission among co-feeding larvae (Nuttall, 2019a). By this means, the low prevalence of transovarial infections may be augmented to yield much higher numbers of nymphal infections and, therefore, make a substantial contribution to virus survival. Opportunities for such augmentation of vertically transmitted infections take place in the field, where a low prevalence of tick-borne encephalitis virus infection in *I. ricinus* larvae has been recorded. Comparable results have been documented for the Colorado tick fever virus and the Crimean-Congo hemorrhagic fever virus, whereas higher filial infection prevalence was reported for the African swine fever virus (Yadav et al., 2019; Hughes et al., 2021).

MICROCLIMATIC CONDITIONS AT TICK-PATHOGEN INTERFACE

The distribution and abundance of ticks are influenced by macro and microclimatic changes, travel, land use, human behavior, and habitat modification. These factors also influence the demography of tick-borne pathogens around the globe. Resurgence, the emergence of new diseases, is also influenced by population growth, shifting, grazing, and transboundary transportation of animals for the economy and politics. Intrinsic changes and extrinsic factors both are enabling factors for tick-borne diseases (Pfäffle et al., 2013; Baneth, 2014; Dantas-Torres, 2015). Ticks are very susceptible to climate. They spend most of their lifetime in the environment and all life cycle stages are dependent on climate variability. Although vegetation and host availability modulate the dynamics of their population,

the climate is the major driver for the absence or presence of ticks (Esser et al., 2019). Ticks adapt to vegetation or microclimatic conditions for their survival and development. Host availability concerning time and space is very important for bionomics. Environmental characteristics (rainfall, humidity, and temperature), host characteristics (age, sex, and bodily condition), and management strategies (animal husbandry and land use) all influence tick loads (Kemal et al., 2016).

Shelter and protection under harsh climatic conditions are other drivers for questing ticks because questing ticks are more vulnerable to these conditions. Poor tick management tactics and large-scale transhumance migration of cattle in search of water and pasture during the dry season are causes of excessive tick infestations in several regions (Mirkena et al., 2018). The wet season is found favorable for the progression of ticks and tick-borne diseases, as they require a humidity level of 85–90%. Both the poor health of animals and the wet season are enabling factors for tick burden and illnesses. In tropical dry lands, the wet season is marked by moderate to heavy rainfall, increased humidity, increased plant cover, and an increase in the availability of appropriate hosts (Medlock et al., 2013; Vander Waal et al., 2017). The rainy season, as compared to the dry season, provides more promising micro-climatic conditions for tick mass reproduction and dissemination in hosts (Esser et al., 2019). After a few months of drought, cow mortality owing to tick-borne illnesses (East Coast fever or anaplasmosis) was found to be greater than that seen in the rainy season (Chepkwony et al., 2020).

Drought conditions verily enhance the abundance of ticks as the animals' body condition deteriorates and results in mortalities (Brown et al., 2014). Vander Waal et al. (2017) discovered that during the dry season, parasites, such as ticks, fleas, and mites, were more commonly exchanged in watering locations than during the rainy season. Temperature, with relatively low humidity, leads to the desiccation of eggs and interrupts the life cycle of ticks. Low water in the environment also leads to water stress in adult ticks.

TICK MANAGEMENT

Tick burden was found significantly lower in intensively managed ranches than in ranches managed with the transhumance management scheme. Nonetheless, tick loads on cattle are found to be reduced under intensive management systems with the utilization of acaricides and typically limited host mobility. In contrast, transhumance, which is a key adaptation for pastoralist societies, has been demonstrated to have a favorable impact on parasite distribution and disease dynamics, since animals from nearby areas are likely to bring ticks with them (Mutavi et al., 2018). The epidemiology of ticks and tick-borne diseases is being influenced by dynamic interactions between the abiotic and biotic factors (Wikel, 2018b). Seminal studies have given the concept that zoonotic pathogens and vectors related to them live in distinct habitats that provide the concept of landscape epidemiology or natural nidality of vectored transmissible diseases. Diving into the cellular and molecular level of interaction of tick-host-pathogen, studies

provide seminal knowledge of the establishment, pathogenesis, and characterization of the pathogens' transmission and novel clues for control of pathogens and their vectors.

EFFECT OF HEAT SHOCK PROTEINS ON TICKS

Heat shock and other stress-related responses are helpful for the modulation of ticks and pathogen infections (Espinosa et al., 2017). Stress response proteins (SRPs) and heat shock proteins (HSPs) provide cells with a higher level of tolerance against harsh environments and protect organisms from damage. Glutathione-S-transferase, metallothioneins, ferritin, and selenoproteins have been reported to be involved in various stress situations, such as blood-feeding, pathogen infections, tick attachment, oxidative stress, and heat shock (Busby et al., 2012; Galay et al., 2014; Siddiqi et al., 2016; Hernandez et al., 2019).

Various studies reported that stress response is induced by pathogen infection and heat shock (Rosche et al., 2021; Neelakanta and Sultana, 2022). However, under the natural pathogen-vector relationship, there is no significant interaction between HSPs and SRPs and reflection of the mechanism of co-evaluation. High temperatures and blood-feeding mainly affect the questing speed of ticks under the overexpression of sublethal, HSP 20, and HSP 70. Ticks acquire pathogens from reservoirs while feeding on them and transmit them to a host after multiplication in the gut wall. At the tick-pathogen interface, a virus has to overcome salivary gland barriers and midgut in the body of a tick (Benelli, 2020).

ROLE OF IMMUNITY IN TICK-PATHOGEN INTERFACE

Ticks' immunity is only dependent on innate immunity, and there is no adaptive immunity, so viruses invade ticks and evade the host immune system, and keep themselves safe from the phagocytosis, nodulation, encapsulation, and secretions of hemolymph (innate immunity) of ticks (McNally and Bloom, 2013). Additional antiviral innate response is dependent on RNAi, which limits virus replications (Migné et al., 2022). Metagenomic studies elucidated that endosymbiont and other pathogens are also present in ticks at the same time (Papa et al., 2017). Tick saliva is the key factor for the increasing pace of tick fauna. Ticks are capable of modulating their saliva, which is a predisposing factor for bloodsucking. As the modulation results in the successful acquisition of feed, this makes ticks successful in the environment and increases pathogen transmission (Wikel, 2013, 2018a; Kotál et al., 2015b; Chmelar et al., 2016a,b). Molecular technologies, such as genomics, metagenomics, functional genomics, proteomics, transcriptomics, and metabolomics, are advanced tools for the rapid detection of pathogens and understanding their complex pathways at the tick-pathogen interface. Saliva makes the cutaneous environment of a host favorable for blood-feeding, transmission, and establishment of infections and infectious agents by deviation or suppression of host pain, inflammation,

hemostasis, adaptive and immune defenses, and wound healing (Wikel, 2013, 2018b; Kotál et al., 2015b; Chmelar et al., 2016a,b; Kazimírová et al., 2017).

The first complex study on tick saliva was carried out by analyzing cDNA libraries on bases of expression (Karim and Ribeiro, 2015). Initial transcriptome characterization of salivary glands was under protein constituent complexity and conducted by applying high throughput sequencing technology (Wikel, 2018b). Combined proteomics and transcriptomics analyses provide deep knowledge to understand functional genomics. Pathogens are not entirely silent in ticks but may also affect vector survival, gene expression, and behavior. These are some factors that cause variations in the tick-pathogen relationship. New generation sequencing will help provide more insights into the tick-pathogen interface.

MITIGATION STRATEGIES FOR TICK-BORNE VIRUSES

Ticks have emerged as a vector for virus transmission with unique features, including lengthened life span and multiplex development, prolonged feeding periods, characteristic digestion of blood in the midgut, and hematophagy throughout life stages, making them a successful vector for virus transmission while contributing to the failure to control tick-borne diseases. Tick control methods can be clumped into chemical, non-chemical, and genetic manipulation, biological control, herbal acaricide, use of biopesticides, and vaccination using tick antigens (Manjunathachar et al., 2014).

ACARICIDAL CONTROL

Until now, tick control is still mainly based on the use of acaricides to encounter tick-related issues and economic losses. Unfortunately, unjustified and extensive use of acaricides has led to some serious concerns comprising the development of acaricidal resistance in ticks, residual effects in milk and meat, and eco-unfriendliness. Moreover, mutations in genes associated with drug susceptibility have also been reported to be leading to the development of resistance. Furthermore, it is resulting in a rise in the lethal dose of drugs for a particular determined species. Currently, a combination of various acaricidal drugs by combining potent active ingredients is widely being used to make the mechanisms of action diverse and minimize the emergence of tick resistance (Domingos et al., 2013). This is a strong signal for the future use of chemical-based acaricide for tick control, as it is still the backbone of tick control strategies. However, the fact cannot be ignored that wide dependence on acaricide usage is not expendable and demands the attention of researchers to avoid the spread of tick-borne viral infections.

VACCINES AND GENETIC MANIPULATION

One reason for the availability of comparatively fewer vaccines to control TBV is that infectious diseases have a worse epidemiological impact than tick-borne viral diseases. The

development of a vaccine that particularly interferes with the transmission of tick-borne viruses can aid to overcome the challenge (Kazimírová et al., 2017). Tick feeding exerts certain effects on the host's immune system expressing the complex aspects of host-tick interaction. The slow feeding habit of ticks accompanied by immunomodulatory and immunosuppressive components of their saliva made ticks survive longer on a host (Tirloni et al., 2014). Besides this protective mechanism, the salivary components also act as antigens to trigger immune responses resulting in acquired resistance of a host. However, this form of resistance by the host is transitory, suggesting that ticks have eluded the host's immune system (Kitsou et al., 2021).

The effectiveness of a vaccine greatly depends on the magnitude and persistence of an antibody, although repeated booster is essential for maximum efficacy. The commercially available anti-*Boophilus* vaccine containing BM86 antigen has been found effective. However, DNA anti-tick vaccines are in inception. It is believed that plasmid-injected DNA molecules directly enter the nucleus and remain as episomal DNA inside the nucleus, generating protective antigens if a cell lives. The uninterrupted *in vivo* formation, processing, and presentation of antigens to T cells in DNA vaccinated animals help to maintain maximum antibody titer resultantly avoiding the need for the repeated boosters (Rego et al., 2019).

A tick control strategy comprising a vaccine based on a recombinant tick gene exhibits promising results. It demonstrates several advantages, as it is cost-effective, reduces acaricidal application, and minimizes the prevalence of tick-borne diseases by reducing the exposure of animals to infected ticks. However, the efficacy of such a vaccine widely depends on geographical distribution and tick species (de la Fuente et al., 2007). Tick cell lines have played a significant role in the identification of tick protective antigens to produce a wide range of vaccines for controlling tick-borne pathogens. Cell lines obtained from susceptible and resistant ticks, gene manipulated cell lines, and cell lines promoting the growth of intracellular tick-borne pathogens generated *in vitro* can assist to decrease the prevalence of tick-borne diseases (Al-Rofaai and Bell-Sakyi, 2020).

USE OF ENDOSYMBIONTS

Endosymbionts can be a potential tick control strategy, but unfortunately, it is still unexplored. Few studies in the past have reflected on the identification and characterization of endosymbionts of ticks (Azagi et al., 2017). Ticks depend on the host's blood, the only source of nutrition providing all the essential nutrients for their growth and development. Ticks do have primary endosymbionts that are transmitted maternally or vertically through progenies. This association between ticks and endosymbionts can be beneficial for an arthropod host. Since endosymbionts are necessary for an arthropod host, removal of these organisms would make the survival of the arthropod host difficult. Studies on physiology and genetics would be required for the manipulation of this symbiotic interface. Along with that, microbiological, chemotherapeutic, and immunological approaches will also be required (Budachetri et al., 2018).

BIOLOGICAL CONTROL

Natural enemies of ticks include parasitoid wasps, insectivorous birds, nematodes, *Bacillus thuringiensis* bacteria, and deuteromycete fungi (Bassiana, Beauveria, and Metarhizium). The biocontrol potential of entomopathogenic fungi for tick control has been examined in various laboratory bioassays (Ebani and Mancianti, 2021). Conidia have been found effective when applied on an animal host under field and semi-field conditions but greatly depend on the behavior of the tick species infesting and the animal host involved.

Various species of fungi were reported as pathogenic to a wide range of tick species and cause high mortality in susceptible species, such as *R. microplus*. Similarly, *M. anisoplae* can also aid in the management of the tick population with relatively fewer adverse effects on the environment. Moreover, it has been reported as potentially effective against a wide range of arthropods and, thus, can cause the death of non-target species (Azagi et al., 2017). Some parasitoid *Ixodiphagus hookeri* wasps can parasitize various forms of ticks, such as larvae and nymphs. It has been suggested that the odor from tick host animals attracts parasitoid wasps (Sormunen et al., 2019). Moreover, 42 nematode strains have shown an anti-tick activity with varying degrees of virulence. At higher concentrations and under optimal conditions, nematodes can kill engorged female ticks before they lay eggs. It is also said that nematodes normally do not attack ticks, but using a tick as bait can help to detect some aggressive strains of tick pathogenic nematodes (Singh et al., 2018).

Some entomopathogenic bacteria, such as *B. thuringiensis*, exhibit mortality in ticks, specifically the larval form of ticks, and higher mortality rates were recorded with an increase in spore concentration. This control strategy offers potential for the control of ectoparasites (Ebani and Mancianti, 2021).

GENETIC MANIPULATION USING RNA INTERFERENCE

RNA interference is an extensively used gene silencing technique for the genetic manipulation of ticks. It has been proved as an effective tool to identify and characterize tick-pathogen interference, tick protective antigens, and screening. It is a nucleic acid-based reverse genetic method used to determine gene function and its possible effects on the metabolic pathway by disrupting gene expression. Four methods, namely, injection, soaking, feeding, and virus production, of dsRNA have been implied to deliver dsRNA for RNA interference in ticks (Niu et al., 2018).

Through this technique, a large number of genes can be recognized as potent candidates for a vaccine. This approach is relatively cheap and requires minimum use of laboratory animals. Selected antigens, after characterization and evaluation, can be produced as recombinant proteins that can be used for vaccine trials (Sudhakar et al., 2013). To understand better and utilize this approach, dsRNA-induced RNAi mechanism should be clarified and refined, since it can elaborate the tick-virus interface and can

play a role in vaccine development and control of transmission of tick-borne viruses.

CONCLUSION

Based on the above-mentioned discussion, it can be concluded that tick-borne viruses are a major threat to public health, and tick-virus interaction is the key point of the spread of these infections. Different factors both from the side of ticks and viruses are involved in virus replication and blockage in tick saliva and midgut. By controlling/ modifying the proteomics of tick saliva, transmission routes, and vector control strategies, the damage caused by tick-borne viruses can be minimized. We are hopeful that this review will enhance the public perception regarding these viruses and tick-virus interaction and will

provide insight into future investigations regarding their control using the factors involved at the tick-virus interaction level.

AUTHOR CONTRIBUTIONS

All authors equally contributed in manuscript writing and editing. All authors contributed to the article and approved the submitted version.

ACKNOWLEDGMENTS

We are thankful to Professor Emeritus Thomas J Nolan of Penn State University Pennsylvania, United States for assisting with English grammar review and improving the manuscript significantly.

REFERENCES

- Ali, A., Fernando Parizi, L., Garcia Guizzo, M., Tirloni, L., Seixas, A., Silva Vaz, I., et al. (2015a). Immunoprotective potential of a rhipicephalus (boophilus) microplus metalloprotease. *Vet. Parasitol.* 207, 107–114. doi: 10.1016/j.vetpar.2014.11.007
- Ali, A., Khan, S., Ali, I., Karim, S., da Silva Vaz, I., and Termignoni, C. (2015b). Probing the functional role of tick metalloproteases. *Physiol. Entomol.* 40, 177–188. doi: 10.1111/phen.12104
- Al-Rofaai, A., and Bell-Sakyl, L. (2020). Tick cell lines in research on tick control. *Front. Physiol.* 11, 152. doi: 10.3389/fphys.2020.00152
- Althouse, B. M., and Hanley, K. A. (2015). The tortoise or the hare? Impacts of within-host dynamics on transmission success of arthropod-borne viruses. *Philos. Trans. R. Soc. B Biol. Sci.* 370, 20140299. doi: 10.1098/rstb.2014.0299
- Assumpção, T. C., Mizurini, D. M., Ma, D., Monteiro, R. Q., Ahlstedt, S., Reyes, M., et al. (2018). Ixonnexin from tick saliva promotes fibrinolysis by interacting with plasminogen and tissue-type plasminogen activator, and prevents arterial thrombosis. *Sci. Rep.* 8, 4806. doi: 10.1038/s41598-018-22780-1
- Austyn, J. M. (2017). Dendritic cells in the immune system-history, lineages, tissues, tolerance, and immunity. *Microbiol. Spectr.* 4, 4–6. doi: 10.1128/9781555819194.ch10
- Azagi, T., Klement, E., Perlman, G., Lustig, Y., Mumcuoglu, K. Y., Apanaskevich, D. A., et al. (2017). Francisella-like endosymbionts and Rickettsia species in local and imported Hyalomma ticks. *Appl. Environ. Microbiol.* 83, e01302–e01317. doi: 10.1128/AEM.01302-17
- Balashov, Y. S. (1972). Blood-sucking ticks (ixodidae)-vectors of disease of man and animals. *Misc. Pib. Entomol. Soc. Am.* 8, 161–376.
- Baneth, G. (2014). Tick-borne infections of animals and humans: a common ground. *Int. J. Parasitol.* 44, 591–596. doi: 10.1016/j.ijpara.2014.03.011
- Barker, D. M., Ownby, C. L., and Krolak, J. M. (1984). The effects of attachment, feeding, and mating on the morphology of the type I alveolus of salivary glands of the lone star tick, *Amblyomma americanum* (L.). *J. Parasitol.* 70, 99–113. doi: 10.2307/3281931
- Benelli, G. (2020). Pathogens manipulating tick behavior—through a glass, darkly. *Pathogens* 9, 664. doi: 10.3390/pathogens9080664
- Bente, D. A., Forrester, N. L., Watts, D. M., McAuley, A. J., Whitehouse, C. A., and Bray, M. (2013). Crimean-Congo hemorrhagic fever: history, epidemiology, pathogenesis, clinical syndrome and genetic diversity. *Antiviral Res.* 100, 159–189. doi: 10.1016/j.antiviral.2013.07.006
- Bhowmick, B., and Han, Q. (2020). Understanding tick biology and its implications in anti-tick and transmission blocking vaccines against tick-borne pathogens. *Front. Vet. Sci.* 7, 319. doi: 10.3389/fvets.2020.00319
- Bichaud, L., de Lamballerie, X., Alkan, C., Izri, A., Gould, E. A., and Charrel, R. N. (2014). Arthropods as a source of new RNA viruses. *Microb. Pathog.* 77, 136–141. doi: 10.1016/j.micpath.2014.09.002
- Binnington, K. C. (1978). Sequential changes in salivary gland structure during attachment and feeding of the cattle tick, *Boophilus microplus*. *Int. J. Parasitol.* 8, 97–115. doi: 10.1016/0020-7519(78)90004-8
- Blisnick, A. A., Foulon, T., and Bonnet, S. I. (2017). Serine protease inhibitors in ticks: an overview of their role in tick biology and tick-borne pathogen transmission. *Front. Cell. Infect. Microbiol.* 7, 1–24. doi: 10.3389/fcimb.2017.00199
- Bournez, L., Umhang, G., Moinet, M., Richomme, C., Demerson, J.-M., Caillot, C., et al. (2020). Tick-borne encephalitis virus: seasonal and annual variation of epidemiological parameters related to nymph-to-larva transmission and exposure of small mammals. *Pathogens* 9, 518. doi: 10.3390/pathogens9070518
- Brault, A. C., Savage, H. M., Duggal, N. K., Eisen, R. J., and Staples, J. E. (2018). Heartland virus epidemiology, vector association, and disease potential. *Viruses* 10, 498. doi: 10.3390/v10090498
- Brown, L., Medlock, J., and Murray, V. (2014). Impact of drought on vector-borne diseases-how does one manage the risk?. *Public Health.* 128, 29–37. doi: 10.1016/j.puhe.2013.09.006
- Brzezinski, K. (2019). *Examining the effects of cold on gut epithelial permeability in locusta migratoria (Master's dissertation)*. Carleton University, Ottawa, ON, Canada.
- Budachetri, K., Kumar, D., Crispell, G., Beck, C., Dasch, G., and Karim, S. (2018). The tick endosymbiont candidate *Midichloria mitochondrii* and selenoproteins are essential for the growth of rickettsia parkeri in the Gulf Coast tick vector. *Microbiome* 6, 1–15. doi: 10.1186/s40168-018-0524-2
- Bullard, R., Allen, P., Chao, C. C., Douglas, J., Das, P., Morgan, S. E., et al. (2016). Structural characterization of tick cement cones collected from in vivo and artificial membrane blood-fed lone star ticks (*Amblyomma americanum*). *Ticks Tick. Borne. Dis.* 7, 880–892. doi: 10.1016/j.ttbdis.2016.04.006
- Burthe, S. J., Schäfer, S. M., Asaaga, F. A., Balakrishnan, N., Chanda, M. M., Darshan, N., et al. (2020). Reviewing the ecological evidence-base for management of emerging tropical zoonoses: kysanur forest disease in india as a case study. *PLoS Negl. Trop. Dis.* 15, e0009243. doi: 10.21203/rs.3.rs-35351/v1
- Busby, A. T., Ayllón, N., Kocan, K. M., Blouin, E. F., De La Fuente, G., Galindo, R. C., et al. (2012). Expression of heat shock proteins and subolesin affects stress responses, Anaplasma phagocytophilum infection and questing behaviour in the tick, Ixodes scapularis. *Med. Vet. Entomol.* 26, 92–102. doi: 10.1111/j.1365-2915.2011.00973.x
- Cabezas-Cruz, A., Alberdi, P., Ayllón, N., Valdés, J. J., Pierce, R., Villar, M., et al. (2016). Anaplasma phagocytophilum increases the levels of histone modifying enzymes to inhibit cell apoptosis and facilitate pathogen infection in the tick vector Ixodes scapularis. *Epigenetics* 11, 303–319. doi: 10.1080/15592294.2016.1163460
- Carvalho-Costa, T. M., Mendes, M. T., Da Silva, M. V., Da Costa, T. A., Tiburcio, M. G. S., Anhê, A. C. B. M., et al. (2015). Immunosuppressive effects of *Amblyomma cajennense* tick saliva on murine bone marrow-derived dendritic cells. *Parasit. Vect.* 8, 22. doi: 10.1186/s13071-015-0634-7

- Chen, Z., Liu, Q., Liu, J. Q., Xu, B. L., Lv, S., Xia, S., et al. (2014). Tick-borne pathogens and associated co-infections in ticks collected from domestic animals in central China. *Parasit. Vect.* 7, 237. doi: 10.1186/1756-3305-7-237
- Chepkwony, R., Castagna, C., Heitkönig, I., Van Bommel, S., and Van Langevelde, F. (2020). Associations between monthly rainfall and mortality in cattle due to East Coast fever, anaplasmosis and babesiosis. *Parasitology* 147, 1743–1751. doi: 10.1017/S0033182020001638
- Chmelar, J., Calvo, E., Pedra, J. H. F., Francischetti, I. M. B., and Kotsyfakis, M. (2012). Tick salivary secretion as a source of antihemostatics. *J. Proteomics* 75, 3842–3854. doi: 10.1016/j.jprot.2012.04.026
- Chmelar, J., Kotál, J., Karim, S., Kopacek, P., Francischetti, I. M. B., Pedra, J. H. F., et al. (2016b). Sialomes and mialomes: a systems-biology view of tick tissues and tick-host interactions. *Trends Parasitol.* 32, 242–254. doi: 10.1016/j.pt.2015.10.002
- Chmelar, J., Kotál, J., Kopecký, J., Pedra, J. H. F., and Kotsyfakis, M. (2016a). All for one and one for all on the tick-host battlefield. *Trends Parasitol.* 32, 368–377. doi: 10.1016/j.pt.2016.01.004
- Chmelar, J., Kotál, J., Langhansová, H., and Kotsyfakis, M. (2017). Protease inhibitors in tick saliva: the role of serpins and cystatins in tick-host-pathogen interaction. *Front. Cell. Infect. Microbiol.* 7, 216. doi: 10.3389/fcimb.2017.00216
- Clark, J. J., Gilray, J., Orton, R. J., Baird, M., Wilkie, G., Filipe, A., et al. (2020). Population genomics of louping ill virus provide new insights into the evolution of tick-borne flaviviruses. *PLoS Negl. Trop. Dis.* 14, e0008133. doi: 10.1371/journal.pntd.0008133
- Coons, L. B., and Lamoreaux, W. J. (1986). *Developmental Changes in The Salivary Glands of Male and Female Dermacentor Variabilis (Say) During Feeding*. University Florida-IFAS. Florida Medical Entomology Lab.
- Dantas-Torres, F. (2015). Climate change, biodiversity, ticks and tick-borne diseases: the butterfly effect. *Int. J. Parasitol. Parasites Wildl.* 4, 452–461. doi: 10.1016/j.ijppaw.2015.07.001
- Dantas-Torres, F., Chomel, B. B., and Otranto, D. (2012). Ticks and tick-borne diseases: a one health perspective. *Trends Parasitol.* 28, 437–446. doi: 10.1016/j.pt.2012.07.003
- De Castro, M. H., De Klerk, D., Pienaar, R., Rees, D. J. G., and Mans, B. J. (2017). Sialotranscriptomics of *Rhipicephalus zambeziensis* reveals intricate expression profiles of secretory proteins and suggests tight temporal transcriptional regulation during blood-feeding. *Parasit. Vect.* 10, 384. doi: 10.1186/s13071-017-2312-4
- de la Fuente, J., Kocan, K. M., Almazán, C., and Blouin, E. F. (2007). RNA interference for the study and genetic manipulation of ticks. *Trends Parasitol.* 23, 427–433. doi: 10.1016/j.pt.2007.07.002
- de la Fuente, J., Villar, M., Cabezas-Cruz, A., Estrada-Peña, A., Ayllón, N., and Alberdi, P. (2016). Tick–Host–Pathogen interactions: conflict and cooperation. *PLoS Pathog.* 12, e1005488. doi: 10.1371/journal.ppat.1005488
- De Meneghi, D., Stachurski, F., and Adakal, H. (2016). Experiences in tick control by acaricide in the traditional cattle sector in Zambia and Burkina Faso: possible environmental and public health implications. *Front. Public Health* 4, 239. doi: 10.3389/fpubh.2016.00239
- Díaz-Martín, V., Manzano-Román, R., Oleaga, A., and Pérez-Sánchez, R. (2015). New salivary anti-haemostatics containing protective epitopes from *ornithodoros moubata* ticks: assessment of their individual and combined vaccine efficacy. *Vet. Parasitol.* 212, 336–349. doi: 10.1016/j.vetpar.2015.08.005
- Domingos, A., Antunes, S., Borges, L., and Rosario, V. E. (2013). Approaches towards tick and tick-borne diseases control. *Rev. Soc. Bras. Med. Trop.* 46, 265–269. doi: 10.1590/0037-8682-0014-2012
- Dou, D., Revol, R., Östbye, H., Wang, H., and Daniels, R. (2018). Influenza A virus cell entry, replication, virion assembly and movement. *Front. Immunol.* 9, 1581. doi: 10.3389/fimmu.2018.01581
- Ebani, V. V., and Mancianti, F. (2021). Entomopathogenic fungi and bacteria in a veterinary perspective. *Biology* 10, 479. doi: 10.3390/biology10060479
- El Shoura, S. M. (1987). Spermiogenesis ultrastructure in the tick argas (persicargas) arboreus (*Acari: Ixodoidea: Argasidae*). *J. Med. Entomol.* 24, 532–535. doi: 10.1093/jmedent/24.5.532
- Espinosa, P. J., Alberdi, P., Villar, M., and Cabezas-Cruz, A. (2017). “Heat shock proteins in vector-pathogen interactions: The anaplasma phagocytophilum model,” in *Heat Shock Proteins in Veterinary Medicine and Sciences*, eds A. Alexander, A. Asea, and P. Kaur (Cham; New York, NY: Springer), 375–398.
- Esser, H. J., Mögling, R., Cleton, N. B., Van Der Jeugd, H., Sprong, H., Stroo, A., et al. (2019). Risk factors associated with sustained circulation of six zoonotic arboviruses: a systematic review for selection of surveillance sites in non-endemic areas. *Parasit. Vect.* 12, 265. doi: 10.1186/s13071-019-3515-7
- Estevés, E., Maruyama, S. R., Kawahara, R., Fujita, A., Martins, L. A., Righi, A. A., et al. (2017). Analysis of the salivary gland transcriptome of unfed and partially fed *Amblyomma sculptum* ticks and descriptive proteome of the saliva. *Front. Cell. Infect. Microbiol.* 7, 476. doi: 10.3389/fcimb.2017.00476
- Estrada-Peña, A., and de la Fuente, J. (2014). The ecology of ticks and epidemiology of tick-borne viral diseases. *Antiviral Res.* 108, 104–128. doi: 10.1016/j.antiviral.2014.05.016
- Estrada-Peña, A., and de la Fuente, J. (2018). The fossil record and the origin of ticks revisited. *Exp. Appl. Acarol.* 75, 255–261. doi: 10.1007/s10493-018-0261-z
- Estrada-Peña, A., Roura, X., Sainz, A., Miró, G., Solano-Gallego, L. (2017). Species of ticks and carried pathogens in owned dogs in Spain: results of a one-year national survey. *Ticks tick-Borne Dis.* 8, 43–52. doi: 10.1016/j.ttbdis.2017.02.001
- Fawcett, D. W., Binnington, K., and Voigt, W. P. (1986). The cell biology of the ixodid tick salivary gland. *Morphol. Physiol. Behav. Biol. Ticks* 22–45.
- Fialová, A., Cimburek, Z., Iezzi, G., and Kopecký, J. (2010). Ixodes ricinus tick saliva modulates tick-borne encephalitis virus infection of dendritic cells. *Microbes Infect.* 12, 580–585. doi: 10.1016/j.micinf.2010.03.015
- Galay, R. L., Miyata, T., Umemiya-Shirafuji, R., Maeda, H., Kusakisako, K., Tsuji, N., et al. (2014). Evaluation and comparison of the potential of two ferritins as anti-tick vaccines against *Haemaphysalis longicornis*. *Parasit. Vectors* 7, 1–10. doi: 10.1186/s13071-014-0482-x
- Gao, Y., Zhao, C., Wang, W., Jin, R., Li, Q., Ge, Q., et al. (2016). Prostaglandins E2 signal mediated by receptor subtype EP2 promotes IgE production *in vivo* and contributes to asthma development. *Sci. Rep.* 6, 20505. doi: 10.1038/srep20505
- Ghafar, A., Gasser, R. B., Rashid, I., Ghafoor, A., and Jabbar, A. (2020). Exploring the prevalence and diversity of bovine ticks in five agro-ecological zones of Pakistan using phenetic and genetic tools. *Ticks Tick. Borne. Dis.* 6, 483–488. doi: 10.1016/j.ttbdis.2020.101472
- Gharbi, M., and Aziz Darghouth, M. (2014). A review of hyalommascupense (*Acari: Ixodidae*) in the maghreb region: from biology to control. *Parasite* 21, 2. doi: 10.1051/parasite/2014002
- Ghosh, S., and Nagar, G. (2014). Problem of ticks and tick-borne diseases in India with special emphasis on progress in tick control research: a review. *J. Vector Borne Dis.* 51, 259–270.
- Godsey, M. S. Jr., Rose, D., Burkhalter, K. L., Breuner, N., Bosco-Lauth, A. M., Kosoy, O. I., et al. (2021). Experimental infection of *Amblyomma americanum* (*Acari: Ixodidae*) with bourbon virus (*Orthomyxoviridae: Thogotovirus*). *J. Med. Entomol.* 58, 873–879. doi: 10.1093/jme/tj aal191
- Gondard, M., Temmam, S., Devillers, E., Pinarello, V., Bigot, T., Chrétien, D., et al. (2020). RNA viruses of amblyomma variegatum and rhipicephalus microplus and cattle susceptibility in the french antilles. *Viruses* 12, 144. doi: 10.3390/v12020144
- Grabowski, J. M., Offerdahl, D. K., and Bloom, M. E. (2018). The use of *ex vivo* organ cultures in tick-borne virus research. *ACS Infect. Dis.* 4, 247–256. doi: 10.1021/acsinfecdis.7b00274
- Grisi, L., Leite, R. C., Martins, J. R. S., Barros, A. T. M., Andreotti, R., Cançado, P. H. D., et al. (2014). Reassessment of the potential economic impact of cattle parasites in Brazil. *Rev. Bras. Parasitol. Vet.* 23, 150–156. doi: 10.1590/S1984-29612014042
- Guglielmone, A. A., Robbins, R. G., Apanaskevich, D. A., Petney, T. N., Estrada-Peña, A., and Horak, I. G. (2014). *The Hard Ticks of the World*. Dordrecht: Springer. doi: 10.1007/978-94-007-7497-1
- Hackenberg, M., Langenberger, D., Schwarz, A., Erhart, J., and Kotsyfakis, M. (2017). In silico target network analysis of *de novo*-discovered, tick saliva-specific microRNAs reveals important combinatorial effects in their interference with vertebrate host physiology. *RNA* 23, 1259–1269. doi: 10.1261/rna.061168.117
- Hart, C. E., and Thangamani, S. (2021). Tick-virus interactions: current understanding and future perspectives. *Parasit. Immunol.* 43, e12815. doi: 10.1111/pim.12815

- Hayward, J., Sanchez, J., Perry, A., Huang, C., Valle, M. R., Canals, M., et al. (2018). Erratum: ticks from diverse genera encode chemokine-inhibitory evasin proteins. *J. Biol. Chem.* 292, 15670–15680. doi: 10.1074/jbc.M117.807255
- Heath, W. R., and Carbone, F. R. (2013). The skin-resident and migratory immune system in steady state and memory: innate lymphocytes, dendritic cells and T cells. *Nat. Immunol.* 14, 978–985. doi: 10.1038/ni.2680
- Heinze, D. M., Carmical, J. R., Aronson, J. F., Alarcon-Chaidez, F., Wikel, S., and Thangamani, S. (2014). Murine cutaneous responses to the rocky mountain spotted fever vector, *Dermacentor andersoni*, feeding. *Front. Microbiol.* 5, 198. doi: 10.3389/fmicb.2014.00198
- Hernance, M. E., and Thangamani, S. (2018). Tick-virus-host interactions at the cutaneous interface: the nidus of flavivirus transmission. *Viruses* 10, 362. doi: 10.3390/v10070362
- Hernandez, E. P., Talactac, M. R., Fujisaki, K., and Tanaka, T. (2019). The case for oxidative stress molecule involvement in the tick-pathogen interactions-an omics approach. *Dev. Comp. Immunol.* 100, 103409. doi: 10.1016/j.dci.2019.103409
- Holding, M., Dowall, S. D., Medlock, J. M., Carter, D. P., Pullan, S. T., Lewis, J., et al. (2020). Tick-borne encephalitis virus, United Kingdom. *Emerg. Infect. Dis.* 26, 90. doi: 10.3201/eid2601.191085
- Hubálek, Z., and Rudolf, I. (2012). Tick-borne viruses in Europe. *Parasitol. Res.* 111, 9–36. doi: 10.1007/s00436-012-2910-1
- Hughes, H. R., Velez, J. O., Fitzpatrick, K., Davis, E. H., Russell, B. J., Lambert, A. J., et al. (2021). Genomic evaluation of the genus *Coltivirus* indicates genetic diversity among colorado tick fever virus strains and demarcation of a new species. *Diseases* 9, 92. doi: 10.3390/diseases9040092
- Jelinski, J. W. (2016). *Painless Hematophagy: The Functional Role of Novel Tick Metalloproteases in Pain Suppression*.
- Jore, M. M., Johnson, S., Sheppard, D., Barber, N. M., Li, Y. I., Nunn, M. A., et al. (2016). Structural basis for therapeutic inhibition of complement C5. *Nat. Struct. Mol. Biol.* 23, 378–386. doi: 10.1038/nsmb.3196
- Kannangara, D. W., and Patel, P. (2018). Report of non-lyme, erythema migrans rashes from New Jersey with a review of possible role of tick salivary toxins. *Vect. Borne Zoo. Dis.* 18, 641–652. doi: 10.1089/vbz.2018.2278
- Karim, S., Budachet, K., Mukherjee, N., Williams, J., Kausar, A., Hassan, M. J., et al. (2017). A study of ticks and tick-borne livestock pathogens in Pakistan. *PLoS Negl. Trop. Dis.* 11, e0005681. doi: 10.1371/journal.pntd.0005681
- Karim, S., and Ribeiro, J. M. C. (2015). An insight into the salivome of the lone star tick, *Amblyomma americanum*, with a glimpse on its time dependent gene expression. *PLoS ONE* 10, e0131292. doi: 10.1371/journal.pone.0131292
- Kaufman, W. R., and Sauer, J. R. (1982). "Ion and water balance in feeding ticks: mechanisms of tick excretion," in *Physiology of Ticks*, eds F. D. Obenchain and R. Galun (London: Elsevier), 213–244.
- Kazimirová, M., and Štibrániová, I. (2013). Tick salivary compounds: their role in modulation of host defences and pathogen transmission. *Front. Cell. Infect. Microbiol.* 4, 43. doi: 10.3389/fcimb.2013.00043
- Kazimirová, M., Thangamani, S., Bartíková, P., Hermance, M., Holíková, V., Štibrániová, I., et al. (2017). Tick-borne viruses and biological processes at the tick-host-virus interface. *Front. Cell. Infect. Microbiol.* 7, 339. doi: 10.3389/fcimb.2017.00339
- Kemal, J., Muktar, Y., and Alemu, S. (2016). Distribution and prevalence of tick infestation in cattle in Babille district, eastern Ethiopia. *Livest. Res. Rural Dev.* 28, 1–9. doi: 10.1155/2016/9618291
- Kemp, D. H., and Tatchell, R. J. (1971). The mechanism of feeding and salivation in *Boophilus microplus* (Canestrini, 1887). *Zeitschrift für Parasit.* 37, 55–69. doi: 10.1007/BF00259545
- Khoo, C. C. H., Piper, J., Sanchez-Vargas, I., Olson, K. E., and Franz, A. W. E. (2010). The RNA interference pathway affects midgut infection- and escape barriers for Sindbis virus in *Aedes aegypti*. *BMC Microbiol.* 10, 130. doi: 10.1186/1471-2180-10-130
- Kim, D., Maldonado-Ruiz, P., Zurek, L., and Park Y. (2017). Water absorption through salivary gland type I acini in the blacklegged tick, *Ixodes scapularis*. *PeerJ* 5, e3984. doi: 10.7717/peerj.3984
- Kim, D., Šimo, L., and Park, Y. (2014). Orchestration of salivary secretion mediated by two different dopamine receptors in the blacklegged tick *Ixodes scapularis*. *J. Exp. Biol.* 217, 3656–3663. doi: 10.1242/jeb.109462
- Kim, T. K., Tirloni, L., Pinto, A. F. M., Moresco, J., Yates, J. R., da Silva Vaz, I., et al. (2016). *Ixodes scapularis* tick saliva proteins sequentially secreted every 24 h during blood feeding. *PLoS Negl. Trop. Dis.* 10, 1–35. doi: 10.1371/journal.pntd.0004323
- Kitsou, C., Fikrig, E., and Pal, U. (2021). Tick host immunity: vector immunomodulation and acquired tick resistance. *Trends Immunol.* 42, 554–574. doi: 10.1016/j.it.2021.05.005
- Klein, M., Brühl, T.-J., Staudt, V., Reuter, S., Grebe, N., Gerlitzki, B., et al. (2015). Tick salivary sialostatin L represses the initiation of immune responses by targeting IRF4-dependent transcription in murine mast cells. *J. Immunol.* 195, 621–631. doi: 10.4049/jimmunol.1401823
- Koči, J., Šimo, L., and Park, Y. (2014). Autocrine/paracrine dopamine in the salivary glands of the blacklegged tick *Ixodes scapularis*. *J. Insect. Physiol.* 62, 39–45. doi: 10.1016/j.jinsphys.2014.01.007
- Kotál, J., Langhansová, H., Lieskovská, J., Andersen, J. F., Francischetti, I. M. B., Chavakis, T., et al. (2015a). Modulation of host immunity by tick saliva. *J. Proteomics* 128, 58–68. doi: 10.116/j.jprot.2015.07.005
- Kotál, J., Langhansová, H., Lieskovská, J., Andersen, J. F., Francischetti, I. M. B., Chavakis, T., et al. (2015b). Modulation of host immunity by tick saliva. *J. Proteomics* 128, 58–68. doi: 10.1016/j.jprot.2015.07.005
- Kotsyfakis, M., Anderson, J. M., Andersen, J. F., Calvo, E., Francischetti, I. M. B., Mather, T. N., et al. (2008). Cutting edge: immunity against a "silent" salivary antigen of the lyme vector *Ixodes scapularis* impairs its ability to feed. *J. Immunol.* 181, 5209–5212. doi: 10.4049/jimmunol.181.8.5209
- Kotsyfakis, M., Schwarz, A., Erhart, J., and Ribeiro, J. M. C. (2015). Tissue- and time-dependent transcription in *Ixodes ricinus* salivary glands and midguts when blood feeding on the vertebrate host. *Sci. Rep.* 5, 9103. doi: 10.1038/srep09103
- Kramer, L. D., and Tavakoli, N. P. (2021). *Viruses of terrestrial mammals in Studies in Viral Ecology*, ed S. J. Hurst (John Wiley and Sons Ltd), 541–583.
- Krolak, J. M., Ownby, C. L., and Sauer, J. R. (1982). Alveolar structure of salivary glands of the lone star tick, *Amblyomma americanum* (L.): unfed females. *J. Parasitol.* 68, 61–82. doi: 10.2307/3281326
- Kurscheid, S., Lew-Tabor, A. E., Valle, M. R., Bruyeres, A. G., Doogan, V. J., Munderloh, U. G., et al. (2009). Evidence of a tick RNAi pathway by comparative genomics and reverse genetics screen of targets with known loss-of-function phenotypes in *Drosophila*. *BMC Mol. Biol.* 10, 26. doi: 10.1186/1471-2199-10-26
- Labuda, M., Jones, L. D., Williams, T., and Nuttall, P. A. (1993). Enhancement of tick-borne encephalitis virus transmission by tick salivary gland extracts. *Med. Vet. Entomol.* 7, 193–196. doi: 10.1111/j.1365-2915.1993.tb00674.x
- Latif, A. A., Putterill, J. F., de Klerk, D. G., Pienaar, R., and Mans, B. J. (2012). Nuttalliellana maqua (*Ixodoidea: Nuttalliellidae*): first description of the male, immature stages and re-description of the female. *PLoS ONE* 7, e0041651. doi: 10.1371/journal.pone.0041651
- Leal, B. F., Alzugaray, M. F., Seixas, A., Da Silva Vaz, I., and Ferreira, C. A. S. (2018). Characterization of a glycine-rich protein from *Rhipicephalus microplus*: tissue expression, gene silencing and immune recognition. *Parasitology* 145, 927–938. doi: 10.1017/S0031182017001998
- Lee, W.-S., Webster, J. A., Madzokere, E. T., Stephenson, E. B., and Herrero, L. J. (2019). Mosquito antiviral defense mechanisms: a delicate balance between innate immunity and persistent viral infection. *Parasit. Vect.* 12, 165. doi: 10.1186/s13071-019-3433-8
- Lemasson, M., Caignard, G., Unterfinger, Y., Attoui, H., Bell-Sakyi, L., Hirschaud, E., et al. (2021). Exploration of binary protein-protein interactions between tick-borne flaviviruses and *Ixodes ricinus*. *Parasit. Vect.* 14, 1–17. doi: 10.1186/s13071-021-04651-3
- Lledó, L., Giménez-Pardo, C., and Gegúndez, M. I. (2020). Epidemiological study of thogoto and dhori virus infection in people bitten by ticks, and in sheep, in an area of Northern Spain. *Int. J. Environ. Res. Public Health* 17, 2254. doi: 10.3390/ijerph17072254
- Madani, T. A., and Abuelzein, E. T. M. E. (2021). Alkhurma hemorrhagic fever virus infection. *Arch. Virol.* 166, 2357–2367. doi: 10.1007/s00705-021-05083-1
- Manjunathachar, H. V., Saravanan, B. C., Kesavan, M., Karthik, K., Rathod, P., Gopi, M., et al. (2014). Economic importance of ticks and their effective control strategies. *Asian Pac. J. Trop. Dis.* 4, S770–S779. doi: 10.1016/S2222-1808(14)60725-8

- Mans, B. J., De Castro, M. H., Pienaar, R., De Klerk, D., Gaven, P., Genu, S., et al. (2016). Ancestral reconstruction of tick lineages. *Ticks Tick. Borne. Dis.* 7, 509–535. doi: 10.1016/j.ttbdis.2016.02.002
- Mans, B. J., Gothe, R., and Neitz, A. W. H. (2004). Biochemical perspectives on paralysis and other forms of toxicoses caused by ticks. *Parasitol.* 129, 95–111. doi: 10.1017/S0033182003004670
- Mans, B. J., and Neitz, A. W. H. (2004). Adaptation of ticks to a blood-feeding environment: evolution from a functional perspective. *Insect Biochem. Mol. Biol.* 34, 1–17. doi: 10.1016/j.ibmb.2003.09.002
- Mansfield, K. L., Jizhou, L., Phipps, L. P., and Johnson, N. (2017). Emerging tick-borne viruses in the twenty-first century. *Front. Cell. Infect. Microbiol.* 7, 298. doi: 10.3389/fcimb.2017.00298
- Martina, B. E., Barzon, L., Pijlman, G. P., de la Fuente, J., Rizzoli, A., Wammes, L. J., et al. (2017). Human to human transmission of arthropod-borne pathogens. *Curr. Opin. Virol.* 22, 13–21. doi: 10.1016/j.coviro.2016.11.005
- Mccoy, K. D., Léger, E., and Dietrich, M. (2013). Host specialization in ticks and transmission of tick-borne diseases: a review. *Front. Cell. Infect. Microbiol.* 3, 57. doi: 10.3389/fcimb.2013.00057
- McNally, K. L., and Bloom, M. E. (2013). “The Tick-Virus Interface” in *Viral Infection Global Change*, ed S. K. Singh (John Wiley and Sons Ltd), 603–616.
- Medlock, J. M., Hansford, K. M., Bormane, A., Derdakova, M., Estrada-peña, A., George, J., et al. (2013). Artikel ixodes ricinus Europa, 2013. *Parasit. Vect.* 6, 1. doi: 10.1186/1756-3305-6-1
- Meekins, D. A., Kanost, M. R., and Michel, K. (2017). Serpins in arthropod biology. *Semi. Cell. Dev. Biol.* 62, 105–119. doi: 10.1016/j.semcdb.2016.09.001
- Migné, C. V., Hönig, V., Bonnet, S. I., Palus, M., Rakotobe, S., Galon, C., et al. (2022). Evaluation of two artificial infection methods of live ticks as tools for studying interactions between tick-borne viruses and their tick vectors. *Sci. Rep.* 12, 491. doi: 10.1038/s41598-021-04498-9
- Mirkena, T., Waleign, E., Tewolde, N., Gari, G., Abebe, G., and Newman, S. (2018). Camel production systems in Ethiopia: a review of literature with notes on MERS-CoV risk factors. *Pastoralism* 8, 30. doi: 10.1186/s13570-018-0135-3
- Moming, A., Yue, X., Shen, S., Chang, C., Wang, C., Luo, T., et al. (2018). Prevalence and phylogenetic analysis of crimean-congo hemorrhagic fever virus in ticks from different ecosystems in Xinjiang, China. *Virol. Sin.* 33, 67–73. doi: 10.1007/s12250-018-0016-3
- Monfared, A. L., Mahmoodi, M., and Fattahi, R. (2015). Prevalence of ixodid ticks on cattle, sheep and goats in Ilam County, Ilam Province, Iran. *J. Parasit. Dis.* 39, 37–40. doi: 10.1007/s12639-013-0267-8
- Morozova, O. V., Panov, V. V., and Bakhvalova, V. N. (2020). Innate and adaptive immunity in wild rodents spontaneously and experimentally infected with the tick-borne encephalitis virus. *Infect. Genet. Evol.* 80, 104187. doi: 10.1016/j.meegid.2020.104187
- Mudenda, L., Pierlé, S. A., Turse, J. E., Scoles, G. A., Purvine, S. O., Nicora, C. D., et al. (2014). Proteomics informed by transcriptomics identifies novel secreted proteins in *Dermacentor andersoni* saliva. *Int. J. Parasitol.* 44, 1029–1037. doi: 10.1016/j.ijpara.2014.07.003
- Mulenga, A., Kim, T., and Ibelli, A. M. G. (2013). A mbyomma americanum tick saliva serine protease inhibitor 6 is a cross-class inhibitor of serine proteases and papain-like cysteine proteases that delays plasma clotting and inhibits platelet aggregation. *Insect Mol. Biol.* 22, 306–319. doi: 10.1111/imb.12024
- Mutavi, F., Aarts, N., Van Paassen, A., Heitkönig, I., and Wieland, B. (2018). Techne meets Metis: Knowledge and practices for tick control in Laikipia County, Kenya. *NJAS Wageningen J. Life Sci.* 86–87, 136–145. doi: 10.1016/j.njas.2018.08.001
- Nazar, M., Khan, M. N. M. A. M. A. Q. S. N. Q. S. A., Shah, A. A., Rahman, S. U., Khan, I. I. U. I. I., Ullah, A., et al. (2013). Prevalence and risk factors of anaplasmosis in cattle and buffalo populations of district Khanewal, Punjab, Pakistan. *Glob. Vet.* 22, 146–153. doi: 10.1590/s1984-29612013000200038
- Neelakanta, G., and Sultana, H. (2022). Tick saliva and salivary glands: what do we know so far on their role in arthropod blood feeding and pathogen transmission. *Front. Cell. Infect. Microbiol.* 11, 816547. doi: 10.3389/fcimb.2021.816547
- Niu, J., Taning, C. N. T., Christiaens, O., Smagghe, G., and Wang, J.-J. (2018). “Rethink RNAi in insect pest control: challenges and perspectives. *Adv. Ins. Physiol.* 55, 1–17. doi: 10.1016/bs.aip.2018.07.003
- Nodari, E. F., Roma, G. C., Furquim, K. C. S., De Oliveira, P. R., Bechara, G. H., and Camargo-Mathias, M. I. (2012). Degenerative process and cell death in salivary glands of *Rhipicephalus sanguineus* (Latreille, 1806) (Acari: Ixodidae) semi-engorged female exposed to the acaricide permethrin. *Microsc. Res. Tech.* 75, 1012–1018. doi: 10.1002/jemt.22025
- Nuttall, P. A. (2013). Tick-borne viruses. *Biol. Ticks* 2, 180–210.
- Nuttall, P. A. (2019a). Tick saliva and its role in pathogen transmission. *Wien. Klin. Wochenschr.* 131, 1–12. doi: 10.1007/s00508-019-1500-y
- Nuttall, P. A. (2019b). Wonders of tick saliva. *Ticks Tick. Borne. Dis.* 10, 470–481. doi: 10.1016/j.ttbdis.2018.11.005
- Páleníková, J., Lieskovská, J., Langhansová, H., Kotsyfakis, M., Chmelař, J., and Kopecký, J. (2015). Ixodes ricinus salivary serpin IRS-2 affects Th17 differentiation via inhibition of the interleukin-6/STAT-3 signaling pathway. *Infect. Immun.* 83, 1949–1956. doi: 10.1128/IAI.03065-14
- Palta, S., Saroa, R., and Palta, A. (2014). Overview of the coagulation system. *Indian. J. Anaesth.* 58, 515–523. doi: 10.4103/0019-5049.144643
- Pantchev, N., Pluta, S., Huisinga, E., Nather, S., Scheufelen, M., Vrhovec, M. G., et al. (2015). Tick-borne diseases (borreliosis, anaplasmosis, babesiosis) in German and Austrian dogs: status quo and review of distribution, transmission, clinical findings, diagnostics and prophylaxis. *Parasitol. Res.* 114, 19–54. doi: 10.1007/s00436-015-4513-0
- Papa, A., Tsioka, K., Kontana, A., Papadopoulos, C., and Giadinis, N. (2017). Bacterial pathogens and endosymbionts in ticks. *Ticks Tick. Borne. Dis.* 8, 31–35. doi: 10.1016/j.ttbdis.2016.09.011
- Parizi, L. F., Ali, A., Tirloni, L., Oldiges, D. P., Sabadin, G. A., Coutinho, M. L., et al. (2018). Peptidase inhibitors in tick physiology. *Med. Vet. Entomol.* 32, 129–144. doi: 10.1111/mve.12276
- Pekáriková, D., Rajská, P., Kazimirová, M., Pechánová, O., Takáč, P., and Nuttall, P. A. (2015). Vasoconstriction induced by salivary gland extracts from ixodid ticks. *Int. J. Parasitol.* 45, 879–883. doi: 10.1016/j.ijpara.2015.08.006
- Perner, J., Kropáčková, S., Kopáček, P., and Ribeiro, J. M. C. (2018). Sialome diversity of ticks revealed by RNAseq of single tick salivary glands. *PLoS Negl. Trop. Dis.* 12, e0006410. doi: 10.1371/journal.pntd.006410
- Pfäffle, M., Littwin, N., Muders, S. V., and Petney, T. N. (2013). The ecology of tick-borne diseases. *Int. J. Parasitol.* 43, 1059–1077. doi: 10.1016/j.ijpara.2013.06.009
- Preston, S. G., Majtán, J., Kouremenou, C., Rysnik, O., Burger, L. F., Cabezas Cruz, A., et al. (2013). Novel immunomodulators from hard ticks selectively reprogramme human dendritic cell responses. *PLoS Pathog.* 9, e1003450. doi: 10.1371/journal.ppat.1003450
- Raney, W. R., Perry, J. B., and Hermance, M. E. (2022). Transovarial transmission of heartland virus by invasive asian longhorned ticks under laboratory conditions. *Emerg. Infect. Dis.* 28, 726. doi: 10.3201/eid2803.210973
- Rashid, M., Rashid, M. I., Akbar, H., Ahmad, L., Hassan, M. A., Ashraf, K., et al. (2019). A systematic review on modelling approaches for economic losses studies caused by parasites and their associated diseases in cattle. *Parasitology* 146, 129–141. doi: 10.1017/S0033182018001282
- Rego, R. O. M., Trentelman, J. J. A., Anguita, J., Nijhof, A. M., Sprong, H., Klempa, B., et al. (2019). Counterattacking the tick bite: towards a rational design of anti-tick vaccines targeting pathogen transmission. *Parasit. Vect.* 12, 229. doi: 10.1186/s13071-019-3468-x
- Reid, H. W. (2019). “Louping-ill,” in *The Arboviruses: Epidemiology and Ecology*, ed T. P. Monath (London: CRC Press), 117–136.
- Rock, D. L. (2021). Thoughts on African swine fever vaccines. *Viruses* 13, 943. doi: 10.3390/v13050943
- Rodriguez, S. E., McAuley, A. J., Gargili, A., and Bente, D. A. (2018). Interactions of human dermal dendritic cells and langerhans cells treated with hyalomma tick saliva with crimean-congo hemorrhagic fever virus. *Viruses* 10, 381. doi: 10.3390/v10070381
- Rodriguez-Vivas, R. I., Jonsson, N. N., and Bhushan, C. (2018). Strategies for the control of Rhipicephalus microplus ticks in a world of conventional acaricide and macrocyclic lactone resistance. *Parasitol. Res.* 117, 3–29. doi: 10.1007/s00436-017-5677-6
- Rosà, R., Andreo, V., Tagliapietra, V., Baráková, I., Arnoldi, D., Haufler, H. C., et al. (2018). Effect of climate and land use on the spatio-temporal variability

- of tick-borne bacteria in Europe. *Int. J. Environ. Res. Public Health* 15, 732. doi: 10.3390/ijerph15040732
- Rosche, K. L., Sidak-Loftis, L. C., Hurtado, J., Fisk, E. A., and Shaw, D. K. (2021). Arthropods under pressure: Stress responses and immunity at the pathogen-vector interface. *Front. Immunol.* 11, 629777. doi: 10.3389/fimmu.2020.629777
- Roshdy, M. A., and Coons, L. B. (1975). The subgenus persicargas (*Ixodoidea: Argasidae: Argas*). 23. Fine structure of the salivary glands of unfed A. (P.) arboreus Kaiser, Hoogstraal, and Kohls. *J. Parasitol.* 61, 743–752. doi: 10.4081/ijas.2007.s2.939
- Sajid, M. S., Iqbal, Z., Khan, M. N., Muhamamd, G., and Iqbal, M. U. (2007). Effect of hyalomma ticks (*Acari: Ixodidae*) on milk production of dairy buffaloes (*Bos bubalus bubalis*) of Punjab (Pakistan). *Ital. J. Anim. Sci.* 6, 939–941. doi: 10.1016/j.ijas.2007.s2.939
- Sajid, M. S., Iqbal, Z., Shamim, A., Siddique, R. M., Hassan, M. J., and Rizwan, H. M. (2017). Distribution and abundance of ticks infesting livestock population along Karakorum highway from Mansehra to Gilgit, Pakistan. *J. Hell. Vet. Med. Soc.* 68, 51–58. doi: 10.12681/jhvms.15556
- Schuijt, T. J., Bakhtiari, K., Daffre, S., Deponte, K., Wielders, S. J. H., Marquart, J. A., et al. (2013). Factor XA activation of factor v is of paramount importance in initiating the coagulation system: lessons from a tick salivary protein. *Circulation* 128, 254–266. doi: 10.1161/CIRCULATIONAHA.113.003191
- Schwarz, A., Valdés, J. J., and Kotsyfakis, M. (2012). The role of cystatins in tick physiology and blood feeding. *Ticks Tick. Borne. Dis.* 3, 117–127. doi: 10.1016/j.ttbdis.2012.03.004
- Shi, J., Hu, Z., Deng, F., and Shen, S. (2018). Tick-borne viruses. *Virol. Sin.* 33, 21–43. doi: 10.1007/s12250-018-0019-0
- Siddiqi, M. K., Shahein, Y. E., Hussein, N., and Khan, R. H. (2016). Effect of surfactants on Ra-sHSP1-A small heat shock protein from the cattle tick *Rhipicephalus annulatus*. *J. Mol. Struct.* 1119, 12–17. doi: 10.1016/j.molstruc.2016.04.002
- Siddique, R. M., Sajid, M. S., Iqbal, Z., and Saqib, M. (2020). Association of different risk factors with the prevalence of babesiosis in cattle and buffalos. *Pakistan J. Agric. Sci.* 57, 517–524. doi: 10.21162/PAKJAS/19.8626
- Sidorenko, M., Radzijeuskaja, J., Mickevičius, S., Bratčikoviene, N., and Paulauskas, A. (2021). Prevalence of tick-borne encephalitis virus in questing *Dermacentor reticulatus* and *Ixodes ricinus* ticks in Lithuania. *Ticks Tick. Borne. Dis.* 12, 101594. doi: 10.1016/j.ttbdis.2020.101594
- Šimo, L., Kazimirova, M., Richardson, J., and Bonnet, S. I. (2017). The essential role of tick salivary glands and saliva in tick feeding and pathogen transmission. *Front. Cell. Infect. Microbiol.* 7, 281. doi: 10.3389/fcimb.2017.00281
- Šimo, L., Koči, J., Kim, D., and Park, Y. (2014). Invertebrate specific D1-like dopamine receptor in control of salivary glands in the black-legged tick *Ixodes scapularis*. *J. Comp. Neurol.* 522, 2038–2052. doi: 10.1002/cne.23515
- Šimo, L., Koči, J., and Park, Y. (2013). Receptors for the neuropeptides, myoinhibitory peptide and SIFamide, in control of the salivary glands of the blacklegged tick *Ixodes scapularis*. *Insect Biochem. Mol. Biol.* 43, 376–387. doi: 10.1016/j.ibmb.2013.01.002
- Singh, N. K., Goolsby, J. A., Shapiro-Ilan, D. I., Miller, R. J., Setamou, M., and de Leon, A. A. P. (2018). Effect of immersion time on efficacy of entomopathogenic nematodes against engorged females of cattle fever tick, *Rhipicephalus* (= *Boophilus*) *microplus*. *Southwest. Entomol.* 43, 19–28. doi: 10.3958/059.043.0120
- Solano-Gallego, L., Sainz, Á., Roura, X., Estrada-Peña, A., and Miró, G. (2016). A review of canine babesiosis: the European perspective. *Parasit. Vect.* 9, 336. doi: 10.1186/s13071-016-1596-0
- Sormunen, J. J., Sippola, E., Kaunisto, K. M., Vesterinen, E. J., and Sääksjärvi, I. E. (2019). First evidence of ixodiphagushookeri (*Hymenoptera: Encyrtidae*) parasitization in finnish castor bean ticks (*Ixodes ricinus*). *Exp. Appl. Acarol.* 79, 395–404. doi: 10.1007/s10493-019-00437-6
- Soulsby, E. J. L. (1982). Helminths, Arthropods and Protozoa of Domesticated Animals. 7th Edn. London: Bailliere Tindall.
- Sprygin, A., Pestova, Y., Wallace, D. B., Tuppurainen, E., and Kononov, A. V. (2019). Transmission of lumpy skin disease virus: a short review. *Virus Res.* 269, 197637. doi: 10.1016/j.virusres.2019.05.015
- Štibráňová, I., Lahová, M., and Bartíková, P. (2013). Immunomodulators in tick saliva and their benefits. *Acta Virol.* 57, 200–216. doi: 10.4149/av_2013_02_200
- Sudhakar, N. R., Manjunathachar, H. V., Karthik, K., Sahu, S., Gopi, M., Shanthaveer, S. B., et al. (2013). RNA interference in parasites: prospects and pitfalls. *Adv Anim Vet Sci* 1, 1–6.
- Suppan, J., Engel, B., Marchetti-Deschmann, M., and Nürnberger, S. (2018). Tick attachment cement—reviewing the mysteries of a biological skin plug system. *Biol. Rev.* 93, 1056–1076. doi: 10.1111/brv.12384
- Talactac, M. R., Hernandez, E. P., Hatta, T., Yoshii, K., Kusakisako, K., Tsuji, N., et al. (2021). The antiviral immunity of ticks against transmitted viral pathogens. *Dev. Comp. Immunol.* 119, 104012. doi: 10.1016/j.dci.2021.104012
- Tang, J., Fang, Y., Han, Y., Bai, X., Yan, X., Zhang, Y., et al. (2015). YY-39, a tick anti-thrombosis peptide containing RGD domain. *Peptides* 68, 99–104. doi: 10.1016/j.peptides.2014.08.008
- Thompson, R. E., Liu, X., Ripoll-Rozada, J., Alonso-García, N., Parker, B. L., Pereira, P. J. B., et al. (2017). Tyrosine sulfation modulates activity of tick-derived thrombin inhibitors. *Nat. Chem.* 9, 909–917. doi: 10.1038/nchem.2744
- Tian, Y., Chen, W., Mo, G., Chen, R., Fang, M., Yedid, G., et al. (2016). An immunosuppressant peptide from the hard tick *Amblyomma variegatum*. *Toxins* 8, 133. doi: 10.3390/toxins8050133
- Tirloni, L., Kim, T. K., Pinto, A. F. M., Yates, J. R., da Silva Vaz, I., and Mulenga, A. (2017). Tick-host range adaptation: changes in protein profiles in unfed adult ixodes scapularis and *Amblyomma americanum* saliva stimulated to feed on different hosts. *Front. Cell. Infect. Microbiol.* 7, 517. doi: 10.3389/fcimb.2017.00517
- Tirloni, L., Reck, J., Terra, R. M. S., Martins, J. R., Mulenga, A., Sherman, N. E., et al. (2014). Proteomic analysis of cattle tick rhipicephalus (boophilus) microplus saliva: a comparison between partially and fully engorged females. *PLoS ONE* 9, e94831. doi: 10.1371/journal.pone.0094831
- Tomás-Cortázar, J., Martín-Ruiz, I., Barriales, D., Pascual-Itoiz, M. Á., De Juan, V. G., Caro-Maldonado, A., et al. (2017). The immunosuppressive effect of the tick protein, Salp15, is long-lasting and persists in a murine model of hematopoietic transplant. *Sci. Rep.* 7, 10740. doi: 10.1038/s41598-017-11354-2
- Tsatsaris, A., Chochlakakis, D., Papadopoulos, B., Petsa, A., Georgalis, L., Angelakis, E., et al. (2016). Species composition, distribution, ecological preference and host association of ticks in Cyprus. *Exp. Appl. Acarol.* 70, 523–542. doi: 10.1007/s10493-016-0091-9
- Turell, M. J. (2020). “Horizontal and vertical transmission of viruses by insect and tick vectors,” in *The Arboviruses: Epidemiology and Ecology*, ed T. P. Monath (London: CRC Press), 127–152.
- Ullah, S. A. K. M., and Kaufman, W. R. (2014). Salivary gland degeneration and ovarian development in the Rocky Mountain wood tick, *Dermacentor andersoni* stiles (*Acari: Ixodidae*): I. Post-engorgement events. *Ticks Tick. Borne. Dis.* 5, 569–574. doi: 10.1016/j.ttbdis.2014.03.012
- Uslu, U., Sajid, M. S., Ceylan, O., and Ejaz, A. (2019). Prevalence of hard ticks (*Acari: Ixodidae*) in spur-thighed tortoise (*Testudo graecaibera*) population of Konya. *Eurasian J. Vet. Sci.* 35, 158–164. doi: 10.15312/EurasianJVetSci.2019.239
- Valdés, J. J. (2014). Antihistamine response: a dynamically refined function at the host-tick interface. *Parasit. Vect.* 7, 491. doi: 10.1186/s13071-014-0491-9
- Vander Waal, K., Gilbertson, M., Okanga, S., Allan, B. F., and Craft, M. E. (2017). Seasonality and pathogen transmission in pastoral cattle contact networks. *R. Soc. Open Sci.* 4, 170808. doi: 10.1098/rsos.170808
- Wernersson, S., and Pejler, G. (2014). Mast cell secretory granules: armed for battle. *Nat. Rev. Immunol.* 14, 478–494. doi: 10.1038/nri3690c
- Wikel, S. (2013). Ticks and tick-borne pathogens at the cutaneous interface: Host defenses, tick countermeasures, and a suitable environment for pathogen establishment. *Front. Microbiol.* 4, 337. doi: 10.3389/fmicb.2013.00337
- Wikel, S. K. (2018a). Tick-host-pathogen systems immunobiology: an interactive trio. *Front. Biosci. Landmark* 23, 265–283. doi: 10.2741/4590
- Wikel, S. K. (2018b). Ticks and tick-borne infections: complex ecology, agents, and host interactions. *Vet. Sci.* 5, 60. doi: 10.3390/vetsci5020060
- Yadav, P. D., Whitmer, S. L. M., Sarkale, P., Fei Fan Ng, T., Goldsmith, C. S., Nyayanit, D. A., et al. (2019). Characterization of novel reoviruses wad medani

- virus (orbivirus) and kundal virus (coltivirus) collected from hyalomma anatolicum ticks in india during surveillance for crimean congo hemorrhagic fever. *J. Virol.* 93, e00106–e00119. doi: 10.1128/JVI.00106-19
- Yang, X., Gao, G. F., and Liu, W. J. (2022). Powassan virus: a tick borne flavivirus infecting humans. *Biosaf. Heal.* 4, 30–37. doi: 10.1016/j.bsheat.2021.12.007
- Yoshii, K. (2019). Epidemiology and pathological mechanisms of tick-borne encephalitis. *J. Vet. Med. Sci.* 81, 343–347. doi: 10.1292/jvms.18-0373
- Yu, X., Zhou, Y., Cao, J., Zhang, H., Gong, H., and Zhou, J. (2017). Caspase-1 participates in apoptosis of salivary glands in *Rhipicephalus haemaphysaloides*. *Parasit. Vect.* 10, 225. doi: 10.1186/s13071-017-2161-1
- Yun, S. M., Song, B. G., Choi, W., Roh, J. Y., Lee, Y. J., Park, W., et al. (2016). First Isolation of severe fever with thrombocytopenia syndrome virus from haemaphysalis longicornis ticks collected in severe fever with thrombocytopenia syndrome outbreak areas in the Republic of Korea. *Vect. Borne Zoo. Dis.* 16, 66–70. doi: 10.1089/vbz.2015.1832
- Zivcec, M., Scholte, F. E. M., Spiropoulou, C. F., Spengler, J. R., and Bergeron, É. (2016). Molecular insights into crimean-congo hemorrhagic fever virus. *Viruses* 8, 106. doi: 10.3390/v8040106

Conflict of Interest: The authors declare that the research was conducted in the absence of any commercial or financial relationships that could be construed as a potential conflict of interest.

Publisher's Note: All claims expressed in this article are solely those of the authors and do not necessarily represent those of their affiliated organizations, or those of the publisher, the editors and the reviewers. Any product that may be evaluated in this article, or claim that may be made by its manufacturer, is not guaranteed or endorsed by the publisher.

Copyright © 2022 Maqbool, Sajid, Saqib, Anjum, Tayyab, Rizwan, Rashid, Rashid, Iqbal, Siddique, Shamim, Hassan, Atif, Razzaq, Zeeshan, Hussain, Nisar, Tanveer, Younas, Kamran and Rahman. This is an open-access article distributed under the terms of the Creative Commons Attribution License (CC BY). The use, distribution or reproduction in other forums is permitted, provided the original author(s) and the copyright owner(s) are credited and that the original publication in this journal is cited, in accordance with accepted academic practice. No use, distribution or reproduction is permitted which does not comply with these terms.



The Potential Vector Competence and Overwintering of West Nile Virus in Vector *Aedes Albopictus* in China

Ying-mei Zhang^{1†}, Xiao-xia Guo^{1†}, Shu-fang Jiang², Chun-xiao Li¹, Dan Xing¹, Heng-duan Zhang¹, Yan-de Dong¹ and Tong-yan Zhao^{1*}

¹ State Key Laboratory of Pathogen and Biosecurity, Beijing Institute of Microbiology and Epidemiology, Beijing, China, ² First Medical Center, Chinese People's Liberation Army (PLA) General Hospital, Beijing, China

OPEN ACCESS

Edited by:

Shu Shen,
Wuhan Institute of Virology (CAS),
China

Reviewed by:

Han Xia,
Key Laboratory of Special Pathogens
and Biosafety, Wuhan Institute
of Virology (CAS), China
Nohemi Cigarroa,
Universidad Autónoma de Yucatán,
Mexico

*Correspondence:

Tong-yan Zhao
tongyanzhao@126.com

[†]These authors share first authorship

Specialty section:

This article was submitted to
Virology,
a section of the journal
Frontiers in Microbiology

Received: 03 March 2022

Accepted: 20 April 2022

Published: 02 June 2022

Citation:

Zhang Y-m, Guo X-x, Jiang S-f,
Li C-x, Xing D, Zhang H-d, Dong Y-d
and Zhao T-y (2022) The Potential
Vector Competence
and Overwintering of West Nile Virus
in Vector *Aedes Albopictus* in China.
Front. Microbiol. 13:888751.
doi: 10.3389/fmicb.2022.888751

West Nile virus (WNV) is an arbovirus, which causes widespread zoonotic disease globally. In China, it was first isolated in Jiashi County, Kashgar Region, Xinjiang in 2011. Determining the vector competence of WNV infection has important implications for the control of disease outbreaks. Four geographical strains of *Aedes Albopictus* (*Ae. Albopictus*) in China were allowed to feed on artificial infectious blood meal with WNV to determine the infection and transmission rate. The results indicated that four strains of *Ae. Albopictus* mosquitoes could infect and transmit WNV to 1- to 3-day-old Leghorn chickens. The infection rates of different strains were ranged from 16.7 to 60.0% and were statistically different ($\chi^2 = 12.81$, $p < 0.05$). The highest infection rate was obtained from the Shanghai strain (60.0%). The transmission rates of *Ae. Albopictus* Shanghai, Guangzhou, Beijing, and Chengdu strains were 28.6, 15.2, 13.3, and 6.7%, respectively. Furtherly, the results reveal that *Ae. Albopictus* Beijing strain infected orally can transmit WNV transovarially even the eggs are induced diapausing. The study confirmed that WNV could survive in the diapause eggs of *Ae. Albopictus* and could be transmitted to progeny after diapause termination. This is of great significance for clarifying that the WNV maintains its natural circulation in harsh environments through inter-epidemic seasons.

Keywords: West Nile virus, *Aedes Albopictus*, infection, transmission, overwinter, diapausing

INTRODUCTION

West Nile virus (WNV) is an important zoonotic arbovirus of the family *Flaviviridae* (Heinz et al., 2000). It was first isolated in Africa in 1937 and circulated in a transmission cycle involving mosquitoes and birds (Gray and Webb, 2014; Chancey et al., 2015). West Nile fever is a global emerging disease. There are a large variety of habitats for migrating birds and resident birds in mainland China. Infectious migrating birds likely were important in WNV amplification (Julian et al., 2002). Therefore, there would be an endemic risk of WNV in China. Serological results for WNV infection in birds and humans suggested that enzootic transmission existed in China (Li et al., 2013). The human infections of WNV were reported in 2013 in Xinjiang (Lu et al., 2014; Cao et al., 2017, 2019). WNV was isolated from mosquitoes firstly in Xinjiang in western China

(Lu et al., 2014; Zhang et al., 2021). Therefore, increasing geographic distribution and circulation of WNV infection in mainland China should be noted.

West Nile virus has been isolated in 43 different ornithophilic *Culex* mosquito species that include *Aedes* and *Ochlerotatus* (Centers for Disease Control and Prevention [CDC], 2003). In China, four *Culex* mosquitoes were confirmed to be capable of WNV infection and transmission (Jiang et al., 2010). *Aedes Albopictus* (*Ae. Albopictus*) Skuse is widely distributed in mainland China with a range extending from south to Hainan Island, north to Shenyang in Liaoning Province, west to Tianshui and Longnan in Gansu Province, and southwest to Motuo in Tibet in China (Lu, 1990). Viral isolation and vector competence studies have established the efficiency of *Ae. Albopictus* in the transmission of more than 20 arboviruses (Paupy et al., 2009). *Ae. Albopictus* is considered a classic bridge vector between zoonotic arboviruses and humans due to its opportunistic feeding behavior (Paupy et al., 2009; Fortuna et al., 2015).

The study on the susceptibility of three North American *Ae. Albopictus* strains (Frederick County, Maryland, FRED strain; Cheverly, MD, CHEV strain; Chambers and Liberty counties, Texas, TAMU strain) to WNV revealed that the susceptibility of the strain from a Hawaiian source (OAHU strain) and TAMU was similar, but different from the FRED and CHEV strains (Sardelis et al., 2002). Currently, little is known about whether *Ae. Albopictus* plays a role in WNV transmission in China. Due to the widespread distribution in China, along with its opportunistic feeding behavior, ecological adaptability, and propensity, the aim of the present study was to evaluate the vector competence of *Ae. Albopictus*. The study presents the oral susceptibility and vector competence of four geographical strains of *Ae. Albopictus* to WNV. Four *Ae. Albopictus* strains are crossing subtropical and temperate regions of China. The results would deepen to the understanding of WNV infection and transmission in different mosquito strains. It would enhance the system of surveillance and control of vectors to prevent the outbreak of WNV in China.

Aedes Albopictus egg undergoes facultative diapause as the mechanism for surviving unfavorable environments, such as winter or arid and frigid environments (Hong et al., 1971). Therefore, the egg diapause mechanism may contribute to arbovirus preservation. A previous study has confirmed that the Japanese encephalitis virus can survive in dried infected *Ae. Albopictus* eggs for 2 months (Rosen et al., 1978). Additionally, dengue virus 2 was detected in diapause eggs of *Ae. Albopictus* (Guo et al., 2007) and transmitted to progeny after diapause termination (Guo et al., 2004). Diapausing behavior may provide an important mechanism for the maintenance of arbovirus under adverse climatic conditions. This work is aimed to confirm the possibility of WNV surviving in the cold season and playing a possible role in an endemic cycle in the next year.

MATERIALS AND METHODS

Ethics Statement

The study was conducted in the Animal Biosafety Level 3 (ABSL-3) facility. All of the experimental protocols involving animals were approved by the Laboratory Animal Center of the State

Key Laboratory of Pathogen and Biosecurity, Beijing Institute of Microbiology, and Epidemiology Institutional Animal Care and Use Committee (IACUC, the permit number is BIME 2011-2009). The animals were performed in strict accordance with the recommendations of the Guide for the Care and Use of Laboratory Animals of the National Institutes of Health.

Mosquitoes

Four geographical strains of *Ae. Albopictus* were originally collected in Guangzhou city (GPS location: 23°08'N and 113°14'W) in 1996, Shanghai city (GPS location: 31°15'N and 121°30'W) in 1995, Chengdu city (GPS location: 30°05'N and 102°54'W) in 1996, and Beijing city (GPS location: 39°56'N and 116°20'W) in 1997, respectively. Mosquitoes were maintained at 25 ± 1°C and 75 ± 5% relative humidity (RH) under a 14-h light/10-h dark (LD) photoperiod. F30 generation of *Ae. Albopictus* mosquitoes was used in this study. In addition, the Guangzhou strain and Beijing strain of *Ae. Albopictus* were collected in the wild in 2004 and 2005, separately. Mosquitoes were domesticated to F3 generation in the laboratory for transmission efficiency evaluation.

Virus Strain and Cell Line

The WNV strain (GenBank AY490240) was provided by the Microbial Culture Collection Center, Beijing Institute of Microbiology and Epidemiology. It had been passaged six times in Vero cells. Viral titer was 10^{7.0}–10^{7.5} PFU/ml. Vero cells were cultivated in Dulbecco's modified Eagle's medium (DMEM) (GIBCO™, Invitrogen, Beijing, China) containing 10% fetal bovine serum (FBS) and placed in an incubator of 37°C and 5% CO₂.

Mosquito Infection

Three- to five-day-old female mosquitoes were deprived of glucose solution and water for 24 h prior to infection. The infectious blood meal was composed of 1:1:1 mouse blood and virus and an 8% sugar solution. The viral titer of infectious blood meals was 10^{6.7}–10^{6.9} PFU/ml. Mosquitoes were offered a WNV infectious blood meal for 1 h using a Hemotek membrane feeding system housed in a feeding chamber that was constantly warmed to 37°C. One hundred and fifty engorged female mosquitoes were selected under CO₂ sedation for each geographical strain and transferred to three small cages (50 mosquitoes/cage), respectively. Engorged mosquitoes were reared under CO₂ sedation and incubated under 29 ± 1°C and 80 ± 5% RH with a 14:10 (light:dark) photocycle.

Virus Assay and Reverse Transcription-Polymerase Chain Reaction

West Nile virus-exposed samples were detected by reverse transcription-polymerase chain reaction (RT-PCR). The PCR primers included a pair of universal primers, Primer 1 (P1): 5'-TTG TGT TGG CTC TCT TGG CGT TCTT and Primer 2 (P2): 5'-CAG CCG ACA GCA CTG GAC ATT CATA. The RNA extraction was performed using TRIzol reagent (Invitrogen) according to the recommendations of manufacturers. Viral RNA

extract was transcribed into cDNA using RNA PCR Kit (AMV) version 2.1 [Takara Biotechnology (Dalian) Co., Ltd., Shiga, Japan]. The resulting cDNA was used as a template in the subsequent PCR reaction. The PCR amplifications were carried out through 45 cycles at 94°C for 30 s, 58°C for 30 s, 72°C for 1 min, and final extension at 72°C for 7 min. Further, some WNV-exposed samples were selected randomly to identify by C6/36 culture isolation. Virus isolation was processed as described in Jiang et al.'s (2006) study. That is, the supernatants of infected mosquitoes or Leghorn chicken blood were passed through a filter with pores of 0.22 μ m in diameter and inoculated into duplicate wells of C6/36 cell microplate cultures. After 1.5 h incubation at 37°C, cells were maintained at 37°C in DMEM supplemented with penicillin (100 U/ml), streptomycin (100 μ g/ml), and 5% FBS for 7 days.

Transmission Experiment of Four Geographic Strains of *Aedes Albopictus* to West Nile Virus

Mosquitoes were deprived of glucose solution and water for 24 h after a 14-day incubation period. One mosquito was allowed to feed on one 1- to 3-day-old Leghorn chicken individually for 30 min. After sucking blood, mosquitoes were killed by freezing at 20°C and were ground individually in 1.0 ml of mosquito diluents to test for the presence of the virus by RT-PCR. Then RNA positive samples were inoculated into C6/36 cells to isolate WNV. On day 2 post-sucking, the chicken blood was collected and serum was separated. The serum was then used to detect viral RNA by RT-PCR and to isolate WNV by inoculation into C6/36 cells.

The infection rate describes the number of mosquitoes infected with WNV in their body in relation to the total number of mosquitoes examined. The transmission rate was calculated as the ratio of the number of mosquitoes that can transmit the virus by biting to the total number of infected mosquitoes (Goddard et al., 2002; Tiawsirisup et al., 2005). The transmission efficiency is the percentage of WNV-positive mosquitoes that can transmit the virus by biting in relation to the total number of engorged mosquitoes.

Mosquito Egg Collection

Eggs from the second and third gonotrophic cycles of *Ae. Albopictus* Beijing strain were used in this study. Filter paper used as an oviposition substrate was placed in a small container of water after blood meal. After 3 days, filter papers were removed and kept in humid environment for 48 h. Then, eggs were held in desiccators at 25 \pm 1°C, 90% RH with a daily photoperiod of 14-h light/10-h dark (LD) for 6 days to permit embryonation (Hanson and Craig, 1994). A schematic representation of the experimental design and infection, transmission, and diapause induction is shown in Figure 1.

Diapause Induction and West Nile Virus Detection

Following embryonation, eggs were placed into a light cultivation chamber (HPG-280H) (Guangdong Medical

Instrument Factory Co., Ltd.) and subjected to a 10-h light/14-h dark (LD) photoperiod and 75% RH was controlled constantly with a supersaturated salt solution (Winston and Bates, 1960). The temperature was decreased 5°C every 2 days from 25 to 10°C. At last, eggs were held at a daily photoperiod of 8-h light/16-h dark (LD) and thermoperiod of 10°C:4°C (LD) and 50% RH for 6 weeks. The diapause induction procedure for uninfected eggs was the same. The control group not in diapause (non-diapause) was maintained at 25 \pm 1°C and 14-h light/10-h dark (LD) photoperiod and 75% RH.

Reverse transcription-PCR and virus isolation in C6/36 cells were used to detect WNV in diapausing eggs from the second and third gonotrophic cycles of infected *Ae. Albopictus*. Pools of diapausing eggs (200 eggs per pool) were detected. Minimum infection rates (MIRs) were calculated using Centers for Disease Control and Prevention (CDC) protocols.¹

Diapausing Egg Hatch

Diapausing eggs of *Ae. Albopictus* Beijing strain were submerged in deoxygenated solution (500 mg larval food was added into 500 ml water for 24 h, the dissolved oxygen concentration was about 0.3–0.5 ppm) to terminate diapause. After 24 h, the number of larvae was counted. All samples then were transferred to non-diapausing conditions [25 \pm 1°C and 14-h light/10-h dark (LD)] and hatch was attempted weekly. Unhatched eggs were bleached to clear the chorion to determine embryonation. The bleach solution consisted of 40 g sodium hypochlorite, 10 ml acetic acid, and 1 L of water (Hanson and Craig, 1994). Pools of F1 generation larvae from diapausing and non-diapausing eggs were detected by RT-PCR and virus isolation with C6/36. MIRs were calculated.

Statistical Analysis

The significance of any differences in infection and transmission rates between four geographical strains of *Ae. Albopictus* were tested with Chi-square and Fisher's exact tests implemented in the SPSS (GraphPad Software, San Diego, CA, United States) Version 10.0. Values of $p < 0.05$ were considered significant.

RESULTS

Oral Susceptibility of Four Geographical Strains of *Aedes Albopictus*

Four geographical strains of *Ae. Albopictus* were susceptible to infection with WNV after imbibing the virus dose of 10^{6.7}–10^{6.9} PFU/ml. The infection rates of four different geographical strains of *Ae. Albopictus* are shown in Table 1. The infection rates of different strains tested in the study were ranged from 16.7 to 60.0%. There were significant differences in infection rates between the four strains ($\chi^2 = 12.81$, $p < 0.05$). The highest infection rate was found in the Shanghai strain, which was 60.0%. There was no significant difference between the *Ae. Albopictus* 30 generations and 3 generations mosquito ($\chi^2 = 2.73$, $p > 0.05$) of

¹ <https://www.cdc.gov/westnile/resourcepages/mosqsurvsoft.html>

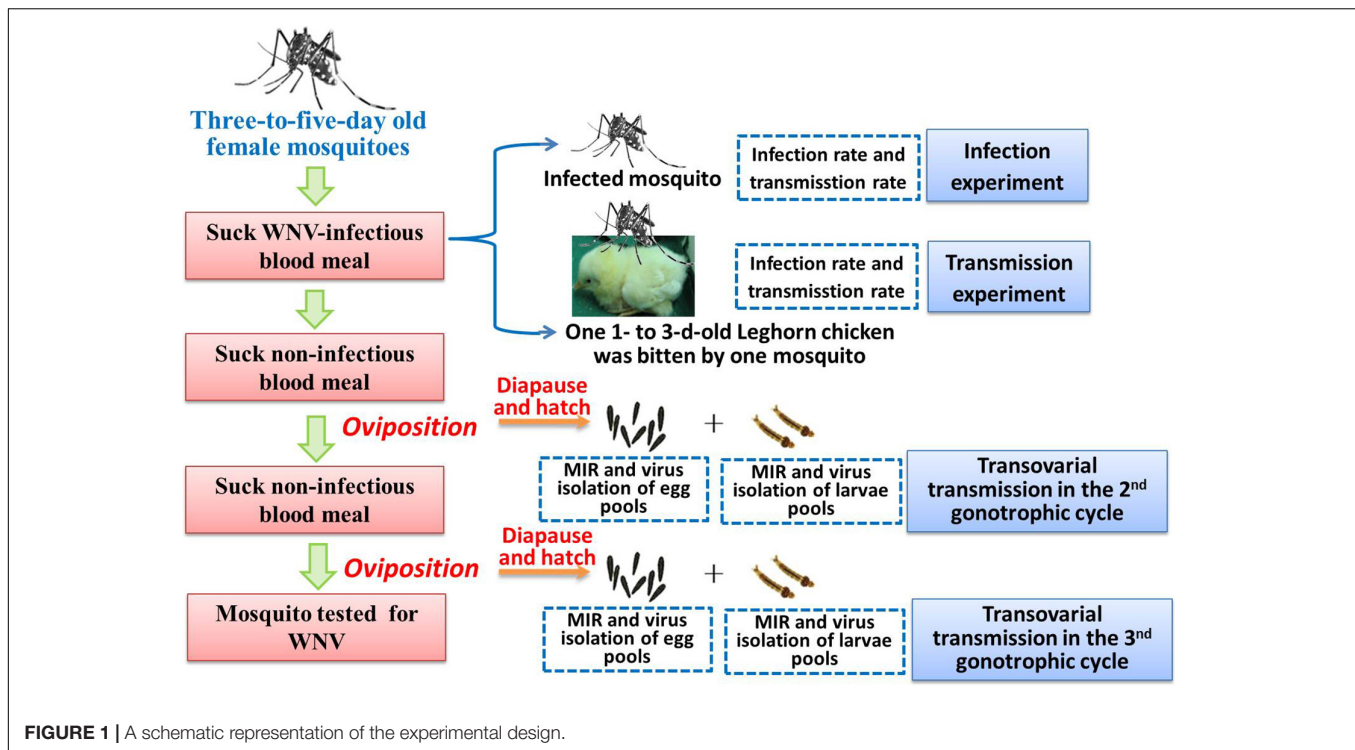


FIGURE 1 | A schematic representation of the experimental design.

Guangzhou and Beijing strains. Four RNA-positive samples were inoculated into C6/36 cells to isolate WNV. Cytopathic effect (CPE) was observed on the fifth day after inoculation.

Transmission Experiment of Four Geographical Strains of *Aedes Albopictus* to West Nile Virus

Four geographical strains of *Ae. Albopictus* were able to transmit WNV to 1- to 3-day-old Leghorn chicken by biting. Transmission rates varied from 40.0 to 47.6% (Table 1). There were no significant differences in transmission rates between the different strains ($\chi^2 = 4.49$, $p > 0.05$). However, there were significant differences in transmission efficiency between the four geographical strains of *Ae. Albopictus* ($\chi^2 = 103.2$, $p < 0.05$). The transmission efficiency of the Shanghai and Chengdu strains was significantly different ($\chi^2 = 5.149$, $p < 0.05$). The Leghorn chickens were bled on the second day for virus assay by RT-PCR. Leghorn chickens had viral RNA in their blood. The serum of three Leghorn chickens was inoculated into C6/36 cells. CPE was observed on the seventh day after inoculation.

West Nile Virus Detection in Diapausing Eggs

Pools of diapausing and non-diapausing eggs (200 eggs per pool) from the second and third gonotrophic cycles were tested by RT-PCR. An amplification product of the predicted size of 408 bp was evident in diapausing eggs. All RNA-positive homogenates of diapausing and non-diapausing eggs were inoculated in C6/36 cells for virus isolation. CPE was observed 4-day post-inoculation in diapausing and non-diapausing eggs. Both the

PCR amplification results and virus isolation in C6/36 cells confirmed that WNV infected diapausing eggs (Table 2).

West Nile Virus Detection in F1 Generation Larvae

West Nile virus was detected in F1 generation larvae from diapausing eggs. An amplification product of the predicted size of 408 bp was evident in F1 generation larvae. RNA-positive samples were inoculated into C6/36 cells to isolate the virus. CPE was observed 6-day post-inoculation in F1 generation larvae. The results showed that WNV can be detected in the larvae hatched from diapausing eggs. The MIR of F1 generation larvae from diapausing eggs was 1:1180 in the second gonotrophic cycle and 1:1120 in the third gonotrophic cycle (Table 3). There were no significant differences in the MIR of F1 generation larvae between diapausing and non-diapausing eggs (1:960 and 1:1120, respectively; $p > 0.05$). There was no significant difference in the MIR in larvae between the second and third gonotrophic cycles ($p > 0.05$).

DISCUSSION

West Nile virus is a re-emerging infectious disease and expands its geographic range in Europe and in other parts of the world (Weaver and Reisen, 2010; Koray et al., 2014). In mainland China, the first WNV isolation from mosquitoes in Xinjiang and the prevalence of fever of viral encephalitis caused by WNV infection has been recorded (Li et al., 2013; Cao et al., 2017, 2019). Therefore, monitoring WNV infection is important for public health in China.

TABLE 1 | Infection rate and transmission rate and transmission efficiency of four geographical *Aedes Albopictus* strains after oral exposure to West Nile virus (WNV).

Strains	Generations	No. tested mosquito	No. infected mosquito	Infection rate (%)	No. infected Leghorn chicken	Transmission rate (%)	Transmission efficiency (%)
Shanghai	30	35	21	60.0 (21/35)	10	47.6 (10/21)	28.6 (10/35)
Chengdu	30	30	5	17.9 (5/28)	2	40 (2/5)	7.1 (2/28)
Guangzhou	30	33	11	36.7 (11/30)	5	45.5 (5/11)	16.7 (5/30)
	3	30	7	23.3 (7/30)	3	42.9 (3/7)	10 (3/30)
Beijing	30	30	9	30.0 (9/30)	4	44.4 (4/9)	13.3 (4/30)
	3	30	5	16.7 (5/30)	2	40 (2/5)	6.7 (2/30)

TABLE 2 | West Nile virus (WNV) detection in diapausing eggs of *Ae. Albopictus* Beijing strain.

Eggs	Gonotrophic cycle	No. pools (200 eggs/pool)	WNV-positive pools	MIR ^a
Diapause	Second	6	1	1:1200
	Third	8	2	1:800
Non-diapause	Second	5	1	1:1000
	Third	6	2	1:600

^aMinimum infection rate (MIR) is the ratio of the number of positive pools to the total number of individuals (eggs) tested.

TABLE 3 | West Nile virus (WNV) detection in F1 generation larvae hatched from diapausing eggs of *Aedes Albopictus* (*Ae. Albopictus*) Beijing strain.

Mosquito stage	Gonotrophic cycle	No. pools (total number)	WNV-positive pools	MIR ^a
Larvae from diapausing eggs	Second	13 (1180)	1	1:1180
	Third	12 (1120)	2	1:1120
Larvae from non-diapausing eggs	Second	10 (960)	1	1:960
	Third	13 (1300)	2	1:650

^aMinimum infection rate (MIR) is the ratio of the number of positive pools to the total number of individuals (larvae) tested.

Vector competence refers to the intrinsic permissiveness of an arthropod vector to infection, replication, and transmission of the virus. In the present study, the infection rate, transmission rate, and transmission efficiency of WNV in four geographical strains of *Ae. Albopictus* from China were evaluated. Our results showed that four geographical strains of *Ae. Albopictus* were susceptible to infect with WNV after imbibing the virus dose of $10^{6.7}$ – $10^{6.9}$ PFU/ml. In nature, wild birds (e.g., crows) can produce viral titers of 10^8 PFU/ml (Cao et al., 2019), and the viral titers $10^{6.7}$ – $10^{6.9}$ PFU/ml are used in this study should be representative of the dose exposed to mosquitoes in nature. Therefore, *Ae. Albopictus* is able to infect WNV by bloodsucking. The Leghorn chicken bitten by infectious mosquitoes can be infected with WNV, which is the direct evidence for *Ae. Albopictus* as a potential vector. Current studies mostly agree that the main vector of WNV is *Culex*, most *Culex* species are bloodthirsty for bird and play an important role in the WNV maintenance and spread in nature. However, the habit of bloodthirsty birds may reduce the danger of transmitting the virus to mammals, such as humans and horses. The opportunistic

feeding behavior of *Ae. Albopictus* could transmit WNV from the amplifying bird hosts to mammals and act as “bridge vectors.” Currently, both virus isolation in the field and transmission experiments in the laboratory indicate that *Ae. Albopictus* is able to transmit WNV and is a possible bridge vector for WNV (Turell et al., 2001; Sardelis et al., 2002). Once the number of virus-infected birds and the population of *Aedes* mosquitoes increased, the danger of WNV transmission from the natural cycle of mosquito to bird to susceptible animals, such as humans and horses, is heightened.

The latitude of *Ae. Albopictus* distribution is also extremely wide, being present in regions south of 41°N and with the highest density of south 32°N (Lu, 1990). Different geographic strains of *Ae. Albopictus* have been shown to vary in their susceptibility to the dengue virus (Woodring et al., 1996). The present study found that four geographic *Ae. Albopictus* strains from both south and north of China were able to infect and spread WNV, with significantly higher transmission rates for the Shanghai strain, and a lower transmission rate for the Beijing, Chengdu, Guangzhou strains. There were significant differences in transmission efficiency between the four geographical strains of *Ae. Albopictus* ($p < 0.05$). *Ae. Albopictus* should therefore be considered a WNV vector in regions of China. The results indicated that *Ae. Albopictus* exhibits geographic variation in vector competence to WNV. A further study on the genetic basis of vector infection and the competence of different geographic strains to transmit WNV should be conducted. In addition, statistical analysis indicated that there were no significant differences between a laboratory strain and field strain on WNV susceptibility ($p > 0.05$). The results showed that there was no significant effect of generation on susceptibility to WNV.

Egg diapause is an essential condition for *Ae. Albopictus* to overwinter and/or survive in harsh environments through inter-epidemic seasons. Eggs from two gonotrophic cycles of WNV-infected mosquitoes were collected and induced diapause. The present study confirmed that WNV can live in the overwintering diapause eggs of *Ae. Albopictus* and transmit to the offspring, which plays a positive role in maintaining the survival and long-distance transmission of the virus under adverse conditions. At the same time, *Ae. Albopictus* is widely distributed in China, and China's climate conditions are complex. Most areas in the north are cold and dry in winter, and the RH is basically maintained at about 50%, while most areas in the south are cold and humid in winter, and the RH is maintained at about 75%. The results of this study show that WNV can survive in the diapause eggs of *Ae. Albopictus* at 50% RH and transmit to the offspring,

which suggests that WNV may maintain its transmission cycle in nature through the diapause eggs of *Ae. Albopictus* in both cold and dry areas. This may be of great significance in the natural epidemic of diseases. Accordingly, more attention should be paid to *Ae. Albopictus* eggs in vector control for WNV outbreak management at temperate latitudes.

DATA AVAILABILITY STATEMENT

The original contributions presented in the study are included in the article/supplementary material, further inquiries can be directed to the corresponding author.

ETHICS STATEMENT

The animal study was reviewed and approved by the Laboratory Animal Center of the State Key Laboratory of Pathogen and

Biosecurity, Beijing Institute of Microbiology and Epidemiology Institutional Animal Care and Use Committee (IACUC, the permit number is BIME 2011-2009).

AUTHOR CONTRIBUTIONS

T-YZ designed the study. Y-MZ, S-FJ, DX, and H-DZ carried out the data acquisition and analysis. X-XG wrote the manuscript. C-XL and Y-DD supervised the study. All authors reviewed the manuscript.

FUNDING

This study was supported by grants from the Infective Diseases Prevention and Cure Project of the National Ministry of Public Health of China (no. 2017ZX10003404).

REFERENCES

- Cao, L., Fu, S., Lu, Z., Tang, C., Gao, X., Li, X., et al. (2019). Detection of West Nile virus infection in viral encephalitis cases, China. *Vector Borne Zoonotic Dis.* 19, 45–50. doi: 10.1089/vbz.2018.2.275
- Cao, L., Fu, S., Lv, Z., Tang, C., Cui, S., Li, X., et al. (2017). West Nile virus infection in suspected febrile typhoid cases in Xinjiang, China. *Emerg. Microbes Infect.* 6:e41. doi: 10.1038/emi.2017.27
- Centers for Disease Control and Prevention [CDC] (2003). *Entomology*. Atlanta, GA: Centers for Disease Control and Prevention.
- Chancey, C., Grinev, A., Volkova, E., and Rios, M. (2015). The global ecology and epidemiology of West Nile virus. *Biomed. Res. Int.* 2015:376230. doi: 10.1155/2015/376230
- Fortuna, C., Remoli, M. E., Severini, F., Di Luca, M., Toma, L., Fois, F., et al. (2015). Evaluation of vector competence for West Nile virus in Italian *tegomyia albopicta* (= *Aedes albopictus*) mosquitoes. *Med. Vet. Entomol.* 29, 430–433. doi: 10.1111/mve.12133
- Goddard, L. B., Roth, A. E., Reisen, W. K., and Scott, T. W. (2002). Vector competence of California mosquitoes for West Nile virus. *Emerg. Infect. Dis.* 8, 1385–1391. doi: 10.3201/eid0812.020536
- Gray, T., and Webb, C. E. (2014). A review of the epidemiological and clinical aspects of West Nile virus. *Int. J. Gen. Med.* 7, 193–203. doi: 10.2147/IJGM.S59902
- Guo, X. X., Zhao, T. Y., Dong, Y. D., Jiang, S., and Lu, B. L. (2004). Transmission of dengue-2 virus by diapausing eggs of *Aedes albopictus*. *Acta Entomol. Sin.* 47, 424–428.
- Guo, X. X., Zhao, T. Y., Dong, Y. D., and Lu, B. L. (2007). Survival and replication of dengue-2 virus in diapausing eggs of *Aedes albopictus* (Diptera: Culicidae). *J. Med. Entomol.* 44, 492–497. doi: 10.1603/0022-2585(2007)44[492:sarodv]2.0.co;2
- Hanson, S. M., and Craig, G. B. (1994). Cold acclimation, diapause and geographic origin affect cold hardiness in eggs of *Aedes albopictus* (Diptera: Culicidae). *J. Med. Entomol.* 31, 192–201. doi: 10.1093/jmedent/31.2.192
- Heinz, F. X., Collett, M. S., Purcell, R. H., Gould, E. A., Howard, C. R., and Houghton, M. (2000). “Family Flaviviridae,” in *Virus Taxonomy: Classification and Nomenclature of Viruses*, eds M. H. van Regenmortel, C. M. Fauquet, D. H. Bishop, E. B. Carstens, M. K. Estes, S. M. Lemon, et al. (San Diego, CA: Academic Press), 859–878.
- Hong, H. K., Shim, J. C., and Young, H. Y. (1971). Hibernation studies of forest mosquitoes in Korea. *Korean J. Entomol.* 1, 13–16.
- Jiang, S. F., Zhang, Y. M., Guo, X. X., Dong, Y. D., Xing, D., Xue, R. D., et al. (2010). Experimental studies on comparison of the potential vector competence of four species of culex mosquitoes in China to transmit West Nile Virus. *J. Med. Entomol.* 47, 788–790. doi: 10.1603/ME08292
- Jiang, S. F., Zhao, T. Y., Zhang, Y. M., Dong, Y. D., and Guo, X. X. (2006). Detection of West Nile virus in experimentally infected mosquitoes and Leghorn chicken by RTPCR. *Acta Parasitol. Med. Entomol. Sin.* 13, 21–24.
- Julian, K. G., Eidson, M., Kipp, A. M., Weiss, E., and Petersen, L. R. (2002). Early season crow mortality as a sentinel for West Nile virus disease in humans, northeastern United States. *Vector Borne Zoonotic Dis.* 2, 145–155. doi: 10.1089/15303660260613710
- Koray, E., Filiz, G., Ozge, E. K., Kerem, O., Sepandar, G., Taner, K., et al. (2014). Serological, molecular and entomological surveillance demonstrates widespread circulation of West Nile virus in Turkey. *PLoS Negl. Trop. Dis.* 8:e3028. doi: 10.1371/journal.pntd.0003028
- Li, X. L., Fu, S. H., Liu, W. B., Wang, H. Y., Lu, Z., Tong, S. X., et al. (2013). West Nile virus infection in Xinjiang, China. *Vector Borne Zoonotic Dis.* 13, 131–133. doi: 10.1089/vbz.2012.0995
- Lu, B. L. (1990). *Vector of Dengue Fever and its Prevention and Control in Mainland China*. GuiZhou: Gui Zhou People's Press, 51–55.
- Lu, Z., Fu, S. H., Cao, L., Tang, C. J., Zhang, S., Li, Z. X., et al. (2014). Human Infection with West Nile Virus, Xinjiang, China, 2011. *Emerg. Infect. Dis.* 20, 1421–1423. doi: 10.3201/eid2008.131433
- Paupy, C., Delatte, H., Bagny, L., Corbel, V., and Fontenille, D. (2009). *Aedes albopictus*, an arbovirus vector: from the darkness to the light. *Microbes Infect.* 11, 1177–1185. doi: 10.1016/j.micinf.2009.05.005
- Rosen, L., Tesh, R. B., Lien, J. C., and Cross, J. H. (1978). Transovarial transmission of Japanese encephalitis virus by mosquitoes. *Science* 199, 909–911. doi: 10.1126/science.203035
- Sardelis, M. R., Turell, M. J., O'Guinn, M. L., Andre, R. G., and Roberts, D. R. (2002). Vector competence of three North American strains of *Aedes albopictus* for West Nile virus. *J. Am. Mosq. Control Assoc.* 18, 284–289.
- Tiawisirisup, S., Platt, K. B., Evans, R. B., and Rowley, W. A. (2005). A Comparison of West Nile Virus transmission by *Ochlerotatus trivittatus* (COQ), *Culex pipiens* (L.), and *Aedes albopictus* (Skuse). *Vector Borne Zoonotic Dis.* 5, 40–47. doi: 10.1089/vbz.2005.5.40
- Turell, M. J., O'Guinn, M. L., Dohm, D. J., and Jones, J. W. (2001). Vector competence of North American mosquitoes (Diptera: Culicidae) for West Nile virus. *J. Med. Entomol.* 38, 130–134. doi: 10.1603/0022-2585-38.2.130
- Weaver, S. C., and Reisen, W. K. (2010). Present and future arboviral threats. *Antiviral Res.* 85, 328–345. doi: 10.1016/j.antiviral.2009.10.008
- Winston, P. W., and Bates, D. H. (1960). Saturated solutions for control of humidity in biological research. *Ecology* 41, 232–237. doi: 10.2307/1931961
- Woodring, J. L., Higgs, S., and Beaty, B. J. (1996). “Natural cycles of vector borne pathogens,” in *Biology of Disease Vectors*, eds W. C. Marquardt and B. J. Beaty (Boulder, CO: University of Colorado Press), 51–72.

Zhang, Y. P., Lei, W. W., Wang, Y., Sui, H. T., Liu, B., Li, F., et al. (2021). Surveillance of West Nile virus infection in Kashgar Region, Xinjiang, China, 2013–2016. *Sci. Rep.* 11:14010. doi: 10.1038/s41598-021-93309-2

Conflict of Interest: The authors declare that the research was conducted in the absence of any commercial or financial relationships that could be construed as a potential conflict of interest.

Publisher's Note: All claims expressed in this article are solely those of the authors and do not necessarily represent those of their affiliated organizations, or those of

the publisher, the editors and the reviewers. Any product that may be evaluated in this article, or claim that may be made by its manufacturer, is not guaranteed or endorsed by the publisher.

Copyright © 2022 Zhang, Guo, Jiang, Li, Xing, Zhang, Dong and Zhao. This is an open-access article distributed under the terms of the Creative Commons Attribution License (CC BY). The use, distribution or reproduction in other forums is permitted, provided the original author(s) and the copyright owner(s) are credited and that the original publication in this journal is cited, in accordance with accepted academic practice. No use, distribution or reproduction is permitted which does not comply with these terms.



Dengue Virus-2 Infection Affects Fecundity and Elicits Specific Transcriptional Changes in the Ovaries of *Aedes aegypti* Mosquitoes

OPEN ACCESS

Edited by:

Shu Shen,
Wuhan Institute of Virology (CAS),
China

Reviewed by:

Ana Beatriz Barletta Ferreira,
Clinical Center (NIH), United States
Shufen Li,
Wuhan Institute of Virology (CAS),
China

*Correspondence:

Fabiana Feitosa-Suntheimer
ffeitosa@bu.edu

†Present address:

Tonya M. Colpitts,
Director of Virology, Infectious
Diseases Research, Moderna
Therapeutics Inc., Cambridge, MA,
United States

‡These authors have contributed
equally to this work

Specialty section:

This article was submitted to
Virology,
a section of the journal
Frontiers in Microbiology

Received: 28 February 2022

Accepted: 23 May 2022

Published: 23 June 2022

Citation:

Feitosa-Suntheimer F, Zhu Z,
Mameli E, Dayama G, Gold AS,
Broos-Caldwell A, Troupin A,
Rippe-Brooks M, Corley RB,
Lau NC, Colpitts TM and
Londoño-Rentería B (2022) Dengue
Virus-2 Infection Affects Fecundity
and Elicits Specific Transcriptional
Changes in the Ovaries of *Aedes
aegypti* Mosquitoes.
Front. Microbiol. 13:886787.
doi: 10.3389/fmicb.2022.886787

Fabiana Feitosa-Suntheimer^{1,2*}, Zheng Zhu^{2,3†}, Enzo Mameli^{1,2,4‡}, Gargi Dayama³,
Alexander S. Gold^{1,2}, Aditi Broos-Caldwell^{1,2}, Andrea Troupin⁵, Meagan Rippee-Brooks⁶,
Ronald B. Corley^{1,2}, Nelson C. Lau^{2,3,7}, Tonya M. Colpitts^{1,2†} and
Berlin Londoño-Rentería^{5,8}

¹ Department of Microbiology, Boston University School of Medicine, Boston, MA, United States, ² National Emerging Infectious Diseases Laboratories, Boston University, Boston, MA, United States, ³ Department of Biochemistry, Boston University School of Medicine, Boston, MA, United States, ⁴ Department of Genetics, Harvard Medical School, Blavatnik Institute, Boston, MA, United States, ⁵ School of Public Health and Tropical Medicine, Tulane University, New Orleans, LA, United States, ⁶ Department of Biology, Missouri State University, Springfield, MO, United States, ⁷ Genome Science Institute, Boston University, Boston, MA, United States, ⁸ Department of Entomology, Kansas State University, Manhattan, KS, United States

Dengue fever (DF), caused by the dengue virus (DENV), is the most burdensome arboviral disease in the world, with an estimated 400 million infections each year. The *Aedes aegypti* mosquito is the main vector of DENV and transmits several other human pathogens, including Zika, yellow fever, and chikungunya viruses. Previous studies have shown that the pathogen infection of mosquitoes can alter reproductive fitness, revealing specific vector-pathogen interactions that are key determinants of vector competence. However, only a handful of studies have examined the effect of DENV infection in *A. aegypti*, showing a reduction in lifespan and fecundity over multiple blood meals. To provide a more comprehensive analysis of the impact of DENV infection on egg laying and fecundity, we assessed egg laying timing in DENV-2 blood-fed mosquitoes (infected group) compared to mock blood-fed mosquitoes (control group). We confirmed a significant decrease in fecundity during the first gonadotrophic cycle. To further investigate this phenotype and the underlying DENV-2 infection-dependent changes in gene expression, we conducted a transcriptomic analysis for differentially expressed genes in the ovaries of *A. aegypti* infected with DENV-2 vs. mock-infected mosquitoes. This analysis reveals several DENV-2-regulated genes; among them, we identified a group of 12 metabolic genes that we validated using reverse transcription-quantitative PCR (RT-qPCR). Interestingly, two genes found to be upregulated in DENV-infected mosquito ovaries exhibited an antiviral role for DENV-2 in an *Aedes* cell line. Altogether, this study offers useful insights into the virus-vector interface, highlighting the importance of gene expression changes in the mosquito's ovary during DENV-2 infection in the first gonadotrophic cycle, triggering antiviral responses that may possibly interfere with

mosquito reproduction. This information is extremely relevant for further investigation of *A. aegypti*'s ability to tolerate viruses since virally infected mosquitoes in nature constitute a powerful source of supporting viruses during intra-epidemic periods, causing a huge burden on the public health system.

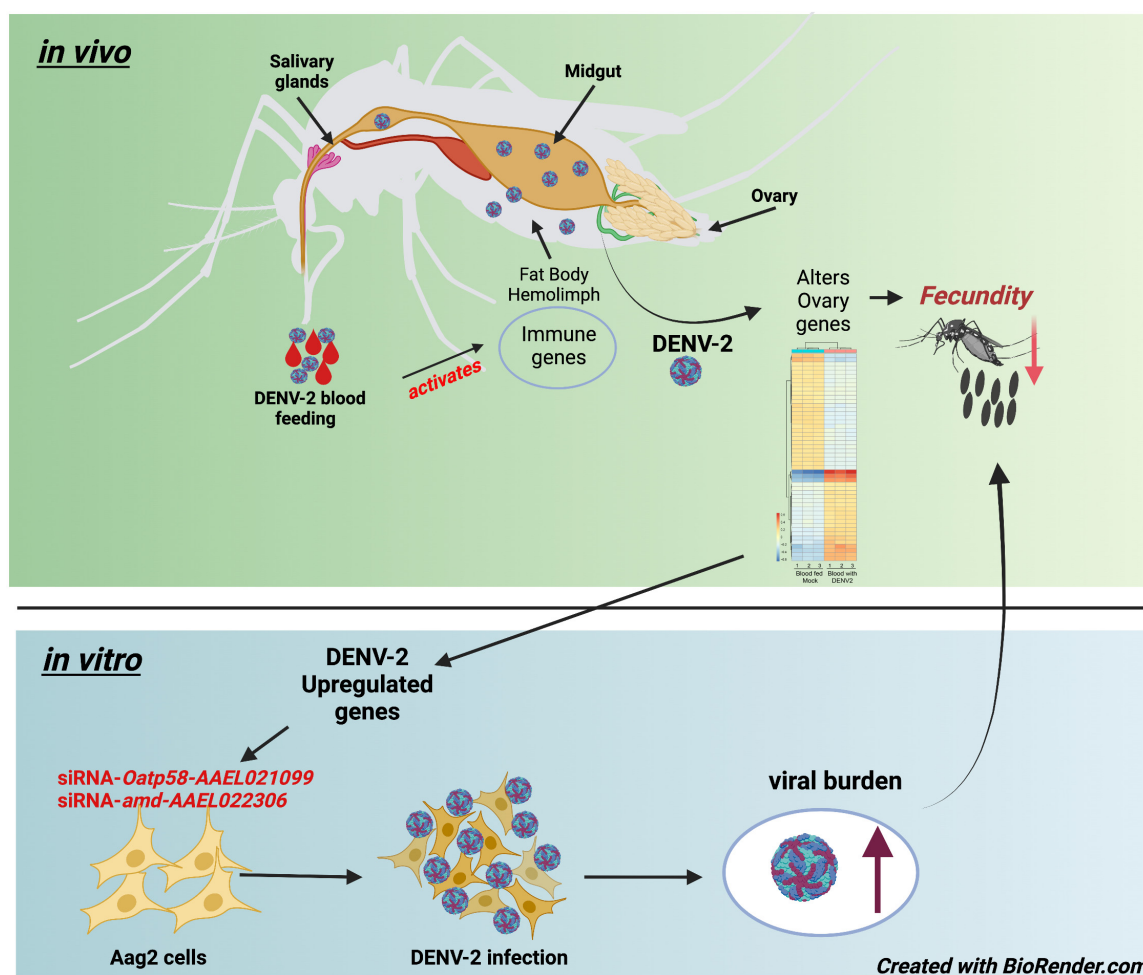
Keywords: *Aedes aegypti*, dengue, host-pathogen interaction, gene expression, mosquito fecundity

INTRODUCTION

Among emerging and pandemic viruses posing a global threat, dengue fever (DF), caused by dengue virus (DENV), is the most prominent arboviral disease in the world. The World Health Organization (WHO) reports an estimated 100–400 million dengue infections per year worldwide (WHO, 2022) with the largest number of cases reported in 2019. The U.S. Centers for Disease Control and Prevention (CDC) also notes that 40% of the world's population is at risk for DF (CDC, 2021). Dengue virus serotypes 1–4 (DENV 1–4) are the etiologic agents of dengue fever that lack effective therapies because of ineffective attempts at vaccine development (Izmirly et al., 2020). For example,

the only available FDA-approved dengue vaccine, Dengvaxia®, has major restrictions on large-scale administration in afflicted countries where dengue fever is endemic. This is due to the problematic side effect of antibody-dependent enhancement (ADE) in a vaccinated patient being previously infected with a DENV serotype different from that of the vaccine antigen (Halstead, 2016).

Research efforts are still needed to better understand how *Aedes aegypti* serves as the main vector of DENV and several other arboviruses, including yellow fever virus (YFV), Zika virus (ZIKV), and chikungunya virus (CHIKV). Although *A. aegypti*'s natural habitats are restricted to tropical and temperate areas, climate change and economic development have increased the



GRAPHICAL ABSTRACT | *Aedes aegypti* first gonadotrophic cycle is altered by DENV-2 infection.

density of human populations in the geographic range of mosquitoes, where feeding on humans contributes to expanding mosquito populations and an increase in vector-borne disease cases (Weaver and Barrett, 2004). For example, a recent study suggested a 3.2–4.4% increase in the *A. aegypti* population, and municipal insecticide spraying programs do not represent environmentally sustainable measures to stop the continuing spread of arboviral diseases (Iwamura et al., 2020).

Therefore, there is a relevant need to improve our understanding of how DENV is sustained in mosquitoes after an infectious blood meal as well as investigate its transmission to humans through subsequent infectious mosquito bites. Humans are considered the reservoir for all DENV serotypes (DENV 1–4) in endemic areas of the world, while primates serve as the reservoir for the sylvatic transmission cycle. Furthermore, other authors have suggested that mosquitoes serve as viral reservoirs due to their ability to transmit viruses to vertebrate hosts (Wu et al., 2019). As an example, a study showed that the same DENV serotypes were detected circulating in wild-collected larva and patients' serum during an outbreak in Sri Lanka (Wijesinghe et al., 2021). After mosquitoes feed on a viremic host, the blood meal is processed in the mosquito midgut, where the virus will infect the midgut epithelial cells and start replicating (Rückert and Ebel, 2018). However, after ingestion of the virus with the bulk of the blood nutrients, the viral particles eventually escape the first barrier of infection, the midgut barrier, to then spread throughout the hemolymph and infect the mosquito hemocytes, fat body, ovaries, and eventually salivary glands (Novelo et al., 2019). After the extrinsic incubation period (EIP) has passed, the infected mosquitoes can then spread arbovirus to several humans through subsequent blood meals (Chan and Johansson, 2012; Carrington and Simmons, 2014; Koh et al., 2018).

Although mosquito somatic tissues, such as the midgut, hemocytes, fat body, and salivary glands, have been previously investigated for their responses to, and capacity for, arbovirus replication (Franz et al., 2015), ovaries have been historically understudied due to the lower viral burden in this tissue. Nevertheless, the viral load in the ovaries is still sufficient for vertical transmission or venereal transmission by infected-born males mating with females (Sánchez-Vargas et al., 2018). The same mechanism of transmission was observed in *A. albopictus* infected with another important flavivirus, ZIKV, where the mosquitoes infected *via* the congenital route could transmit ZIKV to immunocompetent mice (Lai et al., 2020). In field collected *A. aegypti* infected with ZIKV, the vertical transmission was observed as well as the fitness cost of infection in the progeny, showing a reduction in the number of eggs hatched, and slow larvae development (Chaves et al., 2019). Although there is clear evidence of vertical transmission of flaviviruses in *Aedes* mosquitoes, it remains unclear how the mosquito immunity responds to viral infection and what the cost of infection is in mosquito reproduction. The combined events of vertical and venereal transmission are also believed to maintain the virus circulating in wild mosquitoes. Thus, the importance of mosquito ovaries as a site of viral replication, as well as the possible link between activation of mosquito innate immune response in this tissue and mosquito reproduction, warrant further investigation.

The mosquito gonadotrophic cycle is well synchronized starting 1 h after blood feeding with the activation of the 20-hydroxyecdysone (20E) pathway and production of yolk protein precursors (YPPs) by the fat body (Hansen et al., 2014). At 72 h after blood feeding, eggs are fully developed, and females start to search for sites to lay their eggs, usually on the inner walls of artificial containers with fresh water (Day, 2016). Female mosquitoes require a blood meal to initiate the vitellogenesis process by the fat body, which will lead to the intake of proteins to start egg production in the ovaries (Attardo et al., 2005). Although mosquito blood feeding of humans is the key route of pathogenic vectoring capacity and a direct need for mosquito reproduction, the effect of viral infection on mosquito ovary function is poorly investigated. To explore the hypothesis that mosquito ovaries are an important tissue intersecting viral replication and mosquito reproduction, we first conducted a study to investigate the impact of DENV-2 infection on the fecundity of *A. aegypti* females. During the first gonadotrophic cycle, we observed a significant reduction in the number of eggs from DENV-infected mosquitoes compared to uninfected counterparts. We then investigated the changes in the ovary transcriptome of *A. aegypti* 3 days after receiving a DENV-2 blood meal (infected group) compared to mock blood-fed mosquitoes (control group). We highlight several genes with physiological and metabolic functions in the ovary that are changing in expression levels during DENV infection. Some DGEs from the mosquito ovary analysis also appeared to be differentially expressed in the mosquito *A. aegypti* Aag2 cell line when subjected to DENV infection. Interestingly, two genes found to be upregulated in DENV-infected mosquito ovaries exhibited an antiviral role for DENV-2 in an *Aedes* cell line. Overall, our study shows that despite the mosquito's high tolerance to DENV-2 infection *via* blood meal, the ovaries undergo physiological responses to DENV-2 infection as early as 3 days after receiving an infectious blood meal, as reflected by specific transcriptome changes and a reduced fecundity rate of egg laying. Finally, this study set the basis for further investigation of mosquito genes involved in the specific response to DENV infection. These genes possibly orchestrate the delicate balance between immunity and reproduction and contribute to sustaining vector competence. New insights into mosquito tolerance factors could offer new opportunities for vector control strategies aimed at interrupting viral transmission.

MATERIALS AND METHODS

Mosquitoes, DENV-2 Infection, and Blood Feeding

Aedes aegypti colony (Rockefeller strain) was obtained from Tulane University. Mosquitoes were maintained in rearing chambers in a secure insectary (arthropod containment level 3) ACL-3 in the NEIDL, following rearing conditions as described by Araujo et al. (2020).

For the transcriptome experiments, human blood from a donor was used (The Blood Center, New Orleans, LA, United States). Briefly, blood in EDTA was centrifuged, and

plasma was separated and inactivated at 56°C for 1 h. Red blood cells (RBCs) were washed three times with 0.01 M PBS and reconstituted with autologous plasma. For the infection, the blood mixture was then added in a 1:1 ratio to the supernatant from either the DENV-2 culture or uninfected cells. For the feeding experiments, 7–10 day old female *A. aegypti* mosquitoes were starved for 24 h before the feeding. Mosquitoes were fed for 30 min. Engorged females were sorted and kept in the incubator for 3 days with a 10% sucrose solution provided on day 3 after feeding, ovaries from all live mosquitoes were dissected in 0.01M PBS, and RNA was extracted as described below. Midguts were tested for the presence of infection with DENV using reverse transcription-quantitative PCR (RT-qPCR).

For RT-qPCR validation of genes and egg laying, pre-mated females at 7 days old were transferred to individual cups and fasted for 24 h prior to the DENV-2 blood meal or mock blood meal. Females were infected *via* feeding on a Hemotek Feeding System, and an infectious blood meal composed of mice blood and DENV-2 (2.7×10^7 ffu/ml) supernatant at a 1:1 dilution was given to the mosquitoes (infected group). For the mock blood feeding (control group), females were fed with clean blood composed of Vero-E6 cell supernatant and mouse blood at a 1:1 dilution. The blood was freshly collected from Balb/C mice through cardiac puncture and placed in a heparin-coated tube according to standard procedures approved by IACUC PROTO201900005. The whole blood was centrifuged at 3,000 rpm for 10 min to separate plasma and RBCs. RBCs were washed three times in 0.01M PBS to remove anticoagulants, and plasma was heat-inactivated at 56°C for 1 h. RBCs were resuspended with plasma and used immediately for mosquito blood feedings. Mosquitoes were allowed to feed for 30 min. Engorged females from each group were sorted into cups and provided with a 10% sucrose solution and returned to the incubator. Ovaries from females of each group were dissected in 0.01M PBS 3 days after blood feeding. Carcasses from the DENV-infected group were tested for DENV-2 using RT-qPCR, and a pool with the corresponding positive ovaries was used in the RT-qPCR for validation of the volcano plot genes. Individual egg-laying females were placed in individual tubes with 10% sucrose provided. Eggs were counted daily, from 3 to 7 days after receiving a blood meal.

Cell Cultures and Virus

The *A. aegypti* embryonic-derived cell line, Aag2 (gift from Dr. Michael J. Conway), was cultivated at 28°C in an incubator with 5% CO₂ in high glucose Dulbecco's Modified Eagle's Medium, DMEM (Gibco), supplemented with 10% heat-inactivated fetal bovine serum (FBS) (Gemini), 1% Tryptose Phosphate Broth (Gibco), and Antibiotic-Antimycotic (Gibco). Aag2 cells were used for *in vitro* validation of gene expression from selected genes.

The dengue virus 2, New Guinea C (DENV-2-NGC) strain was obtained from BEI resources. The virus was passaged into Vero-E6 cells and cultured for 5 days in high glucose DMEM (Gibco) medium supplemented with 2% heat-inactivated FBS (Gemini) at 37°C in an incubator with 5% CO₂. After visualization of

cytopathic effect (CPE), the viral supernatant was centrifuged, spun down for 10 min at 4,000 rpm, and filtered using a 0.45 (μm) syringe filter. The virus was harvested and aliquoted in cryotubes and stored at -80°C freezer to use for the mosquitoes' infectious blood meal. DENV-2 was also passaged into Vero-E6 cells for focus forming assay (ffa) and the viral titer was obtained.

RNA Sequencing

A pool of 100 ovaries was dissected in 0.01M PBS from females 3 days post DENV-2 blood feeding (DENV infected) and the 100 ovaries from the control group, 3 days post uninfected blood feeding (mock). This was performed in triplicate, and gene expression of infected ovaries was compared to the uninfected control group. Tissues were homogenized in 100 μl of RNA lysis buffer using a pestle and an additional 500 μl of buffer was added to each sample. Total RNA was extracted from infected and uninfected samples using the Qiagen RNeasy Plus Mini-Kit (Qiagen, 74136) per the manufacturer's instructions. RNA sequencing was performed from mosquito samples in three biological replicates by outsourcing to Genewiz, which conducted poly(A) selection and standard strand-specific single-end RNA sequencing (RNA-Seq) library construction and sequencing on a NextSeq 500 instrument. A total of six FASTAQ files were generated and deposited at the NIH NCBI Sequence Read Archive (SRA) under the BioProject accession # PRJNA786000.

Bioinformatics Analysis of RNA Sequencing Data

For quality control, 6 FASTQ files (3 from mock and 3 from DENV infected) were first inspected using FastQC (REF: Andrews S. FastQC: a quality control tool for high throughput sequence data, 2010) to assess any bias due to read quality and length and to confirm the linker adapters had been trimmed. Using the STAR aligner (Dobin A. STAR: ultrafast universal RNA-seq aligner, 2013), RNA-seq reads were then mapped to the reference genome of *A. aegypti* (strain Liverpool AGWG, assembly AaegL5) downloaded from VectorBase (2022), but an additional assignment of *Drosophila* gene names from FlyBase (Thurmond et al., 2019) was appended to enhance the identification of the mosquito gene's machine-generated names.

As the standard analysis of DEGs based solely on *p*-values yielded an intractably large list of gene candidates, we modified our approach to filter for robustly affected genes. First, we looked at mosquito gene annotations that have gene ID, such as AAEL##### as described in the mosquito database (VectorBase, 2022) by appending the gene name of the *Drosophila melanogaster* ortholog from FlyBase (Thurmond et al., 2019).

After batch correction and initial filtering in R, overall relatedness can be observed within the mock and DENV-2 infected samples as seen by the clustering in the principal component analysis (PCA) plot (Supplementary Figure 1A). Using estimated read counts, the transcriptomes below the threshold value (est. read count < 1 across all samples) were further filtered using R. Correction was done for batch effects using DESeq2 (Love et al., 2014; Supplementary Figure 1A) for 2 PCAs before and after batch correction. Differential gene

expression (DGE) analysis was then performed using DESeq2 as well as EdgeR (Robinson et al., 2009) to generate a robust list of DEGs. In each result set, the most significant DEGs were determined ($FDR < 0.05$), and a intersect analysis (Venn diagram) showed approximately 91% overlap of DEGs from DESeq2 results (**Supplementary Figure 1B**). Thus, DESeq2 results were utilized for downstream analysis.

A heatmap was generated to show the top 50 upregulated and downregulated DEGs. Furthermore, the significant DEGs ($FDR < 0.05$) were filtered for a base mean expression value of 150, and 12 highly expressed genes were picked for validation using RT-qPCR as highlighted in the volcano plot and the heatmap. Gene Ontology (GO) analysis was performed on significant DEGs ($FDR < 0.05$) using VectorBase's annotation tool (Ashburner et al., 2000; VectorBase, 2022). The top entries for biological processes, molecular functions, and cellular components, were picked based on an FDR cutoff of 0.005 and excluding GO terms containing 1,000 genes or more to focus on specialized terms.

Mosquito Fecundity Assay

Mosquito egg laying assays were performed in two biological replicates. Two groups of pre-mated females, 7–10 days old, were used for this assay. DENV-2 infected and mock mosquitoes were blood-fed using a Hemotek Feeding System as previously described. The viral titer used in the infectious blood meal was 2.5×10^7 focus forming units (ffu). Engorged females were sorted into individual 50 ml Falcon tubes for egg laying. Each tube was closed with a piece of mesh cloth and secured with an elastic band. A cotton ball with 10% sucrose was placed on the top of each tube for subsequent feeding of mosquitoes. At approximately 60 h post blood feeding, a strip of wet filter paper was placed inside each tube to allow oviposition. The egg counting started at 3 days post blood feeding and ended at 7 days post blood feeding when females were not laying any more eggs. At the end of the experiment, at 7 days post infection (7 DPI), each mosquito was homogenized for total RNA extraction using the QIAshredder (Qiagen, 79656) and the Qiagen RNeasy Plus Mini-Kit (Qiagen, 74136). Individual mosquitoes were tested for DENV-2 by RT-qPCR using the QuantiFast SYBR Green RT-PCR Kit (Qiagen, 204156). Viral burden from individual mosquitoes was obtained by using a standard curve from an *in vitro* transcription of standard DENV-2 RNA as described below. Only positive females were considered for the egg counting final graph.

Reverse Transcription-Quantitative PCR Validation of Gene Expression of Selected Genes and Immune Genes

A total of 12 genes were chosen for RT-qPCR validation. At 3 days after infected blood feeding (DENV-2 infected) and uninfected blood feeding (mock), ovaries of 10 females (DENV-2 infected) and ovaries of 10 females (mock) were dissected in 0.01M PBS and homogenized in RLT plus buffer for total RNA extraction per manufacturer's instructions using the QIAshredder (Qiagen, 79656) and RNeasy Plus Mini Kit (Qiagen, 74136). Individual carcasses of DENV-2 blood-fed mosquitoes were homogenized

as described and RNA extracted to be tested for DENV-2, and only the ovaries from positive carcasses were considered for the RT-qPCR assay as described below:

The *in vitro* transcription of standard DENV-2 RNA (ssRNA) was obtained following the methods described by Araujo et al. (2020), using 5 μ g of total RNA from DENV-2 NGC infected Vero-E6 cells. The first strand was generated using SuperScript III (Invitrogen, 18080051) with random hexamers, and the cDNA generated was used in PCR reaction with the T7 promoter sequence added to the forward primer DENV2_T7-5'-TAATACGACTCACTATAGGGAGAGCAGATCTCTGATGAA TAACCAACG-3' and the reverse primer DENV2_Env_RC: 5'-CATTCCAAGTGAGAATCTCTTTGTCA-3'. PCR cycles of 95°C for 3 min, followed by 35 repeated cycles of 95°C for 30 s, 62°C for 30 s, and 72°C for 1 min. PCR products were used as a template for the *in vitro* transcription using the MEGAscript T7 Transcription Kit (AMB13345).

Absolute quantitation of viral burden per mosquito was obtained using the RNA from carcasses as a template in the one-step RT-qPCR reaction using the QuantiFast SYBR Green RT-PCR Kit (Qiagen) and a CFX96 Touch Real-Time PCR Detection System (Bio-Rad, California, United States) and calculated using a 10-fold dilution series of DENV2 ssRNA as a standard.

The relative gene expression for all 12 genes selected for validation of RNA-Seq and the immune pathway genes were normalized against the *A. aegypti* actin gene using the $2^{-\Delta\Delta CT}$ method. Primers used for these assays were designed using the Primer-BLAST tool available online (Ye et al., 2012). All of the primers used in this study can be found in **Supplementary Table 1**.

Gene Silencing in Aag2 Cell Line

Transfection of siRNA on Aag2 cells was performed using Lipofectamine 3000 (Thermo Fisher Scientific) according to the manufacturer's instructions. The siRNA sequences can be found in **Supplementary Table 1**. Briefly, 5×10^4 cells were seeded into 24-well plates 1 day before transfection. After cells achieved 90% confluency, 10 pmol of gene-targeting siRNA or scrambled siRNA control was mixed with Lipofectamine 3000 (Thermo Fisher Scientific) and Opti-MEM® (Gibco), which was then used to transfect Aag2 cells. At 72 h post transfection, the siRNA-transfected cells were inoculated with DENV-2 at a multiplicity of infection (MOI) of 1 for 2 h at 30°C and 5% CO₂ incubator. At 2 h post infection (hpi), the inoculum was removed, and the cells were washed once with high glucose DMEM (Gibco). Following washing, DMEM (Gibco) supplemented with 2% FBS was then added to the cells. Time points (cell lysates and viral supernatant) were collected at 24 hpi. Cell lysates were harvested in the RLT buffer by adding beta-mercaptoethanol (β -ME), RNA was extracted using the RNeasy Plus Mini Kit (74106, Qiagen), and RNAi efficiency was validated using qRT-PCR. Cell culture supernatants were collected, and viral titers were obtained by ffa as described. Viral RNA was extracted using the QIAamp Viral RNA Kit (52906, Qiagen). DENV load was then quantified by RT-qPCR using SYBR Green and DENV-2 ssRNA as standard, as we previously described.

Focus Forming Assay

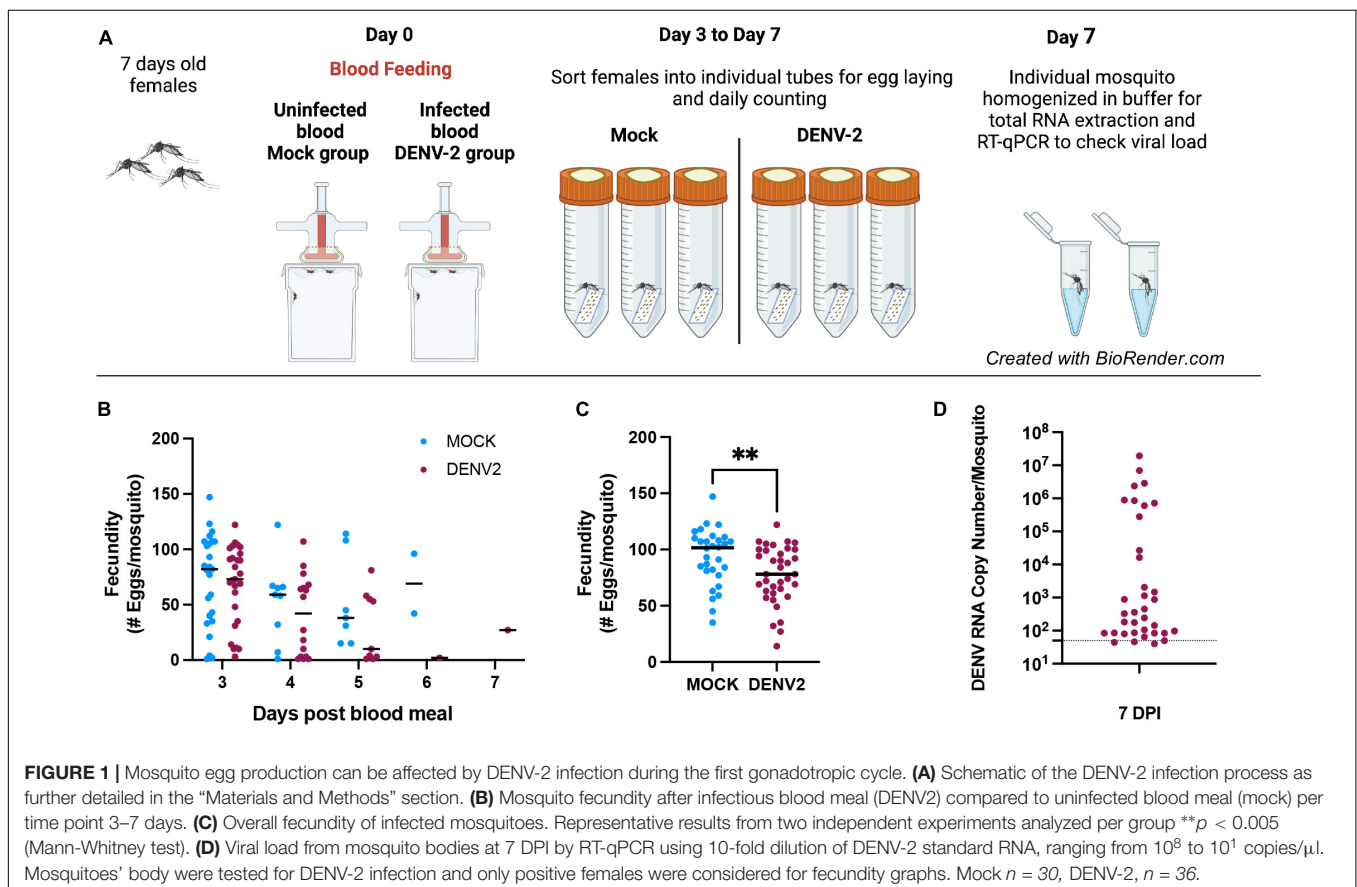
Following dengue infection, cell supernatants from siRNA-transfected Aag2 cells were collected to measure infection by a focus-forming assay. Vero-E6 cells were seeded in 96-well plates at a density of 10,000 cells per well and cultured in DMEM (Gibco) supplemented with 10% heat-inactivated fetal bovine serum (FBS) (Gemini) and 1% penicillin/streptomycin (Gibco) at 37°C in an incubator with 5% CO₂. At 24 h after seeding, Vero-E6 cells were treated with 100 µl of supernatants from infected cells in a serial 10-fold dilution from undiluted to 10⁻⁷ diluted in DMEM (Gibco) for 2 h at 37°C in an incubator with 5% CO₂. After this time, the supernatant was removed, the cells were washed with PBS, and 100 µl of overlay consisting of a 1:1 ratio of DMEM:2% FBS media and 5% carboxymethyl cellulose was added to the cells. Infection was allowed to progress for 5 days, after which the overlay was aspirated, and cells were washed with 0.01M PBS, then fixed with 4% paraformaldehyde (Thermo Fisher Scientific) supplemented with 0.1% Triton X-100 (Thermo Fisher Scientific) for 30 min at room temperature. The fixing solution was then aspirated, and cells were washed with 0.01M PBS again, then blocked with 1% bovine serum albumin (BSA) (Millipore Sigma B6917) in 0.01M PBS at room temperature for 1 h. Following this time, the blocking buffer was removed and cells were incubated with flavivirus group antigen-antibody [D1-4G2-4-15 (4G2)] (Novus Biologicals, NBP-52709, Centennial,

CO., United States) diluted 1:1,000 in 1% BSA in 0.01M PBS for 2 h at room temperature. After this time, the antibody was removed, cells were washed 3 times with 0.01M PBS, and cells were incubated with IRDye® 680RD Goat anti-Mouse IgG Secondary Antibody (LI-COR® Biosciences, Lincoln, NE, United States) diluted 1:1,000 in 1% BSA in 0.01M PBS for 2 h at room temperature. After this time, the antibody was removed, and cells were washed 3 times with 0.01M PBS. PBS was aspirated and cells were allowed to dry. Focus forming assays were performed in duplicate. Foci were identified by the detection of DENV E-specific signal in the 700 nm channel using the Odyssey CLX300 Near-Infrared Fluorescence Imaging System (LI-COR® Biosciences, Lincoln, NE, United States) and counted and reported as focus forming units (FFU).

RESULTS

DENV-2 Reduces Fecundity in *Aedes aegypti* During the First Gonadotrophic Cycle

We aimed to examine the impact of DENV infection on mosquito fecundity. For this, we fed mated 7–10-day old *A. aegypti* females with uninfected blood (mock) vs. blood containing DENV-2 (Figure 1A). We observed that during the first gonadotrophic



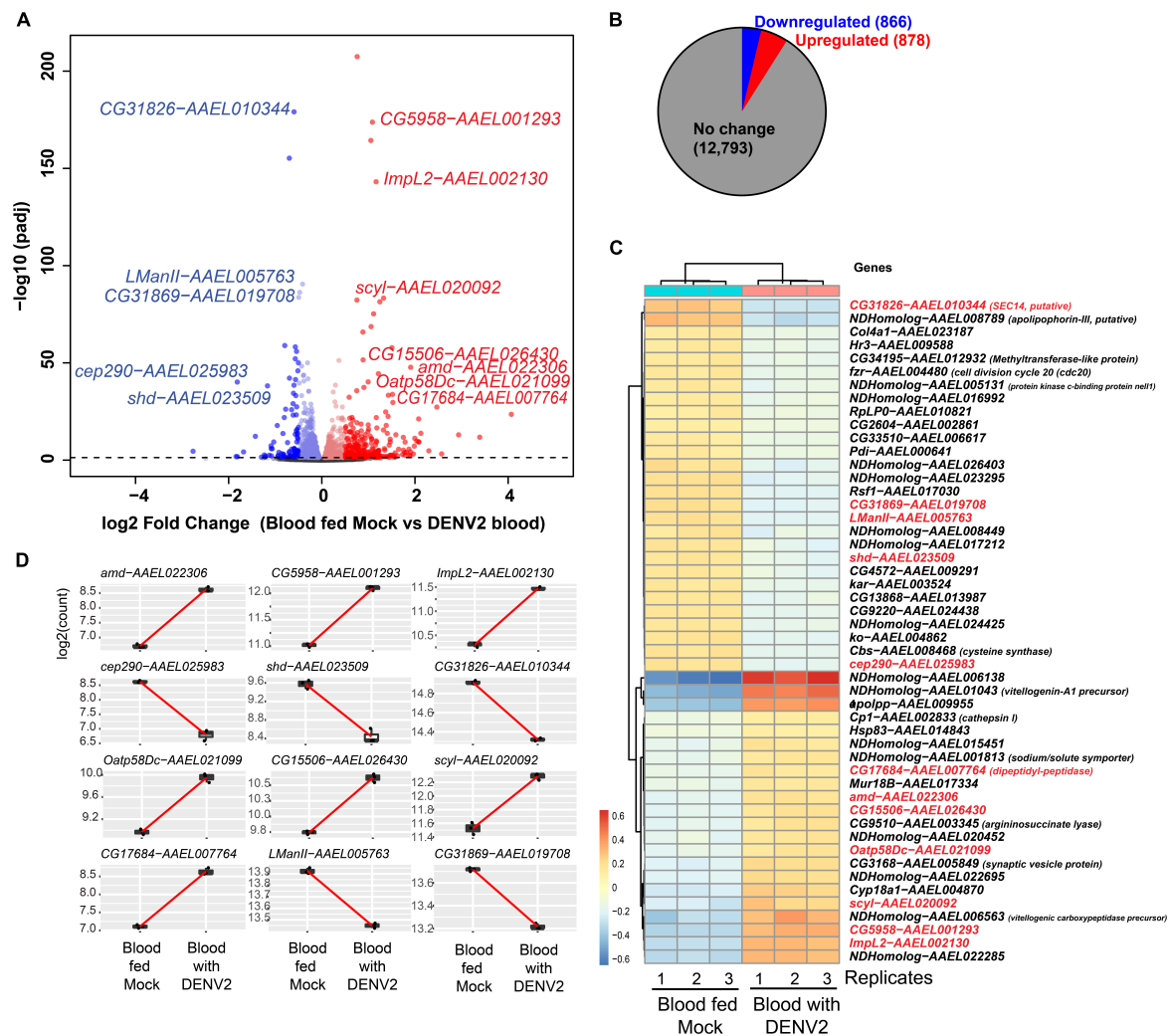


FIGURE 2 | Differential gene expression analysis of *Aedes aegypti* ovaries transcriptomes 3 days after DENV-2 blood feeding vs. mock blood feeding. **(A)** Volcano plot of differentially expressed genes (DEGs) from *A. aegypti* ovaries RNA-seq libraries. **(B)** Fractional proportion of the ovarian DEGs relative to all other *A. aegypti* transcripts. **(C)** Heatmap displaying the top 50 DEGs, and in red text labels are the 12 genes selected for additional downstream studies because the base-mean expression > 200 RPM [or log2(7.6)]. *Drosophila* gene names are shown except for mosquito-specific genes that are named *NDHomolog* because there was no *Drosophila* homologs to be assigned. **(D)** Highlighting the 12 ovarian gene read counts indicate the robustness of the expression change in the read sequencing counts between replicates and the base-mean expression > log2(7.6).

cycle, the females in the DENV-infected group laid significantly fewer eggs compared to females in the mock blood-fed group. In our fecundity assay, we counted eggs daily from 3–7 days post blood feeding (mock or DENV), and we did not observe significant differences in the timing of oviposition, with most mosquitoes laying most of their eggs 3 days post blood meal (**Figure 1B**). In the mock group, the average number of eggs laid per female was 93 eggs/female from a total of 30 females analyzed. In the DENV-2 infected group, the average number of eggs laid was 77 eggs/female from a total of 36 females. These data show a reduction of 22.5% in fecundity from the DENV-2-infected mosquitoes (**Figure 1C**). After egg laying, we confirmed that each female mosquito was infected with DENV using RT-qPCR to detect from 10^1 to 10^8 viral copies. The ratio of DENV-2

infection in the mosquitoes was 50% in the first gonadotrophic cycle alone (**Figure 1D**).

A Search for Genes Affected in *Aedes aegypti* Ovaries Upon DENV-2 Infection

Since blood feeding triggers changes in complex gene expression in females (Giraldo-Calderón et al., 2020), we wondered if the impact that DENV had on the first gonadotrophic cycle could be linked to an alteration of gene expression profiles during blood feeding. Therefore, we performed RNA-seq and transcriptomic analysis of differentially expressed ovarian genes in *A. aegypti* females at 3 days after DENV-2 blood feeding compared to females at 3 days after uninfected blood feeding (mock). As the

TABLE 1 | *Aedes aegypti* ovarian genes with differential expression in blood feeding with DENV-2 selected for RT-qPCR validation.

VectorBase gene ID	VectorBase description	<i>Drosophila</i> ortholog name	<i>Drosophila</i> ortholog gene function
Unregulated genes selected for validation			
AAEL022306	Unspecified product	<i>amd</i>	A methyl dopa-resistant (<i>amd</i>) encodes a carboxy-lyase involved in catecholamine metabolism, i.e., adrenaline, epinephrine
AAEL002130	Ecdysone inducible protein L2, putative	<i>ImpL2</i>	Ecdysone-inducible gene L2. Exhibits insulin binding activity. Involved in several processes, including negative regulation of phosphatidylinositol 3-kinase signaling; positive regulation of entry into reproductive diapause; and regulation of insulin receptor signaling pathway.
AAEL001293	Unspecified product	<i>CG5958</i>	Predicted to have phosphatidylinositol bisphosphate binding activity. PIP2 is a minor phospholipid component of cell membranes.
AAEL021099	Unspecified product	<i>Oatp58Dc</i>	Organic anion transporting polypeptide 58Dc (<i>Oatp58Dc</i>) encodes a membrane transporter implicated in renal elimination of organic compounds including ouabain and methotrexate. In the perineural glia of the blood brain barrier, the product of <i>Oatp58Dc</i> protects the brain from potentially toxic organic anions in the hemolymph.
AAEL026430	Unspecified product	<i>CG15506</i>	No known functions associated, highest express in <i>Drosophila</i> pupation
AAEL020092	Unspecified product	<i>scyl</i>	Scylla inhibits cell growth by regulating the Tor pathway upstream of the Tsc1-Tsc2 complex and downstream of Akt1. Acts as cell death activator during head development
AAEL007764	Dipeptidyl-peptidase	<i>CG17684</i>	Predicted to have serine-type peptidase activity. Predicted to be involved in proteolysis. Is expressed in adult head and spermatozoon. Human ortholog(s) of this gene implicated in amyotrophic lateral sclerosis; asthma; autosomal dominant non-syndromic intellectual disability 33; and spinal muscular atrophy.
Downregulated genes selected for validation			
AAEL023509	Unspecified product	<i>Shd</i>	Shade (<i>shd</i>) encodes 20-hydroxylase and is responsible for converting Ecdysone into 20-hydroxyecdysone, the active form of the steroid. It is required in all tissues that produce active Ecdysone and thus contributes to larval moulting, metamorphosis, growth, neuroblast diversity and egg chamber maturation
AAEL025983	Unspecified product	<i>cep290</i>	Centrosomal protein 290 kDa (<i>Cep290</i>) encodes a cytoplasmic protein located in the cilium transition zone, which assists in the compartmentalization of the cilium in sensory cilia, and the ciliary tip in sperm flagella. Its roles include coordinated movement behavior and sperm motility
AAEL010344	SEC14, putative	<i>CG31826</i>	Predicted to have phosphatidylinositol bisphosphate binding activity. PIP2 is a minor phospholipid component of cell membranes.
AAEL005763	Lysosomal alphananase	<i>LManII</i>	Lysosomal α -mannosidase II (<i>LManII</i>) encodes a mannosyl-oligosaccharide 1,2- α -mannosidase involved in the degradation of asparagine-linked carbohydrates of glycoproteins.
AAEL019708	Unspecified product	<i>CG31869</i>	No known functions associated, widely expressed in many tissues and all stages of <i>Drosophila</i> .

standard analysis of DEGs based solely on *p*-values yielded an intractably large list of gene candidates, we modified our approach to filter for robustly affected genes. First, we looked at mosquito gene annotations that have gene IDs, such as AAEL##### as described in the mosquito database (VectorBase, 2022) by appending the gene name of the *Drosophila melanogaster* ortholog from FlyBase (Thurmond et al., 2019).

After batch correction and initial filtering in R, overall relatedness can be observed within the mock and DENV-2 infected samples as seen by the clustering in the PCA plot (Supplementary Figure 1A). Using DESeq2 from a total of 14,537 DEGs, we identified that 1,744 (12%) genes were significant at an FDR cutoff of 0.05, of which 878 (6%) were upregulated, while 866 (6%) genes were downregulated in the DENV-2 infected pool (Figures 2A,B). The top 50 DEGs can be observed in the heatmap (Figure 2C). From the volcano plot and heatmap, we chose 12 DEGs for the validation of gene expression by qRT-PCR since this technique is powerful in validating gene expression due to its sensitivity and precision. From the list of 12 genes, seven were upregulated, namely, *amd*-AAEL022306,

CG5958-AAEL001293, *ImpL2*-AAEL002130, *Oatp58Dc*-AAEL021099, *CG15506*-AAEL026430, *scyl*-AAEL020092, *CG17684*-AAEL007764, and five were downregulated, namely, *cep290*-AAEL025983, *shd*-AAEL023509, *CG31826*-AAEL010344, *LManII*-AAEL005763, and *CG31869*-AAEL019708. These 12 genes (Figure 2D) are shown to be between the most upregulated or most downregulated (basemean > 150), highlighted in red in the heatmap. We also searched for the ortholog using FlyBase to find the predicted function of those 12 genes. The *Drosophila* ortholog gene function of each of the 12 genes can be found in Table 1. The table illustrates the utility of appending the *Drosophila* gene ortholog name to the mosquito gene ID from Vectorbase because 8/12 of these genes lacked a functional description in the 2021 edition of Vectorbase. However, all of these genes had a clear *Drosophila* ortholog for which Flybase contained a rich functional annotation for the gene. A trend of metabolic and physiology-regulation functions is apparent in this list of genes, with functions such as carboxy-lase for *amd*-AAEL022306, membrane transport in *Oatp58Dc*-AAEL021099, dipeptidyl-peptidase in *CG17684*-AAEL007764, and lysosomal alpha-mannosidase in *LManII*-AAEL005763.

Gene Ontologies of Ovarian DEGs From a DENV-2 Infectious Blood Meal

To explore the functional annotation trends more broadly beyond the 12 validated DEGs, we subjected all the significant DEGs (FDR < 0.05) to a Gene Ontology (GO) analysis, which was aided by the *Drosophila* ortholog names. At Benjamini-Hochberg corrected p -values < 0.05, we identified enriched biological processes, molecular functions, and cellular components among the significant mosquito ovary DEGs impacted by DENV-2 blood meal (**Figure 3**). A trend of physiological and metabolic functions was also apparent in these GO terms, such as peptide metabolic and translation processes, as well as ribosome and translation activity functions.

The general overview of the GO results showed a trend of downregulated genes within the GO biological process in the mosquitoes' ovaries after DENV-2 blood meal (**Figure 3** upper panel). This lowering of the biological process may be related to a decreased number of eggs observed in the first gonadotrophic cycle of the infected mosquitoes.

Specific Differential Gene Expression Changes Validated in *Aedes aegypti* Ovaries During DENV-2 Infection

From the gene expression results shown by the heatmap, we selected 12 DEGs for validation by qRT-PCR (**Figure 4A**). We chose 12 genes to have a better representation of the transcriptome and focus on a search for virally regulated genes. We performed two independent biological replicates of groups of mosquitoes that were fed uninfected blood (mock) vs. a DENV2-infected blood meal. At 3 days post blood feeding, we dissected the ovaries and tested the female carcasses to confirm DENV-2 infection. We used pools of DENV-2 positive ovaries for the RT-qPCR validation assay. As anticipated, all 12 DEGs we tested exhibited similar directional gene expression changes between the RNAseq experiment and the RT-qPCR experiment. Interestingly, two DEGs (amd-AAEL022306 and Oatp58Dc-AAEL021099) after qRT-PCR assay were confirmed to be most upregulated, with over a 3-fold increase, among the 12 selected genes (**Figure 4B**). However, these two genes were the best candidates for further investigation.

We decided to compare the gene expression of these two genes (*amd*-AAEL022306 and *Oatp58Dc*-AAEL021099) with that of an *A. aegypti* eggshell organization factor 1 (EOF1) (Isoe et al., 2019). The EOF1 was recently identified and plays a role in the formation and melanization of the eggshell. Our results using DENV-2 blood-fed females and mock-fed females, 3 days after feedings, showed no differences in the DENV-2-infected mosquitoes compared to the mock-infected ones (**Supplementary Figure 2**).

Specific DEGs From the *Aedes aegypti* Ovary Transcriptome During DENV-2 Infection Also Display Responses in DENV-2 Infection of the Aag2 Cell Line

We hypothesize that DEGs from the *A. aegypti* ovary transcriptome may regulate host responses to DENV-2 infection

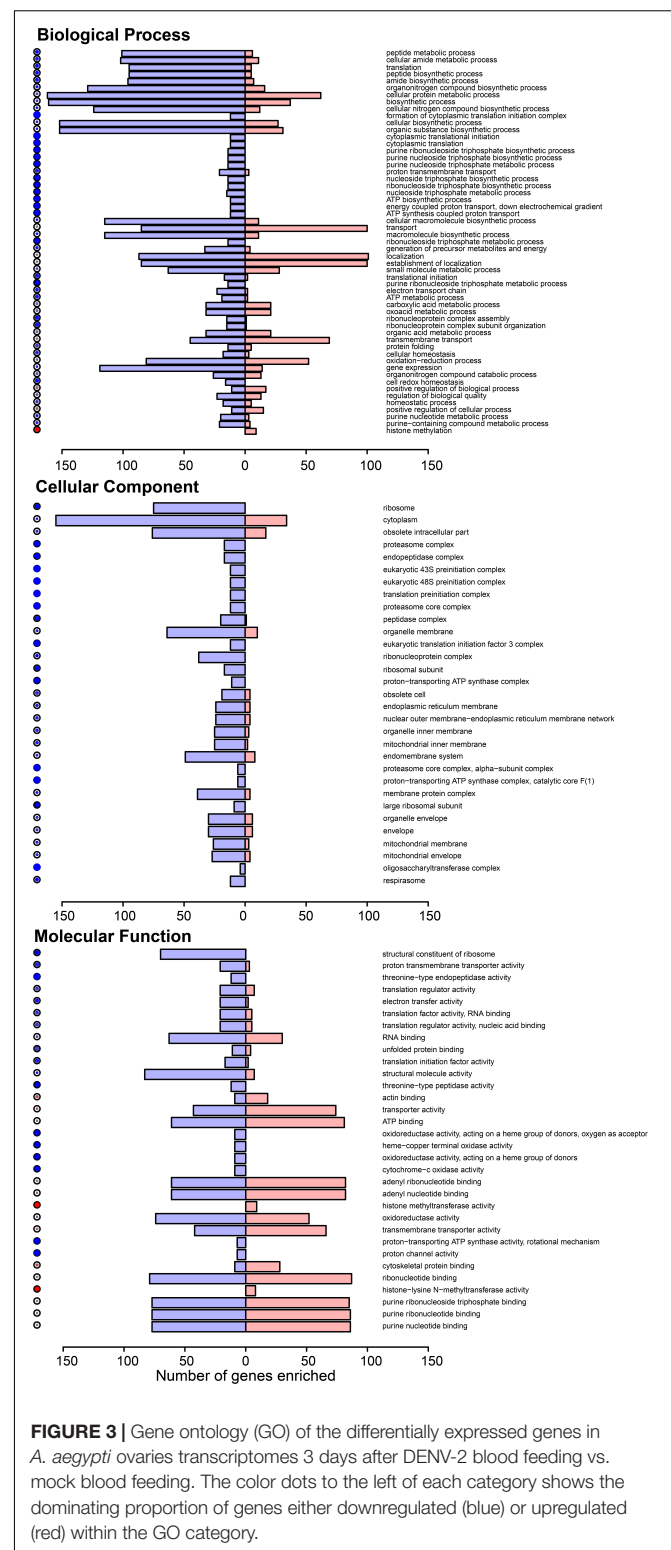
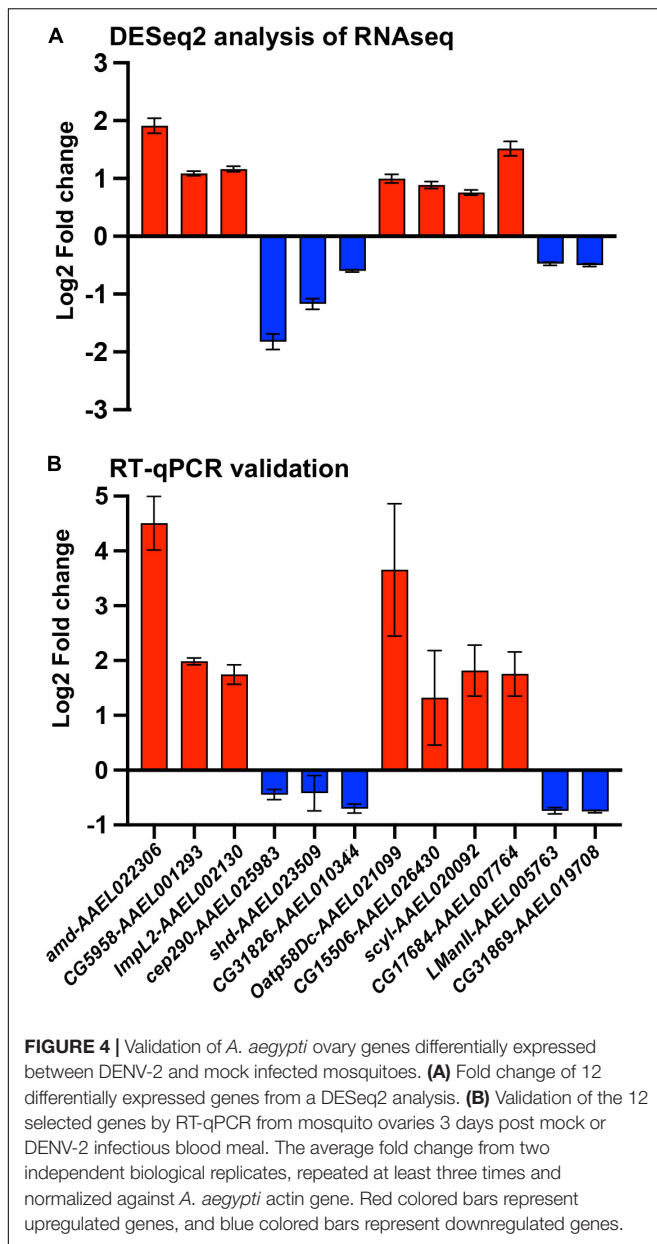


FIGURE 3 | Gene ontology (GO) of the differentially expressed genes in *A. aegypti* ovaries transcriptomes 3 days after DENV-2 blood feeding vs. mock blood feeding. The color dots to the left of each category shows the dominating proportion of genes either downregulated (blue) or upregulated (red) within the GO category.

and modulate fecundity. Using an *in vitro* approach, we chose to investigate the roles of the most upregulated genes from the RT-qPCR validation assays using the Aag2 cell line. This cell line has been shown to recapitulate the immune responses found in adult mosquitoes (Zhang et al., 2017; Li M. J. et al., 2020;



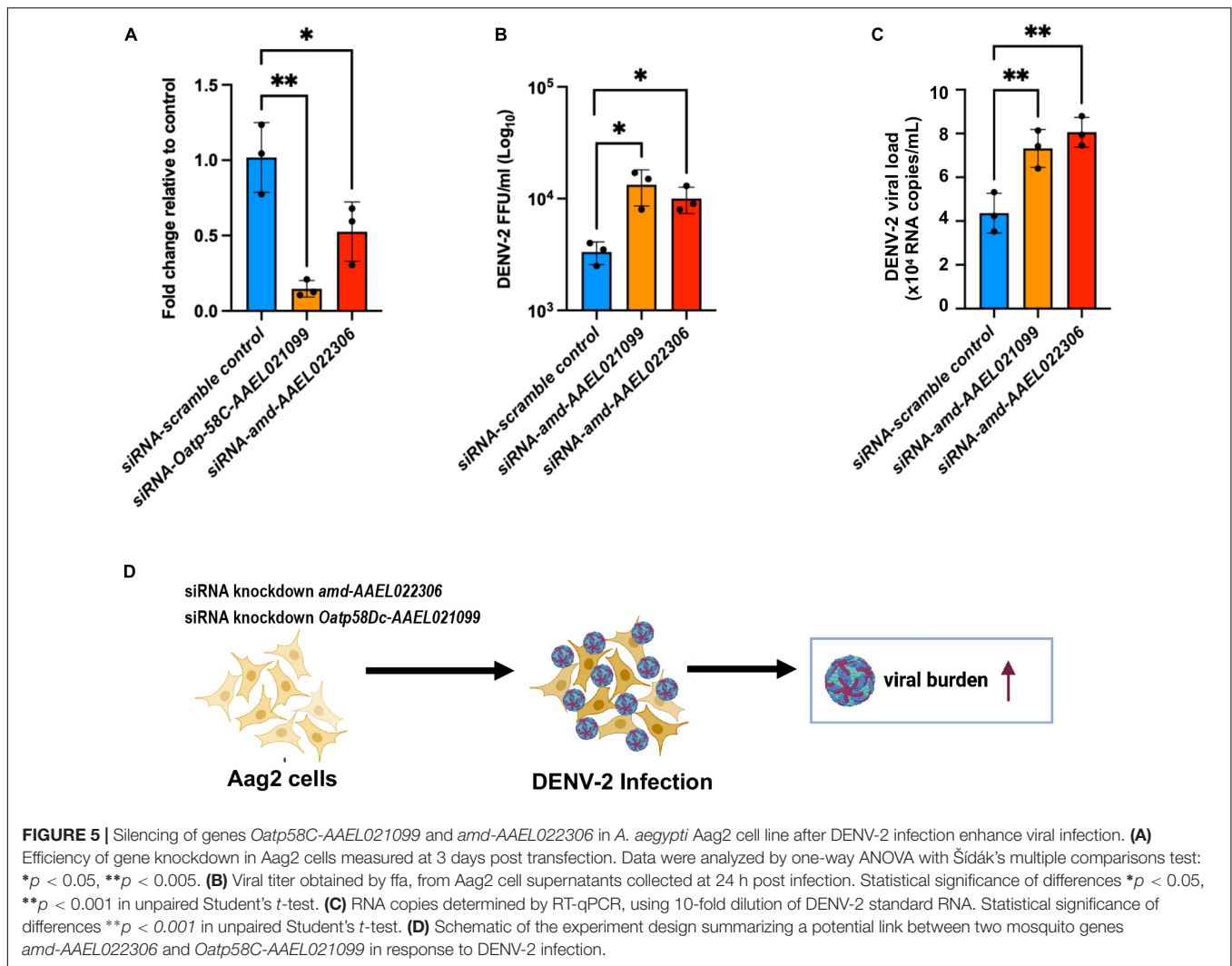
Rosendo Machado et al., 2021). Aag2 cells have been used to experimentally validate mosquito immune pathways (Russell et al., 2021) and to elucidate the mechanisms of antimicrobial peptides (AMP) (Zhang et al., 2017). The advantage of using Aag2 cells to study antiviral immunity genes is that they are much simpler to infect and perform small interfering RNA (siRNA) gene knockdowns than *in vivo* methods. In our Aag2 cell assays, we observed the ideal peak knockdown at 3 days post siRNA transfection of *Oatp58Dc-AAEL021099* and *amd-AAEL022306* in Aag2 cells measured by RT-qPCR (Figure 5A). Following 3 days after knockdown, we infected the cells with DENV-2 at an MOI of 1. At 24 h post infection (24 hpi), cell culture supernatant was collected, and the viral titers were determined by ffa (Figure 5B). We also checked the viral loads by RT-qPCR

(Figure 5C). We observed an increase in DENV-2 RNA copies in Aag2 cells after siRNA-mediated knockdown of either *Oatp58Dc-AAEL021099* or *amd-AAEL022306* compared to cells with the control scrambled siRNA, indicating a potential role of these genes in the mosquito antiviral response (Figure 5D). The same phenotype was observed by Ramirez and Dimopoulos (2010) when silencing MyD88 in laboratory strains of *A. aegypti*, DENV titers were increased in the mosquito's midgut.

DISCUSSION

In this study, we observed that DENV-2 has an impact on the first gonadotrophic cycle of *A. aegypti*. Our data show that infected females lay significantly less number of eggs compared with females that were fed uninfected blood at the first gonadotrophic cycle. Although our data are discordant with a previous report by Sylvestre et al. (2013) where the authors observed a reduction in fecundity observable only at the third and subsequent gonadotrophic cycles, many factors could be affecting mosquito response to infection in laboratory settings, including specific mosquito strain, viral titer, feeding regimens, and others. Other reports suggest a similar reduction in fecundity starting in the first gonadotrophic cycle in the case of infection of *A. aegypti* with alphaviruses such as Mayaro virus (Alto et al., 2020), CHIKV virus (Sirisena et al., 2018), and with flaviviruses such as ZIKV (Petersen et al., 2018). There is not much attention or in-depth studies showing details on the impact of DENV and other members of the Flavivirus genus on the fecundity and fertility of *Aedes* mosquitoes. This is extremely important considering that mosquitoes, males and females, and the eggs are potential natural viral reservoirs (Sánchez-Vargas et al., 2018). Virally infected mosquitoes in nature constitute a powerful source of supporting viruses during intra-epidemic periods and a huge burden on public health (Chung et al., 1998). Studies in *Anopheles* mosquitoes show stimulation of the mosquito immune system by a pathogen and a direct cost within their reproduction and life span (Ahmed and Hurd, 2006; Araujo et al., 2011). For example, in *Anopheles gambiae*, authors used lipopolysaccharide (LPS) to generate a strong immune response that resulted in the upregulation of several immune genes, proposing that immune responses affect egg production *via* induction of apoptosis in the ovarian follicular cells, and this may be one of the mechanisms that lead to a reduction in egg production (Ahmed and Hurd, 2006). A few studies in *Aedes* spp. showed a viral impact on egg laying. CHIKV infected *A. aegypti*, for example, directly impacted the fitness of the mosquitoes by a low survival rate and a decreased number of eggs laid (Sirisena et al., 2018). Moreover, a recent study showed that infection with DENV changes the preference of where to lay their eggs by modifying the expression of selected genes associated with the olfactory learning processes, suggesting that DENV infection may not only impact the number of eggs laid but also the choice of where to deposit them (Gaburro et al., 2018).

Previous studies demonstrated that mosquito immune responses are modulated by blood feeding and that these changes continue through 3 days after ingesting an infectious blood meal



when the females are ready to lay their eggs. Blood alone, without the presence of any pathogen, activates and upregulates immune-related genes (Giraldo-Calderón et al., 2020). In a recent study, the generation of *GCTL-3^{-/-}Aedes aegypti* by CRISPR/Cas9 resulted in a reduction in DENV-2 infection, upregulation of Toll, IMD, and JAK/STAT immune pathways, a reduction in life span, and a reduction in egg production (Li H. H. et al., 2020). In DENV-resistant mosquitoes, the activation of the JAK/STAT pathway results in a fitness cost by decreased egg production by *Aedes* mosquitoes (Jupatanakul et al., 2017).

The extensive trend of metabolic and physiological functions among this set of ovarian DEGs in response to DENV represents an overlooked area of arbovirology since innate immune pathway genes were absent from our DEG analysis. For instance, the gene *amd-AAEL022306* is predicted to participate in the decarboxylation and deamination of L-dopa to 3,4-dihydroxyphenylacetaldehyde (DHPAA). DHPAA is a highly toxic component since its aldehyde group readily reacts with the primary amino groups of proteins, leading to protein crosslinking and

inactivation (Vavricka et al., 2011). The fact that silencing *amd-AAEL022306* increases DHPAA following DENV infection suggests that it may participate in the inactivation of viral particles.

Similarly, the solute carrier organic anion transporter family member *Oatp58Dc-AAEL021099* was also found to be upregulated in the ovaries of infected mosquitoes. The predicted biological process of this protein is ion/transmembrane transport. Interestingly, the silencing of this gene resulted in an increase in DENV replication in Aag2 cells. In *Drosophila*, *Oatp58Dc* is highly expressed in the Malpighian tubules, and it is associated with anoxia, which is linked with an increase in oxidative stress (Campbell et al., 2019). However, Aag2 cells are known as immune-responsive cells (Fallon and Sun, 2001) and have been validated as a reliable model to study *Aedes* immune responses against pathogens (Barletta et al., 2012). More experiments are needed to evaluate the effect of upregulation of *Oatp58Dc-AAEL021099* and *amd-AAEL022306* on immunomodulatory responses *in vivo*. These data suggest that the two genes identified in our mosquito ovary transcriptome may not be involved in

the formation and melanization of the eggshell. In contrast, the viral upregulation of these two genes displayed characteristics of immune-related genes when compared to genes of the mosquito immune pathway.

Although our future goal will be to test the functional relevance of these DEGs in DENV-2 infected mosquitoes, we were able to assess *in vitro* the relevance of two of the DEGs in an Aag2 cell line, setting forth a platform for further investigation of the role that metabolic and physiologic gene may play in the mosquito immune response to arbovirus infection.

CONCLUSION

By employing new strategies to assess mosquito transcriptomic changes during DENV-2 infection and combining gene annotation information from the *Drosophila* database, in this study, we present that DENV-2 elicited transcriptional signatures in the ovaries of *A. aegypti* and the impact of infection on the reproductive cycle, including the reduction in the number of eggs laid by infected females during the first gonadotrophic cycle. The differential gene expression data, shown in this study, are the first to outline the transcriptional signature of the ovary when the virus is not yet present, indicating that the ovaries are responding to the viral infection as early as 3 days after the female ingests an infectious blood meal. It is possible that DENV activates the immune system and triggers upregulation of ovarian genes, and this early response may directly interfere with the fecundity of the mosquitoes in first egg laying, as we observed a reduced number of eggs laid. Building upon these results, we also identified two DEGs that displayed an antiviral mechanism in response to viral infection in mosquito cell lines, indicating their putative cell-autonomous function in the antiviral response of the mosquito. Future investigations of how the early activation of mosquito host responses to DENV-2 affects the fecundity and reproductive fitness of *A. aegypti* are required and may provide new strategies for mosquito control to halt the spread of arboviruses.

DATA AVAILABILITY STATEMENT

The datasets presented in this study can be found in online repositories. The names of the repository/repositories and accession number(s) can be found below: <https://www.ncbi.nlm.nih.gov/>, SRR17125477; <https://www.ncbi.nlm.nih.gov/>, SRR17125482.

REFERENCES

- Ahmed, A. M., and Hurd, H. (2006). Immune stimulation and malaria infection impose reproductive costs in *Anopheles gambiae* via follicular apoptosis. *Microb. Infect.* 8, 308–315. doi: 10.1016/j.micinf.2005.06.026
- Alto, B. W., Civana, A., Wiggins, K., Eastmond, B., and Shin, D. (2020). Effect of Oral Infection of Mayaro Virus on Fitness Correlates and Expression of Immune Related Genes in *Aedes aegypti*. *Viruses* 12:719. doi: 10.3390/v12070719
- Araujo, R. V., Feitosa-Suntheimer, F., Gold, A. S., Londono-Renteria, B., and Colpitts, T. M. (2020). One-step RT-qPCR assay for ZIKV RNA detection in *Aedes aegypti* samples: a protocol to study infection and gene expression

ETHICS STATEMENT

The animal study was reviewed and approved by the Institutional Animal Care and Use Committee (IACUC). Approved protocol PROTO201900005.

AUTHOR CONTRIBUTIONS

FF-S, TC, and BL-R: conceptualization. FF-S, ZZ, EM, and AG: mosquito and virology assays. AB-C, AT, and MR-B: laboratory assistance. GD and NL: bioinformatic analyses and writing. RC: provide foundational and infrastructural support and oversight. FF-S: initial draft. FF-S and BL-R: final writing, review, and editing. All authors reviewed and provided comments on the text.

FUNDING

This study was supported by the Boston University and the National Emerging Infectious Diseases Laboratories (NEIDL) Director's funding. Pilot funding and NIH grant R21AI129881 to TC; NIH grant R01-GM135215 and the Wing-Tat Lee Foundation award to NL.

ACKNOWLEDGMENTS

We would like to thank Jacquelyn Turcinovic and Varun Raghuram for their assistance in looking at additional RNA-seq datasets. We would also like to thank Florian Douam for the helpful discussion and critical comments on the manuscript. We acknowledge support from Norbert Perrimon and assistance from Devin Kenney, Aoife O'Connor, Giulia Unali, and Collen Thurman from NEIDL Animal Core, in the mosquito's blood feedings.

SUPPLEMENTARY MATERIAL

The Supplementary Material for this article can be found online at: <https://www.frontiersin.org/articles/10.3389/fmicb.2022.886787/full#supplementary-material>

during ZIKV infection. *Parasit. Vectors* 13:128. doi: 10.1186/s13071-020-4002-x

- Araujo, R. V., Maciel, C., Hartfelder, K., and Capurro, M. L. (2011). Effects of *Plasmodium gallinaceum* on hemolymph physiology of *Aedes aegypti* during parasite development. *J. Insect Physiol.* 57, 265–273. doi: 10.1016/j.jinsphys.2010.11.016
- Ashburner, M., Ball, C. A., Blake, J. A., Botstein, D., Butler, H., Cherry, J. M., et al. (2000). Gene ontology: tool for the unification of biology. *Nat. Genet.* 25, 25–29. doi: 10.1038/75556
- Attardo, G. M., Hansen, I. A., and Raikhel, A. S. (2005). Nutritional regulation of vitellogenesis in mosquitoes: implications for anaerobiosis. *Insect Biochem. Mol. Biol.* 35, 661–675. doi: 10.1016/j.ibmb.2005.02.013

- Barletta, A. B. F., Silva, M. C. L. N., and Sorgine, M. H. F. (2012). Validation of *Aedes aegypti* Aag-2 cells as a model for insect immune studies. *Paras. Vectors* 5:148. doi: 10.1186/1756-3305-5-148
- Campbell, J. B., Overby, P. F., Gray, A. E., Smith, H. C., and Harrison, J. F. (2019). Genome-wide association analysis of anoxia tolerance in *Drosophila melanogaster*. *G3: Genes, Genom. Genet.* 9, 2989–2999. doi: 10.1534/g3.119.400421
- Carrington, L. B., and Simmons, C. P. (2014). Human to mosquito transmission of dengue viruses. *Front. Immunol.* 5:290. doi: 10.3389/fimmu.2014.00290
- CDC. (2021). *Areas with Risk of Dengue*. Atlanta: CDC.
- Chan, M., and Johansson, M. A. (2012). The Incubation Periods of Dengue Viruses. *PLoS One* 7:e50972. doi: 10.1371/journal.pone.0050972
- Chaves, B. A., Junior, A. B. V., Silveira, K. R. D., Paz, A. D. C., Vaz, E. B. D. C., Araujo, R. G. P., et al. (2019). Vertical Transmission of Zika Virus (Flaviviridae, Flavivirus) in Amazonian *Aedes aegypti* (Diptera: Culicidae) Delays Egg Hatching and Larval Development of Progeny. *J. Med. Entomol.* 56, 1739–1744. doi: 10.1093/jme/tjz110
- Chung, Y. K., Lam-Phua, S. G., Lee, K. M., Yong, R., Lim, L. K., Chow, V. T., et al. (1998). Monitoring of dengue viruses in field-caught *Aedes aegypti* and *Aedes albopictus* mosquitoes by a type-specific polymerase chain reaction and cycle sequencing. *Am. J. Trop. Med. Hyg.* 58, 578–586. doi: 10.4269/ajtmh.1998.58.578
- Day, J. F. (2016). Mosquito oviposition behavior and vector control. *Insects* 7:65. doi: 10.3390/insects7040065
- Fallon, A. M., and Sun, D. (2001). Exploration of mosquito immunity using cells in culture. *Insect Biochem. Mol. Biol.* 31, 263–278. doi: 10.1016/s0965-1748(00)00146-6
- Franz, A. W. E., Kantor, A. M., Passarelli, A. L., and Clem, R. J. (2015). Tissue barriers to arbovirus infection in mosquitoes. *Viruses* 7, 3741–3767. doi: 10.3390/v7072795
- Gaburro, J., Paradkar, P. N., Klein, M., Bhatti, A., Nahavandi, S., and Duchemin, J. B. (2018). Dengue virus infection changes *Aedes aegypti* oviposition olfactory preferences. *Sci. Rep.* 8:13179. doi: 10.1038/s41598-018-31608-x
- Giraldo-Calderón, G. I., Calle-Tobón, A., Roza-López, P., Colpitts, T. M., Park, Y., Rua-Urbe, G. L., et al. (2020). Transcriptome of the *aedes aegypti* mosquito in response to human complement proteins. *Int. J. Mol. Sci.* 21, 1–19. doi: 10.3390/ijms21186584
- Halstead, S. B. (2016). Licensed dengue vaccine: public health conundrum and scientific challenge. *Am. J. Trop. Med. Hyg.* 95, 741–745. doi: 10.4269/ajtmh.16-0222
- Hansen, I. A., Attardo, G. M., Rodriguez, S. D., and Drake, L. L. (2014). Four-way regulation of mosquito yolk protein precursor genes by juvenile hormone-, ecdysone-, nutrient-, and insulin-like peptide signaling pathways. *Front. Physiol.* 5:103. doi: 10.3389/fphys.2014.00103
- Isoe, J., Koch, L. E., Isoe, Y. E., Rascón, A. A., Brown, H. E., Massani, B. B., et al. (2019). Identification and characterization of a mosquito-specific eggshell organizing factor in *Aedes aegypti* mosquitoes. *PLoS Biol.* 17:e3000068. doi: 10.1371/journal.pbio.3000068
- Iwamura, T., Guzman-Holst, A., and Murray, K. A. (2020). Accelerating invasion potential of disease vector *Aedes aegypti* under climate change. *Nat. Commun.* 11:2130. doi: 10.1038/s41467-020-16010-4
- Izmirly, A. M., Alturki, S. O., Alturki, S. O., Connors, J., and Haddad, E. K. (2020). Challenges in Dengue Vaccines Development: pre-existing Infections and Cross-Reactivity. *Front. Immunol.* 11:1055. doi: 10.3389/fimmu.2020.01055
- Jupatanakul, N., Sim, S., Angleró-Rodríguez, Y. I., Souza-Neto, J., Das, S., Poti, K. E., et al. (2017). Engineered *Aedes aegypti* JAK/STAT Pathway-Mediated Immunity to Dengue Virus. *PLoS Negl. Trop. Dis.* 11:e0005187. doi: 10.1371/journal.pntd.0005187
- Koh, C., Allen, S. L., Herbert, R. I., McGraw, E. A., and Chenoweth, S. F. (2018). The transcriptional response of *Aedes aegypti* with variable extrinsic incubation periods for dengue virus. *Genom. Biol. Evol.* 10, 3141–3151. doi: 10.1093/gbe/evy230
- Lai, Z., Zhou, T., Liu, S., Zhou, J., Xu, Y., Gu, J., et al. (2020). Vertical transmission of zika virus in *aedes albopictus*. *PLoS Negl. Trop. Dis.* 14:1–16. doi: 10.1371/journal.pntd.0008776
- Li, H. H., Cai, Y., Li, J. C., Su, M. P., Liu, W. L., Cheng, L., et al. (2020). C-Type Lectins Link Immunological and Reproductive Processes in *Aedes aegypti*. *iScience* 23:101486. doi: 10.1016/j.isci.2020.101486
- Li, M. J., Lan, C. J., Gao, H. T., Xing, D., Gu, Z. Y., Su, D., et al. (2020). Transcriptome analysis of *Aedes aegypti* Aag2 cells in response to dengue virus-2 infection. *Parasites and Vectors* 13:421. doi: 10.1186/s13071-020-04294-w
- Love, M. I., Huber, W., and Anders, S. (2014). Moderated estimation of fold change and dispersion for RNA-seq data with DESeq2. *Genom. Biol.* 15:550. doi: 10.1186/s13059-014-0550-8
- Novelo, M., Hall, M. D., Pak, D., Young, P. R., Holmes, E. C., and McGraw, E. A. (2019). Intra-host growth kinetics of dengue virus in the mosquito *Aedes aegypti*. *PLoS Pathog.* 15:e1008218. doi: 10.1371/journal.ppat.1008218
- Petersen, M. T., da Silveira, I. D., Tática-Ferreira, A., David, M. R., Chouin-Carneiro, T., van den Wouwer, L., et al. (2018). The impact of the age of first blood meal and zika virus infection on *aedes aegypti* egg production and longevity. *PLoS One* 13:e0200766. doi: 10.1371/journal.pone.0200766
- Ramirez, J. L., and Dimopoulos, G. (2010). The Toll immune signaling pathway control conserved anti-dengue defenses across diverse *Ae. aegypti* strains and against multiple dengue virus serotypes. *Dev. Comparat. Immunol.* 34, 625–629. doi: 10.1016/j.dci.2010.01.006
- Robinson, M. D., McCarthy, D. J., and Smyth, G. K. (2009). edgeR: a Bioconductor package for differential expression analysis of digital gene expression data. *Bioinformatics* 26, 139–140. doi: 10.1093/bioinformatics/btp616
- Rosendo Machado, S., van der Most, T., and Miesen, P. (2021). Genetic determinants of antiviral immunity in dipteran insects – Compiling the experimental evidence. *Dev. Comparat. Immunol.* 119:104010. doi: 10.1016/j.dci.2021.104010
- Rückert, C., and Ebel, G. D. (2018). How Do Virus–Mosquito Interactions Lead to Viral Emergence? *Trends Parasitol.* 34, 310–321. doi: 10.1016/j.pt.2017.12.004
- Russell, T. A., Ayaz, A., Davidson, A. D., Fernandez-Sesma, A., and Maringer, K. (2021). Imd pathway-specific immune assays reveal nf- κ b stimulation by viral rna pamps in *aedes aegypti* aag2 cells. *PLoS Negl. Trop. Dis.* 15:1–23. doi: 10.1371/journal.pntd.0008524
- Sánchez-Vargas, I., Harrington, L. C., Doty, J. B., Black, W. C., and Olson, K. E. (2018). Demonstration of efficient vertical and venereal transmission of dengue virus type-2 in a genetically diverse laboratory strain of *Aedes aegypti*. *PLoS Negl. Trop. Dis.* 12:e0006754. doi: 10.1371/journal.pntd.0006754
- Sirisena, P. D. N. N., Kumar, A., and Sunil, S. (2018). Evaluation of *Aedes aegypti* (Diptera: culicidae) life table attributes upon chikungunya virus replication reveals impact on egg-laying pathways. *J. Med. Entomol.* 55, 1580–1587. doi: 10.1093/jme/tjy097
- Sylvestre, G., Gandini, M., and Maciel-de-Freitas, R. (2013). Age-Dependent Effects of Oral Infection with Dengue Virus on *Aedes aegypti* (Diptera: Culicidae) Feeding Behavior, Survival, Oviposition Success and Fecundity. *PLoS One* 8:e59933. doi: 10.1371/journal.pone.0059933
- Thurmond, J., Goodman, J. L., Strelets, V. B., Attrill, H., Gramates, L. S., Marygold, S. J., et al. (2019). FlyBase 2.0: the next generation. *Nucleic Acids Res.* 47, D759–D765. doi: 10.1093/nar/gky1003
- Vavricka, C., Han, Q., Huang, Y., Erickson, S. M., Harich, K., Christensen, B. M., et al. (2011). From L-dopa to dihydroxyphenylacetaldehyde: a toxic biochemical pathway plays a vital physiological function in insects. *PLoS One* 6:e16124. doi: 10.1371/journal.pone.0016124
- VectorBase. (2022). *Vector Base Bioinformatics Resources For Invertebrate Vectors of human Pathogens*. Available online at <https://vectorbase.org/vectorbase/app> (accessed January, 2022).
- Weaver, S. C., and Barrett, A. D. T. (2004). Transmission cycles, host range, evolution and emergence of arboviral disease. *Nat. Rev. Microbiol.* 2, 789–801. doi: 10.1038/nrmicro1006
- WHO. (2022). *Dengue and severe dengue*. Available online class <https://www.who.int/news-room/fact-sheets/detail/dengue-and-severe-dengue> (accessed December, 2021).
- Wijesinghe, C., Gunatilake, J., Kusumawathie, P. H. D., Sirisena, P. D. N. N., Daulagala, S. W. P. L., Iqbal, B. N., et al. (2021). Circulating dengue virus serotypes and vertical transmission in *Aedes* larvae during outbreak and inter-outbreak seasons in a high dengue risk area of Sri Lanka. *Parasites Vectors* 14:614. doi: 10.1186/s13071-021-05114-5

- Wu, P., Yu, X., Wang, P., and Cheng, G. (2019). Arbovirus lifecycle in mosquito: acquisition, propagation and transmission. *Expert Rev. Mol. Med.* 21:e1. doi: 10.1017/erm.2018.6
- Ye, J., Coulouris, G., Zaretskaya, I., Cutcutache, I., Rozen, S., and Madden, T. L. (2012). Primer-BLAST: a tool to design target-specific primers for polymerase chain reaction. *BMC Bioinform.* 13:134. doi: 10.1186/1471-2105-13-134
- Zhang, R., Zhu, Y., Pang, X., Xiao, X., Zhang, R., and Cheng, G. (2017). Regulation of antimicrobial peptides in *Aedes aegypti* Aag2 Cells. *Front. Cell. Infect. Microbiol.* 7:22. doi: 10.3389/fcimb.2017.00022

Conflict of Interest: TC was employed by the Moderna Inc.

The remaining authors declare that the research was conducted in the absence of any commercial or financial relationships that could be construed as a potential conflict of interest.

Publisher's Note: All claims expressed in this article are solely those of the authors and do not necessarily represent those of their affiliated organizations, or those of the publisher, the editors and the reviewers. Any product that may be evaluated in this article, or claim that may be made by its manufacturer, is not guaranteed or endorsed by the publisher.

Copyright © 2022 Feitosa-Suntheimer, Zhu, Mamei, Dayama, Gold, Broos-Caldwell, Troupin, Rippee-Brooks, Corley, Lau, Colpitts and Londoño-Renteria. This is an open-access article distributed under the terms of the Creative Commons Attribution License (CC BY). The use, distribution or reproduction in other forums is permitted, provided the original author(s) and the copyright owner(s) are credited and that the original publication in this journal is cited, in accordance with accepted academic practice. No use, distribution or reproduction is permitted which does not comply with these terms.

Advantages of publishing in Frontiers



OPEN ACCESS

Articles are free to read
for greatest visibility
and readership



FAST PUBLICATION

Around 90 days
from submission
to decision



HIGH QUALITY PEER-REVIEW

Rigorous, collaborative,
and constructive
peer-review



TRANSPARENT PEER-REVIEW

Editors and reviewers
acknowledged by name
on published articles

Frontiers

Avenue du Tribunal-Fédéral 34
1005 Lausanne | Switzerland

Visit us: www.frontiersin.org

Contact us: frontiersin.org/about/contact



REPRODUCIBILITY OF RESEARCH

Support open data
and methods to enhance
research reproducibility



DIGITAL PUBLISHING

Articles designed
for optimal readership
across devices



FOLLOW US

@frontiersin



IMPACT METRICS

Advanced article metrics
track visibility across
digital media



EXTENSIVE PROMOTION

Marketing
and promotion
of impactful research



LOOP RESEARCH NETWORK

Our network
increases your
article's readership